STRUCTURAL, STRATIGRAPHIC AND METAMORPHIC GEOLOGY OF LOWER PROTEROZOIC ROCKS IN THE COWELL/CLEVE DISTRICT, EASTERN EYRE PENINSULA.

VOLUME I



by

Allan John Parker
B.Sc. (Hons), Adelaide

Department of Geology and Mineralogy
University of Adelaide

March, 1978

VOLUME I

	PAGE
TABLE OF CONTENTS	I
LIST OF FIGURES	VII
SUMMARY	XIV
STATEMENT OF ORIGINALITY	XVII
ACKNOWLEDGEMENTS	XVIII
CHAPTER I INTRODUCTION	1
1.1 REGIONAL SETTING	1
1.2 PREVIOUS WORK	3
1.3 PRESENT INVESTIGATION	10
1.4 TERMINOLOGY	11
CHAPTER II LITHOLOGY	15
2.1 INTRODUCTION	15
2.2 THE METASEDIMENTARY ROCKS	16
2.2.1 Quartzite Petrography	17
2.2.2 Layered Migmatites, Gneisses and Schists	21
2.2.3 Dolomites and Calc-Silicates	26
2.2.4 Amphibolite Petrography	31
2.2.5 Iron Formation Petrography	35
2.3 THE GRANITIC ROCKS	37
2.3.1 Plug Range Granite Gneiss	37
2.3.2 Middle Camp Granite	39
2.3.3 Narridy Creek Granite	40
2.3.4 Minor Intrusives	42
CHAPTER III MESOSCOPIC STRUCTURE	46
3.1 INTRODUCTION	46
3.2 BASIC STRUCTURAL ELEMENTS	47
3.2.1 D_1 Deformation	47

3.2.2 D_2 Deformation 48

3.2.3 D_3 Deformation 54

3.2.4 Mylonite Deformation (D_m) 59

3.2.5 D_4 Deformation 62

3.2.6 Brittle Deformation 64

CHAPTER IV MACROSCOPIC STRUCTURE 65

4.1 INTRODUCTION 65

4.2 ORIENTATION DATA 65

4.2.1 Wangaraleednie Subarea 65

4.2.2 Mt. Millar/Morowie Subarea 67

4.2.3 Narridy Creek Subarea 71

4.2.4 Middle Camp Subarea 74

4.2.5 Ullabidinie Subarea 75

4.2.6 Plug Range Subarea 77

4.3 PEGMATITE ORIENTATIONS 78

4.4 SUMMARY DISCUSSION AND REGIONAL CORRELATION 80

CHAPTER V STRATIGRAPHY 87

5.1 INTRODUCTION 87

5.2 SUMMARY DESCRIPTION OF LOCAL SEQUENCES 87

5.2.1 Wangaraleednie Subarea 87

5.2.2 Mt. Millar/Morowie Subarea 89

5.2.3 Middle Camp Subarea 93

5.2.4 Ullabidinie Subarea 94

5.2.5 Plug Range Subarea 94

5.3 INTERPRETATION AND DISCUSSION 96

5.3.1 Sedimentary Record 97

5.3.2 The Basement Controversy 100

5.3.3 Origin of Amphibolites 102

5.3.4 An Upper Iron Formation 104

5.4 CONCLUSIONS AND REGIONAL APPRAISAL 106

5.5 STRUCTURAL IMPLICATIONS 110

APPENDIX A. CHEMICAL ANALYSIS A1

APPENDIX B. GEOCHRONOLOGY B1

VOLUME II PAGE

TABLE OF CONTENTS

CHAPTER VI MICROSTRUCTURE 1

6.1 INTRODUCTION 1

6.2 D_1 DEFORMATION 1

6.2.1 The Fabric 1

6.2.1.1 S_1 fabric 2

6.2.1.2 F_1 folding 5

6.2.2 D_1 Fabric Development 6

6.2.2.1 Significant of S_1 6

6.2.2.2 Origin of S_1 8

6.3 D_2 DEFORMATION 10

6.3.1 The Fabric 10

6.3.1.1 Semipelites 10

6.3.1.2 Other Lithologies 15

6.3.2 D_2 Fabric Development 19

6.3.2.1 Relationship of Fabric to Strain 19

6.3.2.2 Mechanism of layer Silicate Orientation 24

6.3.3 Summary of D_2 Microfabric 30

6.4 D_3 DEFORMATION 31

6.4.1 The Fabric 31

6.4.1.1 Semipelites 31

6.4.1.2 Other lithologies 35

6.4.1.3 Narridy Creek Granite 39

6.4.2 Development of D_3 Fabric 42

6.4.2.1 Relationship of Fabric to Strain 42

6.4.2.2 Development of S_3 42
6.4.2.3 Development of D_3 Quartz Textures 45
6.4.3 Summary of D_3 Microstructures 58
6.5 MYLONITE DEFORMATION 59
6.5.1 The Fabric 59
6.5.1.1 Mica recrystallization Stage 60
6.5.1.2 Feldspar recrystallization Stage 62
6.5.2 Summary and Discussion 68
6.6 D_4 DEFORMATION 71
6.6.1 The Fabric 71
6.6.1.1 Crenulations 71
6.6.1.2 Planar S_4 Elements 72
6.6.2 Discussion 75
6.7 BRITTLE (post D_4) DEFORMATION 76
6.7.1 The Fabric 76
6.7.2 Discussion 78
CHAPTER VII METAMORPHISM 80
7.1 INTRODUCTION 80
7.2 OUTLINE OF METAMORPHIC EVOLUTION 81
7.3 M_{1-2} METAMORPHISM 82
7.3.1 Summary of Mineral Parageneses 83
7.3.2 Discussion 84
7.3.2.1 Evidence for two separate events, M_1 and M_2 84
7.3.2.2 Pelitic and semi-pelitic parageneses 87

7.3.2.3 Carbonate parageneses 92

7.3.2.4 Metabasite parageneses 97

7.3.2.5 Eulysite parageneses 98

7.3.3 T-P Conditions 99

7.4 M_3 METAMORPHISM 105

7.4.1 Summary of Observed Mineral Associations 106

7.4.2 Discussion 108

7.4.3 P-T Conditions 112

7.5 M_4 METAMORPHISM 113

7.5.1 Summary of mineral parageneses 113

7.5.2 Discussion 114

7.5.3 P-T Conditions 116

7.6 SUMMARY OF METAMORPHISM 116

CHAPTER VIII CONCLUSIONS AND TECTONIC IMPLICATIONS 119

8.1 SUMMARY OF CONCLUSIONS 119

8.1.1 Lithology 119

8.1.2 Stratigraphy 120

8.1.3 Igneous, Metamorphic and Structural Evolution 121

8.1.4 Regional Correlation 124

8.2 TECTONIC IMPLICATIONS 126

REFERENCES CITED 130

APPENDIX C Tectonic relationships between the Proterozoic Gawler and Willyama Orogenic Domains, Australia. By R.A. Glen, W.P. Laing, A.J. Parker and R.W.R. Rutland.

LIST OF FIGURES

Enclosed in pocket at rear of Volume II

Plan 1 Geological Map : Portion of Eyre Peninsula (Scale 1:253 440)

Plan 2 Geological Map of the Cowell/Cleve District, Eyre Peninsula (Scale 1: 20 000)

VOLUME I

Figure No.		Facing Page No.
1.1	Locality plan	2
1.2	Synopsis of previous stratigraphic nomenclature on Eyre Peninsula	5
2.1	Regional variation in quartzite lithology	19
2.2	Distribution of migmatite gneisses	24
2.3	Modal compositions of semipelitic gneisses	24
2.4	Modal compositions of amphibolites	32
2.5	Modal compositions of granitic rocks	38
3.1	Location of subareas and simplified geology	46
3.2	Plate - F_2 folds in semipelitic rocks	49
3.3	t' plots for various F_2 and F_3 folds	50
3.4	Plate - L_2 lineations in semipelitic gneisses	51
3.5	Plate - L_2 quartz rodding in quartzites	52
3.6	Plate - F_2 folds in calcsilicates, amphibolite and Plug Range granite gneiss	53
3.7	Plate - F_3 folds in semipelitic rocks	55

3.8	Plate - F_3 folds in quartzite, Plug Range granite gneiss and Middle Camp granite	56
3.9	Plate - Narridy Creek granite	58
3.10	Plate - Mylonite zone - F_3 folds and slaty mylonite	59
3.11	Plate - Mylonite zone in Mindrow Creek	60
3.12	Plate - D_4 structures	62
4.1	Structural map and stereodiagrams of the Wangaraleednie Subarea	66
4.2	Structural cross sections of the Wangaraleednie Subarea	67
4.3	Structural map and stereodiagrams of the Mt. Millar/Morowie Subarea	68
4.4	Structural cross sections of the Mt. Millar/Morowie Subarea	68
4.5	Deformation of F_2 and L_2 lineations in the Mt. Millar/Morowie Subarea	69
4.6	Structural geology of the Calcookara Subarea	71
4.7/4.8	Fabric elements in the Narridy Creek Subarea	72
4.9	Structural map and stereodiagrams of the Middle Camp Subarea	74
4.10	Structural cross sections of the Mattu[illegible] area	76
4.11	Structural geology of the Ullabidinie Subarea	77
4.12	D_4 features in the Ullabidinie Subarea	77

4.13	Structural map of the Plug Range Subarea	78
4.14	Structural cross sections of the Plug Range Subarea	78
4.15	Synoptic stereodiagrams and the assumed style of F_3 in the Cowell/ Cleve district	81
4.16	Synoptic stereodiagram and deformation of F_2 and L_2 structures by F_3	82
4.17	Regional correlation of the structural evolution	84
5.1	Location of key stratigraphic cross sections	87
5.2	Geological cross-sections in the Wangaraleednie Subarea	88
5.3	Geological cross sections in the Mt. Millar Subarea	90
5.4	Geological cross sections in the Morowie Subarea	91
5.5	Geological cross sections in the Middle Camp Subarea	93
5.6	Geological cross sections in the Plug Range Subarea	94
5.7	Comparative stratigraphy of the sub-areas	96
5.8	Geochemistry of amphibolites	103
5.9	Structural geology of the Cleveley/ Glenhaven area	105

5.10A	Stratigraphic correlation in the Cleve Uplands	106
5.10B	Stratigraphy of the Middleback Ranges	108
5.10C	Inferred stratigraphy of southern Eyre Peninsula	109
5.11	Interpretative geological map and sections	111

Appendix A

A1	Location of geochemical samples	
A2	Location of geochemical samples	

Appendix B

B1	Location of geochronology samples	

VOLUME II

6.1	Plate - S_1 mica	2
6.2	Plate - S_1 sillimanite and M_1 garnet	3
6.3	Plate - F_1 folds	5
6.4	Typical F_2 folds	10
6.5	Plate - F_2 fold hinges in semipelitic rocks	11
6.6	Plate - S_2 fibrolite beards and M_2 feldspar	13
6.7	M_2 garnet and L_2 mica lineation	14
6.8	Plate - elongate fibrolite pods and domainal S_2 in quartzites	15
6.9	Plate - L_2 parallel quartz pods	16
6.10	Plate - D_2 fabrics in amphibolites	17
6.11	Distribution of strain in idealized folds	19
6.12	Development of L_2 lineations	21

6.13	Plate - progressive development of S_2 domainal schistosity	25
6.14	F_3 folds in semipelites	31
6.15	Plate - F_3 hinges in semipelites	32
6.16	Plate - quartz, mica and feldspar textures in tight F_3 folds	33
6.17	Plate - S_3 mica	34
6.18	Plate - F_3 folds in banded diopside quartzite	35
6.19	Textural categories of quartzites	37
6.20	Regional variation in D_3 quartz textures	37
6.21	Plate - dolomite, phlogopite and serpentine textures	38
6.22	Plate - clinopyroxene deformation, recovery and recrystallization	38
6.23	Plate - D_3 fabrics in the Narridy Creek granite	40
6.24	Plate - D_3 recovery and recrystallization of plagioclase	41
6.25	Plate - S_3 mica films and tension veins	44
6.26	The crystallographic preferred orientation of quartz	50
6.27	Old and new grain relationships in quartzites	50
6.28	Plate - F_m fold hinges and S_m mica	61
6.29	Plate - mylonite specimens MY-1 and 2	63
6.30	Plate - D_m plagioclase	64
6.31	Plate - mylonite specimens MY-3 and 4	64

6.32	Plate - slaty mylonite specimens MY-5 and 6	65
6.33	Plate - D_m plagioclase and microcline recrystallization	66
6.34	Plate - mylonitic "fluid" phase	66
6.35	Plate - D_4 features	71
7.1	Mineral parageneses of pelitic and semi-pelitic rocks	80
7.2	ACF and AKF diagrams for M_{1-2}	81
7.3	The migmatite zone in relationship to macroscopic folding	82
7.4	Comparative summary of migmatitic and non migmatitic semi-pelites	89
7.5	Chemical restrictions on rocks containing staurolite	91
7.6	M_{1-2} carbonate parageneses	92
7.7	Plate - dolomite-calcsilicate association	93
7.8	T-X_{CO_2} topology for reactions (6) to (10)	95
7.9	Zonation of hornblende colour	97
7.10	P-T conditions of M_1	102
7.11	P-T conditions for M_1 - II	103
7.12	P-T conditions for M_2	105
7.13	T-X_{CO_2} topology for carbonate rocks during M_3	111
7.14	P-T conditions for M_3	113
7.15	Synopsis of M_{1-2}, M_3 and M_4 mineral parageneses and P-T conditions	117

8.1	Chronology of events in the Cleve Uplands	126
8.2	Interpretative cross section through Middle Camp, Mt. Millar and Mt. Desperate	128

SUMMARY

The structural and petrological development of (?) Lower Proterozoic rocks during the Middle Proterozoic Olarian orogeny has been studied in detail within a small area between Cowell and Cleve on Eyre Peninsula. Several major fold deformations have been recognized and the resolution of their macroscopic effects has enabled a specific stratigraphic succession to be reconstructed. That succession has been highly metamorphosed and intruded by various granitic bodies and a detailed analysis of the microstructure has identified several specific events and related them to the deformational evolution. Preliminary geochronology has put some constraints on the timing of those events during the Olarian orogeny.

Four principal periods of deformation are identified. The first of these, D_1, was a high grade fabric forming deformation. It does not appear to have been a major fold deformation but because of a lack of suitable data a definite conclusion could not be reached. The second deformation, D_2, was a major fold deformation that produced macroscopic folds of isoclinal style with pervasive, high grade axial fabrics (L - S). It affected the entire study area and produced inclined or recumbent folds. D_3, the third major deformation, in contrast to D_2, produced macroscopic upright folds of tight but not isoclinal style. Axial fabrics were only weakly developed, but there was considerable variation in strain and two highly strained zones with strong D_3 fabrics have been delineated. Mylonites are developed in one of these and the progressive development of slaty mylonite from an incipient D_3 fabric is described. D_3 quartz textures and crystallographic

fabrics also vary throughout the area and their progressive development is also discussed. The final major period of ductile deformation, D_4, produced mesoscopic folds and crenulations but did not contribute greatly to the macroscopic geometry. Crenulations of pre-existing fabrics were developed during each of the D_2, D_3 and D_4 deformations but each set has its own characteristics which when considered together outline steps in the development of crenulation cleavages and schistosities.

The stratigraphy defined by the resolution of macroscopic D_2 and D_3 folds consists principally of a basal calcsilicate/quartzite unit overlain by a sequence of dolomites, iron formations, amphibolites and semipelitic and pelitic gneisses. The whole sequence is assigned to the Hutchison Group but the quartzite unit and the succession of rocks containing the iron formations have been compared with the Warrow Quartzite of southern Eyre Peninsula, and the Middleback Group of the Middleback Ranges respectively. The stratigraphy defined in this study can be closely correlated with sequences throughout Eyre Peninsula and indeed is similar to sequences of similar age throughout the world. This is discussed along with brief discussions on the nature of the basement to the Hutchison Group, the origin of the amphibolites, the presence of two iron formations and the structural implications of the stratigraphy.

The metamorphic evolution of the region can be considered as a single major cycle with pulses of recrystallisation promoted by deformation. The main phase (s) of metamorphism, M_{1-2}, was associated with the D_1 and D_2 deformations. It was a high grade, low to medium pressure event of upper amphibolite

facies, that locally produced migmatites. Two separate phases of M_{1-2} have been recognized in some areas and it is suggested that M_1 was the main event with M_2 only slightly modifying it. Subsequent phases of metamorphism, M_3 and M_4, were of retrogressive nature and did not greatly alter the M_{1-2} assemblages except in zones of intense strain such as the mylonite zone. They were associated with the D_3 and D_4 deformations respectively and were of upper greenschist facies.

Three major granitic bodies, all previously referred to as the Flinders Group, have been identified. The Plug Range granite gneiss is believed to be basement to the Hutchison Group, the Middle Camp granite was intruded just prior to or during D_2, and the Narridy Creek granite was intruded during D_3. Hence only the first is considered to belong to the Flinders Group proper.

This thesis contains no material which has been accepted for an award of any other degree or diploma in any University nor, to the best of my knowledge and belief, does it contain any material previously published or written by another person, except where due reference is made in the text.

A.J. Parker

ACKNOWLEDGEMENTS

There is a large number of people to whom I am indebted for their assistance during the course of this study and the preparation of this thesis. To my wife, Julie, my mother, my father and my sister, Kaye, I owe much not only for their assistance with typing of early drafts and drafting of some figures etc., but also for their encouragement and patience.

Whilst in the field I boarded at Cowell with Mrs. Dolly Williams and both she and her family made my stays there very comfortable and enjoyable. They were assisted by the town folk of Cowell, by the local farmers on whose properties I worked, and by the Cowell Football Club (Aussie Rules!).

At the University of Adelaide I was very ably assisted and made many close friends. In particular though, I am indebted to my supervisors, Professor R.W.R. Rutland, Dr. M.A. Etheridge (during the first year and a half) and Dr. P. James (during the subsequent three years), my room-mates, Bill Laing and Dick Glen, colleagues Allan Purvis, Neil Mancktelow, Mark Fanning and Charles Coin, technical assistants Jeff Trevellyan, Ric Barrett and Margy Wright, and all other colleagues and members of staff.

During the last two years of study I received much support from the South Australian Department of Mines and Energy but in particular from Bren Thomson, officers of the Regional Geology section, the drafting branch and the typing pool. The department also assisted with the preparation of some thin sections and, through Dr. A. Webb of the Australian Mineral Development Laboratories, with the preliminary geochronology.

Other persons who have assisted me during the course of my studies are Nick Lemon and other personel of the B.H.P. Co. Ltd. at Whyalla, personal friends and family relatives.

CHAPTER 1

INTRODUCTION

1.1 REGIONAL SETTING

In 1914, R. Lockhart Jack made the first historical documentation of the geology of the county of Jervois and wrote:

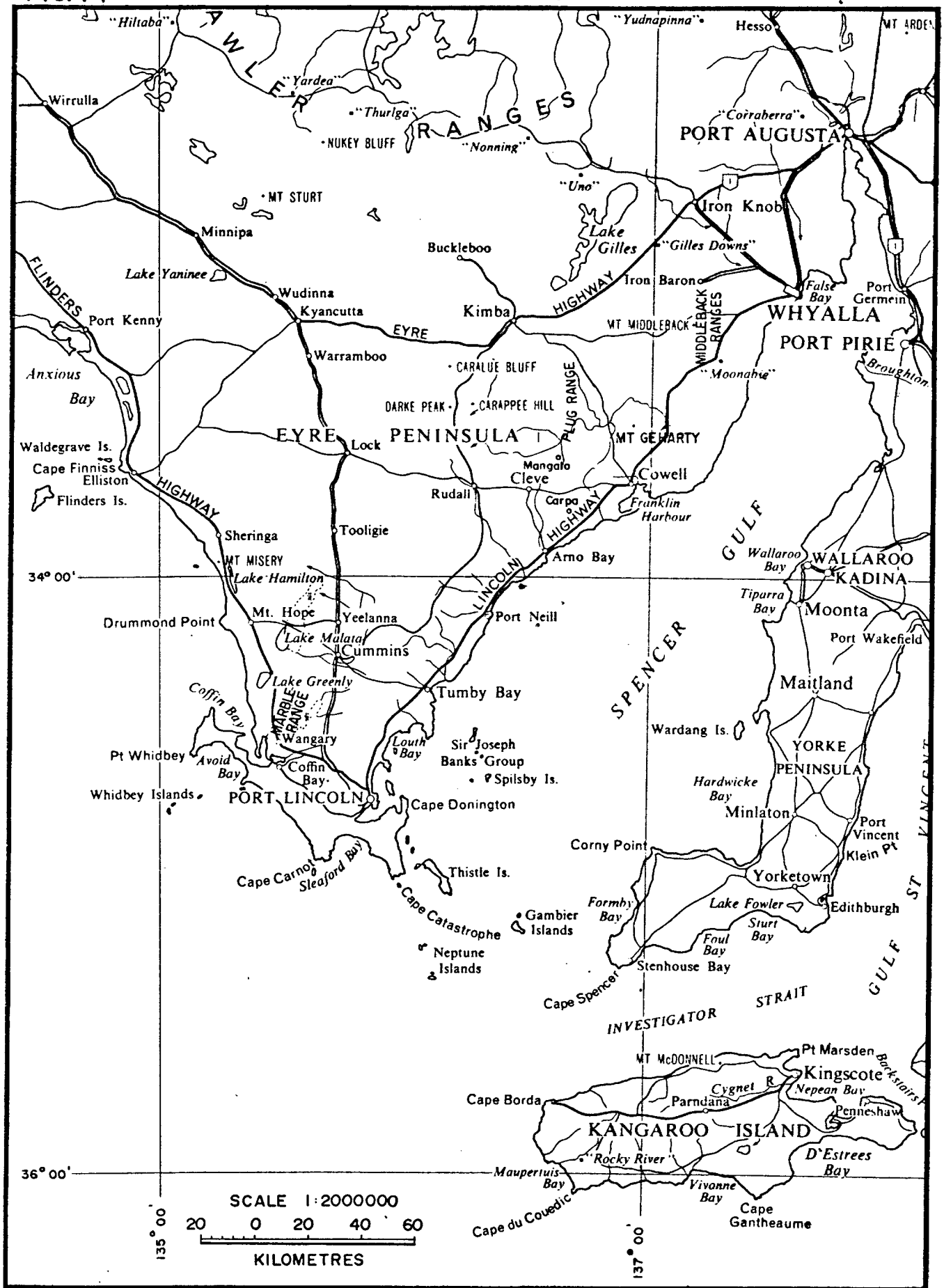
"The outstanding feature in the relief of the country is the metamorphic complex in the centre of the county, where rugged and rounded hills form bold ranges".

Earlier, in 1853, Dr. James McKechnie having left his practice as a physician in Glasgow, was led with his two brothers and a police escort to a fertile valley in the hills called "Wangaraleednie" ("Hill of the West Wind"). So delighted were they with the "highlands that reminded them of romantic old Scotland.....the background chain of hills with their fertile valleys and plains and a view opening out to the blue of the Gulf below....," (Masters, 1950), that they took up a lease and became the first pastoralists to settle in the area. The first police station was subsequently built nearby at a "spring enclosed by rushes and flanked with a green sward of grass....proclaimed 'Yabmana'". (Masters, 1950).

Such was the first occupation of the Franklin Harbour district by pastoralists. They were soon followed by the miners and with the discovery of copper at Wallaroo and Moonta in 1859 and 1861 respectively, copper was soon discovered in the district, and the first mine, the Murninnie Mine, came into operation during 1862.

Today the pastoralists have been replaced by farmers, and much of the land has been cleared for either cultivation or stock grazing. Now there are only scattered remnants of the small mine shafts or prospects which were worked intermittently

FIG. 1-1



LOCALITY PLAN
EYRE PENINSULA SOUTH AUSTRALIA

DEPT. OF MINES AND ENERGY — S.A.

S13210

over the period 1862 to 1952. Although one of the richest assays of silver ever to be mined in Australia came from an ore pod in Atkinson's Mine, the only significant mineral discoveries made in the region are the iron ore resources of the Middleback Ranges to the north, and a jade (nephrite) occurrence in dolomite at Mt. Ghearthy just north of the area covered by this thesis.

This thesis study was undertaken on a part of Jack's Precambrian metamorphic complex. The area is located in the Cleve Uplands midway between Cowell and Cleve (Fig. 1.1) and it covers approximately 170 square kilometres incorporating the historical Wangaraleednie, Yabmana and Middle Camp sites, and many of the region's historical mines such as the Calcookara, Yalpoudnie, Atkinson, Morowie and Mt. Millar mines. Access is good within the area being well served by the main, sealed, Cowell/Cleve road and a network of unsealed, secondary roads. The Cleve road branches off the Lincoln Highway 6.5 km west of Cowell; Cowell is 450 km from Adelaide.

Early geological maps published by the Geological Survey of South Austrlia (Plan 1) show the area to consist of a wide variety of older Precambrian rocks including schists, gneisses, migmatites, granites, quartzites, dolomites, iron formations and amphibolites (Johns, 1957; 1961). These rocks have been complexly folded and subjected to high grade metamorphism.

Outcrop within the study area is sporadic. Northwest of the road between Wangaraleednie and Ulgera Gap, and up to the top of a scarp which represents the edge of a plateau, there is a belt 2-3 km wide of reasonable outcrop. There are some excellent exposures in juvenile creek beds, and most of the hills are scattered with low outcrop. Southeast of

Wangaraleednie-Ulgera Gap road, outcrop is poorer and mainly restricted to the rounded hills. The study area was selected because it represented one of the best exposures on the Cleve Uplands.

The landscape has been described by Laut et al (1977) as,

"Hills on metasediments with short footslopes and fans. The hills and most of the footslopes and fans retain a cover of open scrub and low open woodland used for livestock grazing, but part of the footslopes and fans support a cultural grassland used for rotation cereal cultivation and livestock grazing". The climate is warm and temperate with a mean annual rainfall of 300-425 mm. Mt. Olinthus at 453 m is the highest hill in the region, and represents a relief of some 150 m. Normal relief is of the order of 50 - 100 m. Vegetation is dominated mainly by mallee, but broombush is particularly prominent on quartzite ridges, and sheoaks are prominent on granites. All streams within the area except Salt Creek are shallow and intermittent. Salt Creek is very brackish but flows for most of the year. There are local springs of both fresh and brackish water.

1.2 PREVIOUS WORK

There are only three published works that deal specifically with the geology of the region around Cowell and Cleve: Jack (1914), Johns (1962), and Thomson (1969). There are, however, more detailed accounts of other parts of the peninsula, in particular, the Middleback Ranges, and southern Eyre Peninsula.

HISTORICAL - The first published work on the geology of Eyre Peninsula was that of Mawson (1907). He documented some general aspects of the rocks of southern Eyre Peninsula, recognizing their Precambrian age and identifying some as

obvious metasediments but others as igneous in character.

Jack (1914) extended Mawson's observations to the Cleve Uplands. He recognized the sedimentary components of the complex noting their "intense alteration and crumpling, and evidence of contact metamorphism in the vicinity of injected igneous material".

In his brief descriptions of the quartzites and dolomites he notes the presence of conglomerate in quartzite at Darke's Range and the potential of dolomite as a host for mineralization. Additional to the obvious sedimentary derived rocks, he describes augen gneisses (many of which he believed to have been derived from extreme alteration of sediments), granite, pegmatite dykes, and albitite, one sample of which was traversed by coarse crystals of wernerite (scapolite).

The first detailed petrology to be published was that of Tilley (1920a and b; 1921). He described in explicit detail the petrology of granite gneisses, amphibolites, calc-silicates and dolomites from southern Eyre Peninsula. In so doing he not only established the metamorphic character of those rocks, but he was also the first to group the rocks together and informally name them.

One of the earliest accounts on the geology of the Middleback Ranges is contained in Jack (1922). He described the Iron Knob, Monarch, Prince and Baron ore bodies the mining of which was still in its infancy.

In addition to the above publications, there are numerous records of the early mining activites prior to 1920 contained in the South Australian Reviews of Mining Operations. Few of these relate specifically to the geology; better accounts of the earliest mining operations are contained in Masters (1950) and Johns (1961).

FIGURE 1.2

SYNOPSIS OF PREVIOUS STRATIGRAPHIC NOMENCLATURE ON EYRE PENINSULA

Middleback Ranges		Miles (1954)			Furber and Cook (1976)
		Middleback Group +Gneiss Complex			Middleback Group Gneiss Complex
Cleve Uplands		Johns (1957, 1961)	Whitten (1964)		
		Schist Group/Hutchison Group +Gneiss Group/Flinders Group	Hutchison Group +Flinders Group	Thomson (1969)	
				Hutchison Group Warrow Quartzite +Gneiss Complex	} Cleve Metamorphics
Southern Eyre Peninsula	Tilley (1920a)		Whitten (1966)		
(Marble Range)	Warrow Series *Dutton Series	Johns (1958)	Dutton Metamorphics		Coin (1976)
(Lincoln Uplands) (Southern & Eastern) coastlines	Hutchison Series *Flinders Series (Lincoln & Sleaford Gneisses)	Hutchison Group +Flinders Group	Hutchison Metamorphics **Flinders Gneiss		Hutchison Group **Flinders Group

NB * intrusive into their respective metasedimentary series
** inferred to be basement to the overlying rocks
+ inferred to represent a higher grade of metamorphism with local granitization (of sediments)

STRATIGRAPHY - The stratigraphic nomenclature on Eyre Peninsula is very confusing due to the lack of detailed studies and its redefinition by each and every worker there (Fig. 1.2).

Tilley (1920a) was the first to organize the rocks into some sort of stratigraphic order. He referred all the metasediments of the Lincoln Uplands to the Hutchison Series and then referred all the granitic gneisses, which he believed were intrusive into the Hutchison, to the Flinders Series. On the western coast of southern Eyre Peninsula he erected two additional names, the Warrow Series and the Dutton Series, for the quartzites and granite gneisses respectively.

The next documentation of stratigraphy came from Miles (1954) for the Middleback Ranges. Edwards (1936) had earlier described the metasedimentary sequence in that area as the Iron Ore Series noting their reference to the Mosquito Series on the Geological Map of Australia (Edgeworth, 1932). However, Miles redefined the metasedimentary sequence as the Middleback Group which consisted of the basal Middleback North Dolomite, the Lower Middleback Quartzite, the Cook Gap Schist, and the Upper Middleback Quartzite. This whole sequence was structurally underlain by the Gneiss Complex which he believed was a younger, anatectic type granite.

Johns (1957; 1961) made the next contribution to the nomenclature by reclassifying the rocks yet again. On the 1 mile map series he referred them to a "Gneiss Group" and a "Schist Group" the distinction between the two being quite vague. Both groups contained quartzites and dolomites but the first was dominated by gneisses with minor schist whereas the second was vice versa. In his later publication (Johns, 1961) he redefined the "Gneiss Group" as the Flinders Group and the

"Schist Group" as the Hutchison Group and in so doing redefined Tilley's initial nomenclature. He abandoned the Warrow and Dutton Series referring both to the Flinders Group but retained the name Warrow for the major quartzite horizon within the Flinders Group. His subdivision was based on the concept that the Flinders Group represented metasomatized metasediments whereas the Hutchison Group did not. Because the intensity of this metasomatism was varied in different areas, the boundary between the two groups was necessarily "gradational and.... therefore arbitrarily defined".
In practice his definition is not much different from Tilley's. Both refer to the Flinders Group/Series as granitic and younger than the actual sediments, but however Johns' model is an in situ granitaztion model whereas Tilley's is essentially an intrusive model.

Following on from Johns, Whitten (1964) used the Hutchison Group and Flinders Group in the Miltalie area (near Cowell) commenting that the significant difference between the two groups was the degree of regional metamorphism. He correlated the two approximately with the Middleback Group and Gneiss Complex respectively. However, in his M.Sc. thesis Whitten (1966) modified his ideas. Being concerned mainly with southern Eyre Peninsula, he redefined the stratigraphy to a basal unit, the Flinders Gneisses, overlain by the Hutchison Metamorphics which were subsequently overlain by the Dutton Metamorphics (including the Warrow Quartzite).

The next attempt to define a stratigraphy was by Thomson (1969). In trying to establish a single succession for the whole of Eyre Peninsula, he combined the Middleback Range and southern Eyre Peninsula nomenclatures. Consequently he ended up with three broad subdivisions; a basal Gneiss Complex, the

Warrow Quartzite, and the Hutchison Group. The Gneiss Complex was a confusing mixture of metasediments, migmatites, intrusive granites and basic rocks. It incorporated the Middleback Group and its upper boundary overlapped (!) the lower boundary of the Warrow Quartzite. All the remaining metasediments he included in the Hutchison Group. This whole sequence Thomson called the Cleve Metamorphics.

Such were the published stratigraphies that existed prior to the commencement of work on this thesis. Since then Furber and Cook (1976) have slightly modified Miles stratigraphy for the Middleback Ranges by renaming the Upper and Lower Middleback Quartzites the Upper and Lower Middleback Jaspilites respectively, and by adding a minor sericite quartzite to the base of the sequence.

Coin (1976) in his Ph.D. work mapped the Tumby Bay region of southern Eyre Peninsula and proposed another redefinition of Hutchison and Flinders Groups. His definition however conforms with Tilley's definition in that he refers all metasediments to the Hutchison Group, while the augen and granite gneisses that outcrop down the eastern coast he calls Flinders Group. This is in line with Tilley's classification in that both authors describe the same suite of rocks. However, while Tilley considered the Flinders Group to represent younger intrusives, Coin preferred to think of it as reworked basement (to the Hutchison). Because a major mylonite zone separates the Flinders and Hutchison Groups in this area, the exact relationship between them could not be determined. Coin identified specific intrusive bodies by their locality names (e.g. Moody-Moreenia Adamellite).

STRUCTURE - Previous work describing the deformation of rocks on Eyre Peninsula has been very sketchy. While most workers

have noted the highly deformed character of the rocks, little progress has been made in structural analysis.

Mawson (1907) in addition to noting the deformed nature of the rocks, recorded the presence of a zone "of highly crushed rock". He was referring to what has only just recently been positively identified as a major mylonite zone (Coin, 1976; this thesis).

In the Middleback Ranges, Miles (1954) made a very detailed documentation of folding. He recognized the principal structure of the ranges as a tight syncline of variable plunge but trending approximately north-south. Miles attributed the variation in plunge to cross warping "on a number of broadly parallel northwest-southeast axes".

Johns (1961) also noted the general north-south to northeast-southwest folding which produced tight and relatively upright folds. He believed that they were arranged in an en echelon manner.

One of the more significant structural works is that of Jones (1968). He recognized three periods of folding in the Middleback Ranges; the first period produced isoclinal folds accompanied by transposition, the second also produced tight folds with axial planar fabrics (N.B. these are what Miles mapped on N-S axes), and the third period produced minor conjugate folds and kinks. Jones believed that the variation in plunge of group two folds was a product of inhomogeneous deformation and not due to later crossfolding as proposed by Miles.

Until this particular study was undertaken that was all that was known of the deformational history on Eyre Peninsula. Consequent to this study and that of Coin (1976) a number of minor theses have been carried out by honours students at the

University of Adelaide. Those of Fanning (1975), Flook (1975) and particularly of Clarke (1976) all deal to some extent with the deformational history of southern Eyre Peninsula.

METAMORPHISM - Still one of the principal pioneering metamorphic studies in South Australia is Tilley's work of 1920 and 1921. His work is supplemented, though, by other petrological studies such as those by Miles (1954), Whitten (1966), Barclay (1967), Jones (1968), and Frears (1969). None of these studies however relates to the Cleve Uplands. The South Australian Department of Mines has produced only a few minor unpublished petrological reports (see Rept. No. N.P.N.C. 77/59).

IGNEOUS ACTIVITY - Jack (1914) identified three main groups of granites in the Cleve Uplands

> "(1) The sphene-bearing biotite granite in the hundreds of Moody and Brooker.
>
> (2) The orthogneissic granite of Carappee Hill.
>
> (3) The coarse uncrushed microcline granite of the Charleston massif".

In addition he recognized pegmatite and aplite dykes. Miles (1954) added to Jack's descriptions by considering the first two groups as predating the regional metamorphism and the last group as post-dating that metamorphism. Furthermore he identified two groups of amphibolites, one predating and the other post-dating the intrusion of the older granite suite, and yet a further set of much younger dolerite dykes postdating the regional metamorphism. No other workers have added substantially to the contributions by Jack and Miles.

GEOCHRONOLOGY - Prior to the commencement of this study, the principal dating was that of Compston and Arriens (1968) and Compston et al (1966). They quoted 1780 ± 120 Ma for the regional metamorphism on southern Eyre Peninsula, and 1590 ±

30 Ma for intrusion of the Charleston granite. Since then, however, there has been a profusion of dating cited in literature. Notable amongst these are Cooper et al (1976) who quote dates of 2643 ± 130 Ma for granulite gneisses at Cape Carnot and 1855 ± 10 Ma for the Kirton Point granite gneisses, and Webb and Thomson (1977) who have also recently published dates of 2407 ± 50 Ma and 2350 ± 33 Ma for granites at Whidbey Is. and Glenloth respectively. (see Fig. 1.1).

1.3 PRESENT INVESTIGATION

Because of the complete lack of any detailed studies on the Cleve Uplands, the diversity of opinion between different workers on southern Eyre Peninsula, and the absence of any major works comparing the geology of southern Eyre Peninsula with the Middleback Ranges, the aims of this thesis are of necessity fairly broad. They are:-

1) to map in detail the metamorphic complex,
2) to resolve as clearly as possible the stratigraphy of the Hutchison Group* and to determine the relationship between that group and the Flinders Group*,
3) to unravel the complex igneous, metamorphic and structural evolution of the area, and
4) to correlate the rocks of this area and their evolution with other areas of older Precambrian basement on Eyre Peninsula.

---

*The usage of Hutchison Group and Flinders Group here follows that defined by Coin (1976) for southern Eyre Peninsula. He uses the term Hutchison Group for the main sequence of meta-sedimentary rocks, Flinders Group for the inferred granitic gneiss basement to that sequence, and he refers to younger granites and granite gneisses of intrusive origin by their locality names.

This study was commenced in March 1973. It continued on a full time basis for the 3 years to March 1976 and has been completed on a part time basis since then while working for the South Australian Department of Mines. During the 3 years of full time study, work was equally divided between the field and the laboratory.

The principal emphasis of this study has been on field (especially structural) and petrological observations. Minor geochemical work was undertaken in an effort to solve one or two small problems. Whole rock geochemical analyses were carried out by both the Australian Mineral Development Laboratories (Amdel) and technical assistants of the Department of Geology, University of Adelaide. Some preliminary geochronology was also undertaken by Amdel on samples collected during this study.

To facilitate handling, the thesis has been divided into two volumes. The first volume deals mainly with field observations relating to lithology, the geometry of structures, and stratigraphy. Volume II deals mainly with petrological observations relating to microstructure and metamorphism. Tectonic implications of conclusions reached by this thesis are discussed in the final chapter.

1.4 TERMINOLOGY

A number of words and symbols have been used in a restricted sense in this thesis. Their usage is summarized below.

TEXTURE — the mutual relationships of and between the individual minerals with respect to their size and shape only. Related terms are granoblastic, porphyroblastic poikiloblastic and anastomosing (e.g. Collerson, 1974) qualified by terms such as equigranular, in-equigranular, polygonal, interlobate, and amoeboid

(Moore, 1970), and by grain boundary shapes such as straight, curved, serrated, cuspate or lobate (e.g. Spry, 1969). NB mortar texture will be used in a strictly non-genetic sense.

FABRIC — the mutual relationships of and between minerals with respect to their orientation and distribution in the rock as a whole. Related terms are foliation (including schistosity, crenulation cleavage, and fracture cleavage), lineation and layering (e.g. see Spry, 1969, pp. 207-211).

GNEISS — a medium to coarse grained, foliated metamorphic rock dominantly of quartzo-fedspathic composition and characterized by alternating bands rich or poor in quartz, feldspar and mica.

MIGMATITE GNEISS — a coarse grained gneissic rock in which bands of granitic composition alternate with mafic rich bands.

MYLONITE — after the definition by Bell and Etheridge (1973), "a foliated rock, commonly lineated and containing megacrysts, which occurs in narrow, planar zones of intense deformation. It is often finer grained than the surrounding rocks, into which it grades". The texture and fabric are not necessarily of cataclastic origin.

Related terms are protomylonite (10-50%

matrix) and ultramylonite (90-100% matrix) (Sibson, 1977).

SCHIST — a medium to coarse grained, strongly foliated metamorphic rock consisting dominantly of micaceous minerals.

MICROSTRUCTURE — those features most readily observed in thin section with a microscope.

MESOSTRUCTURE — those features readily observed in hand specimen or outcrop.

MACROSTRUCTURE — those features that become obvious from detailed mapping of the meso-structure.

SYMBOLS

D_1, D_2 etc — deformation episodes, the subscripts referring to their chronological order.

S_o — sedimentary bedding.

S_1, S_2 etc — planar elements produced by a particular deformation, the subscript identifying that deformation episode.

L_1, L_2 etc — linear elements such as mineral lineations and rodding. Subscripts as above.

F_1, F_2 etc — fold axes. Subscripts as above.

M_1, M_2 etc — metamorphic episodes. Subscripts as above.

λ_1, λ_2, λ_3 — the three principal axes of the strain ellipsoid corresponding to the maximum, intermediate, and minimum principal axes respectively (Hobbs et al 1976).

σ_1, σ_2, σ_3 — the three principal stresses corresponding to the maximim, intermediate and minimum principal stresses respectively (Hobbs et al, 1976).

P_t	total pressure
P_f	fluid pressure
P_{H_2O}	partial pressure of water
P_{CO_2}	partial pressure of carbon dioxide
X_{CO_2}	mole fraction of carbon dioxide
T	temperature
Ma	10^6 years

CHAPTER II

LITHOLOGY

2.1 INTRODUCTION

The geology of the area studied in detail is shown in Plan 2. It is dominated by a broad belt of high grade metamorphosed rocks of sedimentary affinity which have been intruded by pegmatitic and aplitic dykes. This belt of metasediments between Ulgera Gap and Wangaraleednie has been previously referred to the Hutchison Group by Johns (1961), but other lesser areas of metasediments have been included in his Flinders Group classification (see Plan 1). The quartzites of Plug Range, the quartzites and dolomites immediately east of Narridy Creek, and the dolomites, quartzites and layered migmatized gneisses to the south and east of Middle Camp are notable instances. These quartzites, dolomites and gneisses are comparable with similar rocks in the main belt of metasediments and as such will be described with them in the broad lithological context of this chapter. Their significance will be discussed in a later chapter when conclusions on their origin and bearing on the stratigraphy of the area will be formulated.

In addition to the metasediments, there are three prominent zones of granitic rocks within the study area and each of these will be considered separately. Johns (op. cit.) grouped them all together under the classification of Flinders Group but because this implies equivalence of character and origin, they will be referred to in this study by their geographical identities. These are the Narridy Creek granite, the Middle Camp granite, and the Plug Range granite gneiss. A discussion of the arguments for or against their classification as younger granites or under the revised usage of Flinders Group

(Coin, 1976) will be undertaken in Chapter V after an appraisal of both their petrological and structural characteristics.

The emphasis in this chapter will be on describing the field relationships, the mesoscopic appearance, and the mineralogy of the individual rock types.

2.2 THE METASEDIMENTARY ROCKS

The belt of metasediments that extends from Ulgera Gap to Wangaraleednie (Plan 2) and the other lesser areas of metasediment embrace a wide spectrum of rock types. The majority of these form major mappable units and include:

(1) The extensive ridge-forming quartzites which constitute an important and persistent marker unit present not only in the study area but throughout the Cleve Uplands and southern Eyre Peninsula.

(2) Valley-forming micaceous gneisses and schists that range from layered migmatites to pelitic mica schists.

(3) The distinctive dolomite and calc-silicate units which display appreciable variation in apparent thickness and continuity and which are particularly prominent in the region east of the Yabmana Fault.

(4) The widespread conformable amphibolites and in particular that unit adjacent to the quartzite.

(5) Iron formations. These are subordinate in the study area but have important correlatives in the Middleback Ranges.

In addition, these units are intruded by numerous pegmatites, aplites and major granite bodies. Basic dykes however have not been observed within the study area although they have been reported in the Middleback Ranges by Miles (1954)

and on southern Eyre Peninsula by Tilley (1921) and Coin (1976).

Thus with such a wide spectrum of lithologies in an area which has been subject to repeated deformation, there results a complex intermingling and repetition. Furthermore, there are many apparent inconsistencies both in sequence and in continuity, such that a complete reconstruction of a stratigraphy is impossible without a prior knowledge of the structure (Chapts. III & IV). Such a reconstruction will be undertaken in Chapter V, but however, since the lithological variations, and especially those across the boundaries of major units, described below are important to the stratigraphy, it is helpful to state the inferred stratigraphy here.

	Upper semipelite/pelite unit
	Upper iron formation
	Lower semipelite unit (with amphibolites)
Hutchison Group	Lower (thin) iron formation
	Dolomite (thin pelite at base)
	Warrow Quartzite
	Basal calc-silicate/dolomite
———————	Assumed Unconformity ———————
Flinders Group	Granite and migmatite gneiss with amphibolites.

2.2.1 Quartzite - Petrography

Quartzites are prominent over much of Eyre Peninsula and within the study area they constitute at least forty percent of the outcropping metasediments. Because of their high resistance to erosion they form prominent physiographical features such as Mt. Olinthus, Plug Range and the majority of ridges. Most of these are flanked by scree slopes which mask the flanking lithologies. However, in road cuttings and in

many of the creek sections cutting down through the ridges, exposures of the unit as a whole are much better, although a complete cross section has not been observed.

The lithology of the quartzites of these ridges ranges from:-

a) pale buff coloured, massive feldspathic quartzite in Plug Range, to

b) flaggy, muscovite rich quartzite with interlayered pelitic schists in the area west of Glenville. Less common are,

c) a pale grey massive, biotite rich, feldspathic quartzite,

d) a white sillimanite quartzite, and

e) a darker buff coloured, layered, calc-silicate rich quartzite.

Within the study area three areas of quartzite are usefully distinguished:

(1) the Plug Range/Mt. Pony area,

(2) the Ulgera Gap/Wangaraleednie area, and

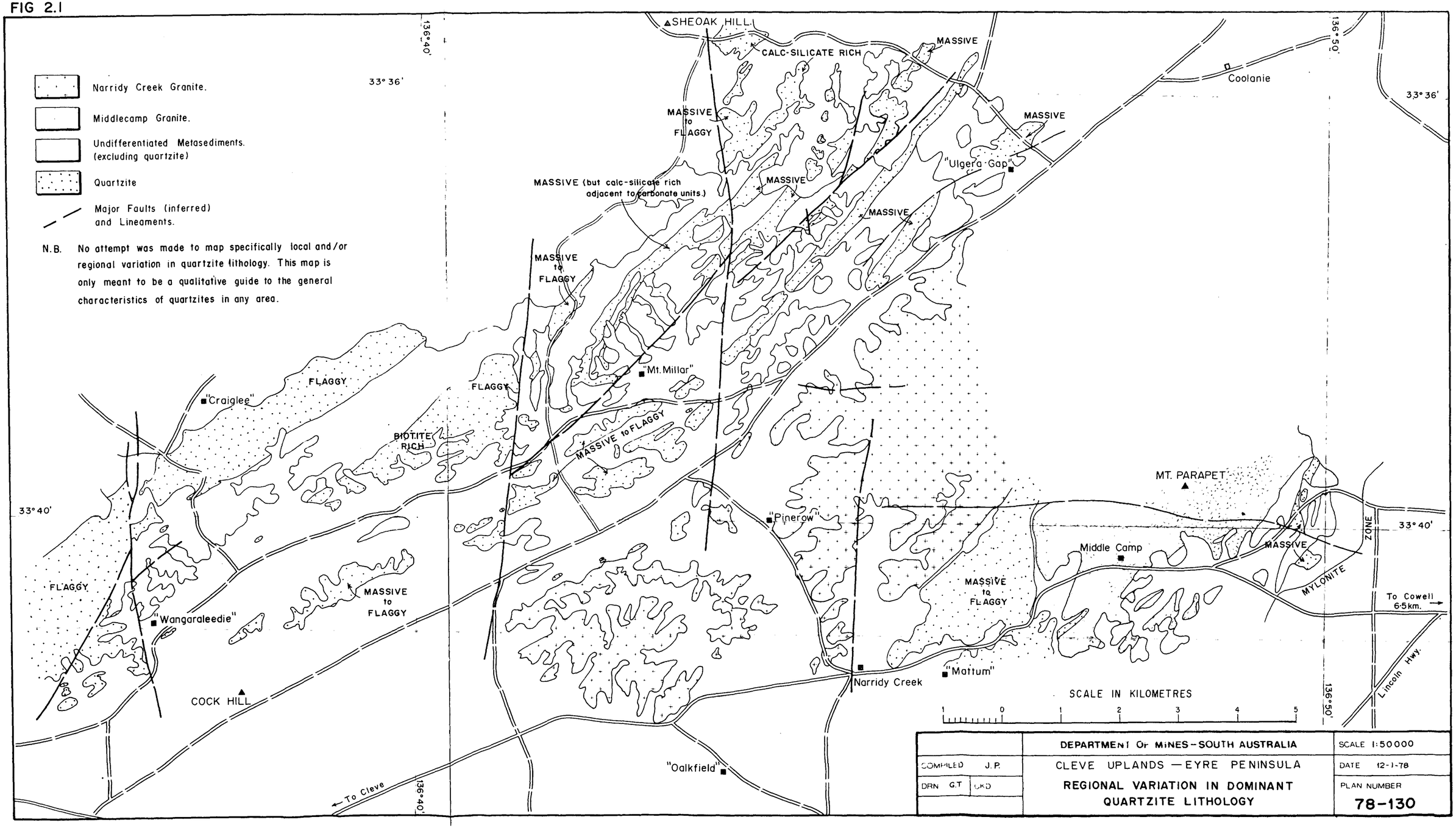
(3) the Narridy Creek/MiddleCamp area.

PLUG RANGE AREA - In the Plug Range area the quartzites are adjacent ot a deformed series of granite gneisses and the inner Plug Range body and the outer Mt. Pony body (see Plan 2) are physically identical. They are essentially massive, medium to coarse grained, feldspathic quartzites of a pale buff to creamy colour, which are neither layered nor well foliated. There are some exceptions however, and these are:

(a) a lensoid white, fine-grained sillimanite quartzite layering on the western flank of Plug Range, and

(b) a broader feldspathic layering which is present at a couple of sites on the southern end of Plug Range and in the outer quartzite unit.

FIG 2.1


Narridy Creek Granite.
Middlecamp Granite.
Undifferentiated Metasediments. (excluding quartzite)
Quartzite
Major Faults (inferred) and Lineaments.
N.B. No attempt was made to map specifically local and/or regional variation in quartzite lithology. This map is only meant to be a qualitative guide to the general characteristics of quartzites in any area.
SHEOAK HILL
CALC-SILICATE RICH
MASSIVE
MASSIVE to FLAGGY
MASSIVE (but calc-silicate rich adjacent to carbonate units.)
"Ulgera Gap"
Coolanie
136°40'
136°50'
33°36'
33°40'
"Craiglee"
"Mt. Millar"
"Pinerow"
"Wangaraleedie"
"Mattum"
"Oalkfield"
Narridy Creek
COCK HILL
FLAGGY
BIOTITE RICH
MT. PARAPET
Middle Camp
MYLONITE ZONE
To Cowell 6·5km.
Lincoln Hwy.
To Cleve
SCALE IN KILOMETRES
1 0 1 2 3 4 5
DEPARTMENT OF MINES - SOUTH AUSTRALIA
SCALE 1:50000
COMPILED J.P.
DRN G.T CKD
CLEVE UPLANDS — EYRE PENINSULA
REGIONAL VARIATION IN DOMINANT QUARTZITE LITHOLOGY
DATE 12-1-78
PLAN NUMBER 78-130

The sillimanite-bearing layers are not continuous but form slightly elongate plates or boudins, 1 cm thick and 5 to 20 cm wide. They are contained in an otherwise massive feldspathic quartzite and the boudins frequently merge into each other to suggest either originally lenticular bedding or the possibility of transposition (cf Turner & Weiss, 1963).

The feldspathic layering is less pronounced and consists of massive quartzite bands up to 10 cm wide separated by thinner, more feldspathic bands a few mm wide.

ULGERA GAP/WANGARALEEDNIE AREA - Quartzites within this main belt of metasediments are of variable lithology. They range from massive feldspathic quartzite to well layered, flaggy and more micaceous quartzite (see Fig. 2.1). A foliation is nearly always present and is very strong in the micaceous rocks. Furthermore, there is frequently a strong quartz rodding.

The massive lithology is similar to the Plug Range quartzite except that it is not as coarse grained. It is interlayered on a broad scale (several metres) with pelitic migmatic gneisses although these are mainly covered by quartzite float. On a mesoscopic scale the quartzite is faintly layered - more so than at Plug Range - and this layering is dominantly feldspathic in nature. This massive lithology predominates in the area east of Yabmana fault where it is associated with the zone of migmatization described in Section 2.2.2. Muscovite is present throughout these quartzites, but only becomes prominent in quartzite transitional to the layered quartzite.

The layered quartzite is also feldspathic but is much more micaceous. Feldspars form thin stringers 1-2 mm wide,

and these are closely associated with thin muscovite layers. Together they impart a fissility to the rock that accounts for its flaggy nature. The layered quartzites are pale buff to creamy yellow coloured, fine to medium grained and very often lineated. The morphology of the layering within these quartzites is varied and obviously grades into the very indistinct feldspathic segregations of the massive lithology. A mineralogical layering and a textural, or grainsize, layering are both commonly present often in association. For example, bands containing more feldspar and muscovite are usually finer-grained than those with less feldspar and muscovite. Layered quartzites are typically interlayered with broad bands of pelitic muscovite-biotite schist and they predominate west of Yabmana fault.

The two other variants of lithology in this area are a pale grey, massive to faintly layered quartzite 2 km west-southwest of Glenville and a calc-silicate quartzite which frequently occurs adjacent to the carbonate units. The pale grey quartzites are mostly fine-grained and contain more biotite and feldspar than typical quartzites.

NARRIDY CREEK/MIDDLE CAMP AREA - Quartzites throughout most of this area are transitional between massive feldspathic quartzite and layered micaceous quartzite. They are thus not unlike those east of Yabmana fault and, in particular, those in the vicinity of Ulgera Gap. They are pale buff to cream coloured, have gneissic interbands and are mainly fine to medium-grained.

In all the above areas the dominant mineral assemblage of the quartzites is quartz, microcline and muscovite with or without one or more of, oligoclase, biotite, sillimanite,

opaque mineral(s) and accessories. Tremolite and diopside are present only in the quartzites adjacent to dolomites and calc-silicates.

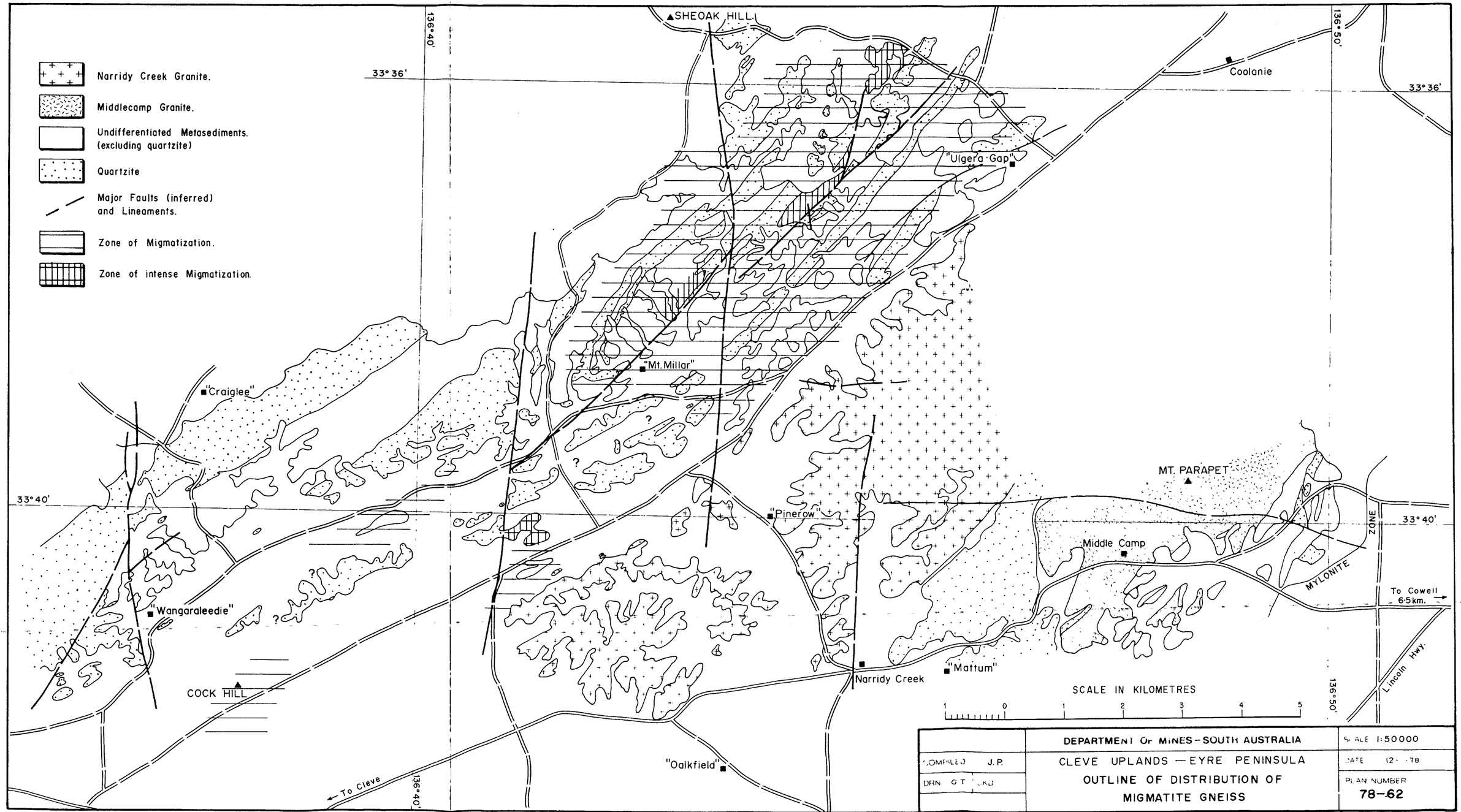
Visual estimates of these minerals are slightly varied, with quartz ranging from 70 to 97 percent but showing a bimodal distribution. Massive quartzite averages 90-95 percent quartz and the bands of micaceous/feldspathic quartzite average about 75 percent quartz. Microcline constitutes from 1 to 20 percent of the whole rock and is very rarely absent. Muscovite, although sometimes absent in the massive lithology, constitutes up to 10 percent of the flaggy lithology. It most commonly makes up 1 to 5 percent of the whole rock volume.

Of the other minerals, plagioclase and biotite most frequently occur and can constitute up to 10 and 6 percent respectively although it is most common for them to be less than half of those figures. Sillimanite is also quite common, particularly in the migmatite zone and at Plug Range, but rarely exceeds 1 percent. Opaque minerals and other accessories such as zircon, sphene, rutile, tourmaline, and apatite only occur in trace amounts but the opaque minerals sometimes form trains parallel to the layering. Sericite and chlorite/semiopaque are present as secondary alteration products of plagioclase and biotite respectively.

2.2.2 Layered Migmatites, Gneisses and Schists

Gneisses and schists within the study area can be broadly categorized into two groups - semipelitic rocks and pelitic rocks. Together they constitute over forty percent of the outcropping metasediments and are best exposed in road cuttings and juvenile creeks. On the hillsides the outcrop is poorer and prone to hillcreep; there are some good outcrops

FIG 2.2


Narridy Creek Granite.
Middlecamp Granite.
Undifferentiated Metasediments. (excluding quartzite)
Quartzite
Major Faults (inferred) and Lineaments.
Zone of Migmatization.
Zone of intense Migmatization.
▲SHEOAK HILL
Coolanie
"Ulgera Gap"
"Mt. Millar"
"Craiglee"
"Pinerow"
MT. PARAPET
Middle Camp
MYLONITE ZONE
To Cowell 6·5km.
"Wangaraleedie"
COCK HILL
"Mattum"
Narridy Creek
"Oalkfield"
To Cleve
Lincoln Hwy.
33°36'
33°40'
136°40'
136°50'
SCALE IN KILOMETRES
1 0 1 2 3 4 5
DEPARTMENT OF MINES - SOUTH AUSTRALIA
SCALE 1:50000
COMPILED J.P.
DRN G.T.
DATE 12-78
CLEVE UPLANDS — EYRE PENINSULA
OUTLINE OF DISTRIBUTION OF MIGMATITE GNEISS
PLAN NUMBER
78-62

but they are invariably weathered and their low relief inhibits good cross-sectional viewing. The sandier, broader channels cutting down through the cultivated areas usually lack outcrop.

The colour of the semipelitic rocks when fresh is a medium to dark grey. Quartz and quartzofeldspathic veins/layers are white to light grey whereas the mafic layers are darker grey to black. When weathered the rocks become brownish - the migmatites go a dark rusty-brownish grey with brownish-yellow pegmatitic segregations, and the micaceous quartzo-feldspathic schists and gneisses stain to a pale yellowish-brown. The colour of the pelitic schists is a silvery to yellowish grey speckled with black spots.

SEMIPELITIC ROCKS - PETROGRAPHY

The lithology of these rocks varies systematically across the area. In the area between the Wangaraleednie and Yabmana faults, the semipelitic rocks consist mainly of quartz-veined schists and gneisses. However in the area east of the Yabmana fault they range from quartz-veined schists and gneisses to well layered, migmatitic schists and gneisses. In fact, it has been possible to subdivide the area into broad zones characterized by either non-migmatized rocks - the quartz veined rocks - or migmatized rocks.

The distribution of the migmatite gneisses and the unmigmatized quartzofeldspathic schists and gneisses is shown in Figure 2.2. There are two areas of intense migmatization where the leucosome (Mehnert, 1968) accounts for a major portion of the total rock. In the vicinity of Morowie Mine this pegmatitic part exceeds 50 per cent and approaches 75 per cent of the rock composition. Similar migmatization

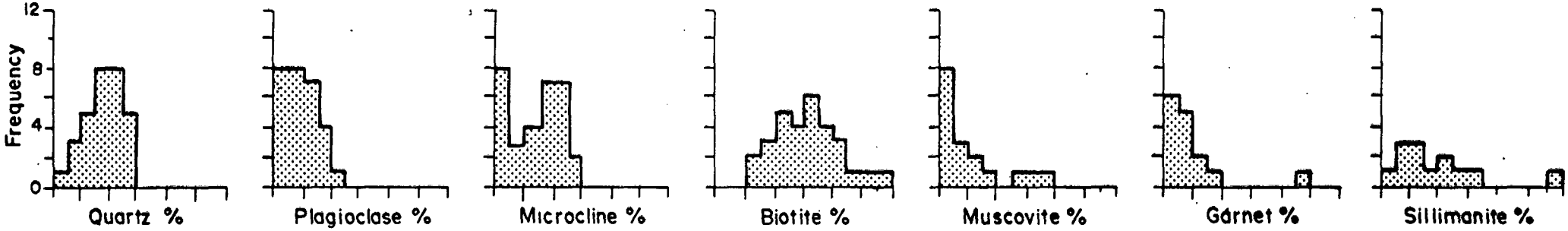
occurs in the core of the Mt. Millar antiform where the leucosome constitutes up to 50 per cent of the total rock. Elsewhere, surrounding these areas, the degree of migmatization gradually falls off until the leucosomatic part becomes effectively negligible and the only pegmatite occurs as long discordant dykes. This corresponds with a change in the overall mineralogy which will be outlined below and represents a transition in lithology from layered migmatites into unmigmatized schists and gneisses more typical of the area to the west of Yabmana fault. It therefore follows that the boundary between migmatite and nonmigmatite zones (Fig. 2.2) is not a sharp discontinuity with migmatites on one side and unmigmatized schists and gneisses on the other. Rather it is a gradational boundary that represents at least qualitatively the appearance of prominent quartzofeldspathic segregation.

Layering is ubiquitous in the semipelites. Within the migmatites it is defined by pegmatitic segregations and quartzofeldspathic layers 5-15 mm wide, by thin wispy layers of biotite (and also of sillimanite) 0.5-1.5 mm wide, and often by bands of garnet 5-10 mm wide. A strong layer parallel schistosity is nearly always present, but not necessarily to the exclusion of other schistosities. Likewise, in the unmigmatized micaceous quartzofeldspathic schists and gneisses there is a good mineralogical layering defined by quartz, feldspar, mica and garnet. The scale is of the same order as within the migmatites and there is also a strong layer-parallel schistosity.

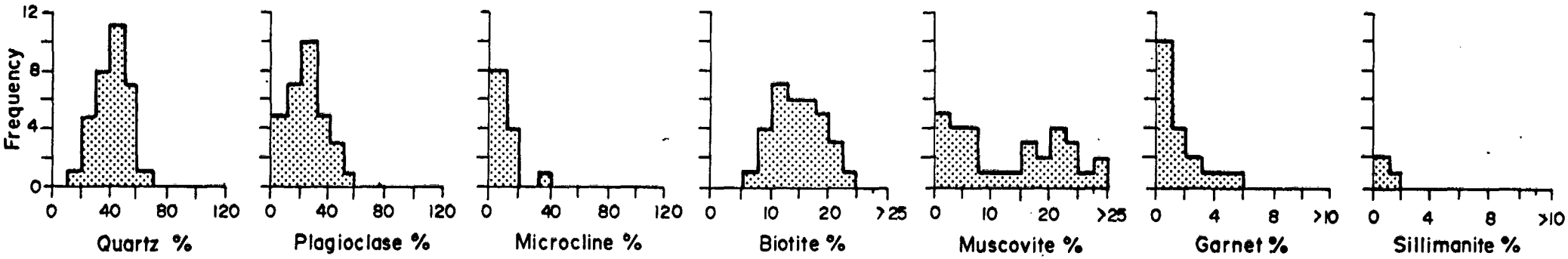
In addition to the mineralogical layering, but related to it, is a grain size variation. This is particularly obvious

FIG. 2-3

MIGMATITE ZONE



NON-MIGMATITE ZONE



S 13211

MODAL COMPOSITIONS OF SEMIPELITIC GNEISSES

DEPT. OF MINES AND ENERGY - S.A

in the non-migmatized rocks where the quartz veins and the mica rich layers are medium-grained in contrast to the average fine grainsize of the rest of the rock. The migmatites show this to a lesser extent because although the pegmatitic segregations are somewhat coarser than the rest, the overall grainsize is medium to coarse.

The mineralogy of the semipelites is summarized in Figure 2.3 and has been arranged to contrast the essential mineralogical differences between migmatized and non-migmatized rocks. There are significant differences in the mineralogy between these two "end members", and these, along with the gradational nature of the boundary of migmatization, will be discussed in Chapter VII under Metamorphism. Plagioclases are mainly of oligoclase/andesine composition.

PELITIC ROCKS - PETROGRAPHY

The three distinctive lithologies included within this category are the biotite-muscovite (-sillimanite) schists, their migmatized equivalents the biotite-feldspar-sillimanite gneisses, and the podded sillimanite gneisses. All are associated with the quartzite unit but in particular the first two are associated with the quartzite/dolomite boundary while the third is associated with the quartzite/calc-silicate boundary. Additionally, the schists and their migmatized variants are also present "below" the quartzite/dolomite boundary interbedded with the quartzite.

The mica schists are medium-grained rocks which are frequently strongly crenulated. They contain minor quartz and quartzofeldspathic lenses 0.1-1 mm wide which gradually become more prominent towards the migmatized zone. Such migmatized pelites resemble the migmatized semipelites but

contain less quartz and plagioclase.

The podded gneiss is pale to medium grey in colour, massive, medium-grained and relatively homogeneous with creamy white pods of sillimanite. It is foliated but not layered, and the pods which are approximately 5 mm x 5 mm x 10 mm in size, are flattened parallel to this foliation.

West of Yabmana fault, muscovite is the dominant mineral in the pelitic schists and constitutes from 40 to 70 percent of the total rock. It typically constitutes over 50 percent, but with the onset of migmatization this decreases to that point where muscovite is only a minor component and has been apparently substituted by potassium feldspar. Sillimanite is uncommon in muscovite-rich schists but becomes more prominent with this feldspar until east of Yabmana fault it can comprise up to 20 percent of the rock. It then occurs as disseminated fine to very fine needles and as wispy fibrolitic pods associated with micaceous layers.

Quartz and biotite are the other two major components of the schists and corresponding gneisses. Quartz varies between 10 and 30 percent of the bulk composition and tends to be slightly elongate parallel to the foliation. Biotite constitutes between 10 and 20 percent of the total rock and like muscovite is strongly idioblastic. Minor components rarely absent are tourmaline and garnet - both of similar habit to those within the semipelites - and less commonly, apatite, zircon and opaque minerals.

By comparison, the podded sillimanite gneisses are slightly coarser grained than the schists and typically the K-feldspars are poikiloblastic. They consist of K-feldspar 40 - 50 percent, biotite 15 - 25 percent, muscovite 0 - 3 percent, sillimanite 5 - 20 percent, quartz 10 - 15 percent, plagioclase 5 - 10 percent and trace tourmaline, zircon, garnet and opaque mineral(s).

2.2.3 Dolomites And Calc-Silicates

Metamorphism of carbonate rich sediments within the study area has produced a variety of rocks, the most conspicuous being the massive dolomites and the well layered calc-magnesian silicates. They are easily recognized by their subdued outcrop and by the characteristic abundance of lime in the top soil. Furthermore the omnipresence of the flora Gahnia ancistrophylla growing in the soils immediately overlying the carbonates and of a white lichen speckled over the dark coloured outcrop, is characteristic.

In addition to the two main groups, dolomites and layered calc-silicates, there are three other related lithologies. They are a chert, an unusual, massive, diopside-tremolite rock, and a calc-silicate banded amphibolite. The first two are included here, but the third is included in the following section on amphibolites.

DOLOMITES - PETROGRAPHY

The dolomites outcrop throughout the study area and with very few exceptions are closely allied with the major quartzite unit. They are mainly pale coloured, commonly white to pale grey, and frequently contain yellowish green to brown serpentine nodules. They weather to a medium or dark brown and any calc-silicate minerals or serpentine are highlighted because of their resistance to erosion.

Typical dolomite is mostly massive, medium-grained and holocrystalline. However, it is sometimes layered and/or cross-cut by veinlets and veins of calcite. The layering consists of alternating bands rich and poor in either serpentine nodules and/or calc-silicate minerals, and these bands vary in width from 1 to 20 mm. The veinlets are narrow,

irregular bodies rarely exceeding 1 mm in width and are accompanied by broader veins of calcite up to 10 mm wide. In addition to the main layering and veining there are also bands a few cm wide of massive serpentine, and narrow stylolitic laminae of opaque minerals. Often associated with the serpentine bands are veins up to 5 mm wide of chrysotile asbestos.

The composition of dolomites varies within the study area. Within those areas characterized by migmatitic gneisses, the typical mineralogy is a serpentinous dolomite with serpentine constituting up to 25 per cent of the rock volume, and the carbonate minerals varying from pure dolomite in monomineralic rocks to nearly pure calcite in rocks or bands very rich in serpentine (cf Tilley, 1921). The serpentine nodules range in size from 0.1 mm to over 3 mm, and they are generally subspherical in shape. Tremolite is not commonly present east of Yabmana fault, but there are bands of diopside and calcite which alternate with serpentine bands. To the west of Yabmana fault and in other unmigmatized areas the association dolomite-calcite-tremolite and/or diopside occurs sporadically within otherwise massive dolomites. Serpentine is absent in these regions.

Other minerals present in the dolomites are forsterite as trace relics in serpentine nodules, phlogopite with occasional chlorite replacement, quartz, scapolite, garnet, apatite and opaque minerals. These rarely total to more than 5 per cent of the whole rock.

CALC-SILICATES - PETROGRAPHY

This section includes those rocks which contain the prominent calc-magnesian minerals, pyroxene and amphibole. They are invariably well layered but grade into other more

massive lithologies such as dolomite and quartzite.

The characteristic lithology is a distinctively well layered rock with layers ranging from thin laminations up to bands 25 or more mm wide. These layers are defined mainly by the predominance of either diopside or feldspar and consequently they weather out preferentially. Their colour is varied: when weathered it ranges from a cream (quartzofeldspathic layers) to a dark brown or black colour (inosilicate layers), but when fresh varies from white to various shades, both dark and light, of grey and greenish grey. The layering is almost invariably folded and exhibits quite spectacular outcrop.

The mineralogy of these calc-silicate rocks is quite varied but is characterized by prominent diopside and feldspar. Diopside itself ranges from 10-50 percent of the total rock and plagioclase from 5-75 percent - the lower figure resulting from intense sericitization which when accounted for would raise the figure to more like 40 percent. The composition of plagioclase ranges from andesine to bytownite but the majority are in the upper calcic end of this series. Microcline content varies from trace to 40 percent. Quartz usually constitutes less than 5 percent but does reach 20 percent with prolific ribbon development, and actinolite/tremolite is usually only minor although it too can reach 20 percent as a more intense uralitization of the pyroxene.

The common carbonate mineral is calcite and this occurs in only minor quantities less than 10 percent: it fills fractures and occurs as interstitial grains of probable secondary origin. Sphene is rarely absent and commonly constitutes 1-3 percent. Sericite can amount to nearly 45 percent in some rocks, but other phyllosilicates - phlogopite,

muscovite, biotite and chlorite - rarely exceed 5 percent. Other minerals of trace or minor quantities are clinozoisite and other epidotes, scapolite, tourmaline and opaque minerals. The epidote group minerals are related to the sericitization and are of secondary origin.

This characteristic lithology grades into both dolomite and quartzite. Calc-silicates of the dolomite association grade into narrow bands of pyroxene 10 mm wide within either massive dolomite or sepentinous dolomite. Their mineralogy is diopside 40 - 60%, dolomite/calcite 25 - 50%, tremolite 5 - 20% and minor quartz, opaque mineral, sphene and feldspar. Calcite usually predominates over diopside, especially when tremolite is present, but an interesting association has been recorded which suggests that calcite is secondary and that diopside-dolomite was originally prominent (see Chapt. VII). Opaque minerals are usually confined to carbonate bands whereas sphene and feldspar are restricted to diopside-quartz interbands.

Calc-silicates of the quartzite association grade into typical quartzites with traces of inosilicates. Typically they are layered, medium grained, and of a pale greenish-grey colour (speckled with black spots) weathering to a buff colour. The layering is defined by narrow monomineralic stringers or lenses of quartz, feldspar or calcite and broader bands enriched in either diopside, feldspar or calcite. A typical mineralogy of this association is quartz prominent 30-40 percent or more, plagioclase 40-50 percent, microcline 15-20 percent, sphene 1-3 percent, and minor opaque minerals, tourmaline, epidote and sericite. Plagioclase in any of the calc-silicate rocks is always heavily sericitized but twinning, when it can be seen, indicates that it is of bytownite composition.

CHERTS - PETROGRAPHY

Cherts are of very limited occurrence in the thesis area and occur only as small isolated lenses within the large, massive dolomite bodies. They are more common in the meta-sediments near Ullabidinie Reservoir than in the main Ulgera Gap - Wangaraleednie area, but in both areas they are of subdued outcrop, mostly being observed as float boulders.

In hand specimen they are white to medium grey, finely laminated rocks of typical microscopic grain size. The layering is regular and individual laminations range in width from 0.01 mm up to 0.5 mm. They are defined by slight grain size variations of quartz, and by thin laminae of phyllosilicate. In the more micaceous rocks these laminae are strongly contorted and folded and the overall grain size is coarser (being < 0.02 mm in the finest layers and 0.05-0.1 mm in the others). Because of their fine grainsize they are very hard, massive and difficult to fracture.

The mineralogy of the cherts ranges from almost pure quartz rocks (99 percent quartz with traces of opaque mineral and phyllosilicate), to rocks containing 85 percent quartz and 15 percent of mainly phyllosilicate with some opaque minerals and zircon. The phyllosilicate is either sericite or more frequently, as in the southeast of the area, chlorite.

DIOPSIDE-TREMOLITE ROCK

This is a very conspicious rock of restricted occurrence which is closely associated with calc-silicates and indeed generally conformable with them. It outcrops as broad, pegmatite-like bodies, 25 to 50 metres wide, is very coarse grained (up to and greater than 10 cm) and is a pale greenish white in colour. It is composed mainly of diopside (> 90 percent) with scattered vug like cavities partially infilled

with tremolite. Calcite and, rarely, quartz, are accessories totalling up to 4 percent of the rock.
Crystallographically, the diopside is slightly iron rich and has a maximum extinction angle, $\gamma \wedge c$, of 41 degrees. Exsolution lamellae parallel to (100) are frequent.

2.2.4 Amphibolite Petrography

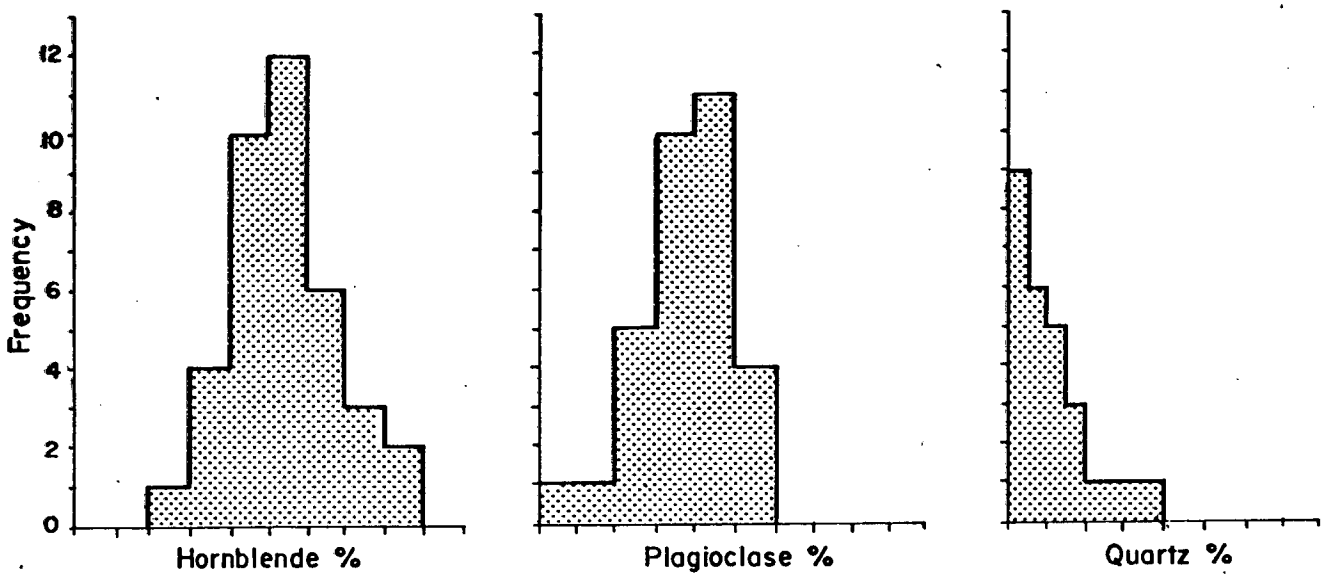
Grossly conformable amphibolites are prominent throughout the study area. They occur as sill like bodies within the Plug Range granite gneiss, within the metasediments and within the Narridy Creek granite deformed zone. In the main metasedimentary belt of this study they form a conspicuous unit at the quartzite/semipelite boundary where they are associated with dolomite and iron formation. However they also occur within the semipelitic gneisses and schists higher in the sequence (see Chapt. V.).

The amphibolite rocks are easily recognized by their relatively massive, homogeneous appearance and by their dark brown to black colour. As outcrop they are subdued by comparison with the gneisses and the quartzite, but a characteristic dark brown soil frequently attests to their presence beneath. Furthermore, the flora is poorer on amphibolite bands than over adjacent rocks and broom brush is notably absent. Consequently, amphibolite bands can be readily located on aerial photographs as areas darker and with less overgrowth than the surrounding ground. This is particularly useful in cultivated paddocks although the contrast may not define precise boundaries. Both a creamy white and a pale green lichen coexist together on weathered outcrop.

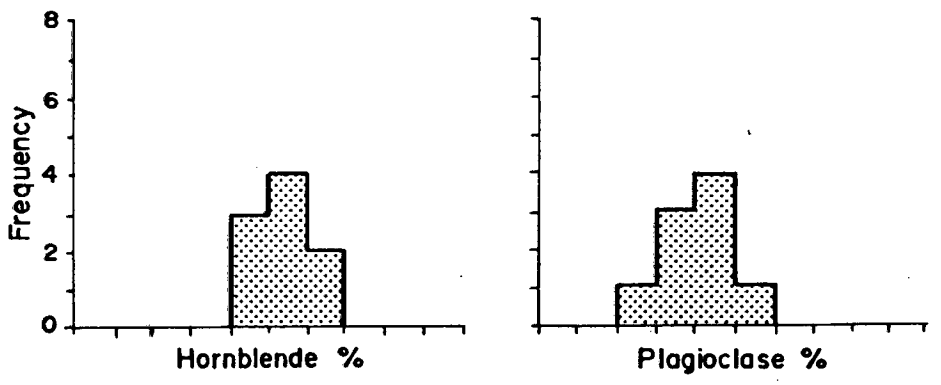
The main unit consists of four components, (A) a massive schistose lithology, (B) a massive porphyroblastic lithology,

FIG. 2-4

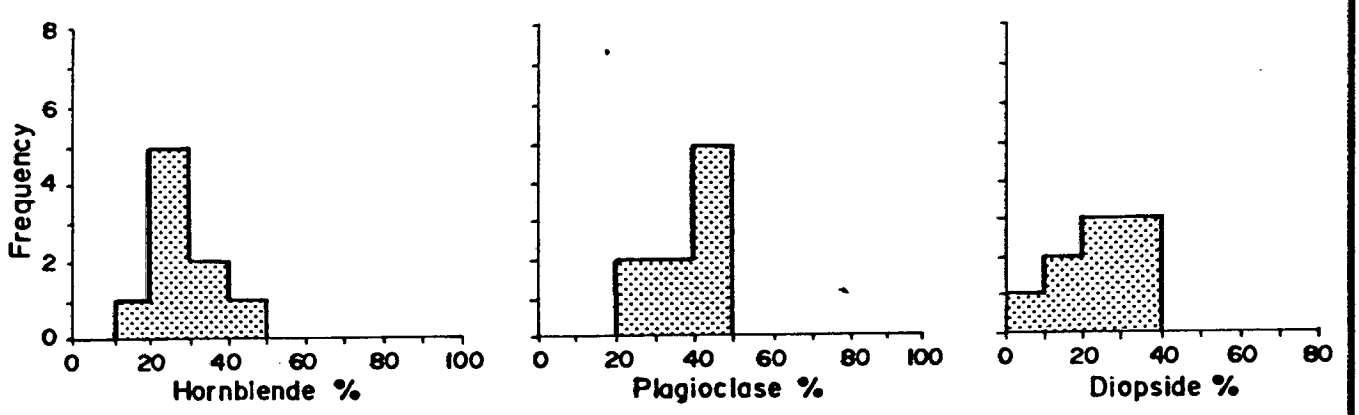
SCHISTOSE AMPHIBOLITES



PORPHYROBLASTIC AMPHIBOLITES



LAYERED AMPHIBOLITES



MODAL COMPOSITIONS OF AMPHIBOLITES

S13212

DEPT. OF MINES AND ENERGY – S.A.

(C) a well layered lithology, and (D) a eulysite lithology. The first of these accounts for over 90 percent of the total exposed amphibolite, and the other three groups occur as bands rarely exceeding a few metres in width and usually completely enclosed by the schistose lithology. Their occurrence is not restricted to any particular horizon within the unit although the porphyroblastic rock can often be found near the "upper" semipelitic boundary. Broad bands such as these cannot be traced for any great distance due to poor outcrop.

SCHISTOSE AMPHIBOLITE

Rocks of this category are characterized by their schistose, homogeneous textures. They are essentially massive and non layered though there is sometimes a weak layering defined by thin creamy-white feldspar and/or quartz veins, by a subtle grain size banding (of hornblende), and by thin, wispy lenticules of sphene or opaque. In general, however, they are equigrained, of fine grainsize, and range from non schistose to strongly schistose rocks often with an accompanying mineral streaking and lineation. They are dark brown to black when weathered, dark grey to black when fresh and are speckled by creamy white grains of feldspar. They are relatively dense rocks by comparison with the gneisses.

The mineralogy of the schistose amphibolites is dominated by hornblende and plagioclase. Their modal compositions are shown in Figure 2.4 and indicate that the typical mode is 45-60 percent hornblende and 35-45 percent plagioclase. The other components are much less abundant and consist of sphene 1-2 percent rarely up to 4 percent, opaque minerals 1-2 percent and again rarely up to 5 or more percent, quartz

absent or less than 4 percent in the main bulk but up to 25 percent in veined rocks, biotite in minor quantities, and in trace amounts the minerals calcite, diopside, alkali feldspar and garnet. Sericite and also a colourless epidote group mineral are common as secondary alteration products, mainly of feldspar, and can constitute up to 35 and 10 percent respectively in some rocks.

PORPHYROBLASTIC AMPHIBOLITE

These amphibolites are dense, massive, non-layered rocks of similar colour to the schistose rocks. They are characterized by equant shaped, xenoblastic porphyroblasts of hornblende 1-5 mm in size set in a fine-grained, weakly schistose matrix of plagioclase and hornblende. The porphyroblasts themselves are mostly unoriented single crystals of strained hornblende, but sometimes they consist of decussate aggregates of medium sized hornblende. The matrix is similar to the schistose lithology but less strongly foliated.

Modal compositions of this group of rocks are equivalent to those of the schistose amphibolites and the overall hornblende and plagioclase modes are essentially the same (Fig. 2.4). However, due to the partitioning of hornblende into the porphyroblasts, the groundmass is proportionately richer in plagioclase than the typical schistose amphibolite. The accessory minerals are also present in similar quantities.

LAYERED AMPHIBOLITE

In contrast to the homogeneous textures of the former categories, this rock type is characterized by a colour/mineralogical layering within the scale of a hand specimen.

The major part of the rock is a strongly schistose amphibolite identical in texture and fabric to that above, but it alternates with pale greenish white to greenish grey layers

ranging in width from thin wispy lenticules up to continuous, parallel bands 10 mm wide. When weathered these pale coloured bands assume a reddish brown hue which stands out against the dark brown colour of the rest. Their internal textures are homogeneous, fine grained and equigranular.

The dominant minerals of the layered rocks and their relative whole rock abundances are shown in Figure 2.4. Plagioclase is most abundant at 40-50 percent, then hornblende 20-40 percent, and diopside 15-35 percent. Within the individual layers, the hornblende rich layers are identical to schistose amphibolite modes and the diopside plagioclase bands contain diopside 30-45 percent and plagioclase 50-65 percent. Of the lesser minerals, sphene and calcite are rarely absent and each can amount to 4 percent. Opaque minerals are less common, usually less than 1 percent, and again sericite and epidote are common as secondary alteration products. Sericitization of plagioclase is most intense adjacent to diopside.

EULYSITE

There have been only three occurrences noted within the study area of iron rich rocks which are classified in this category. They are all narrow, lensoid bodies less than a metre wide wholly enclosed within schistose amphibolite. Hence they are considered to be separate from the banded iron formation. In hand specimen they are dense, massive rocks of medium to coarse grainsize, weakly foliated, and with a faint layering. When weathered they are dark brown to black often with the polished/tarnished appearance of massive ironstone but the fresh rock is a nondescript, medium to dark brownish grey.

The mineralogy of the eulysite pods is very distinctive. They consist mainly of medium to coarse-grained grunerite or

hypersthene with narrow bands of fine-grained garnet. Grunerite and hypersthene are poikiloblastic with very fine-grained inclusions of garnet, quartz and opaque mineral, and they are poorly aligned into subparallelism with the banding.

The modal composition of 425/161-3 is hypersthene 45 percent, grunerite/cummingtonite 10 percent, garnet 30 percent, and minor quartz and opaque mineral. Of 425/D-96 the mode is grunerite 75 percent, garnet 20 percent, and minor apatite, opaque mineral and quartz.

2.2.5 Iron Formation - Petrography

Iron rich rocks within the study area are subordinate to the four main lithologies described above. However there is a particular horizon in the metasedimentary sequence which is characterized by iron rich assemblages. A chemical study of three such rocks (Appendix A) showed that they contained as much as 25 percent iron. They have therefore been assigned to a specific unit which is additional to those eulysites contained wholly within massive amphibolite bodies (see above).

The iron formation is characterized by three specific lithologies: banded quartzite, grunerite schist, and massive ironstone. Of these, the first is the most prominent, the second is much less prominent and usually found immediately adjacent to the amphibolite, whereas the third category occurs only locally as isolated outcrops or pods associated with the first. Exposure of iron formation is poor but the banded quartzites frequently form minor ridges. Thickness is variable and although it ranges from a couple of metres to over 100 m it is mostly of the order of 5 to 10 m wide.

BANDED QUARTZITE

These are very well banded, non-schistose rocks of buff to off white colour with a yellowish green tinge. They consist of bands 0.5 to 10-20 mm wide of white to pale yellow-green pyroxene and/or dark green-brown to black amphibole, alternating with glassy quartz. Additionally there are bands of disseminated opaque mineral within the quartz and such opaque mineral tends to preferentially accumulate in fold hinges.

Grainsize of these banded quartzites is variable, but in general ranges from fine/medium to coarse. Monomineralic pyroxene bands often contain pyroxenes coarser than 10 mm but in quartz-pyroxene bands pyroxene rarely exceeds 2 mm. Quartz is mainly medium-to fine-grained.

The mineralogy of banded quartzites if quartz 50-85 percent (mainly about 75 percent), and either pyroxene or amphibole up to 50 percent (mainly 10-25 percent). The pyroxene in these rocks is diopside and the amphibole is either a blue-green actinolite/hornblende or grunerite. Grunerite is often intergrown with the blue-green amphibole especially adjacent to quartz bands. Additional minerals are calcite up to 4 percent in pyroxene rich rocks, opaque minerals 0.5-3 percent, garnet and rarely biotite in amphibole rich bands, and trace amounts of accessories and microcline. The absence of feldspar in these rocks distinguishes them from calc-silicate rich quartzites.

GRUNERITE SCHIST

These are relatively massive, foliated rocks similar to schistose amphibolite except that they are strongly quartz veined. They are dark reddish brown to black in colour, fine grained and the quartz veins are long, lenticular and

rarely exceed a couple of mm in width.

Their mineralogy is simple and consists of amphibole 85-90 percent and quartz 10-15 percent with minor opaque and biotite. The amphibole is a complex intergrowth of colourless grunerite and blue-green actinolite or hornblende. Grunerite constitutes at least 60 percent of the amphibole.

MASSIVE IRONSTONE

These massive gossanous rocks are very fine grained and range in colour from ochre yellow through dark brown to black. They are composed almost entirely of massive limonite and additional to being partly porous contain numerous vein-like cavities or vugs. As with each of the above iron formation lithologies, they frequently have a characteristic orangey-red coloured lichen growing on external surfaces.

2.3 THE GRANITIC ROCKS

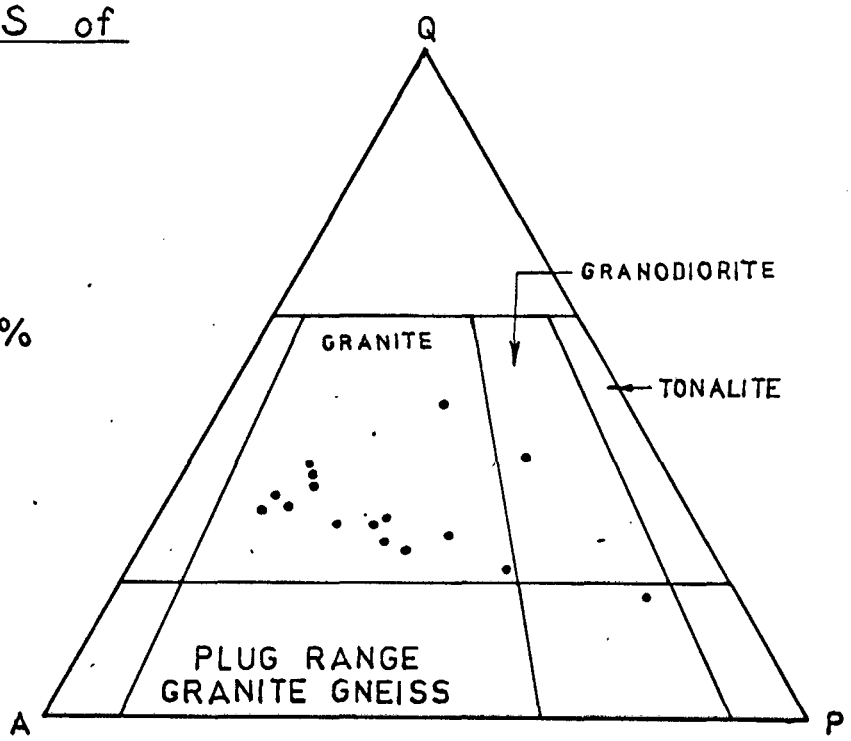
There are three major granitic bodies to be considered here: the Plug Range granite gneiss, the Middle Camp granite, and the Narridy Creek granite. Each of these bodies has its own distinctive characteristics and in particular each can be distinguished by its structural fabric. These structural aspects will be examined in more detail in subsequent chapters whereas in this section the general petrography of the rocks will be described with brief mention of fabric and of preliminary geochronology. Additional to the major granitic bodies there are also several generations of pegmatite and aplite intrusion. These are also considered.

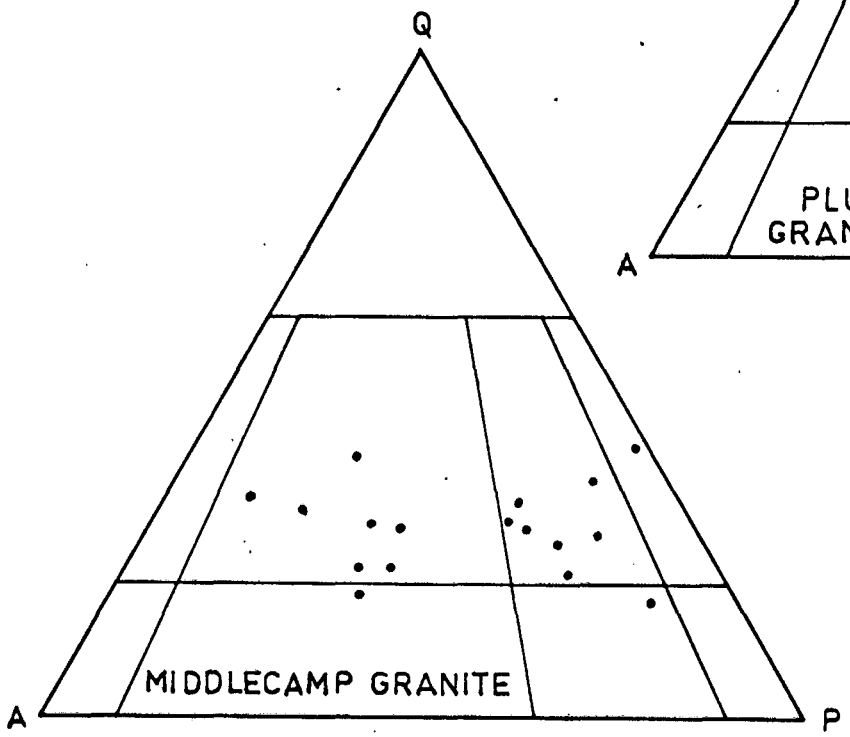
2.3.1 Plug Range Granite Gneiss

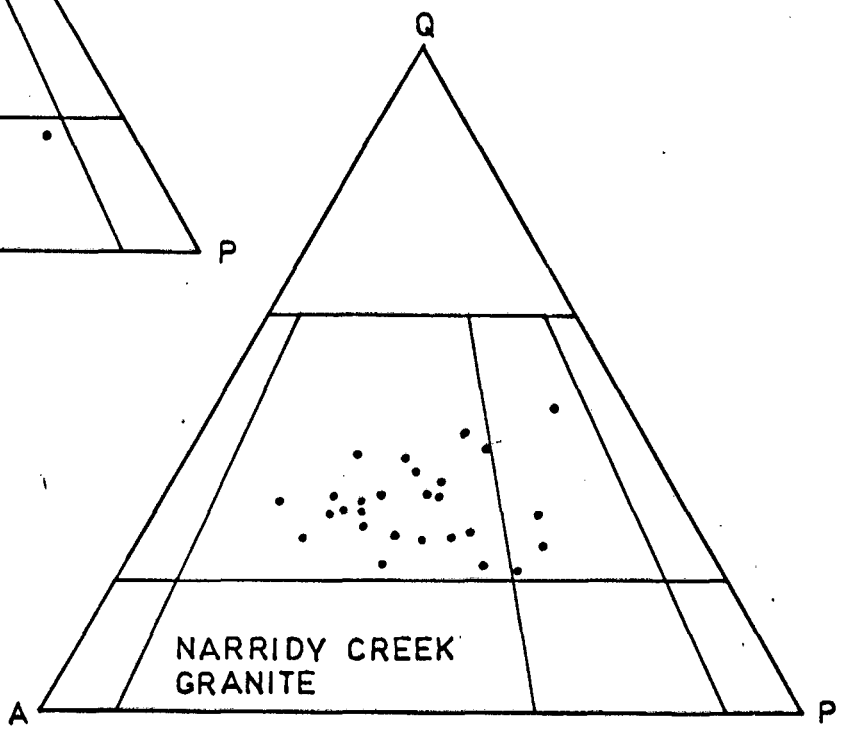
Outcrop of the Plug Range granite gneiss is shown on the main geological plan (Plan 2). It forms low rounded hills or rises which contrast against the steeper ridges of quartzite. In general outcrop is good but its low relief inhibits easy

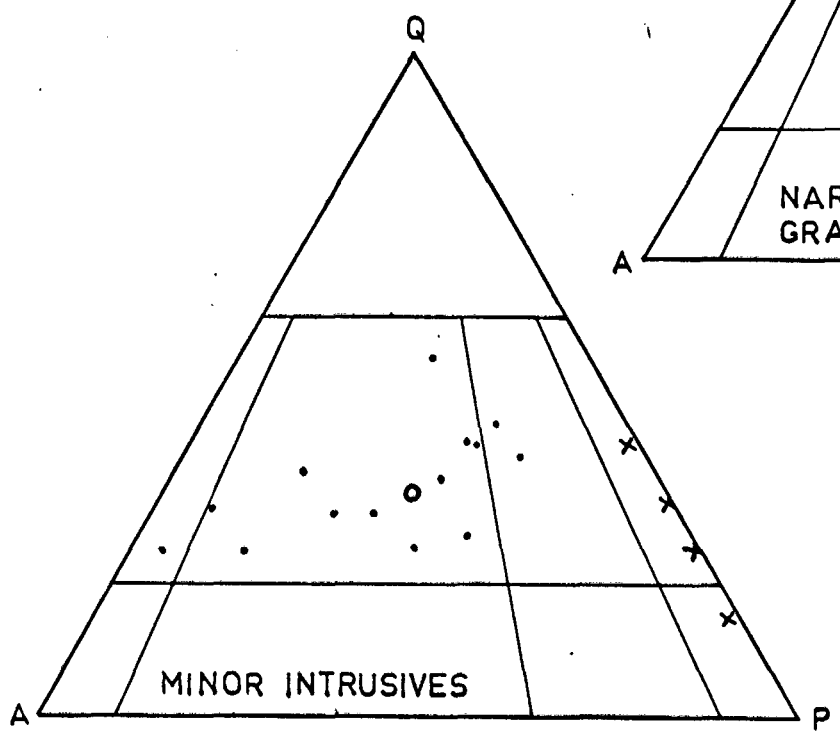
MODAL COMPOSITIONS of GRANITIC ROCKS

Q Quartz
A Alkali feldspar
P Plagioclase
Q + A + P recalculated to 100%
Mafics < 90 %









• Pegmatite
o Fine grained aplite
× Coarse grained aplite

FIG. 2.5

cross sectional viewing. There are however numerous fresh exposures along Salt Creek and these frequently have sub-vertical rock faces.

The granite gneiss itself is medium-to coarse-grained, equigranular, and strongly foliated with a gneissic layering frequently developed. Layers are several millimetres thick and are defined by separate quartzo feldspathic and biotite rich segregations, the latter being somewhat thinner. They are enhanced by conformable pegmatite veins and both these pegmatites and the gneissic layering have been multiply deformed. The colour of fresh gneiss is essentially grey but mottled with pink potassic feldspars.

Compositionally, the Plug Range granite gneiss conforms to a typical granite (IUGS Sub-commission, 1973). Quartz 25 - 40 percent, perthitic microcline 30 - 50 percent, and plagioclase 15 - 40 percent, are the main constituents (Fig. 2.5) but they are supplemented by biotite 10 - 15 percent, minor apatite, zircon, garnet, opaque mineral, and traces of amphibole and sillimanite. Sericite, chlorite, epidote and calcite are present in many rocks as a minor secondary alteration of plagioclase and biotite.

Throughout the area studied in detail the granite gneiss is homogeneous. However, north of the area along strike from typical granite gneiss a coarse augen gneiss has been noted. Compositionally it is similar to the granite gneisses, but it is notably inequigranular and superficially appears to be less deformed. Conformable amphibolite bodies that have been deformed with the granite gneiss are present throughout the area but no xenoliths of rocks of sedimentary affinity have been observed. Therefore, considering all these characteristics, the Plug Range granite gneiss body closely resembles

the Flinders Group gneisses mapped by Coin (1976) between Pt. Neill and Tumby Bay on southern Eyre Peninsula. Coin believed that those gneisses were basement to the Hutchison Group, but because the two groups were separated by a mylonite zone he could not demonstrate positively the relationship between them. In the Plug Range area it has been possible to show how they are related to each other and this is discussed along with preliminary geochronology in Chapter V.

2.3.2 Middle Camp Granite

The Middle Camp granite is well exposed in the hills immediately west of Cowell. It is a distinctive granite gneiss of grey colour and medium grainsize. It is equigranular, foliated and generally massive. Nevertheless it is sometimes layered (gneissic) and often there are thin pegmatite veins parallel to the foliation. Both the foliaton and the conformable pegmatites have been folded but only one generation of fold structures is evident which distinguishes it from the Plug Range and Narridy Creek bodies (see later). Sometimes there are additional pegmatites axial planar to the folds.

The intrusive nature of the Middle Camp granite is clearly evident. In the area east of Middle Camp, granite gneiss and metasediments (mainly dolomite) are complexly intermingled on a macroscopic scale. Outcrop is poor in that area therefore masking the exact nature of granite gneiss/dolomite contacts, but in Mindrow Creek 300 metres southeast of Middle Camp there are rare mesoscopic xenoliths of dolomite completely enclosed within granite.

Along the northwest boundary of the Middle Camp body an intrusive contact is not so obvious. Instead there is a

relatively sharp, conformable contact without xenoliths or other obvious intrusive features.

Preliminary geochronological analysis of the Middle Camp granite on samples collected during this study are outlined in Appendix B. An age of 1650 $\pm$ 35 Ma (and an initial ratio of 0.7098 $\pm$ 0.0013) is indicated.

The composition of the granite gneisses is somewhat variable between typical granite and granodiorite compositions (Fig. 2.5). For the true granites quartz 15-30 percent, K-feldspar 35-50 percent, plagioclase 20-30 percent and biotite/chlorite 5-10 percent are the main constituents, whereas for the granodiorites quartz 15-30 percent, plagioclase 45-60 percent, K-feldspar 10-25 percent and biotite/chlorite 5-10 percent are the main constituents. Sphene and apatite are ubiquitous in the Middle Camp granite as minor components, and other minerals to occur in trace amounts are zircon, opaque mineral, muscovite, amphibole, rutile and calcite. Sericite, epidote, chlorite and actinolite are present as alteration products of plagioclase and biotite.

Considering the composition and texture of the Middle Camp granite there appears to be a close association between it and the second category of biotite-sphene granites outlined by Jack (1914; see Chapter I). Jack's first category, the Carapee Hill granite gneisses are analogons to the Plug Range granite gneiss, whereas his third category, the coarse, undeformed Charleston Granite, is distinctively different from anything mapped in the study area.

2.3.3 Narridy Creek Granite

There are two specific zones within the Narridy Creek granite: a central zone of massive, essentially non-foliated to weakly foliated granite and a broad northwestern zone of

strongly foliated granite gneiss.

The central massive granite is medium-grained, equigranular and has a mottled pink colour. It forms low, rounded hills and is well exposed in Narridy Creek proper.

The northwestern foliated granite is variable in nature. It grades from a porphyritic, medium to coarse grained augen gneiss to a medium grained, equigranular granite gneiss. The variation is outlined in more detail in a later chapter but in summary it grades from coarse augen gneiss at or near the northwestern boundary to finer grained gneiss adjacent to the massive central zone. Assumed xenoliths of country rock metasediment are common and in particular between the Calcookara and Yabmana faults. They are manifest as mesoscopic (some are larger) patches or (?) blocks of metasediment completely surrounded by granite gniess. It is suggested that the greater proportions of country rock here may represent roof pendants over the granite body. The foliation throughout this zone is very constant in orientation, is sometimes strongly linear, and has only been locally overprinted (see later). Amphibolites conformable with the gneissosity are common and they often stretch for several kilometres parallel to the foliation. They also have strong L-S fabrics suggesting that they were emplaced with the granite (N.B. their planar ribbon-like development denies a xenolithic origin for them).

This variation in lithology of the Narridy Creek granite is believed to reflect continuous intrusion/crystallization during a deformational episode. As such the northwest outer zone represents the first phase to intrude and crystallize whereas the massive central zone represents the final, possibly post tectonic, phase. The amphibolites in the outer zone may

be related to the final phase(s).

An attempt has been made to date the massive granite during the course of this work but a very poor figure of 1643 $\pm$ 303 Ma (with an initial ratio 0.7240 $\pm$ 0.1780) was obtained (see Appendix B). The high initial ratio is no doubt partly consequent upon contamination by the older metasediments. However alternatively, it may represent partial remobilization of an older granitic basement analogous to the Plug Range granite gneiss (see Appendix B and Chapt. V). This hypothesis cannot be overruled since in a magmatic intrusive model the origin of the amphibolites is enigmatic whereas in a remobilized Plug Range situation amphibolites already exist within the granite.

The composition of the Narridy Creek granite as a whole is fairly uniform and typical of a true granite (Fig. 2.5) and there are no major variations between the inner and outer zones. Quartz 20-40 percent, K-feldspar 20-50 percent, plagioclase 20-50 percent, muscovite 3-7 percent, and biotite/chlorite 2-3 percent are the main constituents. They are accompanied by minor or trace amounts of opaque mineral, garnet, zircon and the secondary alteration products sericite and chlorite (N.B. the sericite is distinct from the muscovite. Muscovite occurs as scattered deformed plates of primary crystallization. Their presence is inconsistent with the Plug Range granite gneiss though this may be a metamorphic effect).

2.3.4 Minor Intrusives

PEGMATITES

Rocks in this category constitute the main bulk of minor intrusives within the metasediments and granites. They include the large, prominent pegmatite dykes and the smaller pegmatitic pods which form in fold hinges and which represent

only a minor migration of fluid. The dykes consist of massive, light coloured, coarse grained pegmatite typified by a major dyke running approximately parallel to and about 1-1.5 km west of the Yabmana fault. This particular dyke varies from a single dyke a couple of metres wide, to a cluster of parallel dykes spread over a width of 20 or more metres. There is no major mineralogical zonation across them. In other areas in the central migmatite zone, amoeboid patches of pegmatite are mixed up with gneiss and can constitute over 25 percent of the total exposure. They resemble pegmatites outside the migmatite zone but too little work was done to quantitatively substantiate this.

Mineralogically, the pegmatites are composed mainly of quartz, plagioclase and alkali feldspar in the approximate proportions shown in Figure 2.5. In addition they also frequently contain tourmaline up to 5 percent, muscovite 1-8 percent, and biotite from traces to 5 percent. Accessories include garnet, opaque mineral, zircon and apatite. Plagioclase is incipiently to partially sericitized and is predominantly oligoclase - andesine (An_{25-35}). Grains are generally ragged in outline, and many have narrow unsericitized coronas. Patch antiperthite is quite common in the plagioclases. Alkali feldspar ranges from microcline to perthitic orthoclase and it is mostly quite coarse-grained, ragged and anhedral. Of the remaining minerals, tourmalines are green brown in colour and mostly occur as unorientated, non-zoned, elongate prisms. The micas are generally subhedral and may be orientated to define a weak, non-pervasive foliation. They may also be kinked.

FINE GRAINED APLITE

This particular rock is of restricted occurrence having been only observed in the Calcookara subarea (see Fig. 4.6).

It was first recognized here by Jack (1914) whence it was described as a variety of aplite known as albitite. Strictly it is not an albitite, but rather, a very fine grained, densely textured and foliated aplite consisting essentially of quartz, oligoclase, microcline and biotite. Its approximate modal composition is recorded in Figure 2.5 Other minerals within the rock are medium sized, embayed crystals of muscovite, fine garnets and scattered opaques.

In the field it is conspicuous by its grainsize and hardness. It is pale off white in colour and the foliation is not bovious. However, unlike most pegmatites, it markedly crosscuts the layering of adjacent rocks, and has been deformed. Of particular interest in one isolated outcrop is the occurrence of long blades of scapolite within the aplite and adjacent to calc-silicate.These blades range in size up to half a metre long and 40 mm across. The variety of scapolite is wernerite (Jack, 1914).

COARSE APLITE

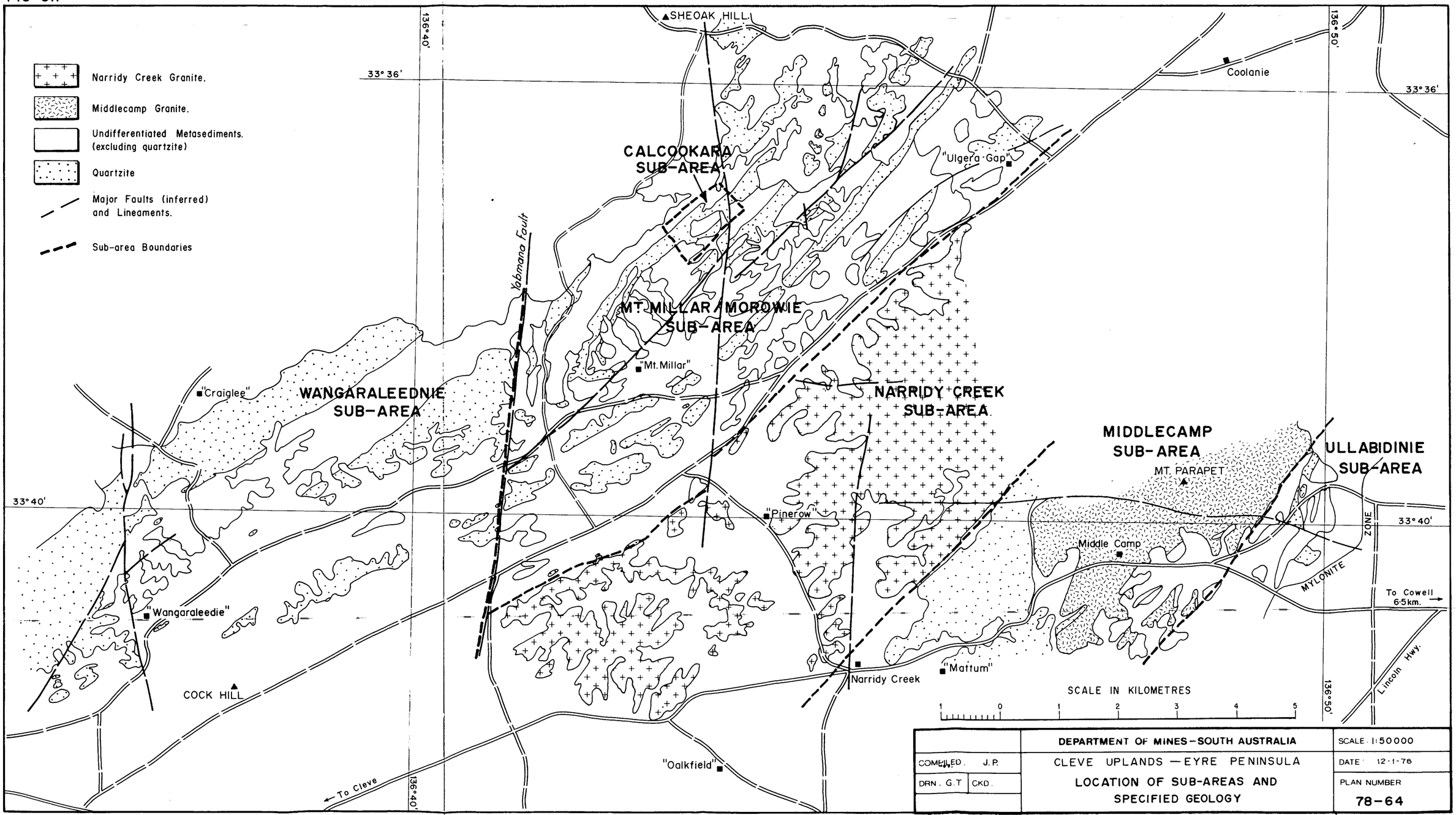
Aplites of this category are medium-to coarse-grained and composed essentially of plagioclase and quartz. As such they can be classed as tonalites (Fig. 2.5).

In the field they appear as white, medium-to coarse-grained, massive dykes generally conformable with the layering and devoid of any mafics. They are not of widespread occurrence although they are more common east of Middle Camp where they are associated with the Middle Camp granite.

In thin section they are porphyroblastic, consisting of coarse-grained plagioclase in a mosaic predominantly of medium-to fine-grained quartz. Plagioclase is the dominant constituent and is a partially sericitized oligoclase (An_{25-30}). It is deformed and displays some spectacular

recovery/recrystallization features whereas quartz forms narrow aggregates of slightly strained polygonal grains. Minor accessories consist of sericite, sphene and, rarely, opaque mineral.

FIG 3.1



	DEPARTMENT OF MINES – SOUTH AUSTRALIA	SCALE 1:50000
COMPILED J.P.	CLEVE UPLANDS — EYRE PENINSULA	DATE 12-1-78
DRN. G.T CKD.	LOCATION OF SUB-AREAS AND SPECIFIED GEOLOGY	PLAN NUMBER 78-64

CHAPTER III

MESOSCOPIC STRUCTURE

3.1 INTRODUCTION

This chapter describes the mesoscopic structural elements observed in the field. Their orientation and macroscopic interpretation follow in Chapter IV, while detailed appraisal of the microstructure follows in Chapter VI.

In the previous chapter it was frequently noted that most lithologies are well layered or banded. No specific sedimentary structures were observed to identify this layering as bedding (S_o), but it is considered to represent bedding because:-

a) its variable nature is more typical of bedding than of a metamorphic layering which is generally more regular particularly with reference to spacing and composition (e.g. Turner, 1941; Ramberg, 1952; Spry, 1969);

b) mesoscopic layering parallels the boundaries of the various macroscopic lithological units;

c) individual units can be traced for several kilometres;

d) a variety of primary rock types are recognized (e.g. quartzite, dolomite, pelite, iron formation); and

e) local sequences can be correlated over large areas.

Throughout the description of meso-, macro-, and microstructure, reference will be made to six major subareas. They are the,

1) Wangaraleednie,

2) Mt. Millar/Morowie (including the Calcookara subarea),

3) Narridy Creek,

4) Middle Camp,

5) Ullabidinie (including the mylonite zone), and

6) Plug Range

subareas as outlined in Figure 3.1. Their recognition as areas in which there is an homogeneity of character was based mainly on the dominant lithology. Thus those areas where either a particular granite or migmatitic gneiss predominates were isolated as separate subareas. However, further subdivision based on structural analysis (e.g. see Hobbs et al, 1976) has been used in certain sectors to demonstrate a particular feature. Most of the subarea boundaries correspond to major dislocations (e.g. Yabmana fault).

3.2 BASIC STRUCTURAL ELEMENTS

3.2.1 D_1 Deformation

The earliest formed planar fabric recognized in the metasediments is a high grade schistosity (S_1) which everywhere parallels the lithological layering, and which can be distinguished from S_2 only in the hinge zones of D_2 structures where it is parallel to the folded layering and overprinted by S_2.* In the granite gneisses only the Plug Range granite gneiss records an S_1 fabric. It is manifest as a strong, pervasive, gneissic layering with a parallel mica schistosity. However that this represents the earliest gneissosity in the Plug Range granite is not evident; there may be an earlier pre D_1 fabric(s) that has been lost during the subsequent deformations.

That the D_1 deformation was a major fold deformation is also not clear although there are some rare folds in the

---

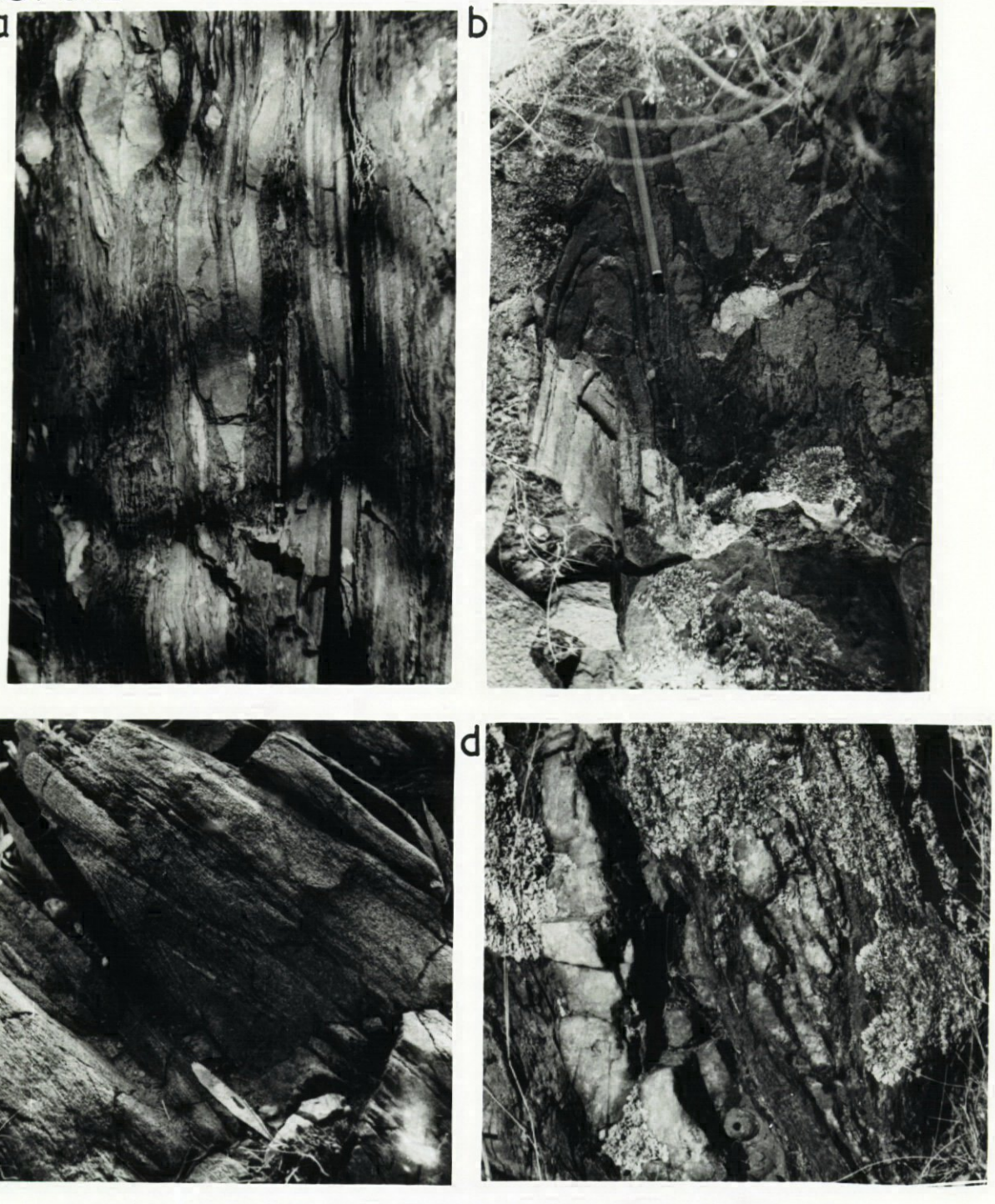
* Because of the isoclinal nature of D_2 folding S_1 and S_2 are commonly parallel in the limbs of F_2 folds. Therefore the normally observed layer-parallel schistosity actually represents the combined effect of D_1 and D_2 strain and will be referred to as S_{1-2}; S_1 and S_2 are reserved for those particular instances where specific overprinting can be demonstrated.

metasediments which by their nature may be related to D_1. These folds fold the lithological layering (S_o) and have a very strong axial plane schistosity which may be S_1; that is, they do not appear to fold any pre-existing fabric. Their form is isoclinal and they approximate very closely to ideal "similar" or Class 2 type folds (Ramsay, 1967). However, apart from the apparent absence of an earlier folded schistosity, they resemble D_2 folds in all respects. Only one fold could be demonstrated to positively antecede the S_2 schistosity. This particular fold (see Fig. 6.3) is an isoclinal, Class 2 fold that has been refolded and overprinted by a strong S_2 schistosity. S_1 is not obvious in hand specimen but it is inferred from thin, elongate quartz pods that lie along transposition surfaces parallel to the axial plane of the fold. It is believed that this fold specimen represents a D_1 fold rather than soft sediment deformation but for a further discussion see Chapter VI.

3.2.2 D_2 Deformation

The second deformation affected the entire study area and was a major ductile event of intense folding which produced tight to isoclinal mesoscopic folds, F_2, with strong, pervasive, axial fabrics, S_2 and L_2. In the migmatitic gneisses the pegmatitic segregations are folded; in the non-migmatitic gneisses quartz veins are folded (although there are some new S_2 parallel veins), in the Plug Range granite gneiss the prominent S_1 gneissosity is folded, and in the Middle Camp granite a strong S_2 schistosity is present. Consequently this deformation post-dated the major metamorphic episode(s) which produced the migmatites and gneissic layering of the Plug Range gneisses, and either postdated or was broadly contemporaneous with the formation of the Middle Camp granite.

FIG. 3.2



Since D_2 variously affected each lithology both within the metasediments and within the granitic bodies each lithology will be considered separately.

SEMIPELITIC GNEISS - Typical D_2 folds from the non-migmatite zone and from the migmatite zone are shown in Figure 3.2. They are more common in the non-migmatite zone of the Wangaraleednie subarea, and in that area they contrast markedly with later overprinted folds which lack the axial fabric. Mesoscopic F_2 folds range in size from those with wavelengths of only a few millimetres up to those with wavelengths of the order of half a metre. Broader F_2 folds are not readily observable but can be reconstructed from detailed mapping of the vergence of mesofolds.

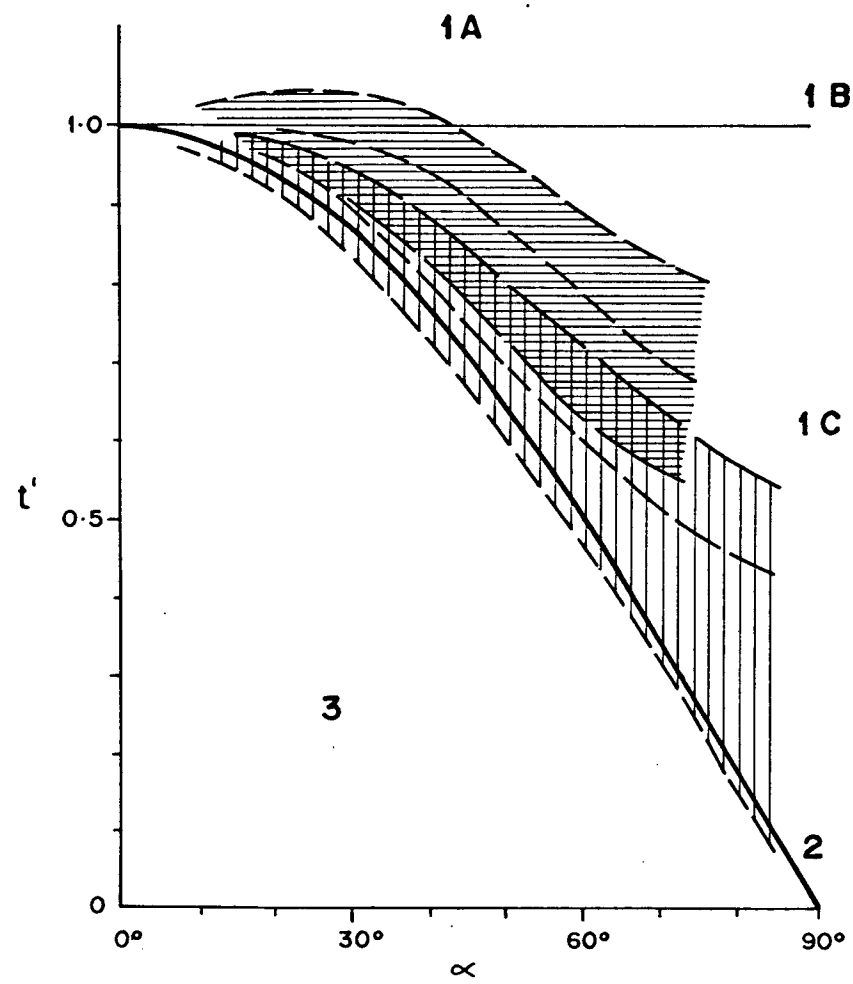
F_2 folds are mainly very tight or isoclinal with small interlimb angles rarely exceeding 10 degrees. The folded layering is considerably thicker in the hinge regions than in the limbs and consequently F_2 resemble "similar" type folds. To demonstrate this, several F_2 folds have been analysed according to Ramsay's classification scheme (1967, pp 360-370).

The system used was that of measuring the orthogonal thickness (t) at various points around a folded layer, calculating the ratio t_α / t_o for the various angles of inclination (α) and plotting that ratio against α. This was carried out on many folds - traced from photographs, hand specimens and thin sections - and was repeated on both psammitic and pelitic (when possible) bands within each fold. the results are shown in Figure 3.3 and indicate that F_2 folds are predominantly

---

Figure 3.2: F_2 folds in semipelitic gneisses. (a), (b) and (c) from non-migmatized rocks in the Wangaraleednie subarea (along the Yabmana cross-section). (d) and (e) from migmatized rocks in the Mt. Millar/Morowie subarea. Note domainal S_2 in (c) and F_3 folds refolding F_2 folds in (e).

FIG 3.3



$t' = \frac{t_\alpha}{t_o}$ where t_α = orthogonal thickness at an angle of inclination = α

F_2 folds Vertical bars.
(approximately at the 90% confidence level.)

F_3 folds Horizontal bars.

Fold classification after Ramsay 1967

t'_α PLOTS FOR VARIOUS F_2 AND F_3 FOLDS WITHIN SEMIPELITIC GNEISSES OF THE HUTCHISON GROUP

of Class 1C type but that they closely approach, and in fact many can be classified as, Class 2 type folds; that is, true "similar" type folds. There was little significant distinction between pelitic and psammitic bands although the former were much more irregular in outline and controlled by the adjacent psammitic bands (see Fig. 3.2B).

Axial fabrics which are rarely absent, are best developed in the non-migmatized gneisses of the Wangaraleednie subarea (Fig. 3.2 A-C). The axial planar S_2 schistosity of F_2 folds in this subarea is a high grade pervasive schistosity which partially obliterates the layer-parallel schistosity of the folded layering. While S_2 is mainly defined by the preferred alignment of micas, it is sometimes additionally defined by a distinct mineral segregation. Such an instance is shown in Figure 3.2C where alternating bands rich or poor in biotite/muscovite and quartz/feldspar have formed on a scale of 0.5-1.00 mm wide. These narrow, evenly spaced bands crosscut the more irregular and broader, folded lithological layering in hinge regions but merge into it in the limbs where both become parallel.

In addition to the axial planar fabric, there is also commonly a linear fabric, L_2, which parallels the F_2 fold axes (Fig. 3.4). This linear fabric is best seen in the non-migmatized gneisses where it is developed as a quartz rod or mullion lineation sometimes associated with a weak mica elongation. The quartz rods are long and continuous, and in section they are mainly of irregular outline but tending to be elliptical in S_2 and S_{1-2}. They are rarely more than a few millimetres across but are generally less than 2 mm.

Mullion type structures are also common and they merge into rod like forms. The mullions are developed on the more quartzo feldspathic layers as a regular corrugation which

FIG. 3.4

a



b



c



parallels the fold axes. This corrugation is of similar form to the rodding, that is, it is commonly 1-2 mm across and cylindrical in length. Both the rodding and mullions appear to represent pinch and swell features in the layering combined with local transposition rather than elongation of discrete objects.

PELITES - In the pelitic schists, there are no recorded mesoscopic features which can be specifically attributed to the D_2 deformation. Rather, the very strong pervasive schistosity which parallels the broad lithological layering represents D_1 and D_2 strain (i.e. S_{1-2}). It is overprinted by D_3 and D_4. There are no prominent pre D_3/D_4 lineations, but occasionally there may be preserved a weak sillimanite pod lineation or even more rarely, a weak tourmaline mineral lineation. The sillimanite pods normally are platy within S_{1-2}, but are sometimes elongate up to 3:1. This elongation when observed, parallels the quartz rodding in adjacent quartzites and semipelites, and is considered to be an L_2 lineation.

QUARTZITES - Within the quartzites, rare F_2 folds are isoclinal and of similar scale and style to those in the semipelites. They have an axial planar S_2 schistosity, but it is not as pervasive as in the semipelites.

The quartzites do however frequently display a very strong rodding (Fig. 3.5). The rods are seen on S_{1-2} and S_2 surfaces, and are defined by very long aggregates of quartz. They are essentially monomineralic, and in cross-section they vary from irregular, equidimensional outlines

---

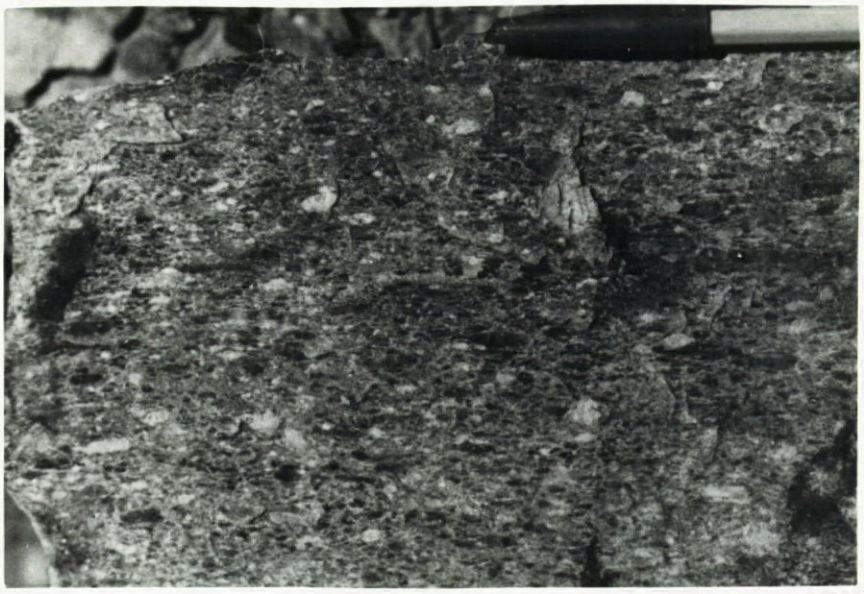
Figure 3.4: L_2 lineations in semipelitic gneisses from the Wangaraleednie subarea. (a) F_2 fold with parallel L_2 lineation deformed by F_4 buckle fold. (b) L_2 lineation (plunging to bottom-left of photo) overprinted by F_3 (shallow) and F_4 (steep) crenulations. (c) L_2 quartz rod with parallel mullions (L_2 oblique to page).

FIG. 3.5

a



b



c



through to elliptical outlines with the long axes lying in the S_{1-2} plane. They merge into mullions developed along the interfaces of quartz and thin feldspar or mica rich layers. The intensity of the rodding is variable throughout the study area and many quartzites lack this linear feature.

DOLOMITES AND CALC-SILICATES - The dolomites in the study area are mainly massive except for a faint, subtle mineralogical banding. Apart from this particular banding they do not contain any observable structural elements which can be attributed directly to D_1 or D_2 strain. The layering itself is quite regular and consistent, but its origin is obscure. It may be bedding because it parallels the broader lithological boundaries, but it may also be of a metamorphic/structural origin as it is also parallel to the S_{1-2} schistosity and layering of the adjacent rocks. Consequently it is considered to be representative of S_{1-2}.

The calc-silicates however, as noted in Chapt. II, are characterized by a prominent layering which displays spectacular folding and records in detail the D_2 deformation. This layering, S_{0-1}, is folded very tightly to isoclinally (Fig. 3.6) and specific overprinting in the Calcookara subarea has established these folds as D_2 structures (see Chapt. IV). The folds are often irregular in cross section and also non-cylindrical suggesting that certain layers (e.g. the carbonate layers) were very ductile during deformation. Elsewhere there are fold cusps (Fig. 3.6B) and limbless folds which imply extreme attenuation and ductility contrast between carbonate and feldspar-rich layers.

AMPHIBOLITE - The most prominent feature of the amphibolites

Figure 3.5: L_2 Quartz rodding in quartzites. (a) and (b) from the Wangaraleednie subarea: (a) parallel to L_2, and (b) perpendicular to L_2. (c) from the Mt. Millar/Morowie subarea 2.2 km SW of Ben Lomond: sub-vertical L_2.

FIG. 3.6

a



b



c



d



is their schistose nature with or without a related mineral lineation. Most amphibolites are massive and non-layered and the schistosity cannot be specifically attributed to either D_1 or D_2. Nevertheless it is deformed by D_3 and consequently is considered as S_{1-2}.

Furthermore, two folds were recorded from a banded amphibolite overprinted by D_3 (Fig. 3.6C). These were isoclinal, of "similar" style, and had both a strong axial planar schistosity and a weak "B" type mineral lineation. (i.e. parallel to fold axes). The folds are equivalent to F_2 in the semipelites and hence the mineral lineation is considered as L_2 and the schistosity as S_2.

PLUG RANGE GRANITE GNEISS - F_2 folds are common in the granite gneiss adjacent to Plug Range. The main gneissosity is S_1 which has been very tightly folded during D_2 producing meso-folds which have wavelengths ranging from 50 to 200 mm and which are essentially of chevron style with minimum interlimb angles of 20 - 25 degrees (Fig. 3.6D). Unlike the semipelitic gneisses, the S_1 gneissosity has remained prominent whilst the D_2 axial plane fabric is subdued. However they have been overprinted by open D_3 folds which firmly establish their D_2 association.

MIDDLE CAMP GRANITE - The earliest recognizable structural feature of the Middle Camp granite is a strong foliation which was folded during D_3.

No earlier fold structures were observed and consequently the foliation is considered to have been derived during D_2 (i.e. it is S_2). It is defined by a strong alignment of

---

Figure 3.6: (a) F_2 folds refolded by F_3 in calc-silicates from the Calcookara subarea. (b) F_2 fold cusps of microcline layer in dolomitic calc-silicate. (c) F_2 folds in layered amphibolite 1.5 km west of Calcookara Mine. (d) Overturned S-vergence F_2 folds within the Plug Range granite gneiss.

biotite, often with narrow (up to 50 mm), subparallel pegmatite veins.

3.2.3 D_3 Deformation

D_3 was responsible for the majority of macroscopic folds observed throughout the study area, and for the production of a prominent fabric in the Narridy Creek granite. In the metasediments D_3 produced mesoscopic folds ranging from broad open warps tens of metres across to fine crenulations of only a few millimetres. The Plug Range granite gneiss was folded into broad open folds and the S_2 schistosity of the Middle Camp granite was buckle folded. Along the eastern edge of the study area, D_3 structures became tighter with the ultimate production of a mylonite zone. The mylonitic deformation although part of D_3 will be treated separately (Sect. 3.2.4).

SEMIPELITIC GNEISSES - The third deformation is characterized by folds and crenulations which are relatively open by comparison with F_2, and which lack a penetrative axial plane fabric. F_3 folds fold both the layering and the layer-parallel schistosities, and in addition often fold a lineation. The folded fabrics, S_{1-2}, S_2 and L_2, remain the predominant fabrics (Figs. 3.4B and 3.7).

The scale and style of F_3 are variable. In the unmigmatized gneisses west of the Yabmana fault, F_3 folds are represented by crenulations, by mesoscopic folds with wavelengths up to 0.5 m, and by much broader and more open warps with a strong crenulation in the hinge areas (Fig. 3.4B and 3.7A). In the migmatite gneisses the crenulations are not prominent. Instead, mesoscopic folds and broader open warps predominate (Fig. 3.2E and 3.7B-C).

The morphology of F_3 varies considerably from curved

FIG. 3.7

a



b



c



d



concentric to either box or chevron type folds. Profiles were measured by Ramsay's scheme (see Sect. 3.2.2), and the results are shown in Figure 3.3. The folds are essentially Class 1C folds, not as tight as F_2, but with hinge regions ($\alpha <$ 40 degrees) of concentric form and limb regions ($\alpha >$ 40 degrees) of Class 1C form. Interlimb angles in the Mt. Millar/Morowie and Wangaraleednie subareas are mainly greater than 30 to 40 degrees and frequently around 60 to 70 degrees. However southeast of the Middle Camp granite F_3 folds become much tighter approaching isoclinal form, and they fall within the region of the overlap of F_2 and F_3 fold styles (Fig. 3.3). Such F_3 folds in migmatized gneisses are similar to F_2 and are difficult to distinguish in the field.

In the majority of F_3 folds throughout the study area there is only an incipient axial fabric. The migmatized gneisses display a wavy, fracture-like cleavage (Fig. 3.7 B-C) which closely approximates the axial planar orientation but which does tend to convergently fan away from that orientation in the limbs. This is particularly so in the pegmatitic segregations whereas in the micaceous layers between them, the converse often holds; that is, it is sometimes divergently fanning*.

The S_3 planes themselves are wavy and discontinuous. They are lined with a dark phyllosilicate and/or opaque, and tend to weather out preferentially. There is no other mineral segregation apparent and while some micas appear to be partly rotated into S_3 orientation, most remain in their S_{1-2}

---

* convergent and divergent are used in the sense described by Ramsay (1967); viz. convergent cleavage fans out from the inner to outer areas.

Figure 3.7: (a) F_3 folds in semipelitic gneiss from the Wangaraleednie subarea. (b) and (c) F_3 folds in migmatite gneisses from the nose of the Mt. Millar antiform. (d) F_3 crenulations (parallel to pen) overprinted by F_4 crenulations in pelitic schist from Range Road, Wangaraleednie subarea.

FIG. 3.8



b



d



a



c

orientation. Flattened sillimanite pods are folded with S_{1-2}.

There are no mineral lineations in the semipelites which can be attributed directly to D_3. However in certain areas F_3 and F_2 have similar orientations in which case the L_2 rodding and mineral lineation assume F_3 parallelism. In other areas however, L_2 lineations are visibly deformed by D_3. Such examples don't show any D_3 mineral elongation but rather an L_3 intersection lineation recording the intersection of S_3 with the folded S_{1-2} surfaces.

PELITIC SCHISTS - West of Yabmana fault, the pelitic schists often show interfering crenulations (Fig. 3.7D) of which the stronger is generally the D_3 crenulation. The angle between the two sets varies up to almost 90 degrees and is dependant on the orientation of S_{1-2}.

The crests of D_3 crenulations are much sharper than the D_4 set and furthermore, the interlimb angle is much smaller and mainly less than 90 degrees. The limbs are essentially symmetrical about the crenulation plane but climb according to the gross structure.

QUARTZITES - Within the massive quartzites, large, open folds occur with wavelengths of several metres or more (Fig. 3.8A) and concentric profiles. In the banded quartzites however, smaller mesoscopic folds are developed. They have wavelengths of 0.2 to 0.5 m, are relatively open with largish interlimb angles, and very frequently fold a lineation (Fig. 3.8B).

Axial fabrics are generally absent in F_3 folds of the quartzites, but a rod or mullion type lineation is sometimes

---

Figure 3.8: (a) Overturned "S"-vergence F_3 folds in relatively massive quartzite 2.2 km north of Wangaraleednie. (b) F_3 folds (parallel to arrow) folding the L_2 quartz rodding in layered quartzite. (c) Broad F_3 warping of the S_1 gneissosity in the Plug Range granite gneiss. (d) Middle Camp granite: F_3 folds (with planar S_3 pegmatite veinlets) folding S_2 parallel pegmatite veins.

developed on one limb only parallel to F_3. This L_3 lineation is superficially identical to the L_2 rodding of the quartzites. S_3 planes are rarely developed.

DOLOMITE, CALC-SILICATE AND AMPHIBOLITE - Within all of these units although minor folds on the scale of less than a metre are present (e.g. in the calc-silicates) the vast majority of D_3 structures are open folds with wavelengths of the order of several to tens of metres. They contrast with the semipelites reflecting their general homogeneous nature; i.e., the folding has developed from buckling of thick bands, and the large wavelength has developed in response to its dependency on thickness of the competent layer (see Ramsay, op cit; p. 375-6).

PLUG RANGE GRANITE GNEISS - In contrast to F_2 in the granite gneiss adjacent to Plug Range, D_3 is represented by very-broad, open warps (Fig. 3.8C). These fold the S_1 gneissosity and F_2 folds, and lack any visible axial fabric.

MIDDLE CAMP GRANITE - Mesoscopic folding of the S_2 schistosity (and S_2 parallel pegmatite veins) is relatively common and is nearly identical to F_3 folding in the migmatite gneisses (Fig. 3.8D). It produces open buckle folds with interlimb angles of about 50-70 degrees. There are no mineral lineations but there is an incipient axial planar S_3 defined by a weak alignment of micas. Also, there are frequently minor, planar, pegmatite veinlets which develop along certain S_3 axial planes (Fig. 3.8D).

NARRIDY CREEK GRANITE - The central body of the Narridy Creek granite, (the granite in Narridy Creek itself) is massive and poorly to non-foliated (Fig. 3.9A).

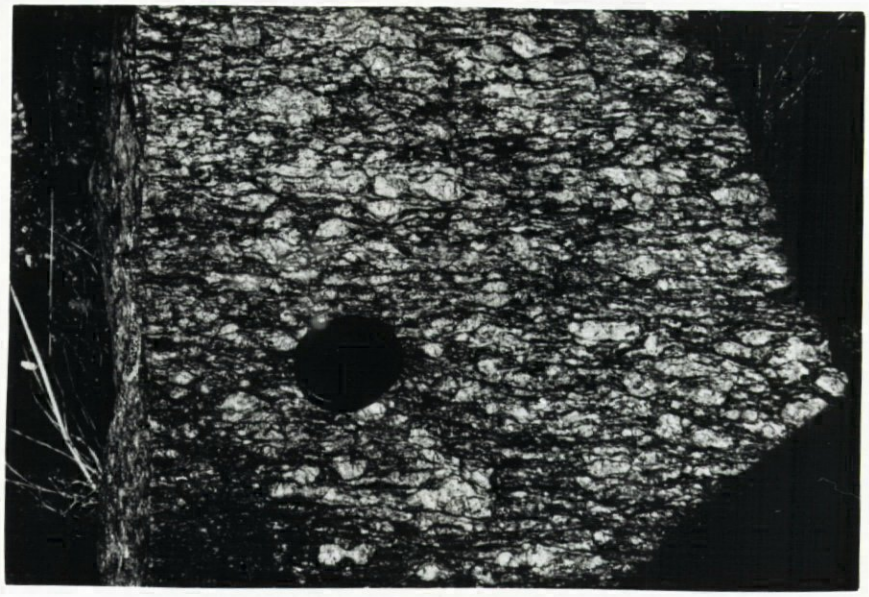
However, along the northwest side of the body there is a broad belt of deformed granite extending from the contact with the metasediments to about 2.5 to 3 km southeast into

FIG. 3.9

a



b



c



the granite. The deformation is manifest as an upright, very strong (though variable), mylonitic type schistosity. It is defined by narrow ribbons of fine grained quartz, feldspar and mica which wrap around augen of medium to coarse feldspar (Fig. 3.9B). The size of the augen varies systematically across the zone and this is examined in the next chapter (Chapter IV).

Locally there is a further development of the S_3 gneissosity into fine grained bands devoid of any relic augen (Fig. 3.9C). These bands vary in width from several millimetres up to 2 m wide, and whilst one boundary is often relatively sharp, the other usually merges gradationally into the adjacent augen textured gneiss.

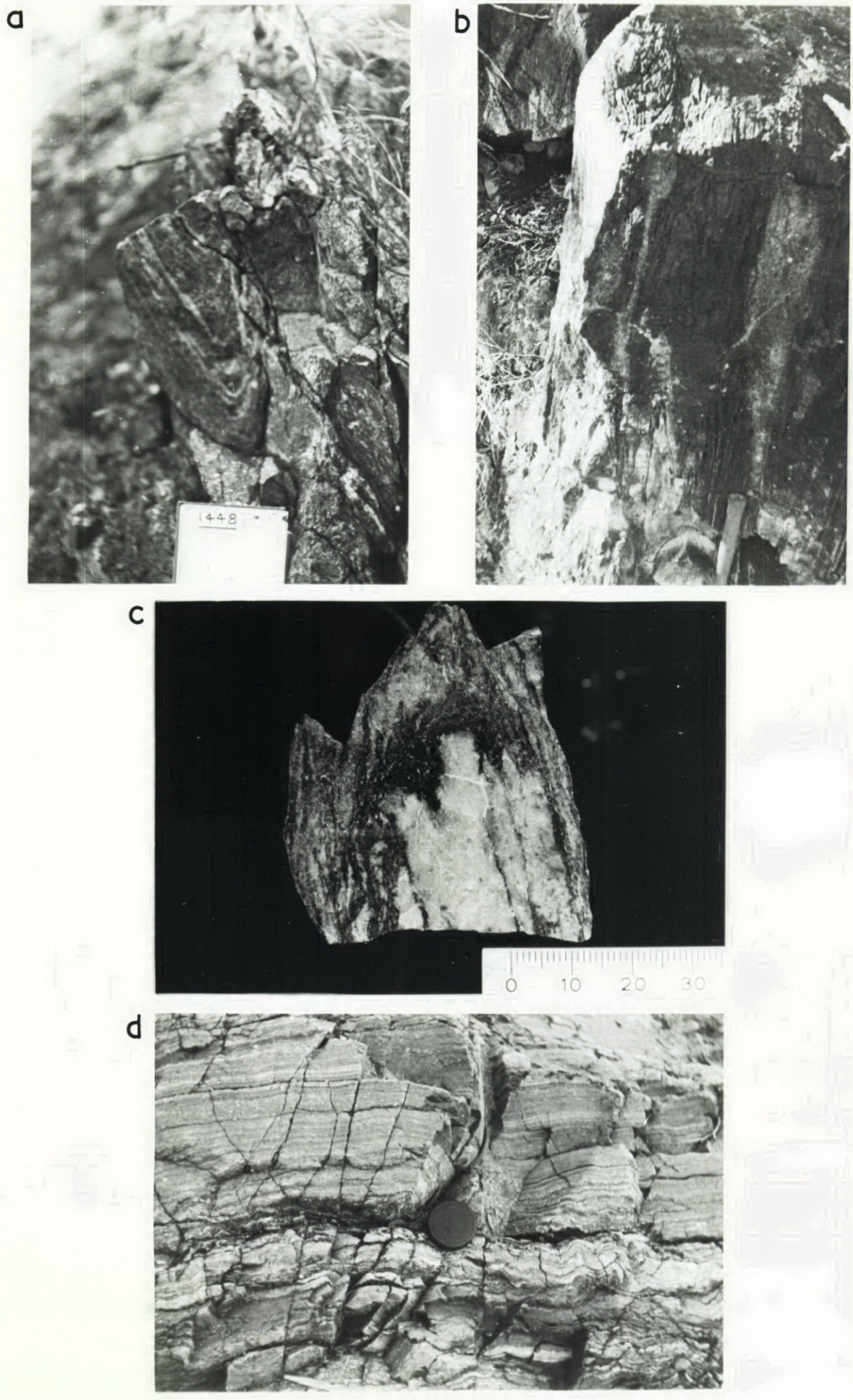
As well as the strong gneissosity there are also scattered areas or bands which display a subhorizontal L_3 rodding. The rodding is much like that of the quartzites and is defined by long, cylindrical aggregates of quartz and feldspar. In section these aggregates are elliptical parallel to S_3 and they range up to 10-15 mm across.

Gneissic xenoliths and the larger areas of metasedimentary schist and gneiss within the borders of the Narridy Creek granite, still retain their S_{1-2} schistosity. However it is invariably strongly crenulated and folded (F_3) with the development of an incipient axial plane schistosity which parallels the granite gneissosity immediately adjacent. The fold axes of these folds and crenulations parallel the rodding within the granite.

Amphibolite bodies in the granite also record the D_3 deformation. The bodies themselves are long and lenticular,

Figure 3.9: Narridy Creek granite (a) Massive granite with garnet/biotite clots. (b) S_3 in coarse augen gneiss southwest of Hill View. (c) Fine grained granite gneiss (left) grading into augen gneiss (right) 2 km northeast of Pinerow.

FIG. 3.10



they parallel the general gneissosity, and they are strongly schistose with a related, well developed lineation. This schistosity always parallels the granite gneissosity, as does the amphibole lineation to the granite rodding, and they are considered to be equivalent (i.e. they are S_3 and L_3 respectively). This is an anomalous situation compared with amphibolites in the metasediments (which have S_{1-2} and L_2 fabrics) and suggests that the amphibolites have been either completely recrystallized during D_3 (which is unlikely in view of the partial recrystallization of the granite - see Chapt. VI) or intruded broadly contemporaneously with intrusion of the massive Narridy Creek Granite. Late or post-orogenic basic intrusions of this nature have been noted on southern Eyre Peninsula (Giddings et al, 1976; Coin, 1976) and would support the latter alternative.

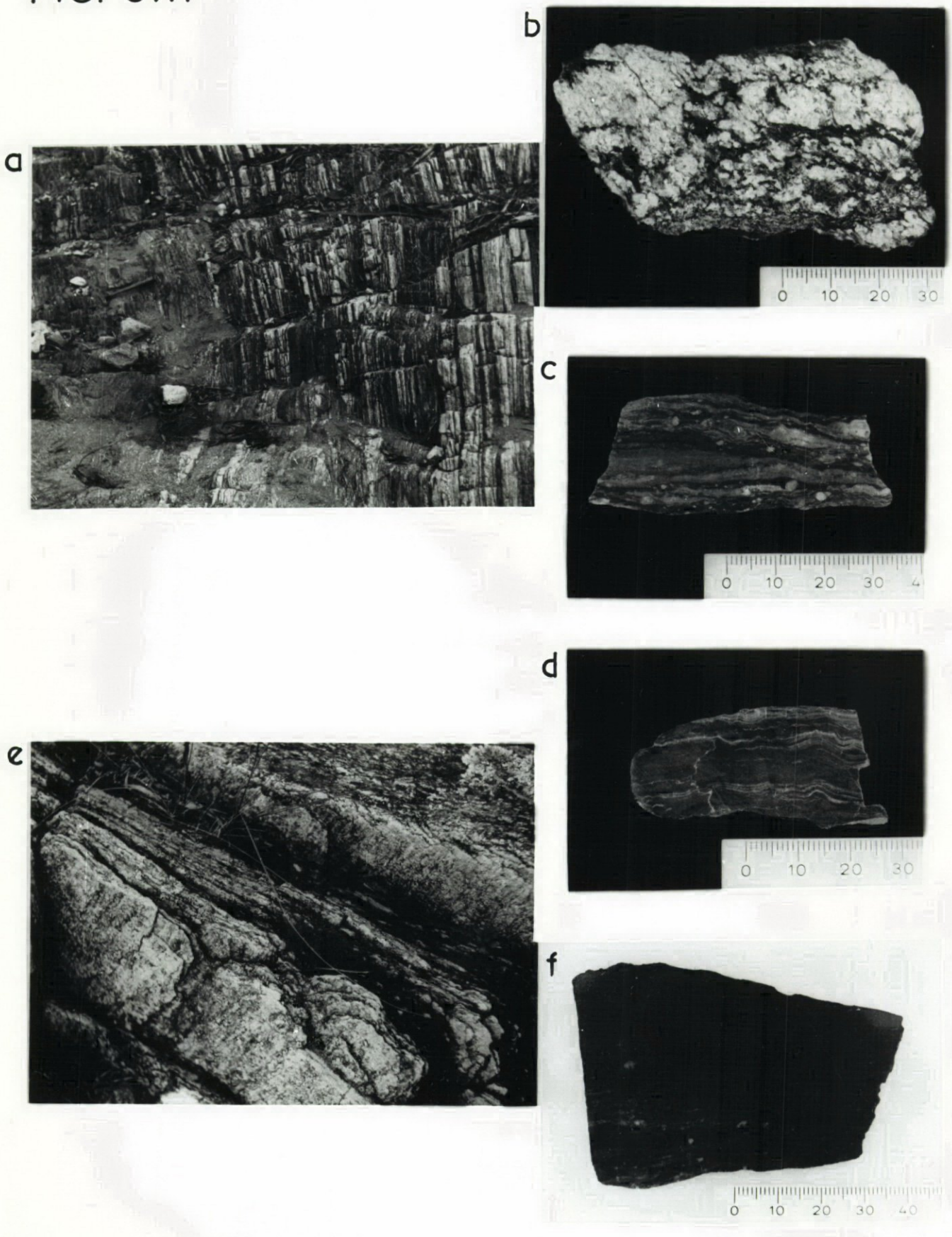
3.2.4 Mylonite Deformation (D_M)

A major mylonite zone is developed along the southeast edge of outcrop in the study area. There are a few other recorded occurrences of mylonite in the study area - particularly near the northwest boundary of the Narridy Creek granite - but these are only of minor extent.

It was noted in the preceding section that F_3 folds in the migmatite gneisses get much tighter and almost isoclinal approaching the mylonite zone (Fig. 3.10A). This is also true of folds within dolomite immediately adjacent to that zone, (Fig. 3.10B), and consequently it appears there is an increase in strain towards the mylonite.

Figure 3.10: (a) Tight F_3 folds in migmatite gneiss adjacent to the mylonite zone. (b) Very tight F_{2-3} folds in weakly layered dolomite immediately adjacent to the mylonite zone. (c) very tight fold in retrograded migmatite gneiss from within the mylonite zone - mylonitized gneiss. N.B. incipient domainal S_M vertical. (d) Typical slaty mylonite with S_M being crenulated by F_4.

FIG. 3.11



Rocks within the zone itself can be subdivided into two broad categories which merge into each other,

(1) mylonitized gneiss,

(2) slaty mylonite.

Most of the zone consists of mylonitized gneiss but there are distinct bands of slaty mylonite developed throughout it. The bands of slaty mylonite vary from 0.2 m wide up to tens of metres wide and are distinguished from mylonitized gneiss on the basis of texture.

Mylonitized gneisses are medium to fine grained, generally equigranular, and still retain the principal characteristics of the host rocks; that is, quartzo feldspathic bands (although maybe transposed) are still distinct and separated from each other by thin micaceous layers (Fig. 3.10C). They grade into the migmatized gneisses outside the zone, and contain numerous very tight to isoclinal folds of F_3 form that have a strong axial planar fabric. This axial fabric (S_m here but equivalent to S_3 outside the zone) is penetrative in hinge zones and progressively develops into a segregation schistosity until ultimately it completely obliterates the original S_{1-2} schistosity.

Slaty mylonite develops from the mylonitized gneiss. It is typical mylonite with scattered, medium sized, relic clasts of feldspar, and long lenticular ribbons of microscopic grained feldspar in a very fine grained micaceous matrix (Fig. 3.11). By contrast with mylonitized gneiss, the original character of the slaty mylonite is not obvious.

Figure 3.11: Mylonite zone in Mindrow Creek. (a) Mylonitized gneiss (right) progressively grading into slaty mylonite (left). (e) L_M lineation on S_M in mylonitized gneiss (from the right hand side of (a)).
(b) mylonitized gneiss from right hand side of (a).
(c) typical mylonite from the centre of (a).
(d) slaty mylonite (N.B. F_4 crenulations) from the left hand side of (a).
(f) discordant "fluid" phase (upper right) truncating slaty mylonite (lower left).

Instead the rock has a distinctive slaty appearance with just the scattered megacrysts and fine grained ribbons of feldspar. The matrix itself is dark green in colour and has a very strong slaty cleavage. The feldspar ribbons have a very finely layered infrastructure and are mostly pink to pinkish-white in colour.

The progressive development of this slaty mylonite is clearly shown in Figure 3.11. Over a matter of three or so metres, a rapid transition in the texture and fabric of the mylonite can be observed. From medium grained mylonitized gneiss there is a progressive transition through varying combinations of matrix, ribbons and clasts into a homogeneous, very fine grained, slaty rock devoid of feldspar clasts. Rarely there may be later veins or pods of quartz which have apparently been introduced after cessation of the mylonitization process. There are also rare isoclinal folds within the slaty mylonite and these appear to fold S_m yet to have S_m axial planar. That is they must have formed after the initial formation of the S_m fabric yet before the cessation of that deformation. They infer a long, continuous process of mylonitization (cf Bell et al, 1973).

Additional to the planar S_m fabric, there is often a strong rod type lineation, L_m, developed on S_m (Fig. 3.11E). It is defined principally by very strongly elongate (>20:1), cylindrical rods of fine grained feldspar which are often accompanied by a chlorite mineral elongation. L_m is seen best in the early and intermediary stages of the mylonite development rather than in the homogeneous slaty mylonite.

Ultimately in the mylonitization process is the production of a "fluid" phase (Fig. 3.11F). This is only a local development which sometimes forms in areas of homogeneous slaty

FIG. 3.12









mylonite. It is massive, dark green in colour, and forms irregular patches which are discordant to the slaty fabric. Although it is apparently of similar composition to the host slaty mylonite, it lacks an internal fabric.

3.2.5 D_4 Deformation

Overprinting both D_3 and D_m fabrics is a crenulation deformation. Its effect on the study area is variable and dependent on both the lithology and initial orientation of the pre-existing fabrics. Predominantly it is east-west oriented, but there is often a conjugate north-north-west orientation also developed.

In the semipelite gneisses and pelitic schists D_4 crenulations are frequently developed. In the gneisses they are associated with gentle warps of the S_{1-2} and L_2 fabrics, whereas in the schists they crenulate the S_{1-2} schistosity overprinting the F_3 crenulations (Figs. 3.4 and 3.7D). These D_4 crenulations are notably different from D_3 crenulations in that they do not have sharp crests nor do they have interlimbs angles less than 90 degrees. Rather, they are gently flexed in the crests and have interlimb angles more of the order of 120 degrees. There is no S_4 fabric in these rocks.

Within the coarser grained migmatized gneisses and pelites, F_4 are the only rarely observed as crenulations. However, in the southeast of the study area (the Ullabidinie subarea) they develop into broad, open, subvertically plunging folds.

Amphibolites reflect D_4 crenulations very well throughout

Figure 3.12: D_4 structures. (a) F_4 crenulations with axial planar S_4 segregations in amphibolite from the Wangaraleednie subarea. (b) F_4 kinkband in quartzite. (c) F_4 warping of S_{1-2} and axial planar S_4 dissolution planes in massive dolomite from the Ullabidinie subarea. (d) S_4 fractures and accompanying "bleaching" of mafic minerals in the Middle Camp granite near Mt. Parapet (S_2 parallels pen).

the study area, (including the Narridy Creek granite) and occasionally also display an incipient feldspathic segregation along S_4 planes (Fig. 3.12A). The crenulations kink the S_{1-2}, S_3, L_2 and L_3 fabrics. Quartzites, dolomites and other metasedimentary units only rarely display D_4 effects. Rare kink bands (Fig. 3.12B) or warps are seen in the quartzites, and the dolomites sometimes have subvertical joints and dissolution planes (cross-cutting S_{1-2}) which may be related to D_4. However, in the Ullabidinie subarea where D_4 is more intense, both the dolomitic layering and tight F_3 folds are folded by broad subvertical buckle folds. Furthermore an incipient, penetrative, fracture cleavage, S_4, has developed axial planar to these folds (Fig. 3.12C). These S_4 planes are akin to narrow dissolution planes and the S_{1-2} layering is destroyed along them.

D_4 has also been recorded in the Middle Camp granite, the Narridy Creek granite and within the mylonite zone. In the Middle Camp granite S_4 fractures are quite common and are unique in the study area. They are shown in Figure 3.12D as discrete fractures less than 2 mm wide infilled with opaque mineral(s) and bounded either side by zones up to 25 mm wide of intense "leaching" of mafics.

The S_3 mylonitic type fabric of the Narridy Creek granite has also been deformed by D_4. In this case, there are kink bands and fractures which are akin to those of the Middle Camp granite. The kink bands often form conjugate pairs and both they and the fractures sometimes have narrow pegmatitic veins along them.

D_4 crenulations and minor buckle folds of S_m in the mylonite zone are shown in Figure 3.10D.

3.2.6 Brittle Deformation

Finally in the deformation of the metamorphic and igenous rocks of the Cowell-Cleve area is a period of brittle faulting. Two specific sets of faults have been observed.

The most obvious set is a north-south trending set of major faults which serve to divide the area into large blocks. These faults are rarely seen in outcrop but are manifest as long linear valleys, and as an offset of lithology. Frequently they have water springs along them and both Yabmana and Calcookara faults are examples of this*.

Wangaraleednie fault which also belongs to this category, has a narrow brecciated zone developed along it. The breccia is a relatively massive, light to dark brown rock with angular fragments of metasediments enclosed within it. Rarely it has silvery slickenslide like planes which impart a weak fabric to it. Breccias have been recorded at some other fault localities and rare feldspathic dykes have been noted along them.

The second set of faults has characteristics much the same as those above. It is generally northeast trending and is typified by the Cowell fault (Lincoln Lineament) which defines the southeast edge of the Cleve Uplands. It has a prominent scarp along it and has apparently been active in recent times. Its coincidence with the mylonite zone infers that that zone has remained a zone of weakness since early Proterozoic time.

---

* Yabmana and Calcookara are local aboriginal names for fresh and brackish water respectively.

CHAPTER IV

MACROSCOPIC STRUCTURE

4.1 INTRODUCTION

This chapter describes:

a) the orientations of the various mesoscopic structural elements;

b) those macroscopic structures which could be reconstructed directly from field observations; and

c) the orientations of the numerous pegmatite sets.

To facilitate these descriptions and to record any spatial variation of the basic elements, each of the subareas outlined in Figure 3.1 is considered individually.

The orientation data recorded in this chapter have been obtained from multiple measurements taken at over two thousand field stations within the study area. All the measurements were taken using a standard magnetic compass fitted with a spirit levelled clinometer. The measurements have been recorded on:

a) general geological and structural maps corrected for a magnetic declination of 6 degrees clockwise from true north; and

b) computer data cards.

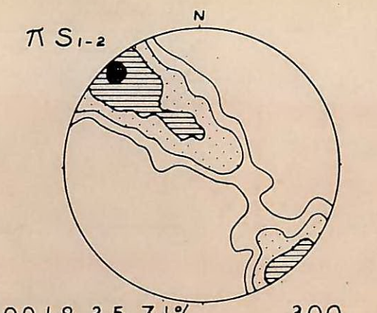
The latter have been processed by the University of Adelaide's updated CDC 6400 computer using a programme derived by Bridges and Etheridge (1974). This particular programme, "ORIENT", produces contoured stereodiagrams. It contours on the hemisphere using polar co-ordinates suitable for printing on either the line printer or graph plotter. All the stereodiagrams are equal area projections (Schmidt nets).

4.2 ORIENTATION DATA

4.2.1 Wangaraleednie Subarea

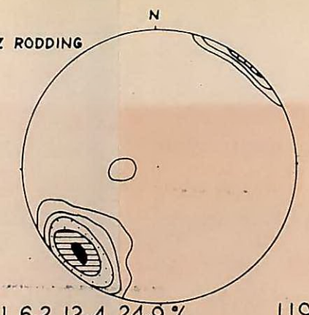
The orientation and distribution of the basic mesoscopic

FIG. 4.1



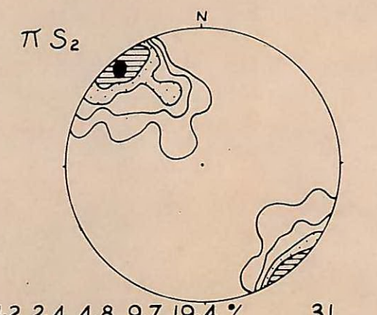
πS_{1-2}

0·9, 1·8, 3·5, 7·1% 300



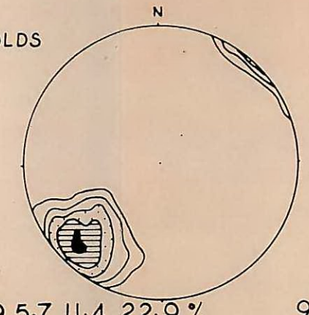
L_2 QUARTZ RODDING

1·5, 3·1, 6·2, 12·4, 24·9% 119



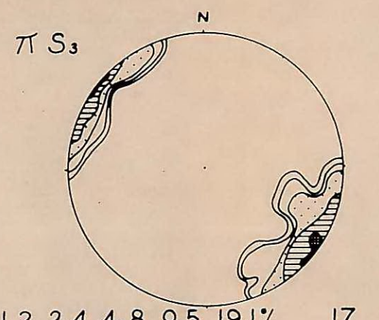
πS_2

1·2, 2·4, 4·8, 9·7, 19·4% 31



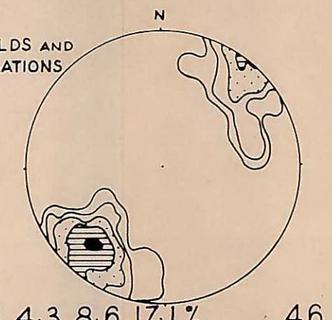
F_2 FOLDS

1·4, 2·9, 5·7, 11·4, 22·9% 93



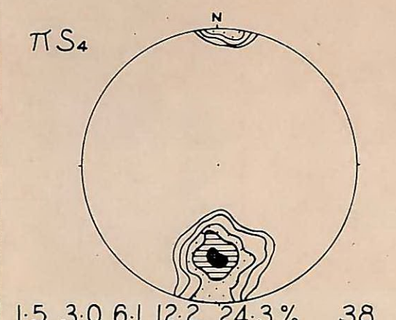
πS_3

1·2, 2·4, 4·8, 9·5, 19·1% 17



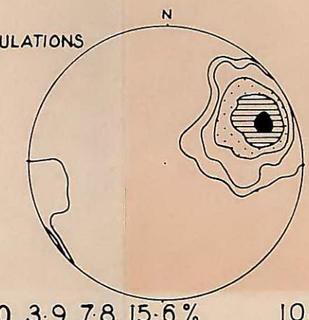
F_3 FOLDS AND CRENULATIONS

1·1, 2·1, 4·3, 8·6, 17·1% 46



πS_4

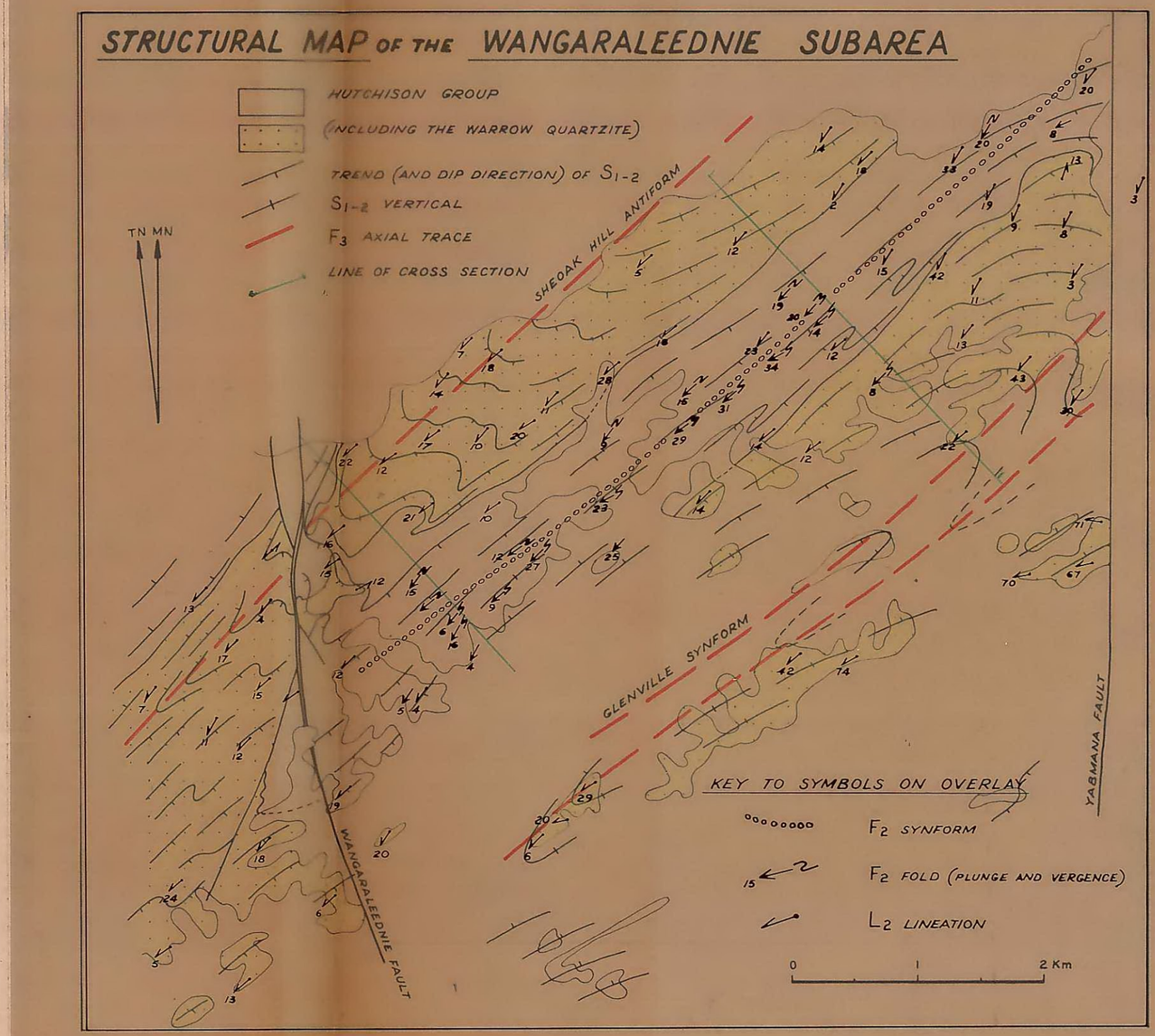
1·5, 3·0, 6·1, 12·2, 24·3% 38



F_4 CRENULATIONS

1·0, 2·0, 3·9, 7·8, 15·6% 104

STERODIAGRAMS OF MESOSCOPIC DATA IN THE WANGARALEEDNIE SUBAREA



structural elements described in the previous chapter are shown in Plan 2 and Figure 4.1. The principal characteristic of this subarea is the omnipresence of a strong, pervasive, layer-parallel schistosity S_{1-2} that is folded about two major D_3 structures, the Glenville synform, and the Sheoak Hill antiform (Fig. 4.1).

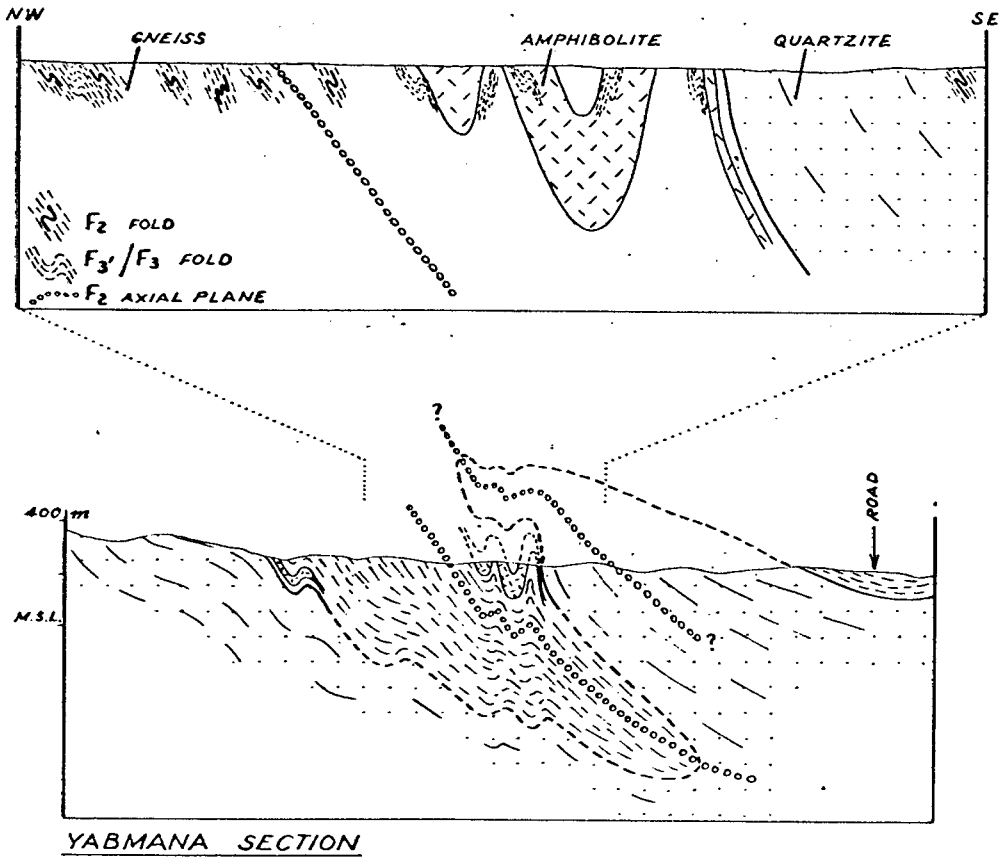
These macroscopic F_3 folds and their associated mesoscopic equivalents trend at approximately 040/220, are essentially upright and relatively open, and are locally cylindrical. They plunge shallowly ($\simeq$20 degrees) towards 200 but this varies from as much as 40 degrees towards 220 to 20 degrees towards 040. F_3 axial planes, S_3, are approximately vertical.

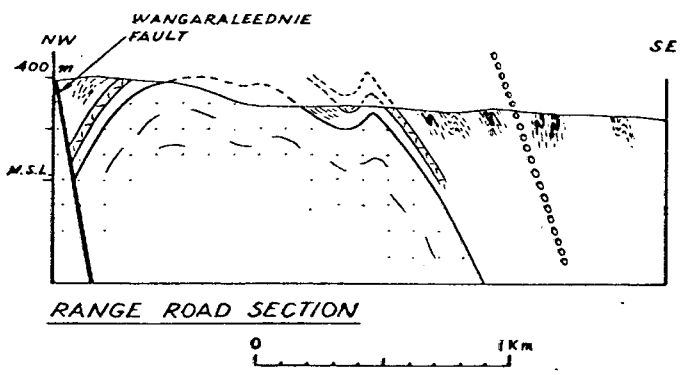
Mesoscopic F_2 folds are quite common in the semipelites but both they and the L_2 rodding, mullions and mineral lineation are subparallel to F_3. However in profile, the L_2 rodding is elliptical and the long axes of the ellipses are folded around D_3 structures.

Macroscopic D_2 structures are not clearly defined. Superficially, the symmetry about a central line through the subarea and the identical lithology of the two major quartzites (both with interbanded pelitic schists), suggests a pre-D_3 structure possibly a D_2 synform. Mesoscopic F_2 folds in semipelites of this region are mostly of dextral vergence but there are several of sinistral vergence. The latter are all located along the southeastern side of the structure (see overlay, Fig. 4.1) where they predominate over dextral F_2. Consequently they infer a D_2 synform and an interpretive profile of that synform and of an <u>inferred</u> complementary antiform are shown in Figure 4.2. The complementary antiform is inferred for two main reasons:

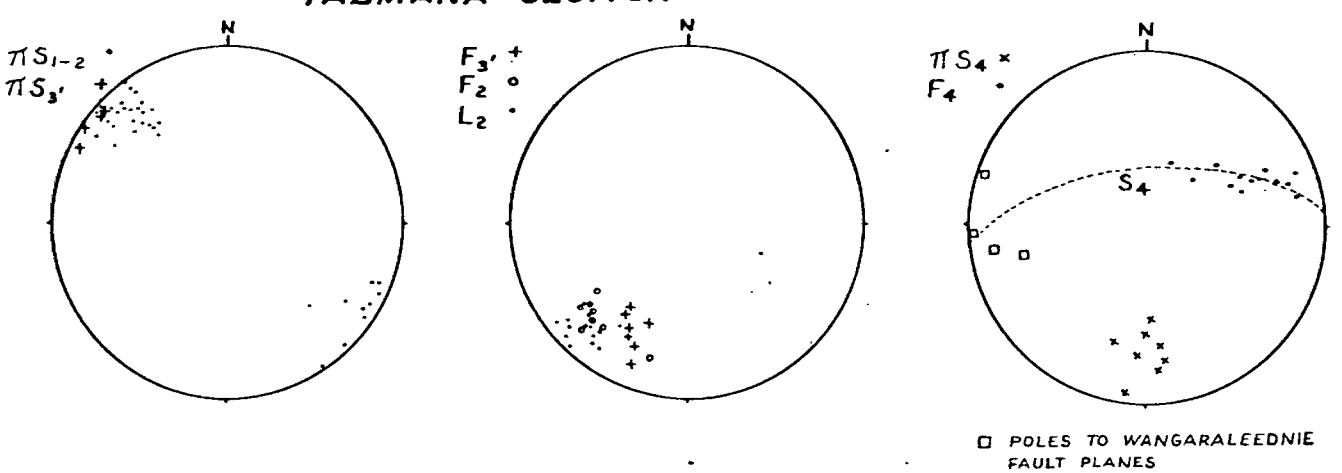
FIG. 4.2

STRUCTURAL CROSS SECTIONS OF THE WANGARALEEDNIE SUBAREA





STEREODIAGRAMS OF FABRIC ELEMENTS ALONG THE YABMANA SECTION



1) the quartzite in its core appears to "disappear" along strike to the southwest which is consistent with a southwesterly plunging antiform; and
2) dolomite and amphibolite along the road southeast of the cross section are believed to be equivalent stratigraphically to those in the main synform thus necessitating a pre-D_3 antiformal structure.

The profiles are complicated by the presence of D_3, structures in the amphibolite along the southeastern limb, but they are firmly believed to be representative of the true structure. The D_3, structures are upright, shallowly plunging folds which plunge towards 205 (see stereodiagrams of Fig. 4.2). They are believed to be related to the D_3 formation but because they are tighter than normal F_3 folds, they are separately identified. It is possible that they may represent an additional, more local deformation.

While all the anteceding structures trend approximately, south-southwest to southwest, D_4 structures are eastwest orientated. S_4 planes strike due eastwest dipping about 60 degrees north and F_4 crenulations and warps, which are of sinistral vergence throughout the subarea, are broadly distributed along S_4 (Fig. 4.1). However, considering just those F_4 and S_4 from the Yabmana section (Fig. 4.2) F_4 specifically spread along S_4; a function of the overprinting of D_4 on an already folded, cylindrical surface.

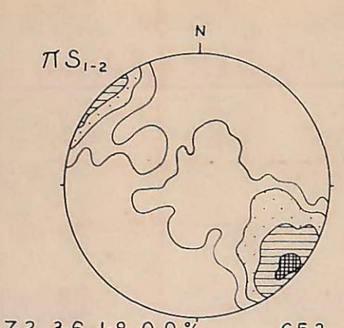
Finally, the major faulting which has conveniently delineated the subareas, is orientated northsouth, and the planar fabric observed in the Wangaraleednie breccia dips steeply (> 60 degrees) to the east (Fig. 4.2).

4.2.2 Mt. Millar/Morowie Subarea

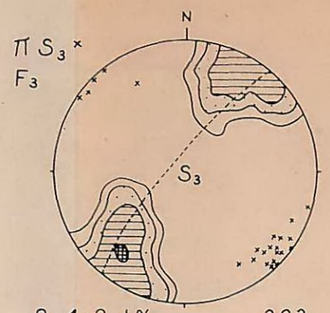
Once again the prominent feature of this subarea is the

FIG. 4.3

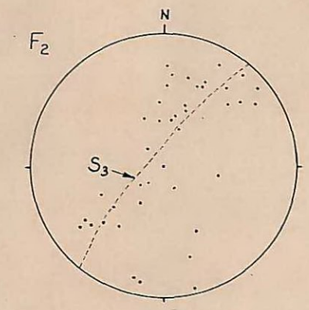
SYNOPTIC STEREODIAGRAMS OF FABRIC ELEMENTS IN THE Mt. MILLAR/MOROWIE SUBAREA



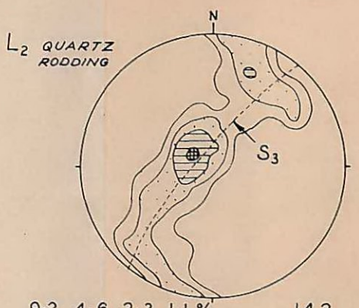
7·2, 3·6, 1·8, 0·9 % 653

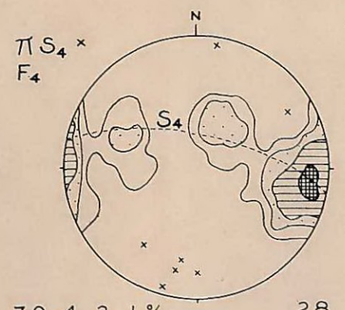


8, 4, 2, 1 % 203



9·2, 4·6, 2·3, 1·1 % 142

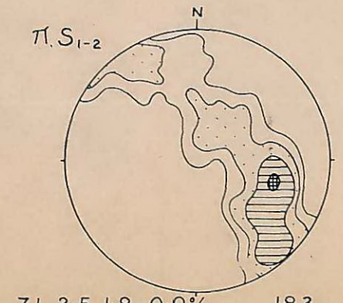




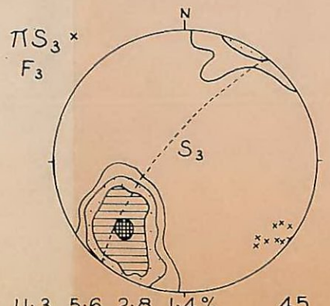
7·9, 4, 2, 1 % 28

NB
CONTOUR INTERVALS (LOWER LEFT) PER 1% AREA.
NUMBER OF POINTS CONTOURED - LOWER RIGHT OF EACH DIAGRAM.

PORTION OF THE MT. MILLAR/MOROWIE ANTIFORM WEST OF CALCOOKARA FAULT



7·1, 3·5, 1·8, 0·9 % 183



11·3, 5·6, 2·8, 1·4 % 45

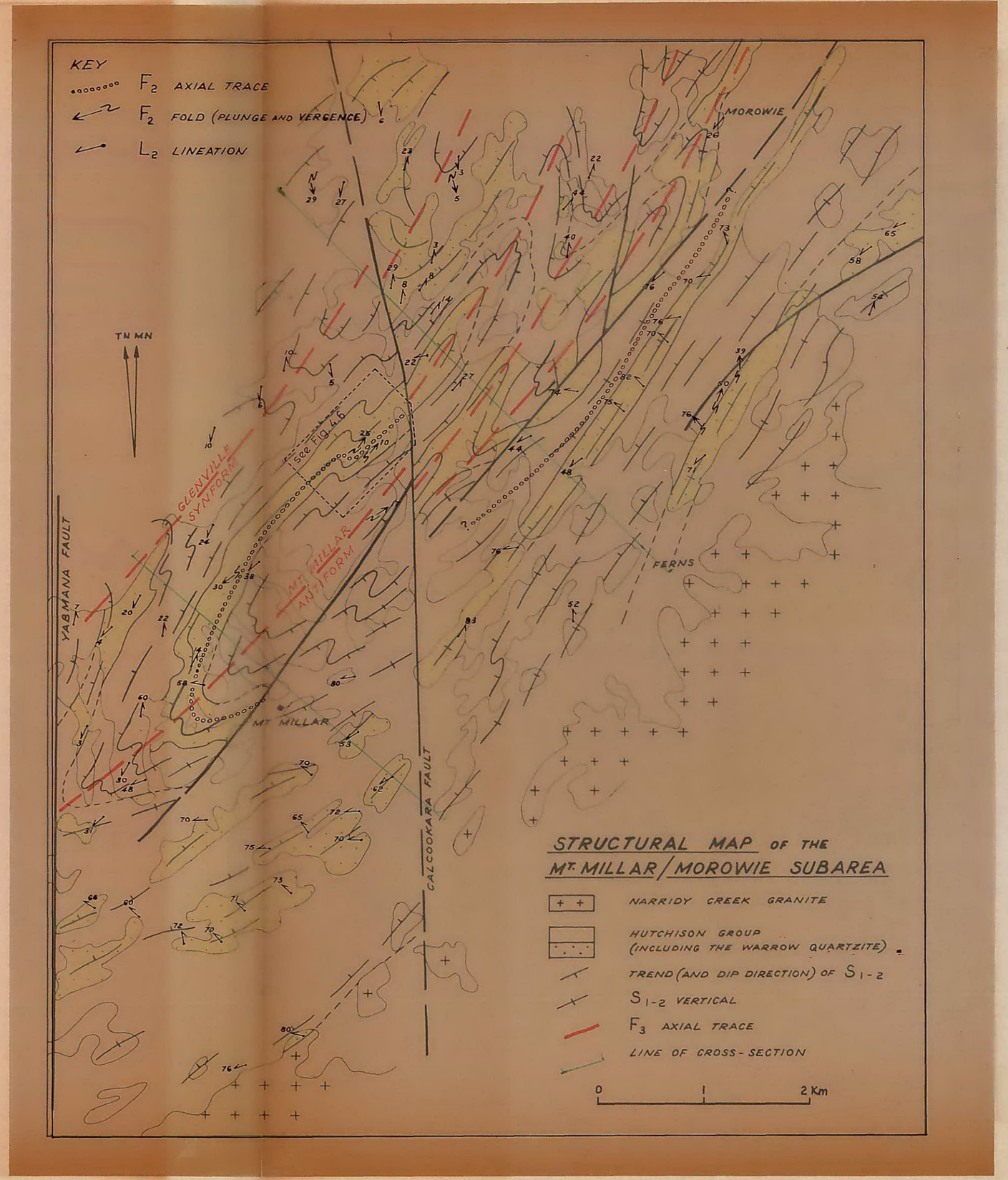
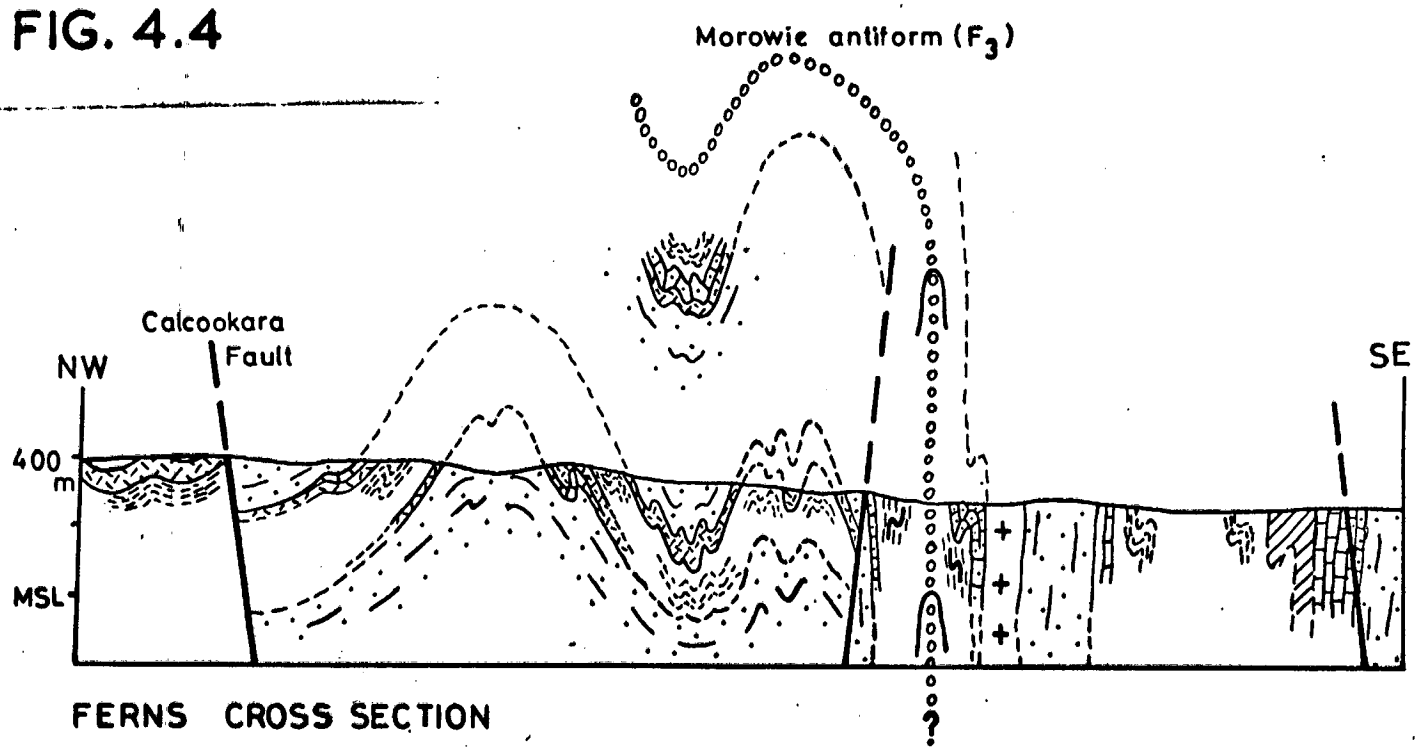
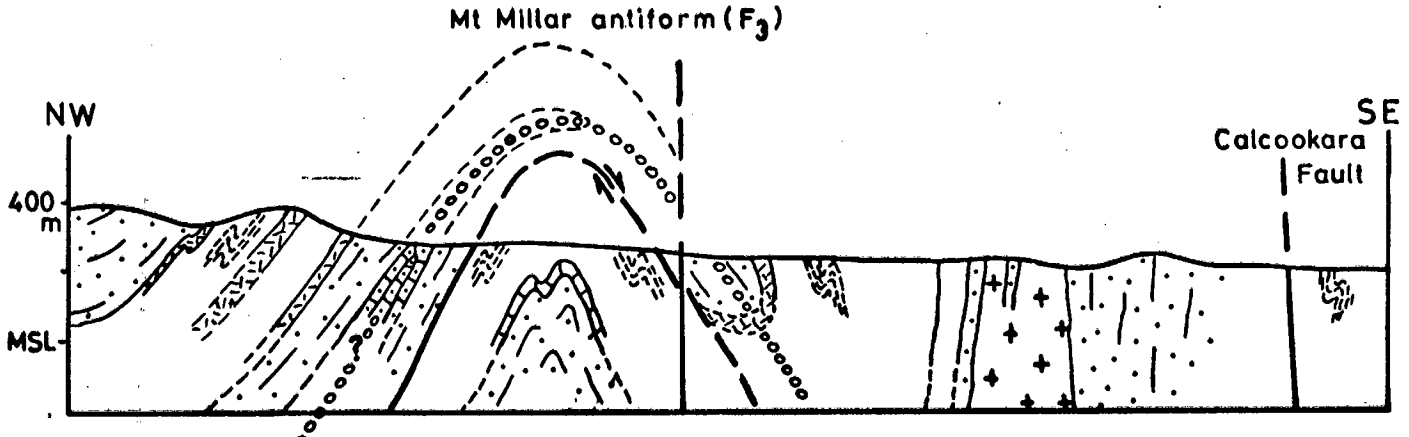


FIG. 4.4



FERNS CROSS SECTION



MT MILLAR CROSS SECTION

granite

semipelitic gneiss

amphibolite

iron formation

dolomite

quartzite

calc silicate

fault

F_2 fold

F_3 fold

inferred axial plane of macroscopic F_2 fold.

0 1 km

folding of the very strong, layer parallel schistosity, S_{1-2}, about upright, relatively open F_3 folds (Plan 2 and Fig. 4.3). There is considerable variation of plunge within the area (Fig. 4.3), but on a local scale D_3 folding is cylindrical. This is demonstrated in Figure 4.3 for the area southwest of the Calcookara subarea on the nose of the Mt. Millar antiform. Here the F_3 folds plunge about 30 degrees towards 225 and the S_3 axial planes dip 75 degrees towards the northwest (c.f. synoptic diagrams). This compares with subhorizontal F_2's in the Calcookara subarea and northeasterly plunging F_3's in some areas east of Calcookara fault (e.g. around Morowie). This variation of F_3 axes is a characteristic of the D_3 deformation.

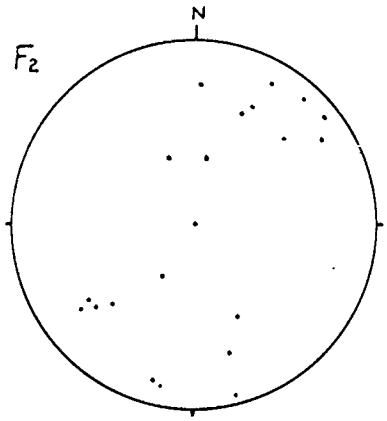
The major F_3 folds are the Mt. Millar/Morowie antiform and the northeasterly extension of the Glenville synform. There may be a synformal structure adjacent to the Narridy Creek granite and passing through Boards Mine but it could not be confirmed. Other F_3 macro-folds are outlined in Plan 2 and Figure 4.3, and interpretive profiles through Mt. Millar and Ferns are shown in Figure 4.4.

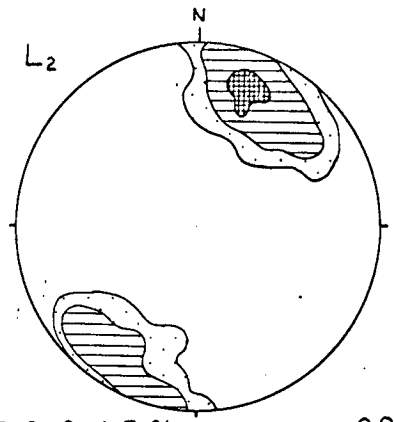
As noted in Chapter III, D_2 folds are less obvious in the migmatitic gneisses east of Yabmana fault. However, linear elements which were attributed to D_2 in the Wangaraleednie subarea are common in the quartzites and amphibolites and they relate a special history. Together with the F_2 axes, they show a unique distribution related to the Mt. Millar/Morowie antiformal axis.

In Figure 4.3 synoptic stereodiagrams of F_2 and the L_2 lineations are illustrated. They show a complex distribution pattern seemingly partly related to S_3. However, when the subarea is subdivided and the quartz rodding, mineral lineations

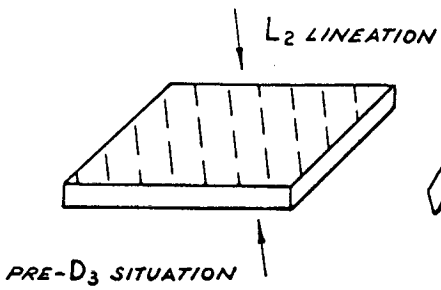
FIG. 4.5

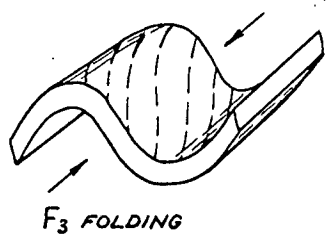
DEFORMATION OF F_2 AND L_2 LINEATIONS NORTHWEST OF Mt. MILLAR / MOROWIE ANTIFORM AXIS

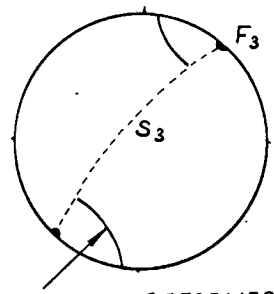




5·9, 3, 1·5 % 68

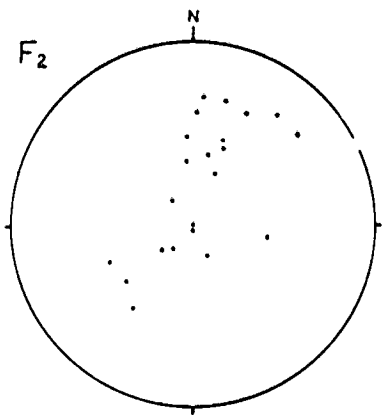


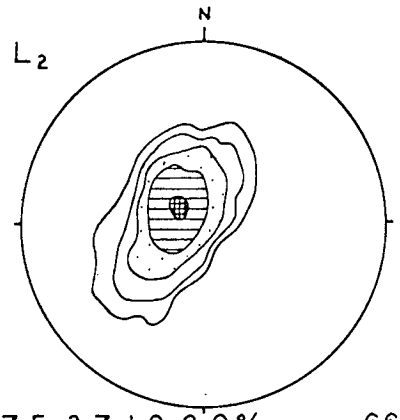




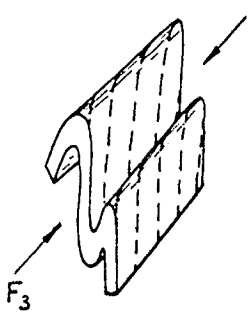
LOCUS OF DEFORMED (BY BUCKLING) L_2 LINEATION

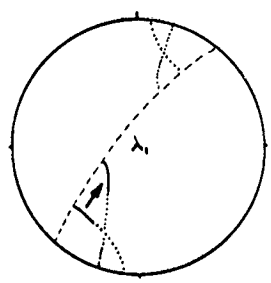
SOUTHEAST OF Mt. MILLAR / MOROWIE ANTIFORM AXIS



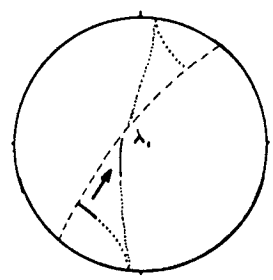


15, 7·5, 3·7, 1·9, 0·9 % 66





FLATTENED BUCKLE FOLD



BUCKLING FOLLOWED BY SIMPLE SHEAR

and F_2 folds on each side of the Mt. Millar/Morowie antiform are considered separately, a more regular distribution becomes apparent.

On the southeast limb of the antiform the lineations and F_2 axes are steeply plunging to the west and northwest (Fig. 4.5). They are spread out along the S_3 plane, and in addition, specifically lie at high angles, indeed nearly at right angles, to the F_3 fold axes. By contrast on the northwestern limb of the antiform, they are mainly at a low angle to the F_3 axes (Fig. 4.5), and define a small circle about the mean position of F_3. As such they are consistent with a model that folds a northsouth trending L_2 lineation about upright, sub-horizontal, northeast-southwest trending F_3 folds. Examples of F_3 mesofolds deforming an earlier lineation of this type and orientation have been recorded from this subarea (Fig. 3.8B) but the relevance and meaning of the macroscopic distribution on the southeast limb are not clear.

The situation that exists on the southeast limb is also represented in Figure 4.5 with clear refolded L_2 lineations in the hinges but with vertically plunging lineations on the limbs. Accepting that the lineations are L_2 and not L_3 (N.B. elsewhere, as in the deformed Narridy Creek granite, L_3 lineations are near horizontal and parallel to F_3), then a model must be constructed which will develop such a distribution. Folding in this region must have developed initially by buckling or flexural slip to give a simple small circle distribution of L_2 as outlined for the northwest limb (Ramsay, 1967). If, after the folds had been initiated, a second process was superimposed on one particular limb, then the resultant L_2 distribution would reflect the combined strain

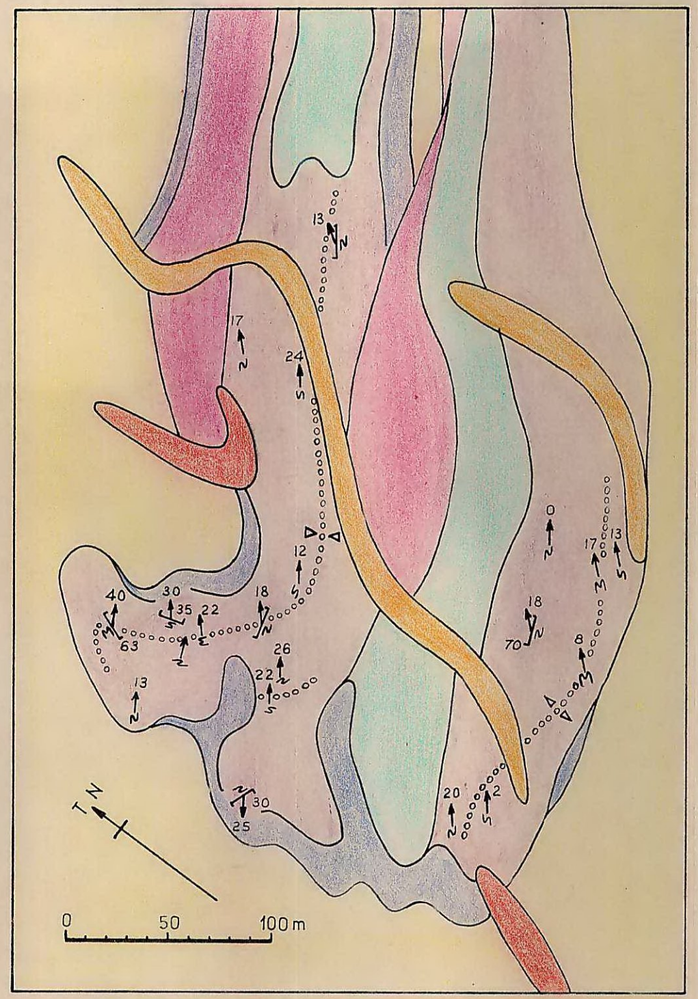
of the two processes. Two processes that are considered here are simple homogeneous flattening and simple shear. Ramsay (op. cit.) discusses these and various other deformation paths, and the type of lineation redistributions that are predicted are sketched in Figure 4.5. Clearly both processes may rotate the L_2 lineation into an orientation that is partially consistent with the observed.

A clue to which process is favoured is given by the microstructure of the quartzites in the region. This is discussed in more detail in the ensuing chapter on microstructure (Chapt. VI) but two very important facts are relevant here. Firstly, the textures of the quartzites on the southeast limb are clearly different from those in the northwest limb implying that the former has suffered a more intense strain. Secondly, the crystallographic fabrics suggest that in those areas where the textures have been significantly modified, there is definitely a component of flattening strain. Hence it is concluded that the rotation of the L_2 rodding represents a superimposed strain over and above the initial buckling, and that that strain represents a more intense flattening maybe with local constriction that has enhanced the linear fabric.

The general paucity of F_2 folds in this subarea has impeded detailed delineation of macroscopic D_2 structures. However in the Calcookara subarea it was possible to outline some important F_2 hinges in well layered calc-silicates being overprinted by D_3 and D_3' structures. The D_3' folds are only of local development and form a north-northeasterly plunging, upright fold pair of dextral vergence (Fig. 4.6)

FIG. 4.6

MAJOR F_2 FOLDS WITHIN CALC-SILICATE ROCKS OF THE CALCOOKARA SUBAREA.



KEY TO SYMBOLS ON MAP ABOVE:

- S_2
- F_2 FOLD (PLUNGE AND VERGENCE)
- MACROSCOPIC F_2 AXIAL TRACE

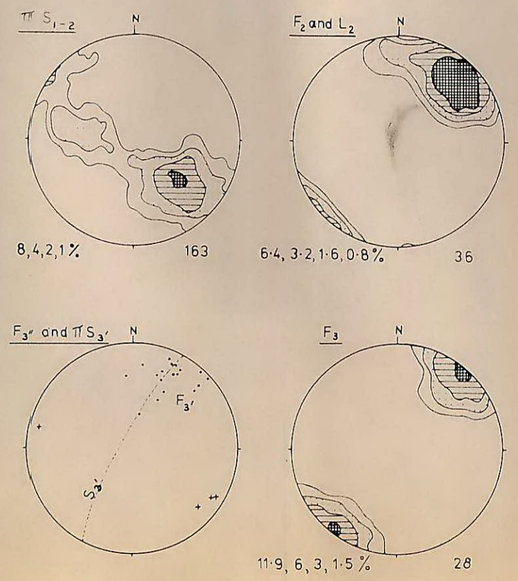
STRUCTURAL GEOLOGY OF THE CALCOOKARA SUBAREA

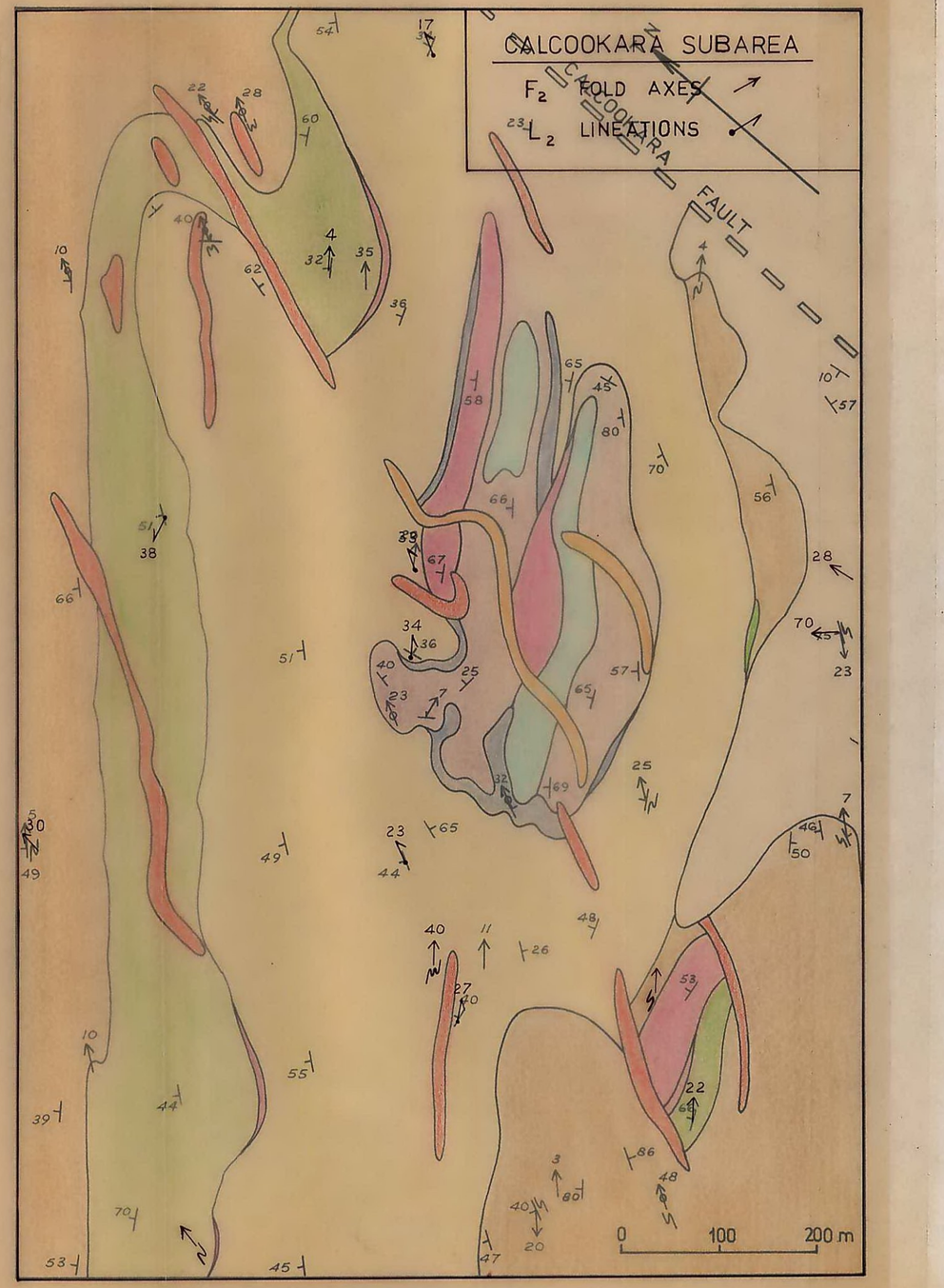
LEGEND:

- PEGMATITE
- FINE GRAINED APLITE
- MIGMATITE GNEISS
- AMPHIBOLITE
- DOLOMITE – MASSIVE
- QUARTZITE
- PODDED SILLIMANITE GNEISS
- CALCSILICATE – LAYERED
- DIOPSIDE – TREMOLITE ROCK

KEY TO SYMBOLS ON MAP TO RIGHT:

- S_{1-2}
- F_3 FOLD (PLUNGE AND VERGENCE)
- $F_{3'}$ FOLD
- MACROSCOPIC $F_{3'}$ AXIAL TRACE





which is responsible for the main redistribution of S_{1-2}. They are tighter than typical D_3 folds in the area but are believed to be related (cf Yabmana cross-section).

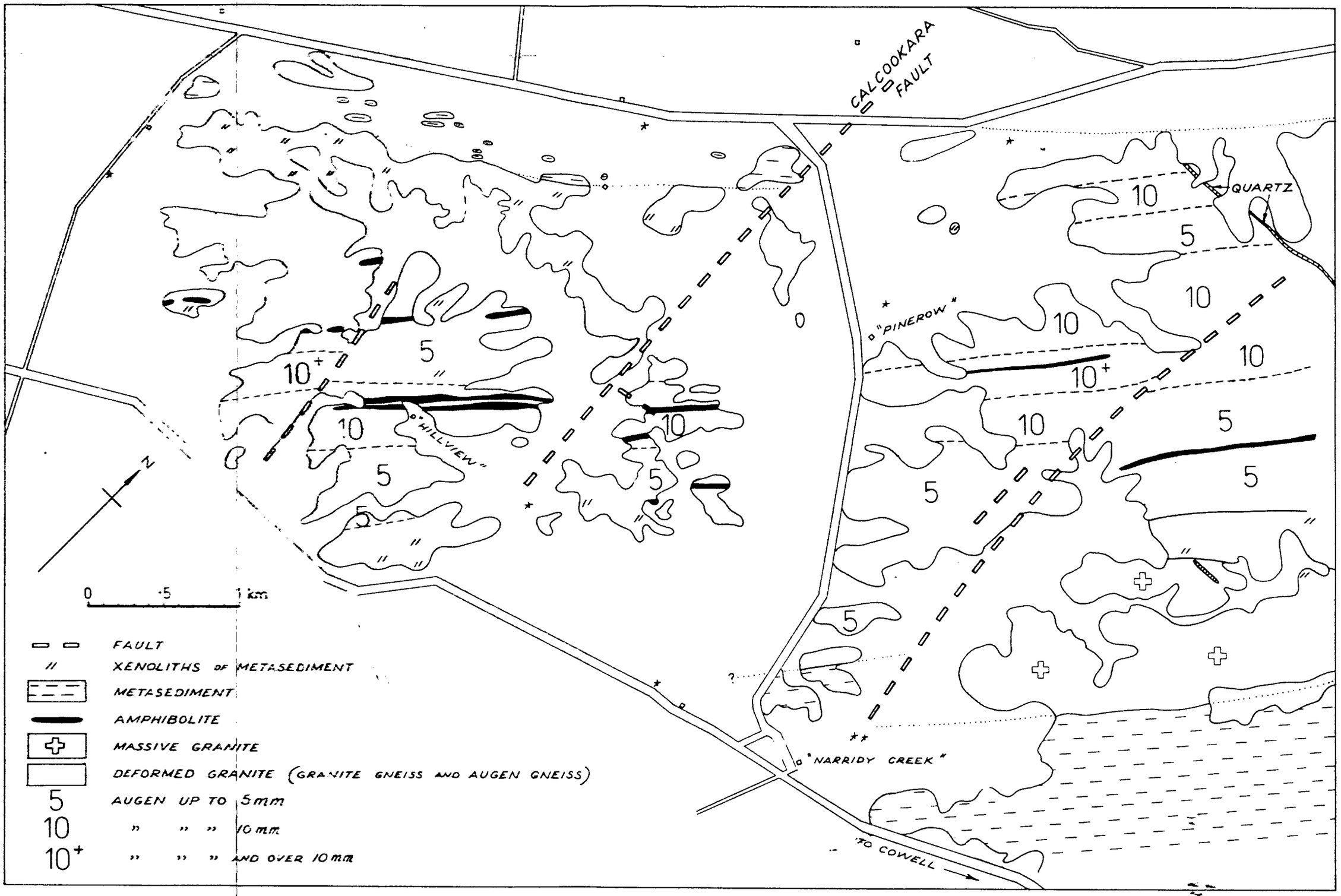
F_2 folds show a small spread in orientation but plunge approximately to the north and northeast. They define discreet macroscopic fold hinges which are folded by D_3 structures and their axial planes swing from steeply dipping northwest through horizontal to shallowly dipping towards the northeast (Fig. 4.6). The overall D_2 structure of this area is antiformal and can be traced outside of the Calcookara subarea around the nose of the Mt. Millar antiform. The discontinuity of dolomite and amphibolite units along its southeastern side, however, suggests that there may be a component of shearing or transposition along that particular limb. This is illustrated in the Mt. Millar cross-section (Fig. 4.4) as a (?) thrust which has been folded by the Mt. Millar antiform. The inferred direction of movement is shown in that sketch diagram.

Other macroscopitc D_2 structures in the Mt. Millar/Morowie area can only be inferred from the symmetry and apparent stratigraphy (see Chapt. V) of lithological units about certain hinge lines. One such major D_2 structure which can be inferred with reasonable confidence occurs east of Atkinsons Mine (see overlay Fig. 4.3; Fig. 4.4). Despite detailed mapping in that region it could not be positively confirmed although typical mesoscopic F_2 folds support the interpretation.

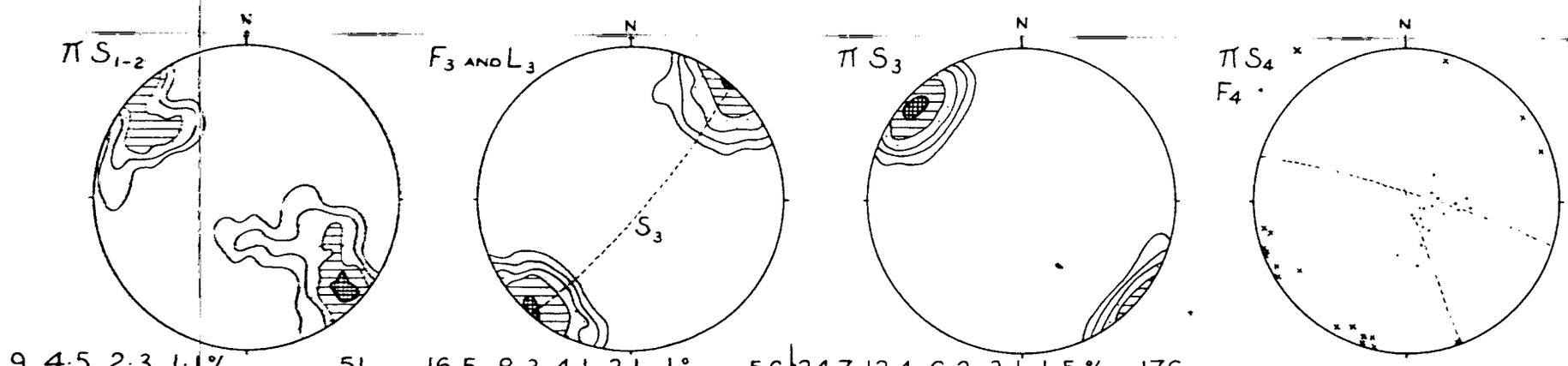
4.2.3 Narridy Creek Subarea

Orientations of the various fabric elements in the deformed zone of the Narridy Creek granite are outlined in Plan 2 and the stereodiagrams of Figure 4.7. They outline:

FIG. 4.8



FABRIC ELEMENTS IN THE NARRIDY CREEK SUBAREA



a) a very strong, pervasive, mylonitic type S_3 schistosity in the granite gneisses striking 040/220 and dipping 82^o southeast;

b) a subhorizontal L_3 lineation within S_3;

c) a general northwest dip of S_{1-2} in the metasedimentary inclusions; and

d) predominantly dextral (looking southwest) vergence F_3 folds and crenulations (in the metasedimentary inclusions) parallel to L_3 (in the granite gneiss).

As previously noted there is a systematic variation in the character of the granite gneiss and its S_3 schistosity. West of the proposed southerly extension of the Calcookara fault (note, no positive evidence for the fault was observed on the field), metasedimentary blocks or inclusions are common for a kilometre or so inside the northwest granite gneiss boundary. They are concentrated in this zone and are associated with numerous pegmatites (dykes, veins and irregular patches) and with granite gneiss. The orientations of S_{1-2} in these metasedimentary inclusions are related to the D_3 deformation (Fig. 4.7) with F_3 axial planes being parallel to S_3 in the granite gneiss. This suggests that the inclusions have not been rotated significantly from their original orientations. Had they been rotated by an intruding magma a more random S_{1-2} orientation would be expected. The actual boundary of the granite gneiss with the metasediments is conformable but sharp, although there are numerous conformable veins of granite gneiss and pegmatite intercalated with the metasediments. It appears to be a relatively passive boundary without any noticeable contact effects. Fine to medium grained granite gneiss dominates in this area but within it there are scattered, concordant (with S_3) amphibolites and local developments of coarse augen gneiss, some with a very

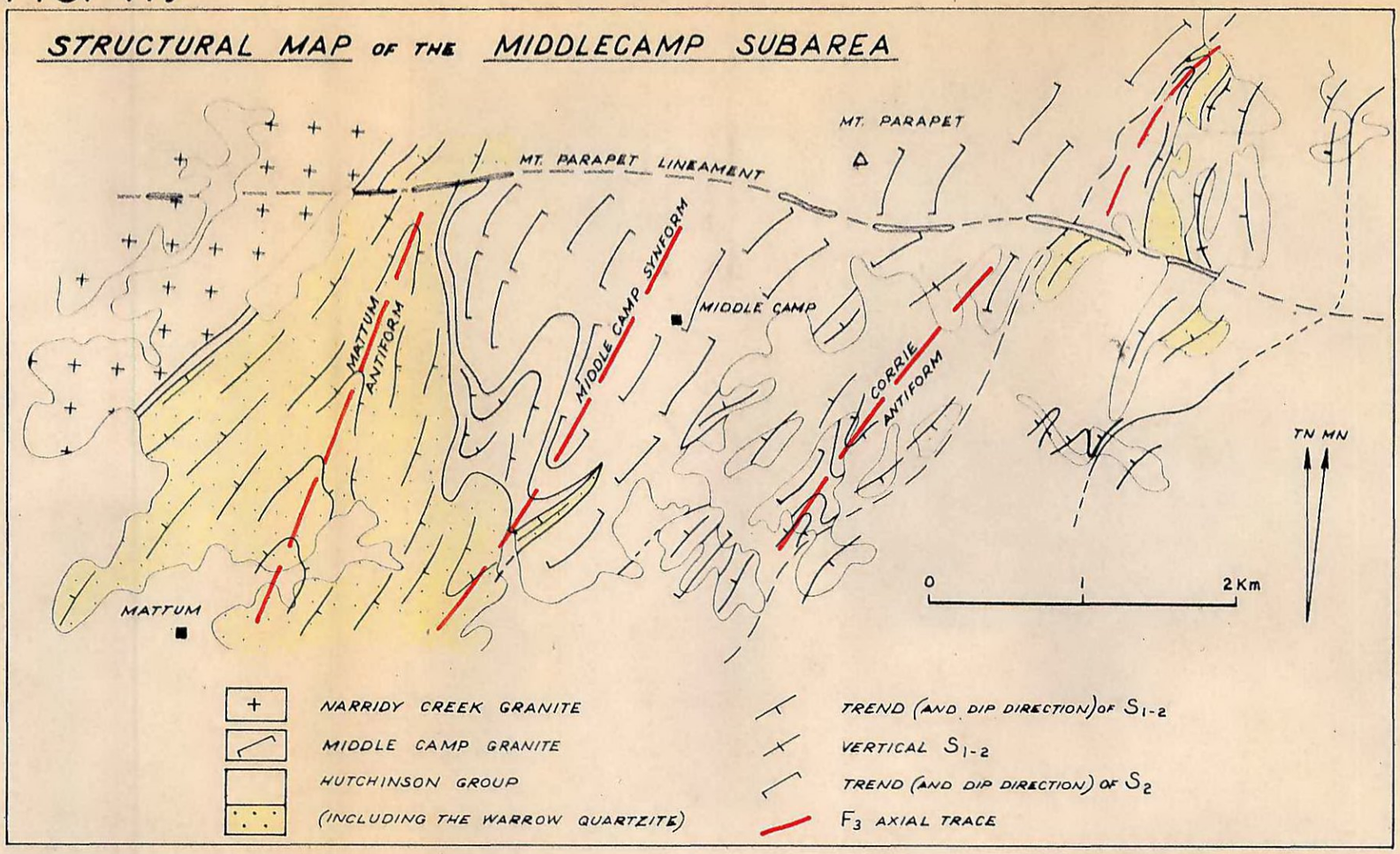
strong linear fabric. Their occurrences are shown in Fig. 4.8 with the best exposures being a coarse (augen > 10 mm) variant and a strongly rodded variant 1.2 km and 0.3 km respectively west-southwest of Hill View.

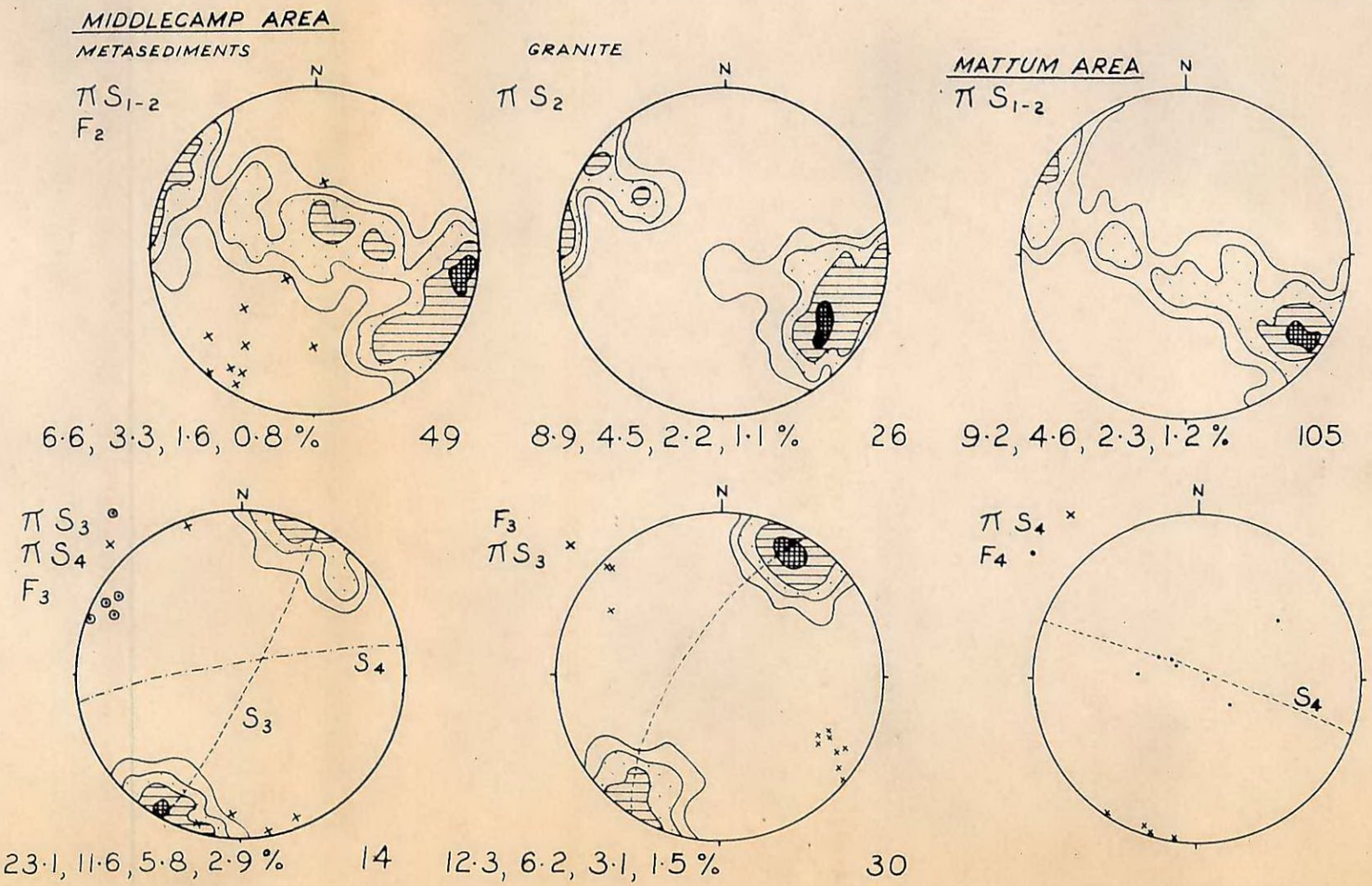
East of the Calcookara fault extension, the augen development is more pronounced. There are fewer metasediment inclusions and the first prominent augen occur less than 0.2 km from the northwest boundary (Fig. 4.8). Various subzones of augen development can be delineated on the basis of the size of the augen, and there is a gradual decrease in size southeast from the centre of the deformed zone towards the massive granite. Boundaries of these subzones are only approximate because the decrease in size is subtle and gradational. Furthermore there is local variation within the subzones delineated as such, and in particular there are scattered, fine grained bands within the coarser subzones. These finer grained bands can be traced for hundreds of metres along strike yet are only one or two metres wide.

The boundary of the deformed zone with the massive Narridy Creek granite is poorly exposed. There is a considerable amount of pegmatite there which accompanies the sub-outcrop and outcrop of granite gneiss and metasedimentary gneiss. Likewise, the boundary of the massive granite with the metasediments is also poorly exposed although it is fairly sharp and conformable with some scattered granitic bands and pegmatites locally intruding the metasedimentary sequence.

The D_4 deformation is represented in the Narridy Creek subarea by kinking of the S_3 foliation within the deformed zone. There are two sets of kink bands, occasionally developed together as conjugate pairs, and these are a dextral set with the kink boundaries (S_4) striking of the order 160/340,

FIG. 4.9


STRUCTURAL MAP OF THE MIDDLECAMP SUBAREA
MT. PARAPET
MT. PARAPET LINEAMENT
MATTUM ANTIFORM
MIDDLE CAMP SYNFORM
MIDDLE CAMP
CORRIE ANTIFORM
TN MN
0
1
2Km
MATTUM
NARRIDY CREEK GRANITE
MIDDLE CAMP GRANITE
HUTCHINSON GROUP
(INCLUDING THE WARROW QUARTZITE)
TREND (AND DIP DIRECTION) OF S1-2
VERTICAL S1-2
TREND (AND DIP DIRECTION) OF S2
F3 AXIAL TRACE


MIDDLECAMP AREA
METASEDIMENTS
π S1-2
F2
N
6·6, 3·3, 1·6, 0·8 %
49
GRANITE
π S2
N
8·9, 4·5, 2·2, 1·1 %
26
MATTUM AREA
π S1-2
N
9·2, 4·6, 2·3, 1·2 %
105
π S3
π S4
F3
N
S4
S3
23·1, 11·6, 5·8, 2·9 %
14
F3
π S3
N
12·3, 6·2, 3·1, 1·5 %
30
π S4
F4
N
S4

and a less frequent, sinistral set striking at about 105/285 (Fig. 4.7). Both sets are subvertical and the kink lineation as defined by the intersection of S_4 and S_3 is also subvertical.

4.2.4 Middle Camp Subarea

The deformational history of the Middle Camp subarea is similar to that in the metasediments northwest of the Narridy Creek granite. The strong, pervasive, S_{1-2} and S_2 schistosities are folded about relatively open F_3 folds which are essentially upright and shallowly plunging.

Specifically, the quartzitic metasediments in the west of the subarea (i.e. the Mattum antiform: see Plan 2), are folded about subhorizontal F_3 axes plunging 10-20 degrees towards 030/210 (Fig. 4.9). S_3 and F_3 axial planes vary in strike from 030 to 040 and in dip from 60-70° northwest to subvertical. The northwest dipping S_3's are mainly along the northwestern side of the subarea with S_3 steepening southeast towards Middle Camp. Those metasediments at or southeast of Middle Camp are folded about essentially upright F_3 folds with subhorizontal axes (Fig. 4.9) and S_2 in the Middle Camp granite itself is likewise folded about these F_3 axes. The main F_3 folds are the Mattum antiform, the Middle Camp synform, and the Corrie antiform.

Mesoscopic D_2 folds are common in the quartzites and gneisses of the Mattum antiform area. They are essentially isoclinal folds and their prevalence has enabled the reconstruction of a major D_2 structure refolded by the Mattum antiform. Good exposure in several creek sections facilitated the construction of three cross-sections across these D_2 and D_3 structures, and they are shown in Figure 4.10. The F_2 axial plane, S_2, because it has been folded by F_3, defines

a cylindrical surface plunging northeasterly with, on the northwest limb of the Mattum antiform, the D_2 macrostructure being a tight synform plunging shallowly to the southwest.

Most F_2 folds have a quartz rodding lineation parallel to their axes, but occasionally they are at a slight angle. Furthermore, in some F_3 folds there are two lineations; one being folded by F_3, and the other parallel to F_3. Therefore, the quartz rodding in the Mattum subarea cannot be explicitly related to a single deformation or fabric except in those particular cases where either overprinting or association with F_2 or F_3 can be demonstrated.

D_4 in the Middle Camp subarea is not strongly developed. A few open, subvertically plunging warps mainly of sinistral vergence, were recorded in the Mattum subarea, and in the Middle Camp granite several instances of an eastwest fracturing associated with the Mt. Parapet lineament were noted (see Chapter III). These are recorded in Figure 4.9.

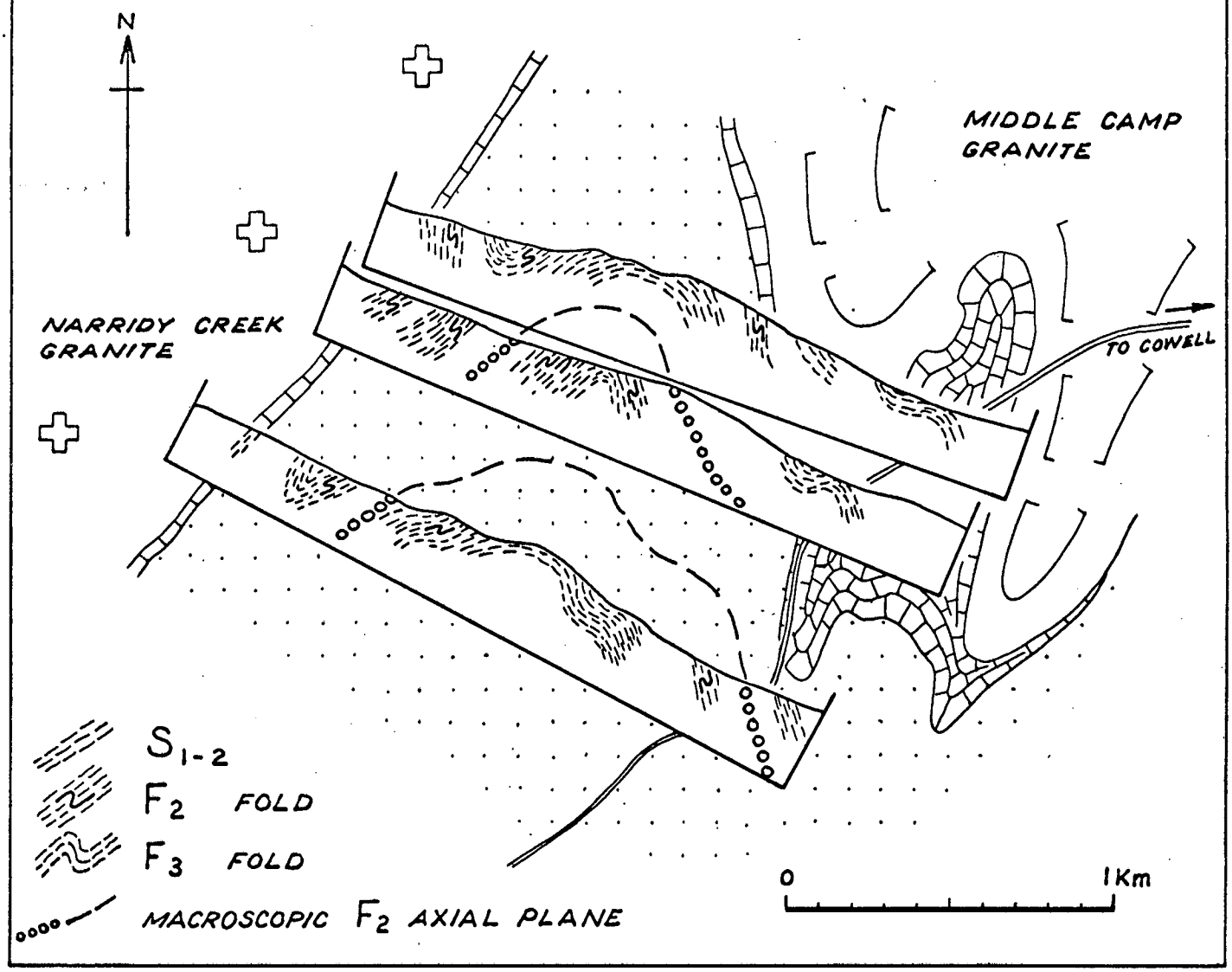
4.2.5 Ullabidinie Subarea

The principal feature of this subarea is the occurrence of the mylonites along its southeastern side. The mylonite zone is of limited exposure being restricted to Mindrow Creek, Ullabidinie Creek and a few isolated outcrops in between. It has however been traced further north outside of the study area, and it defines a prominent zone along the southeastern edge of the Cleve Uplands. It is coincident with a major aeromagnetic feature.

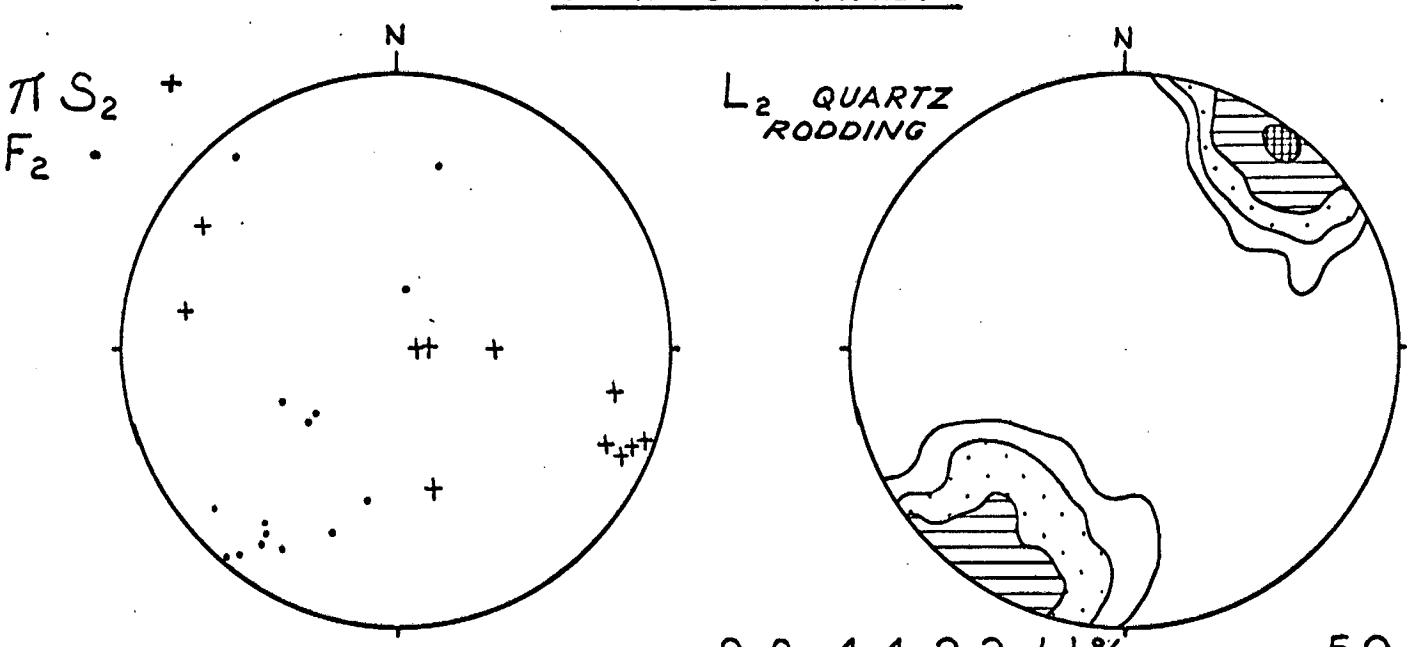
The metasediments adjacent to the mylonite zone in this subarea are very tightly to isoclinally folded. The folds are F_3 in nature and they become noticeably tighter and more isoclinal approaching the mylonite.

FIG. 4.10

STRUCTURAL CROSS SECTIONS OF THE MATTUM AREA



STEREODIAGRAMS OF πS_2, F_2 AND L_2 IN THE MATTUM AREA



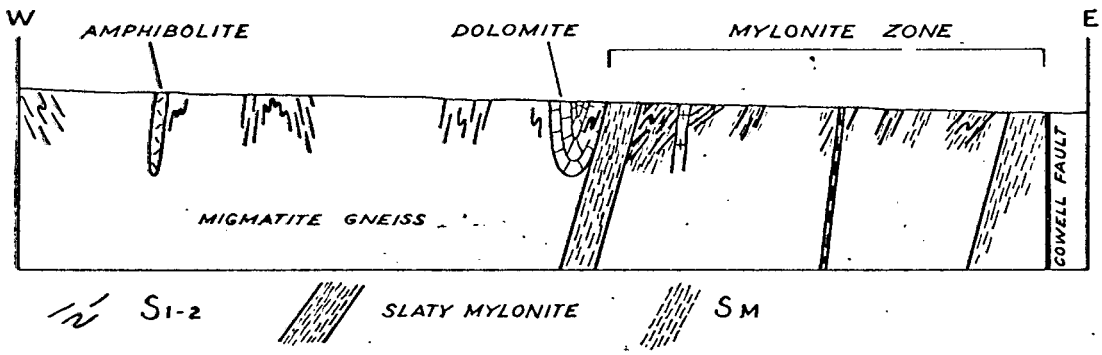
North of the Mt. Parapet lineament, which is a west-northwest to west trending fault or shear zone with accompanying pegmatite and quartz dykes, the apparent continuation of the Corrie antiform is nearly isoclinal in form (see Plan 2). Furthermore D_4 is much stronger than elsewhere in the study area, and consequently the stereodiagrams of S_{1-2} and F_{2-3} (Fig. 4.11) reflect folding about a subvertical F_4 axis rather than the normal distribution of S_{1-2} about northeasterly, subhorizontal F_3 axes. F_{2-3} (F_{2-3} here because F_2 and F_3 cannot be easily distinguished in the field) fold axes are widely dispersed, defining a 50 or 60 degree small circle about the F_4 maximum.

It was noted in the previous chapter that the mylonite zone itself consists mainly of mylonitic gneisses with occasional bands of slaty mylonite. The disposition of the slaty bands within the mylonitic gneisses and their relationship with the adjacent metasediments in Mindrow Creek is shown in the cross-section of Figure 4.11. A distinctive feature of the Mindrow Creek section is that the zone forms the eastern dextral limb of a north-northeasterly plunging D_3 synform and that relic F_3 folds within the zone itself are also of dextral vergence. Furthermore, the slaty mylonite bands are overall slightly steeper dipping than S_M in the mylonitic gneisses away from those bands, even though immediately adjacent to such no perceptible difference can be detected. Allied with the increase in flattening of F_3 folds within the metasediments, and with the corresponding increase in the S_3 development, it appears that the mylonitic deformation and D_3 are intimately related.

The orientations of the D_M fabrics within Mindrow and Ullabidinie Creeks are shown in Figure 4.11. They reflect

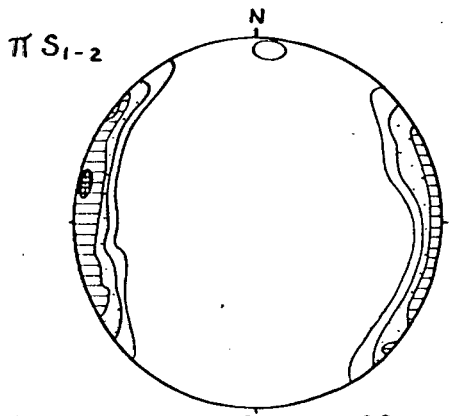
FIG. 4.11

GEOLOGICAL CROSS SECTION THROUGH MINDROW CREEK

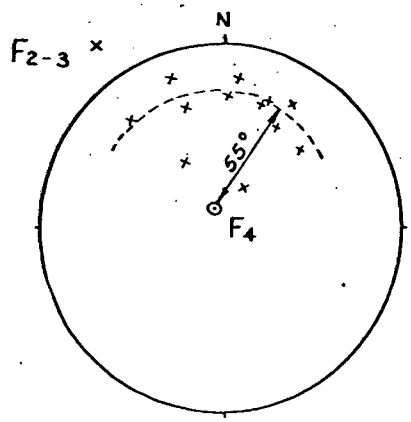


S_{1-2} SLATY MYLONITE S_M

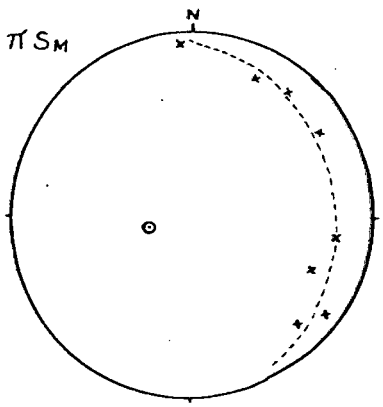
ULLABIDINIE SUBAREA

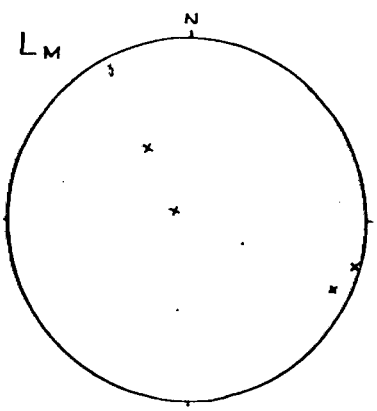


14·2, 7·1, 3·6, 1·8 % 39

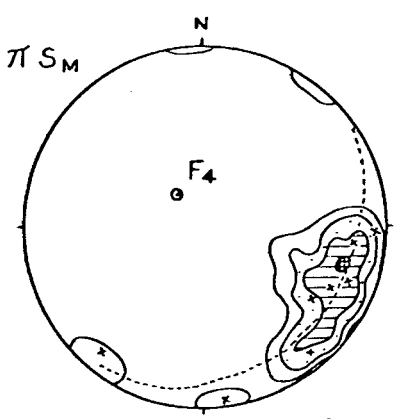


ULLABIDINIE CREEK

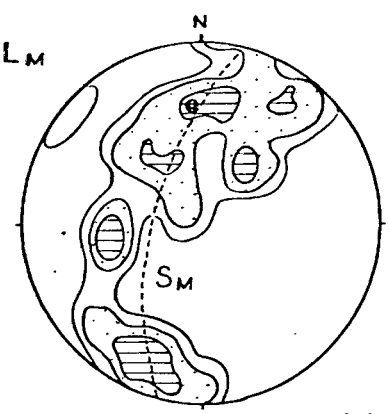




MINDROW CREEK

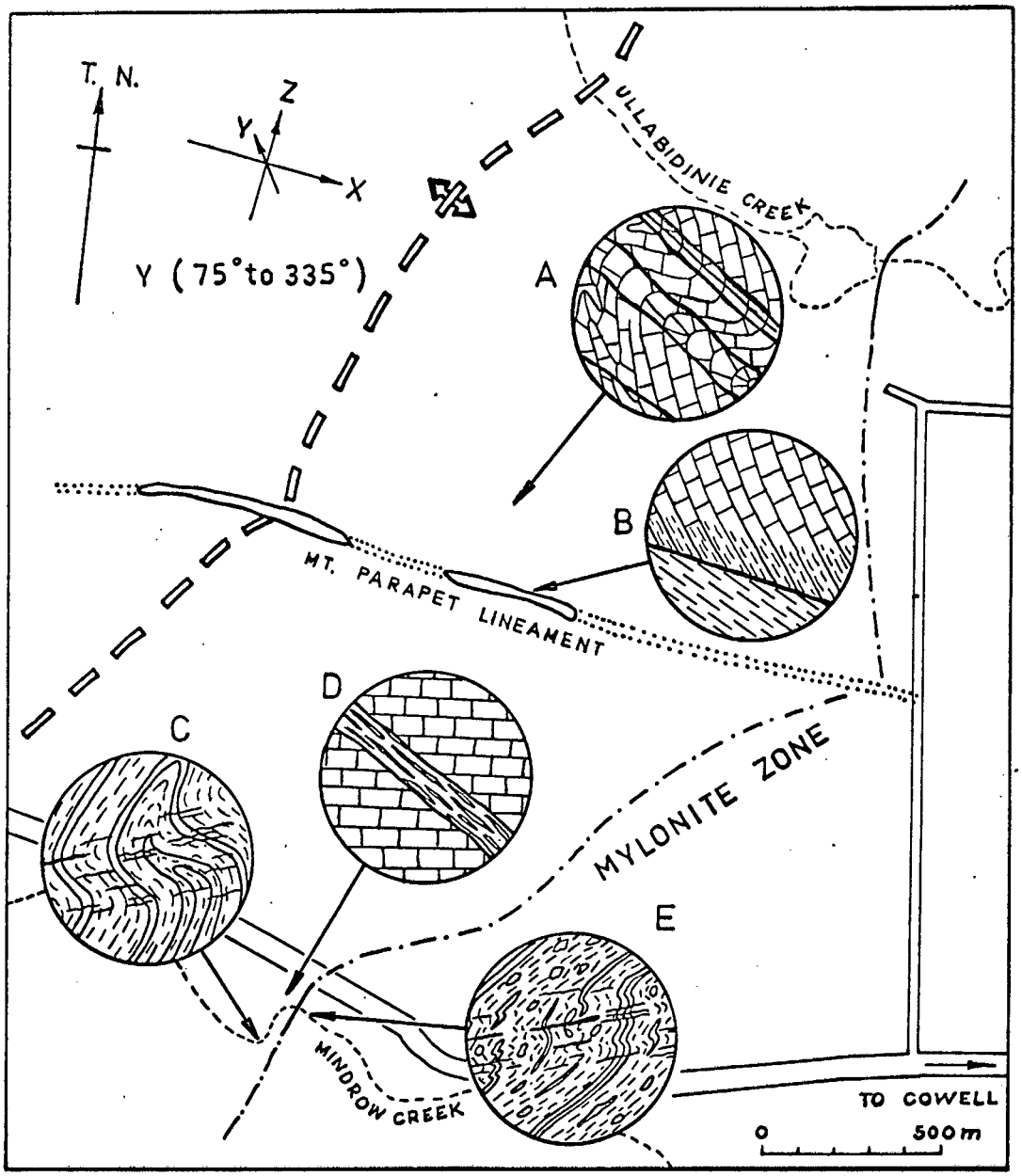


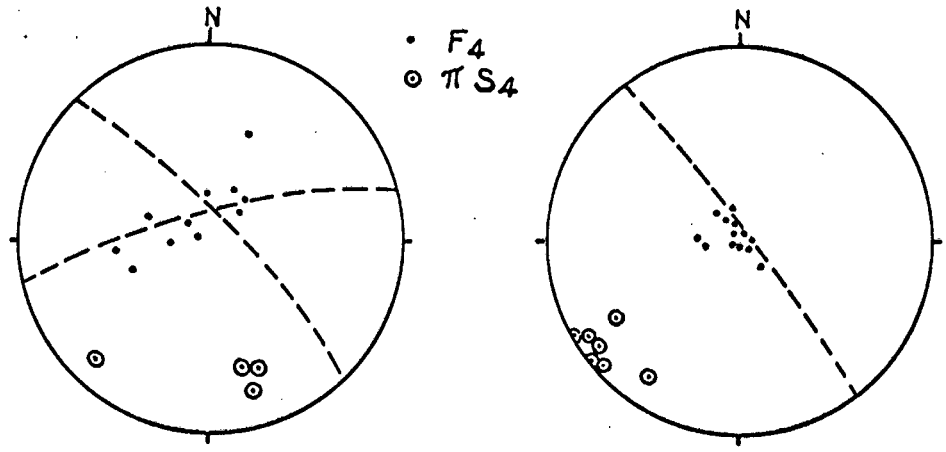
14·4, 7·2, 3·6, 1·8 % 32



7·7, 3·8, 1·9, 1 % 24

FIG. 4.12





MINDROW CREEK

ULLABIDINIE AREA

an originally steep, northwesterly dipping S_M which, like the metasediments, has been folded about subvertical F_4 axes. The mylonitic lineation is also affected by D_4, but an initially random orientation within the S_M plane is inferred by its great circle distribution.

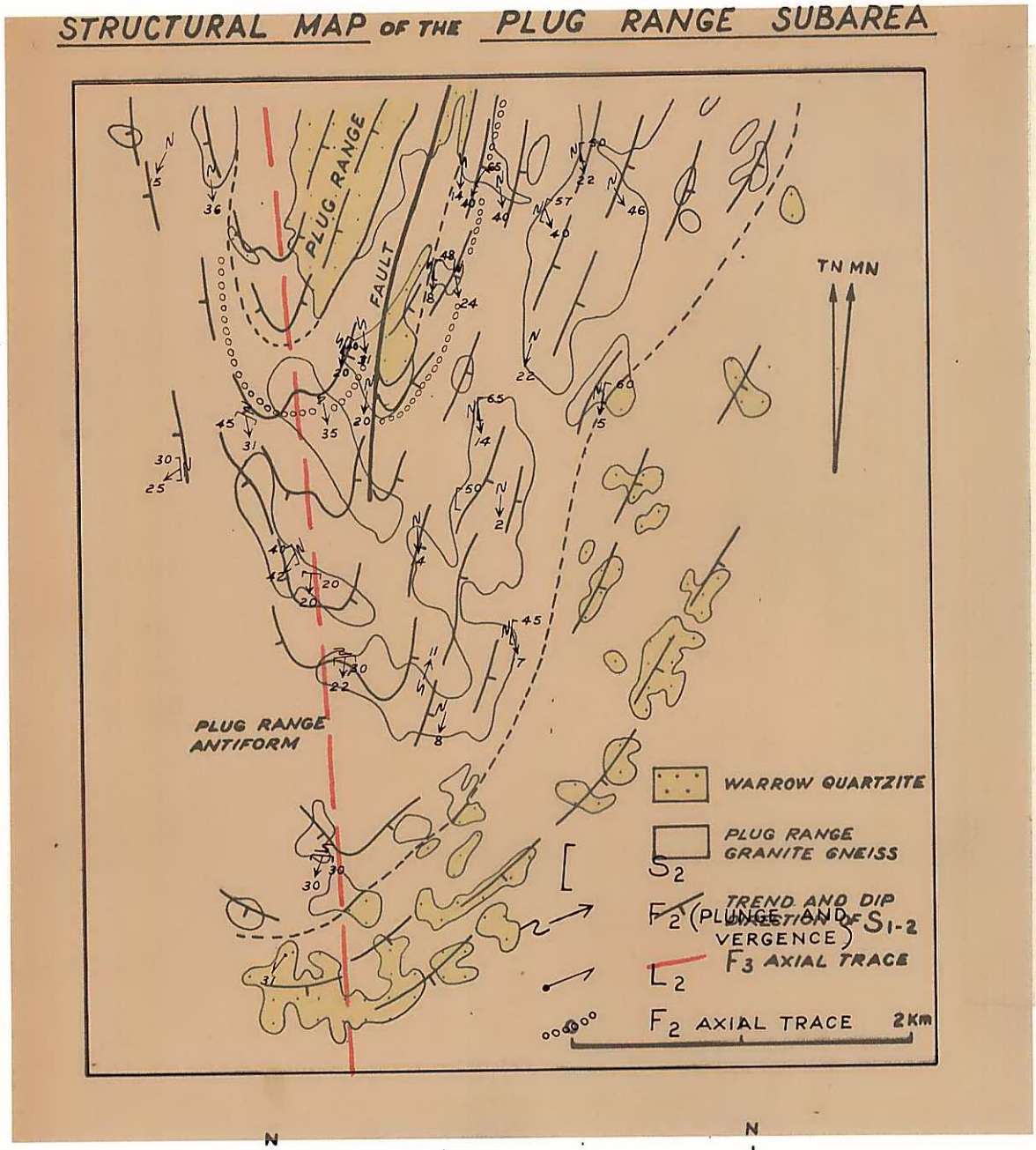
The principal characteristics of the D_4 deformation are outlined in Figure 4.12. North of the Mt. Parapet lineament, D_4 is represented by dextral folds which fold F_{2-3} and which have an incipient, subvertical S_4 fracture cleavage striking northwest. Immediately adjacent to the Mt. Parapet lineament the dolomite swings around to a northwest orientation and changes along strike into an amphibole schist. The schist has a vertical mineral lineation in it, and the schistosity merges into the fracture cleavage of the quartz pegmatite dyke delineating the Mt. Parapet lineament.

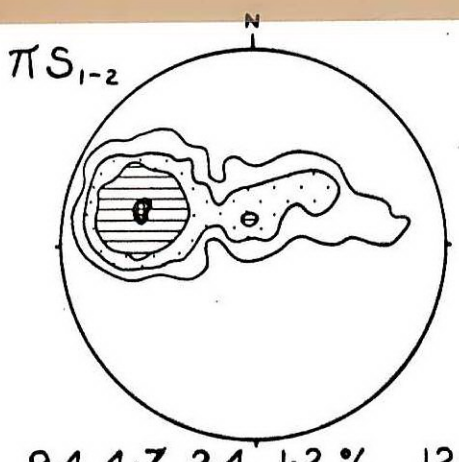
South of the lineament in Mindrow Creek, the migmatite gneisses are folded by sinistral F_4 folds with an incipient S_4 fracture cleavage striking 080 and subvertical in dip. The mylonites are likewise folded by D_4 and immediately adjacent to them in dolomite, a northwest S_4 orientation is defined by a narrow shear zone. Considered together, the two S_4 orientations define a conjugate pair with strain axes oriented as shown in Figure 4.12.

4.2.6 Plug Range Subarea

The main structural feature of the Plug Range subarea is a large open F_3 antiform, the Plug Range antiform. S_{1-2} of the metasediments and S_1 of the intervening granite gneiss are both folded about this broad structure as represented in Figure 4.13, (N.B. the bias towards easterly dipping S_{1-2} reflects the lack of exposure on the western limb). The antiform is a southerly plunging structure and mesoscopic

FIG. 4.13


STRUCTURAL MAP OF THE PLUG RANGE SUBAREA
PLUG RANGE
FAULT
PLUG RANGE ANTIFORM
TN MN
WARROW QUARTZITE
PLUG RANGE GRANITE GNEISS
S_2
F_2 (PLUNGE AND VERGENCE)
TREND AND DIP OF S_{1-2}
F_3 AXIAL TRACE
L_2
F_2 AXIAL TRACE
2Km


N
πS_{1-2}
9·4, 4·7, 2·4, 1·2 %
128

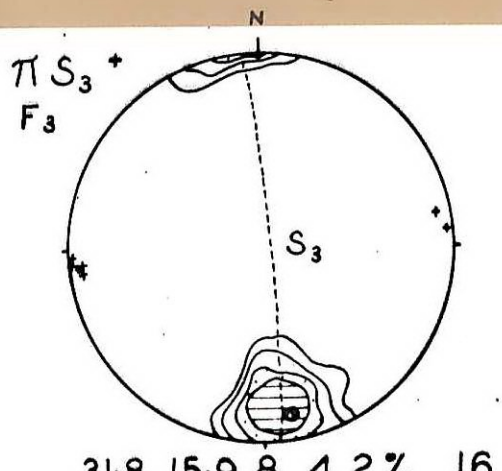
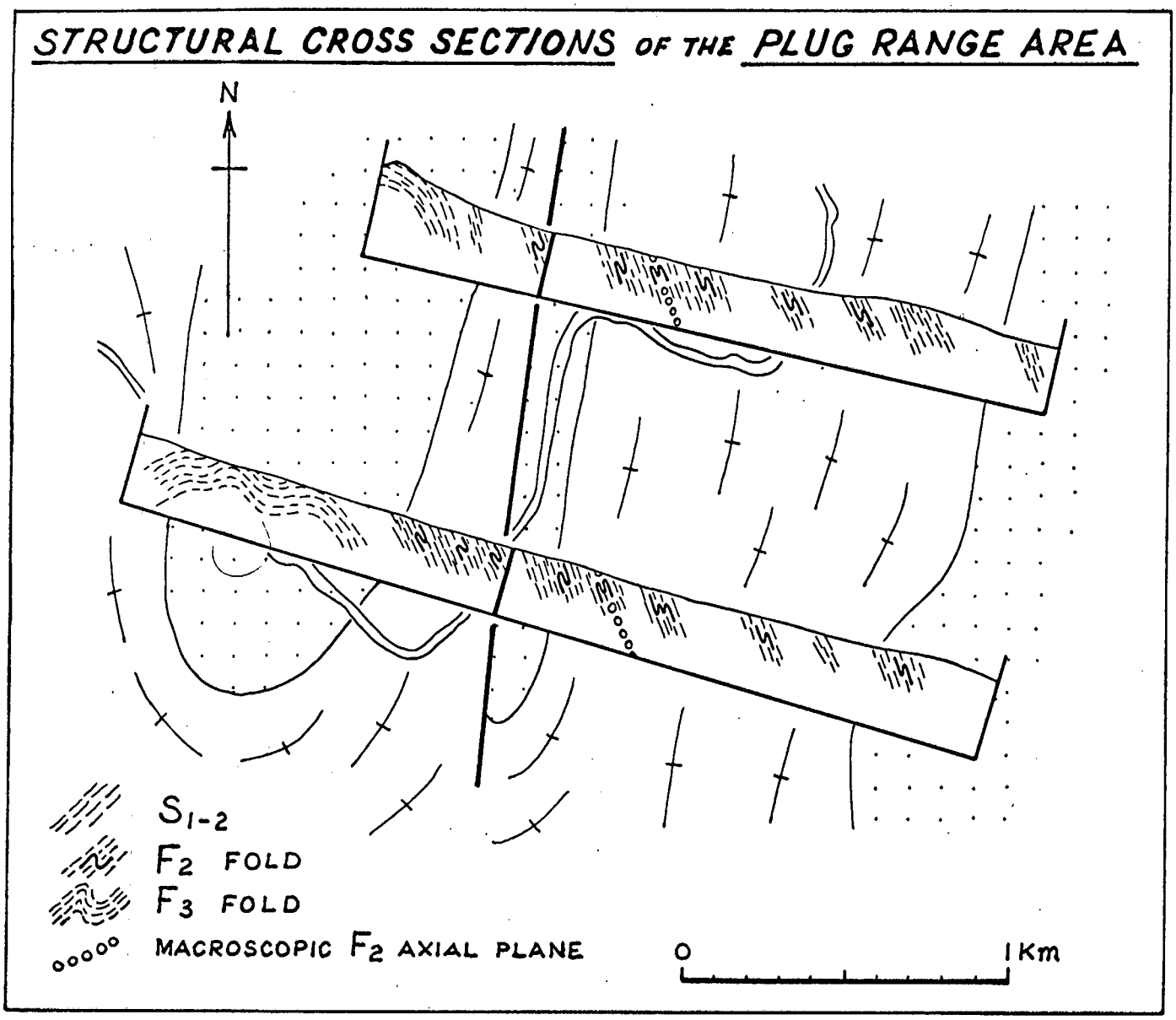
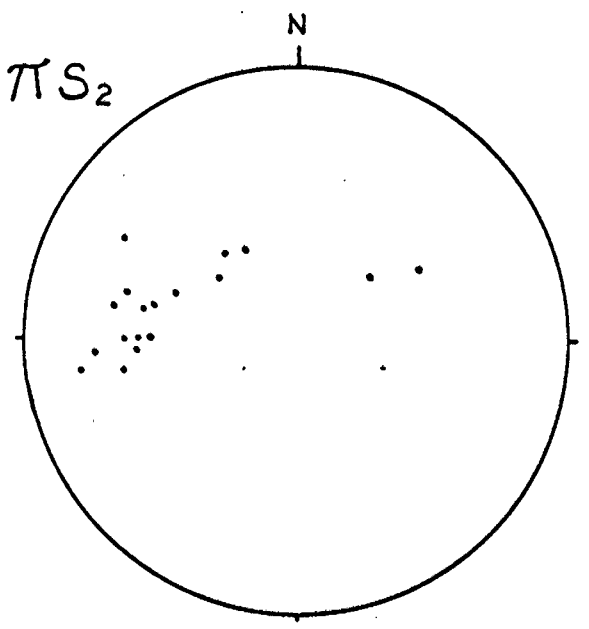
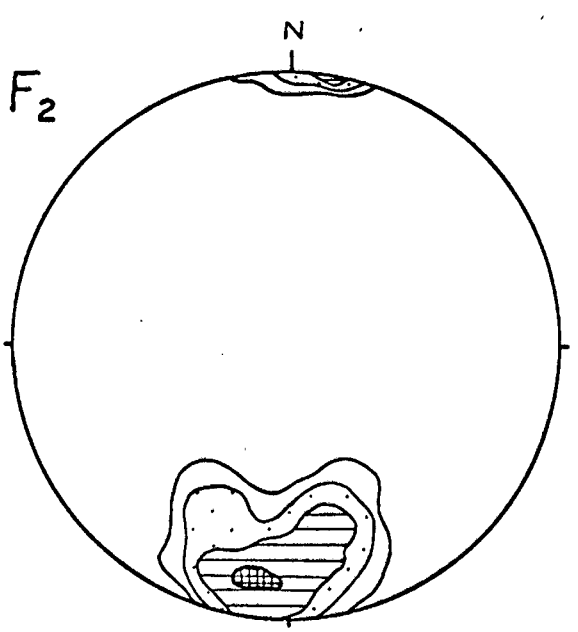

N
πS_3 + F_3
S_3
31·8, 15·9, 8, 4, 2 %
16

FIG. 4.14







16·3, 8·2, 4·1, 2 % 51

F_3 folds - generally broad, monoclinal warping of S_{1-2} - are likewise shallowly plunging (of the order of 20 degrees) to the south. S_3 is a weak fracture cleavage which varies from subvertical to dipping 85 degrees east.

In addition to this major D_3 structure, a major D_2 structure has been mapped on its eastern limb. This feature accounts for the symmetrical disposition of the Plug Range and Mt. Pony quartzites about the granite gneiss, and has been reconstructed from detailed mapping of mesoscopic F_2 folds in the granite gneiss. Two cross sections across this D_2 fold are outlined in Figure 4.14. The macrostructure itself is asymmetric in that its sinistral (looking north) limb dominates most of the subarea and its axial trace is close to the Plug Range quartzite boundary. Furthermore, D_2 folding is more intense in the dextral limb, and some of the metasedimentary units of the eastern boundary of the granite gneiss are absent from the dextral limb. Together these facts suggest that there may be macroscopic D_2 transposition along the dextral limb.

4.3 PEGMATITE ORIENTATIONS

In an earlier chapter, it was noted that there were several different generations of pegmatite intrusion. Two broad categories were recognized - conformable and disconformable. Having now defined the broad deformational history of the study area it is possible to subdivide these categories further, and to relate them to the various deformations.

METASEDIMENTS - The earliest, recognizable development of pegmatite is manifest as layer-parallel pegmatitic segregations within the metasediments. These pegmatitic segregations have an S_{1-2} fabric commonly developed within them, and they have

been deformed during D_2, sometimes with boudinaging or pinch and swell features in the limb regions. In the unmigmatized metasediments these layer parallel segregations are mainly absent but instead are represented by quartz veins which display identical features. Their origin is believed to be related to the D_1/M_1 event (see Chapt. VII).

The second instance of major pegmatization within the metasediments is recorded in the Calcookara subarea by a long, deformed aplite dyke (Fig. 4.6). This fine grained aplite trangresses the major D_2 structures yet is deformed by D_3 structures. Consequently it is considered to have been intruded sometime between the D_2 and D_3 deformations.

During the D_3 deformation, there was local production of pegmatite in the axial regions of major folds. Even on the mesoscopic scale, minor mobilization of pegmatite has occurred with its relocation in hinge areas. On the macroscopic scale, long dykes broadly parallel the axial planes of F_3 folds (e.g. Fig. 4.6). They are subvertical, they crosscut the layering in hinge areas, but in the limbs they subparallel the layering and frequently cannot be differentiated from the earliest formed pegmatites.

Overprinting the above categories are large, massive dykes which trend approximately north-northeast and which are subvertical. They are not widespread but there is one major dyke in the Wangaraleednie subarea which extends for some 3 km (see Plan 2).

PLUG RANGE GRANITE GNEISS - There are numerous S_1 parallel pegmatite veins within the granite gneiss adjacent to Plug Range. They are particularly prevalent on the dextral limb (looking northeast) of the D_2 antiform and they are folded with the gneissosity.

Cross cutting pegmatite veins are less common. There

are two predominant orientations though, striking at about 000 - 015 and 160 - 170 and both dipping subvertically. They post-date D_3.

MIDDLE CAMP GRANITE - As noted in earlier chapters and in Figure 3.8 there are both S_2 parallel and S_3 parallel pegmatite veins in the Middle Camp granite. In addition there are also two other minor dyke sets. They are both subvertical and they trend at approximately 010-020 and 060-070. The latter set are most commonly of slightly earlier invasion as they are often disrupted by the 010-020 set. Both sets are crosscut by D_4 fractures and hence they are between D_3 and D_4 in age.

NARRIDY CREEK GRANITE - There are four main pegmatite groupings in the Narridy Creek granite. Within the deformed zone, there are occasional folded dykes which have the S_3 fabric passing through, there are S_3 parallel dykes which disrupt the above group, and there are two post D_3 sets. The post D_3 sets frequently are associated with narrow shear zones and they form a complementary pair. They are essentially upright dykes and the two dominant trends are 020-030 and 070-080.

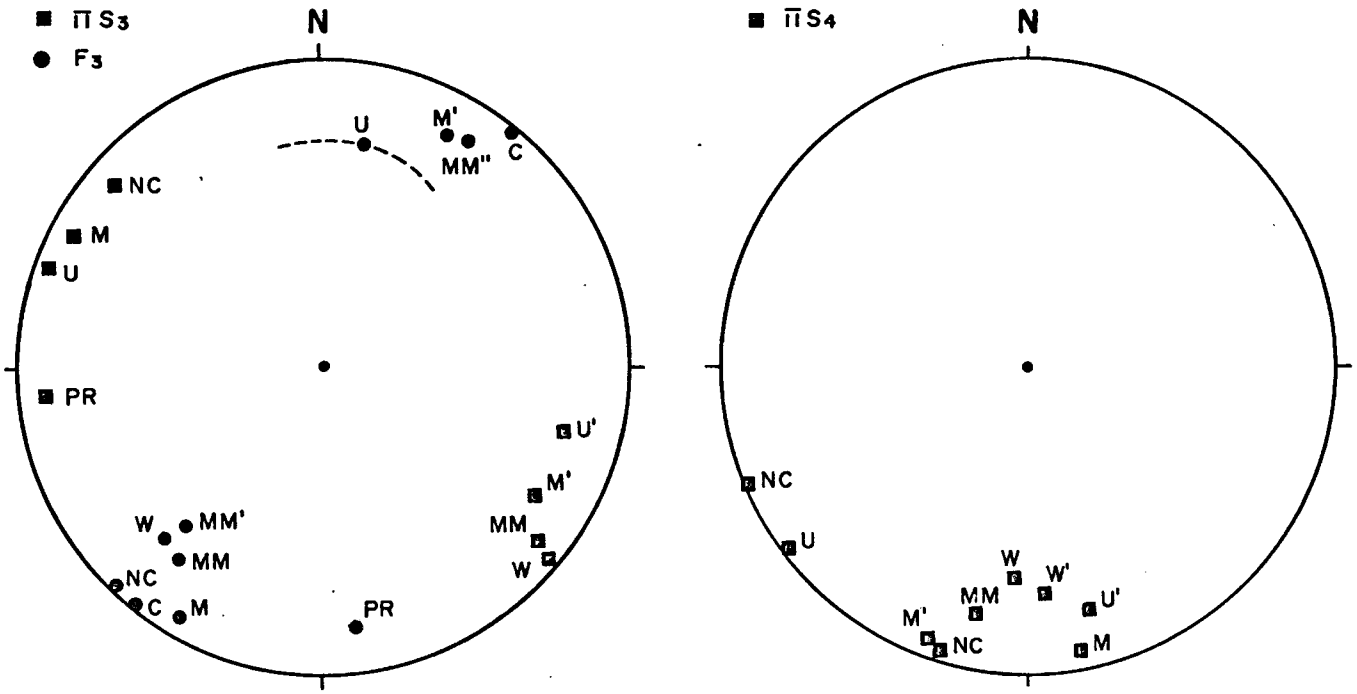
In the massive granite aplite dykes trending at 020-030 are common. They appear to be equivalent to the post D_3 set of that orientation in the deformed zone.

4.4 SUMMARY DISCUSSION AND REGIONAL CORRELATION

On the structure of the Cleve Uplands, Johns (1961) said,

"The ... strata have been deformed by compression and thrown into a system of closely spaced synclines and antiforms... Folding is fairly intense...and, gentle reversals of pitch... give rise to domed and pounded structures. .... here lateral compression directed from the northwest has involved great crustal shortening by the development of steep-limbed folds with broadly arcuate fold axes of a modified en echelon form".

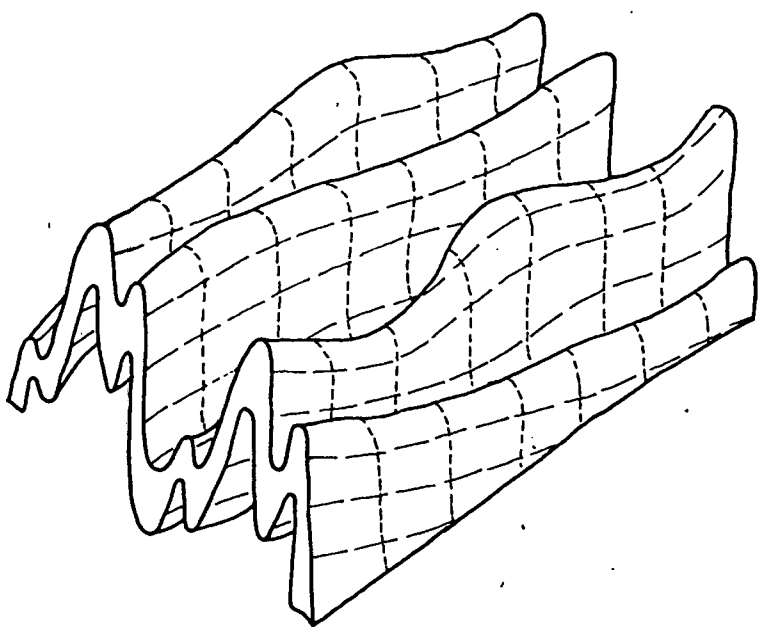
FIG 4.15

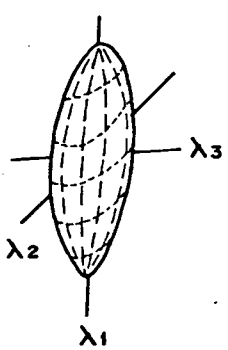


KEY TO SUB-AREAS

C	Calcookara	NC	Narridy Creek
M	Middle Camp	PR	Plug Range
M'	Mattum	U	Ullabidinie
MM	Mt Millar/Morowie	U'	Mylonite Zone
MM'	Mt Millar	W	Wangaraleednie
MM''	Morowie		

SYNOPTIC STEREODIAGRAMS RECORDING THE MAXIMA OF $\bar{\pi}S_3$, F_3 AND $\bar{\pi}S_4$ IN EACH SUB-AREA





Where $\lambda_1 \geqslant \lambda_2 \gg \lambda_3$

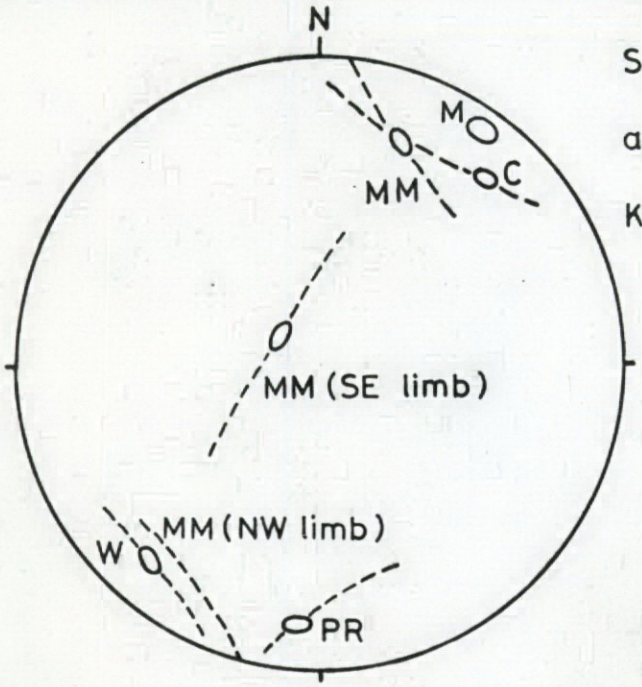
ASSUMED STYLE OF MACROSCOPIC F_3 FOLDS AND THE NATURE OF THE STRAIN ELLIPSOID WHICH IT REPRESENTS

S13225

One of the principal aims of this thesis was to examine in more detail the structure recorded by Johns. Throughout the preceding description it has been emphasized that the major macroscopic folds responsible for the present orientation of the layering are F_3 folds. These folds correspond broadly to those fold structures recorded by Johns (Plan 1) and in fact they display all of the characteristics that Johns noted. Their regional aspects are examined in Figure 4.15. Two specific characteristics are clearly evident; the broad arcuate nature of the fold belt, and the marked reversals of F_3 plunge. The arcuate nature is exemplified by the swing in strike of S_3 and the corresponding swing in trend of F_3. In the Mt. Millar/Morowie, Wangaraleednie and Narridy Creek subareas, S_3 strikes at 040/220. Going east from there, the strike direction progressively changes from that orientation to 030/210 in the Middle Camp subarea and to 020/200 in the Ullabidinie subarea. Reference to Plan 1 will show that a similar strike variation exists to the north of the main study area and in fact S_3 swings around to a 175/355 strike direction in the Plug Range subarea. Even further north, fold trends outlined by Johns suggest that S_3 and F_3 continue to swing around to 160/340. In all areas S_3 is subvertical and F_3 are tight, upright folds with variation of plunge about the horizontal within the S_3 plane.

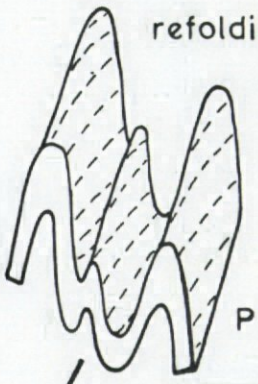
Regionally arcuate fold axes can develop by two main mechanisms; either from local variation in orientation of the stress and/or strain axes, or from a superimposed deformation. Although a suitably orientated superimposed deformation exists in the Cowell region (i.e. D_4 - see Figs. 4.12 and 4.15), it is discounted on the evidence of consistency in orientation of

FIG. 4.16



Synoptic stereodiagram of F_2 and L_2 distributions.

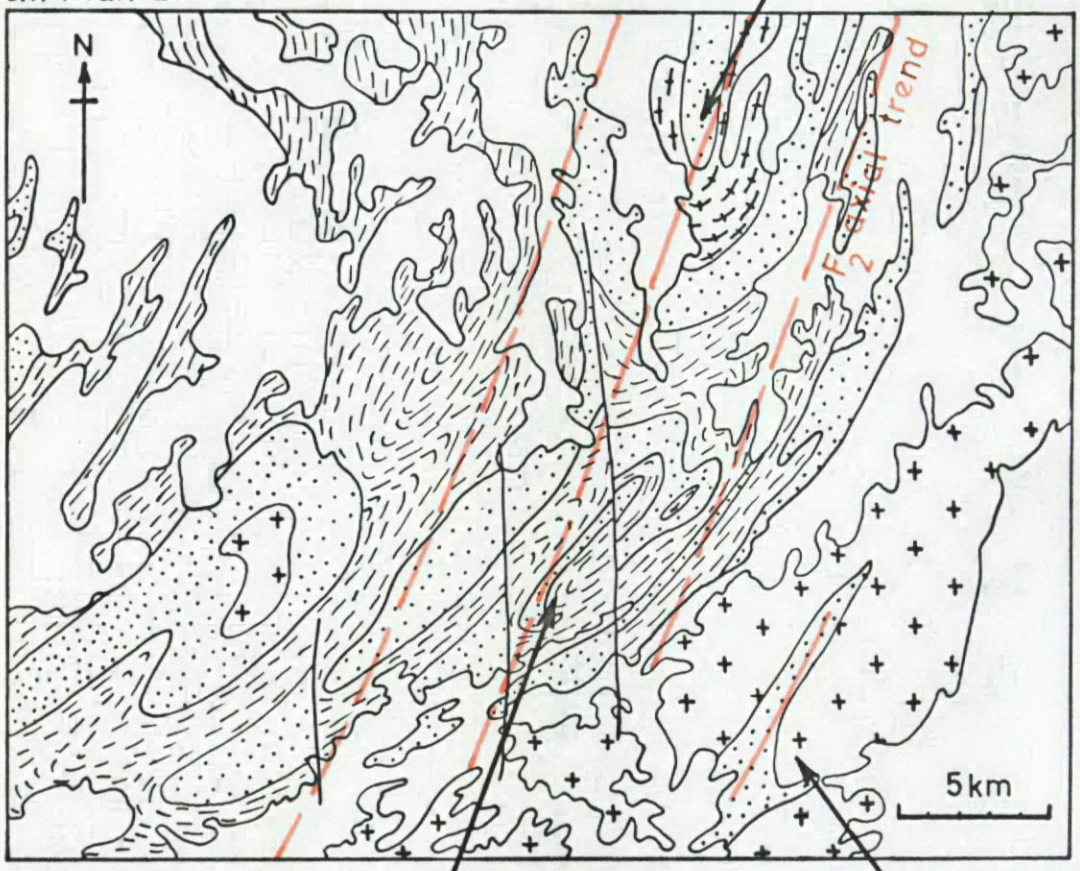
Key to subareas as on Fig. 4.15.

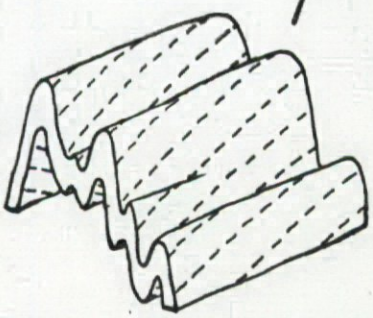


refolding of L_2 by F_3 folds

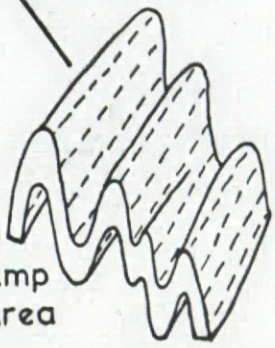
Plug Range Subarea

c.f. Plan 2.





Mt Millar / Morowie Subarea



Middle Camp Subarea

pre F_3 structures. In a D_4 refolding mechanism these features should also be folded, but their present orientations deny this. The situation is examined in Figure 4.16. In the synoptic stereodiagram, the distributions of F_2/L_2 lineations from each of the subareas are summarized. In the northwest limb of the Mt. Millar/Morowie antiform and in the Wangaraleednie subarea, those lineations define small circles about an 040/220 plunging F_3 axis but emanating from a strike trend of about 010 to 030. In the Middle Camp subarea, F_2/L_2 lineations are rather spread out around the F_3 axis which plunges to 030, but in the Plug Range subarea where F_3 axes plunge toward 175, F_2 axes again define a small circle emanating from the 010/020 position. Such distributions are summarized in the sketch block diagrams of Figure 4.16. Together they imply a relatively constant F_2 axial trend (outlined in the plan of Fig. 4.16) which has been folded about variably orientated F_3 axes (Ramsay, 1967). Consequently that variation in F_3 axes (and also S_3) must be due to local variation in orientation of D_3 stress and/or strain axes <u>not</u> a superimposed D_4 deformation.

Looking now at the characteristic variation in plunge of F_3 folds again two mechanisms have been proposed; cross folding, and constriction induced buckling. On the macroscopic scale this is not easily resolved because a constrictional component of strain is effectively equivalent to the type of strain represented by D_4 crenulations. Indeed there is no doubt a component of both. For example in the Mt. Millar/Morowie area where plunge reversals are common, both processes are observed. The flatlying amphibolite northwest of Calcookara shows D_4 cross folding which has demonstrably affected F_3 fold orientations. However the effects are only

small and do not rival outcrops, particularly in the migmatitic gneisses, where mesoscopic plunge variations are readily observed without any form of D_4 overprint. In view of this, a constrictional type model as sketched in Figure 4.15 is here favoured. Such a model has been recognized in many metamorphosed terrains throughout the world (e.g. Rast and Platt, 1957; Ramsay and Wood, 1973; Hopwood, 1977).

Finally, it is appropriate to consider the general aspects of D_3 strain. The type of strain which could have formed the F_3 folds is approximated by an ellipsoid with dimensions of λ_1 greater than or equal to λ_2 which is much greater than λ_3 (Fig. 4.15). The orientation of this ellipsoid would be such that $\lambda_1\lambda_2$ was parallel to S_3 and λ_2 parallel to F_2. Hence in the major part of the study area the maximum compression would be orientated approximately northwest-southeast whereas in the Plug Range area it would be eastwest. Additional to this flattening strain there is no doubt a component of vertical strain manifest by the intrusion of the Narridy Creek granite and by the steeply oriented mylonite zone.

Unlike D_3 structures the original nature and origin of D_2 structures is not clear. Simple unfolding of the superimposed F_3 folds suggests that F_2 folds were isoclinal and either shallowly inclined or recumbent with subhorizontal axes trending 010 to 020 (Fig. 4.16). The strong S and L-S fabrics infer strain conditions approximating between simple flattening and plane strain. Certainly, the features of the D_2 deformation contrast against the D_3 and D_4 deformations. Throughout the area studied, D_2 features are more homogeneous in character and this is well illustrated by the constancy of F_2/L_2 trends. This is believed to reflect a major, intense and widely

Figure 4.17 REGIONAL CORRELATION OF THE STRUCTURAL EVOLUTION

COWELL/CLEVE AREA (this study)	MIDDLEBACK RANGES (Jones, 1968)	SOUTHERN EYRE PENINSULA (Coin, 1976)
D_4 minor east-west crenulations, kinks and fractures. NB weaker conjugate set 150/330	Conjugate folds and kink bands trending 060 and 120.	minor kinking (his D_3)
D_3 major fold deformation - tight upright folds of shallow but variable plunge. S_3 swings from 040/220 (Wangaraleednie subarea) to 340/160 (north of Plug Range). Local intense mylonitization along southeast extent of outcrop (D_M).	Group II folds - tight upright, variable but shallow plunge. Trends are north-south.	mylonite deformation (his D_{2B}) defining southeastern extent of outcropping Hutchison Group. major fold deformation (his D_{2A}) -tight, upright folds of variable but shallow plunge trending northeast-southwest.
D_2 major fold deformation - isoclinal, recumbent folds of shallow plunge trending 010 to 020. Strong L-S fabrics.	Group I folds - isoclinal with local transposition. Strong S fabrics. Trends north-south.	
D_1 major fabric forming deformation - folding not confirmed.		formation of main metamorphic layering (his D_1)

pervasive period of deformation under ductile conditions. Such conditions suggest that D_2 took place while the rocks were deeply buried whereas the later deformations took place at shallower levels of the crust.

Comparing now the structure of the study area with that in the Middleback Ranges and southern Eyre Peninsula there is a good correlation in both sequence and style of deformation. The structure in each of the areas as outlined by Jones (1968) and Coin (1976) respectively is briefly summarized in Figure 4.17. In the Middleback Ranges the sequence and style of deformation is very similar and Jones' Group I and II folds conveniently match up with, respectively, F_2 and F_3 folds of the Cowell region. Jones only recognized mesoscopic Group I folds, but the presence of macroscopic Group I folds has since been confirmed by N. Lemon (BHP Co. Ltd., pers. comm.). Macroscopic Group II folds are however, very prominent and in fact a major Group II synform outlines the backbone of the Middleback Ranges (Miles, 1954). The regular variation in plunge of this synformal structure has been recorded by both Miles and Jones, but they hold different views on its origin; Miles considered that it was due to crossfolding, whereas Jones considered that it was due to constriction parallel to the fold axes. This situation is analogous to that in the Cowell/Cleve region and again there does not appear to be a clear solution. Post Group II kinking in the Middleback Range area is analogous to D_4 crenulation at Cowell, and its conjugate nature suggests a compression parallel to Group II axes. Nevertheless, as at Cowell, that kinking is restricted in its development inferring that it may not be solely responsible for Group II plunge variation.

Correlation of the structural seuqence on southern Eyre Peninsula is not so obvious. Coin (op. cit.) summarized the deformational histories of the Flinders and Hutchison Groups separately as follows, where D and M are used in the same sense as in this thesis and where G represents igneous intrusion.

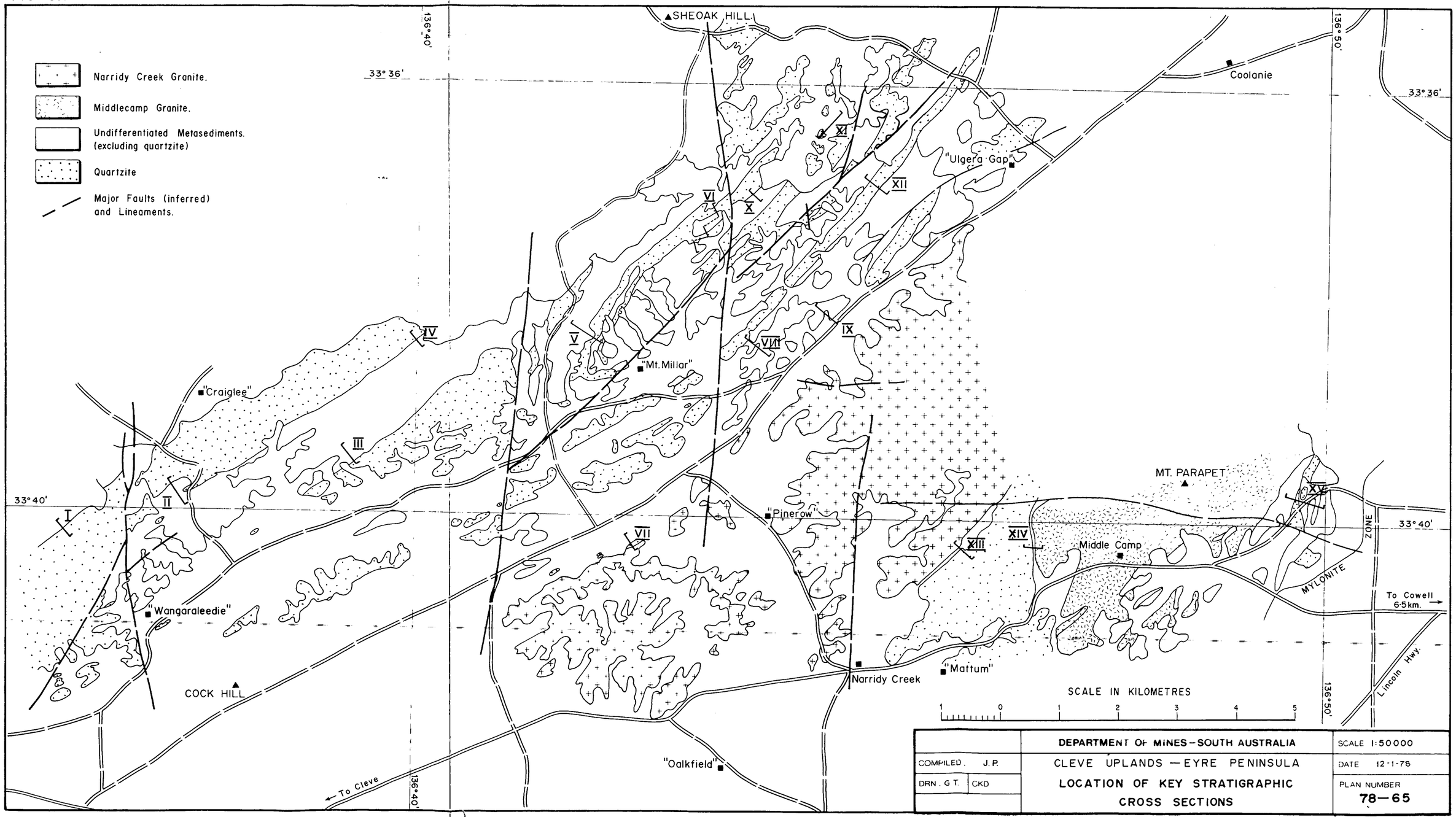
Flinders Group		Hutchison Group
D_1, M_1, G_1		-?
D_2, M_2, G_2		D_1
	early S_3	D_{2A}, M_{2A}, G
D_3, M_3, G_3		
	Later S_M	D_{2B}, (D_M), M_{2B}
D_4		D_3

Within the Hutchison Group metasediments which are regarded as equivalent to those in the Cowell region, Coin attributes the major macroscopic folds to his D_{2A} deformation and the prominent mesoscopic layering folded by D_{2A} structures to an earlier D_1 deformation. These are the structures outlined in Figure 4.17. It appears from reading his thesis and visiting the area, that Coin has grouped all folds in the metasediments together but that in fact there may be two separable groups analogous to F_2 and F_3 of this study. Indeed Coin recognizes earlier folds in the Flinders Group, but he uses this to argue that the Flinders Group gneisses are basement to the Hutchison Group. Other workers on southern Eyre Peninsula (Clarke, 1976; Cooper et al, 1976) generally agree with Coin's Flinders Group structure but they have confined their studies to Flinders Group rocks without considering typical Hutchison Group rocks so therefore they cannot be used as direct evidence.

So in conclusion it is believed that the structural evolution of the Cowell/Cleve region studied in this thesis is typical of a broad fold belt that stretches the length

of the eastern coast of Eyre Peninsula. It involved at least four ductile deformations with at least two of them accompanied by magmatic intrusion. The arcuate nature of the fold belt is consequent to variability of strain during the third major deformation and along with the variability of F_3 plunges within an essentially upright S_3, is seen as a characteristic of that deformation. Local mylonitization was common during D_3 and in particular in a narrow zone along the eastern margin of the peninsula parallel to the fold belt. The preceding D_2 deformation has not been widely recognized, but at least in the northeast of the peninsula it has been identified as a major phase of isoclinal(?), recumbent folding with approximately constant north-south axial trends. Overprinting both D_2 and D_3, the final ductile deformation D_4 affected the entire fold belt although its effects are only locally observed. It represents a period of crenulation and kinking at a high angle to the fold belt.

FIG 5.1


Narridy Creek Granite.
Middlecamp Granite.
Undifferentiated Metasediments. (excluding quartzite)
Quartzite
Major Faults (inferred) and Lineaments.
SHEOAK HILL
136°40'
33°36'
136°50'
Coolanie
"Ulgera Gap"
I
II
III
IV
V
VI
VII
VIII
IX
X
XI
XII
XIII
XIV
XV
"Mt. Millar"
"Craiglee"
"Pinerow"
MT. PARAPET
Middle Camp
33°40'
"Wangaraleedie"
COCK HILL
Narridy Creek
"Mattum"
"Oalkfield"
MYLONITE ZONE
To Cowell 6·5km.
Lincoln Hwy.
To Cleve
SCALE IN KILOMETRES
1 0 1 2 3 4 5
DEPARTMENT OF MINES - SOUTH AUSTRALIA
SCALE 1:50000
COMPILED J.P.
DRN. G.T. CKD
CLEVE UPLANDS — EYRE PENINSULA
LOCATION OF KEY STRATIGRAPHIC CROSS SECTIONS
DATE 12-1-78
PLAN NUMBER 78—65

CHAPTER V

STRATIGRAPHY

5.1 INTRODUCTION

Although the macroscopic structure could not be completely resolved, several major D_2 and D_3 fold structures have been established (Chapt. IV) such that it is now possible to relate particular stratigraphic sequences in one area with those in other areas. During the course of the field study, a number of cross sections were recorded in areas of particular stratigraphic significance. In this chapter these sections are described and compared, firstly within each subarea (Fig. 3.1) and then finally in the overall context of the study area. From there a stratigraphic succession has been established for the study area and it is shown that it is consistent with other sequences throughout northeastern Eyre Peninsula. Reference is made to the sedimentary record, to the nature of the basement of that succession, and to the origin of the amphibolites. Finally the structural implications of the stratigraphy are described and several interpretative cross sections are presented.

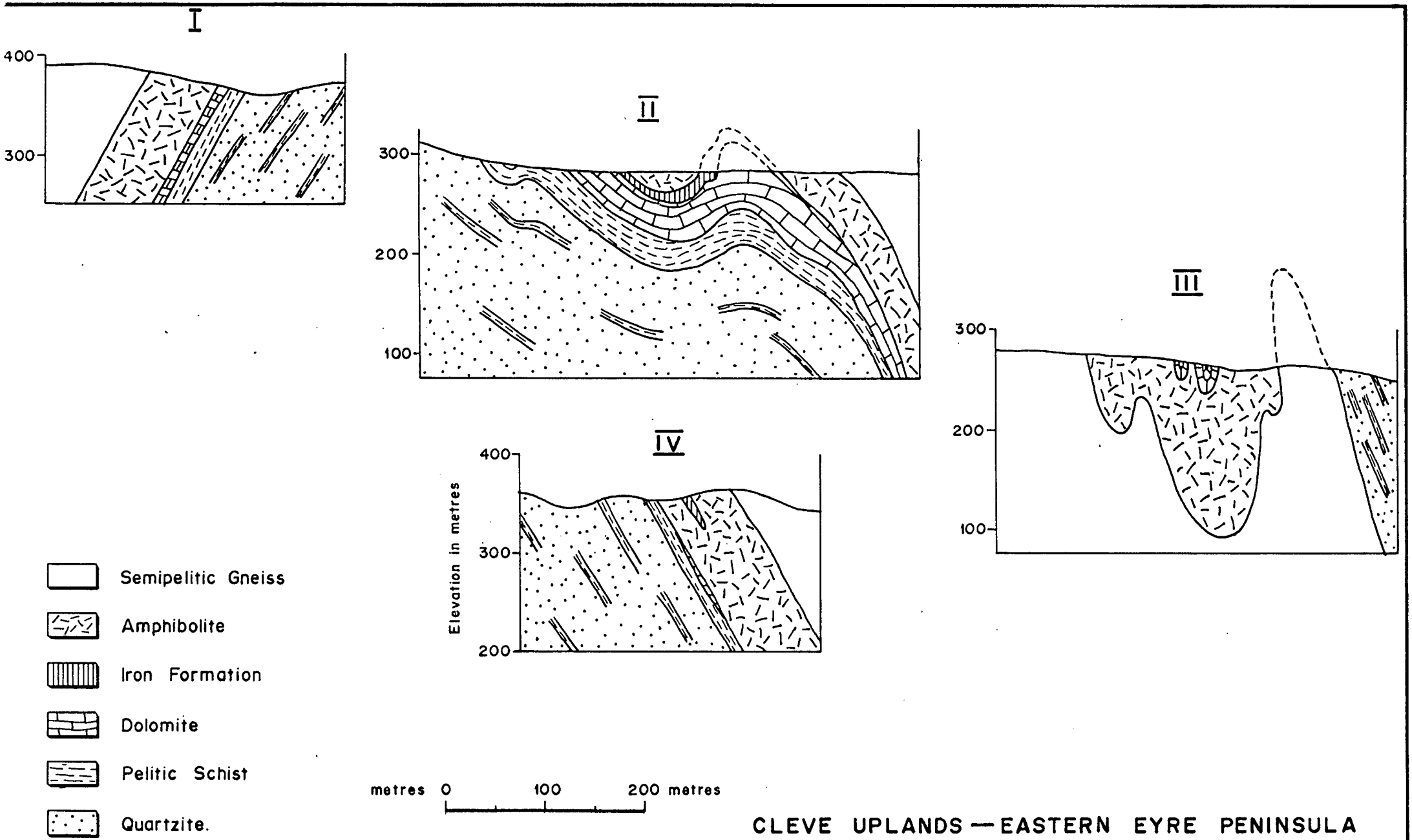
5.2 SUMMARY DESCRIPTION OF LOCAL SEQUENCES

5.2.1 Wangaraleednie Subarea

The combination of reasonable outcrop and a clearly defined macrostructure has enabled a good stratigraphic sequence to be constructed in this subarea. Four sketch sections from localities shown on Figure 5.1 are illustrated in Figure 5.2. There is a close correlation between the stratigraphies depicted by sections I, II, and IV which is expected because they are all related to a single horizon folded by the D_3 antiform (Fig. 4.2 - Range Rd. Section).

Of these sections, the best exposed is section II.

FIG 5.2



For location of sections see plan 78-65

CLEVE UPLANDS — EASTERN EYRE PENINSULA
GEOLOGICAL CROSS-SECTIONS
WANGARALEEDNIE SUB-AREA

The sequence here passes successively through quartzite, pelitic schist, dolomite, iron formation and amphibolite into semipelitic gneiss and schist. The quartzite is both feldspathic and micaceous, and it contains numerous, narrow (≈5-10 m) pelitic schist interbands. There are no recognizable traces of carbonate within this unit and along the boundary between the quartzite and dolomite there is always (in this subarea) a narrow pelitic schist. The dolomite is massive in this section with only a faint layering. It is relatively pure, there being only minor calc-silicate minerals, and there are no major variations across it. However, a patchy pale brown colouring is sometimes present near and adjacent to the iron formation. The iron formation is a typical, well banded amphibole quartzite. It is only very narrow and although they are not exposed, its upper and lower boundaries appear to be sharp. Structurally overlying it, the amphibolite forms a major, very prominent unit. Like the dolomite and iron formation its thickness is quite variable, but in Section II it is of the order of 45 m thick. Both schistose and porphyroblastic lithologies are present, with porphyroblastic amphibolite outcropping as a 2 m wide band along the upper boundary (that is, near the semipelite boundary). The structural upper contact with the semipelitic unit is sharp and apparently conformable. One small, lensoid block of ironstone is present along the well exposed contact, but otherwise semipelitic schist and amphibolite abut against each other. Biotite within amphibolite and amphibole within gneiss a few centimetres either side of the contact is believed to represent local contamination of each unit by the other during metamorphism.

Considering now Section III, in view of the macro-

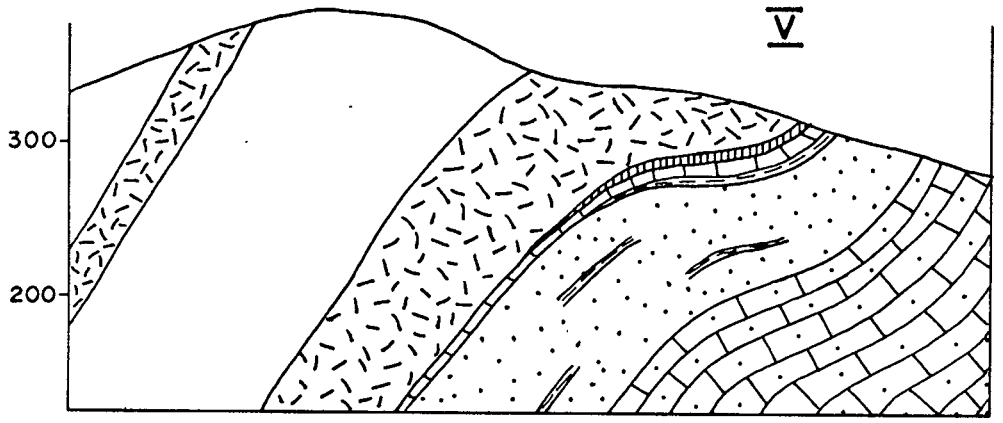
structural interpretation of D_2 folding, (see Figs. 4.1 and 4.2) this particular section is believed to be equivalent stratigraphically to that detailed above. Certainly amphibolite forms a very prominent unit along this horizon adjacent to the quartzite (see Plan 2), which is itself feldspathic and micaceous containing numerous pelitic interbands. Comparing Section III and Figure 4.2 (Yabmana Section) the presence of a minor dolomite horizon in a synformal core places it effectively between the amphibolite and quartzite units. One outcrop of iron formation associated with this dolomite core was recorded northeast along strike from Section III and so is also related to the appropriate horizon. This sequence then, although it does not establish a stratigraphy by itself, does confirm the Range Road section, Section II. Consequently Section II is taken as the type example for the Wangaraleednie subarea.

5.2.2 Mt. Millar/Morowie Subarea

Resolution of the stratigraphy represented by rocks in the Mt. Millar/Morowie subarea is not as straight forward as in the Wangaraleednie subarea. This is due to a more complex fold pattern which could not be satisfactorily unravelled.

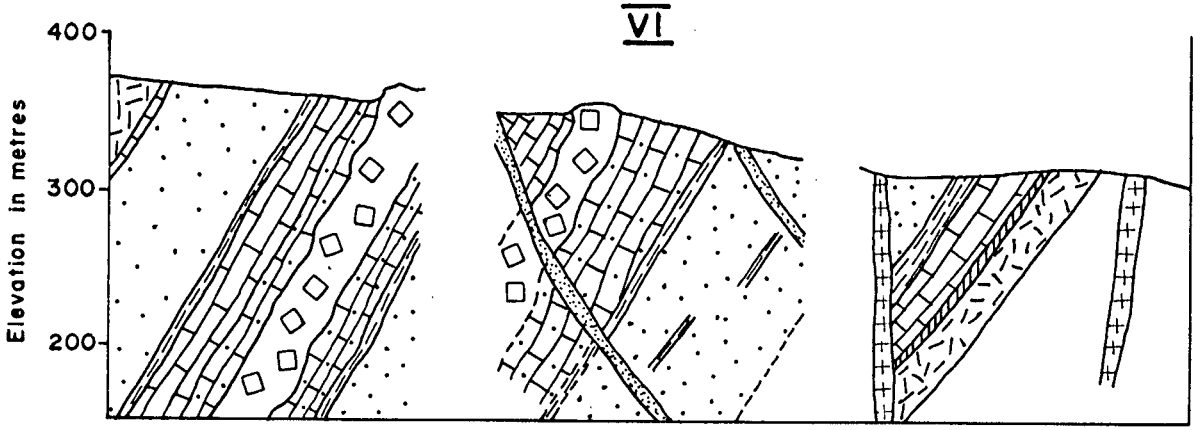
Northwest of the Mt. Millar/Morowie antiform in the Mt. Millar area, the boundary of the quartzite unit (feldspathic and micaceous) with the structurally overlying semipelitic gneisses is an important stratigraphic marker horizon. Metamorphic grade is substantially higher there than in the Wangaraleednie subarea, but there is a similar sequence of units. Pelites have been most notably affected by the metamorphism such that they are now feldspathic gneisses instead of mica schists but semipelitic gneisses likewise

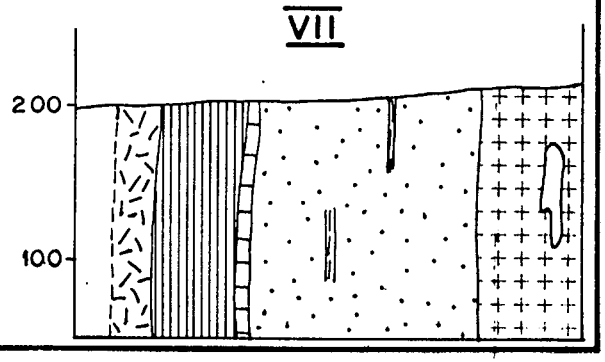
FIG 5.3



Granite (and Pegmatite).
Aplite Dykes.
Semipelitic Gneiss.
Amphibolite.
Iron Formation.
Dolomite.
Pelitic Schist and Gneiss.
Quartzite.
Calc-silicate.
Diopside Rock.

metres 0 100 200 metres



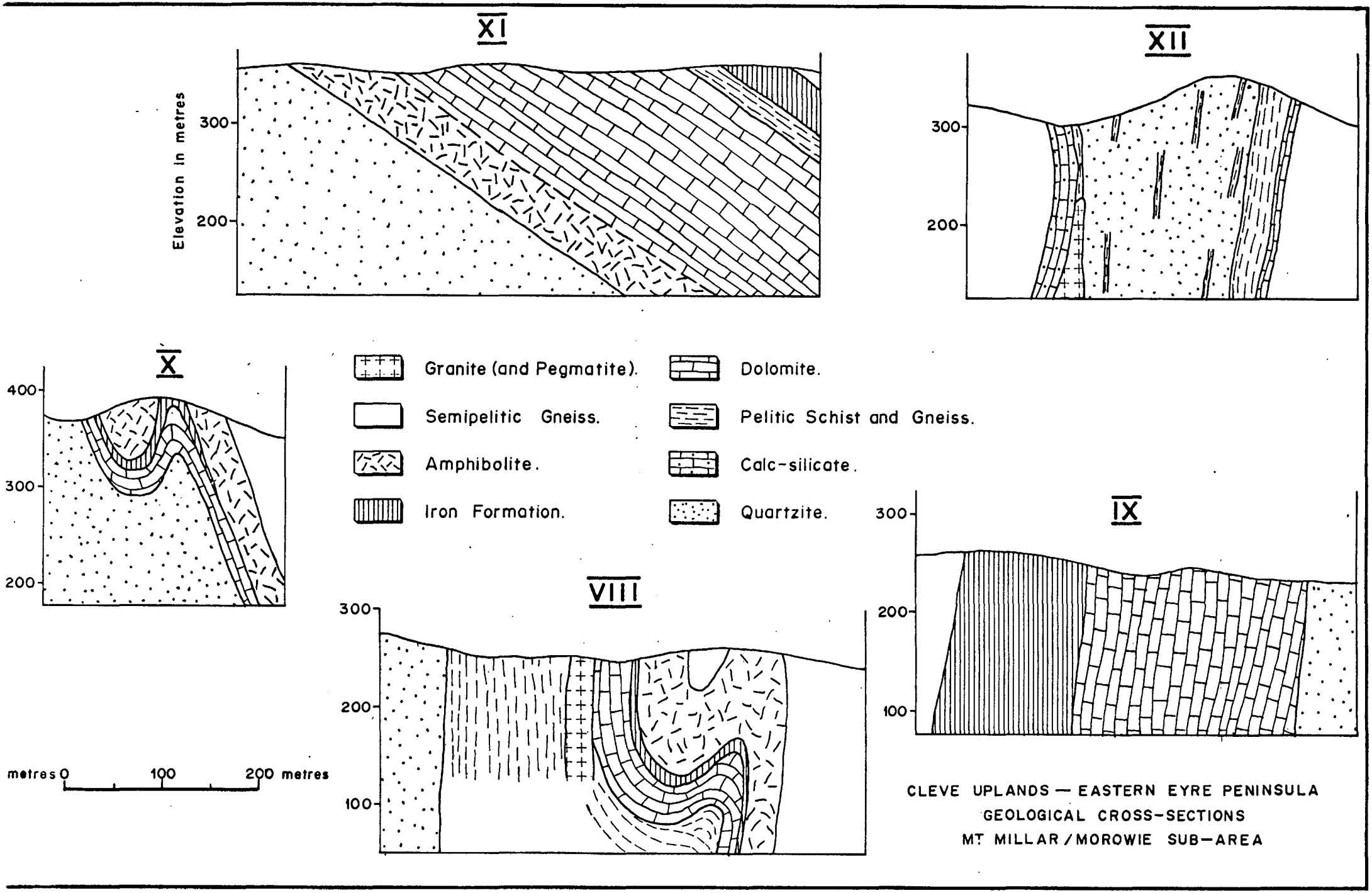


CLEVE UPLANDS — EASTERN EYRE PENINSULA
GEOLOGICAL CROSS-SECTIONS
MT MILLAR / MOROWIE SUB-AREA

have changed character and have been partially migmatized.

The particular horizon in question is detailed in Section V (Fig. 5.3; for location see Fig. 5.1). Ignoring the calc-silicate for the moment, the sequence passes northwest successively from quartzite, through pelitic gneiss, dolomite, iron formation and amphibolite into semipelitic migmatite gneiss. A second amphibolite occurs within the semipelites. The quartzite unit is relatively massive with occasional pelitic gneiss interbands. In some places it contains minor amounts of amphibole and rarely diopside, in addition to mica and feldspar. Between it and the amphibolite are sandwiched a 2 m band of pelitic gneiss, $\sim$ 5 m of massive white dolomite with traces of serpentine, and a 2 m band of quartz-veined grunerite schist (iron formation). The amphibolite is superficially about 60 m thick but reference to Plan 2 shows that this figure is quite variable along strike. Schistose amphibolite is the principal lithology but there are also rare outcrops of porphyroblastic amphibolites, and, along strike from Section I, there are also pods of eulysite within schistose amphibolite. The contact between amphibolite and semipelitic gneiss is sharp and conformable.

The calc-silicate unit identified in Section V outcrops more prominently northeast along strike and is shown in Section VI (see Figs. 5.1 and 5.3). From detailed mapping in this area it has been established that the calc-silicate bodies form the core of an F_2 antiform (refer Chapt. IV and Fig. 4.6). The units either side are roughly symmetrical with respect to this F_2 axis and they define a sequence, starting from the core, of calc-silicate, pelitic gneiss, quartzite with rare interbanded pelitic gneiss, pelitic gneiss, dolomite, iron formation, and amphibolite passing outwards



CLEVE UPLANDS — EASTERN EYRE PENINSULA
GEOLOGICAL CROSS-SECTIONS
MT MILLAR / MOROWIE SUB-AREA

FIG 5.4

into migmatized semipelitic gneisses. The sequence from quartzite to semipelite on either side of the antiform is equivalent to the succession illustrated in Section V, but the core sequence is quite different. The calc-silicates vary in composition without any apparent sequential order although it appears that the very coarse grained diopside rock defines a central core surrounded by well-layered calc-silicates which merge into massive dolomite. The massive dolomite is identical to the "outer" dolomite defining the quartzite/semipelite boundary, but the layered calc-silicates are absent from the "outer" horizon. Between the calc-silicate core and the quartzite, there is commonly a thin, podded, sillimanite gneiss.

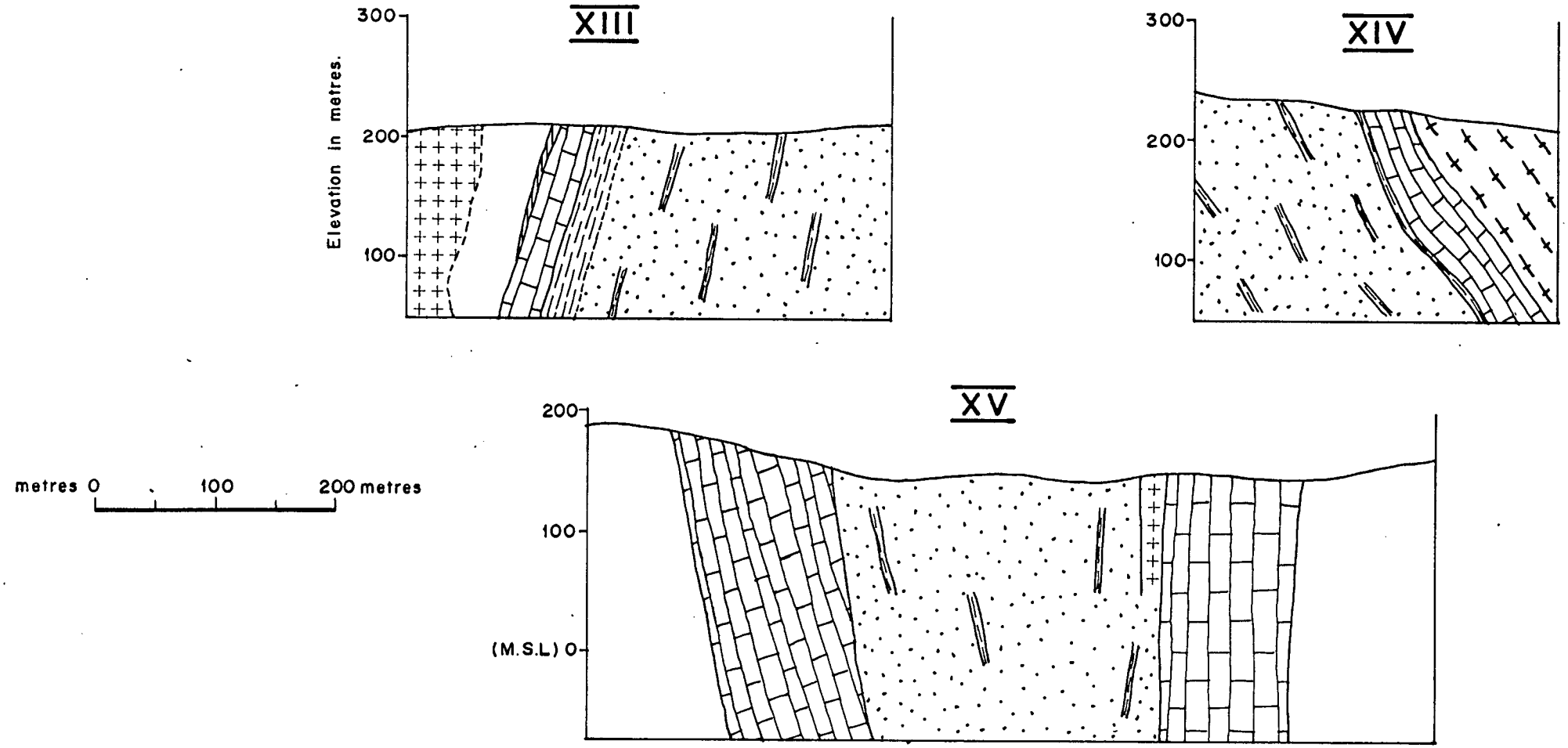
The presence of the "quartzite-pelite-dolomite-iron formation-amphibolite-semipelite" sequence is confirmed at several other localities in the Mt. Millar/Morowie subarea (Figs. 5.1, 5.3 and 5.4). In many sections one or two of the units appear to be absent (or were not recorded due, in part, to incomplete outcrop), however the general sequence is unmistakable. Furthermore there are other quite noticeable variations in thickness of particular units. For example, adjacent to the Narridy Creek granite (Section VII) the iron formation is particularly prominent. It is of the banded quartzite type, and the presence here of numerous F_3 mesoscopic folds deforming this banding suggests that local thickening is a superficial D_3 effect.

Another section of particular interest is Section XII. The macroscopic structure is not clearly understood here, but it has been suggested (Chapt. IV, Fig. 4.4) that this section forms the southeastern limb of a major F_2 structure, probably an F_2 anticline. This would infer that the

sequence shown in Section XII (from northwest to southeast) represents the transition from the inner arc to the outer arc of that F_2 fold structure. On this premise, the F_2 core is defined by migmatized gneiss which passes "upwards" and outwards through, successively, a calc-silicate unit, a thin pelite (with granite developments along strike), quartzite and interbanded gneiss, pelitic schist, dolomite and amphibolite into migmatized semipelitic gneisses. This sequence is very closely analogous to the Section VI sequence with calc-silicates defining the "lower" boundary of the quartzite unit. On the southeastern side of the quartzite the dolomite-amphibolite association is poorly exposed, but that horizon can be traced southwest to Section VIII (Fig. 5.1) where the typical quartzite-pelite-dolomite-iron formation-amphibolite-semipelite succession is again recorded. Porphyroblastic amphibolite and eulysite are present in this section close to the amphibolite/semipelite boundary.

The great thickness of dolomite and iron formation which outcrop southeast of Section XII (see Plan 2) and around Ferns (Section IX), is not clearly understood. Layering in this region is subvertical, of constant orientation and there is no conclusive evidence for thickening due to folding. Furthermore it could not be established if there is a macroscopic F_2 (or F_1?) hinge northwest of it so that it is not known if that dolomite unit is related to any others or not, although intuitively it is believed to be equivalent to the dolomite along the "upper" quartzite/semipelite boundary. Alternatively however it may be a separate unit from a "higher" stratigraphic level. Further work to the northeast of the study area may throw light on this problem.

The status of other major quartzite bodies in the Mt. Millar/Morowie area is also conjectural. Those quartzites



CLEVE UPLANDS — EASTERN EYRE PENINSULA
GEOLOGICAL CROSS-SECTIONS
MIDDLE CAMP SUB-AREA

FIG 5.5

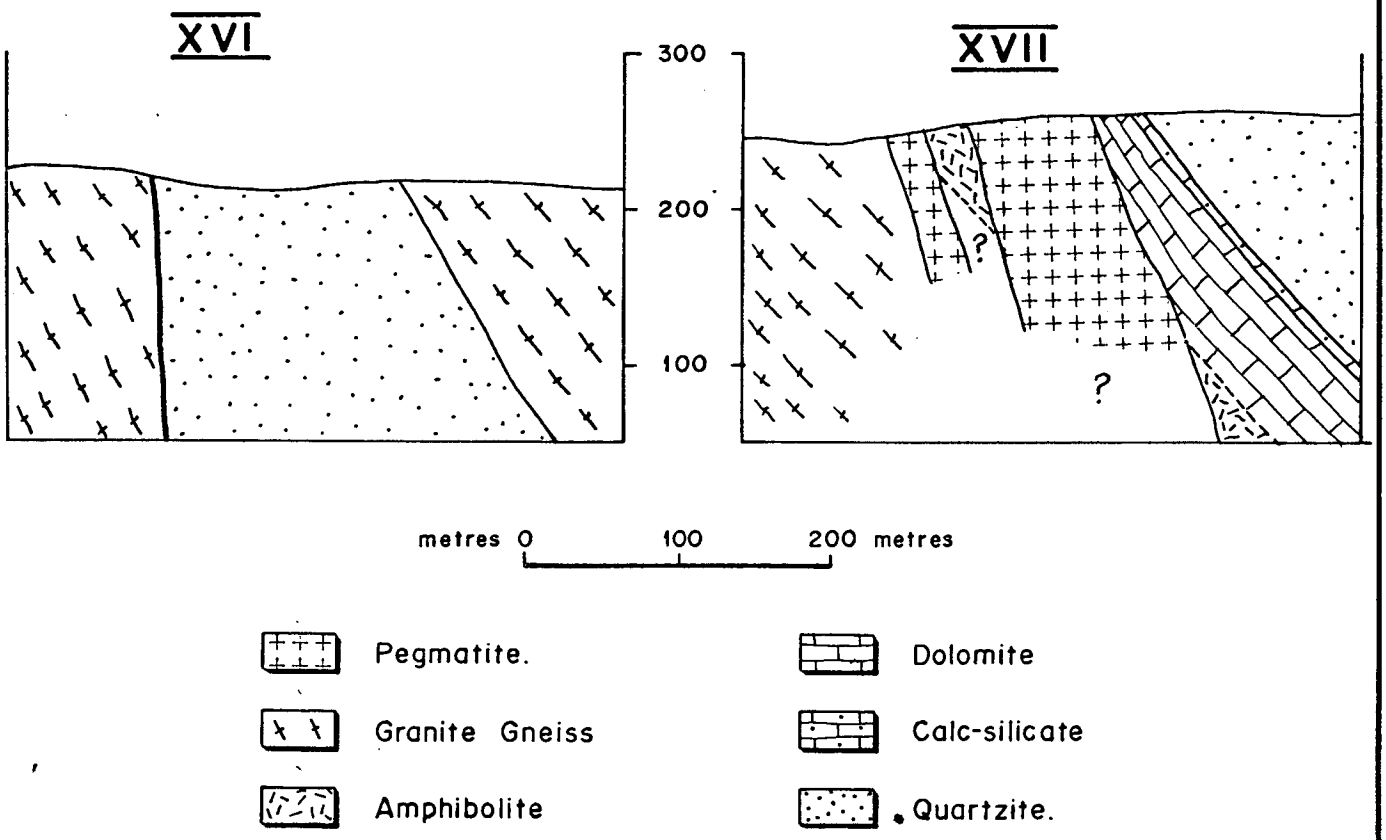
that outcrop at Ulgera Gap, Glenville, Ben Lomond and Atkinson Mine are all lithologically very similar and all have associated dolomites and/or amphibolites along at least one boundary with the semipelitic rocks. However, for them to all be related to one specific quartzite horizon requires several macroscopic F_2 (or $?F_1$) hinges. In most cases these could not be proven, but an interpretation of the structural implications of a single quartzite unit has been detailed and is contained in an ensuing section (Sect. 5.5 and Fig. 5.10). It lends support to a single quartzite unit hypothesis.

In conclusion, the stratigraphy of the Hutchison Group in the Mt. Millar/Morowie subarea can be simplified to that represented by Sections V and VI (Fig. 5.3). It passes successively from migmatite gneiss into a calc-silicate unit, podded sillimanite gneiss, quartzite, pelitic schist, massive dolomite, iron formation and amphibolite into a thick sequence of semipelitic gneisses with minor amphibolite "sills". There may be a second, "upper", iron formation represented in the Ferns area but it is doubted (see Sect. 5.3 and 5.5).

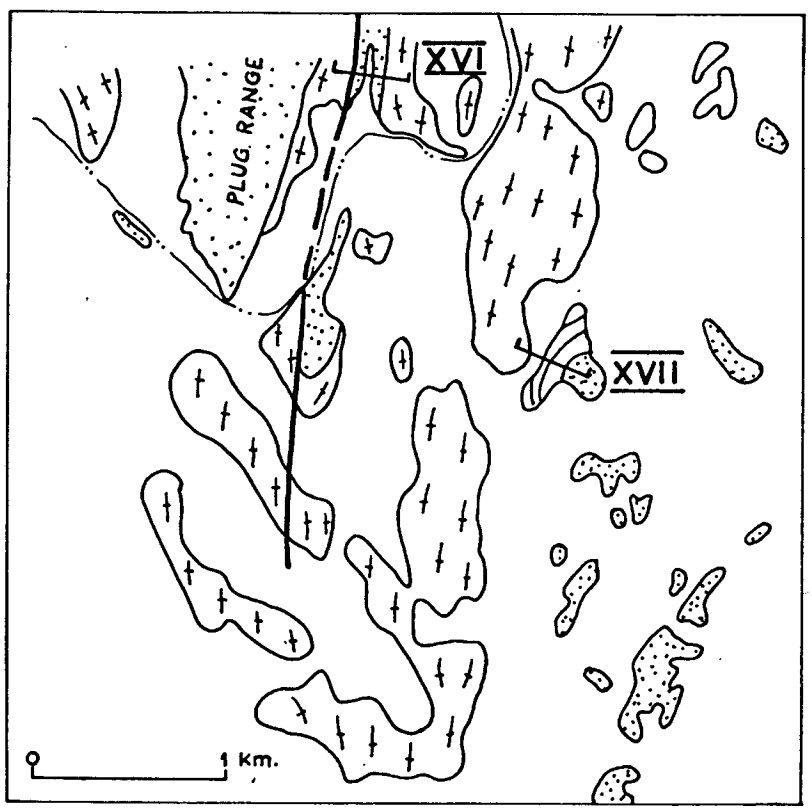
5.2.3 Middle Camp Subarea

Two specific sections are examined here and they are shown in Figure 5.5 (see Fig. 5.1 for locations). In the first of these (Section XIII) there is a clear sequence from typical quartzite with interbanded gneiss through a band of migmatitic gneiss, a massive serpentinous dolomite with a very thin ironstone (and rare banded diopside quartzite), into migmatized, semipelitic gneisses. The Narridy Creek granite intrudes the latter and locally transgresses the quartzite boundary. Although amphibolite is absent here, and in fact from anywhere in the Middle Camp subarea, this

FIG 5.6



LOCALITY



CLEVE UPLANDS — EASTERN EYRE PENINSULA

GEOLOGICAL CROSS-SECTIONS

PLUG RANGE SUB-AREA

S13231

sequence very closely resembles those from the Wangaraleednie subarea and from the "upper" boundary of the quartzite in the Mt. Millar/Morowie subarea. The quartzites and dolomites are analogous and the presence of thin iron formation is also compatible.

The sequence shown in Section XIV on the southeastern side of the D_3 Mattum antiform is theoretically at an equivalent stratigraphic level to the sequence of Section XIII (see Fig. 4.10 in Macrostructure). However in this case the Middle Camp granite abuts against the dolomite and quartzite locally intruding them. The sequence from quartzite through gneiss and dolomite into granite gneiss is comparable.

5.2.4 Ullabidinie Subarea

Only one sketchy section, Section XV, could be constructed here (Figs. 5.1 and 5.5) and again a quartzite-dolomite-gneiss sequence is confirmed. One narrow amphibolite body was observed in Mindrow Creek west of the mylonite zone but it was not near to any dolomite or quartzite, although it was conformable with the surrounding migmatitic gneisses.

5.2.5 Plug Range Subarea

An extremely interesting association of lithologies is present in the Plug Range area that is particularly relevant to the problem of determining the base of the Hutchison Group metasediments. Chapter IV established that there is a major F_2 antiform folded about a large, open D_3 antiform (see Figs. 4.13 and 4.14). The core of that D_2 structure is granite gneiss and it is surrounded by a shell of quartzite. In Sections XVI and XVII (Fig. 5-6) the relationships between quartzite and granite gneiss either side of this D_2 structure are clearly shown.

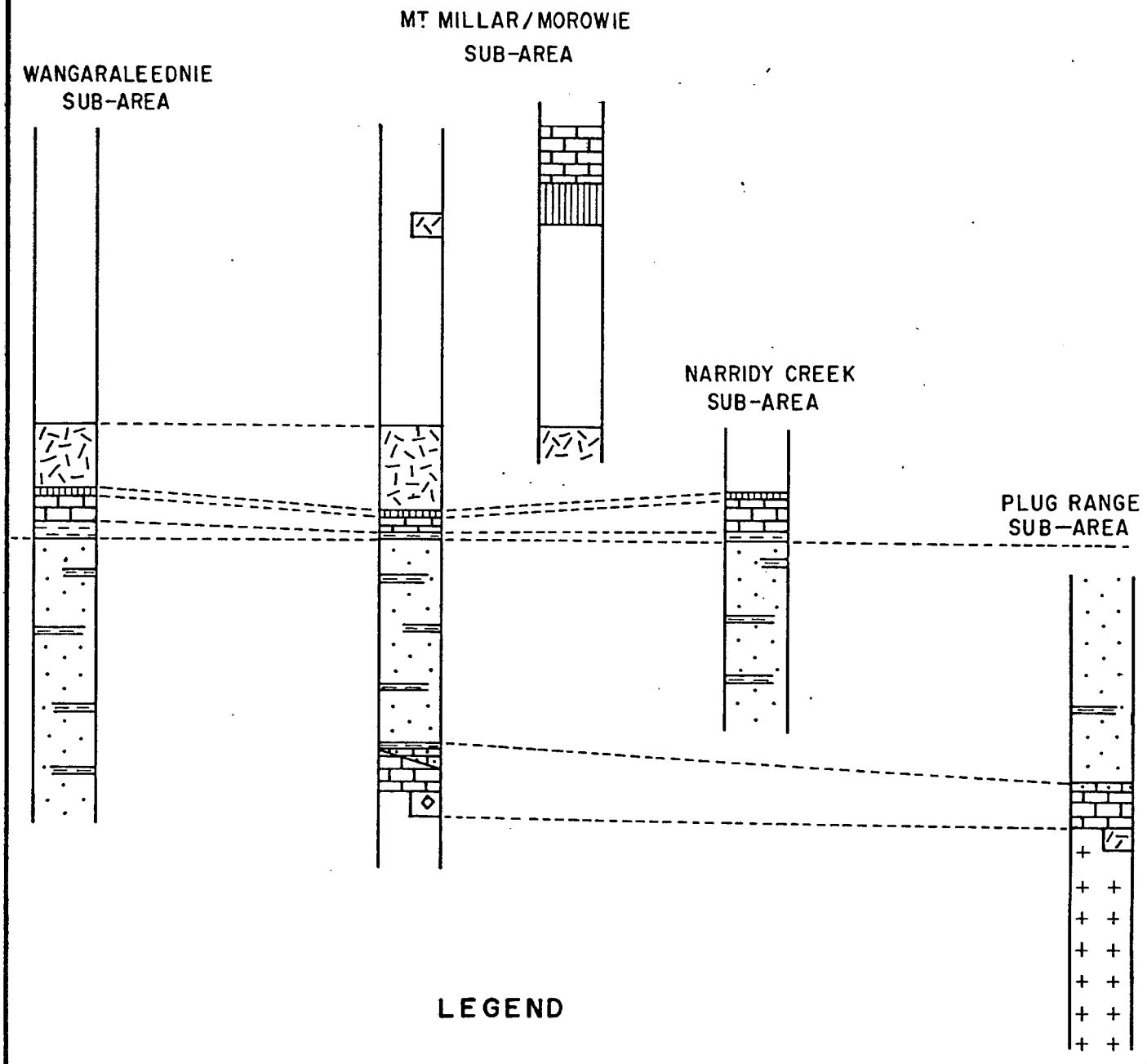
The boundary between the two lithologies on the western

side of the main D_2 antiform (Section XVI) is sharp with outcrops of each only separated by 2 metres. No other lithologies were observed along this contact but if they are present, they are not prominent. A further search north of the area studied may reveal the exact nature of the contact.

East of the main D_2 antiform the boundary between quartzite and granite gneiss is marked by a sequence of rocks from granite gneiss through pegmatite, amphibolite, more pegmatite, dolomite and layered calc-silicate into quartzite (Section XVII). The calc-silicate and amphibolite bodies only locally outcrop, but pegmatites and massive dolomite are common along strike. Not much is known of the pegmatites except that they are coarse-grained and composed mainly of quartz and plagioclase. Their exact orientation also is not known but they are locally discordant and have been represented as such in the sketch section. Their omnipresence along that boundary may, however, have some genetic significance.

Comparing the two sections and their relationship to D_2 meso- and macro-structures, it is believed that the tightness of F_2 mesoscopic folds on the western limb and the assymetry of the macroscopic F_2 limbs (Fig. 4.14) may be consequent to more intense strain on that limb with perhaps local transposition. If this is so then it is possible that the dolomite/calc-silicate bands have been drawn out and locally pinched out along that limb. Alternatively the granite gneiss may be an early, pre D_1 (it has an S_1 fabric) granite intrusive which has intruded to a higher stratigraphic level on the western side. While this cannot be completely precluded the lack of any intrusive bodies, dykes or sills, within the quartzites does not support it. Therefore the

FIG 5.7



LEGEND

- Semipelitic Gneiss and Schist
- Amphibolite
- Iron Formation
- Dolomite
- Pelitic Schist
- Quartzite
- Calcsilicate
- Diopside Rock
- Granite Gneiss

Vertical Scale: 1cm. rep. 50m.

CLEVE UPLANDS — EASTERN EYRE PENINSULA

COMPARATIVE STRATIGRAPHY OF SUB-AREAS

S13207

sequence of rocks represented by Section XVII is taken as the type stratigraphy for the Plug Range area with granite gneiss at the base.

5.3 INTERPRETATION AND DISCUSSION

Accepting that the quartzites throughout the study area represent a single unit, there is a good correlation of local sequences, particularly that sequence of rocks from what has been termed the "upper" quartzite boundary through to semipelitic gneiss. Using the quartzite as a datum, Figure 5.7 has been synthesized to compare the observed sequences outlined in each of the subareas. The quartzite is a good, consistent marker throughout the study area being massive to flaggy, and containing microcline and muscovite as essential constituents. Throughout the area there are minor pelitic interbands: in the lower grade unmigmatized areas these are biotite-muscovite schists, whereas in the migmatized areas, these are biotite-feldspar-sillimanite gneisses.

Although locally there are minor omissions from it, the sequence from quartzite into semipelitic gneiss is very clearly defined by pelite, dolomite and iron formation, with amphibolite forming a prominent marker horizon in the Wangaraleednie and Mt. Millar/Morowie subareas. The semi-pelitic gneisses vary systematically with metamorphic grade from one area to the next but otherwise do not show any pronounced variation with stratigraphic level. Northwest of Mt. Millar there is an amphibolite body (? sill) within the semipelite unit but this is not confirmed elsewhere. Also in the Mt. Millar/Morowie area, the extensive dolomite and iron formation horizons at Ferns raise the possibility of their being a separate "upper" iron formation/dolomite horizon

distinct from the "lower" dolomite/iron formation/amphibolite association.

At the so called "base" of the quartzite unit in the Mt. Millar/Morowie and Plug Range subareas, pelite, dolomite, and importantly, calc-silicate, define the boundary between quartzite and the "underlying" units. The layered calc-silicate and its associated very coarse-grained diopside rock are distinctive because they have not been recorded at the "upper" quartzite boundary. Structurally underlying the quartzite, dolomite and calc-silicate in these subareas are migmatitic gneiss and granitic gneiss. The migmatitic gneiss is more pegmatitic than the migmatized semipelites, but otherwise they are mineralogically similar. The Plug Range granite gneiss is distinctive however and may well be basement to the quartzites.

Despite this simple but convincing correlation between the various subareas, there are several problmes raised. They are:

1) the sedimentary origin with particular reference to the facing direction, of the quartzites, dolomites, semi-pelites and related rocks;
2) the nature and origin of the units "basal" to the quartzite (i.e. the Plug Range granite gneiss);
3) the origin of the amphibolites; and
4) the likelihood of a second "upper" iron formation.

5.3.1 Sedimentary Record

In considering the nature of sedimentation that formed the sequence of quartzites, dolomites, etc., and to determine some sort of certainty on the direction of facing of that sequence, two separate factors are important. They are the likeness of this sequence with classical, less deformed,

less metamorphosed series of Precambrian rocks from other parts of the world, and its relationship with the known structure.

The unique association of dolomite and iron formation overlying a major clastic unit and being overlain by a semi-pelitic unit is a very characteristic association of many of the world's major iron formations deposited around 2,000 Ma ago. Three such examples are: the Transvaal and Northern Cape Province regions of South Africa, the Lake Superior Region of North America, and the Hamersley Basin of Western Australia.

In South Africa the major lower Proterozoic iron formations occur within the Transvaal Supergroup (e.g. see Beukes, 1973). That supergroup consists of a basal clastic unit (Black Reef Formation) overlain by a predominantly chemical unit including major dolomites and iron formations (Olifants River and Ghaap Groups), which is in turn overlain by an arenaceous and argillaceous unit with thin chemical interbands (Griqualand and Pretoria Groups). The major iron formations are considered to be an end member in a carbonate sedimentary cycle (Button, 1973).

Similarly in the Lake Superior Region (e.g. see Bayley and James, 1973) iron formations are associated with chemical sediments (Menominee Group of northern Michigan) which overlies - locally unconformably - coarse clastic and dolomitic units (Chocolay Group), which are themselves overlain by a sequence dominated by greywacke and slate with minor iron formation, dolomite and volcanics (Baraga Group).

Nearer to home in the Hamersley Basin, iron formations are again associated with dolomite in a group of mainly chemical sediments (Hamersley Group). That group is part of

the Mt. Bruce Supergroup (Macleod, 1966) which incorporates a basal unit of interbanded coarse clastics and volcanics (Fortescue Group), the Hamersley Group, and an upper, locally disconformable, unit of greywacke, shale and mainly fine clastics with minor dolomite and iron formation (Wyloo Group).

Comparing thicknesses of each of the above sequences with those inferred from this study is somewhat meaningless because the Cowell region has been much more intensely deformed. Nevertheless the Hutchison Group as envisaged here is substantially thinner than the other sequences. It is believed to be of the order of 1500-2000 m thick whereas the Transvaal Supergroup is commonly 2000-5000 m thick, the Lake Superior sequence can range up to 6000 m thick, and the Mt. Bruce Supergroup is commonly 6000 to 15000 m thick.

In all of the above areas, the stratigraphic sequences are clearly defined and they outline a general sedimentary cycle of coarse clastics sitting unconformably on basement, followed by a period of chemical sedimentation, and then subsequently by a period of deeper, possibly eugeosynclinal sedimentation. Therefore, in drawing a comparison between the sequence described for the Cowell/Cleve area and those of a supposedly equivalent age of sedimentation from elsewhere in the world, a very specific model or style of sedimentation is inferred. Furthermore in drawing this worldwide parallel, not only is a facing direction inferred on the Cowell/Cleve sequence, it also suggests that those units basal to the quartzite may in fact be an older basement to the series.

Accepting this hypothesis that the clastic quartzite unit is the basal unit of the Hutchison Group and that it is overlain by finer grained, deeper water sediments with an

intervening chemical unit of dolomite and iron formation, then it is clear that D_2 antiformal structures which have either granite gneiss, calc-silicate or quartzite as a core are actually true anticlines.

5.3.2 The Basement Controversy

Considering firstly that the Plug Range granite gneiss structurally underlies the quartzite metasediments, and secondly, that from similar metasedimentary sequences around the world quartzites characteristically form the basal unit, then there exists a strong case to suppose that the Plug Range granite gneiss is basement to the Hutchison Group.

In order to test this, several samples were collected and submitted to Amdel for dating. The results are tabled in a progress report by Webb (1977) and included here as Appendix B. They give a Model 3 isochron with an age of 1697 ± 65 Ma and an initial Sr^{87}/Sr^{86} ratio of 0.7340 ± 0.0048. Webb discusses these results briefly and points out that the unusually high initial ratio for rocks of this age implies "reworking" of much older crustal rock (Moorbath, 1975). He estimates that a rock of composition equal to the average of those samples used would take about 450 Ma to increase its Sr^{87}/Sr^{86} ratio to such an initial value. Hence an age of about 2150 Ma can be inferred for the parent material of the Plug Range body. While such an age is younger than the ca. 2600 Ma dates from Cape Carnot (Cooper et al, 1976) and the ca. 2400 Ma dates from the Whidbey Islands (Webb and Thomson, 1977), it is the oldest age yet obtained from the northeastern part of Eyre Peninsula. As such it clearly antecedes by some 450 Ma the major metamorphism affecting the region (ca. 1700 Ma, see Appendix B) and the intrusion of the syntectonic Middle Camp, Carpa and Narridy

Creek granites (ca. 1650 Ma. see Appendix B).

Considering these figures and considering that there is a strong S_1 fabric in the gneiss, there are three possible models for the Plug Range granite gneiss;

1) it could be basement to the Hutchison Group;
2) it could be remobilized basement to the Hutchison Group intruded before D_1, or
3) it could be a basal metasedimentary unit deposited sometime around 2150 Ma.

Of the first two alternatives while an intrusive model cannot be completely overruled, the basement model is preferred because there is a distinct absence of xenoliths of Hutchison Group rocks in the gneiss, and furthermore there are no granite gneiss sills or dykes within the metasediments.

Comparing the first and third models and comparing the figure of 2150 Ma with the likely age of sedimentation for the Hutchison Group rocks it is not clear whether the Plug Range body forms a basement or not. Unfortunately there are no dates available on the sedimentation age of the metasediments. However by drawing a parallel between the Hutchison Group and the worldwide development of iron formations, a likely age of sedimentation is 1900-2200 Ma (Goldich, 1973). The parental material of the Plug Range granite gneiss could therefore be either basement implying a sedimentary age of 1900-2000 Ma for the Hutchison Group, or else it could be a major basal unit of the Hutchison Group that has been granitized. In view of its size, its homogeneity, its relationship with the quartzites etc., and the absolute lack of any recognizable sedimentary features or even interlayered rocks of possible sedimentary origin, the basement alternative is preferred.

Unlike the Tumby Bay region where Coin (1976) somewhat tenuously demonstrated an additional deformation in the Flinders Group rocks, the Plug Range granite gneiss does not. The granite gneiss records a similar structural evolution to Coin's Flinders Group rocks but an extra deformation has been recognized in the Hutchison Group rocks. It is firmly believed that because of the intensity of the D_1 and D_2 deformations any anteceding structures if they existed would have been almost completely overprinted and therefore no longer recognizable. Consequently the apparent lack of pre D_1 structure in the Plug Range body does not necessarily preclude the basement hypothesis.

5.3.3 Origin Of Amphibolites

There are two principal modes of origin for amphibolites:

1) Metamorphosed igneous intrusives (sills) or extrusuives (lava sheets);

2) metamorphosed carbonate-pelite mixtures.

Both modes have been proposed at various times to describe the origin of conformabl amphibolite bodies on Eyre Peninsula. Tilley (1921) considered that they were:

> "metamorphosed igneous rocks (sills) of slightly higher acidity than the normal gabbroid or doleritic type of intrusive",

and Edwards (1936) considered that they represented:

> "basic igneous rocks which, from their interbedded and folded relations with the schists, were either sills intruded before the folding, or more probably, contemporaneous lava flows".

The alternative mode was put up by Johns (1961) who believed them "to represent metamorphosed dolomitic shales".

This problem of distinguishing between amphibolites

FIG. 5.8

GEOCHEMISTRY OF AMPHIBOLITES

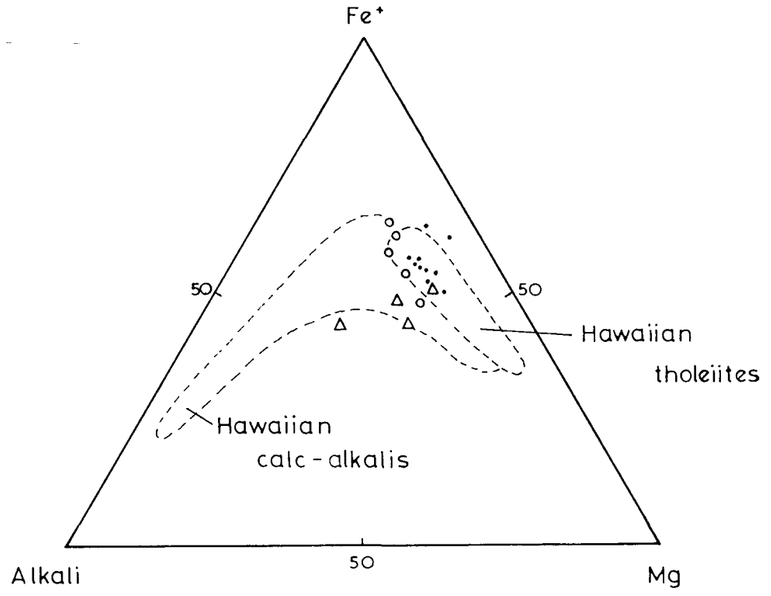
Cleve Uplands, Eastern Eyre Peninsula

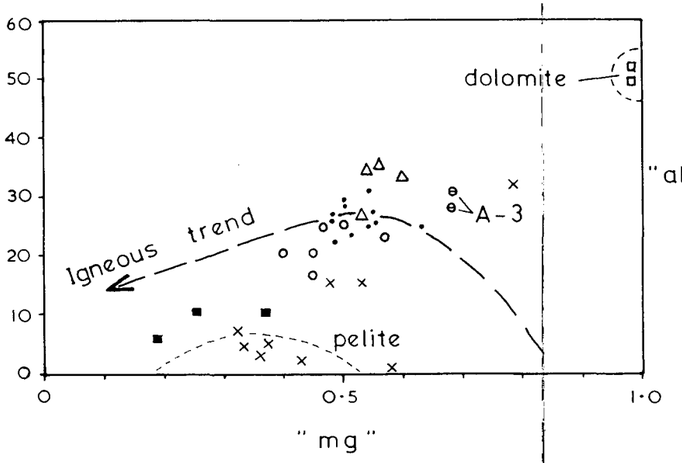
a) Diagrams below compare the amphibolites with the metasediments (after Leake, 1964).

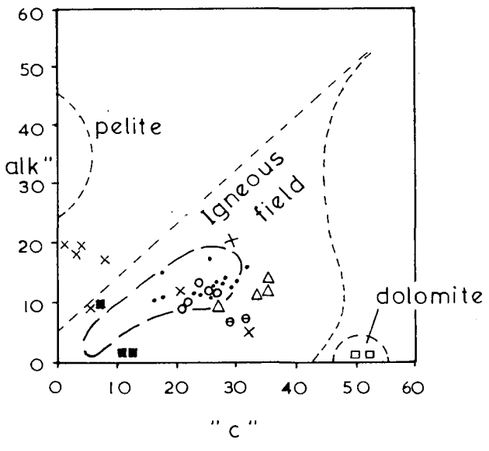
b) Diagrams to the right compare the amphibolites with some basic igneous rocks (after Kuno, 1968).

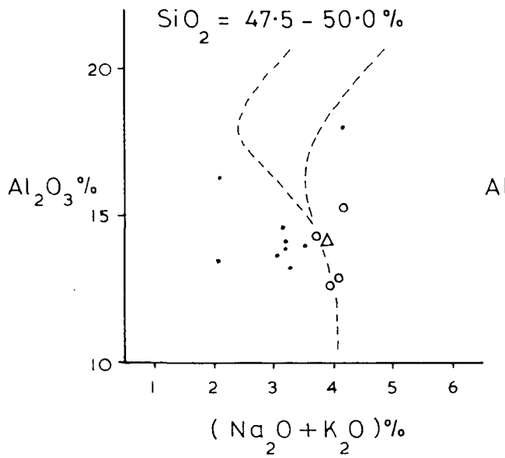
Legend

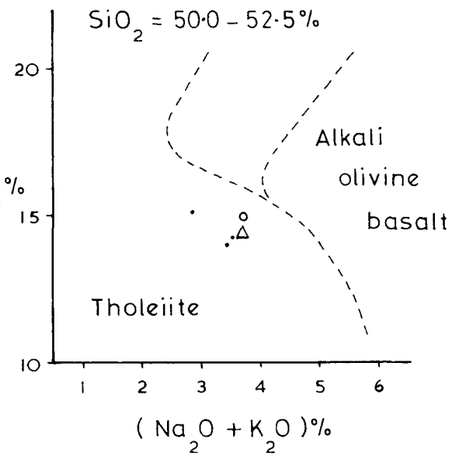
- · Schistose amphibolite
- o Porphyroblastic amphibolite
- Δ Layered (Cpx rich) amphibolite
- × Semipelitic gneiss
- ▪ Iron formation
- ▫ Dolomite

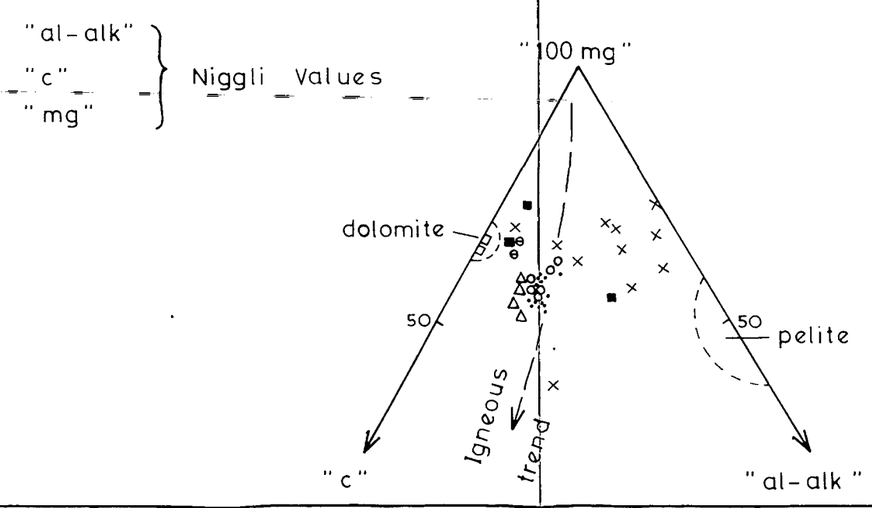


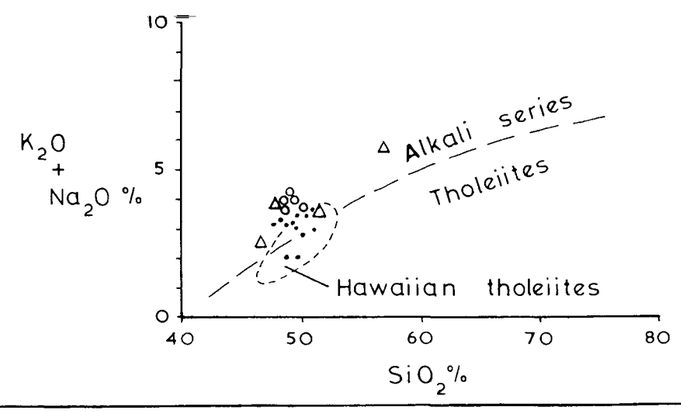












of igneous and sedimentary origin is common to most high grade terrains in the world (e.g. Leake, 1964; van de Kamp, 1968). Often there is no definite solution to the problem, but in the Cowell/Cleve district, there are several features which suggest that an igneous origin, particularly a lava flow, is the most likely. The evidence for this is two fold.

Firstly, both in the field and under the microscope, the amphibolites prove to be relatively massive and homogeneous not only along strike but also across strike. The only major variations are the porphyroblastic and well layered types but these are both of restricted occurrence. Upper and lower boundaries are sharp but there is very minor contamination on the scale of a few centimetres. The porphyroblastic amphibolite may however reflect a boundary condition of metasomatic/metamorphic origin in that it is frequently associated with the upper boundary. Although the amphibolites separate dolomitic and semipelitic rocks, there are no interlayered carbonate or other obvious sedimentary bands.

Secondly, considering the geochemistry of the amphibolites and adjacent rocks, the general field criteria are enhanced (Appendix A; Fig. 5.8). There is very little compositional variation from bottom to top across the major bodies and the boundaries are sharply defined. Their general compositions conform to basic igneous trends (Fig. 5.8) and while they roughly fall midway between dolomite and pelite compositions, there is not a gradational change from dolomite to iron formation to amphibolite to semipelite. In fact the amphibolites lie slightly off the pelite/dolomite trend. Other factors supporting an igneous origin are, the TiO_2:P_2O_5 ratios which are mostly comparable to basalts (i.e. ≈ 10-11, R.W. Nesbitt, pers. comm.), the Fe_2O_3* and Al_2O_3 contents which are also

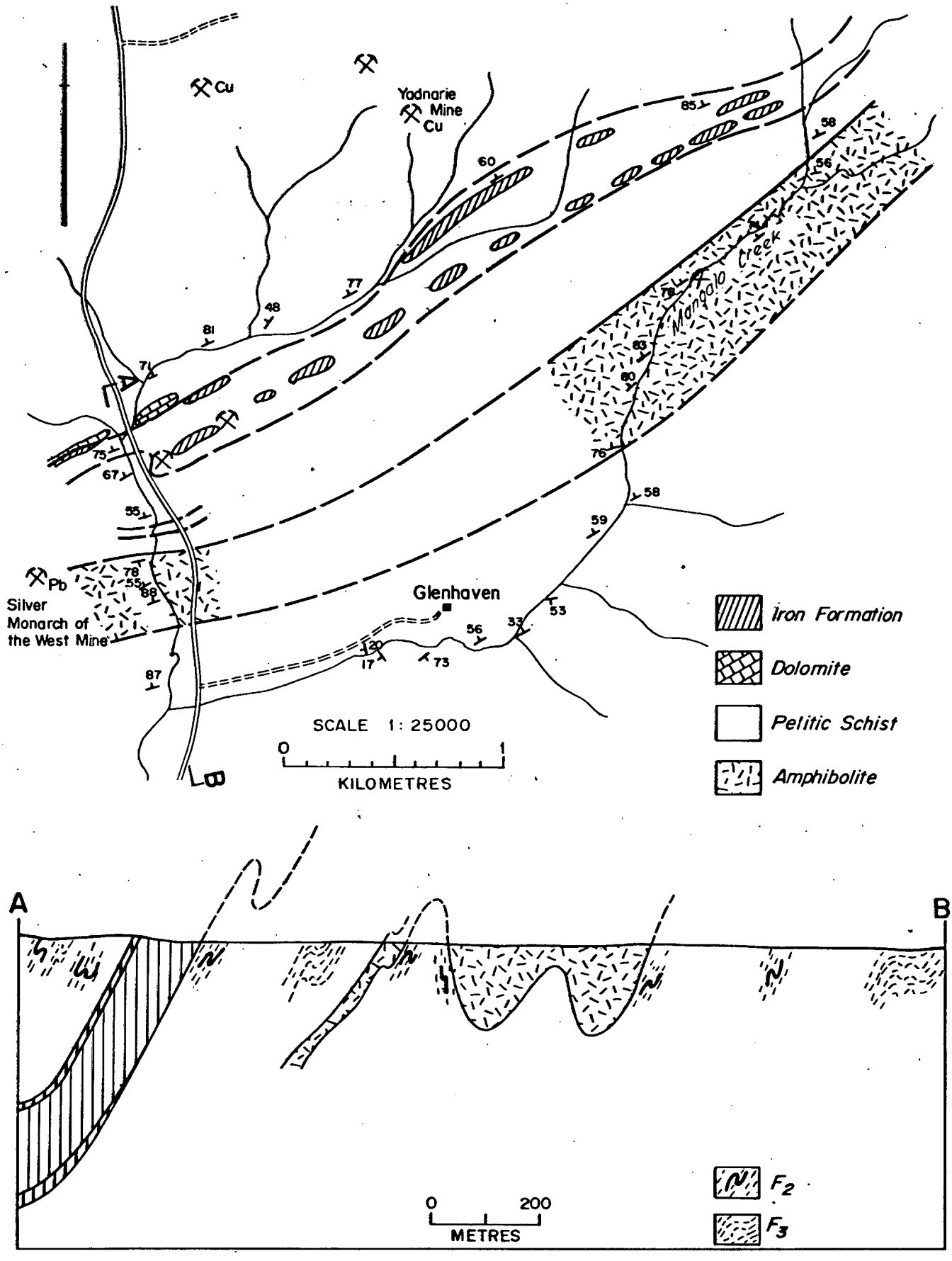
comparable to basaltic rocks (cf sedimentary amphibolites often have Fe_2O_3* > 18%, A. Pruvis, pers. comm.), and the MnO contents which are mainly of the order of 0.2% whereas sedimentary amphibolites often have MnO > 0.4% (A. Purvis, pers. comm.). In addition, the amphibolite compositions are consistent with a quartz theolite parental material (Fig. 5.8).

Consequently it is concluded that an igneous origin is more likely than a sedimentary origin. To distinguish between an intrusive or extrusive origin however is more difficult. On structural grounds, the amphibolites were definitely deformed by the D_2 deformation. However there is no positive evidence of an earlier D_1 fabric (see Chapt. VI) which suggests that they may have been intruded as sills during or after D_1. Against that view though is the gross conformability of the amphibolites at a quite specific stratigraphic horizon thus suggesting an origin related to deposition of the Hutchison Group (i.e. as lava flows). Furthermore the amphibolites are homogeneous bodies and do not reveal any evidence of differentiation which is common in most sills. In either model, however, the absence of feeder dykes is a curious anomaly. Therefore it can only be concluded that the amphibolites are most likely of igneous origin but that the mode of igneous origin is uncertain.

5.3.4 An Upper Iron Formation

The presence or not of a second iron formation has some quite important implications when comparing the local stratigraphy with other parts of Eyre Peninsula. It was suggested above (Section IX, Fig. 5-4) that it was possible the great thickness of banded iron formation and dolomite at Ferns may represent a second iron formation. While this could not be resolved at Ferns and is in fact doubted on a structural

FIG. 5-9



GEOLOGICAL PLAN AND CROSS SECTION OF THE CLEVELEY / GLENHAVEN AREA

DEPT. OF MINES AND ENERGY - S.A.

S13162

interpretation (Sect. 5.5), a second iron formation has been demonstrated to exist in an area northwest of Cleve. In that area, a major iron formation, surrounded on both sides by schists, had been previously mapped by Johns (1961; see Plan 1).

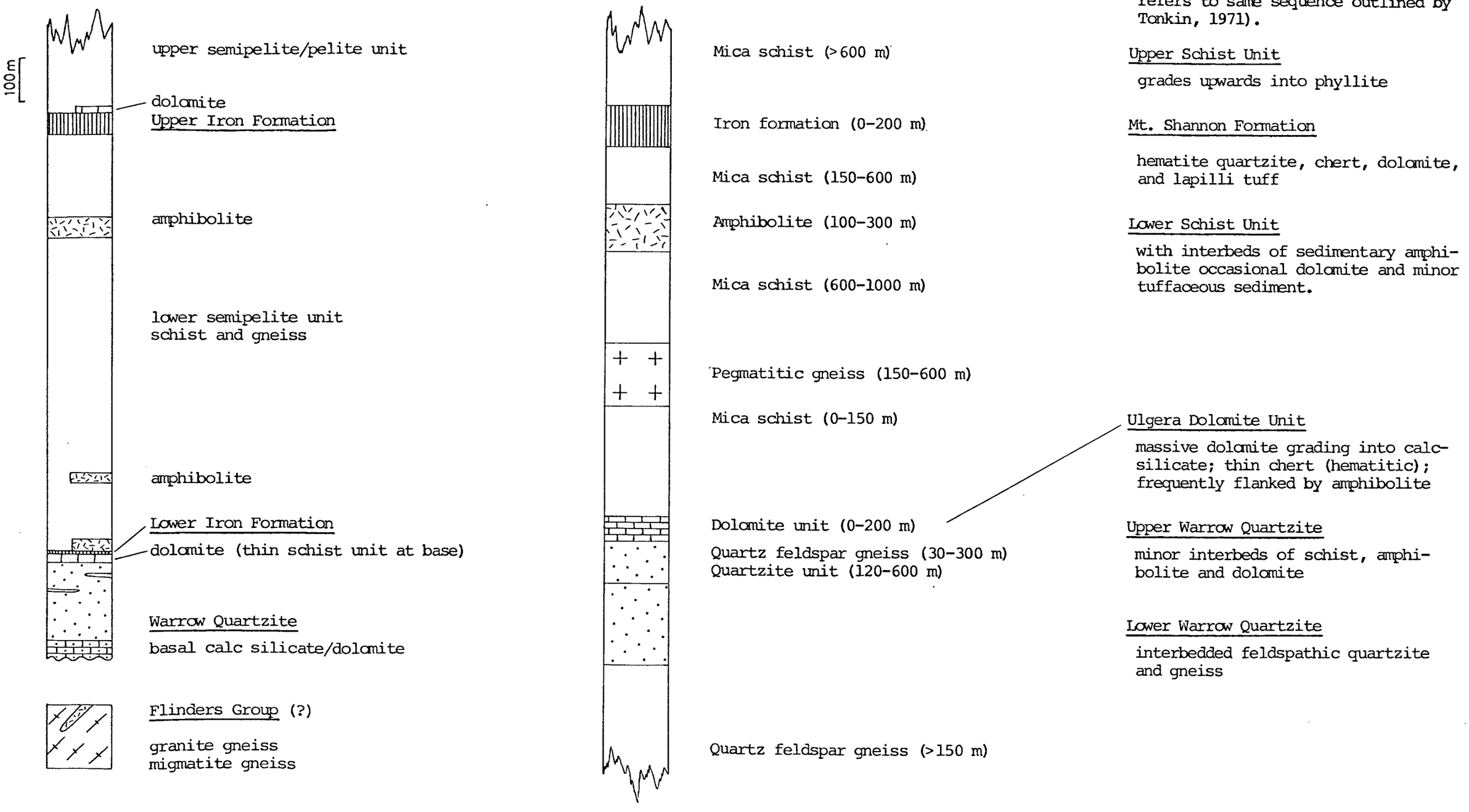
Cleve itself is just south of a major D_3 antiform in which quartzite forms a prominent core. Structurally overlying the quartzite is a thin dolomite band (locally with iron formation) and then a sequence of sempelitic schists and gneisses with scattered conformable pegmatite and amphibolite bodies. Approximately 2.5 km northwest of the quartzite/dolomite contact within the schists and still on the northwest limb of the antiform, is the Mt. Shannon iron formation. A rough sketch map and cross section of this iron formation in the Cleveley/Glenhaven area is shown in Figure 5.9.

In that area, the schists and related rocks are folded by tight F_2 folds with strong axial planar fabrics. These have subsequently been refolded by more open F_3 buckles and crenulations. Both F_2 and F_3 plunge shallowly to the southwest.

Based on this structural interpretation, the sequence exposed in Glenhaven area begins in quartz veined schist and passes successively through amphibolite (blue-green hornblende), schist then iron formation and dolomite, and ends in further quartz veined schist. Such a sequence which is quite remote from major quartzites (i.e. feldspathic quartzites), implies that there is definitely a prominent upper iron formation associated with dolomite. A note worth making here in connection with the Glenhaven area is that there are some minor banded quartzites (of iron formation affinity)

FIGURE 5.10 A

STRATIGRAPHIC CORRELATION IN THE CLEVE UPLANDS, EASTERN EYRE PENINSULA



closely associated with the major amphibolite body. It infers that there may well be some genetic relationship between the origins of these two lithologies.

5.4 CONSLUSIONS AND REGIONAL APPRAISAL

In conclusion then, a stratigraphy can be erected for the complexly folded rocks of this study. That stratigraphy consists of a basal unit, the Flinders Group gneisses, which incorporates the Plug Range granite gneiss and probably the migmatitic gneisses of the Atkinson mine area. That this unit is basement to the overlying rocks could not be positively confirmed by the present study but, however, it is not denied.

Overlying the Flinders Group is the Hutchison Group. It is a metasedimentary unit consisting of basal calc-silicate/dolomite, feldspathic and micaceous quartzite with scattered pelitic schist and gneiss interbands, thin but prominent massive dolomite (with a thin pelitic band separating it from the quartzite below), a thin iron formation, and a thick unit of semipelitic schist and gneiss. Amphibolites are present locally within this sequence and in particular are common above the lower iron formation and dolomite units. Adding to this sequence the sequence exposed northwest of Cleve, then the semipelitic rocks pass upwards into a second iron formation with local dolomite, and finally into further semi-pelitic to pelitic schist. Allowing for the tight folding, a combined thickness from the base of the quartzite to the top of the upper iron formation is estimated at about 1250 m. This broad stratigraphy is shown schematically in Figure 5.10.

Such a stratigraphic succession compares very favourably with unpublished private company work carried out in the Cleve Uplands. Tonkin (1971) of Pacminex Pty. Ltd. mapped

an area west of the Wangaraleednie fault and extending across to and including the Mt. Shannon iron formation. He erected a simple stratigraphy based on the succession of rocks northwest from Cleve to Mt. Shannon. This is shown in Figure 5.10 along with his thickness estimates. He did not take into account any folding and hence his stratigraphy is considerably thicker than conceived by this study. Thomson (1976) also measured off the distance between the quartzite and Mt. Shannon iron formation and without allowing for folding quoted 2000 m as the thickness. While it is not agreed that that figure represents the present thickness of the semipelite unit, it is conceded that it may be more representative of the original thickness prior to deformation.

More recently Duncan (1976) working for Carpentaria Exploration Company Pty. Ltd., over an area including the ex-Pacminex area but extending much further west thereof (across to Rudall and Carappee Hill), concluded that the Cleve/Mt. Shannon section represented a valid working stratigraphy for the Cleve Uplands. He modified Tonkin's section and informally named many of the units (Fig. 5.10). Duncan correctly correlated the basal quartzites with the Warrow Quartzite (see discussion below), but the names "Ulgera Dolomite Unit" and "Lower Schist Unit" are believed to be misleading. As discussed above and shown in Figure 5.4 (Section IX) the massive dolomite of Ulgera Gap, which is the same body as that at Ferns is <u>not</u> typical of that unit immediately overlying the quartzite. Not only is it much thicker than normal, but doubt has been expressed concerning its stratigraphic level. To call the semipelitic unit overlying the dolomite the "Lower Schist Unit" is also misleading because as is clearly detailed in this thesis,

FIGURE 5.10 B

STRATIGRAPHY OF THE MIDDLEBACK RANGES

MILES (1954)

MIDDLEBACK GROUP

Upper Middleback Quartzite

banded hematite quartzites and interbedded schist (150-250 m)

Cook Gap Schists

schist and phyllite (10-300 m)

Lower Middleback Quartzite

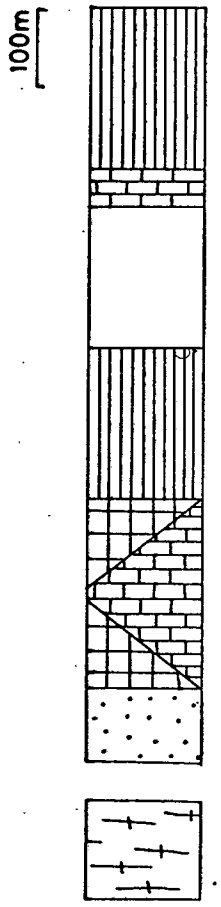
banded hematite quartzites and interbedded schist (150-250 m)

Middleback North Dolomite

cherty (at top) dolomitic marble (60-150 m)

Gneiss Complex

schist, quartzite, migmatitic gneiss, genissic granite



FURBER AND COOK (1976)

unconformity

Upper Middleback Jaspilite

Cook Gap Schist

dolomitic at top

Lower Middleback Jaspilite

Middleback North Dolomite and Carbonate Zones

massive dolomite at base grading to chert at top

Sericite Quartzite

"Gneiss Complex"

ortho and para gneiss and schist

* NB concordant amphibolites (ortho and para) interbedded in sequence

the semipelitic unit represents not only schists and gneisses, but also their migmatitic variants which can no longer be classified as schists.

Going further afield and correlating the stratigraphy of the Cowell/Cleve area with that of the Middleback Ranges, there is also a favourable comparison. The basic stratigraphy of that area, as outlined by Miles (1954) and modified by Furber and Cook (1976), is shown in Figure 5.10. The basal (Warrow) quartzite is not very prominent there but N. Lemon (B.H.P.; pers. comm.) believes that some of the gneissic granites of the "Gneiss Complex" represent partially granitized or assimilated quartzite. This is highlighted in the area east of the Middleback Ranges where Miles' "Gneiss Complex" rocks have large blocks of quartzite and metasediment enclosed within them (e.g. Deep Creek, Wertigo Rock Hole). Thicknesses of the various units of the Middleback Group are also drastically different from the Cowell/Cleve area. The Cook Gap Schist is most notable amongst these, but its progressive thickening from the north end to the south end of the ranges suggests that further south it may thicken even more substantially. This would make it consistent with the stratigraphy of this thesis. Otherwise the remarkable similarity in lithology between the two stratigraphies encourages an informal naming of the sequence from the top of the feldspathic (Warrow) quartzite to the top of the upper (Mt. Shannon) iron formation in the Cowell/Cleve area, as the Middleback Group.

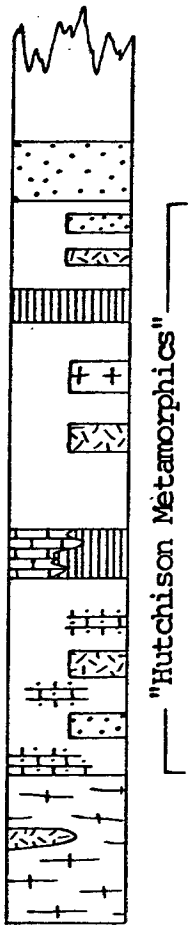
By establishing such a correlation between the Middleback Ranges and the Cowell/Cleve area, the familiar stratigraphic relationships of Thomson (1969) are invalidated. Thomson incorporated the Middleback Group into his "Gneiss" Complex

FIGURE 5.10C

INFERRED STRATIGRAPHY OF SOUTHERN EYRE PENINSULA

WHITTEN (1966)

(Not to scale but total thickness of the Hutchison Metamorphics was inferred to be greater than 10,000 m).



"Hutchison Metamorphics"

"Dutton Metamorphics"

including basal Warrow Quartzite, schist and gneiss.

Sericitic quartzite, schist and amphibolite.

Koppio Jaspilite

Amphibolite, gneiss, schist and pegmatite

Greenpatch Jaspilite

with dolomite

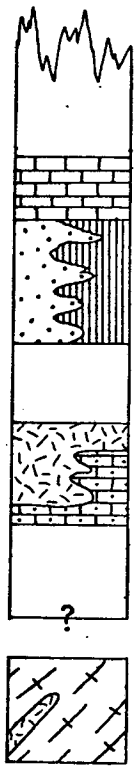
Calc-silicate Horizon with amphibolites, minor schist, gneiss and sericite quartzite

"Flinders Gneiss"

augen gneisses and interlayered amphibolites

COIN (1976)

(Not to scale)



Hutchison Group

Pelitic, semipelitic and minor calc silicate schists

Siliceous Marble and Ophicalcite Unit (graphite schist at base)

Layered quartzite (Warrow equivalent) layered chert and Banded Iron Formation

Garnet schist

Layered amphibolite and layered calc silicate

Pelitic and Quartzofeldspathic Schist

Flinders Group

granitic and augen gneiss

while the Mt. Shannon iron formation he incorporated into the Hutchison Group much higher in the sequence. Such a stratigraphy is now unacceptable. Furthermore besides this obvious anomaly, it is vague and unnecessarily redefines the "Gneiss" Complex and the Hutchison "Group". As detailed in Chapter I of this thesis, Hutchison Group should be kept in the original context portrayed by Tilley (1920) to include all the Lower Proterozoic metasediments. However, a note of caution is afforded here concerning the presence of banded gneisses of metasedimentary affinity in the Cape Carnot area (Fanning, 1975; Cooper et al, 1976) and near Tarcoola (Daly et al, 1968) which are of Archaean age and which should not be confused with the Hutchison Group.

On southern Eyre Peninsula the stratigraphy is quite confusing and no workers have yet been able to satisfactorily resolve it. The two principal documentations are those of Whitten (1966) and Coin (1976) (Fig. 5.10). Whitten's interpretation was very subjective in that he believed the whole region was one large synform with an axis through the Marble Range/Mt. Greenly area. Such an interpretation is poorly founded and ignores the numerous, very tight folds on the eastern side of the peninsula. Coin's interpretation is much better founded, but is still questionable in that he does not present any suitably detailed mapping to support it. However in his defence outcrop is very poor in that region and as noted by Whitten (1966), "all formations cannot... be defined". Within the Hutchison Group, Coin recognizes four main subdivisions, a basal amphibolite and schist unit, a layered quartzite/Banded Iron Formation unit, a major carbonate unit and an upper pelitic/semipelitic schist unit. There are some broad similarities here with the

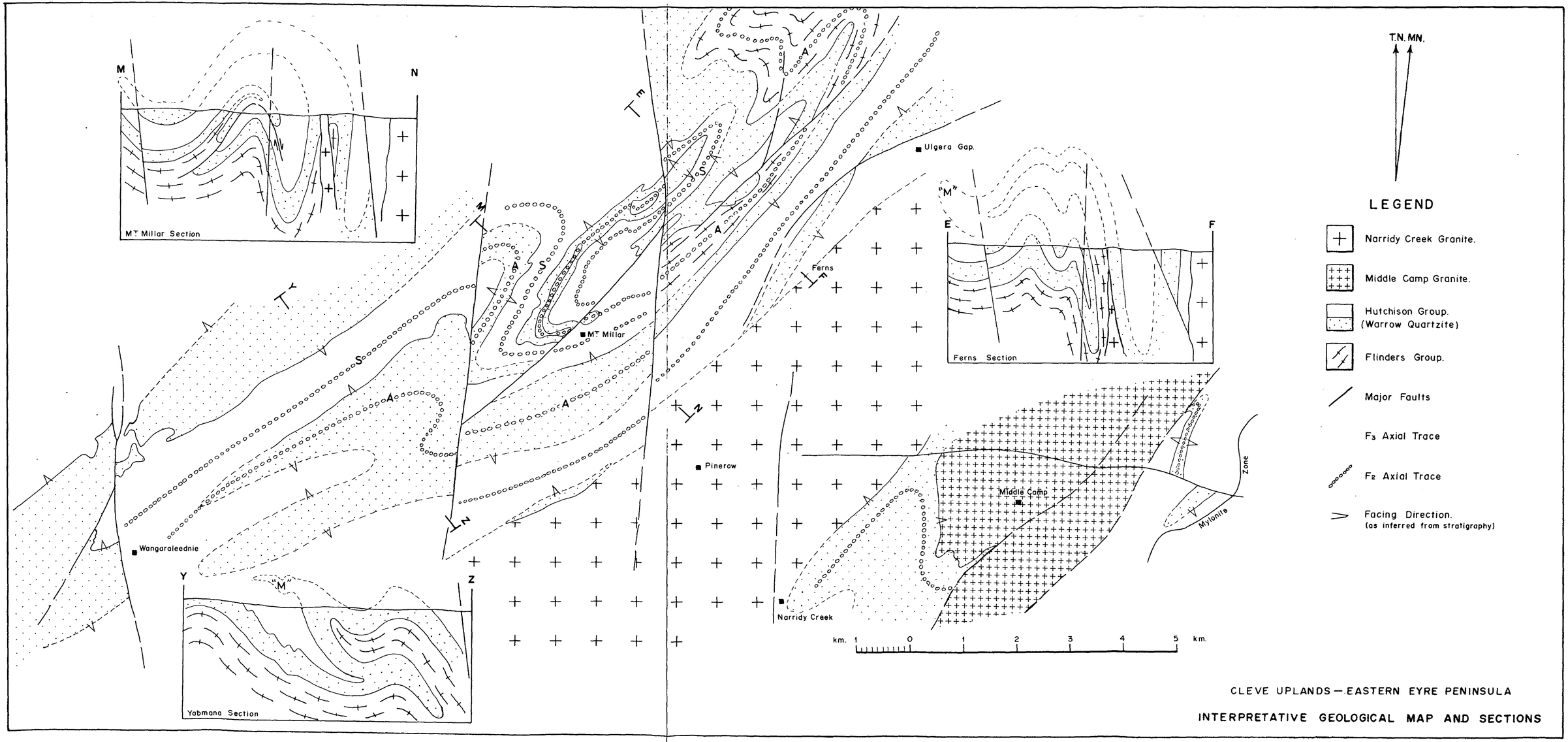
sequence in the Cowell/Cleve area. The principal feature is the layered quartzite to carbonate to schist sequence. This sequence almost certainly correlates with that of this thesis. In particular, the layered quartzite has a very strong likeness to the major quartzite of the Cowell/Cleve area. However, Coin considers that this feldspathic and micaceous quartzite is laterally equivalent to the non-feldspathic banded iron formation! He does not present any evidence to substantiate this, and furthermore his mapping does not show the two ever merging into one another. Therefore the two lithologies may well be separate units.

On the western side of southern Eyre Peninsula, the "type" Warrow Quartzite has been considered by different workers as a unit above the Hutchison Group (Tilley, 1920; Whitten, 1966) and as a unit within the Hutchison Group (Johns, 1961; Thomson, 1969; Coin, 1976). It lies apparently conformably on granitic gneisses dated at ca. 2250-2350 Ma (Webb A.W., pers. comm.) which tentatively makes them (the granite gneisses) part of the older basement. The quartzites are micaceous and feldspathic and are visually identical to those in the Cowell/Cleve area. In fact the geology of this area is analogous to the Plug Range area. Consequently the characteristic feldspathic quartzites of the thesis area are believed to be stratigraphically equivalent to the Warrow Quartzite.

5.5 STRUCTURAL IMPLICATIONS

Having established an informal stratigraphy for the Cowell/Cleve district and having demonstrated that it is consistent with other areas on Eyre Peninsula, it is appropriate to consider what implications that stratigraphy has on the structure of the study area. In Chapter IV several macro-

FIG 5.11



CLEVE UPLANDS — EASTERN EYRE PENINSULA

INTERPRETATIVE GEOLOGICAL MAP AND SECTIONS

78-153

scopic D_2 structures were indicated but however considering the stratigraphy several other macroscopic D_2 structures are necessary. These are outlined in Figure 5.11, an interpretative map outlining the distribution of all the major quartzites and the facing direction implied by the stratigraphy.

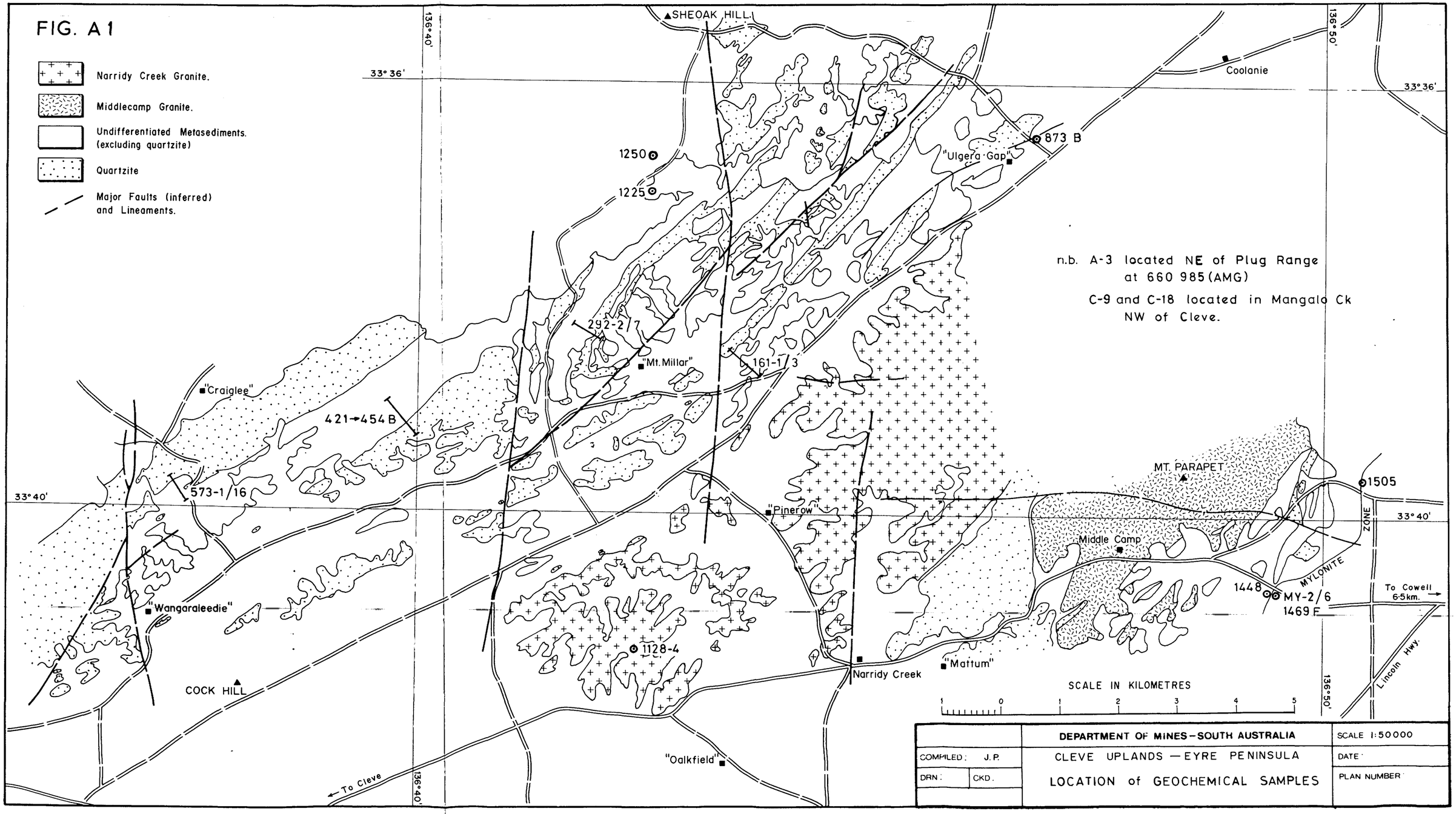
In the Wangaraleednie subarea macroscopic F_2 folds have already been clearly indicated (Fig. 4.2) but in Figure 5.11 a wider, more generalized cross section has been sketched. It illustrates the major F_2 fold pair being refolded about the macroscopic F_3 folds. A similar situation exists in the Mt. Millar/Morowie subarea. The stratigraphy outlines a series of macroscopic F_2 folds which have also been folded about F_3 structures. Interpretive cross sections have been constructed through Mt. Millar and Ferns (cf. Fig. 4.4) and they clearly indicate a major F_2 fold pair-antiform and synform-which is analogous to the F_2 structures of Wangaraleednie subarea. In fact so close is the resemblance that all the antiformal F_2 structures labelled "A" (in Fig. 5.11) and all the synformal F_2 structures labelled "S" (in Fig. 5.11) are believed to be the same macroscopic structures. They have been offset across the various faults throughout the area but otherwise can be traced with a fair amount of confidence.

Perhaps one of the most significant features of these structures is that they confirm the north-south F_2 fold trend implied by the mesoscopic fabric elements (Fig. 4.16). While specific F_2 fold closures are not evident in the field, (at least within the bounds of the study area) they can be easily traced on the interpretive cross sections. One such F_2 fold nose labelled "M" in the Ferns and Mt. Millar sections can

be clearly seen to "move across" the Mt. Millar/Morowie antiform implying an F_2 axial trend oblique to the F_3 trend.

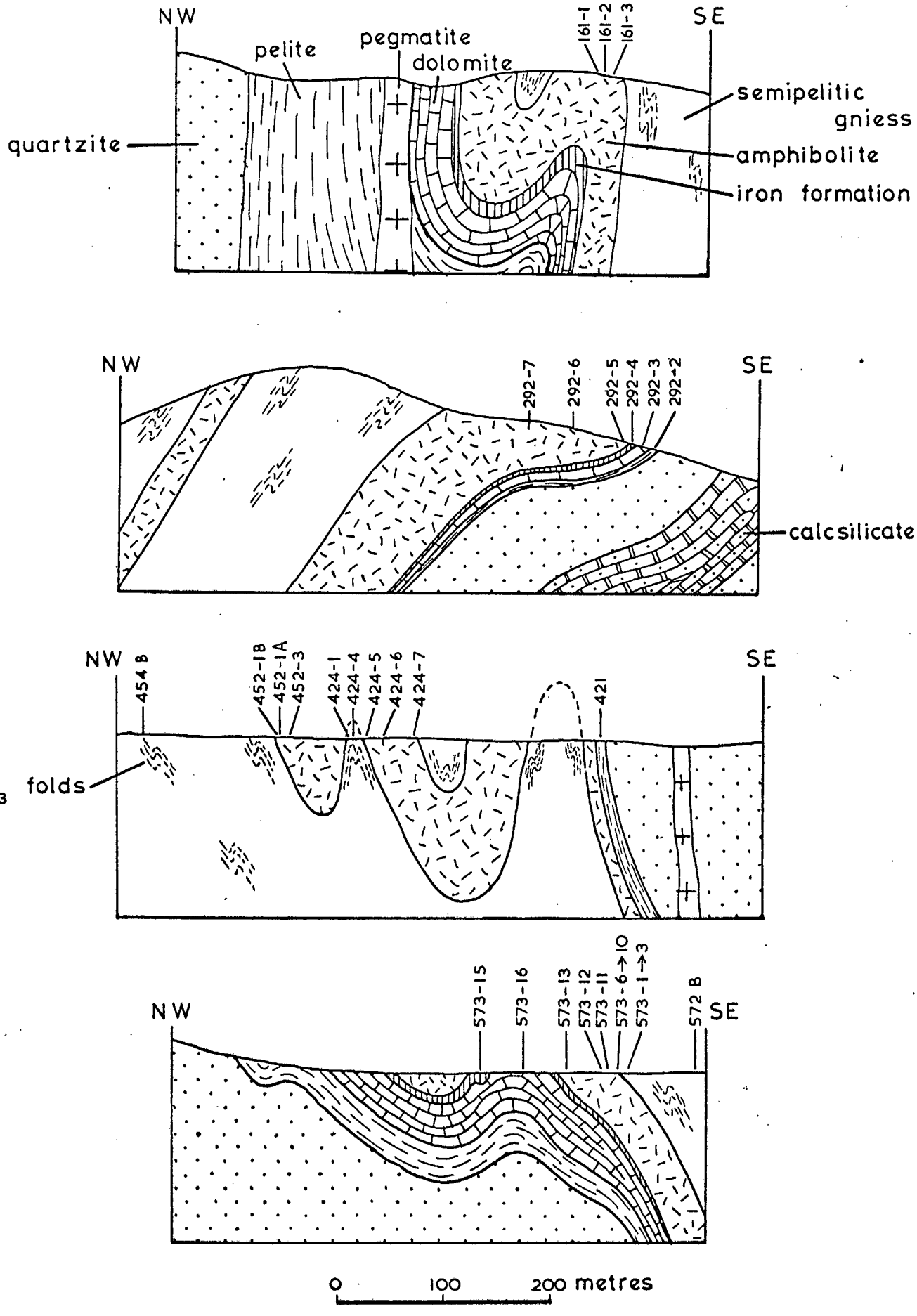
Finally, having been able to apply the stratigraphy to the structural problem and having been able to relate each of quartzite bodies to each other with such a simple refolding mechanism, it must raise the confidence level on the actual stratigraphy itself. That such a stratigraphy has been realized in this part of Eyre Peninsula where deformation, metamorphism and plutonism have all been intense, represents a very major breakthrough in the understanding of the geology of Eyre Peninsula. In the following chapters the physical conditions that were applied to these rocks during their complex evolution will be looked at in more detail.

FIG. A1



	DEPARTMENT OF MINES—SOUTH AUSTRALIA	SCALE 1:50000
COMPILED: J.P.	CLEVE UPLANDS — EYRE PENINSULA	DATE:
DRN: CKD.	LOCATION of GEOCHEMICAL SAMPLES	PLAN NUMBER:

FIG. A2



LOCATION OF GEOCHEMICAL SAMPLES

APPENDIX A

CHEMICAL ANALYSIS

Chemical analyses of 50 rock specimens collected during the course of this study are tabulated below. Their locations and relationships with the stratigraphy are shown in Figures A1 and A2, and their petrographical names and major constituents are listed immediately below.

The symbols are: Bi (biotite), Chl (chlorite) Cpx (clino-pyroxene), Do (dolomite), Ep (epidote), Ga (garnet), Gr (grunerite), Hb (hornblende), Hyp (hypersthene), Kf (K-feldspar), Mu (muscovite-sericite in mylonites), Op (opaque minerals), Pl (plagioclase), Q (quartz), Sph (sphene), Serp (serpentine), Tr (tremolite).

AMPHIBOLITES

A-3	Porphyroblastic lamprophyre (gabbro)	Hb-Cpx-Pl-Kf-Q
C-9	Amphibolite (schistose)	Hb-Pl
161-1	Amphibolite "	Hb-Pl(-Px)
161-2	Porphyroblastic amphibolite	Hb-Pl(-Q)
292-5	Amphibolite (schistose)	Hb-Pl
292-6	Amphibolite "	Hb-Pl
292-7	Amphibolite "	Hb-Pl
424-5	Amphibolite "	Hb-Pl
424-6	Layered amphibolite	Pl-Cpx-Hb
424-7	Amphibolite (schistose)	Hb-Pl-Q(-Bi)
452-1A	Amphibolite "	Hb-Pl
452-1B	Porphyroblastic amphibolite	Hb-Pl
452-3	Layered amphibolite	Pl-Hb-Cpx
573-7	Amphibolite (schistose)	Hb-Pl-Op(-Bi)
573-8	Prophyroblastic amphibolite	Hb-Pl
573-9	Porphyroblastic amphibolite	Hb-Pl
573-10A	Porphyroblastic amphibolite	Hb-Pl-Q-Bi
573-12	Amphibolite (schistose)	Hb-Pl
573-13	Amphibolite "	Hb-Pl
1128-4	Amphibolite "	Hb-Pl
1225	Layered amphibolite	Hb-Pl-Cpx
1250	Amphibolite (schistose to weakly layered)	Hb-Pl(-Cpx)

METASEDIMENTS

C18	Amphibole-mica schist	Hb/Tr-Q-Bi-Pl-Op
161-3	Iron formation	Hyp-Ga-Gr-Op-Q
292-2	Migmatite gneiss	Kf-Bi-Q-Mu-Si
292-3	Dolomite	Do-Serp
292-4	Grunerite schist (iron formation)	Gr/Hb-Q(-Op)
421	Podded gneiss	Q-Pl-Kf-Bi-Mu-Si
424-1	Amphibole gneiss	Pl-Q-Hb-Bi
424-4	Calc-silicate	Pl-Q-Cpx-Hb

454B	Quartzofeldspathic gneiss	Q-Pl-Bi-Mu-Ga
572B	Quartzfeldspathic gneiss	Q-Pl-Mu-Bi-Ga
573-1	Quartzofeldspathic gneiss (/schist)	Q-Pl-Mu-Bi-(-Ga)
573-2	Quartz-feldspar-mica schist	Q-Pl-Mu-Bi-Op
573-3	Quartzofeldspathic gneiss	Pl-Q-Bi-Op
573-6	Ironstone	Op-Pl-Q-Hb
573-10B	Amphibole gneiss	Pl-Hb-Q-Bi
573-11	Quartzofeldspathic gneiss	Q-Pl-Bi-Op-Ga
573-15	Banded quartz-amphibole rock	Gr/Hb-Q(-Ga-Op)
573-16	(552) Dolomite	Do-Tr
878B	Calc-silicate quartzite	Q-Kf-Cpx-Pl-Tr
1448	Migmatite gneiss	Q-Kf-Pl-Bi/Chl-Ga

MYLONITIC ROCKS

MY-2	Mylonitic gneiss	Pl-Q-Kf-Mu-Chl
MY-3	Mylonite	Q-Pl-Chl-Mu-Op
MY-4	Mylonite	Q-Pl-Kf-Chl-Mu
MY-5	Slaty mylonite	Q-Pl-Kf-Chl-Mu
MY-6	Slaty mylonite	Q-Pl-Kf-Chl-Mu
1469F	Mylonite (discordant "fluid" phase)	Feld-Chl-Ep-Sph
1505	Mylonite	Q-Pl-Kf-Ch-Mu

CHEMICAL ANALYSES OF AMPHIBOLITES

Sample No. S.A.D.M. No.	A3 A31/75	A-3	C9 A32/75	161-1 A34/75	161-2	292-5 A38/75	292-6	292-7	424-5
SiO_2	51.06	50.80	48.59	48.77	49.92	49.52	49.05	50.28	50.29
Al_2O_3	9.59	9.87	18.02	14.60	12.93	13.70	13.48	15.08	14.15
Fe_2O_3	2.39	10.18	.67	1.11	16.73	1.14	15.87	12.09	13.70
FeO	6.40		7.00	11.40		10.30			
MnO	.18		.16	.25		.25			
MgO	10.5	11.13	7.44	6.50	5.73	6.57	6.51	7.07	7.41
CaO	13.26	12.27	10.00	11.08	8.70	11.58	11.10	11.54	11.10
Na_2O	1.58	1.73	2.08	2.69	2.88	2.52	1.80	2.54	2.54
K_2O	1.39	1.71	2.03	.43	1.22	.54	.24	.31	.98
TiO_2	.74	.83	.54	1.19	1.80	.91	1.34	.92	1.13
P_2O_5	.18	.28	.02	.06	.15	.06	.11	.09	.16
H_2O^+	1.03		2.07	1.05		1.15			
H_2O^-	.13		.13	.11		.13			
Total	98.44	98.80	98.75	99.22	100.06	98.36	99.50	99.92	101.46
Loss on Ignition		1.13			1.33		1.37	1.45	1.59

Analyses with South Australian Department of Mines numbers were done by the Australian Mineral Development Laboratories. All other analyses were done at the University of Adelaide.

424-6 A39/75	424-7 A40/75	452-1A A41/75	452-1B A42/75	452-3 A43/75	573-7	573-8	573-9 A44/75
51.51	57.28	48.17	50.21	48.11	48.54	48.91	48.57
14.38	15.19	13.25	14.97	14.20	12.65	15.24	14.25
.43	.70	.92	.60	.89	17.03	13.51	1.93
8.10	8.75	12.60	9.70	7.00			10.30
.24	.19	.26	.19	.20			.22
5.64	2.35	7.53	7.69	6.60	5.80	5.99	6.86
13.88	8.65	9.27	9.28	13.15	8.13	10.05	10.41
2.76	1.65	2.34	2.62	2.77	3.40	3.45	3.05
.91	1.26	.88	1.12	1.07	.51	.66	.65
.72	1.55	1.18	.78	.67	2.76	1.63	1.32
.09	.43	.04	.04	.11	.16	.14	.09
1.01	1.18	1.62	2.04	4.30			1.13
.07	.06	.10	.06	.16			.33
99.75	99.23	98.16	99.30	99.24	98.98	99.58	99.10
					.87	.80	

573-10A A45/75	573-12 A46/75	573-13	1128-4 A50/75	1225 A51/75	1250 A52/75
59.17	47.70	49.77	49.68	49.14	46.80
11.90	13.85	13.95	16.23	14.17	14.19
1.91	1.43	14.75	1.00	1.94	.65
8.20	10.30		8.80	8.70	8.95
.50	.34		.18	.20	.25
4.71	8.06	6.48	6.50	6.00	6.76
5.09	10.68	9.90	12.65	11.53	14.77
3.04	1.95	2.86	1.67	2.30	1.98
.99	1.18	.79	.37	.84	.53
.87	.98	1.43	.83	1.10	1.16
<.01	.05	.13	.05	.18	.21
1.63	1.52		1.08	2.08	1.23
.41	.18		.06	.36	.09
98.41	98.22	100.06	99.10	98.54	97.57
		1.50			

CHEMICAL ANALYSES OF METASEDIMENTS

Sample No. S.A.D.M. No.	C-18 A33/75	161-3 A35/75	292-2	292-3 A36/75	292-4 A37/75	421	424-1
SiO_2	50.68	43.99	60.45	2.12	54.96	68.02	64.77
Al_2O_3	13.05	7.25	19.00	.20	1.90	17.32	14.87
Fe_2O_3	2.03	13.56	6.24	<.05	.18	3.53	5.46
FeO	12.10	13.60		.85	25.20		
MnO	.26	11.80		.10	1.92	0.04	
MgO	4.74	4.81	4.22	20.10	8.07	1.70	3.07
CaO	7.20	2.57	.16	30.97	4.03	0.60	4.19
Na_2O	3.22	.03	.63	.02	.30	-	3.89
K_2O	.30	.05	7.82	.05	.12	6.39	1.48
TiO_2	2.84	.25	.62	<.01	.08	0.65	.53
P_2O_5	.47	.23	.06	.03	.28	0.13	.15
H_2O^+	1.28	1.06		.53	1.50		
H_2O^-	.14	.08		.05	.02		
Total	98.30	99.28	99.20	55.02	98.55	98.37	98.41
Loss on Ignition			2.28			1.73	1.08

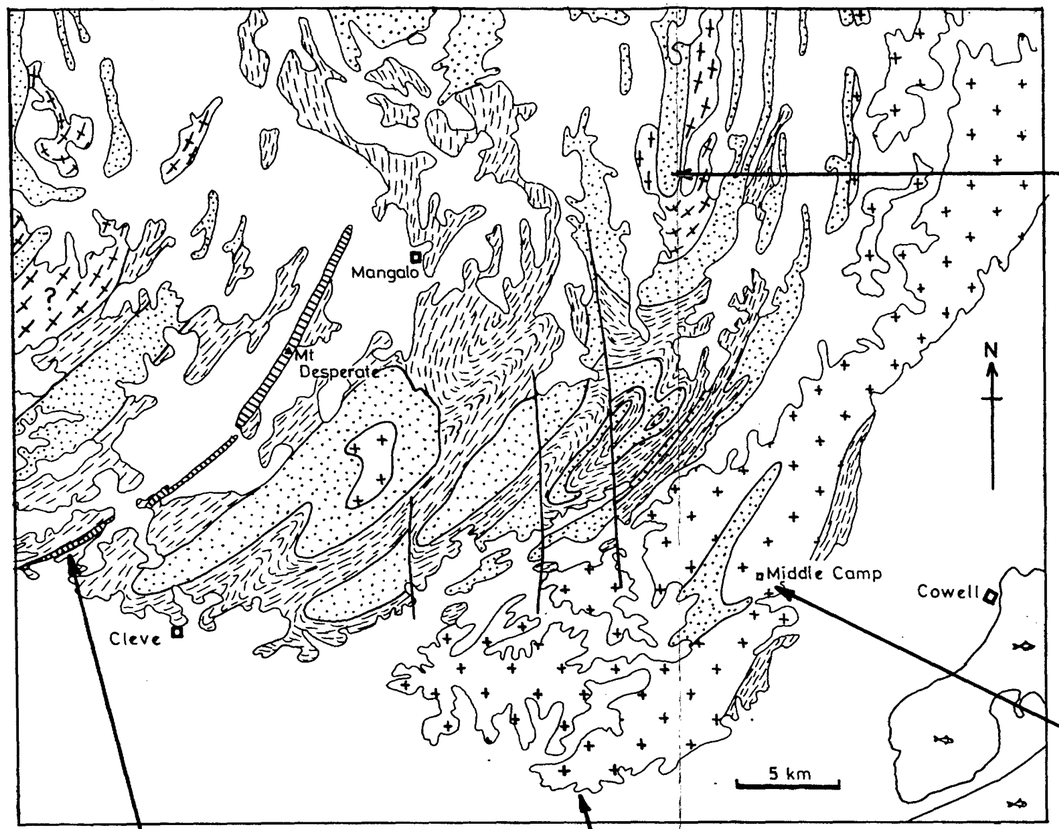
424-4	454B	572B	573-1	573-2	573-3	573-	573-6
57.50	70.02	79.41	67.81	64.86	61.72	62.73	21.35
15.51	13.61	10.44	16.11	17.08	14.84	14.53	5.99
7.98	5.34	2.70	5.88	6.94	11.57	11.52	61.76
	.18						
3.66	1.77	.65	1.68	2.65	2.50	2.47	1.26
9.21	1.13	.99	.71	.66	1.40	1.59	1.32
4.38	-	2.69	2.23	2.10	3.55	3.25	1.45
1.67	2.96	1.83	4.55	5.16	3.21	3.21	.26
.91	0.43	.30	.59	.82	.63	.61	.73
.18	0.12	.08	.13	.16	.13	.21	.13
101.00	95.56	99.09	99.69	100.43	99.55	100.12	94.25
2.24	.88	.52	1.93	2.77	3.14	3.10	10.66

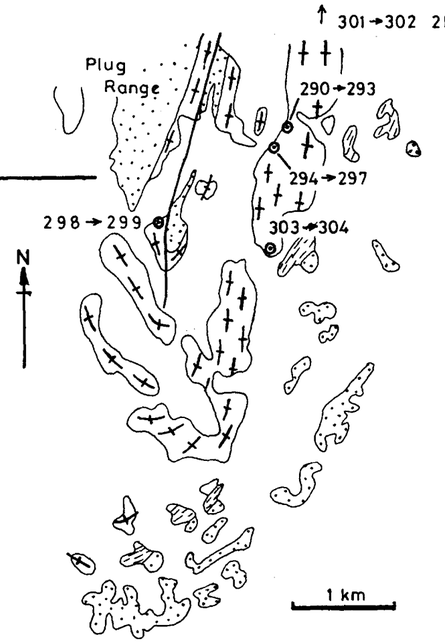
573-10B	573-11	573-15 A47/75	573-16 A48/75	873B A49/75	1448
62.29	59.98	68.80	2.03	74.60	69.08
12.00	16.58	1.25	.53	6.82	14.60
11.07	8.61	.91	<.05	<.05	6.38
		18.00	.80	1.85	
		1.76	.12	.05	0.07
4.98	2.18	3.85	20.40	4.71	2.81
4.85	1.41	2.78	30.20	6.79	1.73
3.19	3.64	.12	.02	.72	-
1.07	5.69	.13	.04	3.39	2.61
.42	.68	.06	.02	.12	.35
.03	.11	.12	.23	.06	.22
		1.29	.41	.44	
		.05	.05	.04	
99.90	98.88	99.11	54.85		97.83
1.96	3.84				1.65

CHEMICAL ANALYSES OF MYLONITIC ROCKS

Sample No. S.A.D.M. No.	MY-2	MY-3	MY-4	MY-5	MY-6	1469F	1505
SiO_2	66.50	71.39	69.16	71.10	69.01	48.44	66.72
Al_2O_3	19.97	15.70	15.25	13.82	15.80	20.08	14.74
Fe_2O_3	2.86	3.03	4.34	4.15	4.73	11.42	5.24
FeO							
MnO	.04	.03	.05	.06	.06	.12	.04
MgO	2.47	2.12	2.81	2.69	2.61	5.91	3.50
CaO	.26	.27	.31	.25	.17	4.84	.68
Na_2O	-	-	-	-	-	-	-
K_2O	2.79	1.69	2.08	2.70	3.80	7.03	6.22
TiO_2	.18	.38	.51	.48	.52	1.18	.71
P_2O_5	.10	.09	.09	.09	.06	.26	.05
H_2O^+							
H_2O^-							
Total	95.17	94.70	94.59	95.34	96.76	99.27	97.90
Loss on Ignition	2.53	1.82	1.97	2.18	2.73	3.67	.89

FIG. B1



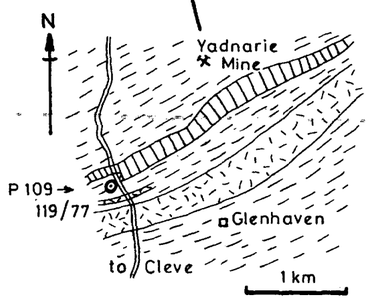


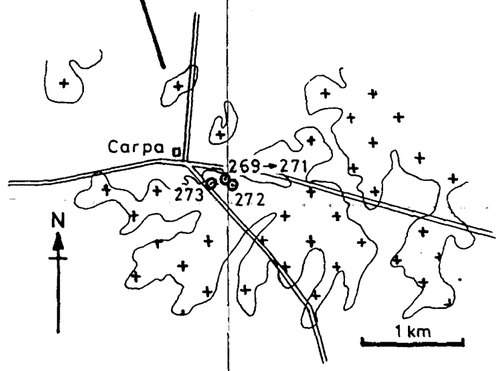
LOCATION of GEOCHRON SAMPLES

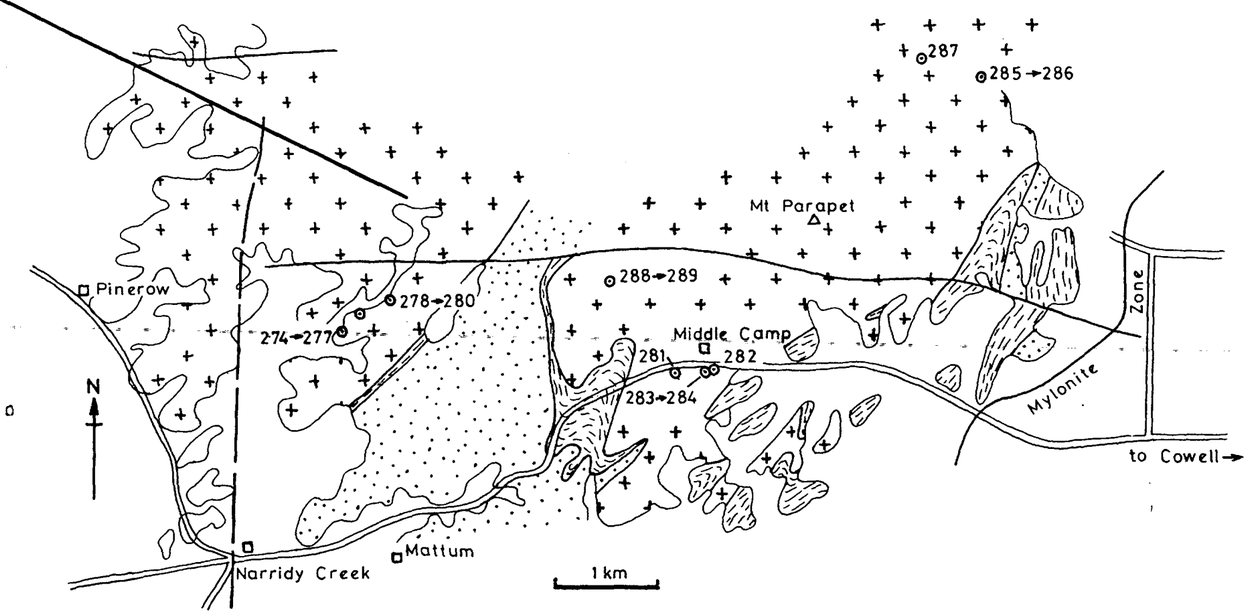
LEGEND

- Fault
- Syn-tectonic granites
- Hutchison Group
  - Iron fm
  - Amphibolite
  - Quartzite
- Pre-tectonic granite gneiss

c.f. Plans 1 and 2.







APPENDIX B

GEOCHRONOLOGY

Preliminary geochronology was carried out by A.W. Webb of the Australian Mineral Development Laboratories on several samples collected during this study. The work was funded by the South Australian Department of Mines and Energy and the assistance of Mr. B.P. Thomson is acknowledged. The locations from where the samples were collected are detailed in Figure B1 and the results are detailed in the following progress reports reproduced here with permission of Dr. Webb and Mr. Thomson.

amdel
The Australian Mineral Development Laboratories

Flemington Street, Frewville, South Australia 5063
Phone Adelaide 79 1662, telex AA82520

Please address all correspondence to Frewville,
In reply quote:

NATA CERTIFICATE AN 1/1/186

8 January 1977

The Director,
Department of Mines,
Box 151,
EASTWOOD SA 5063

GEOCHRONOLOGY OF THE ANCIENT BASEMENT

ROCKS OF THE GAWLER CRATON

Progress Report No. 3

Petrography by: Dr B. G. Steveson

Geochronology by: Dr A. W. Webb

Officer in Charge, Analytical Section: D. K. Rowley

for F. R. Hartley
Director

This laboratory is registered by the National Association of Testing Authorities, Australia. The test(s) reported herein have been performed in accordance with its terms of registration. This document shall not be reproduced except in full.

hjj

GEOCHRONOLOGY OF THE ANCIENT BASEMENT ROCKS OF THE GAWLER CRATON

1. INTRODUCTION

This progress report is the first one for this project to contain geochronological data and differs from previous reports for other projects in that a new decay constant for Rb^{87} has been used. The new value of the decay constant ($\lambda = 1.42 \times 10^{-11}\ y^{-1}$) was recommended at the 25th International Geological Congress in August 1976 and accepted by the geochronologists present at that meeting. The effect of the change is to reduce all Rb-Sr dates reported from Amdel by 2.1%. Changes to the K^{40} decay constants were also suggested but there was not the same enthusiasm amongst those present to accept the proposed new values. However, the effect of a change in K^{40} decay constants would vary with the age of the sample and would be negligible in samples of late Archaean - early Proterozoic age. Hence, it is not intended to use the proposed new constants in this laboratory in the immediately future.

Changes to important published dates for the late Archaean and early Proterozoic are tabulated below.

ROCK UNIT	REFERENCE	AGE
C. Carnot Augen Gneiss	(Cooper et al; 1976)	2587 ± 134
C. Carnot Leuco Gneiss	(Cooper et al; 1976)	2777 ± 583
Whidbey Granite	(Project 1/1/122)	2337 ± 65
Glenloth Granite	(Project 1/1/122)	2300 ± 33
Black Range Dolerite Dyke	(Lewis et al; 1975)	2280 ± 89
Kirton Point Granite Gneiss	(Cooper et al; 1976)	1816 ± 10

2. REVIEW OF PROGRESS

The samples so far examined have been predominantly metamorphic rocks from Eyre and Yorke Peninsulas and the islands of Spencer Gulf. Petrographic descriptions of the Glenloth Granite, gneissic granites from Plug Range and a variety of granitic and basic gneisses from the Tarcoola area have been reported in progress report numbers 1 and 2. The present report contains petrographic descriptions of gneisses from Corny Point and Rb-Sr isotopic analyses on samples from all of the rock types listed above. In addition several K-Ar and Rb-Sr analyses were made on foliated granulites and augen gneisses collected during the helicopter survey of the continental shelf islands and described for Project 1/1/160.

4.4 Gneissic Granites - Plug Range

Fifteen samples of metamorphic rocks from 5 separate localities were submitted for Rb-Sr geochronology. The samples were mainly acid gneisses but a few basic rocks were also present. Twelve samples were analysed and the data are listed in Table 5 and plotted in Fig. 3. Examination of Fig. 3 shows a considerable scatter of the data in a non-linear fashion which can be attributed mainly to three points - P292/76, P300/76 and P301/76. Two of these points are from a locality some distance from the other sampling sites while the third sample is from a basic lens which may not have had the same initial Sr^{87}/Sr^{86} ratio as that of the acid gneisses.

Regression of the remaining 9 analyses showed that there was still a marked scatter beyond that which could be attributable to experimental error. The Model 3 isochron has an age of 1697 ± 65 Ma and an initial Sr^{87}/Sr^{86} ratio of 0.7340 ± 0.0048. The high initial ratio indicates that the material incorporated in the gneiss had resided in the crust for a significant period prior to the metamorphism 1700 Ma ago, or that it had been derived from rocks exceptionally enriched in radiogenic Sr. A rock with a composition equal to the average of the 9 samples used in the regression would take ~450 Ma to increase its Sr^{87}/Sr^{86} ratio from 0.700 to 0.734 i.e. assuming that the samples can be given equal weight in relation to the overall composition of the rock unit and that there has not been any selective concentration or removal of Rb and Sr during metamorphism, the parental material of the gneiss could be about 2150 Ma old.

Thus, these results reinforce conclusions arrived at from other investigations in southern Eyre Peninsula, that, during the early Proterozoic, there were significant additions of new material on and adjacent to the Archaean basement. The Sr isotopic evidence indicates that the material forming the Coffin Bay metasediments, the Plug Range gneissic granite and the augen gneisses of Kirton Point, Spencer Gulf and southern Yorke Peninsula was introduced some time after 2300 Ma ago.

TABLE 5

Rb-Sr Analyses - Plug Range Gneissic Granites

SAMPLE NUMBER		Rb/Sr	Rb^{87}/Sr^{86}	Sr^{87}/Sr^{86}
P291/76	6230 RS 34	1.024	2.9853	0.8059
P292/76	RS 35	0.537	1.5601	0.7624
P293/76	RS 36	2.212	6.5039	0.8942
P294/76	RS37	1.528	4.4695	0.8403
P295/76	RS 38	1.328	3.8791	0.8260
P296/76	RS 39	1.268	3.7032	0.8241
P298/76	RS 41	2.836	8.3730	0.9371
P299/76	RS 42	0.792	2.3053	0.7937
P300/76	RS 43	0.1078	0.3120	0.7314
P301/76	RS 44	1.720	5.0451	0.8692
P303/76	RS 46	1.974	5.7938	0.8757
P304/76	RS 47	2.550	7.5155	0.9190

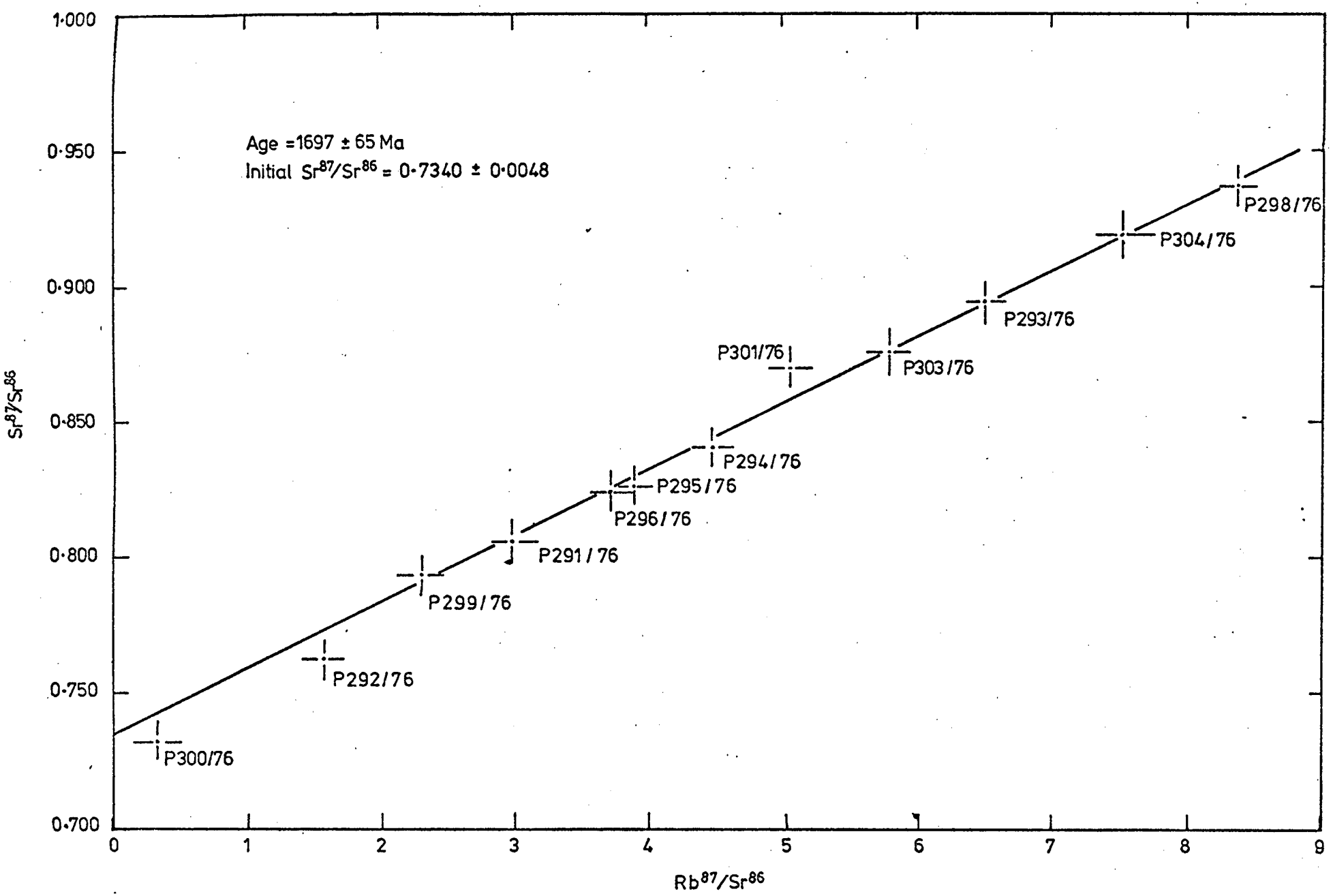


FIG.3: GNEISSIC GRANITE, PLUG RANGE

amdel
The Australian Mineral Development Laboratories

Flemington Street, Frewville, South Australia 5063
Phone Adelaide 79 1662, telex AA82520

Please address all correspondence to Frewville,
In reply quote:

NATA CERTIFICATE AN 1/1/122

24 January 1977

The Director,
Department of Mines,
Box 151,
EASTWOOD SA 5063

GEOCHRONOLOGY OF THE YOUNGER GRANITES OF THE GAWLER BLOCK AND ITS NORTHWEST MARGIN

Progress Report No. 30

to 14 January 1977

Geochronology by: Dr A. W. Webb

Officer in Charge, Analytical Section: D. K. Rowley

for F. R. Hartley
Director

hjj

This laboratory is registered by the National Association of Testing Authorities, Australia. The test(s) reported herein have been performed in accordance with its terms of registration. This document shall not be reproduced except in full.

GEOCHRONOLOGY OF THE YOUNGER GRANITES OF THE GAWLER BLOCK AND ITS NORTHWEST MARGIN

1. REVIEW OF PROGRESS

This Progress Report will be the final one for Project 1/1/122 and contains the Rb-Sr analytical data and interpretation for the Carpa Middlecamp and Narridy Creek Granites. Twenty-one samples of these granites were described in Progress Report No. 29 and fifteen of these samples have subsequently been analysed.

2. GEOCHRONOLOGY

The fifteen Rb-Sr analyses are listed in Table 1 and the data for the Carpa and Middlecamp Granites plotted in Fig. 1. The Rb/Sr ratios of these two granites are low and have contributed to the high errors in the age determinations. The Narridy Creek Granite contrasts with the former two granites in this respect and has exceptionally high Rb/Sr ratios, but the analyses are not plotted on an isochron diagram because the reduction in scale necessary would make the visual display meaningless.

A revised value of the Rb^{87} decay constant ($\lambda = 1.42 \times 10^{-11}\ y^{-1}$) is now being used and the results quoted in this report must be increased by 2.1% to allow comparisons to be made with previously reported Rb-Sr ages from the Gawler Block.

2.1 Carpa Granite

Four samples of this granite were analysed and regression of the analyses produced a Model 1 isochron of 1677 ± 125 Ma with an initial Sr^{87}/Sr^{86} ratio of 0.7124 ± 0.0050. The large uncertainty in the age is due to the low values and restricted range of Rb/Sr ratios and to the small number of samples analysed.

K-Ar age determinations on two samples of biotite from the Carpa Granite, reported in Progress Report No. 8, were 1576 and 1593 Ma. Neither these two samples (P946/71, P947/71) nor most of the samples of the present group, show any petrographic indications of recrystallisation or metamorphism and the reason for the difference between the K-Ar and Rb-Sr dates is obscure. Possibly, there was a considerable time interval between the emplacement of the granite and the time when it had cooled sufficiently to allow retention of radiogenic argon.

2.2 Middlecamp Granite

The samples of this granite, described in Progress Reports Nos 8 and 29, show evidence of extensive recrystallisation and development of a foliation. However, Rb-Sr total rock analyses of 6 samples produced a strongly linear plot on the isochron diagram (Fig. 1) although regression of the analyses indicated a residual variance beyond that due to experimental error. The age of this isochron is 1635 ± 86 Ma and the initial Sr^{87}/Sr^{86} ratio is 0.7108 ± 0.0032.

Most of the residual variance appears to be due to sample P289/76 and when this analysis is dropped from the regression, a Model 1 isochron is produced. The age is not significantly different at 1650 ± 35 Ma (initial Sr^{87}/Sr^{86} = 0.7098 ± 0.0013) but this is preferred because of the better fit of the isochron and the reduced error in the age.

This age is considerably older than the biotite K-Ar age of 1522 Ma (Progress Report No. 8) determined for the granite and the low mineral date could be due to loss of argon during the deformation and recrystallisation event.

2.3 Narridy Creek Granite

The samples of this granite have been partly recrystallised and all contain significant amounts of secondary muscovite. The Rb/Sr ratios are high (12-15), due mainly to fairly low levels of Sr rather than to abnormally high Rb, so the high ratios could be a primary feature of the granite.

The Rb-Sr isotopic analyses show a considerable scatter when plotted on an isochron diagram. The scatter can not be attributed to any one particular analysis and therefore all data were regressed to produce an isochron of 1643 ± 303 Ma with an initial Sr^{87}/Sr^{86} ratio of 0.7240 ± 0.1780. The large errors associated with the isochron age render this determination of little significance and perhaps a K-Ar measurement on the muscovite would give a better estimate of the age of recrystallisation. The significance of the Rb/Sr isochron age could then be evaluated on the basis of this other information.

2.4 Significance of Initial Sr^{87}/Sr^{86} Ratios

All three granites had initial Sr^{87}/Sr^{86} ratios greater than 0.710, indicating a significant degree of contamination by, or assimilation of, pre-existing crustal rocks by the granite magmas.

TABLE 1

Rb-Sr Analyses

SAMPLE NUMBER	LOCALITY	Rb/Sr	Rb^{87}/Sr^{86}	$\#Sr^{87}/Sr^{86}$
Carpa Granite				
P269/76	33° 45 2/3'S, 136° 41½'E	1.005	2.9234	0.7829
P270/76	" "	1.140	3.3190	0.7920
P271/76	" "	1.068	3.1081	0.7878
P272/76	" "	0.668	1.9386	0.7591
Narridy Creek Granite				
P274/76	33° 40 1/6'S, 136° 45 2/3'E	11.170	34.912	1.5499
P276/76	" "	14.580	46.701	1.8245
P277/76	" "	14.020	44.777	1.7916
P279/76	" "	13.230	41.889	1.6940
P280/76	" "	13.030	41.299	1.7058
Middlecamp Granite				
P281/76	33° 40½'S, 136° 48'E	0.669	1.9410	0.7562
P282/76	" "	0.885	2.5707	0.7697
P283/76	" "	1.766	5.1617	0.8324
P285/76	" "	0.255	0.7377	0.7273
P286/76	" "	0.810	2.3523	0.7661
P289/76	" "	0.488	1.4145	0.7462

\# Measured Ratios Normalised to $Sr^{88}/Sr^{86} = 8.3752$

Constants used: $Rb^{85}/Rb^{87} = 2.600$

$\lambda\ Rb^{87} = 1.42 \times 10^{-11}\ y^{-1}$

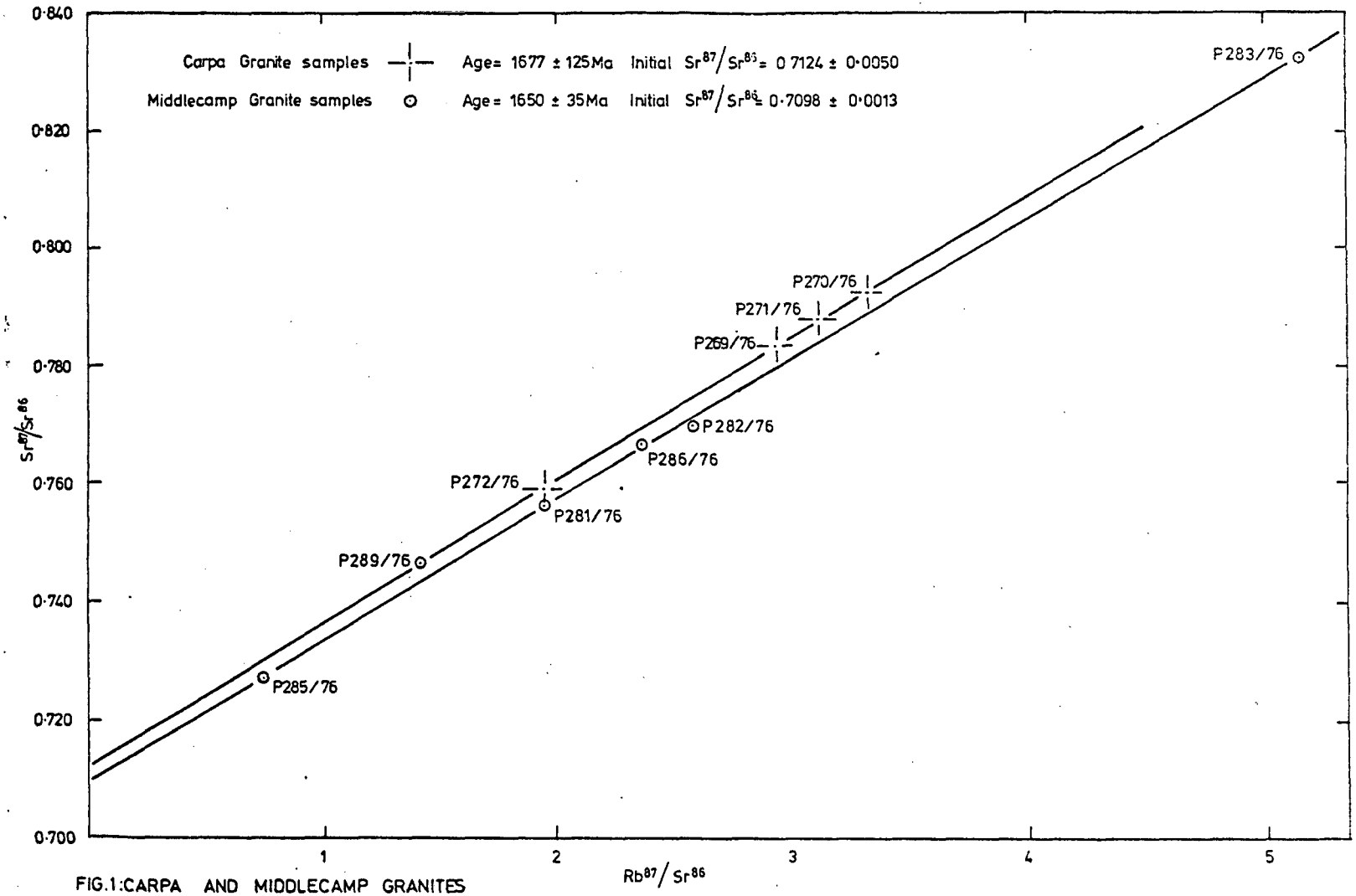


FIG.1:CARPA AND MIDDLECAMP GRANITES

amdel
The Australian Mineral Development Laboratories

Flemington Street, Frewville, South Australia 5063
Phone Adelaide 79 1662, telex AA 82520

Pilot Plant: Osmond Place, Thebarton, Sth. Aust.
Phone Adelaide 43 8053
Branch Offices: Perth and Sydney
Associated with: Professional Consultants Australia Pty. Ltd.

Please address all correspondence to Frewville.
In reply quote:
AN 1/1/126

The Director,
Department of Mines,
Box 151,
EASTWOOD SA 5063

April 1977

GEOCHRONOLOGY OF
STRATIGRAPHICALLY SIGNIFICANT
ROCKS FROM SOUTH AUSTRALIA

Progress Report No. 17 ✓
to 30 April 1977

NB P/R No. 17 of May should be No. 18.
P/R No 18 of May " " No 19.

Report by: Dr A. W. Webb

Officer in Charge, Analytical Section: D. K. Rowley

D. K. Rowley

for F. R. Hartley
Director

hjj

2.5 Cook Gap Schist Equivalents at Mangalo Creek

Nine samples of mica schist were collected over a distance of 70 m across strike along Mangalo Creek, northwest of Cleve. The rock unit underlies the upper iron formation in this area and is therefore the stratigraphic equivalent of the Cook Gap Schists of the Middleback Group.

The samples showed a wide variation in Rb/Sr ratio and the analyses of 8 samples are listed in Table 4 and plotted in Fig. 3. Regression of the analyses produced an MSWD of 23.1, indicating considerable scatter of the data in excess of experimental error. The Model 2 isochron has an age of 1688 ± 76 Ma with an initial Sr^{87}/Sr^{86} ratio of 0.7061 ± 0.0042. The age is identical to that determined for the Plug Range gneissic granite northwest of Cowell and reinforces the interpretation made in Progress Report No. 3 for Project 1/1/186, that the Plug Range gneissic granite was remobilised and intruded at that time. It appears that a major phase of the Kimban Orogeny occurred in the Cleve-Cowell district about 1700 Ma ago.

The initial ratio of the schists is fairly low and it is unlikely that the material forming the schists was derived from an Archaean terrain. Deposition of the original sedimentary material probably occurred during the Lower Proterozoic and hence, if the correlation of these schists with the Cook Gap schist is valid, the iron formations of the Middleback Group must also have been deposited in the Lower Proterozoic.

This conclusion is in agreement with that made in Section 2.1 that there is a difference in age and type between the Mt Christie and Middleback iron formations.

TABLE 4

Rb-Sr Analyses, Biotite Schists from Mangalo Creek

SAMPLE NUMBER	Rb/Sr	Rb^{87}/Sr^{86}	# Sr^{87}/Sr^{86}
P109/77	1.302	3.7928	0.7980
P110/77	0.939	2.7288	0.7733
P111/77	0.734	2.1297	0.7571
P112/77	3.199	9.4462	0.9388
P113/77	1.613	4.7106	0.8239
P115/77	2.657	7.8143	0.8969
P116/77	2.575	7.5632	0.8832
P119/77	1.748	5.1067	0.8276

TABLE 5

Rb-Sr Analyses, Moody Granite

SAMPLE NUMBER	Rb/Sr	Rb^{87}/Sr^{86}	# Sr^{87}/Sr^{86}
P83/77	2.910	8.5740	0.9160
P1002/77	2.688	7.9086	0.9010
P1106/77	2.675	7.8697	0.9002

TABLE 6

Rb-Sr Analyses, Metamorphics at Pt Souttar

SAMPLE NUMBER	Rb/Sr	Rb^{87}/Sr^{86}	# Sr^{87}/Sr^{86}
P154/77	3.989	11.8219	0.9769
P155/77	3.170	9.3524	0.9297
P156/77	2.824	8.3060	0.8976
P157/77	1.677	4.8942	0.8169
P158/77	3.310	9.7705	0.9351
P159/77	3.173	9.3588	0.9269

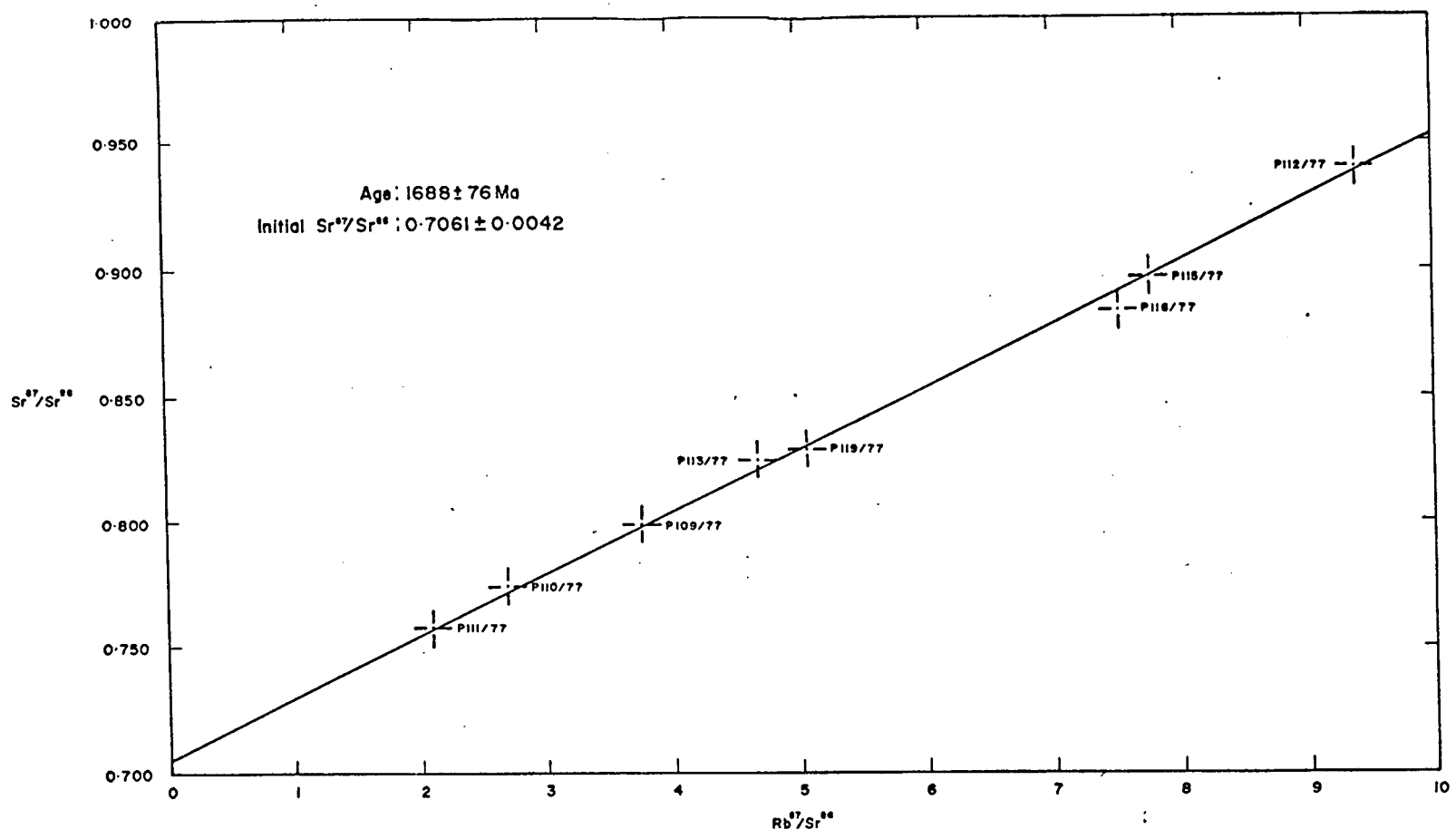
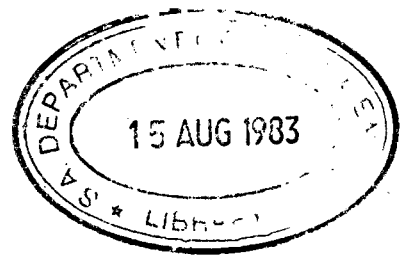


Fig.3 Mica Schists, Mangalo Creek

STRUCTURAL, STRATIGRAPHIC AND METAMORPHIC GEOLOGY OF LOWER PROTEROZOIC ROCKS IN THE COWELL/CLEVE DISTRICT, EASTERN EYRE PENINSULA.

VOLUME II



by

Allan John Parker
B.Sc. (Hons), Adelaide

Department of Geology and Mineralogy
University of Adelaide

March, 1978

TABLE OF CONTENTS

VOLUME II PAGE

TABLE OF CONTENTS

CHAPTER VI MICROSTRUCTURE 1

6.1 INTRODUCTION 1

6.2 D_1 DEFORMATION 1

6.2.1 The Fabric 1

6.2.1.1 S_1 fabric 2

6.2.1.2 F_1 folding 5

6.2.2 D_1 Fabric Development 6

6.2.2.1 Significant of S_1 6

6.2.2.2 Origin of S_1 8

6.3 D_2 DEFORMATION 10

6.3.1 The Fabric 10

6.3.1.1 Semipelites 10

6.3.1.2 Other lithologies 15

6.3.2 D_2 Fabric Development 19

6.3.2.1. Relationship of fabric to strain 19

6.3.2.2 Mechanism of layer silicate orientation 24

6.3.3 Summary of D_2 Microfabric 30

6.4 D_3 DEFORMATION 31

6.4.1 The Fabric 31

6.4.1.1 Semipelites 31

6.4.1.2 Other lithologies 35

6.4.1.3 Narridy Creek Granite 39

6.4.2 Development of D_3 Fabric 42

6.4.2.1 Relationship of Fabric to Strain 42

6.4.2.2 Development of S_3 42
6.4.2.3 Development of D_3 Quartz Textures 45
6.4.3 Summary of D_3 Microstructures 58
6.5 MYLONITE DEFORMATION 59
6.5.1 The Fabric 59
6.5.1.1 Mica recrystallization Stage 60
6.5.1.2 Feldspar recrystallization Stage 62
6.5.2 Summary and Discussion 68
6.6 D_4 DEFORMATION 71
6.6.1 The Fabric 71
6.6.1.1 Crenulations 71
6.6.1.2 Planar S_4 Elements 72
6.6.2 Discussion 75
6.7 BRITTLE (post D_4) DEFORMATION 76
6.7.1 The Fabric 76
6.7.2 Discussion 78
CHAPTER VII METAMORPHISM 80
7.1 INTRODUCTION 80
7.2 OUTLINE OF METAMORPHIC EVOLUTION 81
7.3 M_{1-2} METAMORPHISM 82
7.3.1 Summary of Mineral Parageneses 83
7.3.2 Discussion 84
7.3.2.1 Evidence for two separate events, M_1 and M_2 84
7.3.2.2 Pelitic and semi-pelitic parageneses 87

7.3.2.3 Carbonate parageneses 92

7.3.2.4 Metabasite parageneses 97

7.3.2.5 Eulysite parageneses 98

7.3.3 T-P Conditions 99

7.4 M_3 METAMORPHISM 105

7.4.1 Summary of Observed Mineral Associations 106

7.4.2 Discussion 108

7.4.3 P-T Conditions 112

7.5 M_4 METAMORPHISM 113

7.5.1 Summary of mineral parageneses 113

7.5.2 Discussion 114

7.5.3 P-T Conditions 116

7.6 SUMMARY OF METAMORPHISM 116

CHAPTER VIII CONCLUSIONS AND TECTONIC IMPLICATIONS 119

8.1 SUMMARY OF CONCLUSIONS 119

8.1.1 Lithology 119

8.1.2 Stratigraphy 120

8.1.3 Igneous, Metamorphic and Structural Evolution 121

8.1.4 Regional Correlation 124

8.2 TECTONIC IMPLICATIONS 126

REFERENCES CITED 130

APPENDIX C Tectonic relationships between the Proterozoic Gawler and Willyama Orogenic Domains, Australia. By R.A. Glen, W.P. Laing, A.J. Parker and R.W.R. Rutland.

CHAPTER VI

MICROSTRUCTURE

6.1 INTRODUCTION

This chapter has, like the previous mesoscopic chapter, been subdivided into six sections which consider individually each of the successive deformations D_1 to D_4 with separate sections on the mylonite zone and brittle deformation features. Each section itself has been further subdivided into a fabric subsection in which the particular fabrics are described in detail, a discussion subsection in which the development of the fabrics is discussed, and a brief summary subsection. The fabrics of the semipelitic gneisses are considered in most detail, but brief reference is made to the fabrics of the other lithologies.

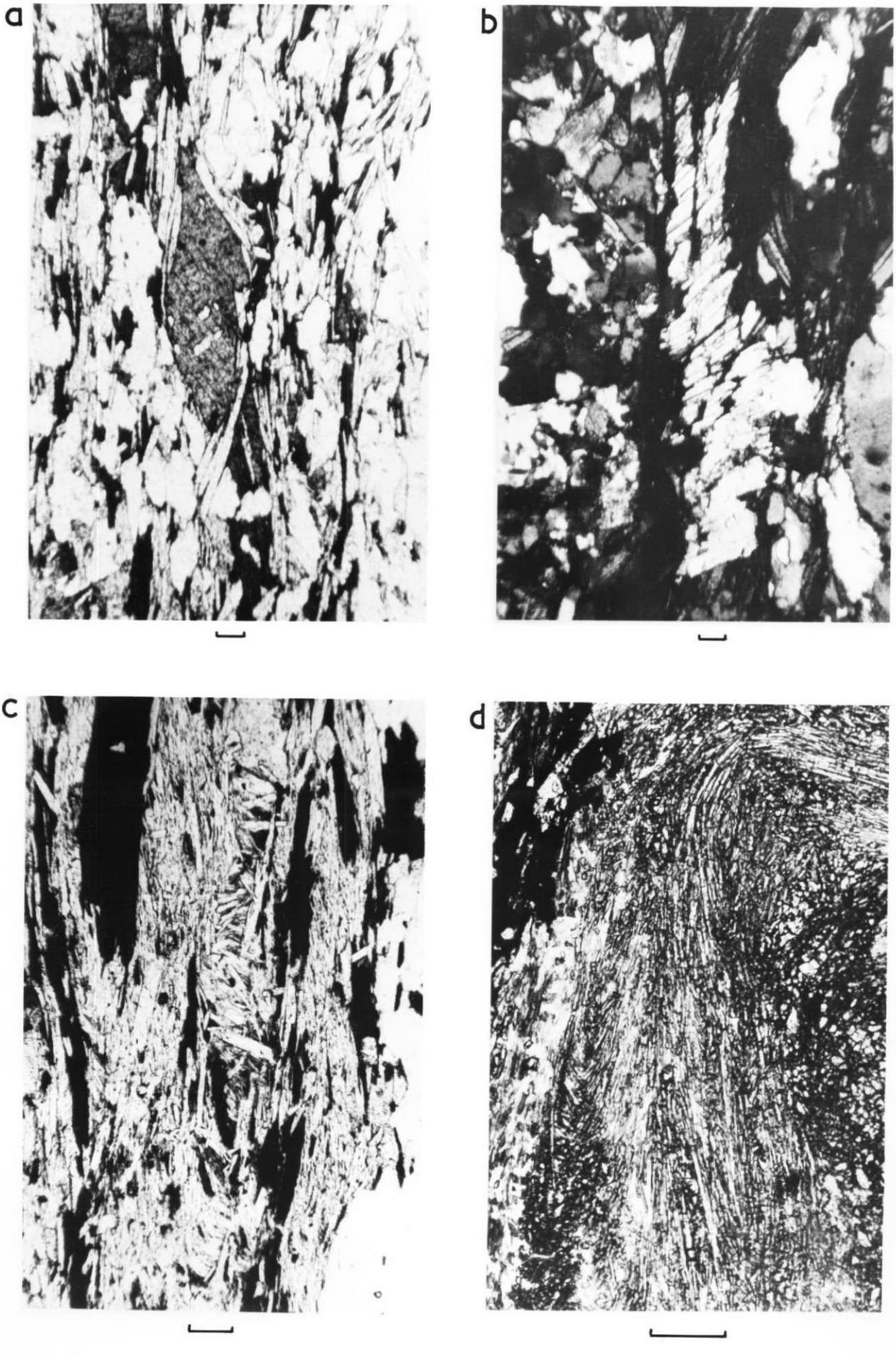
The principal aims of this chapter and the subsequent metamorphism chapter are to establish the nature of the particular fabrics (i.e. the minerals that define them and the strength of any preferred orientation etc.), the physical conditions, metamorphic and tectonic, that are implied by those fabrics, and any variations in those conditions throughout the area in either time or space. There are a few subjects though that are described and discussed in somewhat more detail because they can be applied to much more general problems. These are the developments of crenulation cleavage, quartz crystallographic fabrics and mylonite microstructures.

6.2 D_1 DEFORMATION

6.2.1 The Fabric

As noted in Chapter 3 (Sect. 3.2.1) the prime evidence for a D_1 deformation was the occurrence of a layer parallel planar fabric (S_1) recognizable in the hinges of F_2 folds.

FIG. 6.1



It was noted that some mesoscopic folds apparently lacked these folded elements thus suggesting that they may also antecede F_2 folding. However, subsequent microscopic investigations of many such folds have established that all but one contain evidence of an earlier planar fabric. Furthermore their gross parallelism with, and their similar style to local F_2 folds, and their lack of any F_2 overprinting all support an F_2 origin for them.

6.2.1.1 S_1 fabric

The S_1 fabric as it is observed in F_2 fold hinges is defined by mica, sillimanite, garnet, and quartz or quartzofeldspathic veins. Each of these is described separately below.

S_1 MICA - Within the pelites, semipelites, quartzites and the Plug Range granite gneisses, there are numerous relics of pre F_2/S_2 biotite and muscovite which are commonly parallel or sub-parallel to the layering. They are manifest as,

1) coarse, often augen shaped, single crystals (Fig. 6.1a) wrapped around by and sometimes penetrated by the S_2 schistosity, and with the internal (001) of the mica at a distinct angle to S_2 outside,

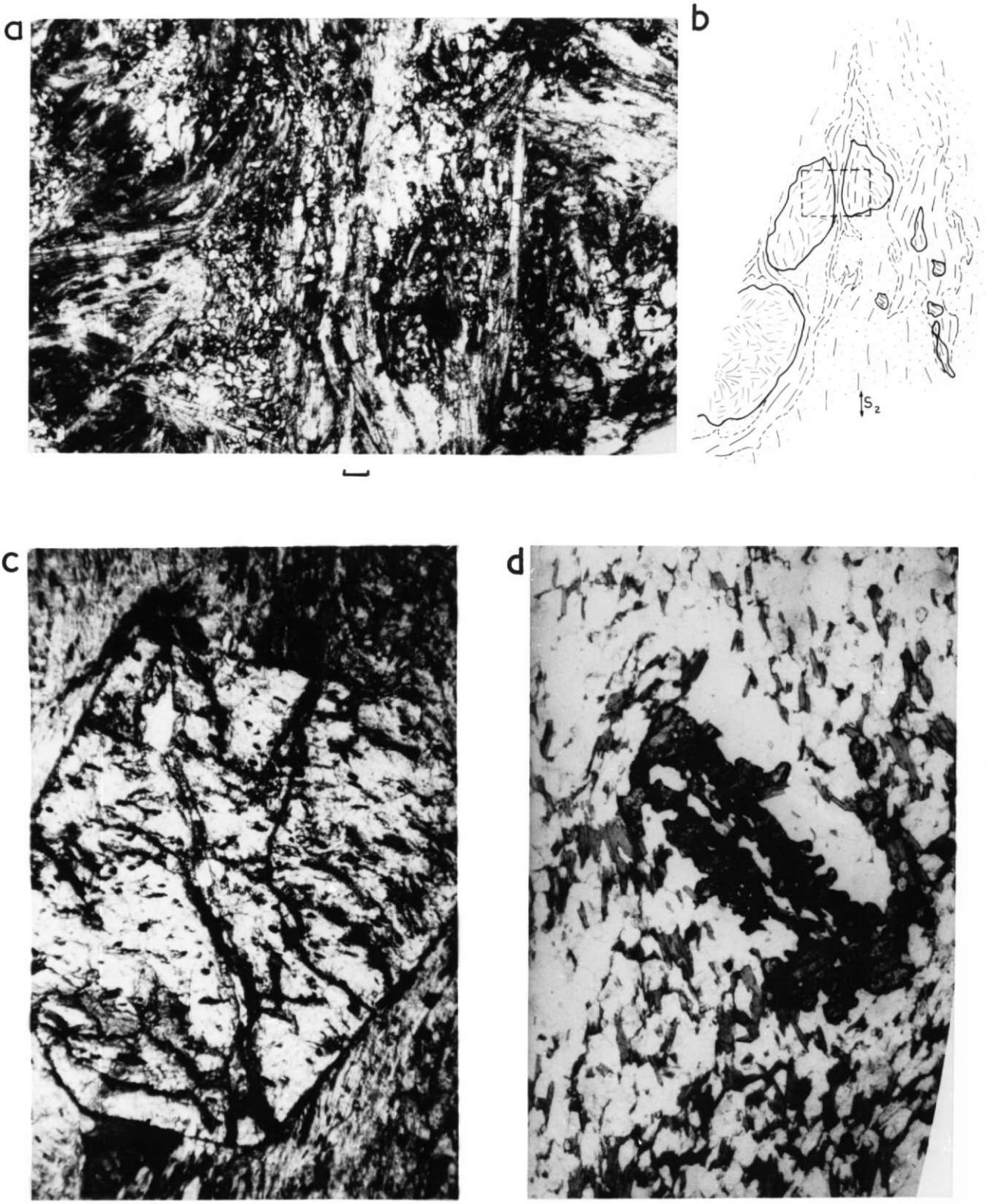
2) coarse, highly embayed single crystals (mainly of muscovite in this case) within S_2 mica films (Fig. 6.1b),

3) elongate, S_2 parallel domains or ribbons of medium grained mica oriented at a high angle to S_2 which wraps around them (Fig. 6.1c), and,

4) coarse multigrained muscovite pods (flattened in S_2) in which the muscovites are randomly oriented.

Figure 6.1: Relic S_1 fabrics: (a) pre-S_2 biotite augen (S_2 vertical) (b) embayed pre-S_2 muscovite relic enclosed within an S_2 mica film (S_2 vertical) (c) elongate S_2 parallel domain of S_1 micas oriented at a high angle to S_2 (vertical). (d) sillimanite pod with an internal, crenulated S_1 fabric (centre left) overprinted by a strong S_2. S_2 has been buckled by F_3 (top right). Bar scale = 0.1 mm.

FIG. 6.2



In nearly all cases the positive identity of a pre-S_2 affinity relies on the recognition of an angular mismatch between (001) of these pre-S_2 micas and S_2 itself. This is because S_1 and S_2 micas are optically identical and cannot be distinguished from each other except on overprinting criteria. There are in fact numerous coarse micas identical to specific S_1 micas but parallel to S_2 and these may be S_1 micas that have been rotated into S_2 parallelism.

While scattered S_1 micas of categories 1) and 2) above do not necessarily infer a planar S_1 fabric (they could be derived from a random pre-S_2 fabric) the third category is firmly believed to do so. The fabrics in those domains are defined not by one grain but by several grains and hence they preclude a random pre S_2 fabric. The formation of these elongate domains which preserve S_1 is discussed in Section 6.3.2 under the development of S_2 from a crenulation cleavage.

S_1 SILLIMANITE - In the migmatitic gneisses of the Mt. Millar/Morowie subarea, pods and films of accicular sillimanite and of fibrolite often record evidence of a pre-D_2 planar sillimanite fabric. Pre-S_2 fibrolite pods are relatively common and they often have S_2 parallel overgrowths (sillimanite beards) surrounding them (see Fig. 6.6). Fibrolite within them is mainly randomly oriented but coarser grained needles are frequently oriented to define a planar layer parallel fabric. In Figure 6.1d accicular sillimanite within such a pod is mainly S_2 parallel, but there are domains in which the earlier S_1 fabric has been preserved. It is crenulated and overprinted

---

Figure 6.2: (a) sillimanite pods with an internal S_1 fabric overprinted by S_2 (vertical). Location of the micrograph is shown in (b) where S_1 is represented by the train of sillimanite pods (heavy outline). (c) and (d) Garnets with internal S_1 fabrics at a high angle to S_2 (vertical). Bar scale = 0.1 mm.

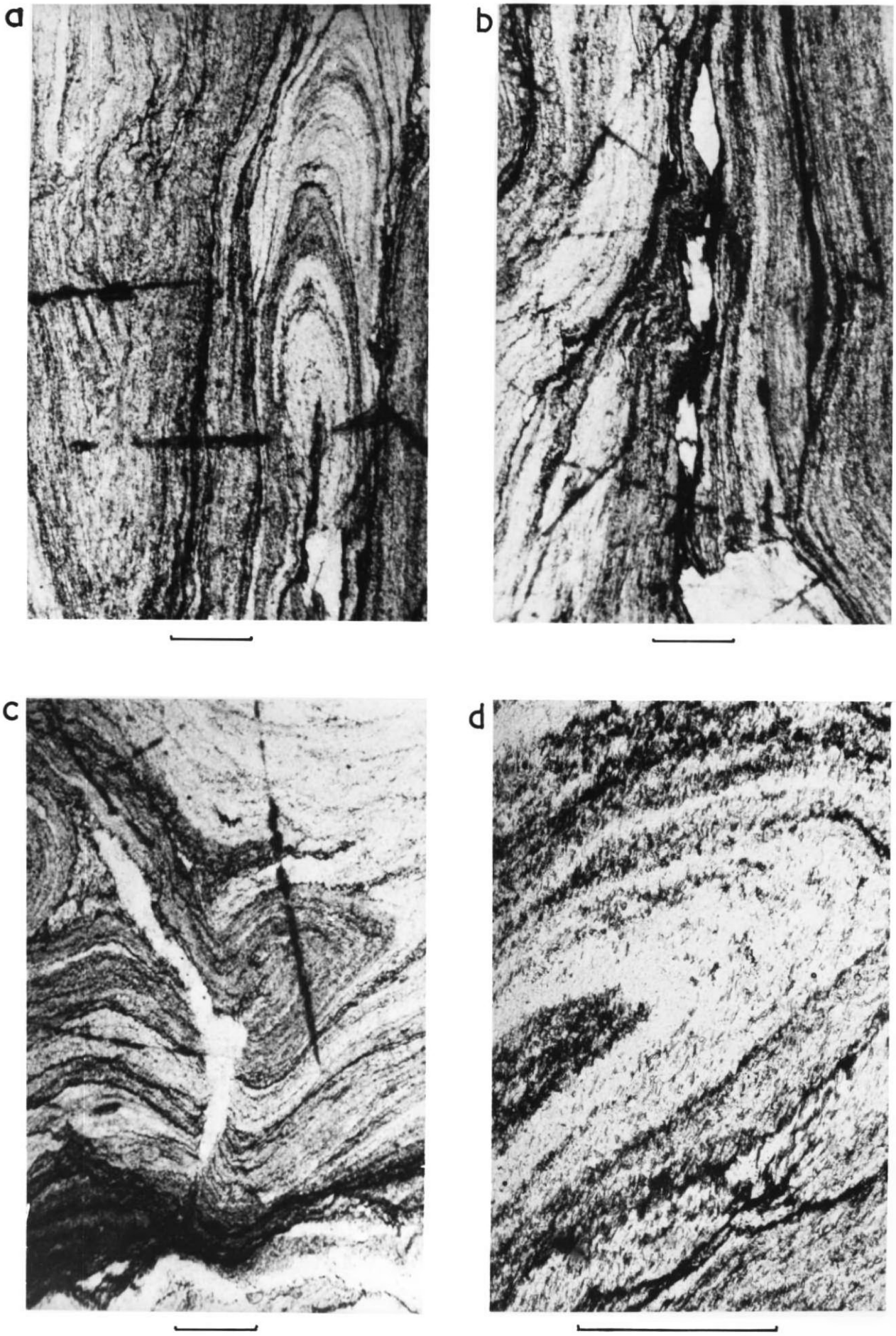
in the limbs by F_2 and S_2 respectively. The original nature of the pods is uncertain, but it is believed that many were formerly layers of sillimanite which have been broken up by a domainal S_2 fabric. This is demonstrated in Figure 6.2 a) and b) where there are clearly two planar fabrics the first being rotated around into the second which is S_2.

S_1 IN GARNET - Planar internal fabrics (S_i) in garnet porphyroblasts are relatively common in semipelitic rocks throughout the study area. They are defined mainly by fine grained mica and quartz inclusions, by bands of minute inclusions, and by the elongation of some of the inclusions. Two examples are shown in Figure 6.2. In both of them S_i is a planar fabric at a distinct angle to S_2. However, in example d) it is also at angle to the primary layering (S_{0-1}) with distinct hooks on each end. This hooked shape of the porphyroblast combined with the tails of finer garnet infers a rotation with respect to S_{0-1} and S_2, and by removing that rotation the garnet becomes elongate in S_{0-1}. Hence it is concluded that the elongate shape of the garnet and its internal fabric defined by elongate quartz grains and biotite preferred orientation, represent a planar pre-S_2 fabric (i.e. $S_i = S_1$). Other examples of pre-S_2 garnets are given in Figure 6.7.

S_1 QUARTZ AND QUARTZO-FELDSPATHIC VEINS - It has already been noted in Chapter 3, that quartz and quartzofeldspathic veins antecede the D_2 deformation. They parallel the lithological layering in all but one instance (see below) and are folded with it.

The one example of a non layer parallel but pre-D_2 quartz vein is at a high angle (80-90°) to the lithological layering and has S_2 overprinted on it. This is an anomalous situation which may represent either a former high angle

FIG. 6.3



S_1 to S_o relationship if the quartz vein represents S_1, or a non-S_1 parallel relationship. The latter interpretation is preferred because mesoscopic S_1 in adjacent gneisses parallels the layering. Therefore, the vein may represent a tensional feature perpendicular to S_1.

6.2.1.2 F_1 Folding

In the previous chapter on the stratigraphy it was concluded that there were no macroscopic F_1 folds necessarily indicated. Therefore, the evidence for folding during D_1 is tenuous and based on only one mesoscopic specimen. Furthermore because of its close proximity to the mylonite zone (only 1.5 km northwest of it) it is possible that the strong overprinting fabric is not S_2 but S_3 or S_M thus making the fold an F_2 fold.

The particular fold specimen is shown in Figure 6.3. The rock is a very fine grained laminated, micaceous chert from a band associated with massive dolomite. It's very fine grainsize contrasts with quartzites from the same vicinity (fine to medium grained) but this is believed to be due to inclusion inhibition (Hobbs et al, 1976, p. 113) of primary grain growth induced by the fine lamination and the fine grained phyllosilicate and opaque mineral content. Consequently the very fine grainsize is considered to be a primary growth feature and not secondary recrystallization during the D_3 or more specifically, D_M deformation.

In thin section, the folds are isoclinal with considerable thickening in the hinges relative to the limbs and with

Figure 6.3: (?) F_1 folds in micaceous chert. S_2 is oriented "northwest" in (a) and (b) but is vertical in (c) and (d). Note transposition of limbs in (a) and quartz pods along dissolution surfaces in (b). (c) and (d) demonstrate the overprinting (?) S_2 fabric. Bar scale = 1 mm.

transposition and dissolution along the limbs such that individual laminations pinch out into dark, stylolite like, dissolution planes (Fig. 6.3a). Quartz veins and pods are not visibly folded by the folds (cf F_2 later this chapter) but rather are associated with the dissolution planes as elongate stringers and pods (Fig. 6.3b). The quartz within the pods is coarse with many pods being single crystals albeit undulose and deformation banded (from later deformations). The dissolution planes are very narrow and lined with opaque and semiopaque minerals. They are layer parallel in the limbs but truncate the layering adjacent to hinge regions.

6.2.2 D_1 fabric development

6.2.2.1 Significance of S_1

Before considering how S_1 may have formed, it is necessary to establish whether the S_1 fabric is a schistosity in its own right or whether it may not be a by-product of the D_2 deformation. There are two mechanisms by which such a fabric can be achieved as a by-product of D_2.

The first mechanism is based on the March model (March, 1932; Hobbs et al, 1976) and is based on passive rotation of micas in response to shortening. Such a model predicts either a symmetric point maximum of poles parallel to λ_3 or an orthogonal pattern of preferred orientation with modes symmetrical about λ_3 depending on whether the initial fabric is random or planar (see Hobbs et al, 1976). In either case it can be argued that if the principal axis of shortening is exactly parallel to (001) of mica then such mica cannot be rotated by a homogeneous strain. Consequently it is possible to get scattered micas at a high angle to S_2 during a single deformation, D_2 irrespective of the initial fabric. However, it is a unique situation that requires those micas that are at a high

angle now to always have been at a high angle and it does not predict rotation of micas from a low angle to a high angle. Therefore in considering the elongate, S_2 parallel domains of micas oriented at a high angle to S_2 (Fig. 6.1c), the planar fabric within them must initially have been a planar fabric because an initially random fabric would predict only scattered high angle grains.

The second mechanism is a preferential growth model which predicts that mica will grow with (001) perpendicular to σ_1 and hence ultimately, in a coaxial strain situation, closely parallel to $\lambda_1\lambda_2$ (Kamb, 1954; Flinn, 1965). While such a model predicts a unimodal fabric it does not discount other orientations and in particular those with σ_1 parallel to (001). Once again, though, this could account for certain of the scattered isolated micas at a high angle to S_2, but it does not account for the S_1 domains.

Allied to the growth mechanism is the Dieterich model. Dieterich (1969) outlined several theoretical models by which a layer parallel schistosity could be developed in the hinge areas of folds without the necessity of there being a pre-existing planar fabric. Dieterich demonstrated that in the hinge areas of certain folds the principal axis of shortening was locally perpendicular to the layering rather than the axial plane. Consequently it is possible to get a bimodal distribution of the type observed; that is, both layer parallel and axial plane parallel orientations. This type of layer parallel fabric development in hinge zones has been clearly demonstrated (e.g. see Roberts and Stromgard, 1972), but, however, it predicts only <u>local</u> layer parallelism, in certain regions of fold hinges. Furthermore it does not predict widespread truncation of micas nor does it

account for S_2 parallel domains of S_1 mica.

Hence it is concluded that the microstructural evidence presented above confirms the existence of a pre-S_2 planar fabric, S_1. The mechanisms briefly outlined above may have enhanced the S_1 fabric, but they are considered to be of only local importance.

6.2.2.2 Origin of S_1

Consequential to the strong overprint of D_2, D_3 and other post D_1 deformations, and because only one possible (?) F_1 fold was recorded, it is impossible to say how S_1 was developed. There are two models for developing such a fabric;

a) by sedimentary settling or compaction, and

b) by tectonic deformation.

They both suppose that micas in general become orientated such that (001) is perpendicular or at least subperpendicular, to the maximum shortening strain whether that be by rotation, preferred nucleation, preferred growth or whatever.

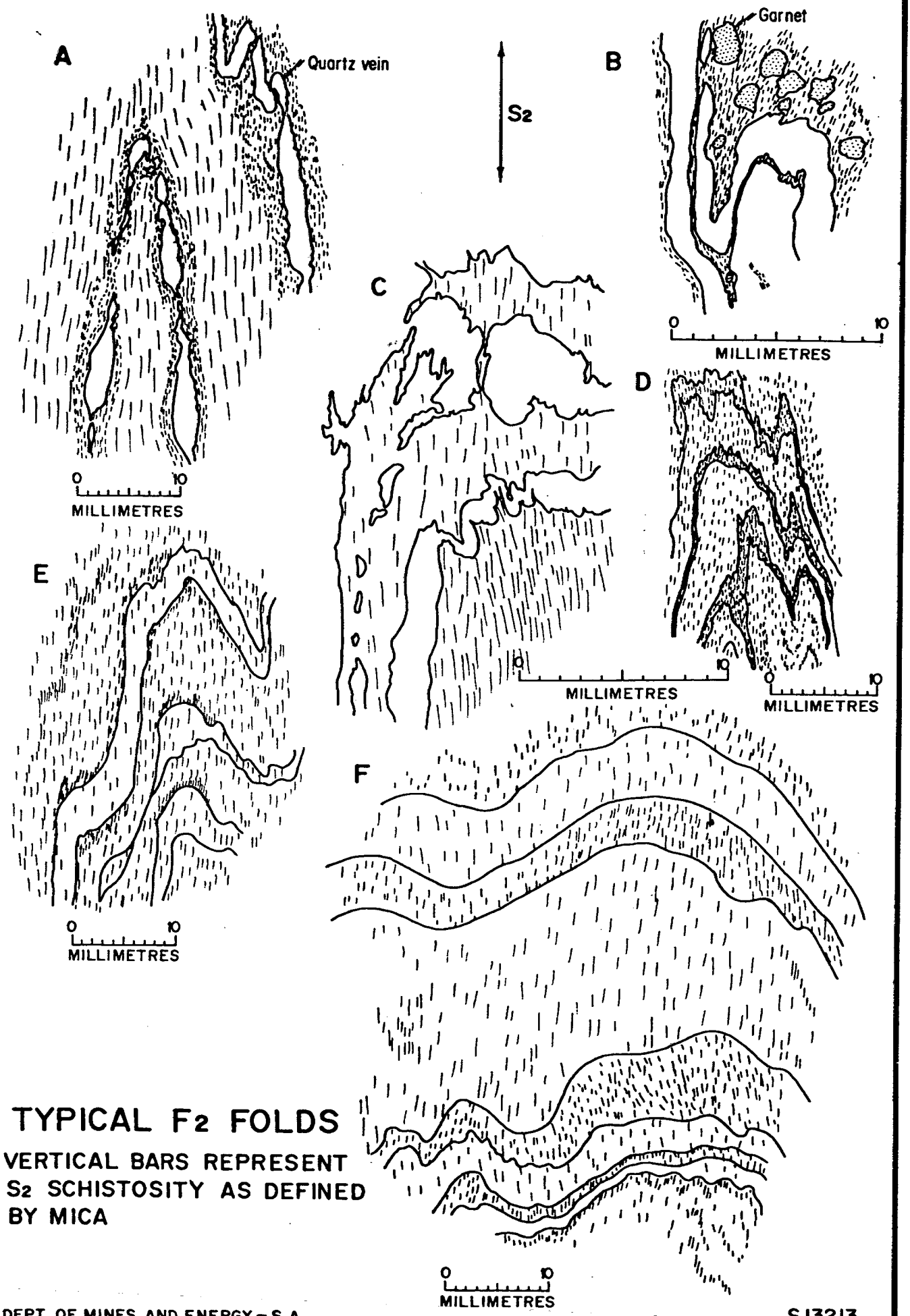
MODEL A - The sedimentary model supposes that sedimentary layer silicates such as clays or detrital micas are either deposited as flakes parallel to bedding or deposited at a distinct angle to bedding but rotated into parallelism during compaction of the sedimentary pile. There is little doubt that such processes do occur and that a strong layer parallel orientation can form this way. Furthermore, such micas can act as nuclei for new grains or can control new grain orientation (mimetic growth; Hobbs et al, 1976) such that a fabric developed during compaction can be enhanced during an imposed metamorphic event even without an accompanying deformation. Examples of this type of fabric formation are common in literature (e.g. see Oertel, (1970); Deelman, (1974); Williams et al, (1969)) and the phenomenon is well known.

MODEL B - The general occurrence of schistosities and other foliations parallel or very closely parallel to the axial planes of folds is also well known and has been well documented (e.g. see Turner and Weiss, 1963; Ramsay, 1967; Hobbs et al, 1976). Furthermore it is a widely held view that isoclinal folds produce layer parallel schistosities in their limbs and that the hinge areas are commonly markedly subdued. Such is the case in areas like Broken Hill for example, where large, macroscopic, isoclinal folds have been confirmed on sedimentary facing criteria (Glen et al, 1977). Here, at Broken Hill in the high grade rocks, there is a very strong, pervasive, layer parallel schistosity developed in the limbs of these isoclinal folds, whereas the hinge areas have been so strongly deformed and overprinted that they are now no longer recognizable. The Broken Hill example is only one of many such examples of this type of early deformation (e.g. see also Ramsay, 1958; Read, 1973; Cooper, 1974; Huddleston, 1976).

Related to this simplified fold model are numerous other more complicated structures such as thrust nappes and fold nappes. These too have been recognized throughout the world (e.g. see Marjoribanks, 1976; Johnson, 1970; Thompson et al, 1968) and in the vast majority of cases they also produce ayer parallel schistosities. Whilst they may represent either extremes of isoclinal recumbent folding or entirely different thrust type tectonics as in the Alps, they are included in this model because they are all characterized by tectonically formed, pervasive, layer parallel schstosities.

To discount either of models A or B is very difficult because of the severe D_2 overprint. The single, (?) F_1 fold example described earlier is the only positive evidence

FIG. 6-4



TYPICAL F2 FOLDS

VERTICAL BARS REPRESENT S2 SCHISTOSITY AS DEFINED BY MICA

DEPT. OF MINES AND ENERGY – S.A.

S 13213

to support a tectonic model since it has been shown that macroscopic D_1 structures are not necessarily required. Therefore it can only be concluded that a sedimentary model is indicated. Indeed the (?) F_1 fold may be a sedimentary structure. However while a sedimentary model may be indicated, it is stressed that a tectonic model cannot be completely precluded.

6.3 D_2 DEFORMATION

6.3.1 The fabric

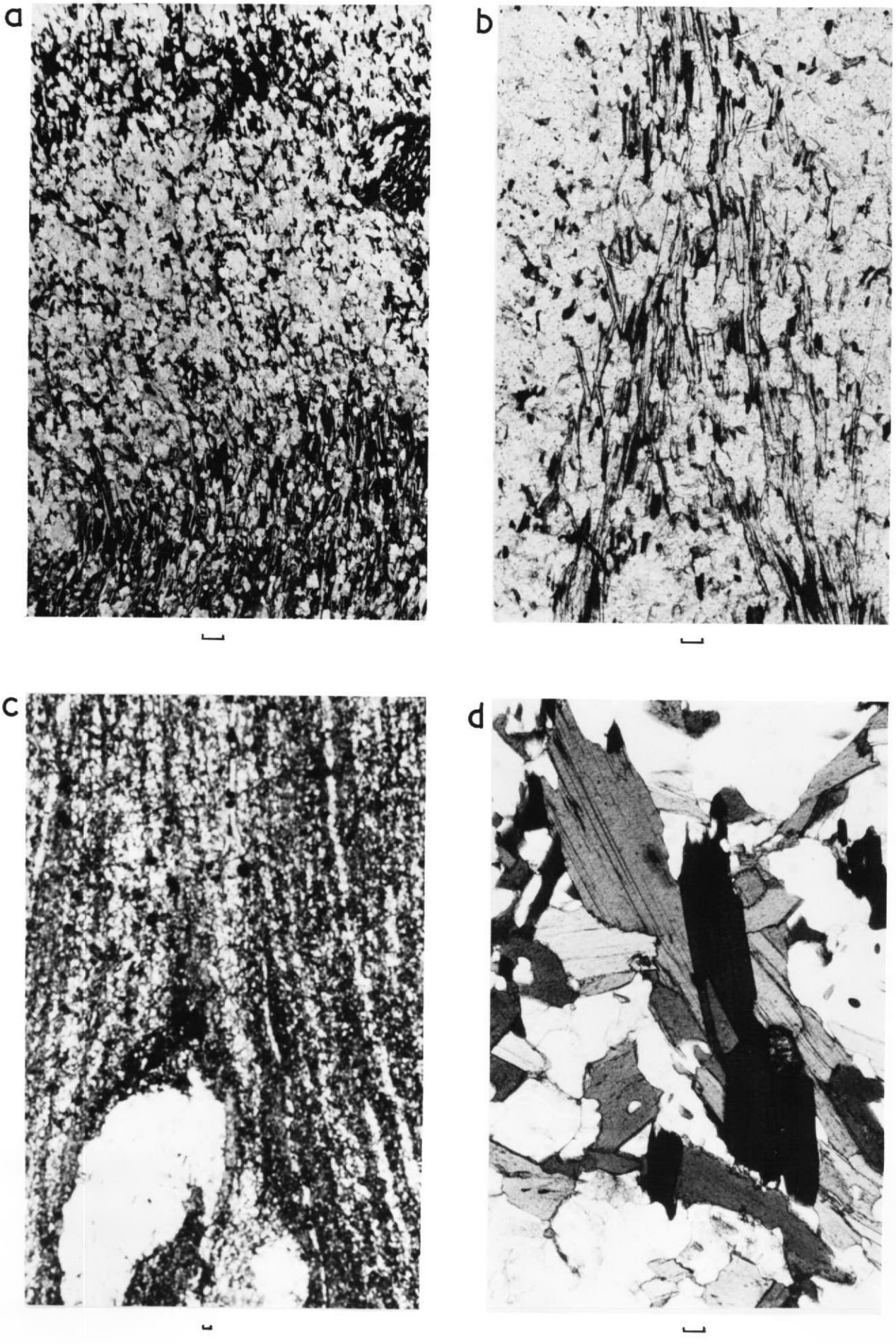
As previously outlined, the D_2 deformation was a major fold event affecting the whole area and producing pervasive planar and linear fabrics. The various lithologies have all been affected by D_2 and they all record F_2 folds and S_2 planar fabrics of essentially the same character. As D_2 is best recorded in the semipelites, the fabrics of those rocks will be described in detail and then a brief comparison of the equivalent fabrics in the other lithologies, will be made.

6.3.1.1 Semipelites

F_2 FOLDS

F_2 folds in general have the form of tightly adpressed multiple fold hinges with limbs parallel or very closely parallel to the axial planar S_2 schistosity (Fig. 6.4). The limbs often display pinch and swell type features ranging from simple mullions to isolated, elongate pods (? boudins) within the S_2 schistosity. This may represent attenuation of the limbs but it was noted in Section 6.2.1.2 that quartz pods were developed as primary features along dissolution planes associated with the (?) F_1 folding. Therefore the observed pinch and swell structure may represent the combined effect of D_1 and D_2 deformation.

FIG. 6.5



Hinges of F_2 folds are varied in form due to the heterogeneous nature of the semipelitic layering. Quartz veins generally have rounded outer arcs and sharp inner arcs, but in the more subtle layers with lower competency contrast, the hinges are more rounded (Fig. 6.4). The latter also have longer wavelengths than folded quartz veins.

Textural characteristics of hinges and limbs are identical. Quartz in the quartz veins is coarse grained and some single grains often span entire hinges without any evidence of strain thus inferring significant recovery and recrystallization.

S_2 SCHISTOSITY

GENERAL - S_2 in the semipelites is defined principally by a strong mica preferred orientation supplemented by a mineral segregation (domainal or differentiated schistosity) and a crenulation schistosity (of the earlier S_1).

In the unmigmatized semipelitic gneisses of the Wangaraleednie subarea it is generally manifest as a homogeneous mica (and locally sillimanite) schistosity with micas uniformly distributed within the individual S_{0-1} bands, and oriented with (001) parallel to the F_2 axial planes (Fig. 6.5a-b). The micas are elongate parallel to S_2 and this is sometimes accompanied by the dimensional preferred orientation of other minerals such as opaque minerals, quartz and feldspar. Muscovite and muscovite/sillimanite pods are flattened within S_2.

Figure 6.5: F_2 fold hinges with strong S_2 (vertical) fabrics. (a) homogeneous (within individual S_{0-1} bands ("east-west" oriented)) mica schistosity (b) homogeneous mica schistosity. (c) domainal schistosity, S defined by folded quartz vein at bottom. (d) S_2 biotite overprinting S_1 biotite in migmatite gneiss. Note pleochroic haloes about minute zircon inclusions. Bar scale = 0.1 mm.

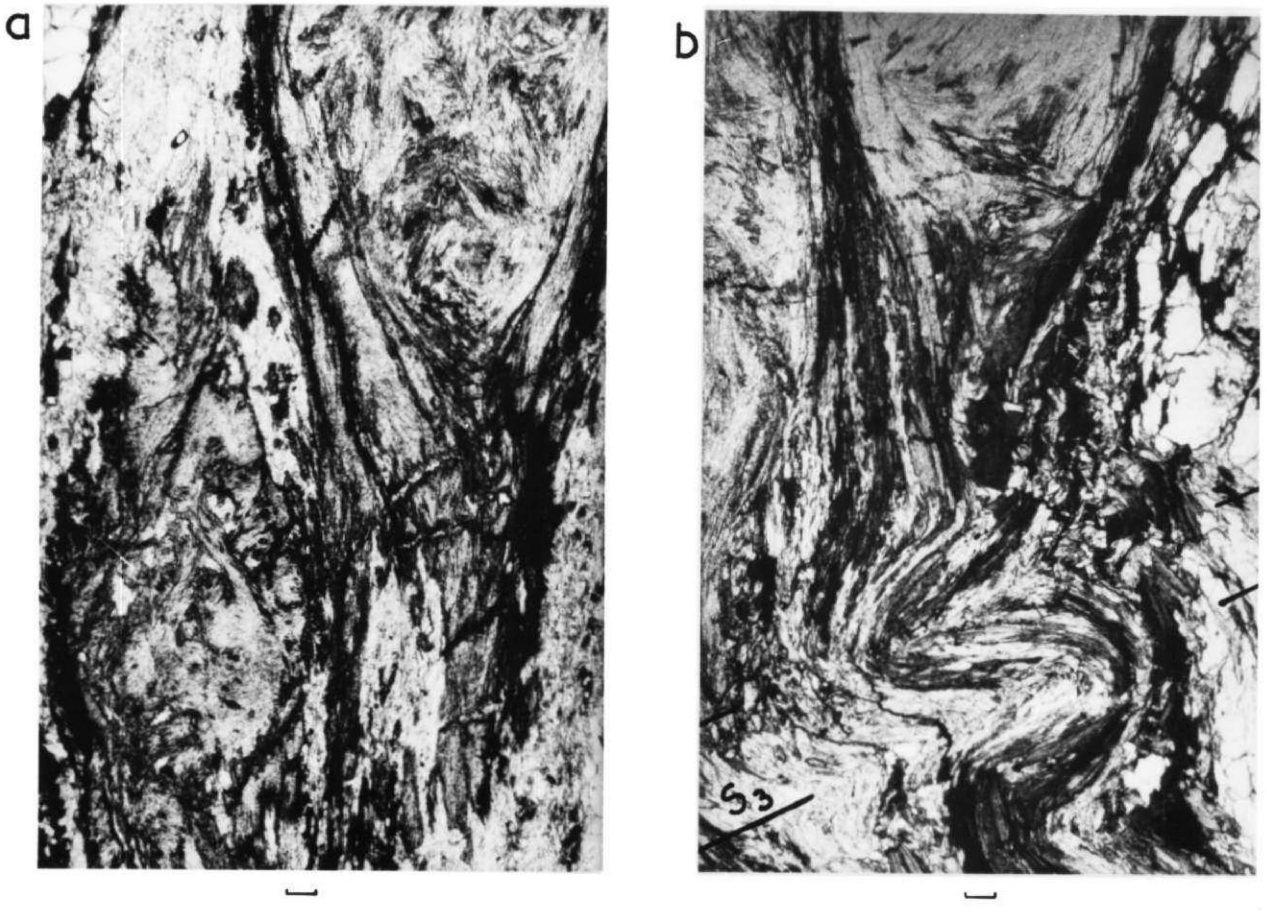
In addition to the mica preferred orientation, a domainal schistosity sometimes develops. It occurs as planar domains richer or poorer in either mica, quartz or feldspar (Fig. 6.5c), and ranging in width from 0.05 mm (one grain wide) to over 0.2 mm. Micas in the mica rich domains are strongly S_2 parallel but in the quartzo feldspathic domains they are scattered in orientation there being two main modes, an S_2 parallel orientation and a high angle (to S_2) orientation.

Associated with the domainal schistosity is sometimes a crenulation schistosity. It is preserved only in the mica rich (S_{0-1}) bands and micas in the long limbs have been rotated into sub-parallelism with S_2. They do however show a slight angular mismatch to S_2 which distinguishes them from new micas recrystallizing along crenulation band boundaries. The crenulation band boundaries are strictly S_2 parallel and they grade into the domainal fabric.

In the migmatized gneisses of the Mt. Millar/Morowie subarea and the granite gneisses of the Plug Range subarea, S_2 is more enigmatic because F_2 folds are less common. Therefore its positive identification as distinct from S_{1-2} is restricted mainly to layer parallel cases where remnants of an earlier fabric could be clearly established and where the layer parallel fabric clearly antecedes D_3.

S_2 in these subareas is represented by two forms of schistosities. The first and prominent form is a high grade mica and sillimanite schistosity defined by the preferred orientation of (001) of mica (Fig. 6.5d), (001) of sillimanite (Fig. 6.2a-b), and by their preferred dimensional orientation. The second form of schistosity is defined by narrow, planar domains of finer grained, recrystallized mica, sillimanite, quartz and feldspar (Fig. 6.1d). The domains are mainly

FIG. 6.6



parallel to the layering and are of the order of 0.05-0.3 mm wide. Their S_2 association is clearly established by remnants of S_1 fabric elements which they often enclose and by F_3 overprinting. They frequently wrap around fibrolite pods and are associated with S_2 parallel overgrowths (Fig. 6.6a).

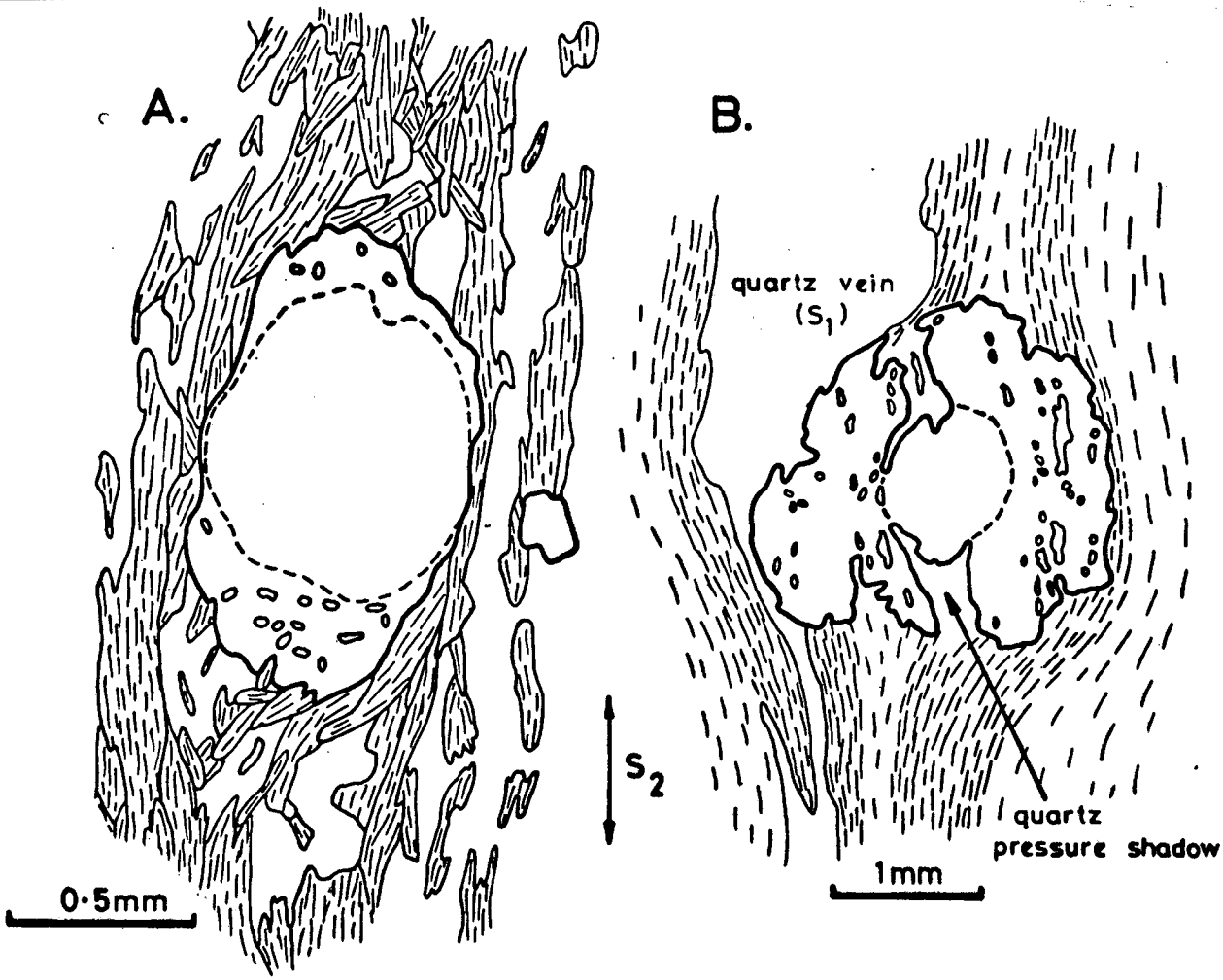
S_2 MICA - There are no recognizable differences between S_1 and S_2 micas except that S_2 micas are penetrative and may be finer grained than S_1 relics. Biotites of both schistosities contain scattered zircon inclusions with sharply defined pleochroic haloes (Fig. 6.5d) and they are of identical colour within any particular specimen.

Mica habit is variable according to the mineralogy of the gneissic layering. In the quartzo feldspathic layers biotite is prominent and distinctively occurs as stumpy, subidioblastic plates with length to breadth ratios (in sections normal to S_2) around 3:1. By contrast, in micaceous layers micas are more idioblastic (because there are more mica-mica interfaces than quartz/mica interfaces, the latter being mainly cuspate or embayed) and they display a more intensive platiness with length to breadth ratios mainly in excess of 5:1.

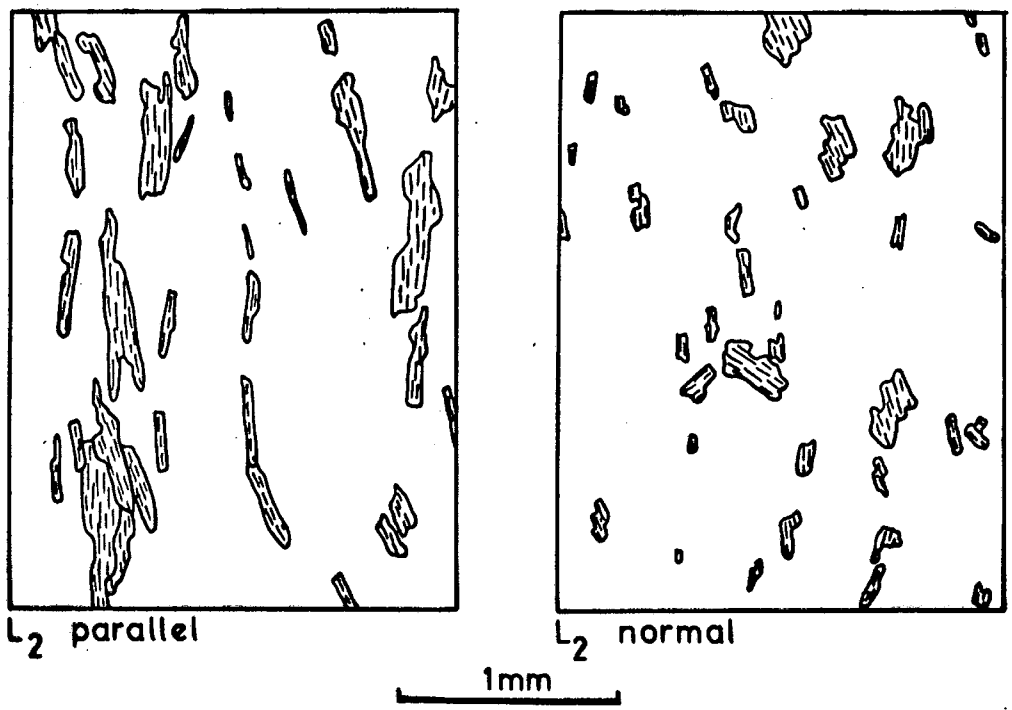
S_2 SILLIMANITE - Sillimanite defining S_2 occurs in three main forms; as fine needles overprinting M_1 fibrolite in pods flattened within the S_2 schistosity, as fine needles within accicular S_{1-2} trains, and as fibrolite beards overprinting fibrolite pods (Fig. 6.6a). Characteristically S_2 sillimanite is penetrative, idioblastic and fine grained.

Figure 6.6: (a) and (b) fibrolite pods with fibrolite/mica beards. S_2 is vertical. Note F_3 crenulations of mica/sillimanite films in (b). (c) and (d) M_2 orthoclase/microcline elongate in S_2 but with an internal S_2 fabric. Note in (d) the deformed S_1 fibrolite remnant ("northwest" oriented). Bar scale = 0.1 mm.

FIG. 6.7



A-B) D_2 garnet overgrowths on pre-D_2 garnet cores



C-D). L_2 mica elongation within psammite bands.

D_2 QUARTZ AND FELDSPAR - Neither quartz nor feldspar contribute greatly to defining S_2 and as illustrated in many of the preceding micrographs (Figs. 5.2-10, 11, 12) a dimensional preferred orientation of either of these minerals is either weak or absent. However, when restrictions on grain growth are imposed by either the gneissic layering or individual mica plates, quartz in particular assumes an S_2 or S_{1-2} parallel elongation. Furthermore, although it is rare, new feldspar that has crystallized during D_2 is also elongate in S_2. One such example from podded sillimanite gneiss in the Calcookara subarea has a poikiloblastic texture with an internal S_{1-2} biotite-sillimanite fabric (Fig. 6.6c-d) and is elongate of the order of 3:1. This elongation is a primary growth feature and not a mechanical flattening.

D_2 GARNET - While garnet does not contribute greatly to the S_2 fabric, there are a few examples of garnet growth during D_2. In Figure 6.7a-b two periods of garnet growth are clearly inferred with the second growing during D_2. In these examples the early garnet is dusty with minute inclusions whereas the later garnet has fine grained quartz and mica inclusions. However, while the outer garnet in both examples is regarded as of D_2/M_2 origin, there is conflicting evidence with respect to the exact timing of garnet growth and deformation in each. In Figure 6.7a the M_2 garnet has grown in a strain shadow site relative to S_2 whereas in Figure 6.7b the M_2 garnet has grown in a site of high strain. Hence it is concluded that there has been a slight diachronism of deformation and garnet growth between the two areas from where these examples came. However, since both examples are from the Wangaraleednie subarea not far removed from each other it is not regarded as a major macroscopic feature (cf MacQueen

and Powell, 1977) though it may be a topic for future investigation.

L_2 LINEATIONS Apart from the quartzites, the best development of an L_2 linear fabrics is in the unmigmatized gneisses of the Wangaraleednie subarea. It is manifest as an extreme elongation within S_2 (> 10:1) of quartz pods and quartzo feldspathic aggregates, as a strong mullioning and, occasionally, as a mica elongation. Neither quartz nor feldspar show any pronounced elongation even within the elongate pods and aggregates, but rather they are essentially equant and subpolygonal. In the general case micas also lack any elongation within S_2, but a common feature of the very mica poor layers is the tendency for biotite to show a preferred elongation parallel to the other lineations (Fig. 6.7c-d).

Migmatite gneisses by contrast to their finer grained, unmigmatized counterparts, generally lack any lineation. However trains of sillimanite needles and fibrolite pods are quite often elongate in S_{1-2}. A clear example is shown in Figure 6.8a-b where a fibrolite pod (now pseudomorphed by sericite) is distinctively elongate (of the order of 10:1 against the 3:1 flattening normal to the lineation) within S_{1-2}.

6.3.1.2 Other lithologies

QUARTZITES - Within the quartzites typical F_2 folds are isoclinal with parallel limbs, axial planes, and axial plane schistosities. S_2 varies according to lithology and in the layered micaceous rocks is mainly a domainal schistosity

Figure 6.8: (a) and (b) elongate sericite (formerly fibrolite) pods defining L_2. (a) is perpendicular to L_2, (b) is parallel to L_2. Note F_3 crenulations with "east-west" oriented S_3 in (a) and "northeast" oriented S_3 in (b). (c) hinge of F_2 fold in layered quartzite showing domainal S_2 schistosity (vertical). S_{0-2} is oriented "east-west". (d) S_2 dissolution plane (vertical) with rotated muscovite. Note the sub-rounded microcline grains. Bar Scale = 0.1 mm.

FIG. 6.8

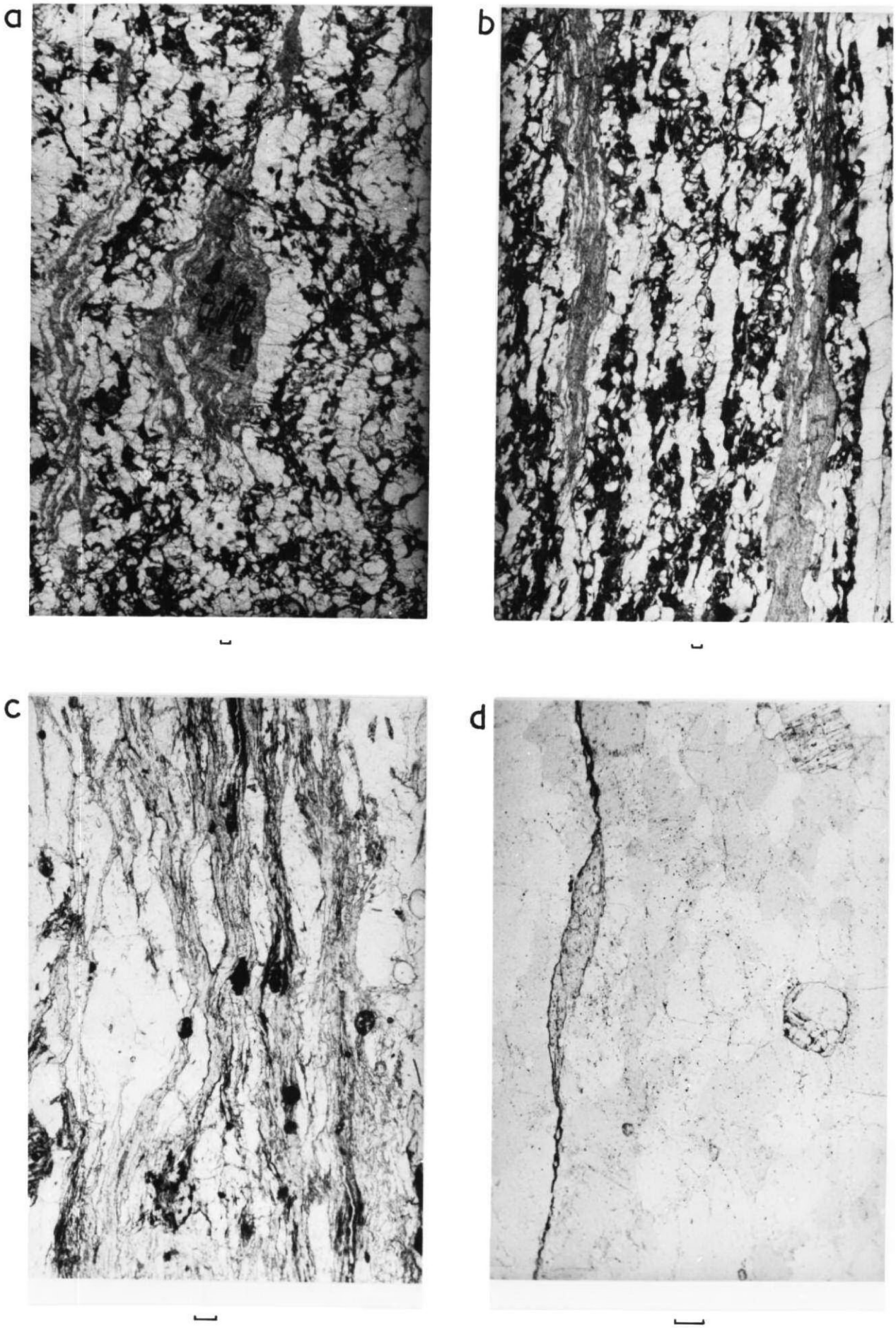
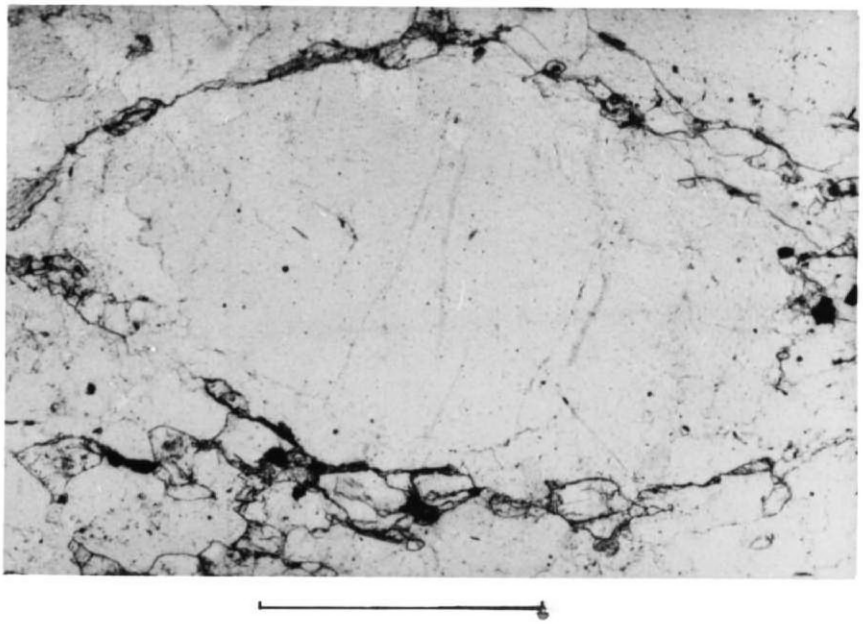
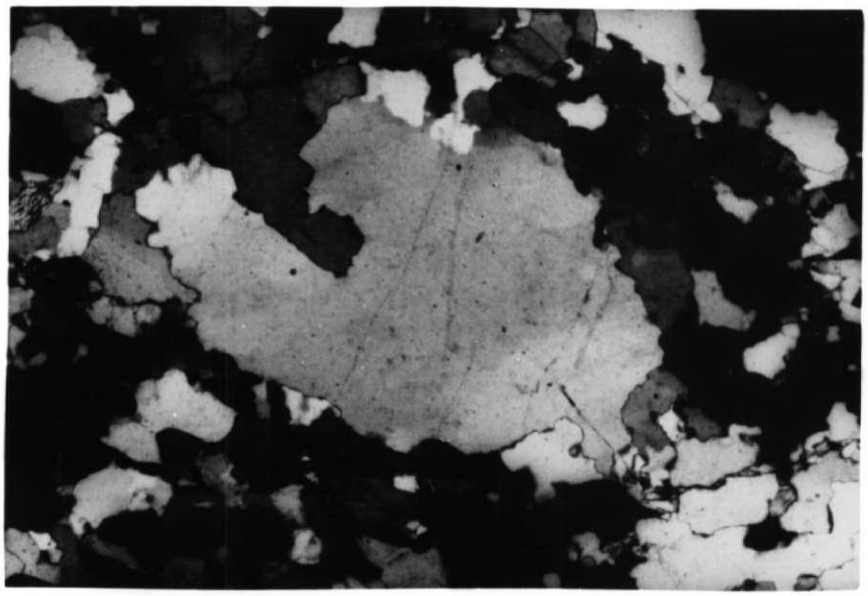


FIG. 6.9

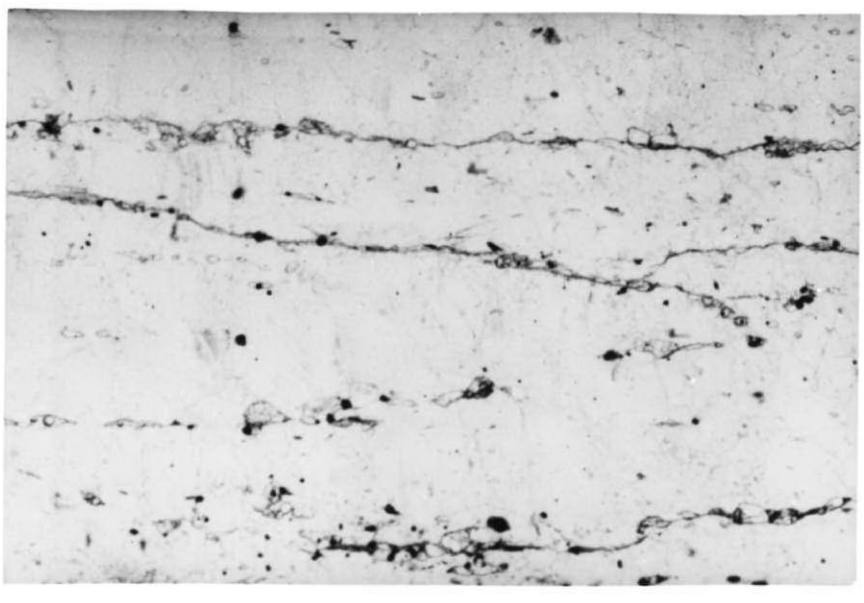
a



b



c



with mica films wrapping around quartz pods or augen (Fig. 6.8c). Within the massive rocks, however, the mica films are substituted by discrete, dissolution or fracture like planes with elongate muscovite and subrounded microcline grains scattered along them (Fig. 6.8d), they also often outline quartz augen in sections normal to S_2 and S_{1-2}.

In addition to these planar features, sillimanite, tremolite and deformed M_1 diopside also contribute to the definition of S_2. Sillimanite and tremolite occur as scattered fine needles within quartz grains while the diopside grains have been kink banded into elongate plates within S_2.

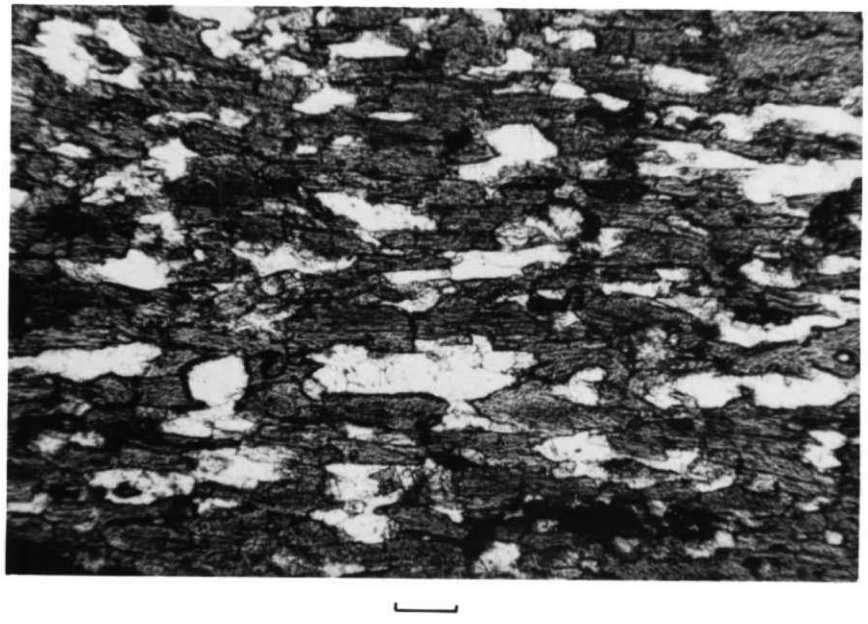
An L_2 lineation is prominent in quartzites throughout the study area. It is variously affected by D_3 and D_4 and this has a marked effect on quartz textures (see Sect. 6.4). The lineation is defined by two features; a strong elongation of quartz and sillimanite pods and aggregates (Fig. 6.9), and a more subtle mica, sillimanite and tremolite mineral lineation. The pods are particularly prominent and they generally have length to breadth ratios (parallel to L_2 but normal to S_2) up to and in excess of 10:1. They are mainly multi-grained aggregates of subpolygonal, relatively equant grains.

AMPHIBOLITES - The principal feature of amphibolites within the metasedimentary sequence is their strong S_2 and L_2 fabric. The F_2 fold illustrated in Chapter III has a good axial planar fabric combined with a weak (in this case) mineral lineation parallel to the fold axis. The planar S_2 fabric is defined by a very strong crystallographic preferred orientation of hornblende (i.e. "b" & "c" axes lying in S_2), by the dimensional

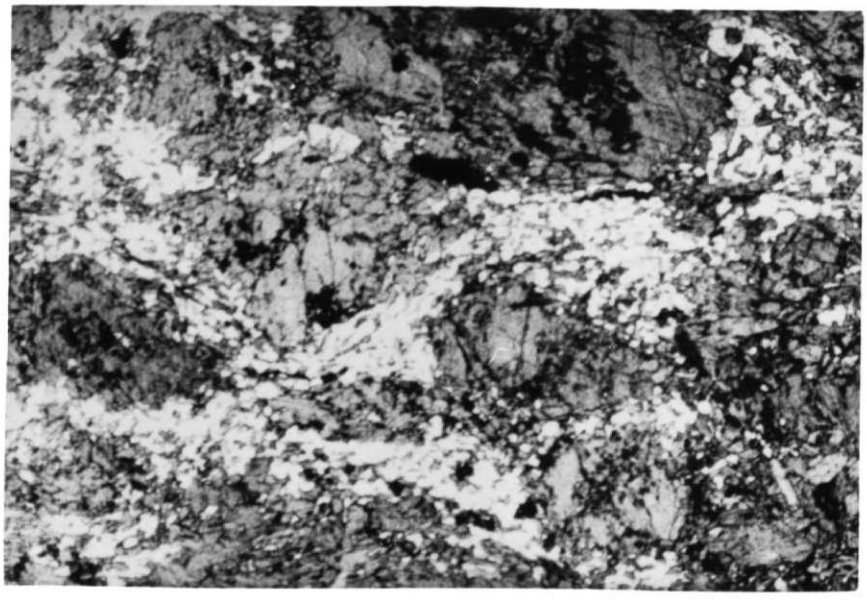
Figure 6.9: (a) quartz pod in section cut perpendicular to L_2. (b) as for (a) but crossed polars. (d) quartz pod, parallel to L_2. Bar scale = 1 mm.

FIG. 6.10

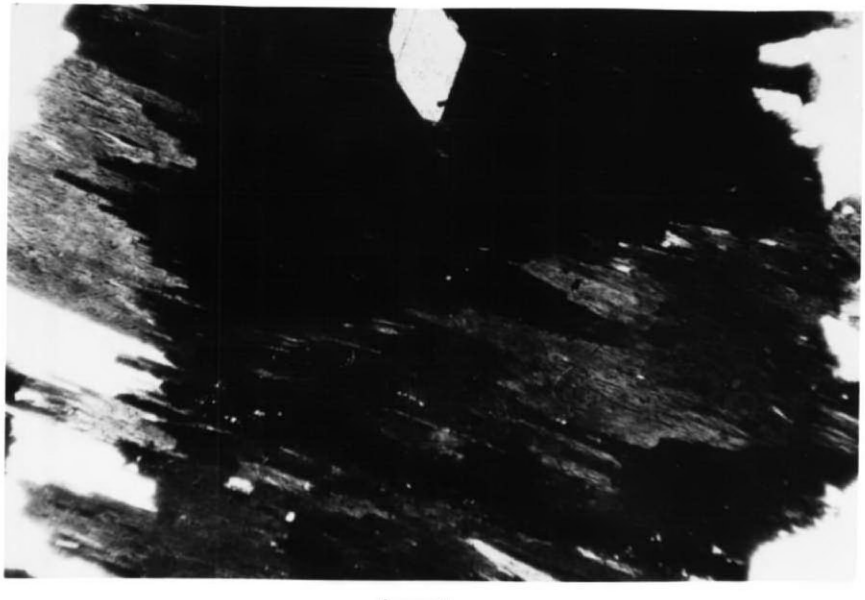
a



b



c



orientation of hornblende, plagioclase, quartz and opaque mineral, by biotite, by wispy lenticular aggregates of sphene and plagioclase, and, occasionally, by platy pyroxenes. The linear L_2 fabric is defined by the strong alignment of hornblende "c" axes within S_2 (Fig. 6.10a). There is no apparent pre-F_2 planar fabric in the amphibolites, but there are pre-F_2 hornblende prophyroblasts (Fig. 6.10b). By contrast with the schistose matrix, these are not crystallographically oriented in any specific direction. They are equidimensional though slightly augen shaped (< 2:1 elongation within S_2), and the S_2 schistosity of the matrix wraps around them. Furthermore they are xenoblastic and have recovery features such as subgrains (Fig. 6.10c). Rarely there are coarse, xenoblastic and unoriented biotite porphyroblasts accompanying the hornblende.

CALC-SILICATES - Both the calc-silicates and in particular the massive dolomites lack strong D_2 fabrics. However there are sufficient micas and chain silicates in the calc-silicates to define at least an S_2 microfabric.

The principal components of S_2 in them are an amphibole (mainly tremolite) preferred orientation, a dimensional orientation of pyroxene and a homogeneous biotite schistosity which truncates stumpy, S_1 relics.

Platy pyroxenes are significant in the calc-silicates because they are of M_1 origin and are commonly elongate parallel to the layering. However, in the cores of F_2 hinges some are elongate parallel to F_2 axial planes hence contributing to S_2. Also there are rare monomineralic pyroxene bands

---

Figure 6.10: (a) Strong hornblende lineation (of "c" axes) in a section cut parallel to L_2. (b) coarse augen of hornblende enclosed in a schistose matrix (S_2 horizontal). (c) subgrains within a coarse hornblende augen. Bar scale = 0.1 mm.

which have medium grained subpolygonal textures. Although a specific relationship could not be established, these bands are considered to represent polygonization during D_2 because they have sharp, curved to cuspate, grain boundaries which contrast against those derived from later (D_3) polygonization (see next section).

True dolomites are massive with granoblastic textures, but layer and chain silicates when they do occur, display weak layer parallel (S_{1-2}) preferred orientations (dimensional and crystallographic). Phlogopite and tremolite are mainly stumpy and often prefer to align along grain boundaries rather than parallel to S_2.

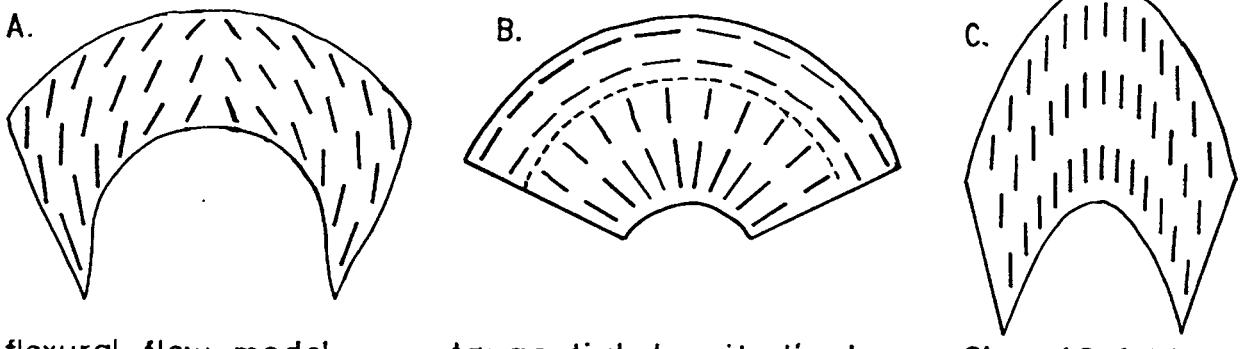
GRANITE GNEISSES - Two very important granitic bodies are affected by D_2; the Plug Range granite gneiss, and the Middle Camp granite. F_2 folds are numerous in the Plug Range body (see meso and macro-structure) and they are specifically characterized by a strong S_1 fabric which is folded and overprinted by a weaker, axial plane S_2 fabric. S_2 is defined by biotite, sillimanite, and less commonly by a weak dimensional orientation of quartz and feldspar. The relationship of S_2 biotite to S_1 biotite is identical to that observed in the migmatized gneisses.

By contrast, the gneissic granites of the Middle Camp body lack any signs of a planar fabric anteceding D_2. In these rocks, the prominent fabric (and only fabric preceding D_3) is S_2. It is defined by the preferred orientation of biotite and sphene, and by a dimensional orientation of feldspar and lenticular quartz aggregates. Biotite sometimes segregates into layers parallel to S_2 but this gneissosity is only weakly defined. The textures of these gneissic granites are enigmatic because of the strong overprint of the

FIG. 6.11

DISTRIBUTION of STRAIN in IDEALIZED FOLDS

after Ramsay (1967), Dieterich (1969), and Hobbs (1971)



flexural flow model

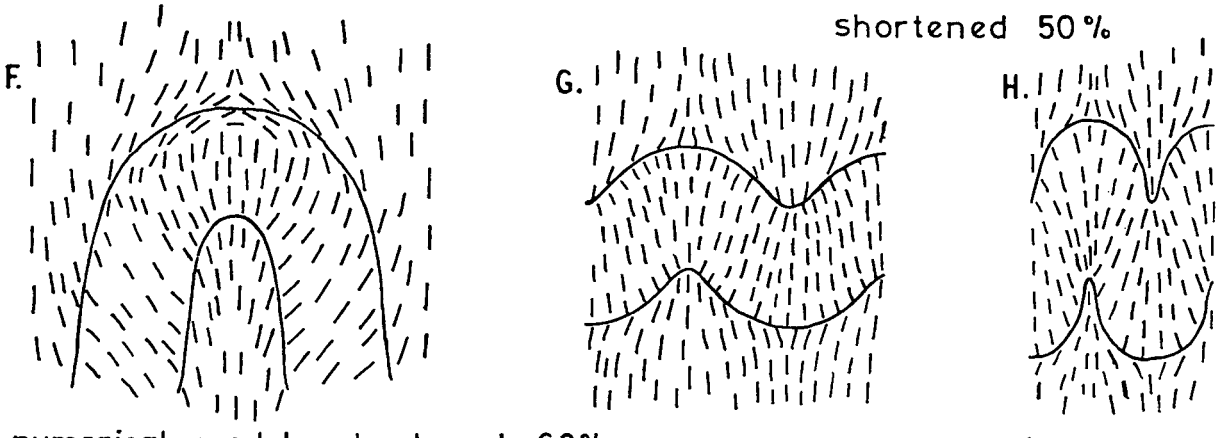
tangential longitudinal strain model

Class 1C fold shortened 50%



ideal Class 2 fold

Class 2 fold shortened 50%

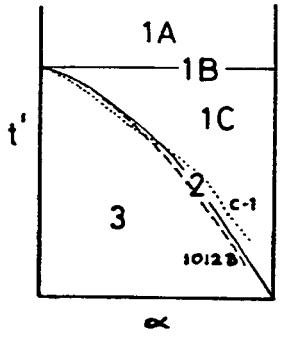


numerical models shortened 63%
viscosity contrast = 42 / 1

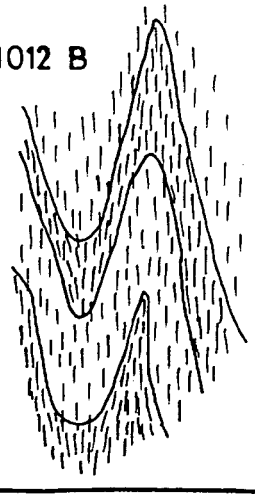
shortened 78%
viscosity contrast = 17-5 / 1

specimen C-1





1012 B



D_3 deformation which has resulted in partial recrystallization. However, it is believed that the original D_2 textures were medium to coarse grained, relatively equant and subpolygonal. Biotite inclusions within the larger plagioclase grains are randomly oriented.

6.3.2 D_2 Fabric Development

6.3.2.1 Relationship of Fabric to strain

ORIENTATION OF S_2 RELATIVE TO $\lambda_1\lambda_2$ - It has not been possible to establish quantitatively the distribution of strain during D_2 because there are no suitable strain markers and furthermore it is not known precisely how both earlier and later deformations have affected the strain at any one point. However it is possible to make some qualitative comments.

To get an idea of the total finite strain resulting from the D_2 deformation, one of the principle guidelines is the style and shape of F_2 folds. This in itself does not give a singular solution to the problem because, as illustrated by Hobbs (1971), the state and distribution of strain within folded layers of identical shape can vary according to, for example, the fold mechanism or the amount of shortening to which that layer was subjected.

To illustrate this, several different theoretical strain patterns have been sketched in Figure 6.11. These sketches are not by any means comprehensive, but they are at least representative of the more likely strain states envisaged.

In Chapter III it was noted that F_2 folds were either of Class 1C or Class 2 form and that they were equivalent to flattened parallel folds where the order of flattening was well in excess of 50%. Therefore they would correspond approximately to any of models C, D, E, G and H of Figure 6.11. Models A, B and F are ruled out because they are essentially

Class 1B folds. It thus follows that any of the strain states represented in those five sketches may be applied to F_2 folds.

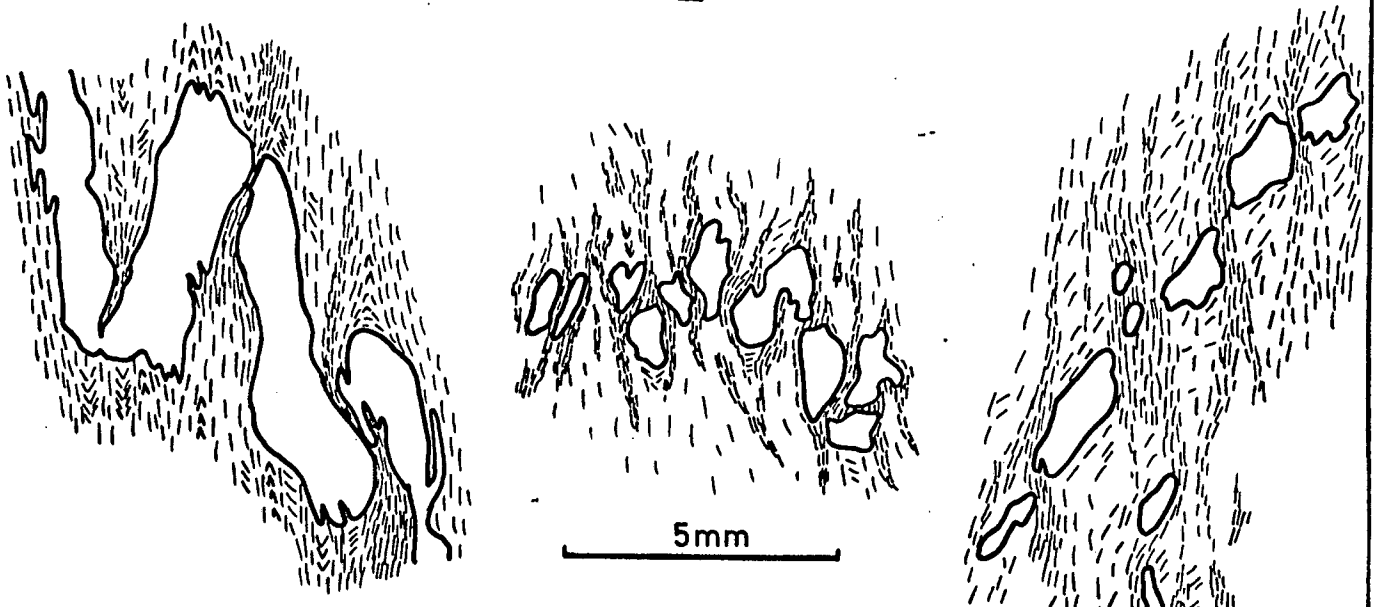
With isoclinal folds of the form of F_2, it is considered that in most limbs, the direction of maximum elongation (in the plane perpendicular to the fold axis) will be very close or parallel to both the layering and the axial plane of the fold. It will in fact be within only a very few degrees of that orientation and hence indiscernible from such.

In the hinge regions of F_2 folds, several cases may exist depending on the various inhomogeneities of both the lithology and deformation. Two particular examples are illustrated heree. Specimen C-1 which approximates to a Class 2 fold can be likened to a single layer system and as such, can be likened to model H. Specimen 1012B also approximates to a Class 2 fold, but it is more akin to a multiple layer system of relatively low viscosity contrast. Therefore it is compared with models C and E. As can be seen, there is clearly a close correspondence between the orientations of $\lambda_1\lambda_2$ and (001) of S_2 mica. In fact, from comparing numerous F_2 folds with theoretical $\lambda_1\lambda_2$ distributions (cf Figs. 6.4 and 6.11) there does appear to be, within the limits of normal observational error, a close parallelism between (001) of S_2 mica and $\lambda_1\lambda_2$ of the finite strain ellipsoid. This is consistent with previously published strain analyses, both natural and experimental, and with theory (e.g. see reviews by Hobbs et al, 1976; Williams, 1977; and Means, 1977).

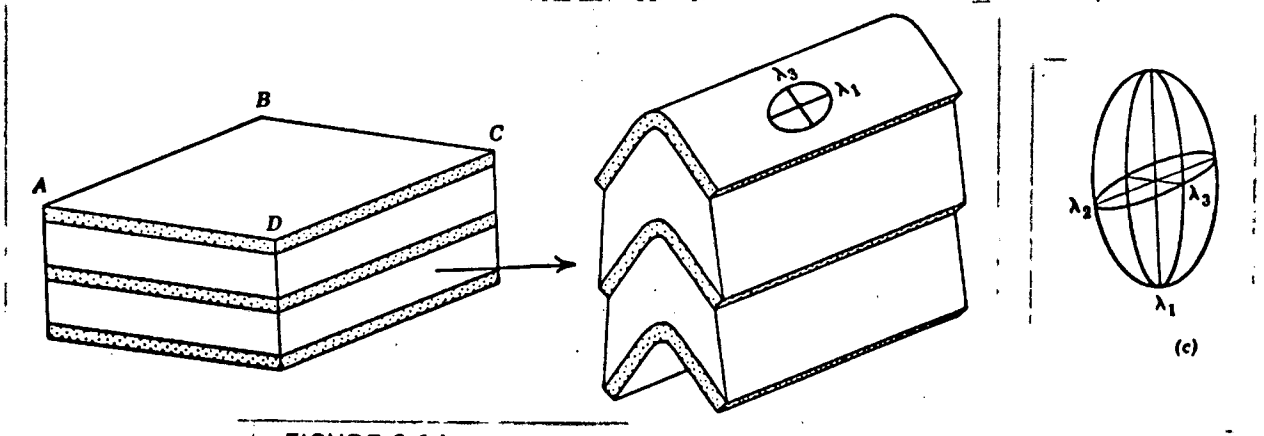
ORIENTATION OF L_2 RELATIVE TO λ_1 - The above discussion was concerned with S_2 and the $\lambda_1\lambda_2$ plane of the strain ellipsoid.

FIG. 6.12

DEVELOPMENT of L_2 LINEATIONS

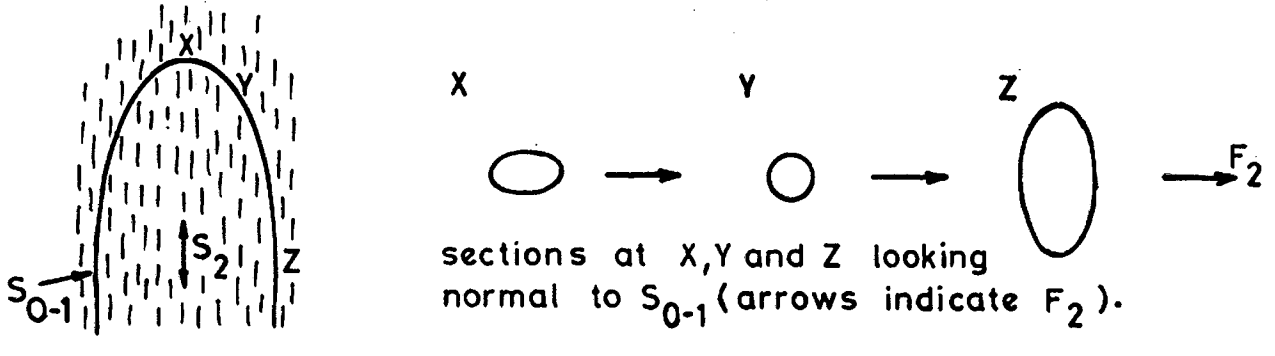


A) progressive formation of quartz rods from intersection of the domainal S_2 with S_1.



B) (from Hobbs et al., 1976)

FIGURE 6.14 Diagram illustrating how the principal axis of extension, in some folded layers, may be parallel to the fold hinge even though the latter is perpendicular to the principal extension axis of mean strain. The dimension of *AD* measured parallel to bedding has decreased during folding but the area of *ABCD* has been maintained by extension parallel to *AB*. The thickness of the competent beds (stippled) is unchanged and λ_1 at any point is these beds is, therefore, papallel to the hinge line. The thickness of the incompetent beds, however, has changed and λ_1 of the mean strain ellipsoid (*c*), for a system of such folds, is perpendicular to the hinge line.



sections at X, Y and Z looking normal to S_{0-1} (arrows indicate F_2).

C) shape and orientation of Schwerdtner's (1970) sectional ellipses on isoclinal folds when λ_1 is perpendicular to F_2.

The relationship between lineations, fold axes and the elongation of the strain ellipsoid is an even more complex problem than the foliation case where only the plane $\lambda_1\lambda_2$ was considered and not the orientation of λ_1 and λ_2 within that plane.

Within the study area, there are a variety of linear features ascribed to L_2 and parallel to F_2 fold axes. These are the quartz rodding, the amphibole lineation and the mica lineation. The principal mechanism for the development of the quartz rodding is related to the formation of domainal S_2 fabrics and as such is an intersection lineation recording the intersection of S_2 and S_{0-1}. It is clearly illustrated in the semipelitic gneisses where the process is initiated by folding of the more competent layers (e.g. quartz veins) accompanied by incipient dissolution and recrystallization of micas along discreet planes (Fig. 6.12a). These planar S_2 features progressively develop into narrow mica domains which transform the competent layers into a series of elongate segments within S_2. Ultimately it produces lensoid rods or aggregates of equant shaped, subpolygonal, recrystallized quartz and feldspar (Figs. 6.8c and 6.9; cf also Fig. 6.2a and b with respect to the formation of sillimanite pods) which represent the intersection of the $\lambda_1\lambda_2$ plane (assuming $S_2 = \lambda_1\lambda_2$, see above) with S_{0-1}. Hence they do not necessarily represent either λ_1 or λ_2.

The amphibole and mica lineations however are in a different category. Because they are mineral lineations they are more likely to reflect elongation directions (i.e. λ_1) than the quartz rodding. Therefore it would be useful to know the orientation of λ_1 and λ_2 relative to F_2 fold axes.

Although in many experimental and natural strain analyses

(e.g. see Cloos, 1971; Wood; 1974) λ_2 is often parallel to fold axes there is no reason why λ_1 should not be parallel to such or to any other orientation in between (for a discussion see Ramsay, 1967 and Hobbs, et al, 1976). In fact it is possible that the λ_1 to fold axis relationship may vary either spatially or during the course of deformation.

Without any strain markers, it is impossible to draw any quantitative conclusions. However, considering the macroscopic pre-D_3 geometry of F_2 fold axes (i.e. subhorizontal; see Fig. 4.16) the total strain ellipsoid may well have been oriented with λ_1 vertical in S_{1-2} and λ_2 parallel to F_2 (assuming $\lambda_1\lambda_2$ parallels S_2). Such an orientation is based on the observation that λ_1 is frequently parallel to the gravitation field. On such a presumption it is immediately inferred that the L_2 lineations parallel λ_2 of the total, macroscopic D_2 strain ellipsoid.

While this λ/L_2 parallelism may be valid on a macroscopic scale it need not be so on a meso or micro scopic scale. For example, Hobbs et al (1976) illustrate a situation that may develop in layered rocks where there is high competency contrast between layers. In that situation λ_1 may parallel the fold axes within the more competent quartzofeldspathic layers even though λ_1 of the total strain ellipsoid is oblique to the fold axes (Fig. 6.12b).

It is considered that this situation is particularly relevant here because it was noted above (e.g. Fig. 6.7c-d) that a mica lineation is <u>only</u> present in the very mica poor bands of the semipelitic gneisses. Hence a λ_1 parallel mica elongation is suggested. Nevertheless, though, it does not seem reasonable to extend this simple, local model to the more widespread amphibole lineation.

There are numerous accounts in literature of the preferred alignment of hornblende parallel to fold axes (e.g. Sturt, 1961; Ramsay and Sturt, 1970; Dallmeyer, 1972) oblique to fold axes (e.g. Vernon and Ransom, 1971), and both parallel and oblique to fold axes (e.g. Schwerdtner, 1970). Schwerdtner placed considerable emphasis on the sectional strain ellipse as the principal controlling factor noting that in isoclinal folds with λ_1 oblique to the fold axes, the long axis of the sectional ellipse is parallel to the axes in the hinge regions but oblique to them in the limbs (Fig. 6.12c). However, it is clear that the preferential alignment depends not only on strain, but also on the orienting mechanism. For example, Ramsay and Sturt (op cite) stressed the importance of body rotation (as in the Jeffrey model) whereas the Kamb model of stress controlled new grain growth may be more applicable in the Broken Hill examples of Vernon and Ransom (op cite). Another alternative which has not received much attention is intracrystalline deformation. Carter and Raleigh (1969) did not believe that this was important in amphiboles (compared with dolomite, quartz, pyroxene and olivine) but since Rooney et al (1975) have demonstrated preferential intracrystalline deformation of hornblende (by mechanical twinning on $(\bar{1}01)$ and translational glide along (100 001), such a mechanism must be important.

From this brief discussion it is clear that there is no straightforward solution to identifying either the mechanism of amphibole orientation or the relationship of that orientation with λ_1 and λ_2. However because a pre D_2 amphibole fabric appears to be absent, it is suggested that the strong L_2/S_2 fabric is principally a growth phenomena rather than a rigid body or intracrystalline rotation. There is no evidence to

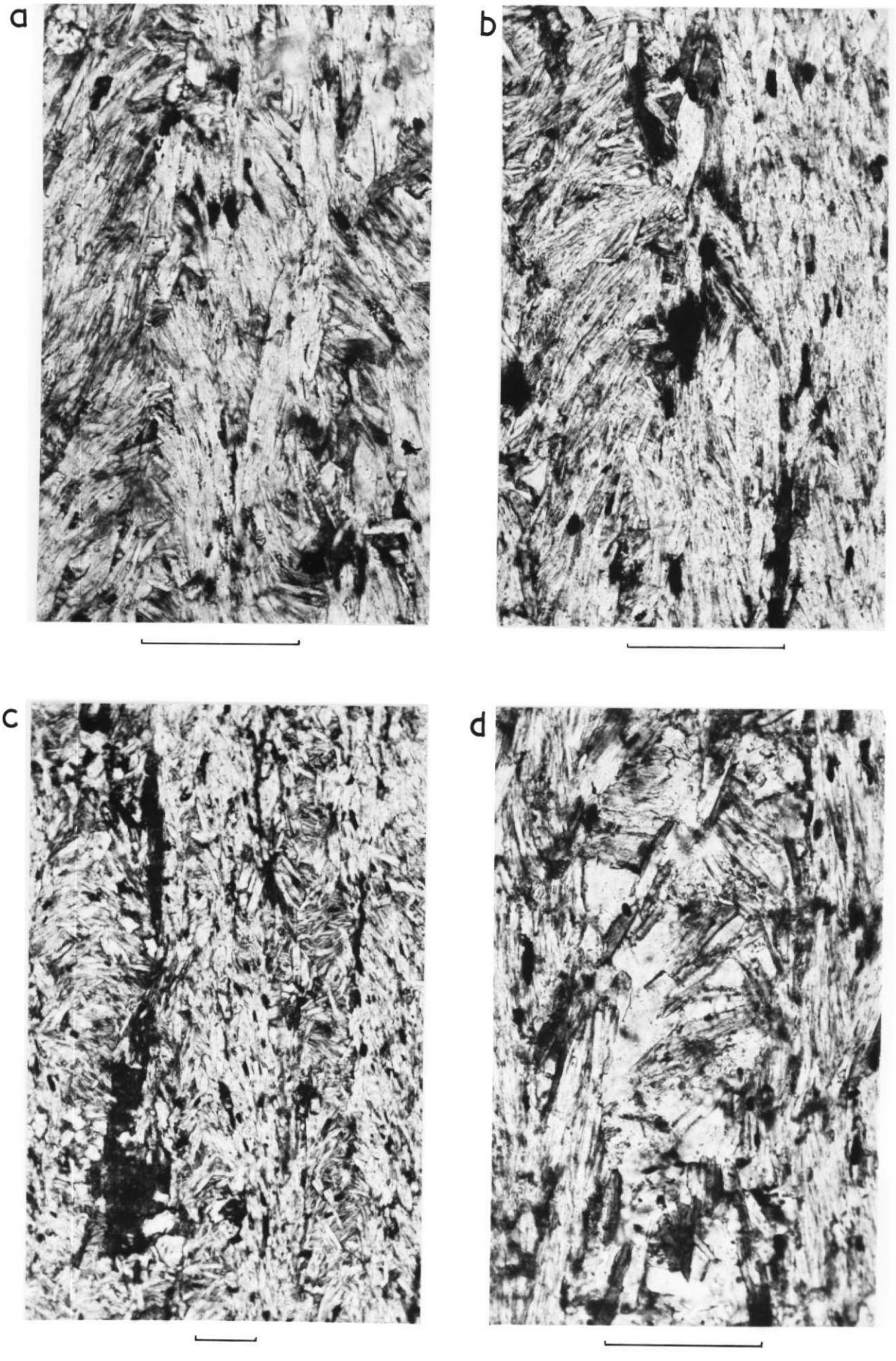
support a λ_1 or λ_2 parallelism (or even parallelism with the long axis of the sectional ellipse) although intuitively a λ_2 parallelism is suggested (see above).

6.3.2.2 Mechanism of Layer Silicate Orientation

In the broadest sense, the mechanisms of preferred orientation of layer silicates can be subdivided into two classes; mechanical rotation and preferrential growth. It is beyond the scope of this thesis to completely review the past and present views pertaining to this topic because such are well covered by Hobbs et al (1976), Williams (1977), and Means (1977). Briefly though, mechanical rotation in response to strain includes the March model (March, 1932): rotation of passive markers in a homogeneous body; and the Jeffery model: rotation of rigid markers in a viscous fluid (Jeffery, 1923). Opposing that, the growth mechanism is essentially based on the Kamb (1954) theory pertaining to the preferred growth of anisotropic minerals of a specific orientation relative to the stress field at the expense of those in less favourable orientations. The exact nature of this preferred growth is not clear however because there is some argument as to whether it is nucleation, pressure solution or preferential recrystallization rather than preferential growth of random nucleii. What is clear though is that this growth mechanism is distinct from the purely rotational mechanism and that no doubt both contribute to the development of all foliations. The problem then becomes one of determining how important a role each plays in the development of a particular foliation.

CRENULATION CLEAVAGE AND DIFFERENTIATION - There is unequivocal evidence that crenulation cleavage makes an important

FIG. 6.13



contribution to the S_2 fabric and that metamorphic differentiation is related to it. Numerous zones or domains containing mica at a distinct angle to the enveloping S_2 schistosity have been noted (e.g. Fig. 6.1c) but more importantly, rare relics of D_2 crenulations have also been observed. Every stage in the transition from simple crenulations with an incipient S_2 fabric, through to the domainal fabric have been recorded, and consequently this uniquely establishes a mechanism of S_2 fabric development. It need not, however, be the only mechanism.

In Figure 6.13 a series of photomicrographs traces this transition within a single specimen of muscovite-biotite-garnet pelitic gneiss from the Wangaraleednie subarea. In the initial stage of development the crenulations have relatively sharply defined though ragged band boundaries, the S_1 micas have been recrystallized to form a series of short but straight segments which interconnect each limb, and there is incipient growth of new mica principally along the crenulation band boundaries, but also as scattered, isolated plates within the limb domains.

With increasing strain and recrystallization, there is concomitant rotation of micas in the long limbs of assymmetrical crenulations and growth of new micas. The rotation becomes such that there is very little discernible difference between their orientation and S_2 and furthermore there is apparently incipient differentiation because these

---

Figure 6.13: Progressive development of S_2 (vertical) from a crenulated S_1 schistosity. (a) crenulated S_1. (b) crenulated S_1 with rotation of right limb into subparallelism with S_2. (c) domainal S_2 fabric with coarse S_2 micas along crenulation band boundaries (lower left). (d) domainal S_2 fabric. Bar scale = 0.1 mm.

strongly rotated limbs are deficient in quartz relative to the obliquely oriented S_1 domains. There is prolific new mica growth a) in zones which were initially band boundaries b) as isolated laths scattered throughout the oblique S_1 domains and c) in S_2 parallel limbs (? mimetic growth). There is exaggerated grain growth of some new S_2 micas whilst other minerals, particularly the opaque minerals, often form elongate shapes in S_2.

The final development in this particular specimen is a penetrative domainal schistosity. Rotation of the long limbs of assymmetrical crenulations and new grain growth in those limbs and along crenulation band boundaries have combined to produce ubiquitously S_2 oriented, planar, mica domains. These alternate with the quartzo feldspathic domains in which the high angle S_1 of the short limbs of assymmetrical crenulations has been preserved but overprinted by scattered, new, S_2 micas. Quartz (and feldspar) of the latter domains is mainly equant in shape and subpolygonal, but when bounded by micas either side becomes elongate. These textures indicate substantial recrystallization of quartz and feldspar.

Considering this example and the common presence of scattered S_1 domains enveloped by S_2, it is clear that the S_2 fabric has developed from the combined mechanism of rotation and new grain growth. Although it is impossible to say which mechanism contributed most to the definition of S_2, it is particularly significant that new grain growth made an important contribution. This contrasts with the superimposed D_3 and D_4 fabrics (see later).

OTHER S_2 SCHISTOSITIES NOT DIRECTLY RELATED TO CRENULATION - Development of S_2 mica orientation in rocks other than the

pelitic rocks or interbands, is more enigmatic. Although there are rare relics of crenulations (e.g. in fibrolite pods) and although some garnets have been shown to have been clearly rotated relative to the S_2 fabric (e.g. Fig. 6.1d), there is no positive evidence to suggest dominance of either a rotational mechanism or a new grain growth mechanism for the formation of S_2. Quartz and feldspar textures are identical to those in the quartzo feldspathic domains of the differentiated layering, (i.e. subpolygonal and equant), hence implying that they have either substantially or even completely recrystallized. This may suggest that the two could be equivalent with respect to development of S_2. In the differentiated layering it was clear that much of the S_2 mica was actually new and had grown in such orientations. The abrupt truncation of S_1 relics, the penetration of S_2 micas (and sillimanite etc.) into quartz veins (and the presence of M_2 overgrowths (Figs. 6.2), certainly support a growth mechanism for at least part of the S_2 fabric. However the contribution of rotation of S_1 micas in the differentiated case was also significant, therefore it can only be concluded that both mechanisms must have contributed to the definition of the penetrative S_2, but with the growth factor being significant.

COMPARISON WITH PREVIOUS WORK - Because the development of a penetrative mica schistosity from a crenulation cleavage is well illustrated here, it is appropriate to compare its development with some of the published material on that topic. There are two broad fields of study; the observational field (e.g. Williams, 1972; Etheridge and Lee, 1975; Knipe and White, 1977; Vernon, 1977), and the experimental field (e.g. Etheridge and Hobbs, 1974; Tullis, 1976).

Both Etheridge and Lee (1975), and Knipe and White (1977), have demonstrated by meticulous examination of natural examples that there is a very strong component of new grain growth in the development of slaty cleavage. Etheridge and Lee considered that the bimodal mica orientation (one bedding parallel and the other cleavage parallel) in their examples was incompatible with a predominantly mechanical rotation and hence concluded that much of the cleavage mica grew in that orientation during deformation. Likewise, Knipe and White were also able to show that the dominant mechanism of mica orientation was syntectonic growth. However they also demonstrated some other relevant features; namely, the growth of new cleavage mica along and parallel to the axial planes of crenulations and the progressive production of an anastomosing fabric starting from the initial crenulations and progressing via a domainal schistosity to a penetrative slaty cleavage.

Vernon (1977) in describing naturally deformed biotite from Broken Hill, considered that both mechanical rotation and new grain growth contributed towards defining a new fabric. Recrystallization and crystallization took place in zones of intense deformation (e.g. kinking) or dilation, and involved the formation and migration of serrated kink band boundaries and the preferred nucleation and/or growth of new mica both in rotated portions of deformed biotite and in areas of least physical constraint and/or greatest transport (e.g. kink band boundaries).

Etheridge and Hobbs quoting from experimental work on the deformation of phlogopite, also demonstrated the importance of kinking or crenulation. They showed that the annealing of bent or kinked micas led firstly to the development of

highly serrated kink band boundaries. Following this, there was rapid nucleation and growth of new grains particularly in the hinges of kinks. These then apparently grew to large new grains with subsequent secondary new grain nucleation and growth within them. The new grain growth was both stress and host controlled and the three most important orientations were (001) parallel to kink band boundary, (001) parallel to (001) of the host (i.e. mimetic growth), and (001) approximately perpendicular to kink band boundary. They also showed compositional differences between new and host grains and consequently concluded that there may have been some chemical driving energy in addition to purely deformational energy (N.B. Vernon also suggested this).

By contrast to those experiments, Tullis (1976) in a similar set of experiments but under different conditions concluded that rotation was the predominant mechanism. Tullis argued that the preferred orientation of mica was exactly as to be expected from the March model and furthermore that textures did not suggest new grain growth. Also Tullis did point out that syntectonic recrystallization produced stronger fabrics and that this was probably related to the reduction of mutual grain interference.

So therefore, in summary, it may be concluded that the crenulation cleavage mechanism of formation of a penetrative schistosity is very important. Both rotation and new grain growth are important processes and it appears from this thesis and the examples cited above that syntectonic recrystallization is fundamental in the production of a strong axial planar fabric. Furthermore, from this and previous work, it is also apparent that there are three broad stages in the development of such planar fabrics.

They are:

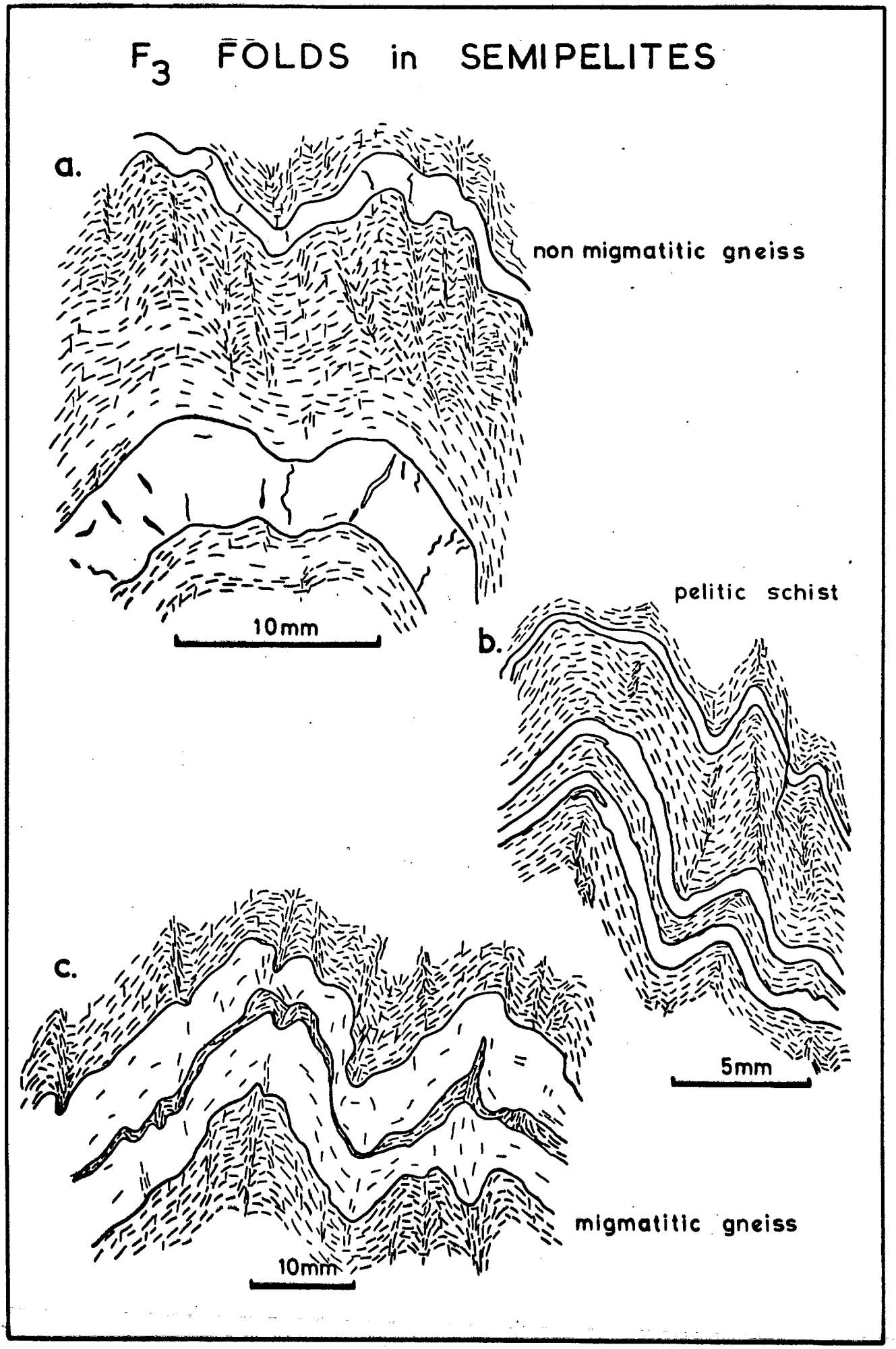
1) crenulation and kinking of a pre-existing fabric,
2) syntectonic recovery of mica with the development of serrated crenulation or kink band boundaries, and incipient new grain growth principally (but not exclusively) along such boundaries (with preferred orientations as outlined by Etheridge and Hobbs, 1974), and
3) widespread new grain growth of a domainal nature facilitated by rotation of a particular limb and the consequent (?) mimetic growth resulting from such. This leads to exaggerated grain growth of some micas.

Etheridge and Hobbs suggested a fourth stage to this involving further new grain growth within the first new grains but this could not be demonstrated in this study. However, the D_2 fabrics of this study have clearly developed through the first two of the above stages and are believed to represent an equilibrium situation at the stage 3 level.

6.3.3 Summary of D_2 Microfabric

In concluding the description and discussion of the D_2 microstructure it is obvious that the very principal characteristic of the D_2 deformation is the tight to isoclinal folding accompanied by a strongly pervasive and penetrative axial S_2 and L_2 fabric. All the microstructures have been developed from the combined processes of mechanical deformation (rotation), recrystallization and new grain growth with the latter being prominent and characteristic of this deformation. Furthermore these combined processes are typical of high grade deformations and they infer that the accompanying metamorphism was at least of the amphibolite facies. For example there has certainly been syn- and probably post-tectonic annealing resulting from the high temperatures of the rocks.

FIG. 6.14


F_3 FOLDS in SEMIPELITES
a.
non migmatitic gneiss
10mm
b.
pelitic schist
5mm
c.
migmatitic gneiss
10mm

Total strain is not known quantitatively but from inferences made it has been concluded that there was certainly a large component of flattening superimposed on the initial folding. From comparison with fold styles it is believed that $\lambda_1\lambda_2$ of the strain ellipsoid closely parallels the axial planes of folds. In addition it is also believed that mica (001) reflect the state of strain and that their orientations are certainly consistent with the $\lambda_1\lambda_2$ distribution.

D_2 fabrics are relatively uniform across the study area although they do vary somewhat according to the primary M_1 textures (i.e. migmatites verses non migmatites). This implies that D_2 was pervasive and that D_2 strain was of relatively constant magnitude. The processes of recovery, recrystallization and crystallization apparently kept pace with them.

Finally, the D_2 fabrics provide further confirmation of the existence of a planar fabric anteceding D_2; that is, they support D_1. There is certainly evidence that there is at least local disruption or minor transposition of the S_1 layering even at this scale, and in addition, that there is considerable variation in thickness of the layering.

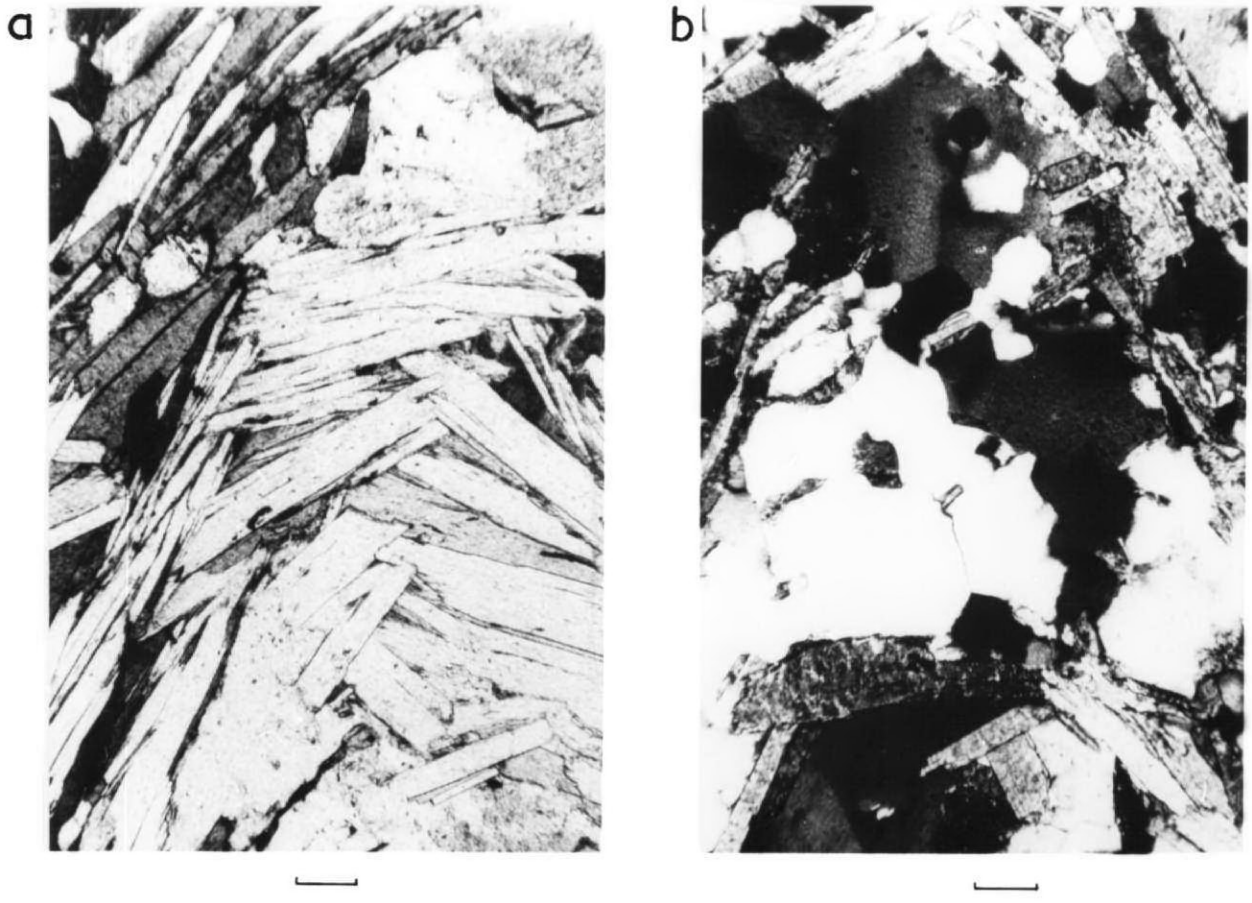
6.4 D_3 DEFORMATION

6.4.1 The Fabric

6.4.1.1 Semipelites

F_3 FOLDS - The nature of F_3 folds in thin section is shown in Figure 14. Characteristically they fold and/or crenulate the prominent layer parallel S_{1-2} schistosity with its associated quartz, muscovite and sillimanite pods, and normally they have an incipient axial plane cleavage; either a fracture like cleavage or a weak alignment of wispy micas. The common form of both F_3 and S_3 is variable throughout the

FIG. 6.15



study area due to variation of intensity of deformation, degree of recovery/recrystallization, and lithology.

In the unmigmatized gneisses of the Wangaraleednie subarea and parts of the Mt. Millar/Morowie subarea broad F_3 warps and buckles consist of tightly adpressed crenulations (Fig. 6.14A) in which S_{1-2} mica has partially recovered and recrystallized to form straight segments separated by highly serrated crenulation (kink) band boundaries (Fig. 6.15a).

In the migmatized gneisses of the Mt. Miller/Morowie subarea tightly adpressed crenulations are restricted to mica/sillimanite layers and occur either as tightly flexed, fine grained sillimanite/mica films, or as kink banded, medium grained S_{1-2} mica with highly serrated kink band boundaries (Fig. 6.15c). Quartzo feldspathic layers buckle rather than crenulate and they are often fractured subparallel to S_3. An important feature of these quartzo feldspathic layers is the nature of quartz and feldspar grain boundaries which, like the fractures, are nearly always lined with a diffuse, rusty brown material consisting in part of phyllosilicate. In addition, along feldspar/feldspar grain boundaries there is often incipient crystallization with minute new grains forming narrow, irregular zones one or two (new) grains wide. This contrasts with the smoothly curved or cuspate, quartz/feldspar grain boundaries.

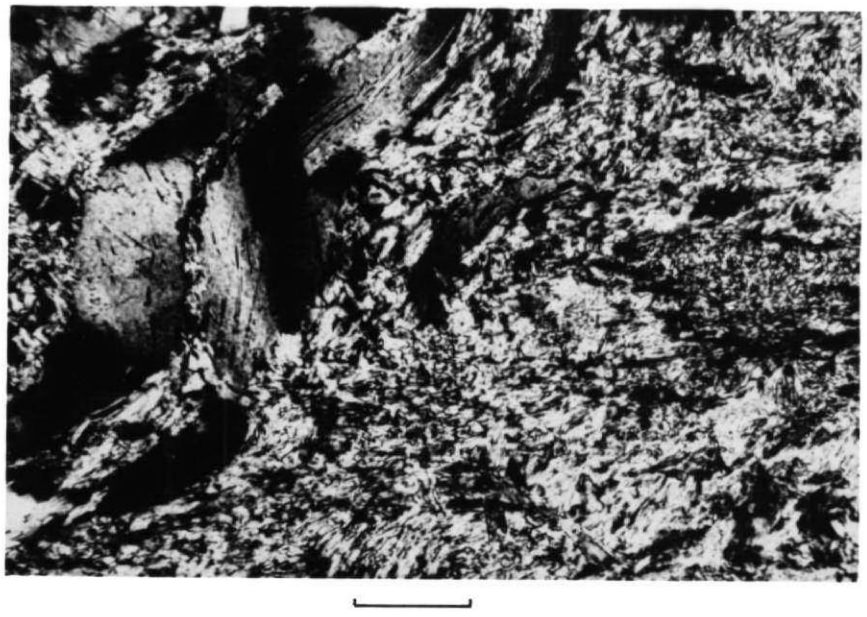
In a few localities, the intensity of D_3 deformation and degree of recovery/recrystallization is such that the normal S_{1-2} textures and fabrics are significantly modified. These localities are, immediately adjacent to the mylonite zone,

---

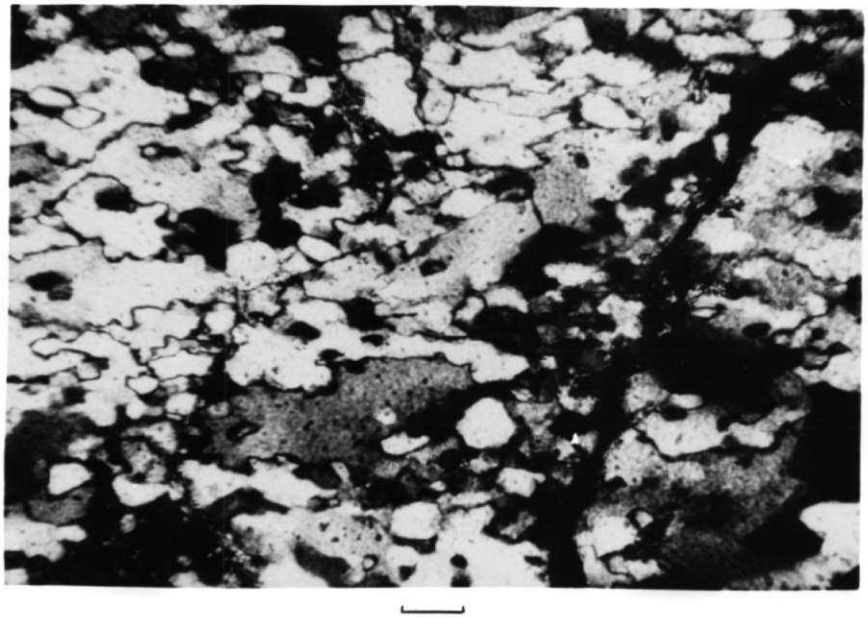
Figure 6.15: (a) and (b) hinges of F_3 crenulations in non-migmatite gneiss (S_3 vertical). (a) micaceous layer, (b) psammitic layer. (c) F_3 hinges in migmatite gneiss (S_3 vertical). Note S_3 fracture cleavage in quartzo-feldspathic band. Bar scale = 0.1 mm.

FIG. 6.16

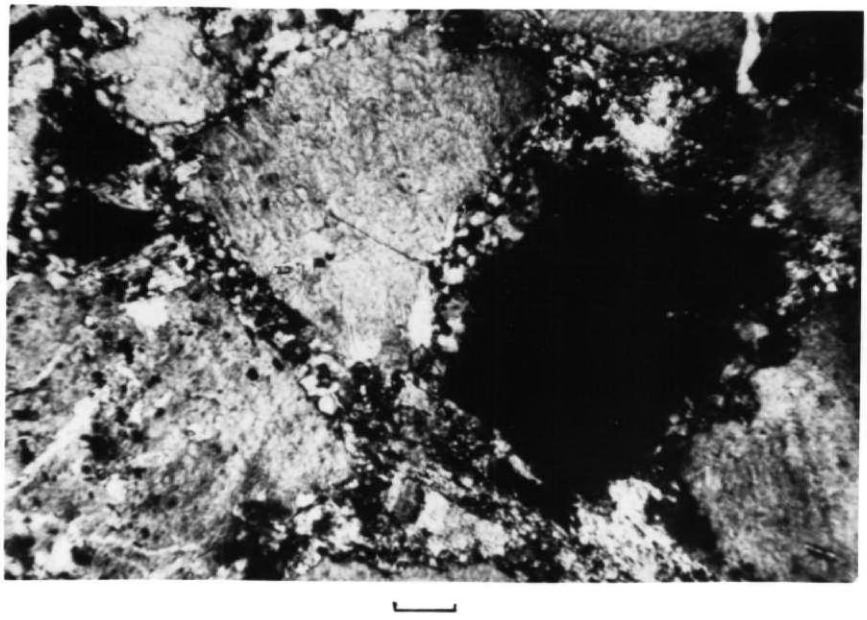
a



b



c



immediately adjacent to and on the northwest side of the Narridy Creek granite and in a few other areas such as in the hinge of the Mt. Millar antiform. There is a gradational variation in D_3 textures and fabrics and in general this gradation goes from northwest to southeast approaching the granite and the mylonite zone.

The effects of this more intense deformation and recrystallization were to further modify quartz textures and to develop tighter crenulations with a stronger axial planar cleavage (Fig. 6.16a). Within less deformed gneisses, quartz grains are typically undulose and/or deformation banded with broadly serrated grain boundaries and scattered new grains derived from rotated subgrains. In the more deformed gneisses, however, quartz grains are strongly undulose with irregular, finely serrated grain boundaries and prolific new grain growth. The new grains are much finer and are sometimes elongate parallel S_3 (Fig. 6.16b).

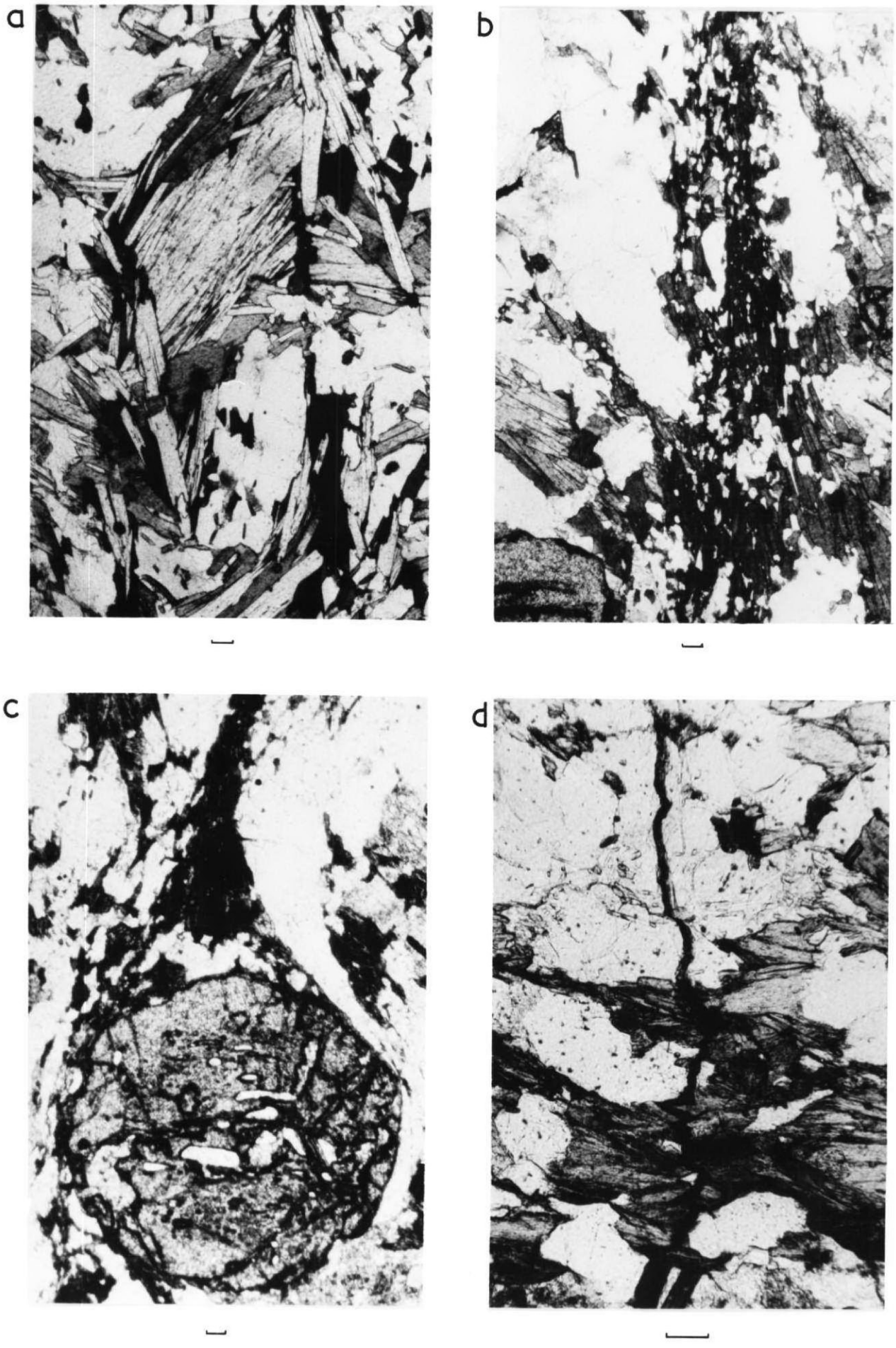
The potassium feldspars too have been further modified, and they have undergone intense recrystallization along grain boundaries to produce distinct zones of very fine new grains (Fig. 6.16c).

S_3 SCHISTOSITY - There are three separate but related features which represent S_3. They are, a mica preferred orientation, a weak dimensional orientation, and an alignment of fractures or dissolution planes. The S_3 fabric is quite heterogeneous but is strongest in the hinges of tight F_3 folds.

S_3 MICA - There are several different mica fabrics which contribute to S_3. They are, scattered medium to fine sized

Figure 6.16: (a) hinge zone of tight F_3 fold. Note the old, deformed quartz grains (including the rotated internal fabric) and the stronger S_3 (horizontal) fabric. (b) new, recrystallized quartz grains from the same specimen as (a) (S_3 horizontal). (c) incipient recrystallization along microcline/microcline grain boundaries from a specimen with similar textures to (a) and (b). Bar scale = 0.1 mm.

FIG. 6.17



grains often associated with and aligned along crenulation or kink band boundaries (Fig. 6.17a), mica beards (Fig. 6.17c), and fine to very fine grained mica films (Fig. 6.17b). In each case (001) of the mica is aligned subparallel to F_3 axial planes and is subidioblastic. Rotated old grains are often augen shaped and in the more deformed specimens have very fine new micas along grain boundaries (cf. Fig. 6.28d).

S_3 DIMENSIONAL ORIENTATION - The dimensional orientation of minerals parallel to S_3 is restricted mainly to S_{1-2} micas that have been rotated and to new S_3 micas. However in certain cases, mainly related to the more intense F_3 folding, both quartz and feldspar can assume an S_3 platiness due to intense recrystallization.

S_3 FRACTURE OR DISSOLUTION PLANES - These particular features are characteristic of the D_3 deformation. They are discrete, wavy, irregular surfaces, crudely parallel to S_3 and lined with a rusty brown semi-opaque material which is in part phyllosilicate. Although they are most common in quartzo feldspathic layers they also truncate micaceous layers where their form is mainly sharply serrated (Fig. 6.17d).

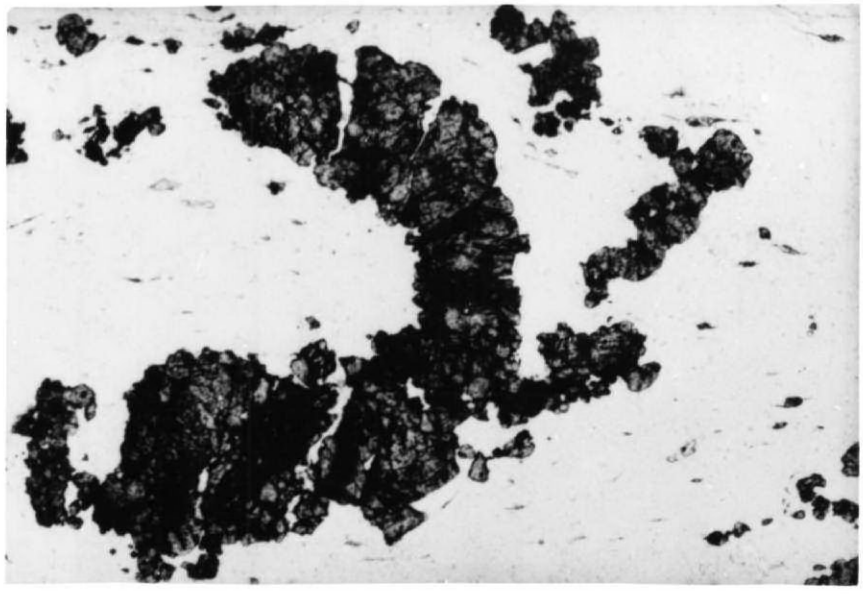
These planar features are also particularly common in garnets (and also pyroxene; see later) where they form straight joint like surfaces traversing entire porphyroblasts including their relatively inclusion free coronas.

In general there is no major displacement either along or across the dissolution surfaces. However, they are sometimes associated with kink band boundaries suggesting that they are genetically related.

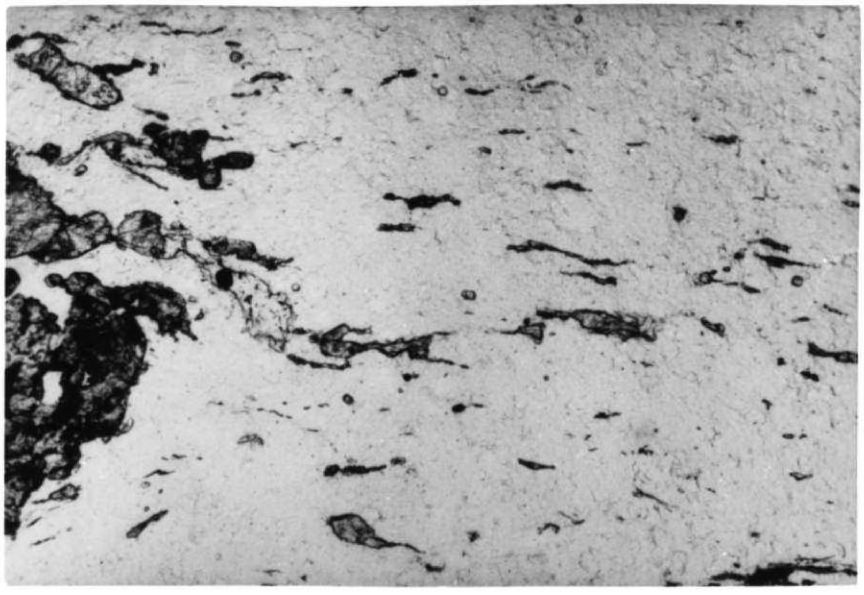
Figure 6.17: (a) F_3 crenulations with new S_3 oriented (vertical) micas. (b) S_3 mica film. S_3 is vertical but S_{1-2} is oriented "west-north-west". (c) S_3 mica beard about a garnet porphyroblast. Note internal, S_{1-2} fabric of garnet (parallels S_{1-2} outside of garnet) and the inclusion free corona. (d) S_3 dissolution surface (vertical) cutting across S_{1-2} (horizontal) but not displacing it. Bar scale = 0.1 mm.

FIG. 6.18

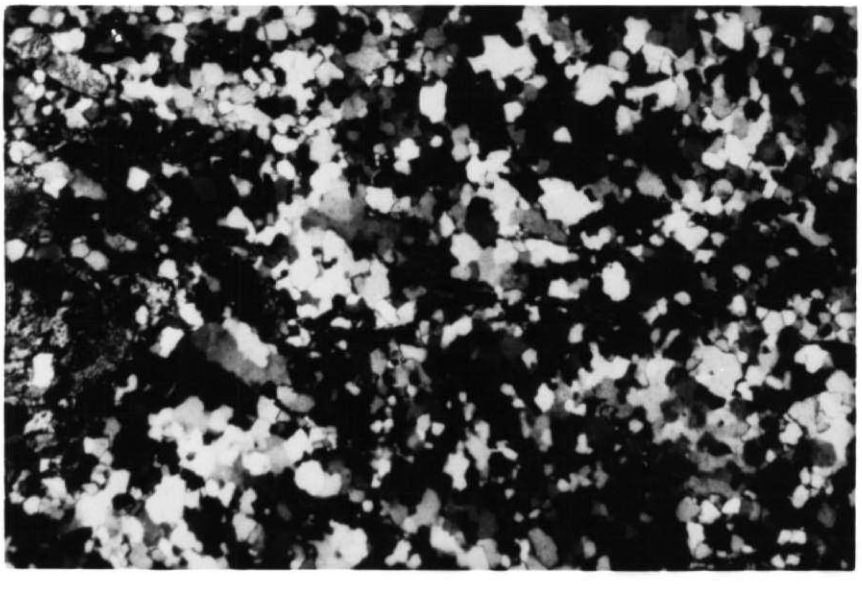
a



b



c



L_3 LINEATION - The only lineations associated with D_3 are those produced by microcrenulation of S_{1-2} and those produced by the intersection of S_3 and S_{1-2}. Consequent to their D_3 recovery and recrystallization, S_{1-2} micas that have been crenulated, naturally lose some of their platiness and become slightly elongate parallel to the crenulation. This is a mechanical feature and not due to preferred growth. Actual S_3 micas do not show any pronounced elongation either parallel or oblique to F_3 axes.

6.4.1.2 Other lithologies

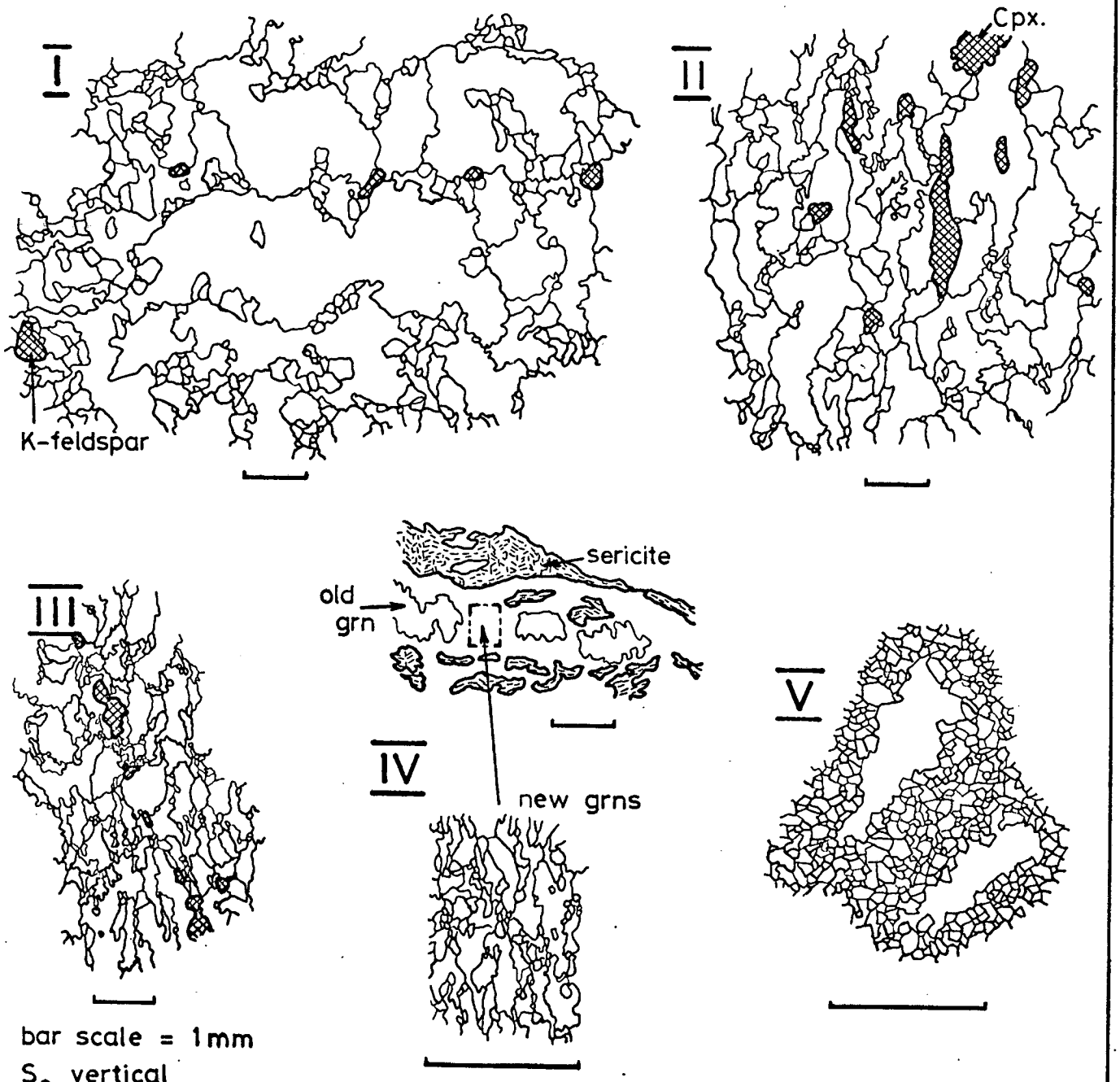
QUARTZITES - Micro crenulations and mesoscopic F_3 folds, although rare, are present in layered, micaceous quartzites and are in general similar to F_3 folds within the semipelites. However, immediately adjacent to the Narridy Creek granite deformed zone there are numerous tight F_3 folds in banded quartzites of the iron formation. One such example is illustrated in Figure 6.18. In microphotograph a), the coarse clinopyroxene has been folded tightly and radial fractures have developed (some being subsequently infilled with quartz). There is a good S_3 schistosity defined by elongate fragments of pyroxene, and, by new amphiboles (Fig. 6.18b) and the quartz has substantially recrystallized to form a subpolygonal mosaic of fine to very fine new grains with scattered relics of older grains recognizable by their size and undulose extinction (Fig. 6.18c).

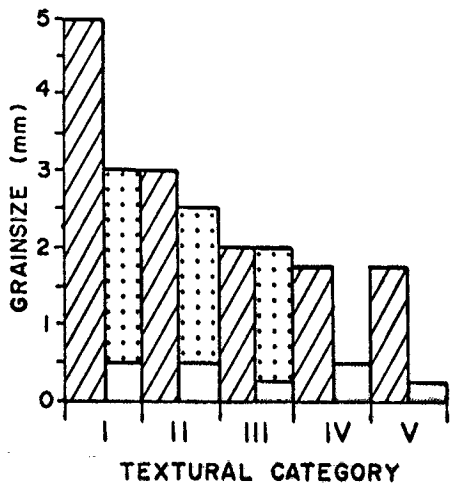
It is clear from this example that the quartz textures have been significantly modified in this area compared with those of Figure 6.9.

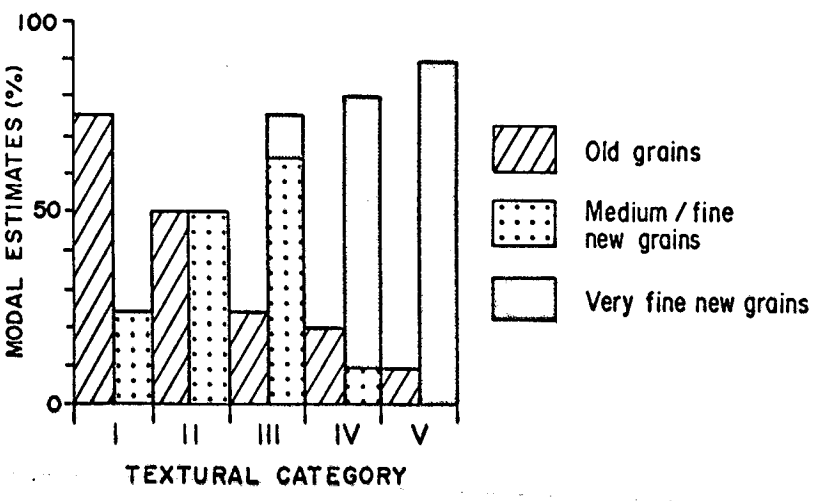
Figure 6.18: a) F_3 folded diopside grain in banded diopside rich quartzite (iron formation). Note the radial, quartz filled tension gashes. S_3 horizontal. (b) S_3 fabric (horizontal) in the hinge zone of the above fold. (c) as for (b) but with crossed polars. Bar scale = 1 mm.

FIG. 6.19

TEXTURAL CATEGORIES of QUARTZITES







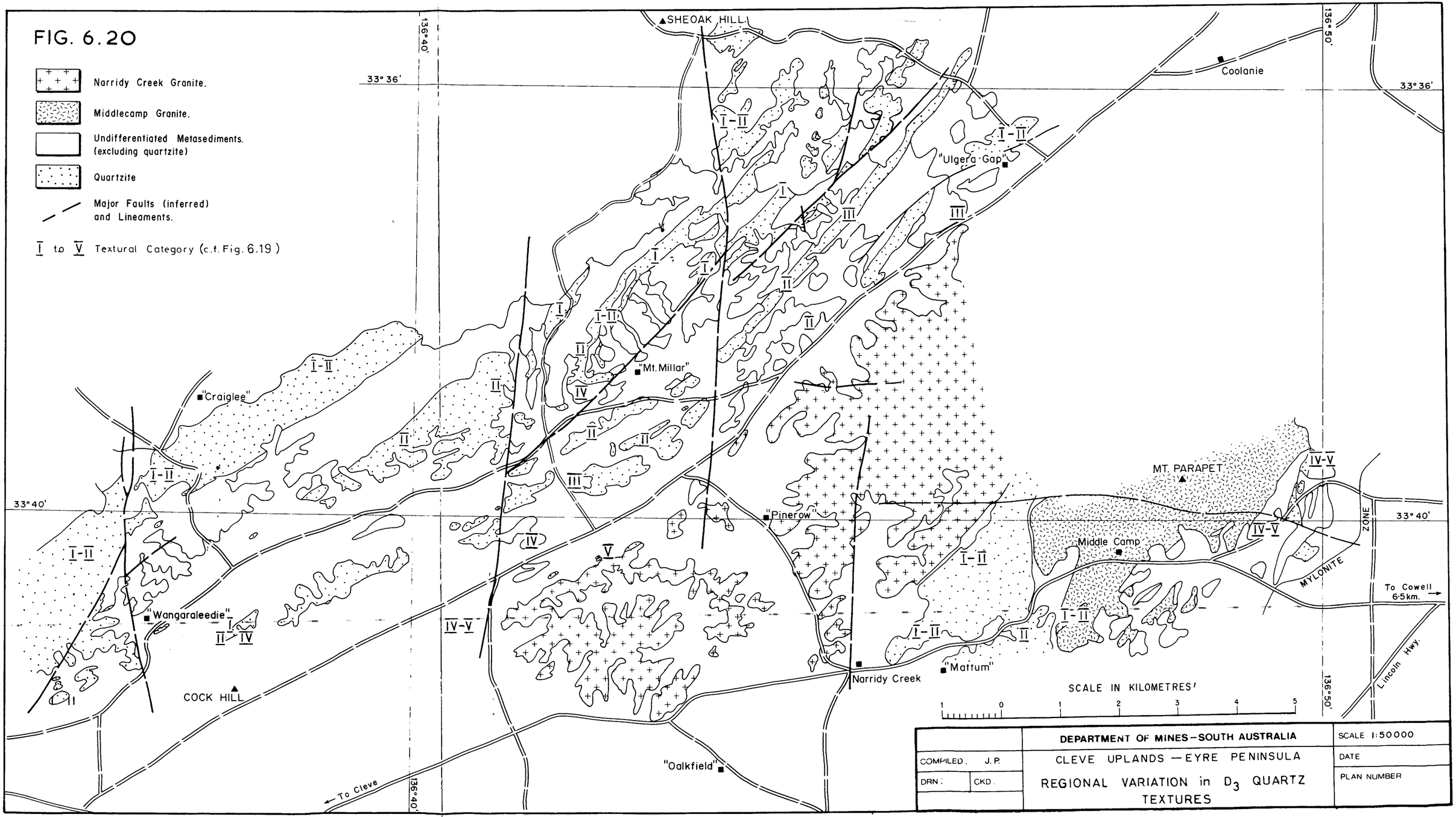
In fact the quartz textures vary considerably throughout the area and can be categorized into five groups on the basis of grainsize, presence and nature of recovery features (e.g. deformational bands), and presence and nature of new grains. These groups as outlined in Figure 6.19 are:

I - Medium to coarse grained and inequigranular with coarse old grains and medium to fine new grains. The old grains are characterized by sharply bounded deformation bands and/or irregularly shaped, medium sized subgrains and they sometimes contain deformation lamellae. New grains are medium in size, also deformation banded, and have clearly developed from rotation of the above subgrains. They are irregular in shape though some are dimensionally elongate parallel to S_3 and their boundaries are serrated or cuspate. Some new grains show further subgrain and new grain formation an order of magnitude smaller .

II - Medium grained with rare coarse grains. Old and new grains are not distinguishable although from comparison with category I they would all appear to be new grains. They are deformation banded (sharply defined), contain both subgrains and deformation lamellae and although of irregular shape with serrated or cuspate grain boundaries, they are commonly dimensionally elongate parallel to S_3.

III - Medium grained predominantly but quite often with bimodal grainsize distribution. The dominant mode is essentially equivalent to category II in size and shape, but deformation bands are poorly defined and grain boundaries are cuspate or lobate, frequently with very fine new grains scattered along them. These new grains are of equivalent size to the lobes and they constitute the minor grainsize mode. Undulosity/ deformation banding is quite marked but deformation lamellae are not common.

FIG. 6.20


Narridy Creek Granite.
Middlecamp Granite.
Undifferentiated Metasediments. (excluding quartzite)
Quartzite
Major Faults (inferred) and Lineaments.
I to V Textural Category (c.f. Fig. 6.19)
SHEOAK HILL
Coolanie
"Ulgera Gap"
"Mt. Millar"
"Craiglee"
"Pinerow"
MT. PARAPET
Middle Camp
MYLONITE ZONE
"Wangaraleedie"
COCK HILL
"Mattum"
Narridy Creek
"Oalkfield"
To Cowell 6.5km.
Lincoln Hwy.
To Cleve
136°40'
136°50'
33°36'
33°40'
SCALE IN KILOMETRES
1 0 1 2 3 4 5
DEPARTMENT OF MINES—SOUTH AUSTRALIA
SCALE 1:50000
COMPILED J.P.
CLEVE UPLANDS — EYRE PENINSULA
DATE
DRN: CKD:
REGIONAL VARIATION in D_3 QUARTZ TEXTURES
PLAN NUMBER

IV - Fine grained with scattered medium sized relics of old ribbon grains. The old grains are strongly undulose with diffuse deformation bands and subgrains of irregular and often lobate shape. New grains are predominantly elongate parallel to S_3, undulose and have very irregular, lobate grain boundaries. However, some new grains are equant and polygonal.

V - Fine to very fine grained with scattered medium sized relics of old ribbon grains. Old grains resemble those of category IV, but new grains form polygonal aggregates of essentially strain free grains with straight grain boundaries.

The principal features of this sequential variation in quartzite textures are the variation in subgrains and deformation bands - from sharply defined to diffuse - , the progressive decrease in grainsize both of old and new grains, and the proportion of old to new (Fig. 6.19). This variation in textures is principally related to three macroscopic structures, the Mt. Millar/Morowie antiform, the deformed zone of the Narridy Creek granite, and the mylonite zone. To the northwest of the Mt. Millar/Morowie antiform there is little variation in quartz textures with categories I and maybe II being characteristic. However, southeast of that structure there is considerable variation. Textures range from categories I to V and can be generalized as a broad, progressive transition from I through to V approaching the boundary of the deformed Narridy Creek granite (Fig. 6.20). Southeast of the Narridy Creek granite in the quartzites of the Mattum area, textures are of categories I, II and sometimes III whereas between the Middle Camp granite and the mylonite zone they range from II through to V with a progressive transition from II to V approaching the mylonite zone.

DOLOMITES AND CALC-SILICATES - Within the dolomites, the principal microscopic features are the modification of dolomite grain textures, and the deformation (e.g. kinking) of accessory minerals phlogopite, tremolite, diopside and serpentine. Dolomite grains are frequently twinned (combined D_2, D_3 and D_4 effect) and although they are essentially equant in shape (Fig. 6.21), their grain shapes are varied from irregular and lobate to subpolygonal and straight. The deformation of phlogopite and serpentine is principally by flexure and kinking (Fig. 6.21 b and c). However, neither feature is clearly of D_3 age so that generation during D_4 cannot be ruled out.

Within the calc-silicates the characteristic microscopic feature of the D_3 deformation is deformation/recovery/recrystallization of diopside and tremolite. For example, tremolite, both primary and some secondary, has been crenulated with incipient recovery/recrystallization to form finer grained, essentially straight but rotated, segments (cf mica).

Diopside, however, has reacted differently. In the cores of F_3 folds, originally coarse grains have undergone partial polygonization (Fig. 6.22) to form fine to medium grained mosaics of "new", equant shaped, pyroxenes with grain boundaries being cuspate to lobate and frequently lined with new quartz, tremolite and calcite. The formation of the "new" pyroxenes is related to subgrain formation and to flexure and kinking of the old grain. From the flexed state, ragged kink band boundaries have formed followed by crystallization of quartz, calcite and tremolite along them (Fig. 6.22).

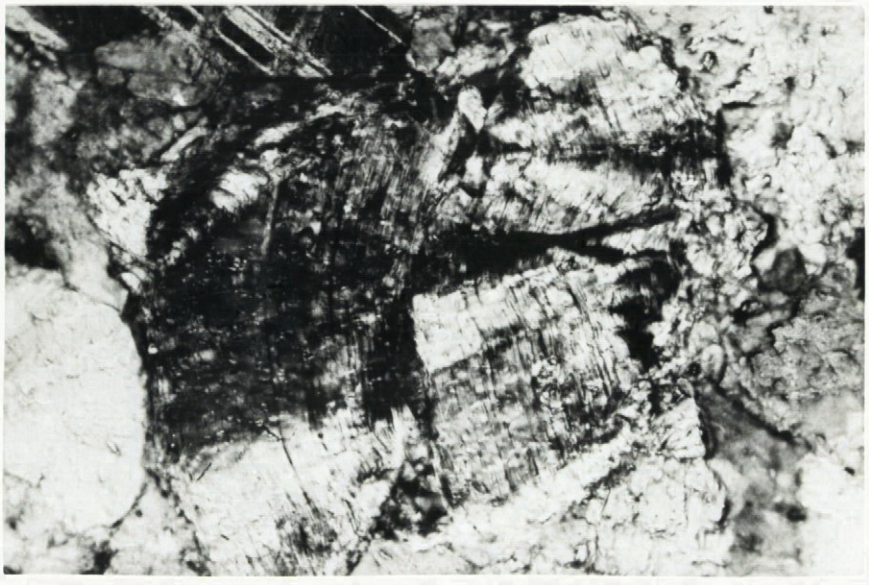
Figure 6.21: (a) dolomite textures in massive dolomite.
(b) kinked phlogopite within massive dolomite.
(c) kink banded serpentine within serpentine nodule (pseudomorph after forsterite) in massive dolomite.
Bar scale = 0.1 mm.

FIG. 6.21

a



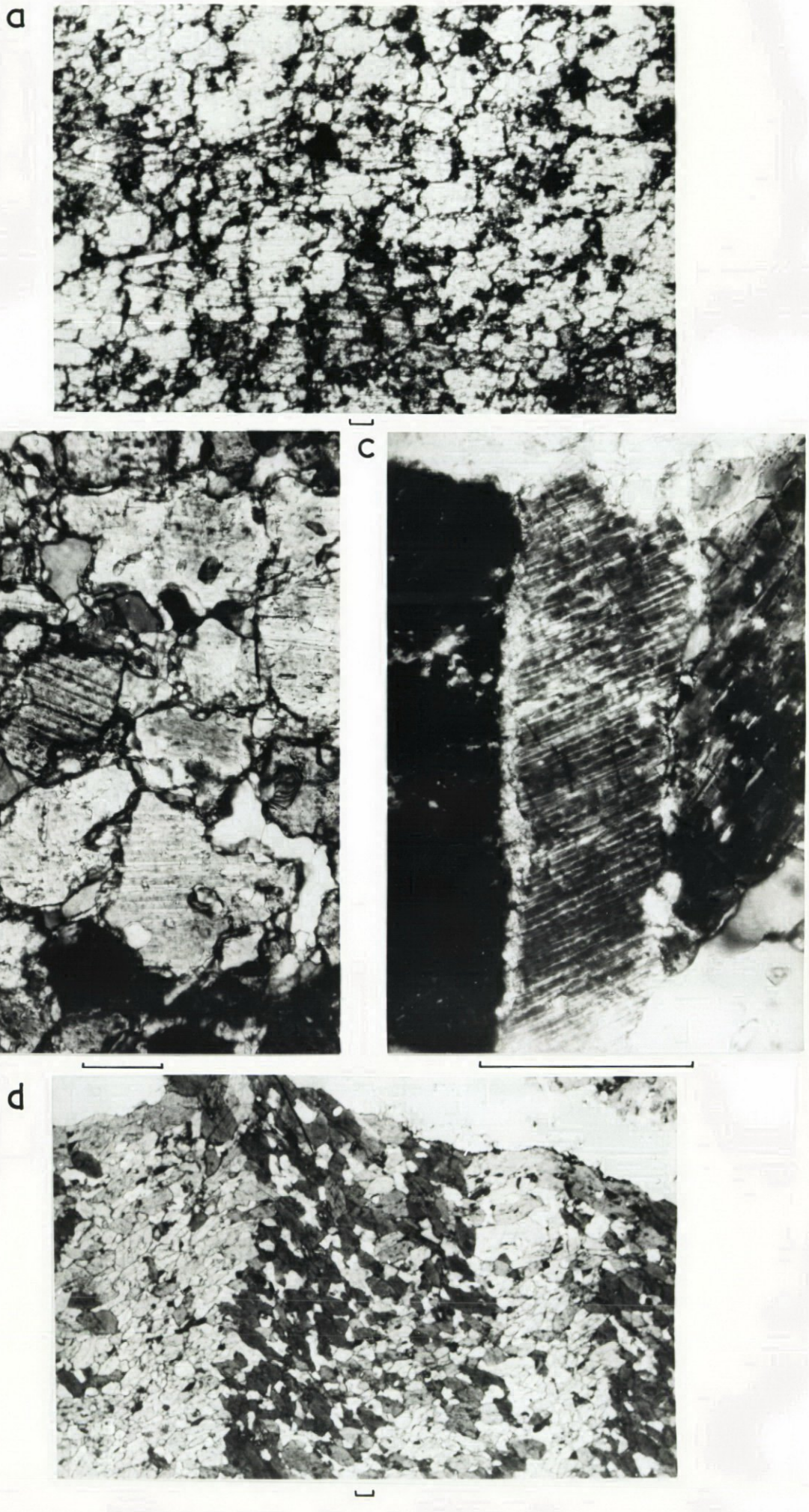
b



c



FIG. 6.22



This type of diopside deformation and recrystallization is diagnostic of D_3 and contrasts with the sharply defined subpolygonal aggregates of D_2 recrystallization.

AMPHIBOLITES - Although broad mesoscopic F_3 folds characterize the amphibolites associated with the metasediments, in thin section small mesofolds and crenulations can be observed folding the main S_{1-2} amphibole schistosity. Like tremolite in the calc-silicates, individual hornblende grains are not flexed but rather have sufficiently recovered and/or recrystallized to form sharply defined crenulation bands (Fig. 6.22d). There is generally no other S_3 parallel fabric.

PLUG RANGE GRANITE GNEISS - Tight mesoscopic F_3 are rare in this body, but those that do occur have similar textures and fabrics to F_3 folds in the migmatite gneisses.

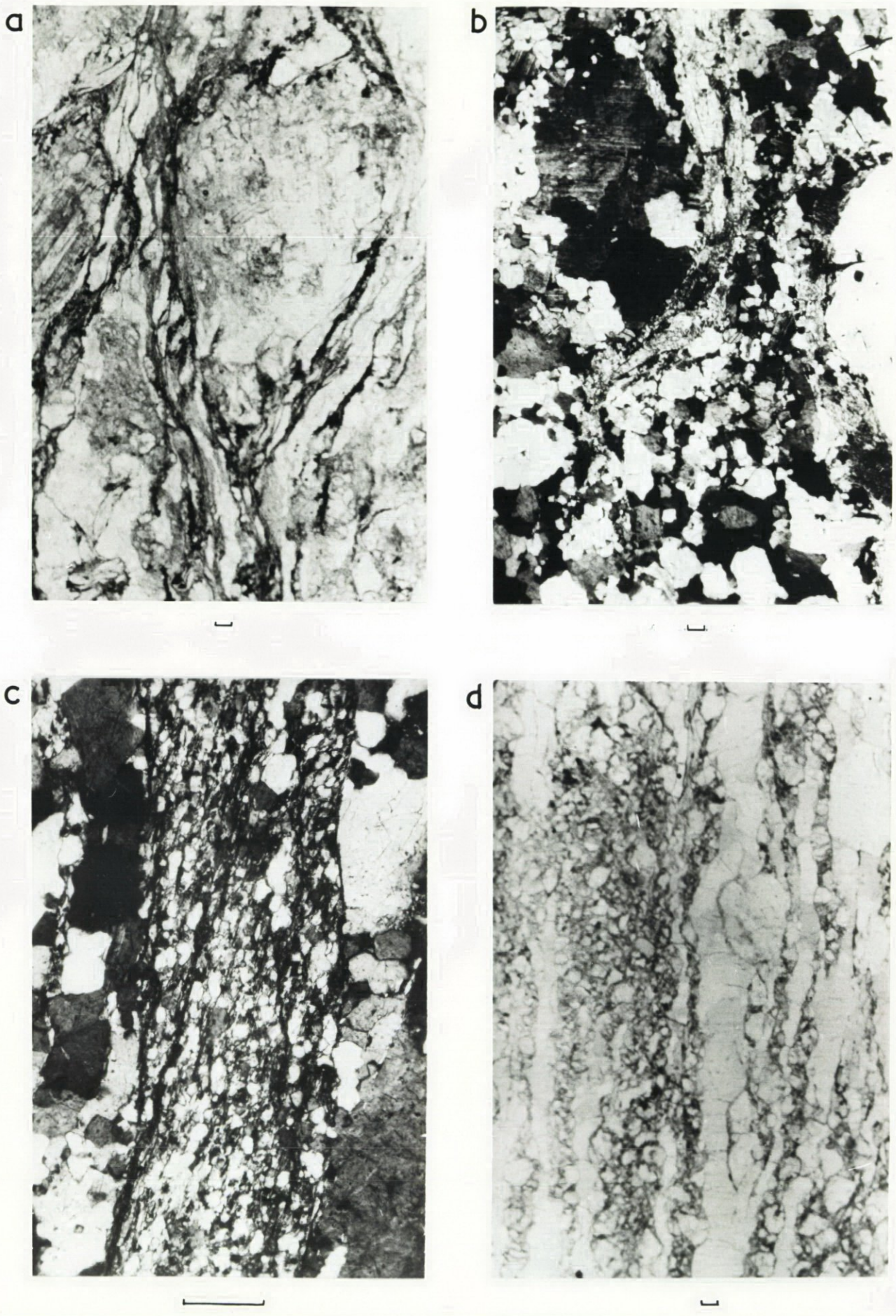
MIDDLE CAMP GRANITE - In addition to folding the S_2 fabric, D_3 also significantly modified quartz and feldspar-textures. Quartz textures range from coarse, subgrained and deformation banded single grains through to polygonal aggregates of equant and weakly undulose, medium sized grains whereas feldspar textures are characterized by incipient recrystallization along feldspar/feldspar (particularly microcline/microcline) grain boundaries to form narrow zones (< 0.1 mm) of very fine new grains. In addition, some individual plagioclases are deformation twinned and have incipient subgrain development.

6.4.1.3 Narridy Creek Granite

Textures of the Narridy Creek granite range from grano-

Figure 6.22: (a)-(c) D_3 diopside recrystallization. (a) subgrains and new grains within a coarse, old grain. (b) new diopside grains with crystallization of quartz, tremolite and calcite along grain boundaries. (c) kinked old grain with crystallization of quartz, tremolite and calcite along kink band boundaries. (d) crenulated S_{1-2} hornblende fabric (horizontal) within amphibolite. S_3 is vertical and both L_2 and F_3 are perpendicular to the section. Bar scale = 0.1 mm.

FIG. 6.23



blastic equigranular to xenoblastic serriate. The massive central granite body has not been greatly affected by D_3 and is mainly medium to coarse grained with granoblastic textures. Micas within it are often flexed or kinked and are sometimes weakly aligned to describe an incipient foliation. Quartz and feldspar also show very minor deformation/recovery/recrystallization but by comparison with the adjacent rocks are relatively undeformed.

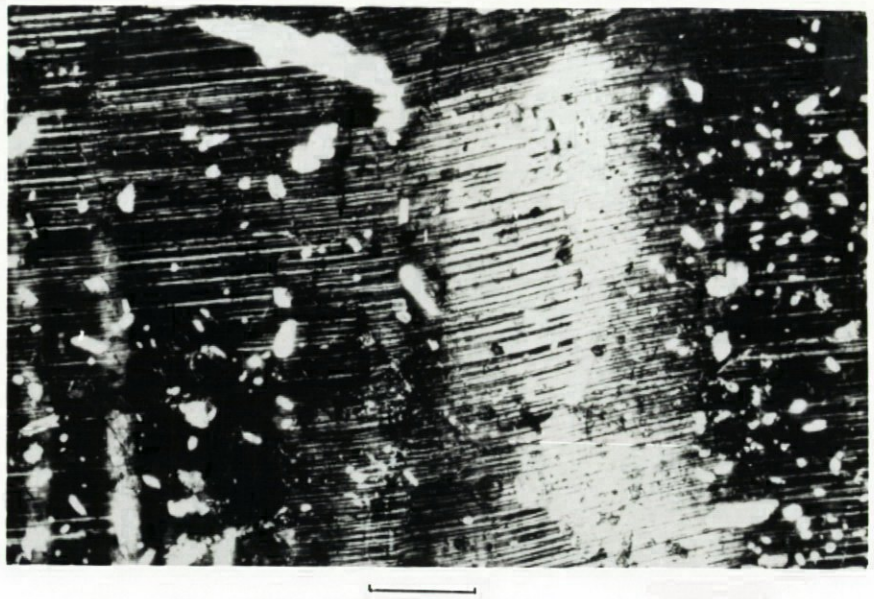
In the deformed zone the granitic augen gneisses are strongly foliated and have granoblastic inequigranular to serriate textures (mortar textures). Texturally they consist of three principal components; coarse feldspar relics (Fig. 6.23a), fine grained subpolygonal matrix of quartz, feldspar and mica (Fig. 6.23b), and narrow planar zones of very fine grained quartz, feldspar and mica (Fig. 6.23c). The augen vary in size, quantity and habit but all have a feldspar core (usually a single crystal, but sometimes multigrained) with tails of fine grained matrix. Some may have mica films or narrow recrystallized zones wrapping around them but others do not. For example, in the area east of Calcookara fault and between the massive granite and an S_3 parallel line through "Pinerow" (see Fig. 4.8) the planar zones are not prominent but in the areas west of Calcookara fault and northwest of "Pinerow" the planar zones are prominent.

In addition to the normal augen textures there are numerous long linear zones, a) of strongly rodded gneiss, and b) of much finer grained, finely layered gneiss lacking

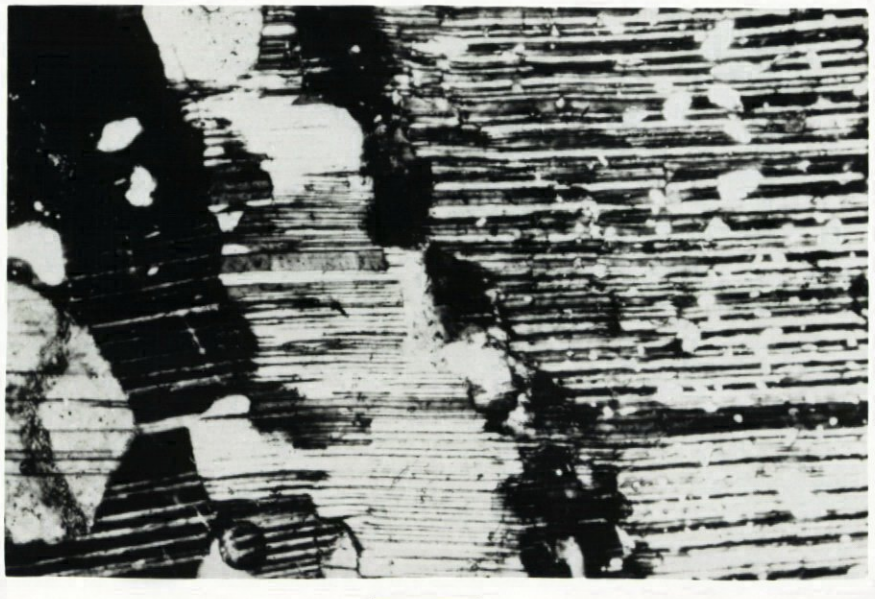
Figure 6.23: Narridy Creek granite (S_3 vertical). (a) augen gneiss texture with coarse feldspar augen wrapped around by very fine grained recrystallized films and matrix. (b) fine grained recrystallized matrix surrounding coarse but subgrained plagioclase (upper left). (c) very fine grained recrystallized domain within fine grained matrix. (d) recrystallized linear fabric (section cut parallel to L_3) Bar scale = 0.1 mm.

FIG. 6.24

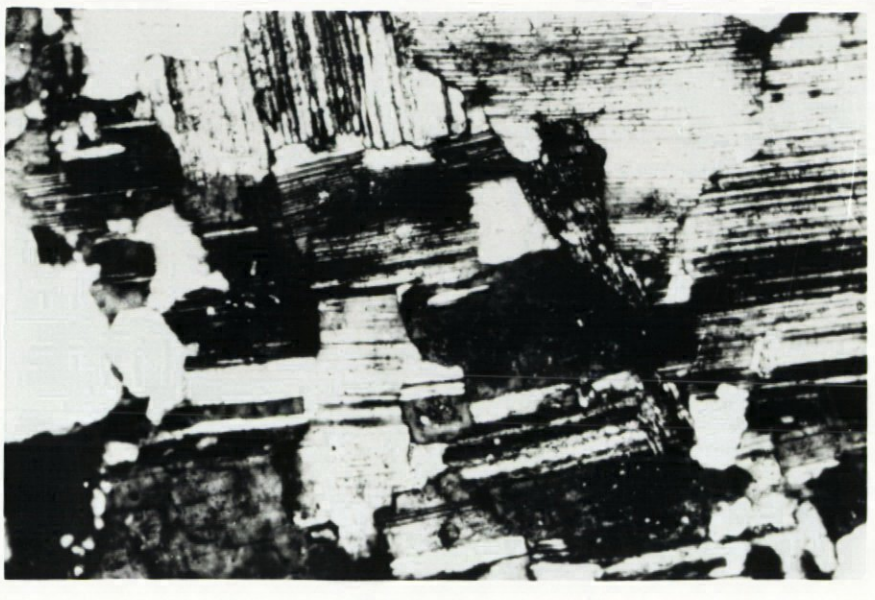
a



b



c



augen. The rodded gneiss is a simple variant of the normal augen texture and is texturally similar to the fine grained matrix. It lacks coarse augen and in cross section (normal to the rodding) it often lacks a strong planar fabric. However, parallel to the lineation there is always a strong fabric defined by elongate quartz ribbons and by aggregates of new, fine grained feldspar (Fig. 6.23d). The rods are elongate > 20:1 parallel to L_3 but only 2 or 3:1 perpendicular to L_3 in the S_3 plane.

The other fine grained variant of the augen gneiss is thought to represent a more intense recrystallization perhaps induced by increased strain in those zones (cf mylonitic zones). The gradation from coarse augen gneiss into finely layered gneiss is seen as a gradational decrease in the amount and size of feldspar augen (accompanied by a slight increase in mica content) while the matrix has remained texturally the same with a strong planar fabric.

Individual quartz, feldspar and mica textures of the granite gneisses are typically D_3 in origin. Quartz ranges from medium sized undulose grains down to very fine new grains, microclines show incipient, very fine new grain growth around their margins but particularly along microcline/microcline grain boundaries, and plagioclases are often deformed. The latter have however behaved quite differently to microcline during deformation and recrystallization because while microcline recrystallized into very fine new grains, plagioclase recovered and subsequently recrystallized by a process related to kinking and subgrain formation. A sequence of micrographs in Figure 6.24 clearly illustrates the progression from flexed twin lamellae

Figure 6.24: Progressive recovery and recrystallization of plagioclase in the Narridy Creek granite. (a) flexed multiple twins. (b) kink banded multiple twins. (c) new grain aggregates. Note deficiency of sericite in new grains. Bar scale = 0.1 mm.

to aggregates of new grains (N.B. the absence of mica inclusions in subgrains and new grains suggesting that intrzcrystalline diffusion is very important in this process).

Amphibolites within the Narridy Creek granite gneiss consist of very strongly aligned green hornblende. The alignment is such as to define a strong lineation and schistosity; that is, b and c axes define S_3 and c axes define L_3. There is no sign of any earlier (pre D_3) textures or fabrics, but S_3 and L_3 are both deformed by D_4 (see later).

6.4.2 Development of D_3 Fabric

6.4.2.1 Relationship of Fabric to Strain

It was demonstrated in Chapter III that F_3 folds approximated to flattened Class 1B folds. In a previous discussion on D_2 strain, this flattening was used as an argument to support a close parallelism of $\lambda_1\lambda_2$ of the D_2 strain ellipsoid with the axial plane of F_2. However in this case where the flattening was not as great and where there is some variation in amount of flattening between hinge and limb (cf Fig. 3.3), it is not possible to infer confidently the distribution of strain around any particular folded layer. Consequently it is impossible to relate the fabric directly to the D_3 strain ellipsoid.

6.4.2.2 Development of S_3

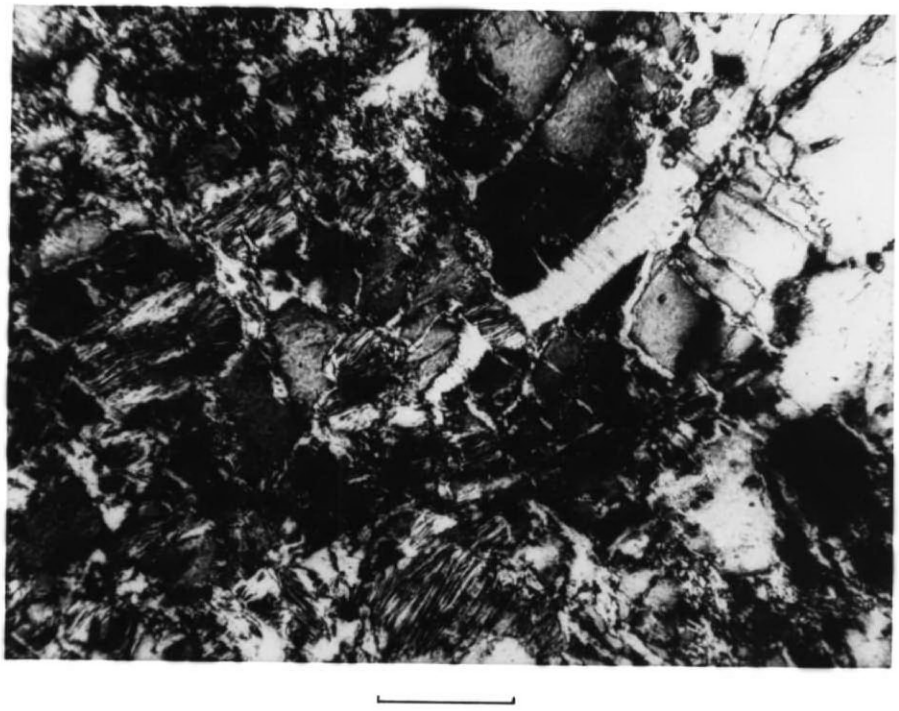
CRENULATION CLEAVAGE - In the discussion on D_2 crenulation cleavage (Sect. 6.3.2.2) it was concluded that there were three main stages of crenulation cleavage development. From the D_3 microstructures described above (see Figs. 6.15a and 6.17a) the first two of these stages are clearly present; that is, the micas have recovered and recrystallized from their flexed state to form straight segments with ragged

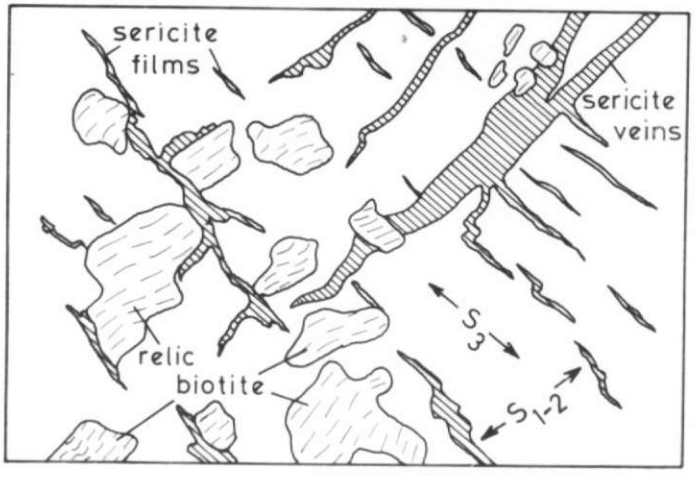
kink or crenulation band boundaries. There has been incipient new grain growth but it is restricted to kink or crenulation band boundaries. Hence, by contrast to D_2 where the typical fabric represents an almost complete progression to the new grain growth stage (State 3), typical D_3 fabrics have only completed the recovery/ recrystallization stage (Stage 2).

MICA FILMS AND MICA BEARDS - Both these features are local zones of intense new grain growth but each represents opposing strain histories; that is, the mica films are narrow, planar zones of high strain whereas the mica beards are annulus shaped zones of low strain or dilation about rigid or semi-rigid particles in a deformed viscous matrix (e.g. see Ghosh et al, 1973; Ghosh et al, 1975). Preferential mica growth in mica beards has been studied by Williams (1972) and he considered various possibilities of oriented nucleation and/or growth relative to either the interface of the rigid particle or the stress field. Although he was unable to make a complete explanation for his observations, he believed that random nucleation followed by preferential growth was the most likely. Nucleation took place on the particle interface and it was those grains that were oriented perpendicular to the interface and also favourably oriented relative to the stress and strain axes (e.g. perpendicular to compression), that grew quickest.

This type of origin accords well with the examples illustrated in this thesis. Furthermore, it is supported by an example illustrated in Figure 6.25. The mica in this case is new mica that has grown in two sets of zones transgressing coarse feldspar grains. Those zones parallel to S_3 are narrow high strain zones equivalent to mica films,

FIG. 6.25





whereas those perpendicular to S_3 are quite broad and represent extension perpendicular to F_3. In both cases despite the fact that one set is in compression and the other in tension the new mica growth is parallel to S_3 and overprints coarse S_{1-2} micas. Therefore it is concluded that D_3 mica films and beards were related processes of new grain growth in direct response to stress and/or strain and that the preferred orientation of mica within them was developed from preferential growth in the direction of least obstruction (i.e. perpendicula to λ_3).

S_3 FRACTURES OR DISSOLUTION PLANES - These irregular, planar features are different from mica films although they have some features in common. The principle difference is that mica films are narrow domains of intense recrystallization whereas the fractures or dissolution planes show no recrystallization but rather, contain diffuse (?) residues of opaque minerals and mica left behind during some deformational diffusion process.

There are three principal processes by which such features may form; either the planes are stylolite like planes formed from pressure solution of certain minerals (e.g. see Durnery, 1972), or they are microfaults (e.g. see Williams, 1972), or they are former channel ways (i.e. no displacement either side) along which certain fluids have moved during the deformation. While all three processes may have contributed the principal feature is that they were channelways. This is supported by the common occurrence of traces of diffuse residues along quartz and feldspar grain boundaries which are believed to represent grain boundary

Figure 6.25: Sericite films and veins transgressing coarse microcline grains. S_{1-2} is orineted "northeast" and S_3 is oriented "northwest". Bar scale = 0.1 mm.

diffusion. Microfaulting is not supported because the surfaces are often serrated (Fig. 6.17d) and generally lack any shear displacement. Likewise the lack of significant displacement normal to the surface does not support a major component of pressure solution.

6.4.2.3 Development of D_3 Quartz Textures

Assuming that recovery of quartz is diagnosed by the presence of deformation bands, deformation lamellae and subgrains (e.g. see White, 1977; Vernon, 1976; Hobbs et al, 1976), and that recrystallization is diagnosed by the presence of distinct new grains, then both of these processes have clearly occurred in quartz. The problems discussed here relate to the timing of those processes, their nature and relative importance, and the physical conditions that they infer. Following that, the crystallographic fabrics of some quartzites are briefly discussed with reference to their associated microstructure and possible mechanism of formation.

TIMING OF RECOVERY/RECRYSTALLIZATION - The two processes of recovery and recrystallization are related to each other and took place approximately simultaneously. This is supported by the unique relationship between deformation bands, subgrains and new grains within any particular specimen. For example, in rocks where the deformation bands are broad and subgrains are large, the corresponding new grains are of similar dimensions, whereas in other rocks where the deformation bands and subgrains are smaller, the new grains are correspondingly smaller. Furthermore it is clear in many examples that while one part of an old grain is undergoing recovery another part has recrystallized. However it is also clear that a certain amount of recovery has preceded

recrystallization in those parts converted to new grains. Therefore while it can be said that the two processes were broadly synchronous, at any particular point within a grain the onset of recovery necessarily preceded the onset of recrystallization.

With respect to the relationship between recovery/recrystallization and deformation it is also clear that the combined processes were syntectonic or dynamic (versus annealing or static recovery/recrystallization), and that the accompanying deformation was D_3. This is seen in the relationship between the textural classification and meso- and macro-D_3 structures, in the elongation of both subgrains and new grains parallel to S_3, and in the presence of undulose extinction and deformation bands within new grains. The latter has been taken by many workers (e.g. see White, 1976, 1977) to infer syntectonic recrystallization although it is believed here that much of it is inherited from the original host grain. However in certain areas, the undulose extinction is partly a superimposed feature resulting from later deformation (D_4). This cannot be completely discounted but because the nature and variation of this undulosity is allied to other D_3 deformation features, a superimposed origin is considered to be untenable on a regional scale. Furthermore the textures are typical of those fabricated in experimental syntectonic recrystallization (e.g. Hobbs, 1968).

SIGNIFICANCE OF RECOVERY AND RECRYSTALLIZATION - Having recognized that both processes occurred during D_3 it is appropriate to consider the role each has played in developing the observed textures. On the basic presumption that new grains represent recrystallization, it immediately

follows (from Fig. 6.19) that there is an increase in degree of recrystallization progressing from categories I to V. In fact, the categories can be considered as "stages" in the process of recrystallization.

In stage I then, recovery is the predominant process. By the migration and annihilation of dislocations (White, 1973, 1976, 1977) the strained old grains have recovered to form sharply defined deformation bands and subgrains. The subgrains are medium sized regions of identical form (i.e. deformation banded) to old grains. They show slight mismatch across sharply defined but irregular boundaries, and they tend to develop preferentially around old grain boundaries. Further away from the cores of old grains they have rotated sufficiently ($>7^{o}$) to be defined as new grains. Hence the initial stage of recrystallization is related to the recovery process and is in fact an extension of that process.

Stage II follows on from Stage I with the progressive formation of new grains by subgrain rotation until there are no large old grains remaining. Recovery and recrystallization are considered to be of equal importance here, but in the next stage, Stage III, recrystallization assumes greater dominance. There are two classes of new grains here. Those of the first class are medium grained and equivalent to Stage II new grains formed by recovery and rotation of subgrains. However, their average size is slightly smaller than Stage II equivalents and furthermore they are much more undulose with diffuse deformation bands. The latter represents an excess of strain energy not dissipated completely by recovery processes. Its presence is of fundamental importance because it provides the driving force behind the

formation of the second class of very fine new grains; that is, it initiates bulging of grain boundaries. Furthermore it implies that the recovery rate was less than the strain rate.

Stage IV textures merge into Stage III textures. They have also developed principally from subgrain rotation. However, becuase of a change in physical conditions the subgrains and the corresponding new grains are much finer. The new grains often have lobate boundaries which are analogous to those in Stage III.

The final stage is an extension of the previous stages and represents almost complete recovery and recrysallization to form very fine, polygonal subgrains that have subsequently rotated to form new grain mosaics.

Emerging from this sequence of recovery and recrystallization is a distinct pattern of microstrutural development. In each of the stages the textures have formed by progressive recovery and recrystallization leading firstly to deformation bands, then to subgrains, and then to new grains. In many cases the new grains themselves have subsequently been deformed and have gone through the same cycle to develop secondary new grains an order of magnitude smaller. What then do the five stages represent in terms of physical conditions?

There are five principal factors which may affect the degree of recovery/recrystallization. They are, temeperature, water content, total strain, strain rate, and nature and orientation of the original crystallographic fabric. All of these factors have been studied previously by many workers both in the field (e.g. Sylvester and Christie, 1968; Wilson, 1973 and 1975; Bell and Etheridge, 1973 and 1976; Marjoribanks, 1976; Bouchez, 1977) and in the laboratory (e.g. Hobbs,

1968; Tullis, 1973; Morrison-Smith et 1976). Consequently there is now well documented evidence to support increased recrystallization with either increased temperature, increased water content, increased strain, increased strain rate, or any combination of such. Unfortunately it has not yet been possible to determine which is the most important condition because in most cited cases, two or more are present at any one time. For example, Sylvester and Christie, and Bouchez, had both temperature and strain increasing together, thus they could not say explicitly that one alone was fundamental. However, they considered strain as the most important condition and it appears from a wide study of literature that this is probably, but not exclusively, so.

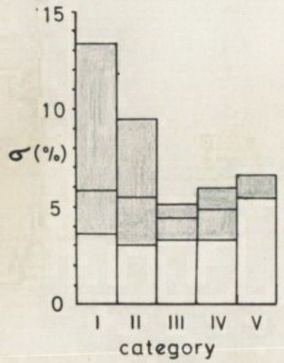
In this study the lack of strain markers means that no quantitative comparison could be made. Nevertheless, it has been noted that the D_3 deofrmation does become gradually more intense going from northwest to southeast towards both the Narridy Creek granite and the mylonite zone. Therefore as the quartz textures do broadly vary accordingly, there exists a prima facie case to support an increase in strain represented by Stages I to V. Temperature also may be important partiuclarly in the development of Stage V textures because there was no doubt a gradient around the syn D_3 Narridy Creek granite. Strain rate also may be considered to be linearly related to strain if the duration of deformation is considered as constant throughout the area.

Consequently without appropriate control over all these factors it is not possible to be any more conclusive than to say that Stage I represents the low strain, low strain rate, and low temperature end of the sequence, whereas Stage V represents the higher strain, higher strian rate, and possibly

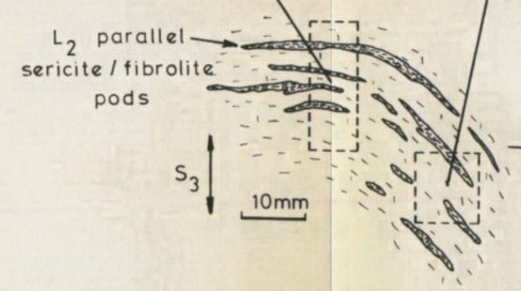
FIG. 6.26

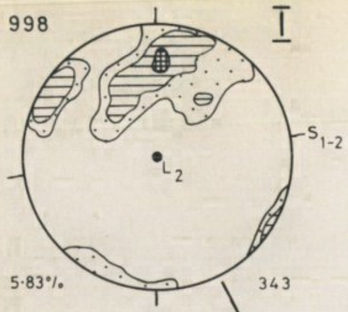
THE CRYSTALLOGRAPHIC PREFERRED ORIENTATION of QUARTZ

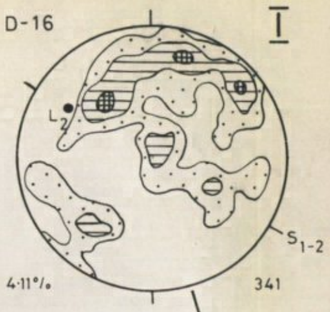
All diagrams are oriented with F_3 normal to the page and S_3 vertical. S_{1-2} and L_2 are indicated.
Contour intervals are 92·5% σ, 46·25% σ, and 23·125% σ where σ = maximum density (lower left of each diagram).
Number of points counted shown at lower right.

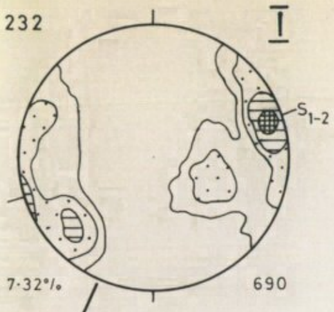


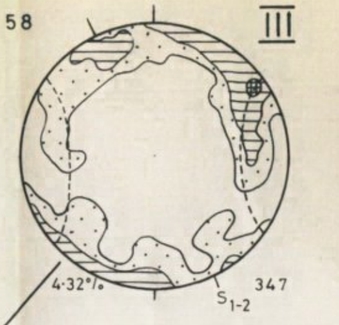
Maximum densities (σ) of all diagrams in each category.

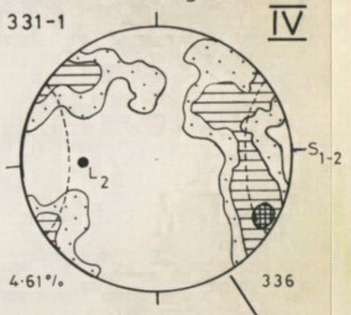


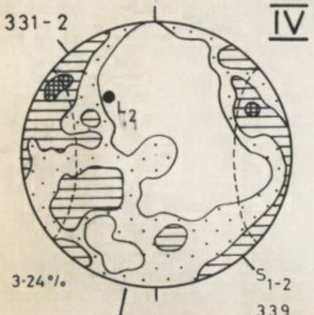


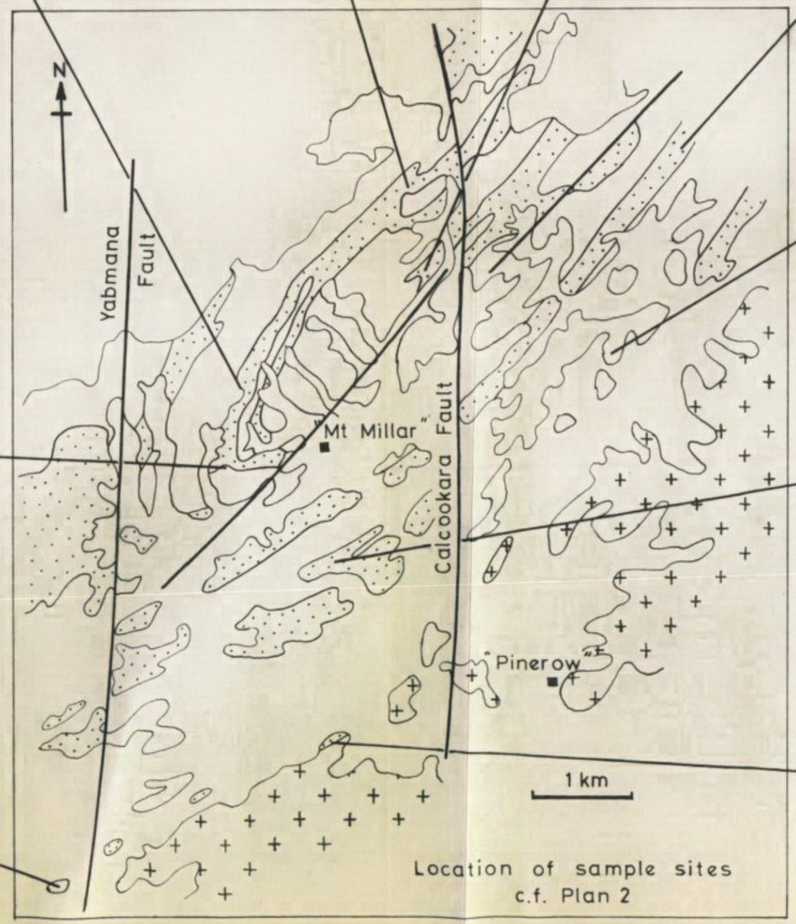


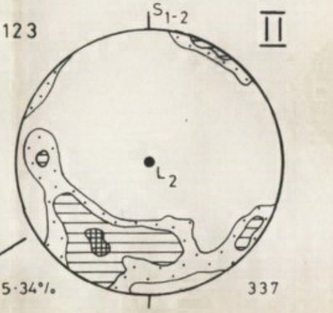


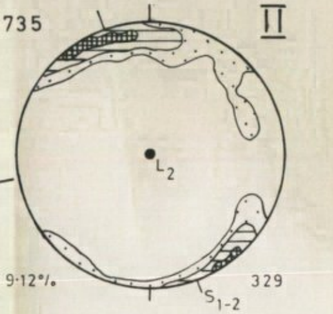


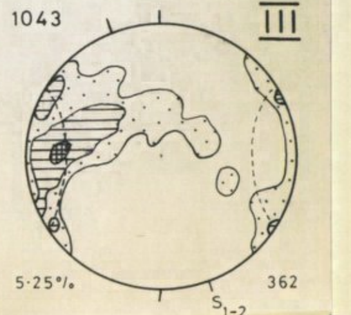


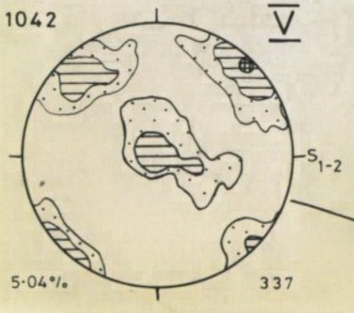












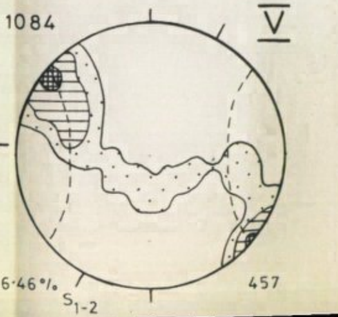
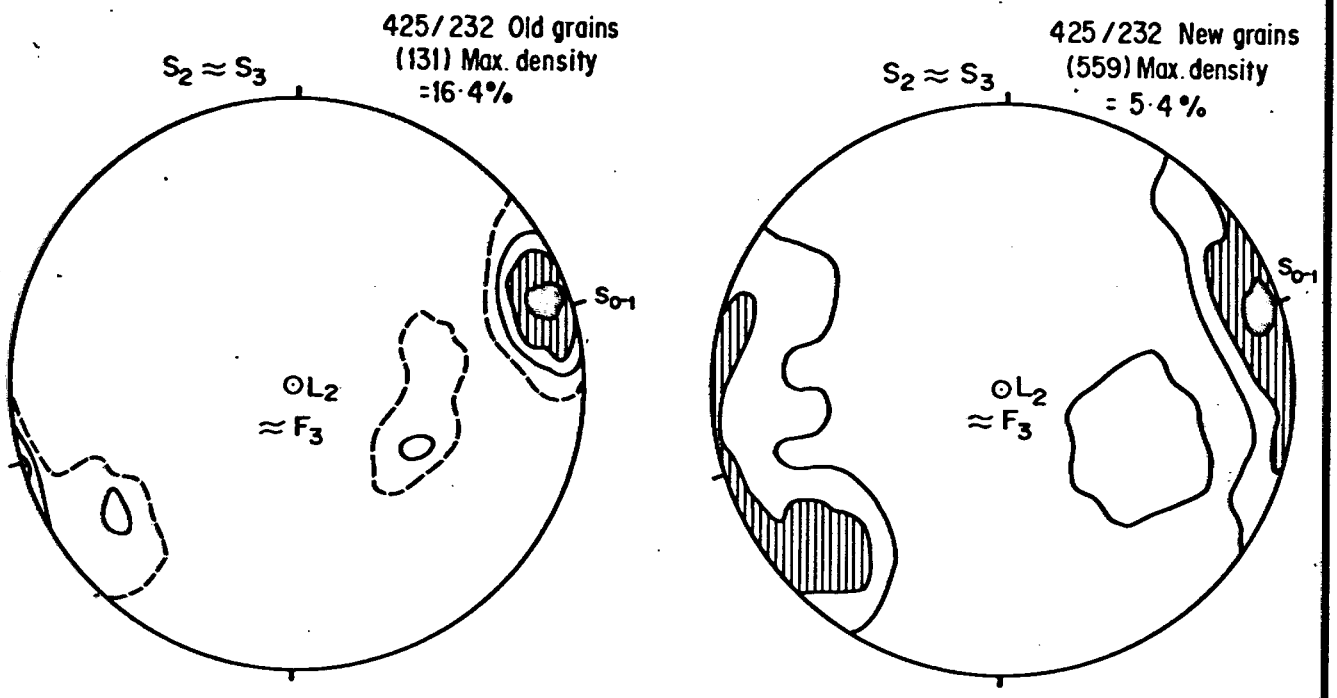
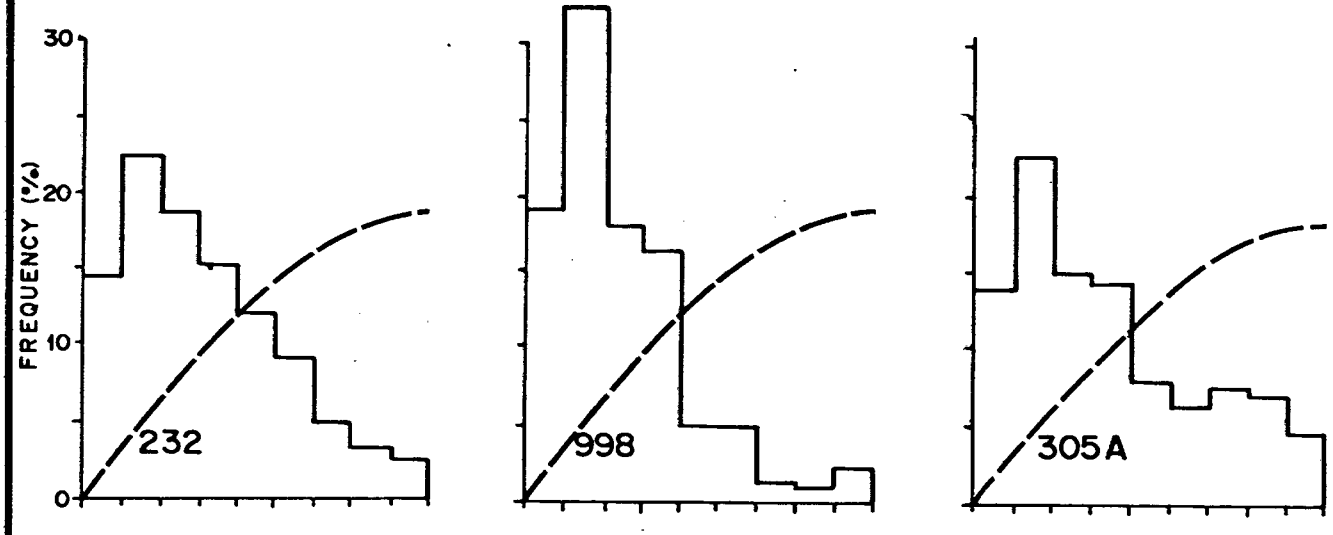


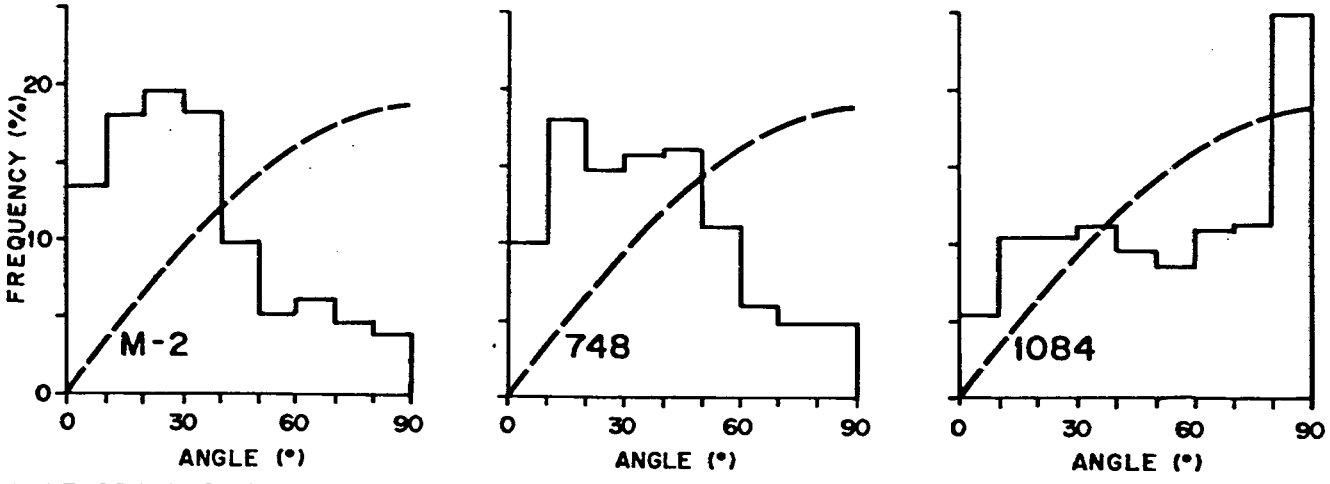
FIG. 6-27



ANGLE OF OLD GRAINS TO ADJACENT NEW GRAINS



NB. Dashed line represents uniform distribution between a random pair of lines (eg. see Ramson, 1971)



DEPT. OF MINES AND ENERGY - S.A

S 13214

higher temperature end. Crystallographic control will be considered in the following section.

QUARTZ C-AXIS FABRICS - Although a full study of quartz lattice orientation is beyond the scope of this theses, 26 fabric analyses have been carried out using a universal stage optical microscope and are included here as an adjunct to the study of quartz microstructures.

Some typical C-axis diagrams of quartzites from part of the study area are shown in Figure 6.26. It is immediately obvious that there is a crystallographic preferred orientation developed in all quartzites though it shows considerable variation in strength, nature, and orientation relative to other fabric elements. However there is a systematic variation which can be related directly to the degree of D_3 microstructural development. Most of the diagrams were based on 300 measurements or more and were contoured by the same method (ORIENT (Bridges and Etheridge, 1974)), therefore they can be considered as compatable.

STAGE I - Depending on the proportion of old grains to new grains, the fabrics of quartzites belonging to this category range from elliptical point maxima (specimen 232) to diffuse partial girdles (specimen D-16). They do not show any consistent relationship to the fabric elements S_{1-2} or S_3, however they often have maxima in either of those planes and normal to either L_2 or F_3. The most striking example is specimen 232.

Comparing old grains with new grains in specimen 232 (Fig. 6.27), the old grains which constitute by far the greater part by volume of the thin section, define a much stronger maximum than the total fabric while the new grains tend to spread out in a partial girdle about that maximum.

No such relationship exists for specimens 998 and D-16, both of which have fewer old grains relative to new grains. Their fabrics define partial girdles with the degree of spread about the maximum being roughly proportional to the abundance of new grains.

STAGE II - Fabrics of quartzites belonging to this group can be considered as an extension of Stage I fabrics; that is they define partial girdles not specifically related to either S_{1-2} or S_3. Although specimen 735 is exceptional, they mostly show greater spread about the point maxima and a lower maximum density than Stage I fabrics.

STAGE III - In keeping with the trend shown from Stage I and II fabrics, Stage III fabrics are even less well defined. They define diffuse girdles with low maximum densities. However, there is an approach to orthorhombic symmetry and the suggestion of initiation of a partial small circle about the pole to S_3 which is absent in the diagrams of previous stages.

STAGE IV - Two very important features can be noted from these fabrics. The first is the symmetry with respect to S_3 and F_3, and the second is the strength of the fabric in relation to the position in the fold.

Firstly, the fabrics, particularly that of specimen 331-1, clearly define partial small circle girdles about the pole to S_3. The opening angle of the girdles is 35-40° about that pole, and the maxima tend to be perpendicular to F_3.

Secondly, the fabric of specimen 331-1 is much better defined, is more symmetrical, and has a higher maximum density than does that of specimen 331-2. Both specimens display identical textures with strong S_3 quartz dimensional

orientation and therefore it is assumed that the total strain in each case is approximately equivalent. Because most other physical conditions (e.g. temperature, water pressure etc.) can be considered as similar over such a small distance, and because both specimens should ideally have started out (prior to D_3) with similar quartz textures and preferred orientation (N.B. orientation of L_2), then the principal factor for the difference in strength appears to be the deformation path. The strain path for that specimen (331-1) from the hinge of the fold can be considered as coaxial homogeneous flattening whereas in the limb it would not have been. Therefore, the strain history, particularly coaxiallity, has been an important control in the development of strong preferred orientation.

STAGE V - Fabrics of quartzites with Stage V textures are strong and consistent with Stage IV fabrics. Complete small circles about the pole to S_3 are not present but the fabrics (particularly that of specimen 1042) have orthorhombic symmetry and maxima which represent the intersection of small circles with the plane perpendicular to F_3.

INTERPRETATION - Any interpretation of the fabrics must take in account the following observations.

1) Stage I quartzites dominated by old grains generally have strong point maximum fabrics (specimen 232 and, to a lesser extent, specimen 998).

2) In Stages I to III with increasing numbers of new grains, that is, with increasing degree of recrystallization, there is a noticeable decrease in the maximum density of the fabrics and a corresponding increase in spread of orientation.

3) In Stages IV and V where there is substantial recrystallization the fabrics essentially define small circle girdles

about the pole to S_3.

4) There is a suggestion of a strong pre-D_3 crystallographic fabric.

1) Considering firstly those quartzites dominated by old grains. On the premise that the degree of recrystallization is proportional to the amount of deformation (strain), then these particular quartzites have not deformed as much as others. There can be two possible explanations for this. The first is the simple case of local variation of intensity of strain from one point to another. The second is the indirect case that says that quartz will deform more readily in certain orientations relative to the stress/strain axes than others. Since there are no specific strain markers, there is no way of proving or disproving the first hypothesis. The second hypothesis has evolved from both yield stress experiments on quartz (e.g. Hobbs et al, 1972) and, more recently, from fabric analyses of deformed rocks containing both highly deformed and relatively undeformed grains (Bouchez, 1977; Mancktelow, in press). The latter have demonstrated that the least deformed grains in a deformed rock commonly are aligned parallel to one of the principal strain axes. Considering the two least deformed specimens in this study it is significant that their point maxima lie close to one of the inferred principal strain axes (N.B. the principal strain axes can only be inferred from the orientations of S_3 and F_3). Although this is not conclusive this hypothesis is considered as a likely explanation for the preservation of old grains in those samples.

2) The second observation cited above is related to the microstructure. In an earlier discussion on the textural development of quartz, it was concluded that new grains

formed by the progressive rotation of subgrains away from their original orientation. Furthermore it was noted that old grains recrystallized first and then with subsequent deformation/ recrystallization, the new grains themselves recrystallized. Obviously, accompanying this increase in degree of recrystallization there is a progressive rotation of c-axes of the new grains away from their original position. So, it immediately follows that with increase in degree of recrystallization, there is an inherent increase in degree of misorientation away from the initial fabric.

Although this explanation accounts for progressive misorientation, it does not predict preferential misorientation in a specific direction. This is, of course, unless there is some internal or external factor influencing it. The two most important factors here are crystallographic control and stress/ strain control.

As in most studies crystallographic control on the development of quartz fabrics cannot be conclusively demonstrated because the complete orientation of quartz axes other than the c-axes is not known. It is known however that certain slip systems and slip directions will be favoured over others (e.g. see Baeta and Ashbee, 1969) and that the operation of certain of these will produce certain fabrics (e.g. see work of Lister in Hobbs et al, 1976; Suzuki, 1970; Tullis et al, 1973).

To examine one aspect of crystallographic control over the type of fabrics observed, the angles between the c-axes of old (host) grains and new (recrystallized) grains have been computed (Fig. 6.27). Previous workers (e.g. Hobbs, 1968; Ransom, 1971; Wilson, 1973; Beland Etheridge, 1976) have shown that quartz often tends to preferentially align

itself such that the angle between its c-axis and those of its neighbours is about 20-40°. This was particularly so in the annealing experiments of Hobbs. However in the examples illustrated here, this tendency is not obviously developed. Instead the angle subtended is characteristically small for specimen 232 of Stage I but increases towards a uniform random distribution (specimen 1084) with increase in degree of recrystallization. This is consistent with the principle of progressive misorientation with degree of recrystallization. Consequently it is concluded that in this study this one aspect of crystallographic control does not have much influence on the preferred orientation of quartz. It suggests that strain and deformation mechanisms were more important in the orienting process.

3) Considering the third major observation, the fabrics of Stage IV and V quartzites, it is useful to compare them with those obtained in theory (Lister in Hobbs et al, 1976), in experiment (Green et al, 1970; Tullis, 1973) and in natural examples (e.g. Marjoribanks, 1976). The mathematical models of Lister predict that small circle girdles about the pole to foliation can be formed from random aggregates in certain conditions. Some of these are basal (only) intracrystalline slip in an essentially plane strain deformation, and combined basal and rhombohedral slip with grain rotation in deformation conditions ranging from homogeneous flattening to plane strain. The effects of combined prismatic and basal slip have also been studied theoretically by Tullis et al (1973) and they predict that with greater amounts of prismatic slip, the opening angle of the small circle should increase.

Small circle girdles about the pole to foliation have also been produced experimentally. Green et al. (op. cit.)

in syntectonic recrystallization experiments on flint in the α quartz field produced point maxima fabrics parallel to the axis of compression at low T and high strain rates, but at higher T and lower strain rates, produced small circle girdles about that axis. Likewise Tullis et al produced almost identical results during similar experiments on quartzites. In addition, though, they demonstrated that the opening angle increased with increase in T or decrease in strain rate, and that the transition from point maxima to small circle girdles approximately corresponded to the onset of recrystallization. All these experiments were done under axial compression and therefore approximate to simple homogeneous flattening.

Small circle girdles have long been recognized in natural quartzites. Furthermore it has been observed that the opening angle does appear to increase with metamorphic grade such that in greenschists it is commonly 25-30°, in amphibolites it is 30-40°, and in granulites it is about 59°. The study by Marjoribanks (1976) is most relevant to this study. He demonstrated that with increasing strain there was a corresponding increase in recrystallization and in development of the c-axis fabric. Furthermore in those examples which approximated to simple flattening he got small circle girdles about the pole to foliation while in others that ranged from that to plane strain, he got fabrics that varied from small circles to single point maxima or great circle girdles on the constrictive side of plane strain. The opening angle in Marjoribanks examples was commonly 30-40° but it decreased to 25° in the high strain specimens.

Assessing much of the available data then, it appears

that the small circle girdle distribution of c-axes about the pole to foliation is characteristic of a flattening deformation closely approximating to simple flattening, whereas a great circle distribution is more characteristic of constrictive strain. On this basic presumption, it is therefore postulated that the quartzites of Stages IV and V have undergone a strain closely approximating to simple flattening. Furthermore the opening angle of 30-40^{o} suggests that the strains and strain rates in these specimens were not very high but rather were of moderate magnitude.

The similarity between these fabrics and the experimental and theoretically produced fabrics cited above, allied with the strain and variability of c-axis orientations within individual grains (both old and new) suggests further that intracrystalline deformation was an important mechanism in the development of the fabrics. However it was noted earlier that many grain boundaries were lined with diffuse rusty brown material presumably a residue of grain boundary diffusion. Consequently grain boundary mechanisms may also have assisted in the rotation of new grains. Therefore, it is believed that the combined processes of intracrystalline and grain boundary deformation were responsible for the development of D_3 preferred orientation.

4) In all the above examples cited from literature, the girdle fabrics were produced from progressive deformation of an initially random fabric. This is not so with this study. Instead, due to the effect of two prior high grade deformations, D_1 and D_2, the fabrics have developed from an initial preferred orientation. Since many of the fabrics have maxima in the S_{1-2} plane normal to the L_2 lineation it is believed that the initial fabric had a prominent point

maximum either in that orientation or very close to it. Fabrics of this type are common in high grade intense deformations where recrystallization and grain growth were strong and pervasive (e.g. see Wilson, 1973). They reflect different physical conditions to those envisaged during D_3.

SUMMARY OF MICROFABRIC - There are several conclusions that are suggested by the above interpretations.

1) A strong crystallographic preferred orientation arising from the D_1 and D_2 deformations has been progressively modified to produce a different preferred orientation in D_3.

2) Fabrics of Stage I to III quartzites reflect progressive misorientation of the D_{1-2} fabric whereas fabrics of Stage IV and V quartzites, where there has been intensive recrystallization, reflect D_3 strain parameters.

3) Fabrics of Stage IV and V quartzites suggest a flattening type D_3 deformation.

4) The mechanism of quartz reorientation during D_3 involved the combined processes of intracrystalline slip (with related recovery) and grain boundary slip.

6.4.2 Summary of D_3 Microstructure

In summary, it is clear that the principal characteristic of the D_3 deformation is the variability and poorer development of axial fabrics, S_3 and L_3, compared to those of the anteceding D_2 deformation. Neither S_3 nor L_3 are pervasive or penetrative, and furthermore they vary in nature and strength not only with lithology (e.g migmatites verses non migmatites) but also with areal distribution.

Although new grain growth along crenulation band boundaries, in mica films, and in mica beards has been emphasized in the above discussion, it is in fact only of minor importance in the development of the dominant D_3 microstructure.

Rather, the textures and fabrics have developed by the combined processes of recovery and recrystallization of S_{1-2} fabrics without prominent new grain growth in the S_3 orientation (cf D_2). Fracture cleavages are prominent and diffusion along them and grain boundaries has been an important process. However, syn-or post-tectonic annealing has not contributed greatly except perhaps in the immediate vicinity of the Narridy Creek granite. Therefore, all the microstructural evidence points towards lower metamorphic conditions than those during D_2 and in fact would suggest upper greenschist to lower amphibolite metamorphic conditions.

The relative magnitude, orientation and distribution of strain during D_3 could not be practically determined. However, allied to the mesostructure, the microstructure suggests that simple homogeneous flattening was an integral and important part of the deformation. Furthermore the broad variation in degree of microstructural development from northwest to southeast towards the Narridy Creek granite and from northwest to southeast towards the mylonite zone infers that the intensity of deformation increased towards those regions. Except within the mylonite zone, neither the strain nor the related strain rate could be regarded as excessive.

Finally, on a microscopic scale, there is relatively little disruption of layering although there is visibly a relative thickening and thinning of it in the hinges and limbs, respectively, of F_3 folds. This varies according to lithology and total strain.

6.5 MYLONITE DEFORMATION

6.5.1 The Fabric

This section is concerned only with the fabrics and

textures of those highly deformed rocks within the mylonite zone. The effects that mylonitization had on the surrounding rocks outside that zone have been covered under the D_3 deformation.

There are two principal stages or categories of fabric development that are observed in the mylonite zone. The first stage is dominated mainly by recrystallization of mica and quartz with incipient recrystallization of feldspar and is here referred to as the mica recrystallization stage. The second stage is a feldspar recrystallization stage.

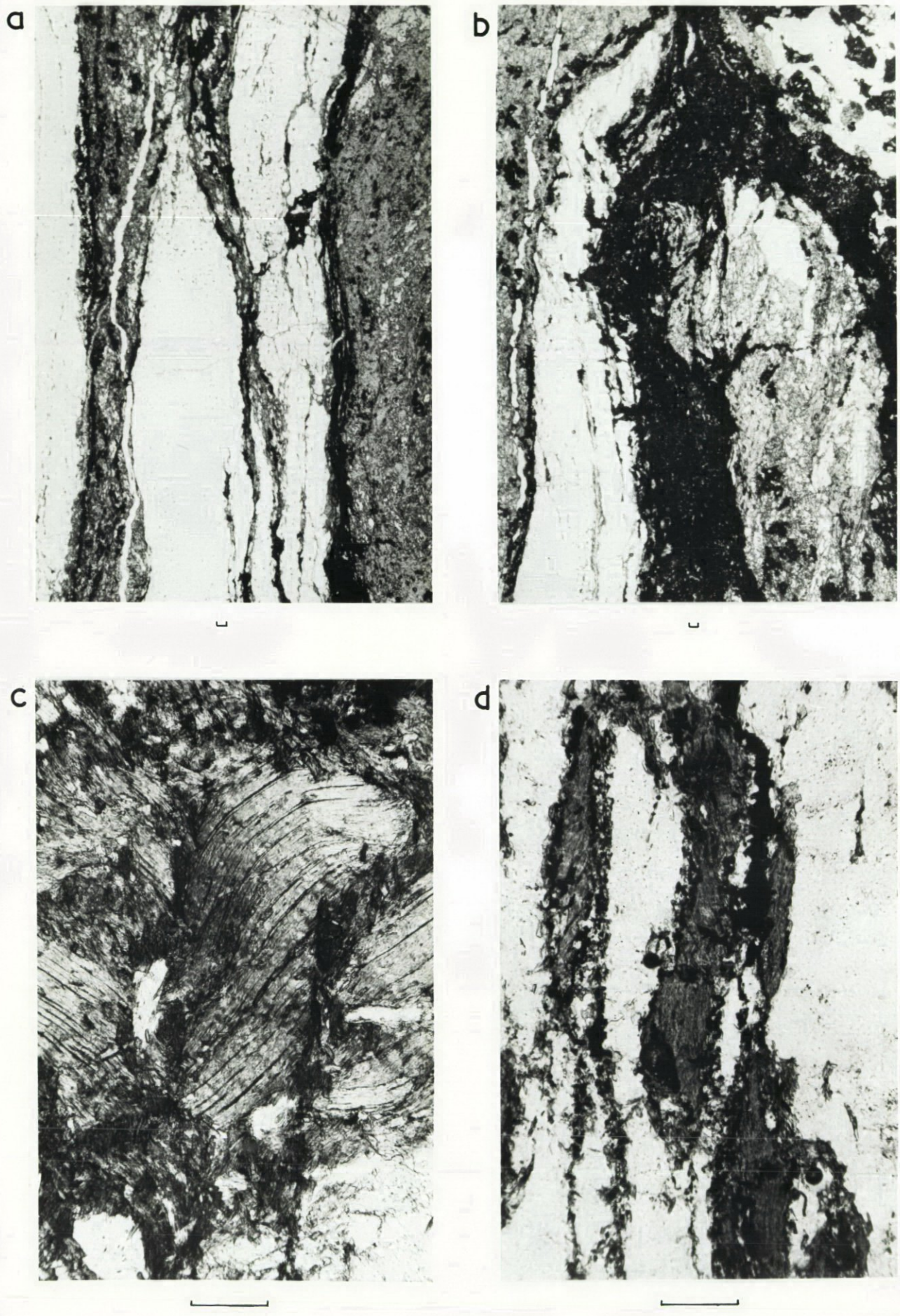
6.5.1.1 Mica Recrystallization Stage

The fabrics and textures of mylonitized gneisses are an extension of D_3 microstructures outside the mylonite zone. There are numerous meso-folds in these rocks and as noted in Chapter III they resemble F_3 folds. However in thin section they have several obvious differences. Firstly, they are noticeably much tighter, secondly they have a strong, penetrative axial fabric, and thirdly, there is considerable disruption of layering.

The tightness of the folds is illustrated in Figure 6.28a-b. In example a the quartz vein has been isoclinally folded with the short intermediate limb having been almost completely pinched out. There is no trace of the S_{1-2} fabric in the hinge and the quartz textures are similar to, though more deformed than, Stage IV D_3 textures. In example b, the discontinuous nature and disruption of the layering is illustrated. S_m, here overprinting a relic S_{1-2} schistosity, is defined by a highly penetrative fracture cleavage which is developing into a domainal schistosity by the recrystallization of mica and semiopaque mineral along it.

It is clear in these examples that there is a new axial

FIG. 6.28



fabric strongly developed. The fabric is a logical progression from S_3 fabrics outside the mylonite zone and there are three main features defining it. They are, a fracture cleavage, a mica preferred orientation and a segregation or domainal schistosity.

The fracture cleavage grades from simple fractures or dissolution planes typical of S_3 outside the mylonite through to complex zones or domains of intense recrystallization; that is, they grade into the domainal schistosity. In fact, it is common for a fracture in one part of a thin section to progressively change into a domainal schistosity in another part.

S_{1-2} micas in mylonitized gneiss, by contrast with their moderately deformed equivalents outside of the zone, are both highly deformed and strongly recrystallized (Fig. 6.28c-d). Kinked or crenulated micas have strongly flexed hinges and there is often prolific, very fine new grain growth along kink band boundaries and wrapping around individual grains. S_m is defined by these new micas, by rotated fragments of old grains and by a dimensional orientation of fine opaque minerals accompanying the new mica growth.

Both biotite and chlorite can constitute S_m and S_{1-2}. In those specimens (mainly very quartz rich) where S_{1-2} is defined by biotite, the newly recrystallized micas are also biotite. However, the new grains are associated with very fine grained opaque and semi-opaque minerals which are not present in the old biotites. In by far the majority of specimens however, the principle micas are chlorite and

---

Figure 6.28: Mylonite zone-mylonitized gneiss. (a) and (b) hinge zones of isoclinal folds with axial planar S_m fabrics (vertical S_m). (c) and (d) biotite recrystallization along kink band boundaries and around the edges of rotated grains. S_m vertical. Bar scale = 0.1 mm.

sericite. Old S_{1-2} micas are still present, but they have been almost completely pseudomorphed by chlorite.

Sericite is abundant in all rocks within the mylonite zone. It is fine grained, sub-idioblastic and forms narrow, lenticular aggregates parallel to S_m. In the hinges of folds, these sericite aggregates are axial planar whereas in the limbs they are essentially layer parallel. They often have scattered remnants of sillimanite, feldspar or biotite (now chlorite) within them and they define the domainal schistosity.

Accompanying recrystallization of mica, there is concomitant recrystallization of quartz, retrogression of garnet and incipient alteration of feldspar. The recrystallization of quartz has led to a variety of fine to medium grained aggregates ranging from subpolygonal and relatively unstrained new grains, to highly undulose and irregularly shaped (?) old grains. Garnets have partially or completely retrogressed to chlorite, and the alteration of feldspar is manifest as a partial sericitization of plagioclase and an incipient grain boundary recrystallization of microcline (cf Fig. 6.16c).

6.5.1.2 Feldspar Recrystallization Stage

This stage of mylonitic microstructural development corresponds exactly with the formation of slaty mylonite. In the previous stage while the S_{1-2} fabric was largely destroyed, the rocks still retained much of their original character (e.g. layering, medium grain size). However, with the recrystallization of feldspar that character is obliterated and replaced by a homogeneous slaty fabric. In Figure 3.11 a band of slaty mylonite displaying its progressive development from mylonitized gneiss, was illustrated. Several

FIG. 6.29

specimens were taken across this band, and they are here labelled MY-1 through to MY-6 with MY-6 representing the homogeneous slaty mylonite. In order to simplify their description, they are grouped together into three groups MY-1 and 2, MY-3 and 4, and MY-5 and 6. It should be noted that all these particular specimens have similar mineral (Q_{30-40} Pl_{30-45} $Kspar_{10-20}$ $Mica_{10-12}$ Acc_{1-5}) and chemical compositions (see Appendix A).

Specimens MY-1 and 2 both display partial recrystallization of feldspar which is manifest as aggregates of fine to very fine new grains both surrounding old grains and sweeping off into long tails on each end (Fig. 6.29). Augen development is pronounced and the textures are typically protomylonitic (Sibson, 1977; Spry, 1969; N.B. this term is used here in a structly non-genetic manner (as does Sibson) whereas Spry implied that it was a crushed rock rather than a recrystallized rock) with the augen or clasts still constituting 45-55% of the total rock. There is a good foliation (S_m) in the rock being defined by mica alignment, quartz ribbons, slightly elongate old feldspars, and trains of newly recrystallized feldspar grains. The micas are mainly fine to very fine grained sericite and chlorite but there are some rare, scattered, medium sized, highly deformed old grains.

The quartz ribbons are very prominent in both specimens. They often occupy pressure shadow sites, but more importantly, individual ribbons are often interconnected across S_m and form very coarse single grains (Fig. 6.29). Figure 6.29c

---

Figure 6.29: Mylonite zone - mylonite specimens MY-1 and MY-2. (a) and (b) coarse feldspar relics in a very fine grained, recrystallized matrix with very coarse, anastomosing ribbons of unstrained quartz. (c) a very coarse single grain of quartz anastomosing new and old feldspar grains. Bar scale = 0.1 mm.

FIG. 6.30

a

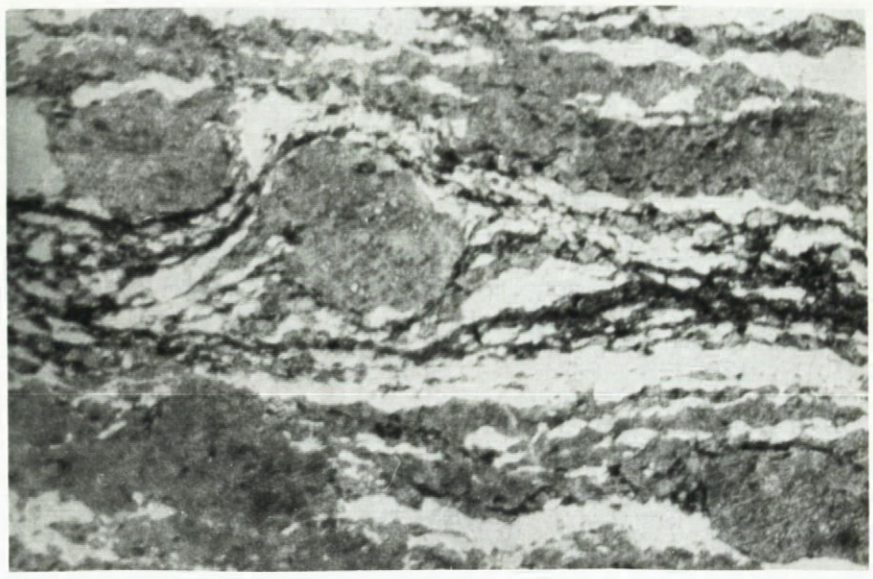


b

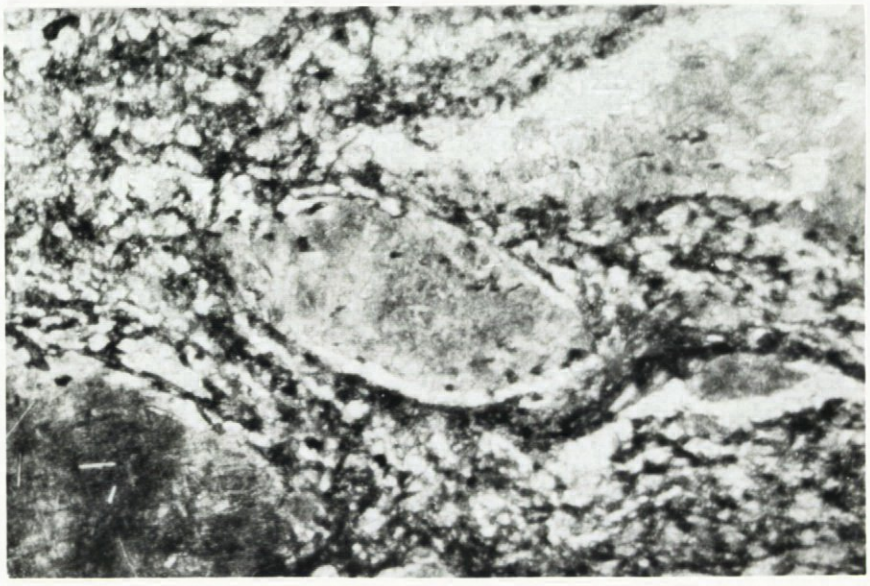


FIG. 6.31

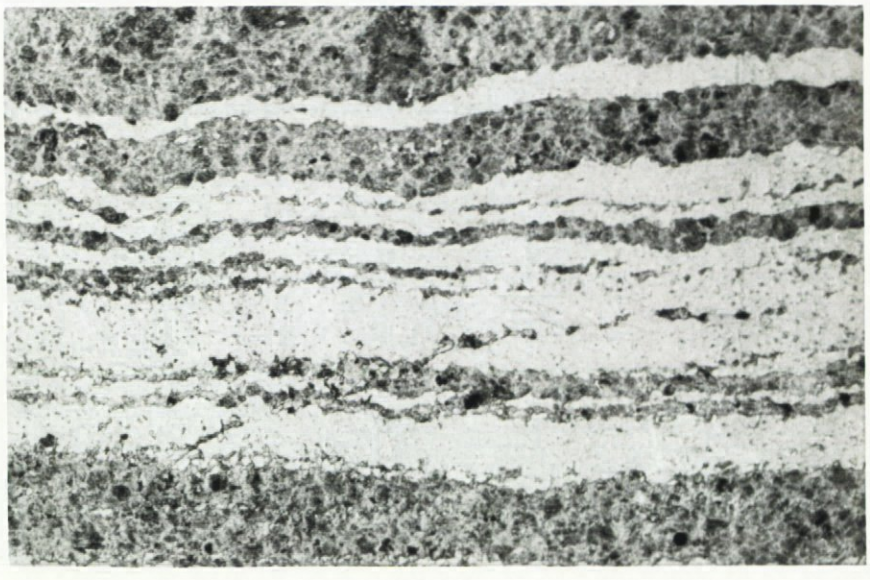
a



b



c



shows a single, relatively unstrained grain anastomosing recrystallized feldspars, while in other areas similar euhedral grains may have subgrains locally developed. This local strain and recovery of otherwise unstrained grains indicates that there was minor, local deformation postdating the final quartz crystallization. Nevertheless though, the quartz crystallization does postdate the major deformation and is a very late stage effect.

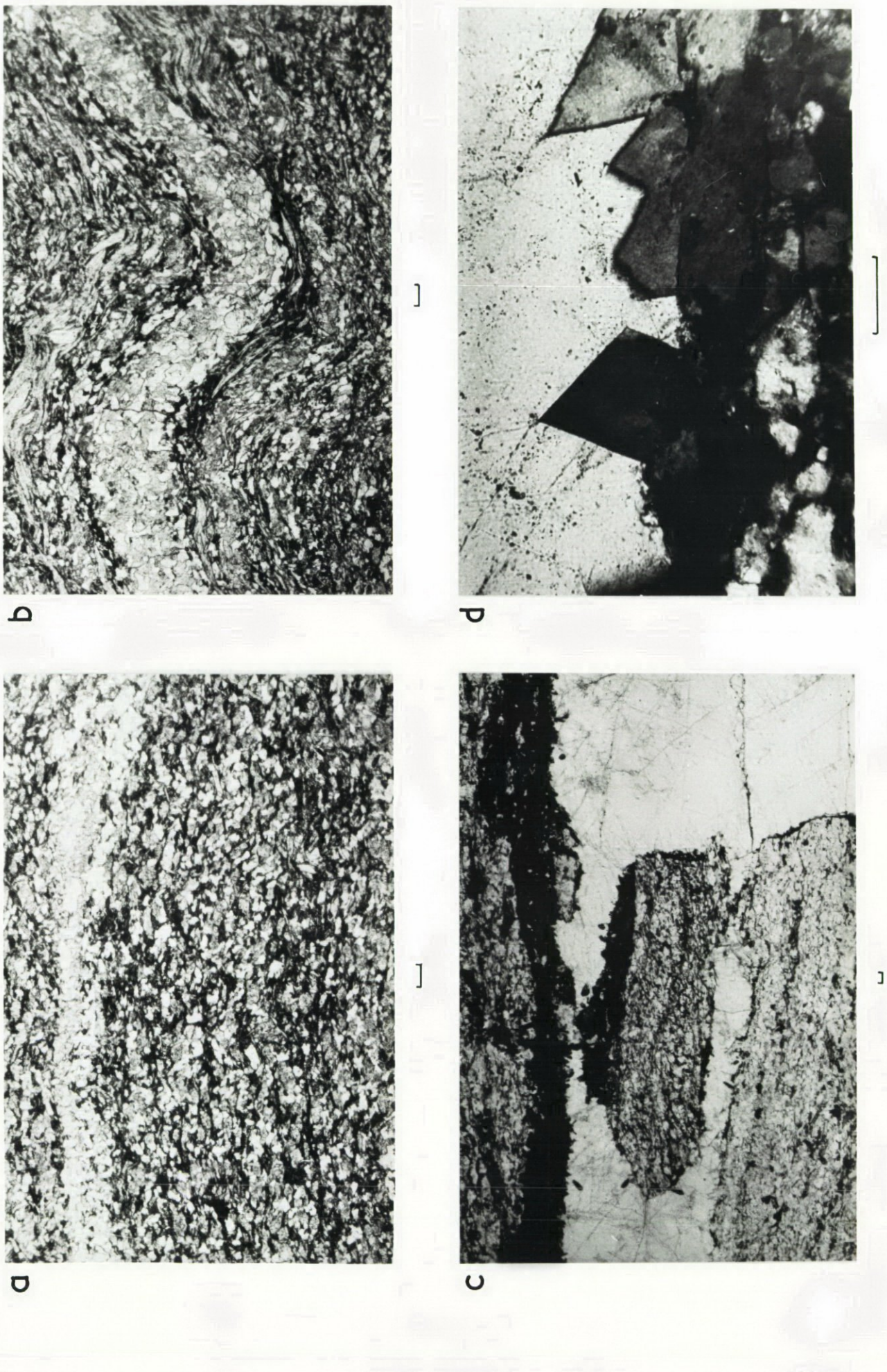
Associated with the quartz ribbons is another very characteristic feature. It is the presence of new plagioclase both as overgrowths on old grains (Fig. 6.30a) and as aggregates of new grains (Fig. 6.30b). In the first case, the old and new grains are optically continuous but the old grains are clearly recognized by their sericitized outlines. Note that the new overgrowth is strikingly euhedral into the quartz ribbon. In example b, the new grains are likewise clear of sericite inclusions but form subpolygonal mosaics.

The next stage of development represented by specimens MY-3 and MY-4 produced typical mylonite textures with only 10-25% augen remaining in a fine grained, strongly foliated matrix (Fig. 6.31). The augen are recrystallized with old grain relics in the cores and they have long tails of new grains which are sometimes strongly elongate to define mesoscopic L_m lineation on S_M (Fig. 6.31c; cf Fig. 6.31a-b).

Figure 6.30: (a) new euhedral plagioclase overgrowth on a sericitized old grain. Note the continuity of twin lamellae. (b) aggregate of new, polygonal plagioclase grains.

Figure 6.31: Mylonite zone - mylonite specimens MY-3 and MY-4. (a) and (b) typical mylonitic texture with scattered coarse feldspars (partly recrystallized) in a fine grained matrix (section normal to L_m). Quartzo feldspathic ribbons (pink in hand specimen) are clearly shown in (a) at the top and bottom separated by a chlorite rich band (cf (b)). (c) fine grained, recrystallized quartzo feldspathic ribbons in a section cut parallel to L_m. Bar scale = 0.1 mm.

FIG. 6.32



Pinkish white quartzo feldspathic bands are characteristic of this stage of development. They consist entirely of alternating ribbons of fine grained highly undulose quartz and fine grained subpolygonal aggregates of recrystallized plagioclase. (Fig. 6.31a and b). They contrast against the dark green slaty matrix which consists of fine grained quartz, feldspar, chlorite, sericite, epidote, sphene and opaque minerals with scattered feldspar clasts.

The third stage of mylonitic development is shown by specimens MY-5 and MY-6 (Fig. 6.32). Both examples have typical ultramylonitic textures, there being fewer than 10% clasts or augen (e.g. in MY-6, augen constitute only 1-2% of the rock), and the matrix is fine grained with a strong slaty schistosity defined by the preferred orientation of chlorite, sericite, some opaque minerals, and to a lesser extent epidote prisms. Quartz and quartzo feldspathic bands are much less prominent and they have homogeneous textures compared with the ribbon textures of MY-3 and MY-4 (compare Figs. 6.31 and 6.32). Micas also are generally homogeneously mixed up in the matrix but some sericite has aggregated in the hinges of post mylonitic, D_4 crenulations (Fig. 6.32b) to form narrow muscovite films.

Another important observation in a specimen equivalent to MY-6, is the presence of late generation quartz veins (Fig. 6.32c-d). They resemble those of MY-1 and 2 (Fig. 6.29) in that they are very coarse grained and unstrained (e.g. in the example shown here there are only two grains),

Figure 6.32: Mylonite zone-slaty mylonite specimens MY-5 and MY-6. (a) typical slaty mylonite. (b) crenulated (by F_4) slaty mylonite with muscovite aggregating in hinges. (c) very coarse, single crystals of quartz anastamosing fragments of slaty mylonite. (d) euhedral plagioclase overgrowths growing on recrystallized matrix grains into quartz grain of (c). Bar scale = 0.1 mm.

FIG. 6.33

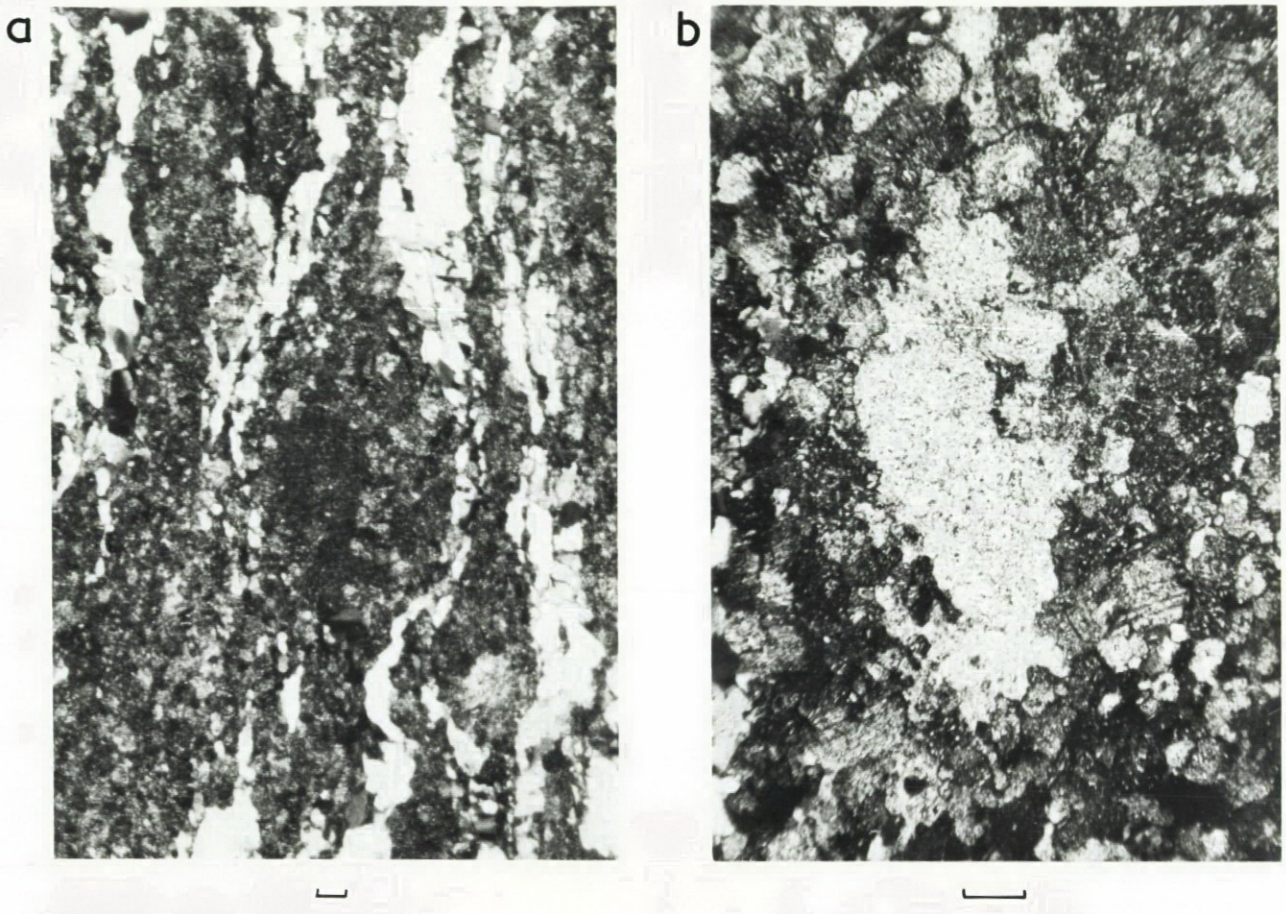
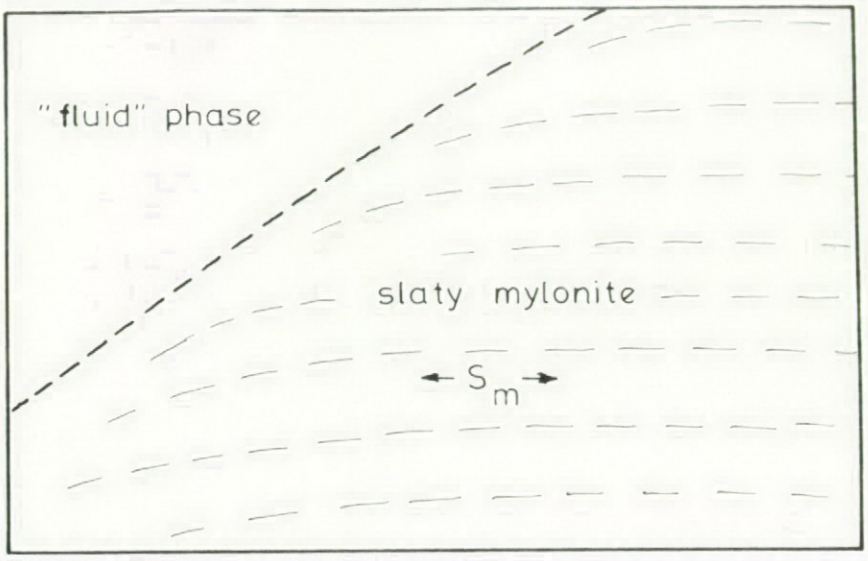
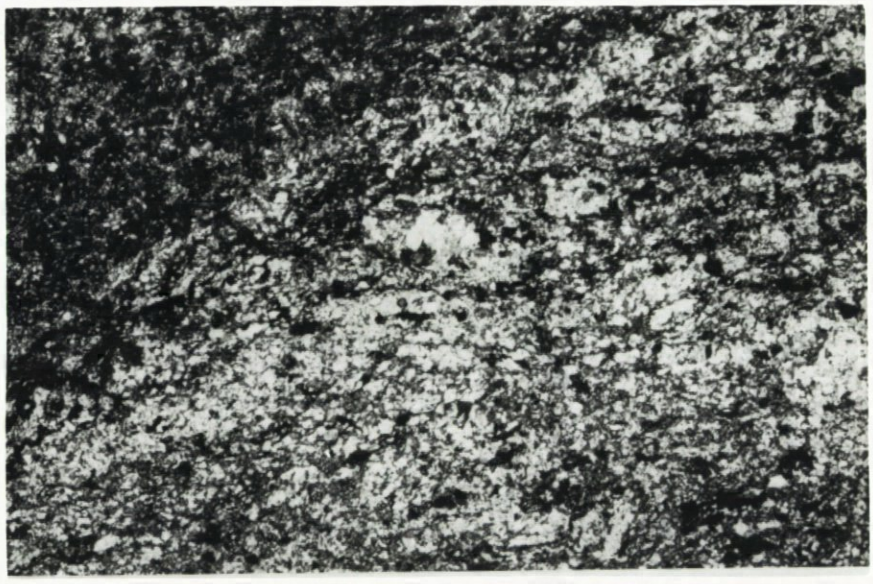


FIG. 6.34

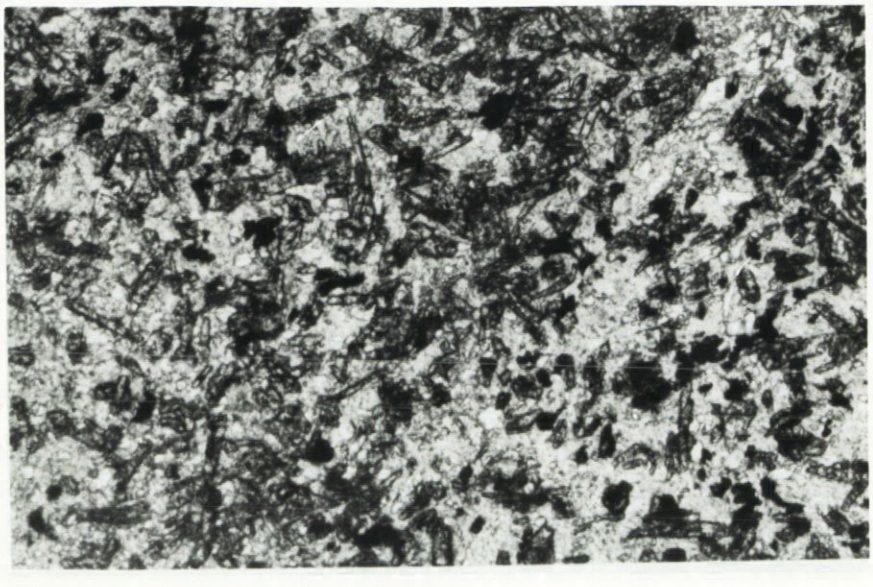
a



b



c



and furthermore they have very fine euhedral feldspar overgrowths growing out from the matrix into them.

Summarizing then the transition from mylonitized gneiss into slaty mylonite, the principle features are the gradual reduction in augen or clasts, the corresponding recrystallization of feldspar, and the progressive mixing up or homogenization of the fabric. The ultimate slaty mylonite bears little resemblance to the original rock although it is of similar overall composition.

An interesting observation in this recrystallization sequence is a comparison of the nature of recrystallization of plagioclase and microcline. As noted in the Narridy Creek granite (Sect. 6.4.1.3 and Fig. 6.24), recrystallization of plagioclase was initiated by recovery of flexed twin lamellae to form subgrains which subsequently rotated to form fine/medium grained aggregates of new grains. Such recovery initiated recrystallization is also clearly present in the mylonitized gneisses and in the initial stages of slaty mylonite development. It is a rapid process and in specimens MY-3 and MY-4 the old plagioclases have completely recrystallized to aggregates of fine, subpolygonal grains. The nature of this recrystallization is clearly shown in Figure 6.33. A relic of the initial old grain remains in the centre of the augen but is surrounded by a mosaic of subpolygonal new grains. These new grains are much finer grained than those outside the slaty mylonite belts and this is believed to be analogous to the decrease in new grain

---

Figure 6.33: Feldspar recrystallization. (a) and (b) Recrystallization of plagioclase from fine subgrains. (c) recrystallization of microcline. (d) as for (c) but crossed polars.

Figure 6.34: Mylonite zone-"fluid" phase. (a) line sketch of (b). (b) "fluid" phase truncating S_m of the slaty mylonite. (c) unoriented epidote prisms in the "fluid" phase. Bar scale = 0.1 mm.

size with increase in strain often recorded in quartz (e.g. D_3 quartzite textures in this study; White, 1977). That the new grains have formed from subgrains of the old host grain is evidenced by aprogressive misorientation of new grains away from the old grain core.

Microcline behaved quite differently to plagioclase during the development of slaty mylonite. These differences were noted even in the mildly deformed rocks outside the mylonite zone, but are much more obvious here. In the mylonitized gneisses microcline shows incipient very fine new grain growth along grain boundaries and along (?) fractures within the grains. In the slaty mylonite specimens MY-1 to MY-5 microcline augen show prolific grain boundary recrystallization (Fig. 6.33c-d) and it is noteworthy that the majority of augen still remaining in specimens MY-5 and MY-6 are predominantly microcline. Although they have many features in common with plagioclase recrystallization (old grain cores surrounded by new grain rims with tails of new grains off each end), the size and nature of new grains differ substantially. Therefore the process of recrystallization appears to have been much slower and more restrictive than in plagioclase. It is believed that this apparently slower rate of recrystallization is related directly to the size of the new grains. Because the new grains are smaller in microcline more energy must be required to completely recrystallize whole grains than would be required to recrystallize whole plagioclase grains.

Finally in the process of mylonitization is the production of an unusual rock which is best considered as a "fluid" phase. It is quite different mineralogically (Q_3 $fleds_{40}$ $mica_{30}$ Ep_{25}) and chemically (see Appendix A), it

lacks any internal fabric (Fig. 6.34) and it cuts across S_m in the slaty mylonite. While it could be considered as an original lithological layering the distinct lack of an internal fabric, the nature of its contact with slaty mylonite and its basic composition suggest that this "fluid" phase was "intruded" into the slaty mylonite late during D_m.

6.5.2 Summary and Discussion

It is clear from the above descriptions that the microstructure of the mylonite series of rocks has developed principally from recrystallization of the various components without significant changes in overall composition. The first evidence of mylonitization was seen in the country rocks adjacent to the mylonite zone. In these rocks, D_3 features noticeably intensified on approaching the mylonitized rocks, folds became tighter, S_3 became much stronger, and there was incipient retrogression.

Within the mylonite zone, it was possible to distinguish two rocks groups, those rocks that still retained much of their original character but which were visibly strongly deformed (the mylonitized gneisses), and those rocks in which the new fabric had obliterated most of the original character (slaty mylonite). Furthermore it was shown that these particular groups corresponded essentially with, firstly, recrystallization of mica, and then subsequently, with recrystallization of feldspar. The importance of recrystallization is emphasized because it was the major mechanism behind the development of the microstructure. Clearly the recrystallization process was a dynamic process as illustrated by its progressive development, by the strong S_M schistosity in the recrystallized matrix, and by the overprint of late stage quartz veins that have clearly

formed subsequent to the main fabric.

Ductile deformation of the rocks is also emphasized by the association of isoclinal folding with the development of the microstructure. No brittle or cataclastic features are present in these rocks and while it may be argued that they have been masked by recrystallization or neo-mineralization subsequent to the cataclastic deformation (e.g. see Christie, 1960) all the available evidence supports a ductile event. This is particularly so when the extreme elongation of many recrystallized aggregates is considered.

Such features are well known to metallurgists as the result of superplasticity of very fine grained aggregates when two or more mineral phases are present (e.g. Hayden et al, (1972); Ashby, 1973; Boullier and Gueguen 1975). Boullier et al have applied some of the metallurgical concepts to mylonites and rightly consider that the principles of superplasticity can be applied to such rocks. Many of the conditions that they believed were significant also apply here; that is, the fine grainsize of the aggregates, the presence of two mineral phases, the polygonal shape of the grains in the aggregates, the extreme elongation of the aggregates, and the movement of grains relative to their original neighbours. As such superplasticity is analogous to drawing froth through a funnel (e.g. see Ashby, 1973).

In concluding that ductile deformation accompanied by dynamic recovery/recrystallization was the prime process of mylonite microstructural development at Cowell, it is appropriate to compare this study with recent concepts. By contrast to Lapworth's (1885) definitions in which the concepts of cataclastic grinding or milling were inherent, recent literature has emphasized the importance of dynamic

recrystallization accompanying ductile deformation (e.g. Bell and Etheridge, 1973; Hobbs et al, 1976; Sibson, 1977). Many of these recent concepts have developed from analogy with metals on which there is a considerable volume of literature. Therefore this study confirms the current views on mylonite development.

More importantly though, it emphasizes the importance of feldspar recrystallization as the prime factor controlling the development of what are normally considered as typical mylonites (Spry, 1969; Siddans, 1977). Bell and Etheridge (1973) erected a basic four stage scheme for the formation of mylonites. Their scheme is summarized in the table below and compared with this study

STAGE	Bell and Etheridge (1973)	This study
1	COUNTRY ROCK NOT VISIBLY DEFORMED	D_3
	- quartz recovery/recrystallization, rare feldspar deformation, micas kinked but only incipient recrystallization	microstructure
2	COUNTRY ROCK VISIBLY DEFORMED	mylonitized
	- mylonite schistosity prominent, feldspar deformation common, significant mica recrystallization	gneiss
3	QUARTZ-FELDSPAR MYLONITE	
	- all remnants of country rock obliterated, feldspar recrystallization significant	slaty mylonite MY-1 to MY-5
4	QUARTZ-FELDSPAR PHYLLITE	slaty mylonite
	- no country rock grains remain, homogeneous fabric	MY-6

There is clearly a positive correlation between microstructural development in their study and that examined here.

What then does the "fluid" phase of this study represent.

In many mylonite zones throughout the world, pseudotachylites have been recorded in asssociation with ultra-mylonites (e.g. see Waters and Campbell, 1935; Philipotts, 1964) and in the opinion of many authors they represent the extreme "crushing" of rocks possibly accompanied by partial fusion. Although there is no evidence of either fusion or crushing in these rocks it is possible that they represent the ultimate development of mylonitization.

With only a very limited occurrence of this rock it is not possible to take this any further than to suggest that, it along with pseudotachylites, may represent a fifth stage in the microstructural sequence.

In conclusion then, this study presents a clear case supporting the concepts expressed by Bell and Etheridge (1973). Those concepts are that ductile deformation and dynamic recrystallization are fundamental in the development of most mylonite microstructures, that typical mylonites form from the active recrystallization of feldspar, and that there are at least four, if not five fundamental stages in mylonitic development across zones of intense deformation.

6.6 D_4 DEFORMATION

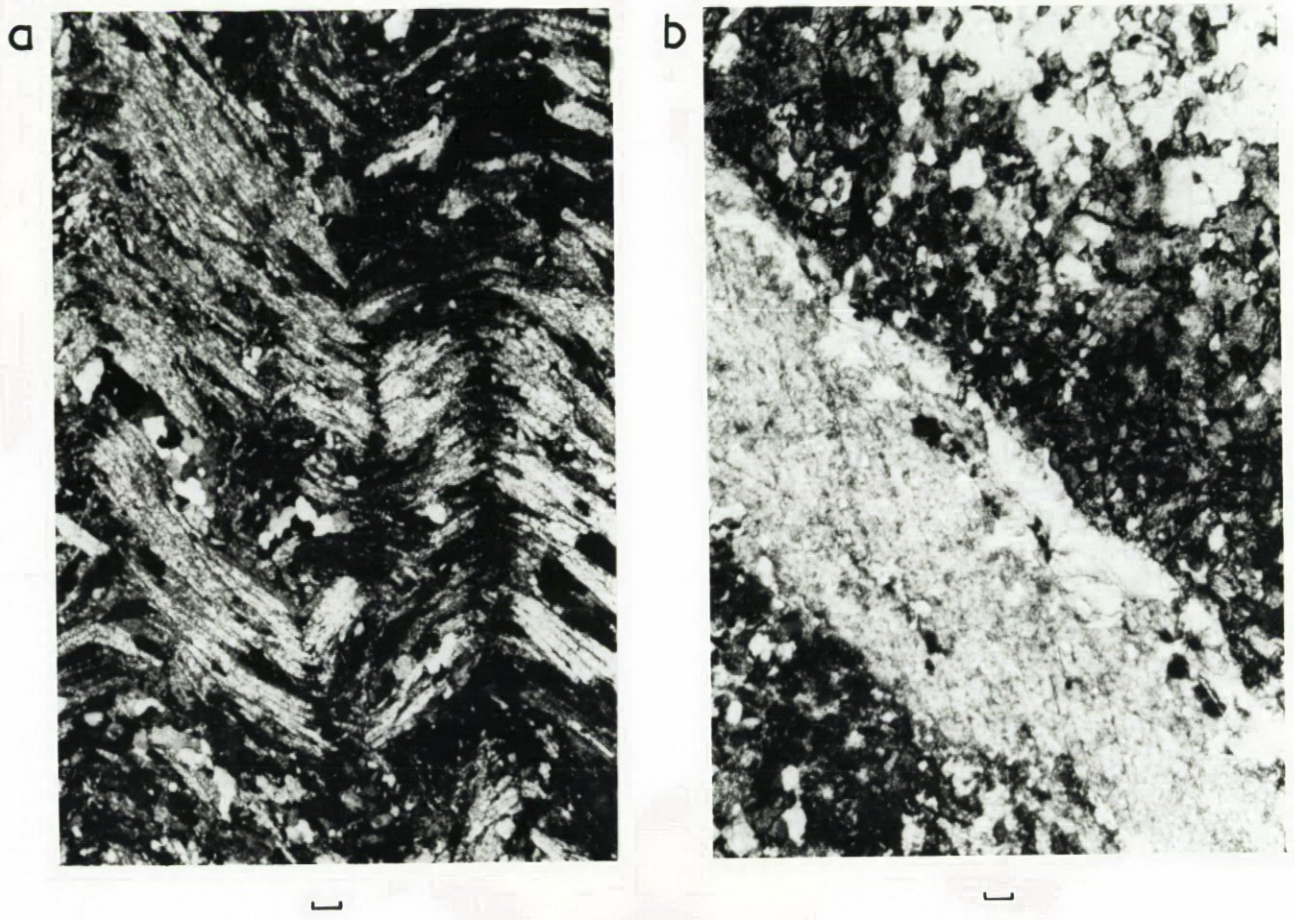
6.6.1 The Fabric

There are two principal categories into which D_4 microstructures fall; crenulations and planar elements.

6.6.1.1 Crenulations

Within the schists D_4 crenulations are manifest as a general flexing of mica lamellae without pronounced recovery or recrystallization (Fig. 6.35a). The crenulations define distinct bands within the rocks, but there is no recovery/recrystallization to form discrete kink band boundaries or straight mica segments as in F_3 crenulations. The rare

FIG. 6.35



segments that do develop are still always flexed.

In the amphibolites because F_4 is always at a relatively high angle to L_2 and ($?L_3$) mineral lineations, F_4 is manifest as crenulations of the long "C" axes of amphibole prisms. By contrast to the flexuring of micas, the amphiboles flex only slightly. Instead, they tend to break up into a few slightly flexed segments. On the short limbs the individual amphiboles are more fractured than on the long limbs, and furthermore there is often incipient quartz feldspar segregation (see below) within them.

D_4 crenulations in the mylonite zone have already been noted (see Fig. 6.32b). Coarser micas (e.g. those that have preferentially formed in F_4 hinges) are mainly flexed but sometimes show incipient recovery to form flexed segments and serrated kink band boundaries. The layered matrix is gently buckled and hinge arcs are mainly rounded.

6.6.1.2 Planar S_4 Elements

S_4 is variously developed according to lithology and intensity of strain and is strongest in the southeast of the study area.

Within the semipelites (and, to a lesser extent, the quartzites), there are two distinct but sometimes related forms. The first form of S_4 is as narrow alteration zones ranging in width from 0.2-5 mm (Fig. 6.35b). They are planar zones of intense retrogression (sericitization of plagioclase, chloritization of biotite, and trails of minute fluid inclusions across quartz) that cut across the rock at an angle to S_{1-2}. They are not sharply bounded and there is

Figure 6.35: (a) F_4 crenulations in pelitic schist. (S_4 vertical). (b) S_4 veinlet infilled with calcite and quartz and accompanied by intense sericitization of the host gneiss adjacent to it (unaltered gneiss in top right corner). Bar scale = 0.1 mm.

generally no obvious displacement across them nor any sign of intense strain within them. However, they are sometimes associated with narrow fracture like veinlets.

These fracture like veinlets are the second form of S_4 and range in width up to 1.5 mm wide. Narrow fractures are lined with opaque mineral(a), but broader veinlets consist of varying proportions of fine to medium grained adularia, calcite, quartz, opaque mineral and scattered relics of the host rock. The S_{1-2} layering can often be traced through them with only minor flexure or displacement.

Within the amphibolites similar veinlets are specifically associated with F_4 crenulations. They are not sharply bounded and are mainly less than 0.5 mm wide. Quartz and feldspar (plagioclase and/or adularia) are the main constituents but can be accompanied by calcite, sphene (often coarser grained than in host), and opaque mineral.

Within dolomites, the most conspicuous S_4 elements are calcite veinlets and dissolution planes. Minor pressure shadow type overgrowths of secondary serpentine, calcite and opaque have been recorded on serpentine nodules but could not be specifically related to D_4 although a related origin is considered most likely. Calcite veinlets are common throughout the area. They are irregularly shaped, crosscut S_{1-2}, and generally consist of coarser calcite than either the host dolomite or calcite.

The most striking effect of D_4 on the dolomites is the production of dissolution planes and an amphibole schist within the Ullabidinie subarea. Dissolution planes axial planar to F_4 warps are narrow, relatively sharply defined fracture like planes or zones that truncate adjacent dolomite grains. The zones range in width up to 1 mm wide and

consist of very fine grained amoeboid calcite with associated fine grained phlogopite, opaque mineral and other accessories. Phlogopite is more abundant in these zones than in the host dolomite. It parallels S_4 whereas S_{1-2} parallel phlogopite adjacent to the zones is often flexed and curved into them suggesting slight displacement of one side relative to the other. Lobate grain boundaries are particularly noticeable in the host dolomite.

As recorded previously (Sect. 4.2.5), the dolomite merges into an amphibole schist adjacent to the Mt. Parapet Lineament (Fig. 4.12). This schist has a very strong S_4 parallel schistosity defined by narrow dissolution planes lined with semi-opaque material, and by a strong preferred alignment of fine to very fine grained tremolite. This S_4 schistosity is oblique to S_{1-2} in the massive dolomite and within it there are scattered, medium grained, porphyroblastic remnants of pre-D_4 tremolite which are randomly oriented and strongly deformed with subsequent subgrains. Amphibole is the principal constituent of the rock (99%) while carbonate is noticeably absent.

Within the Middle Camp granite it was noted that S_4 fractures were particularly prominent near the Mt. Parapet lineament. They are very narrow zones (<0.5 mm) lined mainly with opaque mineral. There is no noticeable displacement across them, but the host rock on either side is substantially affected out to a distance of up to 50 mm. While quartz and feldspar seem to have escaped any effect of D_4 in these zones, biotite has been completely altered into fine grained actinolite. The latter forms accicular radial clusters that penetrate into the adjacent minerals and is responsible for the apparent bleaching of the rock.

6.6.2 Discussion

It is clear that D_4 was neither an intense nor a high grade deformation. The nature of the crenulations within the pelites is quite significant to this point and it fits in well with the first stage of the crenulation model described under the D_2 deformation (Sect. 6.3.2.2). Clearly recrystallization and recovery have not played a major role in the fabric development.

Of all the planar S_4 elements none have produced a pervasive fabric except for the amphibole schist adjacent to the Mt. Parapet lineament. All are restricted in their occurrence but have one feature in common; they are narrow zones along which there has been siginficant modification of the host rock. That modification has been in the form of either partial or complete retrogression of some of the host minerals. In either case it is necessary to add or take away (or both) by means of solution or diffusion certain elements or minerals.

The dissolution planes in the dolomites are the clearest example of this process. The increase in proportions of phlogopite within the dissolution zones and their rotation into parallelism with S_4, can be directly accommodated by the partial loss of carbonate from those zones. This is also believed to be the process behind the formation of the amphibole schist. It has formed immediately adjacent to a zone of high deformation from a dolomite which contained only scattered silicate minerals. Due to preferential solution and removal of the carbonate and no doubt to the introduction of a certain amount of iron and magnesium etc., the dolomite has been converted into a monomineralic amphibole schist. The presence of a quartz pegmatite along the Mt.

Parapet lineament attests to that zone having been a channel-way for migrating or escaping solutions and therefore supporting this model.

It should be recorded here that this model may be significant when considering the origin of gem quality jade (nephrite) north of the study area. That jade occurs as pods within the dolomite and is of retrogressive origin. While it need not necessarily be of D_4 origin, the D_4 model when applied to dolomites which are adjacent to the D_3 associated mylonite zone in that area, could well account for the formation of Cowell jade.

The solution or diffusion controlled model for S_4 dissolution planes in the dolomites can be extended to all S_4 elements. Although there is generally no displacement across S_4 planes or zones, they are all believed to have been formed by diffusion or solution along local heterogeneities set up by D_4 strain. This is obvious in the amphibolites where they are directly associated with F_4 crenulations.

6.7 BRITTLE (post D_4) DEFORMATION

6.7.1 The Fabric

Although exposure of the actual fault breccias is very limited, sufficient specimens were obtained to emphasize their definite cataclastic affinity (c.f. the ductile mylonite deformation). The microstructures are varied in form and four different examples are described. The fourth may not be related to the brittle deformation as there was no other evidence of faulting in its vicinity. Rather it was on the outer arc of a D_3 anticline (in quartzite from Range Rd) and may actually be a D_3 tensional feature. All the

examples however, have one major feature in common; they all have angular fragments of country rock enclosed in a variable matrix.

The first example is from a fault within the deformed zone of the Narridy Creek granite. The breccia consists of angular fragments of the granite gneiss which range in size from very coarse down to very fine. Coarse fragments are angular and frequently fractured with very fine matrix infilling them, finer fragments are mainly single grains of quartz and feldspar which are rounded to well rounded in form, while the matrix is very fine to minute grained and consists of granulated quartz and feldspar accompanied by a red brown semi-opaque material. There is little mica in the matrix and no planar fabric.

In the second example (from Ulgera Gap) angular quartzite fragments are enclosed within a massive dark red-brown semiopaque matrix. Fragments vary in size but in contrast to those above, are strongly elongate in shape such that they define an L-S fabric. This is enhanced by remnants of mica within the matrix, and by thin films of matrix which infill fractures transgressing the fragments. In sections normal to the lineation, the fractures and films of semi-opaque matrix outline a box work fabric.

Thirdly from the Wangaraleednie fault, in addition to patches of breccia like the first described, there are "dykes" of crystalline rock which enclose elongate fragments of very fine grained ultracataclasite resembling the matrix of the Narridy Creek example. Surrounding the fragments is a medium grained crystalline rock consisting of lathes of albite and euhedral crystals of magnetite. Both have been considerably altered subsequent to their crystallization

such that there is now a network of narrow phyllosilicate (yellow-green chlorite) films that cut across the feldspar and magnetite to define an S_5 schistosity. In addition there are also irregular patches of web textured, red-brown, semiopaque mineral. This post D_4 fabric parallels the alignment of the above pre-crystalline fragments.

Finally, the example from Range Rd consists of randomly oriented, angular fragments of quartzite separated by veins of coarsely crystalline quartz. The quartz is very markedly euhedral, there being abundant perfect crystal forms, and it has grown radially out from the quartzite fragments.

6.7.2 Discussion

The Narridy Creek example illustrates a typical cataclasis or brecciation of country rock due to brittle deformation. The fault is narrow and its affects do not spread into the country rock and furthermore country rock fragments within the breccia are also sharply defined with little or no internal strain. There is a progressive breakdown of the coarse angular fragments into fine well rounded fragments and this is analogous to a brittle crushing or milling process. The final product is a very, very fine grained matrix consisting of equant shaped grains derived from the parent mixed in with a considerable amount of iron oxides and other alteration products.

In the Wangaraleednie example, a similar cataclasis has been accompanied by syntectonic intrusion of albite dykes. They have partially anastomosed the breccia enclosing some fragments of it. Subsequent to their crystallization they have been subjected to further deformation which has considerably fractured and altered them. The gross parallelism of early and late deformation is indicated by the parallelism

of each fabric. The origin of the dyke material is not known, but it is postulated that it has come from deeper regions of the fault which have acted either as channelways for diffusion of an albitic phase, or as a heat source for local melting.

CHAPTER VII

METAMORPHISM

7.1 INTRODUCTION

In this chapter the metamorphic evolution is examined in some detail in order to establish what conditions prevailed during the deformation of the gneisses and related rocks.

Although there are a number of ways in which the metamorphic evolution of an area can be studied, the approach adopted here utilizes the microstructural fabric as a "datum". That is, the relationship between the mineral parageneses and the various fabric elements is used to relate a particular paragenesis to a specific metamorphic/structural event. Such an approach has been used successfully by many petrologists to unravell the metamorphic history of complex gneiss terrains (e.g. Zwart, 1963; Tobisch et al, 1970; Cooper, 1974; Ayrton and Ramsay, 1974; Rutland and Etheridge, 1975), although it does have some shortcomings.

Some of the criticisms levelled at this approach have questioned its validity in terrains where there is considerable heterogeneity. No doubt there will always be problems relating to the existence of metastable relics of previous phases, to pseudomorphous replacements of early formed minerals, or to diachronous deformation and metamorphism, but no other method (e.g. using xenoliths within undeformed granites: Toogood, 1976) offers a more comprehensive resolution of the metamorphism. Indeed, the problems of diachronous metamorphism and deformation (or granite intrusion, etc.) over large areas are inherent in any approach. They are in fact part of the overall story and MacQueen and

Powell (1977) and Chadwick (1968) clearly illustrated this in examples where, over large areas, there was diachronism between deformation and metamorphism. Their examples were based on a fabric/mineral paragenesis "datum" (e.g. zoning and inclusion trails in garnets) and they convincingly showed that the deformation and metamorphic "fronts" migrated relative to each order.

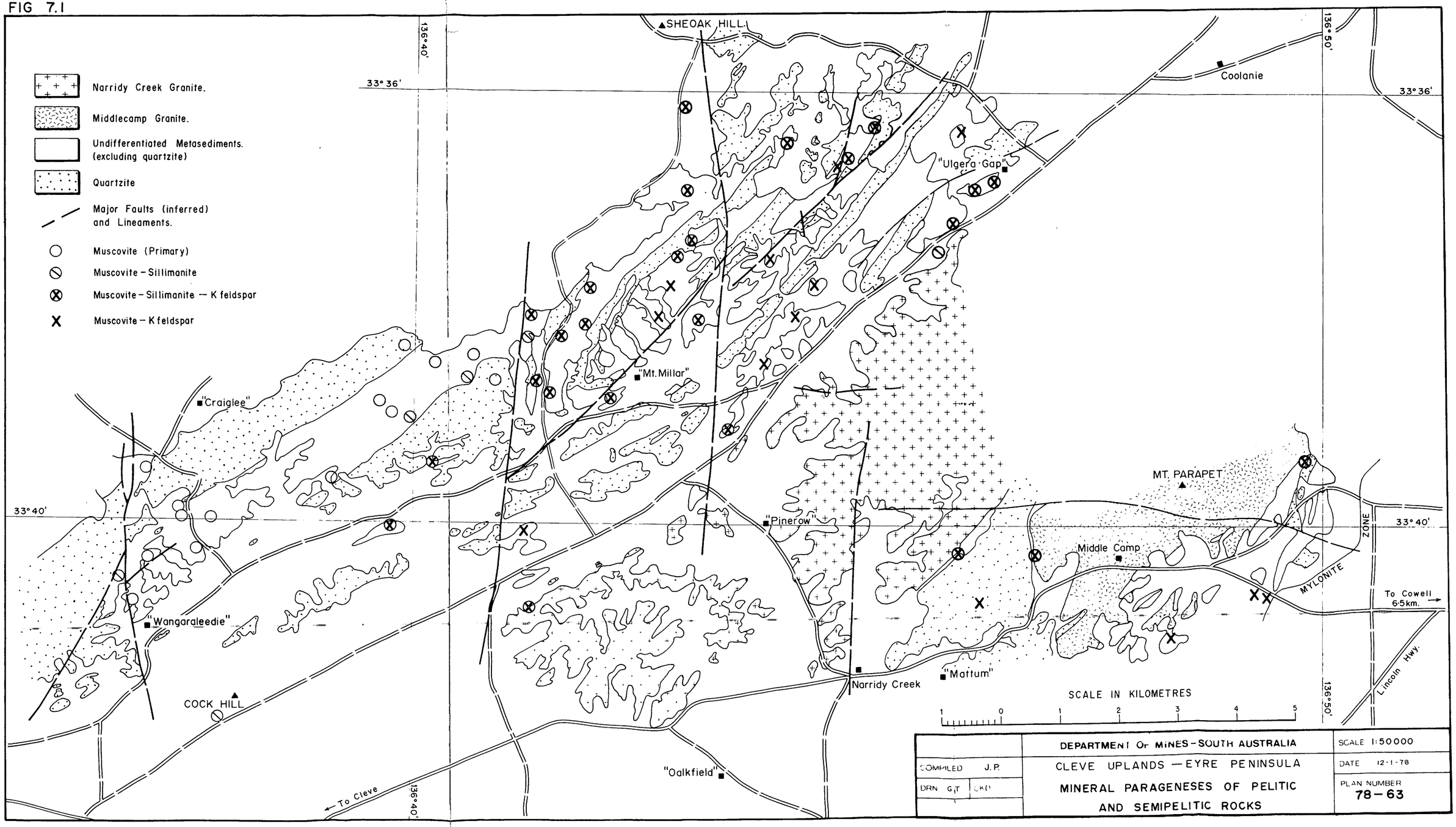
The principal criticism of a fabric "datum" approach however, is its subjectiveness. Neccessarily, because it is based upon the petrologists's interpretation of the fabric, there is an unavoidable subjectivity inherent in relating a particular fabric/mineral paragenesis in one area to that in another. In this study there is a good continuity of structure (see previous chapters) between subareas and furthermore the size of the area is not so large as to expect any major diachronism.

Finally, this study of the metamorphism is based mainly on field and petrological observations with only a very limited number of whole rock analyses. Consequently it has not been possible to make a complete appraisal of the metamorphism.

7.2 OUTLINE OF METAMORPHIC EVOLUTION

Using the microstructural fabric as a "datum", a sequence of metamorphic events is outlined corresponding to the deformational episodes. They are

FIG 7.1


Narridy Creek Granite.
Middlecamp Granite.
Undifferentiated Metasediments. (excluding quartzite)
Quartzite
Major Faults (inferred) and Lineaments.
Muscovite (Primary)
Muscovite – Sillimanite
Muscovite – Sillimanite — K feldspar
Muscovite – K feldspar
▲SHEOAK HILL
136°40'
136°50'
33°36'
Coolanie
"Ulgera Gap"
"Mt. Millar"
"Craiglee"
33°40'
"Pinerow"
MT. PARAPET
Middle Camp
ZONE
MYLONITE
To Cowell 6.5km.
"Wangaraleedie"
COCK HILL
Narridy Creek
"Mattum"
L.incoln Hwy.
SCALE IN KILOMETRES
1 0 1 2 3 4 5
"Oalkfield"
To Cleve
DEPARTMENT OF MINES – SOUTH AUSTRALIA
SCALE 1:50000
COMPILED J.P.
DRN G.T CKD
CLEVE UPLANDS — EYRE PENINSULA
MINERAL PARAGENESES OF PELITIC AND SEMIPELITIC ROCKS
DATE 12-1-78
PLAN NUMBER 78-63

Remarks	Deformation	Metamorphism
local recovery but rare new grain growth	D_4	M_4
local recrystallization/ new grain growth	D_3	M_3
widespread recrystallization/ new grain growth	D_2	M_2
migmatization	D_1	M_1 M_{1-2}
burial metamorphism?	pre D_1	$M_?$

The M_1 and M_2 metamorphic events are very difficult to separate due to intense recrystallization during D_2 and the problem of identification of the fabric without clear overprinting criteria (i.e. the normal S_{1-2} situation). Consequently these two events will be described together (M_{1-2}) but with particular reference to the separate events when such can be determined.

The superimposed metamorphic events, M_3 and M_4, are both retrograde in nature and their imprints are restricted mainly to areas of significant recrystallization such as the mylonite zone and the Mt. Parapet lineament.

7.3 M_{1-2} METAMORPHISM

7.3.1 Summary of Mineral Parageneses

The fundamental M_{1-2} mineral assemblages of the metasediments as outlined in Chapters II and VI are listed below in two categories defined by the migmatite and non-migmatite zones (Fig. 2.2). The distribution of key pelitic and semipelitic mineral assemblages is shown opposite in Figure 7.1.

A) MIGMATITE ZONE

Psammite

1. quartz-microcline-biotite-muscovite-sillimanite (- plagioclase)

2. quartz-bytownite-diopside-microcline-calcite (- tremolite)

Semi-pelite

3. quartz-orthoclase/microcline-oligoclase-biotite-sillimanite (-garnet-muscovite)

Pelite

4. quartz-orthoclase/microcline-biotite-sillimanite-(oligoclase-garnet-muscovite)

Carbonate

5. dolomite

6. dolomite-calcite-forsterite/serpentine

7. dolomite-calcite-forsterite-diopside (-tremolite)

7^{i}. calcite-forsterite/serpentine-diopside

7^{ii}. calcite-diopside-tremolite

8. bytownite/labradorite-diopside-calcite (-quartz-microcline-tremolite)

Metabasite

9. hornblende-andesine/labradorite

10. hornblende-plagioclase-diopside

11. hornblende-andesine-biotite

Eulysite

12. grunerite-garnet-(quartz)

13. hypersthene-garnet (-quartz-grunerite)

14. grunerite-actinolite/hornblende-quartz (-garnet-biotite)

15. diopside-quartz (-tremolite-calcite)

B) NON-MIGMATITE ZONE

Psammite

assemblages 1. and 2.

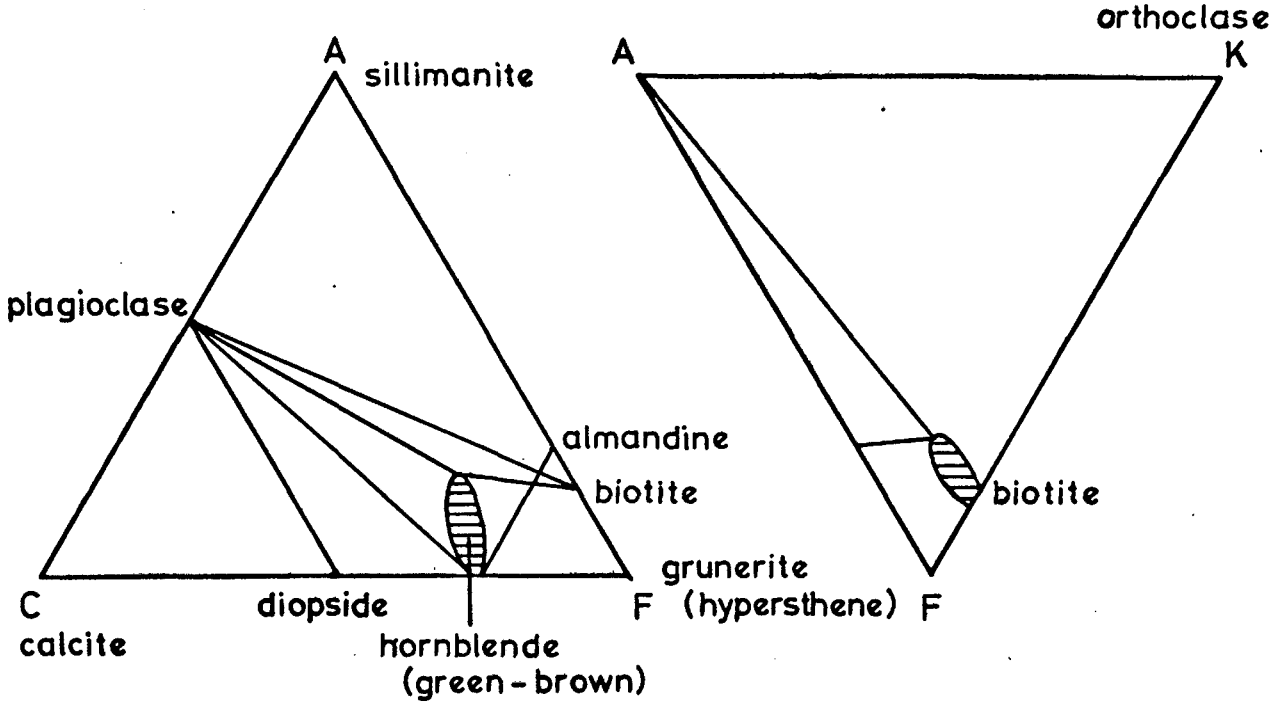
Semi-pelite

16. quartz-oligoclase-biotite-muscovite (-garnet)

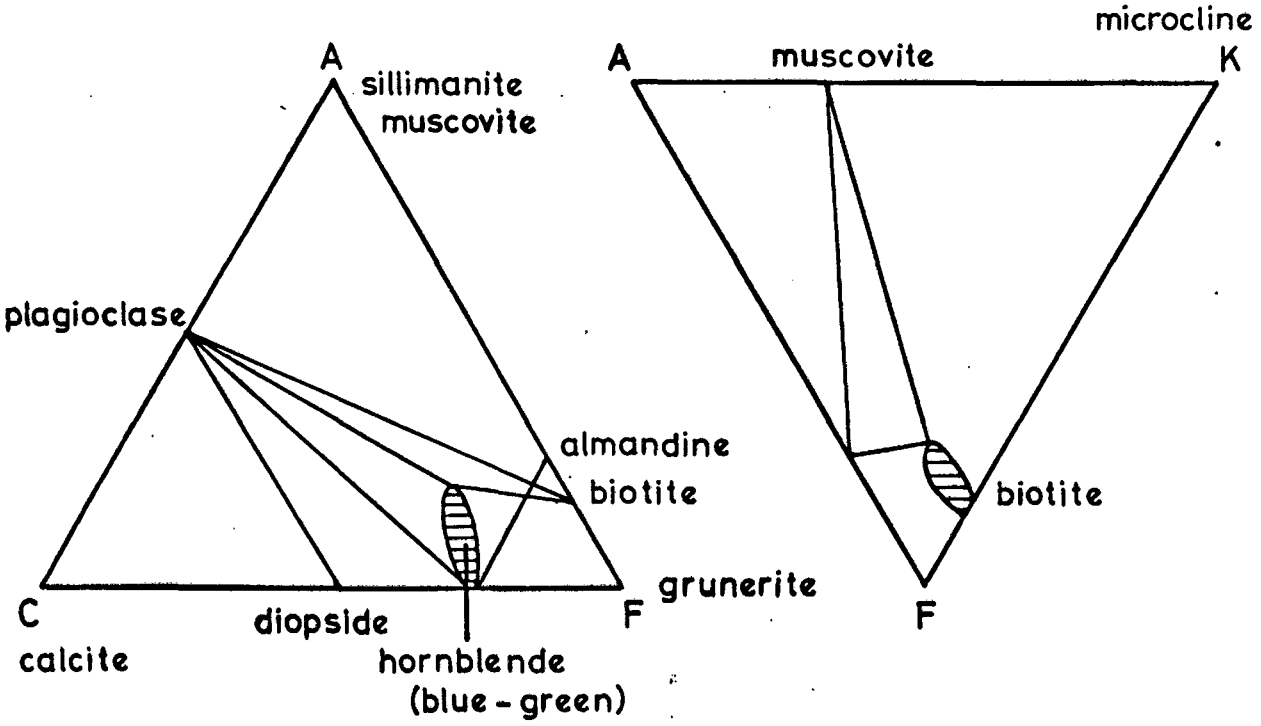
FIG. 7.2

ACF and AKF DIAGRAMS for M_{1-2}

MIGMATITE ZONE



NON MIGMATITE ZONE



17. quartz-oligoclase-biotite-muscovite-microcline (-sillimanite)

Pelite

18. muscovite-biotite-quartz (-oligoclase-garnet)

Carbonate

assemblages 5, 7^{ii}, and

19. dolomite-phlogopite (-quartz)

20. dolomite-diopside (-quartz) N.B. reacting to form 7^{ii}.

21. diopside-tremolite-quartz (-calcite)

Metabasite

assemblages 9, 10 and 11

Eulysite

assemblage 14

The complete parageneses of the migmatite and the non-migmatite zones are summarized in the ACF and AKF diagrams of Figure 7.2. These diagrams have been constructed from the mineral associations listed above using average rock and mineral compositions defined by Poldevaat (1955), but with the aid of geochemical data included in Appendix A. SiO_2 - CaO - MgO phase diagrams for siliceous carbonates within the two zones are shown later in Figure 7.6.

7.3.2 Discussion

7.3.2.1 Evidence for two separate events, M_1 and M_2.

On the basis of overprinting relationships established in the previous "Microstructure" chapter, there is clearly strong evidence supporting two high grade metamorphic events, M_1 (pre D_2) and M_2 (syn D_2). Although complete mineral parageneses for each of these events could not be established, those minerals that could be specifically related to either M_1 or M_2 in pelitic and semipelitic rocks are tabled below.

	Migmatite zone	Non-migmatite zone
M_1	sillimanite	minor sillimanite
	garnet	garnet
	microcline/orthoclase	minor microcline (in semi-pelites and quartzites only)
	biotite	biotite
	embayed muscovite relics	muscovite
M_2	sillimanite	minor sillimanite
	garnet	garnet
	orthoclase (minor)	biotite
	biotite	muscovite
	muscovite (minor)	

The most important fact though is the timing of the widespread migmatite formation.

The concept of zonation of the metasediments into two regions with a transitional zone between them, is a simplified model representing a progressively increasing grade of metamorphism. This progression is dominated,

a) by the initiation of apparent melting of the semi-pelites
b) by the breakdown of muscovite in the presence of quartz within pelitic and semipelitic rocks,
c) by the widespread formation of sillimanite, and
d) by the progressive mineralogical changes in the carbonate rocks.

It is supplemented by incipient breakdown of grunerite within eulysites of the central migmatite zone, by the absence of staurolite and cordierite in pelitic rocks, by the absence of $Al_2 SiO_5$ polymorphs other than sillimanite,

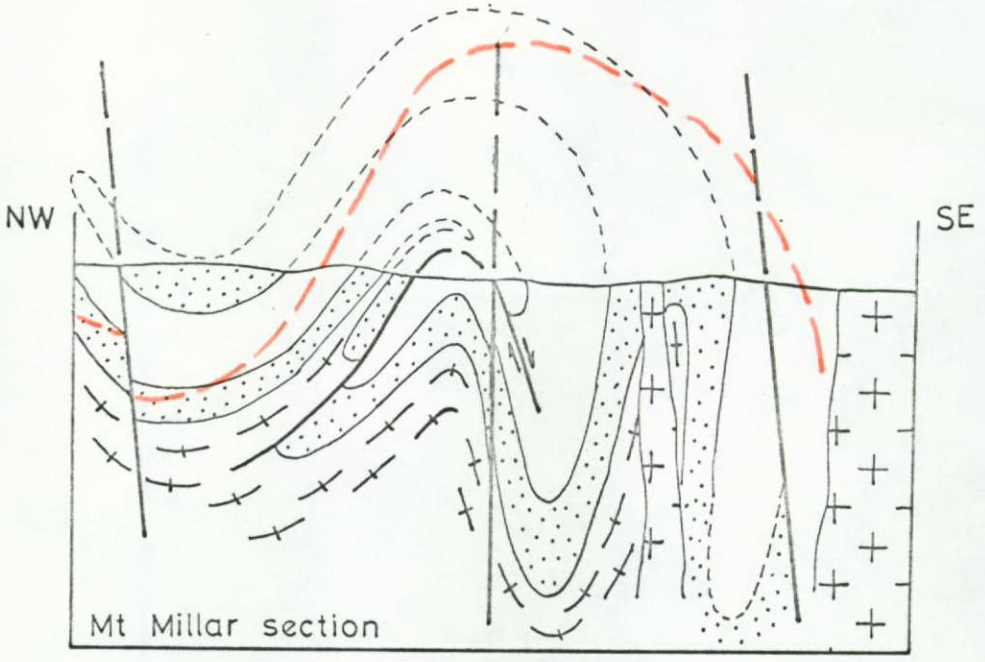
by the systematic variation of biotite colour; that is, in the non-migmatite zone biotites are dark brown in colour whereas in the migmatite zone they are red-brown in colour; and by the systematic colour variation of hornblende (see below). While the last five of these could not be specifically associated with either M_1 or M_2 , the first four features, a) to d), are believed to represent the M_1 event. There are several reasons for this.

On both mesoscopic and microscopic scales, quartzo feldspathic segregations which have been identified as the principal feature of the migmatization, have been clearly deformed during D_2 (e.g. see Fig. 3.2 and Fig. 6.4). Likewise in the non-migmatite zone quartz veins have been also clearly deformed during D_2 hence there is good evidence on this scale for an M_1 origin for both the quartzo feldspathic segregations and the quartz veins. The widespread production of sillimanite is also believed to be pre D_2 in origin. As was clearly illustrated in Chapter VI (Figs. 6.2 and 6.6), much of the sillimanite was deformed during D_2 to produce flattened pods within the S_2 fabric and overprinted by a second, less prominent S_2 parallel sillimanite preferred orientation. Such was also the case with garnet and K-feldspar and in fact, within the pelitic and semipelitic rocks, D_2 was characterized by widespread recrystallization of pre-existing assemblages rather than widespread crystalli-zation of new mineral associations. Therefore, it is concluded that at least on a mesoscopic and microscopic scale, the principal event was M_1.

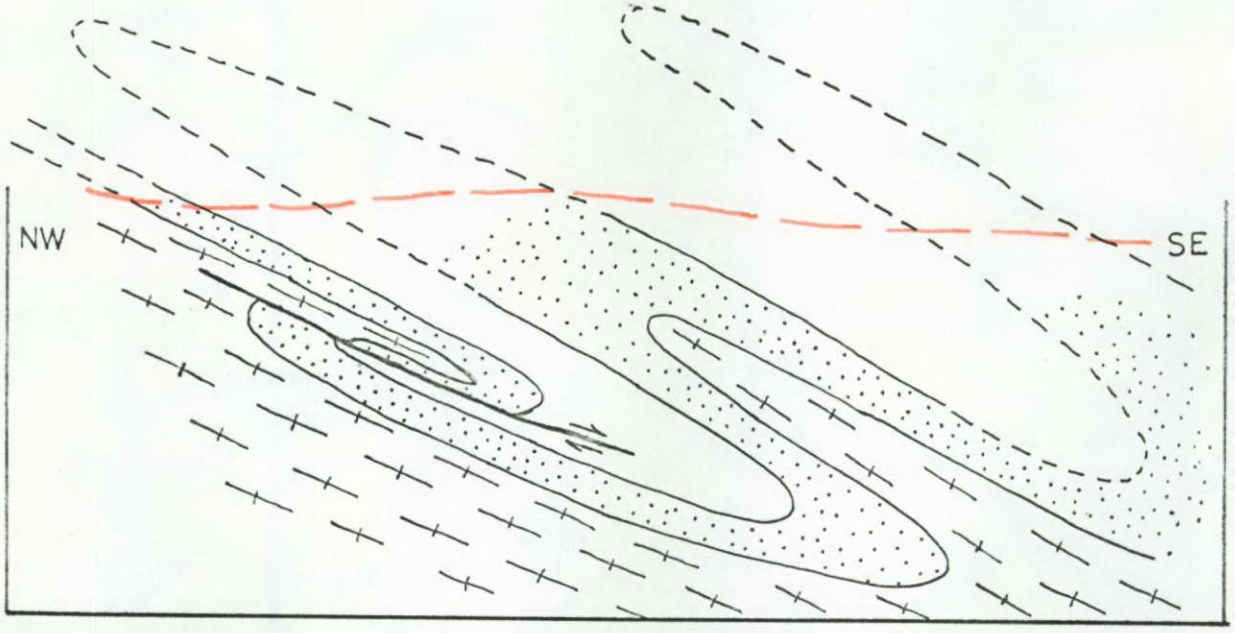
On a macroscopic scale, however, this is not so clearly supported. In Figure 2.2 the broad distribution of migmatized rocks was illustrated. If that distribution is

FIG. 7.3

The Migmatite Zone in Relationship to Macroscopic Folding



A) the infered position of the migmatite "front" (c.f. Fig. 5.11).



B) the inferred position of the migmatite "front" after removing the effects of the D_3 deformation.

compared with the interpretative structural cross-sections derived in Figure 5.11 and reproduced in Figure 7.3, it can be seen that the simplest model when unfolded (i.e. when the F_3 folds are removed), infers an M_2 (or even post D_2) origin for the widespread migmatization. For an exclusively M_1 origin (i.e. pre D_2) one would expect the migmatite "front" to have been deformed by F_2 folds.

This problem could not be resolved within the scope of this thesis. The map showing the distribution of iso-grads and migmatization is the simplest interpretation based on the available outcrop. It is conceivable however that the front is actually much more complex both on the map and on Figure 7.3. Even so the general trend of the front is clearly across the stratigraphic succession and the axial trace of the macroscopic F_2 folds. This may mean that while the principal migmatization may have been an M_1 feature there was continued advance of the "front" during M_2. Therefore, near the isograd the e.g. K-feldspar-sillimanite assemblage would be exclusively M_2 whereas away from the isograd it would be recrystallized M_1.

7.3.2.2 Pelitic and semipelitic parageneses

ORIGIN OF QUARTZO-FELDSPATHIC SEGREGATIONS - There are four main modes of origin that have been postulated for migmatite formation (for a discussion, see Mehnert, 1968). They are,

1) in situ crystallization of the original (S_o) banding,
2) lit-par-lit injection of a granitic magma,
3) partial melting (anatexis), and
4) metasomatism.

Since the quartzo feldspathic layers are not composi-

tionally comparable with any layers in equivalent non-migmatized gneisses the first of these is rejected. Secondly, the introduction of substantial amounts of granitic magma is also untenable because for one, the bulk compositions of equivalent migmatized and non-migmatized rocks are broadly compatible (see Appendix A and later this discussion), and for another, there are no obvious "feeders" to the majority of pegmatitic segregations many of which are simple lensoid bodies.

Therefore it is believed that either the third or fourth mode of origin was responsible for the segregation of quartz and feldspar. Macroscopic metasomatism is not inferred for the same reasons against the magmatic injection model, but micro or mesoscopic metasomatism cannot be disproven. However the nature of the segregations suggests an anatectic origin and this is supported by the composition of the segregations which approximates to a melt, and by the coarse accessories such as apatite which are only very fine grained outside them.

BREAKDOWN OF MUSCOVITE - As in many medium to high grade areas throughout the world, the breakdown reactions of muscovite,

1. muscovite + quartz → orthoclase + sillimanite + H_2O
2. muscovite + quartz + plagioclase → orthoclase + sillimanite + more clacic plagioclase + H_2O

are of fundamental importance in this study. In unmigmatized rocks muscovite is ubiquitous and sillimanite is of restricted occurrence being mainly confined within coarse megacrysts of muscovite. However, with the first signs of migmatization, viz. the first appearance of prominent pegmatitic segregations in semi-pelitic rocks, sillimanite appears as clusters of

FIGURE 7.4

COMPARATIVE SUMMARY OF NON-MIGMATITIC AND MIGMATITIC SEMI-PELITES

	Non-Migmatites	Migmatites
TEXTURES	granoblastic sub-polygonal equigranular	granoblastic interlobate inequigranular
Grainsize	fine 0.1-0.2 mm	medium 0.2-2.0 mm
Pegmatitic Segregations	no	yes
MODES		
Quartz	45%	40%
Plagioclase	20%	15%
K-feldspar	5%	40%
Biotite	15%	15%
Muscovite	20%	2%
Almandine	1%	1%
Sillimanite	trace	2%
MINERALOGY		
Plagioclase	An_{20-25}	An_{20-30}
K-feldspar	microcline	perthitic microline/ orthoclase
Biotite	brown	red-brown
Muscovite	idioblastic	embayed when present

needles within biotite layers.

This situation is one that has parallels in migmatite terrains throughout the world. In North America there are analogies in southeastern British Columbia, the Canadian Shield and in particular in the northwest Adirondack Mountains of Vermont and New Hampshire where Engel and Engel (1958) noted that sympathetically with the disappearance of muscovite,

> "...the average plagioclase becomes more calcic, biotite changes from greenish brown through successive shades of brown, reddish brown to deep red brown, quartz content decreases, grain size increases and segregational banding appears in the gneiss."

All these observations are consistent with the transition observed in this study and outlined in Figure 7.4. Furthermore, the importance of sillimanite and orthoclase is also brought out by analogy with rocks from the Scottish Caledonides. Here Chinner (1966) noted,

> "the close correspondence between the areas occupied respectively by sillimanite-bearing, gneissic (i.e. migmatitic), and potassium-feldspar-bearing rocks'

he suggested that,

> "the formation of the three was approximately synchronous and resulted from the same cause."

The cause as detailed by Chinner in this case, was the combined effect of the reaction muscovite + quartz (probably in the presence of plagioclase) and the partial melting of the gneisses. However, whilst he considered these processes as synchronous (i.e. in time) Chinner was able to define zones where melting was initiated prior to the breakdown of muscovite and zones where muscovite was completely absent

(i.e. the sillimanite-orthoclase zone).

In the Cowell/Cleve area the transition from non-migmatites to migmatites is paralleled by the breakdown of muscovite. Within the transitional zone muscovite-quartz co-exists with both sillimanite-potassium feldspar and pegmatitic segregations. It is therefore inferred that the two processes - the breakdown of muscovite and the initial melting - were approximately concomitant in both time and space.

Winkler (1967) examined this situation in his discussion on anatexis and points out that the melting behaviour of rocks containing muscovite and not potassium feldspar is very similar to "normal" rocks composed of quartz-potassium feldspar-plagioclase. He points out that in place of equation 1 above, another reaction of the form:

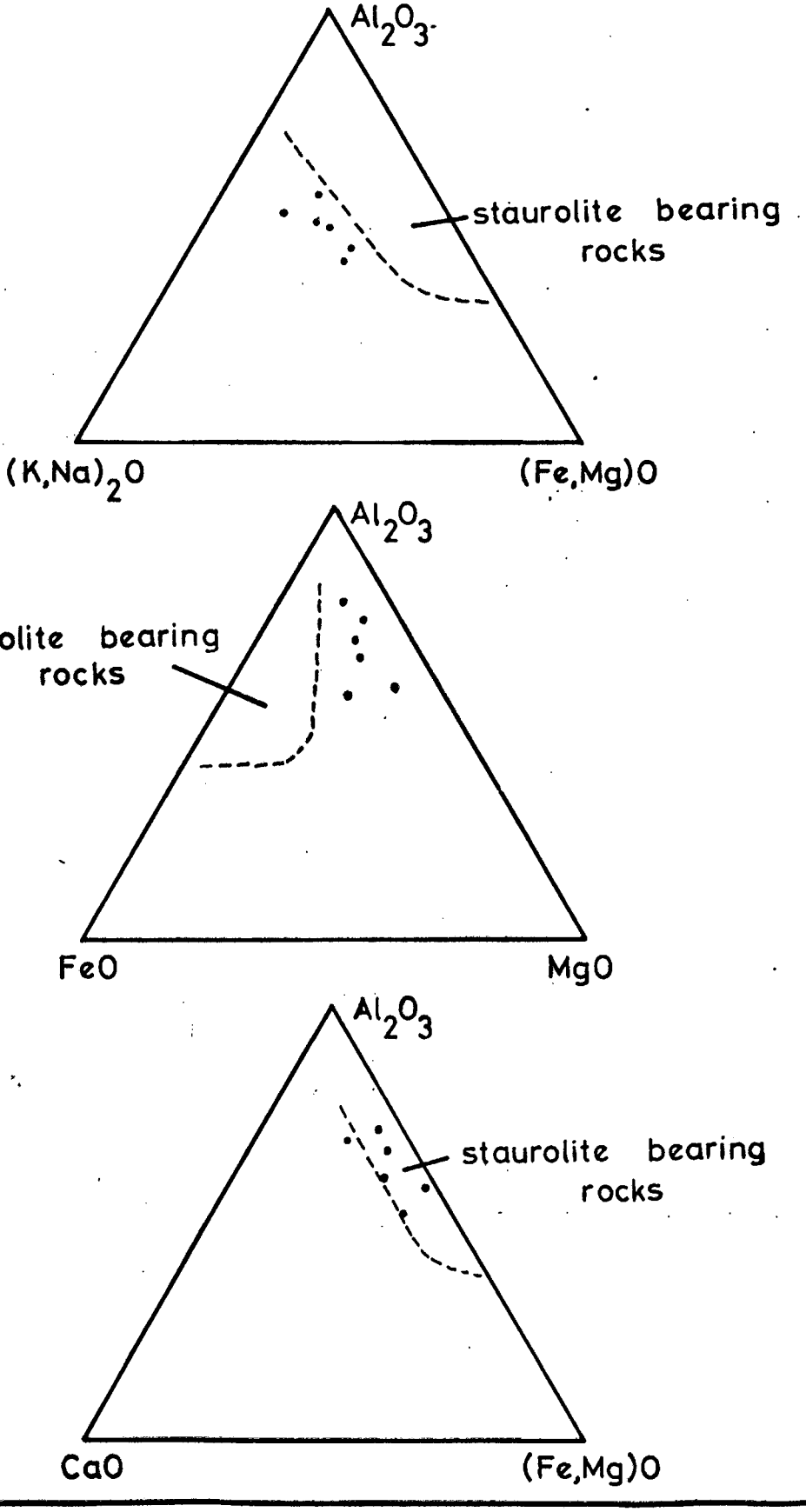
3. muscovite + quartz + plagioclase → K-feldspar-plagioclase-quartz components in the melt + more calcic plagioclase + sillimanite + H_2O

can be written which is probably more applicable. In fact this reaction accounts for observations made in this study area, namely that pegmatitic segregations are composed mainly of potassium feldspar and quartz with lesser amounts of plagioclase, and that the sillimanite is associated with biotite and plagioclase (slightly more clacic) in the residual part of the rock. Carmichael (1969) ascribes this common occurrence of sillimanite with biotite to the relative immobility of aluminium with respect to the other components such as silica, sodium and potassium. As is observed in non-migmatized rocks, muscovite, which would be the source of aluminium, is closely allied with biotite in mica rich layers. With muscovite reacting according to equation 3 and

FIG. 7.5

CHEMICAL RESTRICTIONS on ROCKS CONTAINING STAUROLITE

after Hoschek (1967)



producing a melt, this would then leave behind aluminium to form the observed sillimanite.

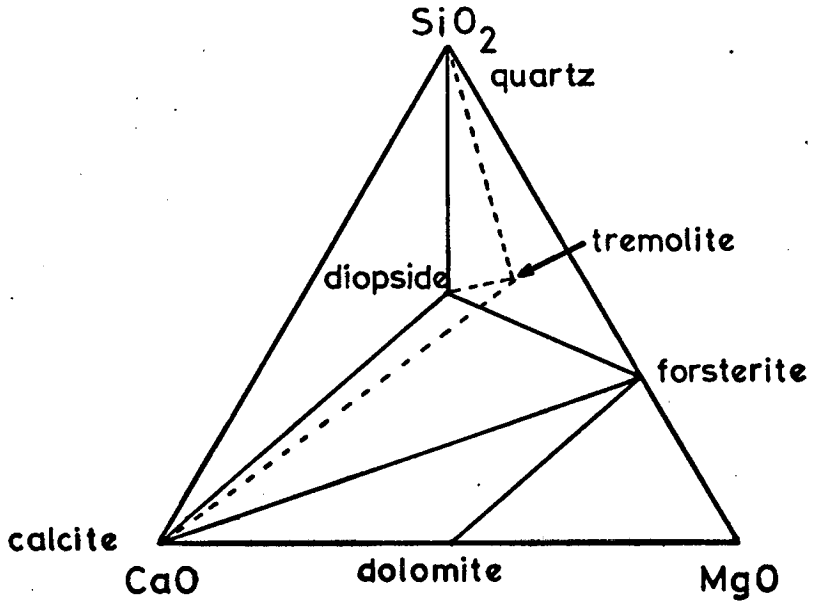
Reaction 3 as written infers substantial changes to the overall mineralogy, so it is useful to compare modal compositions of the semi-pelites before and subsequent to its effect. The modal compositions were detailed in Figure 2.3 and outlined in Figure 7.4. They infer appreciable loss of muscovite, quartz and some plagioclase, and appreciable gain of potassium feldspar and sillimanite. Except for perhaps plagioclase, this is exactly what reactions 1 to 3 would predict. Plagioclase according to reactions 2 and 3 should not decrease appreciably but rather, become more calcic. It was observed that there may indeed be a very slight increase in the An content of the residual plagioclase in the migmatites and furthermore it is believed that the plagioclase decrease is only superficial because much if not all of it can be accounted for by the perthitic veinlets and stringers in K-feldspar.

STAUROLITE AND CORDIERITE - It is useful to consider these two minerals and the significance of their absence from the study area. In most metamorphic terrains, staurolite is generally of limited occurrence being restricted to rocks with specific Mg/(Fe+Mg) ratios (Winkler, 1976). Therefore to test if there were rocks of suitable composition in the study area, a brief breakdown of several whole rock analyses was made along the lines suggested by Hoschek (1967; see also Winkler, 1976). Hoschek defined broad compositional fields for those rocks with or without staurolite. While they are only a qualitative guide the results shown in Figure 7.5 imply that most of the pelitic and semi-pelitic rocks lie outside that field for which staurolite

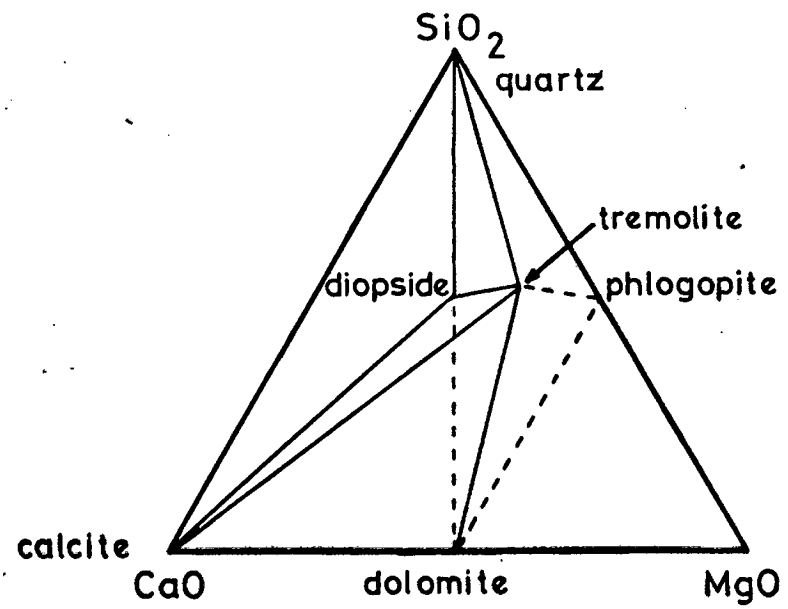
FIG. 7.6

M_{1-2} CARBONATE PARAGENESES

MIGMATITE ZONE



NON MIGMATITE ZONE



should be expected. Consequently it is believed that the absence of staurolite is primarily a result of unsuitable rock compositions and does not necessarily mean that the metamorphic conditions were above or below its stability field.

Cordierite has not been recorded in the area under discussion, although it has been noted in gneisses and amphibolites recovered from drilling 9 km northeast of Mt. Parapet (SADM Rept. No. NPNC 77/59). Its absence and the prominence of almandine garnet are significant and their relevance is discussed by Currie (1971, 1974), Hensen and Green (1971) and Winkler (1976). They examined the reaction,

4. 3 cordierite → 2 garnet + 4 sillimanite + 5 quartz

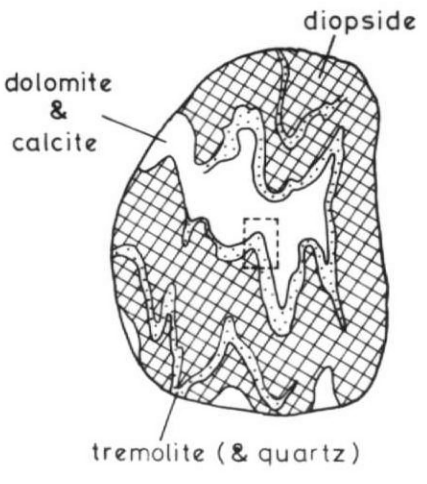
at various temperatures, pressures and Fe/(Fe+Mg) ratios and were able to define specific T-P fields in which either cordierite, garnet or both existed at certain Fe/(Fe+Mg) ratios of the initial rock. The resultant fields were essentially independent of temperature but sensitive to pressure changes - at moderate to high pressures almandine only is stable, at moderate pressures almandine and cordierite coexist, and at low pressures cordierite only exists. Consequently, since cordierite is absent and almandine is abundant within the study area, there appears to be a prima facie case for the regional pressures in that area to have surpassed those in which cordierite is stable. This of course, supposes that the bulk rock compositions were suitable for the formation of cordierite.

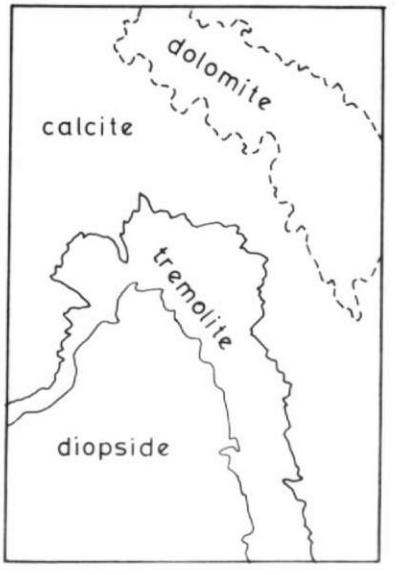
7.3.2.3 Carbonate Parageneses

The M_{1-2} carbonate parageneses of the Cowell area are graphically represented in Figure 7.6. Insufficient work and lack of suitable rocks (particularly in the non-migmatite

FIG. 7.7




diopside
dolomite
&
calcite
tremolite (& quartz)


dolomite
calcite
tremolite
diopside

areas) has prohibited complete parageneses to be reconstructed, but some important mineralogical changes are evident.

NON-MIGMATITE ZONE

Within the non-migmatized rocks, the carbonates are represented mainly by relatively pure dolomites sometimes with phlogopite and sometimes with calc-silicates. Of the latter, a unique dolomite-calcite-tremolite-diopside association has been recorded (Fig. 7.7) which is important in the understanding of the carbonate paragenesis. In this example, successive bands of diopside, tremolite, calcite and dolomite have been folded by F_3 folds and the textures suggest that an original dolomite-diopside assemblage has been partially replaced by tremolite and calcite; that is, it suggests a reaction of the form.

5. Tremolite + 3 calcite → dolomite + 4 diopside + CO_2 + H_2O

but in direction from right to left.

By analogy with standard texts (Turner 1968, Winkler, 1967; Miyashiro, 1973) this is a retrogressive reaction. However, in recent literature (Skippen, 1974; Slaughter et al, 1975) equilibria relationships have been established by experimental and thermodynamic principles which account for the observed relationships by either a slight increase in the total fluid pressure or by a decrease in X_{CO_2} at constant temperature (Fig. 7.8; N.B. the low X_{CO_2} stability field for dolomite diopside is not considered here because

---

Figure 7.7 : (a) zonation of diopside, tremolite, calcite and dolomite in calcsilicate bands from the Wangavaleednie subarea. (b) key to minerals in (a). (c) location of (a) and (b) with respect to mesoscopic layering and F_3 folds (S_3 vertical). Bar scale = 1 mm.

it is based on disequilibrium assemblages in partly retrogressed rocks, A.C. Purvis, pers. comm.).

MIGMATITE ZONE (including Plug Range Subarea)

Parallel to the outgoing of muscovite and incoming of sillimanite-orthoclase in pelites, carbonate rocks display a progression from rocks devoid of forsterite to rocks with prominent forsterite. Although the forsterite is now almost completely hydrated to serpentine pseudomorphs, its original dominance is manifest by scattered, embayed relics enclosed within the serpentine.

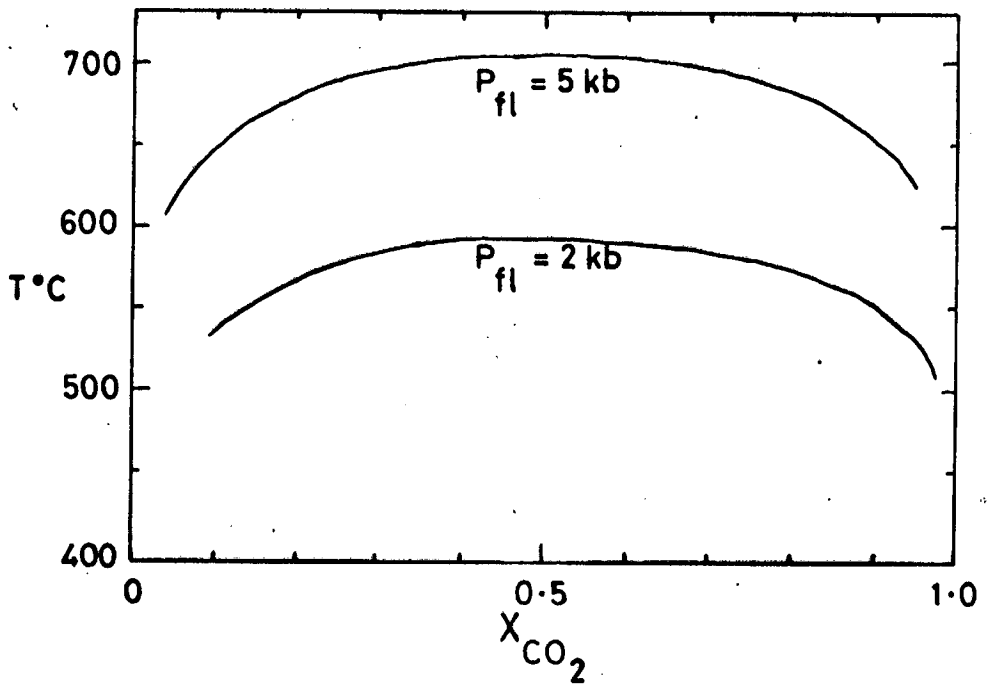
Within the main zone of migmatites, the prominent M_{1-2} siliceous carbonate assemblages are forsterite-calcite-dolomite and diopside-tremolite-calcite. In addition there is a third important assemblage of dolomite-calcite-forsterite-diopside which is restricted to carbonates from the Plug Range subarea.

Considering the prograde progression from non-migmatite assemblages to those of the migmatite zone there are many different reactions which can account for the incoming of forsterite (Glassley (1975) outlined twelve for example). However, only four principal reactions are considered. They are:

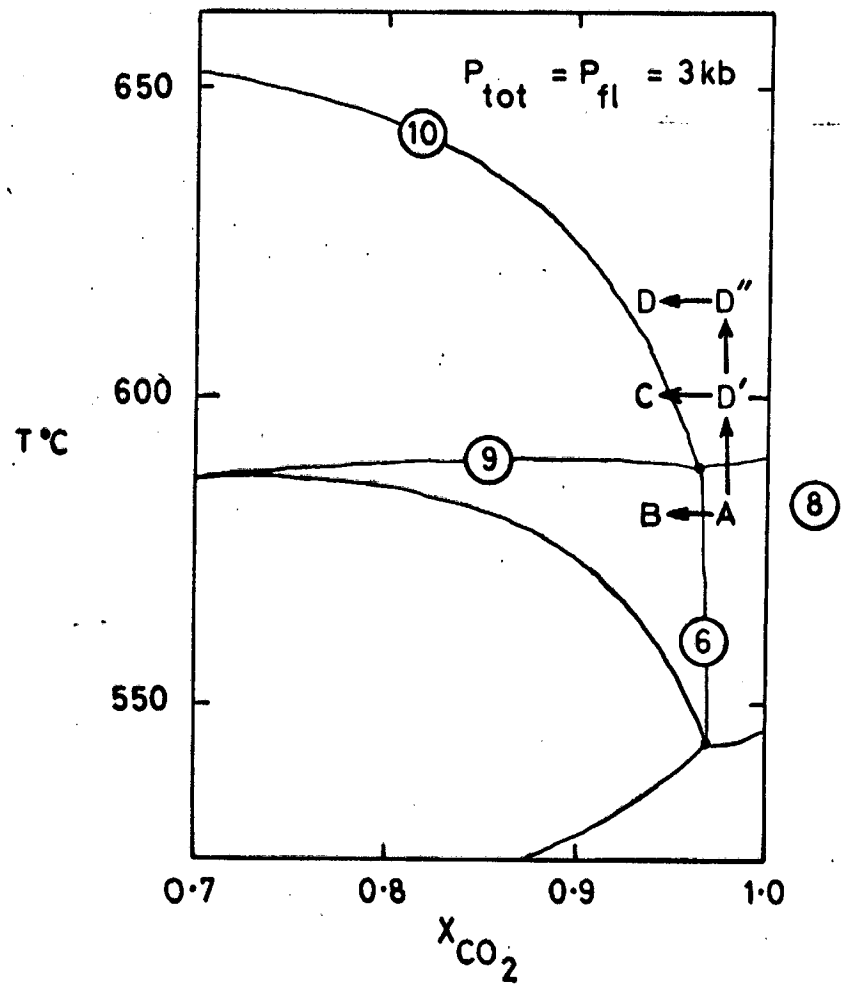
7. 2 phlogopite + 7 dolomite → 6 forsterite + 7 calcite + spinel + vapour (7 CO_2, H_2O, K_2O, 2F)
8. diopside + 3 dolomite → 4 calcite + 2 forsterite + CO_2
9. tremolite + 11 dolomite → 8 forsterite + 13 calcite + $9CO_2+H_2O$
10. 3 tremolite + 5 calcite → 11 diopside + 2 forsterite + $5CO_2+3H_2O$

In all three reactions (7) to (9) calcite is consequential

FIG. 7.8



A) $T-X_{CO_2}$ topology for reaction (6) after Slaughter et al(1975).



B) $T-X_{CO_2}$ topology for reactions (6) to (10) after Skippen(1974).

to the formation of forsterite, which accounts for the common observation of alternating dolomite and calcite-forsterite bands (see also Tilley, 1920a).

In order to evaluate the effect and relevance of each of these, once again the recent work of Skippen is invaluable. He calculated equilibrium curves for reactions (8) to (10) at various fluid compositions, pressures and temperatures. The results are significant because they demonstrate firstly, that equations (8) and (9) occur at approximately the same temperature and secondly, that reaction (10), although its limits of uncertainty overlap those of reaction (9), generally takes place at higher temperatures. Reaction (7) according to Glassley (op. cit.) also takes place at equivalent temperatures to reactions (8) and (9).

Consequently the production of the observed carbonate parageneses in the migmatites involves two specific reaction paths, depending on the initial assemblage. For example, if the initial assemblage was dolomite-diopside, then it would react according to reaction (8) to produce forsterite and calcite but, alternatively, if the initial assemblage was tremolite-calcite-dolomite, then it would react according to reaction (9) to produce forsterite and calcite. Looking at an appropriate phase diagram adopted from Skippen's work (Fig. 7.8b) these two reaction paths are represented respectively by the transition from A to D' and B to C. Reaction A to D' however does not account for tremolite in the final product so an additional reaction, reaction (10) from right to left, is required to produce the assemblage C which is the observed assemblage in dolomites from the migmatite zone.

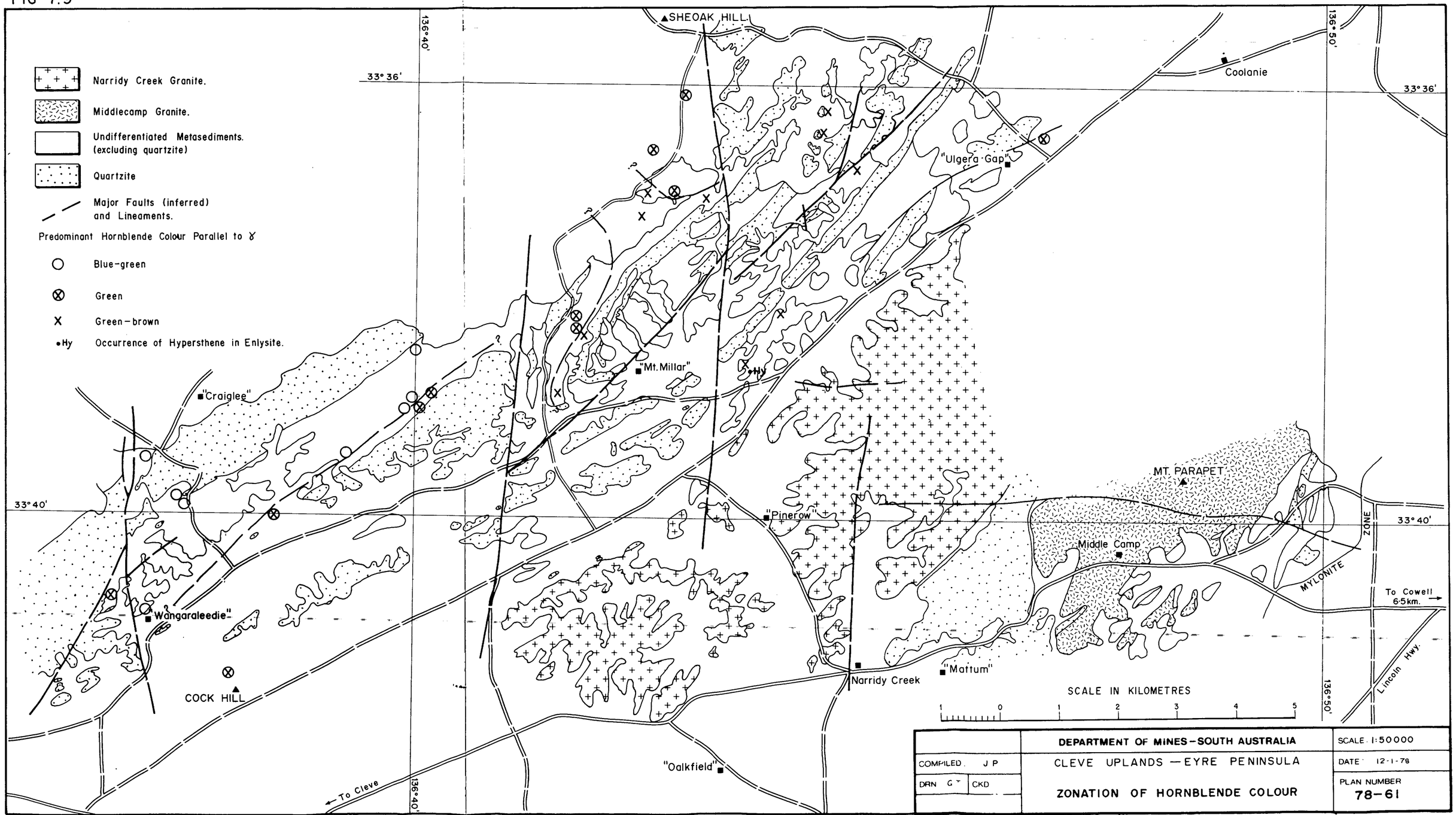
Considering the mode of occurrence of tremolite in the carbonates, a clue to its origin is recorded by a xenolith,

within the Middle Camp granite. In that xenolith, there are scattered relics of highly embayed diopside enclosed within and partially pseudomorphed by a medium grained aggregate of tremolite. This situation is analogous to the tremolite-calcite replacement described from the non-migmatized area. However in this case other carbonates in and around the granite indicate an initial forsterite-diopside-calcite assemblage. Therefore the implication is that during intrusion of the Middle Camp granite (hence sometime during the D_2 deformation) the diopside was significantly replaced by tremolite representing a hydration reaction from D' to C on Figure 7.8b.

Consequently, the conclusion is drawn here that the initial prograde metamorphism, M_1, produced assemblages A to D' in the non-migmatized and migmatized zones respectively. Then, during the second phase of metamorphism, M_2, there was a slight hydration of the system - related to intrusion of the Middle Camp granite - which produced tremolite by the reactions (6) and (10) respectively. Extending this to the stable diopside-forsterite-calcite assemblages devoid of tremolite in the Plug Range area simply requires an initial M_1 upgrading from D' to D'' followed by M_2 hydration to D. It is possible, however, that the Plug Range area escaped the hydration event in which case an upgrading from D' to D'' is not required.

A final point on carbonate rocks is a note on plagioclase compositions. It was recorded in Section 2.2.3, that the majority of plagioclases fall into the calcic end of the series with anorthite content greater than 70 percent. This is in keeping with calc-silicates from southern Eyre Peninsula (Tilley, 1920b), and siliceous carbonates from sillimanite

FIG 7.9


Narridy Creek Granite.
Middlecamp Granite.
Undifferentiated Metasediments. (excluding quartzite)
Quartzite
Major Faults (inferred) and Lineaments.
Predominant Hornblende Colour Parallel to Y
Blue-green
Green
Green-brown
•Hy Occurrence of Hypersthene in Enlysite.
SHEOAK HILL
Coolanie
"Ulgera Gap"
"Mt. Millar"
"Craiglee"
"Pinerow"
MT. PARAPET
Middle Camp
MYLONITE ZONE
"Wangaraleedie"
COCK HILL
Narridy Creek
"Mattum"
"Oalkfield"
To Cowell 6·5km.
Lincoln Hwy.
To Cleve
33°36'
33°40'
136°40'
136°50'
SCALE IN KILOMETRES
1 0 1 2 3 4 5
DEPARTMENT OF MINES—SOUTH AUSTRALIA
SCALE 1:50000
COMPILED J P
DRN G Y CKD
CLEVE UPLANDS — EYRE PENINSULA
DATE 12-1-78
ZONATION OF HORNBLENDE COLOUR
PLAN NUMBER 78-61

zones throughout the world (Wenk, 1970; Soper and Brown, 1971).

7.3.2.4 Metabasite Parageneses

The only major variations in amphibolites between the non-migmatite and the migmatite zones are compositional changes in hornblende and plagioclase.

	Non-migmatite Zone	Migmatite Zone
colour of hornblende	green to blue-green	green to green-brown
Plagioclase composition	An_{18} - An_{45}	An_{40} - An_{55}

The areal distribution of hornblende colour is shown in Figure 7.9. From the shape of the green-brown "isograd" in the Mt. Millar/Morowie subarea it is clear that it has been folded about the D_3 Yabmana synform indicating at least a pre D_3 origin. However it is not clear if it represents M_1 or M_2.

The amphiboles that describe this variation define the principal schistosity S_{1-2}. Porphyoblasts within the same rocks do not necessarily conform with them and, for instance in the Range Road area, porphyroblasts have been noted to have green-brown cores grading outwards into the blue-green colour of the schistose amphiboles that wrap around them. Such schistose amphiboles define the L_2 mineral lineation and have been strongly oriented or reoriented during D_2. Hence it is believed that the colour vatiations may reflect M_2 conditions rather than M_1.

Similar colour changes of hornblende have been recorded at Broken Hill (Binns, 1965) and they infer an increase in grade of metamorphism. Binns noted that sympathetically with the progression from the sillimanite-muscovite zone into the sillimanite-orthoclase zone there was a change in

hornblende colour from blue-green through green to green-brown. This is a common feature of migmatite terrains (Miyashiro, 1973) and has been accounted for by relative increases in TiO_2 parallel to those which account for the change in colour of biotite from brown to red-brown (Binns, 1965).

Compositional changes in plagioclase with increasing grade likewise have been well documented and for example in the Central Alps of Switzerland, Wenk (1970) recorded the appearance of plagioclases with An> 50 percent in amphibolites coincident with the appearance of migmatites. The increase in An Content is allied to compositional changes in hornblende and it is the availability of Ca from actinolite breakdown which influences the plagioclase composition. The higher An content of plagioclase in the layered amphibolites is related to the higher CaO contents of those particular rocks (see Appendix A).

7.3.2.5 Eulysite Parageneses

Important among this category of rocks are the grunerite schists and the first appearance of hypersthene within the migmatite zone. The grunerite schists are characterized by crystallographically parallel intergrowths of green/blue green hornblende and colourless grunerite and are a stable M_{1-2} association throughout most of the study area.

The appearance of hypersthene in a restricted occurrence within the migmatite zone however, is significant and is one which has been recorded in highly metamorphosed iron formations. Klein (1966) for example, noted a quartz-carbonate-grunerite-orthopyroxene assemblage within the staurolite-kyanite zone of SW Labrador, but in a later paper (1973) related the widespread occurrence of orthopyroxene to the

sillimanite zone. In the Cowell/Cleve area, orthopyroxene has been first recorded well into the migmatite zone (hence also well into the sillimanite zone) and consequently it is inferred that its appearance is at a higher temperature than the sillimanite-orthoclase isograd. However, biotite and hornblende are still stable in associated lithologies which therefore infers that the appearance of orthopyroxene in eulysites precedes the breakdown of those minerals in pelitic and mafic rocks respectively.

The particular reaction which is relevant to the incoming of hypersthene is,

11. grunerite → hypersthene + SiO_2 + H_2O

Recently, Forbes (1977) has experimentally studied the breakdown of grunerite to form fayalite at various total pressures and oxygen fugacities and concludes that it is a valuable asset in determining metamorphic conditions. Bonnischer (1975) in a study on the Biwabik Iron Formation, Minnesota has shown that fayalite and hypersthene appear at approximately equivalent P-T regimes, and that the breakdown of grunerite/cummingtonite to either one depends upon the Fe/(Fe+Mg) content. If that is high then fayalite is formed whereas high Mg leads to orthopyroxene. Consequently it is possible to draw some conclusions from Forbes' experiments. These will be used in the following section to determine P-T conditions of the M_{1-2} metamorphism. Reactions relating to the origin of grunerite, actinolite, and diopside from ferrodolomite and quartz rich sediments are outlined in Klein (1966, 1973).

7.3.3 T-P Conditions

Finally in this discussion on the M_{1-2} metamorphism of rocks in the Cowell-Cleve area, it is appropriate to assess

the T-P conditions and the metamorphic grade recorded by the mineralogical changes during the climatic M_{1-2} metamorphic event.

Within the pelitic and semi-pelitic rocks, considerable emphasis has been placed on the critical reaction muscovite-quartz going to orthoclase-sillimanite and its related anatexis. This reaction has been widely studied and recently has assumed particular importance as a critical grade determinator (Winkler, 1976). Winkler in abandoning the almost universal facies series nomenclature, has adopted this reaction and partial anatexis as the basis of his subdivision of medium from high grade. The combination of partial anatexis and the breakdown of muscovite are broadly independant of pressure: that is, they are mainly dependant on increase in temperature. Consequently in order to place some limits on pressure other factors are required, and here Winkler uses both the polymorphs of Al_2SiO_5 and the almandine-cordierite inter-relationships to divide his broad "grade" domains into smaller subdomains. If Winkler's system is followed in the study area, then the resultant P-T domain is necessarily defined by those fields in which sillimanite and almandine are stable and in which the transition from muscovite-sillimanite assemblages to sillimanite-orthoclase assemblages is observed to be coincident with incipient anatexis.

Such a situation represents a transition from the sillimanite-almandine zone of Winkler's medium grade to the almandine zone of his high grade. In the more normal facies series classification this represents a transition from the sillimanite-muscovite (-almandine) sub-facies to the sillimanite-orthoclase (-almandine) sub-facies of the upper

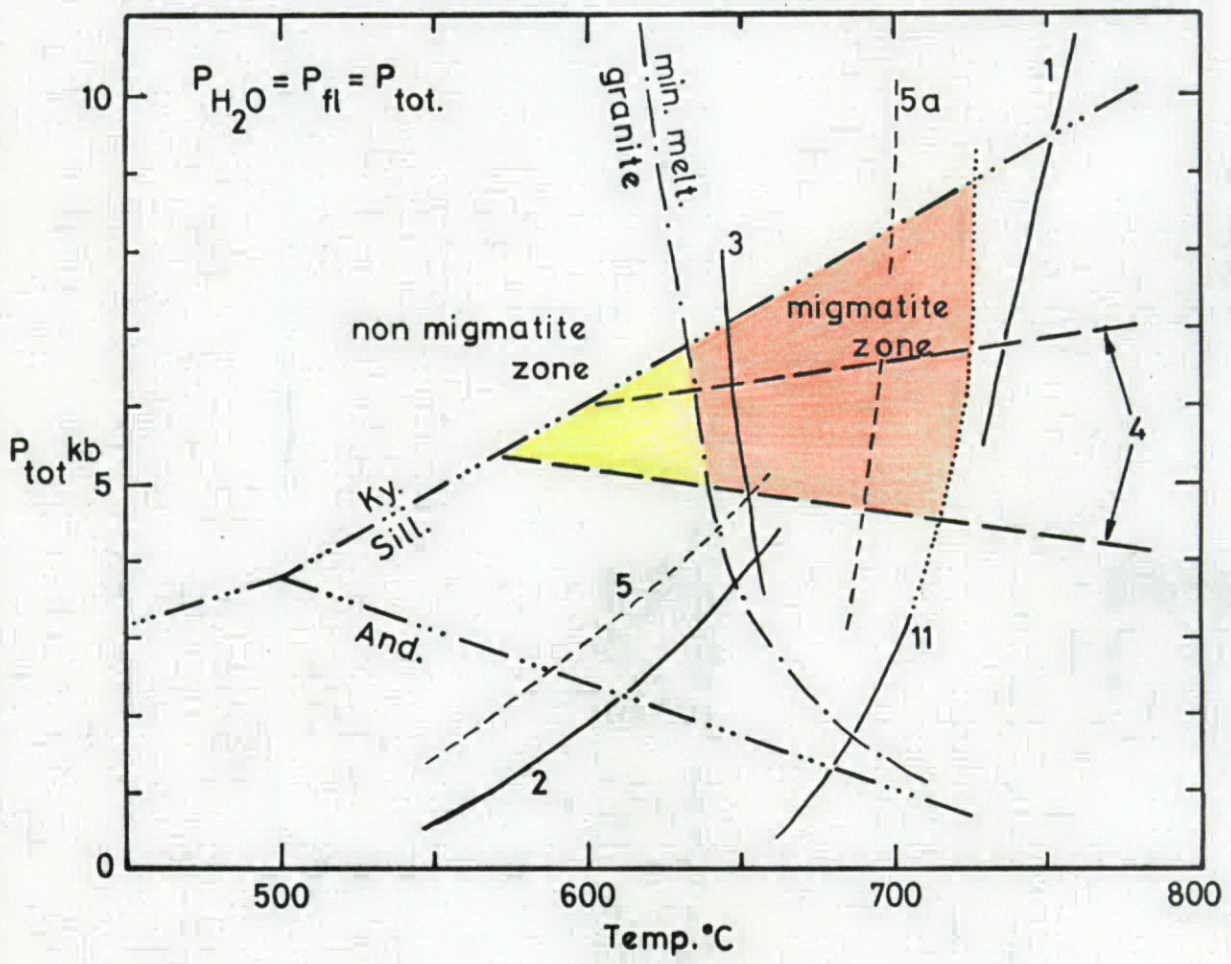
amphibolite facies (Turner, 1968; Winkler, 1967; Hyndman, 1972). It is analogous to similar well-documented transitions in British Columbia (Hyndman, 1968), Adirondack Mountains, New York (Engel and Engel, 1958), in parts of Scotland (Chinner, 1966), and in parts of the Swiss Alps (Wenk, 1970).

In considering these similar transitions recorded from other parts of the world it is noteworthy that they mostly represent medium pressure type metamorphism, something akin to the classical Barrovian type metamorphism but perhaps of slightly lower pressure; that is, below the kyanite isograd. Read (1973) in an extension of Hyndman's (1968) study in British Columbia, considered that such a metamorphic series was midway between Barrovian and Buchan type metamorphism and subsequently labelled it as "Slocan" type metamorphism.

Having qualitatively defined the metamorphic conditions it is useful to consider the specific reactions described in the text above and to compare them with theoretical and experimental work. Because of the large number of experiments which have been carried out on many of the reactions, it has been necessary to select certain work and to reject others. The aluminosilicate phase diagram is classical in this respect and only that of Holdaway (1971) has been used since that has the most widespread acceptance. However it must be noted that many other workers are in close agreement on the position of the sillimanite/kyanite boundary which is the most relevant here. Secondly, without having any garnet analyses, it was necessary to select suitable curves for the cordierite to almandine transition. In this case, an FeO/(FeO + MgO) ratio of 0.65 was chosen because it is most representative of the bulk composition of "normal" gneisses and schists

FIG. 7.10

P-T CONDITIONS of M_1



1) partial melting of muscovite + quartz in absence of plagioclase.

2) breakdown of muscovite + quartz (Kerrick, 1972).

3) musc + qtz + Ab + H_2O = Liquid + sill (Storre and Karotke, 1971).

4) almandine / cordierite stability for FeO / (MgO + FeO) = 0·6 (Currie, 1971).

5) staurolite + musc + qtz breakdown (Hoschek, 1969).

5a) staurolite + quartz breakdown

11) upper limit of grunerite breakdown (Forbes, 1977).

alumino silicate curves from Holdaway (1971)

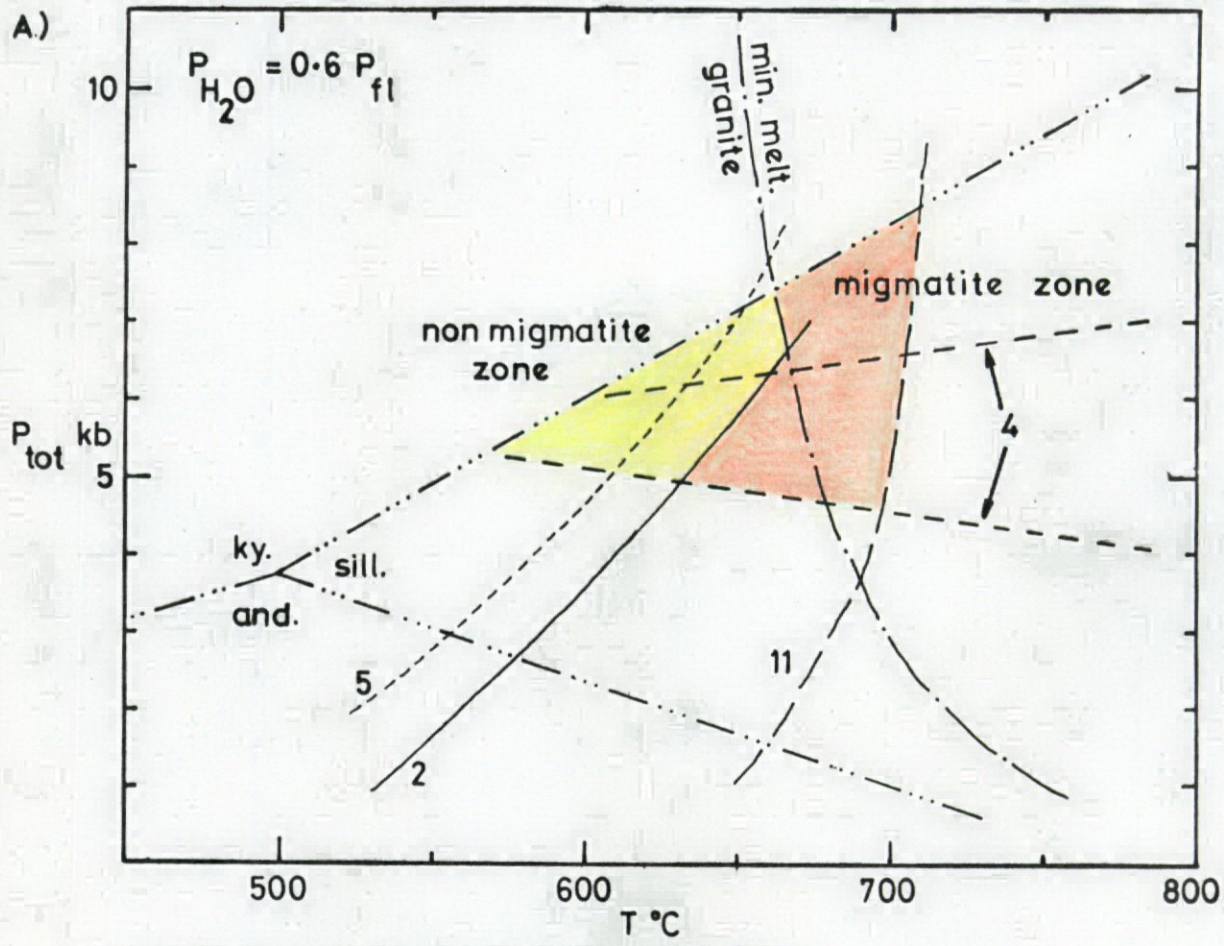
(Poldervaart, 1955). However, this ratio may be higher and for example may be as high as 0.8 in which case the curves would be lowered by about 0.5 kb. Currie's (1971) experimental curves have been used in preference to others (e.g. Hensen and Green, 1971) because his experiments were done in a temperature range relevant to this study.

The T-P fields which are consequently defined by these experimental and theoretical curves under the specific condition of $P_{H_2O} = P_{total}$ are shown in Figure 7.10. They suggest pressures between 5 and 7 kb and temperatures (a) in the non-migmatite zone, of 600 - 650°C, and (b) in the migmatite zone, in excess of 650° but not greater than 725°C. This upper limit in the migmatite zone is inferred after extrapolating Forbes' (1977) data on grunerite breakdown. The particular curve shown (curve 11) is his maximum stability limit for grunerite at moderately high oxygen fugacites. At lower oxygen fugacites the curve moves to the left by up to 50°C implying an upper temperature limit for the migmatite zone of 675° instead of 725°C. Intuitively this seems to be more realistic. The validity of these grunerite breakdown curves is confirmed by curve (1) which represents the partial melting of quartz-muscovite in the absence of plagioclase; that is, the partial melting of muscovite rich quartzites. As muscovite is stable in plagioclase free quartzites throughout the study area, this temperature condition apparently has not been reached.

The field as it has been depicted, represents the total region where almandine is stable. However, if the absence of cordierite is considered, the field is appreciably narrowed to that region of the diagram where almandine only is stable; that is, above the upper curve of (4). This then infers

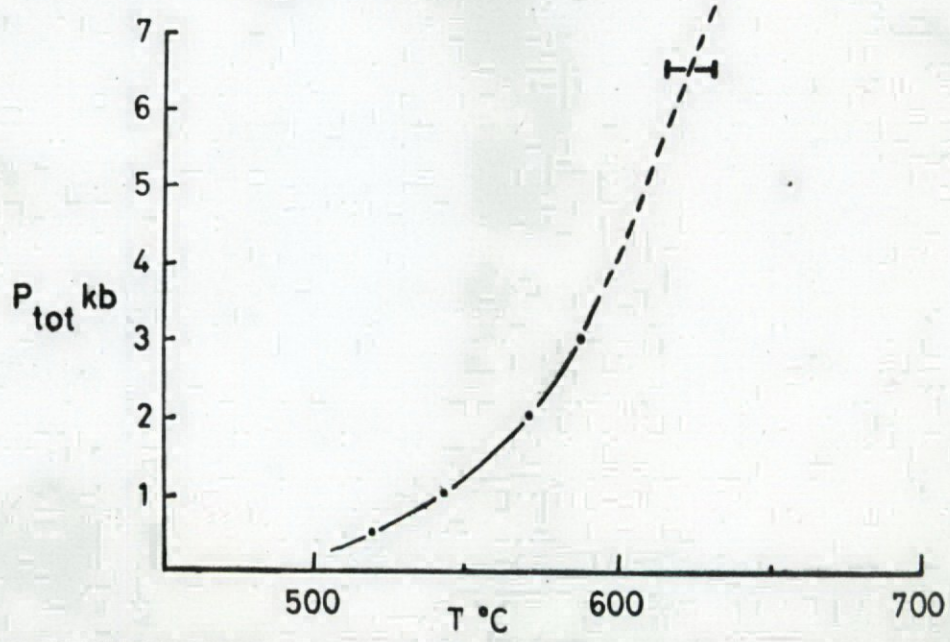
FIG. 7.11

P-T CONDITIONS for $M_I - \underline{\underline{II}}$



see text and Fig. 7.10 for explanation.

B) approximate P-T conditions for the first appearance of forsterite at $X_{CO_2} = 1{\cdot}0$ (after Skippen, 1974).



pressure conditions of between 6-7 Kb rather than the 5-7 Kb estimation above.

The definition of such a P-T field has one shortcoming if the absence of staurolite is considered to be a function of metamorphic grade rather than of rock composition. This is implied by curves (5) and (5A) which represent the breakdown of staurolite in the presence of quartz with or without muscovite respectively. Under the $P_{H_2O} = P_{fluid}$ conditions pertaining to Figure 7.10, this infers that staurolite should be present given a suitable rock type. Alternatively however, it is possible that, (1) curve (5) and (5A) are not representative, or (2) the $P_{H_2O} = P_{fluid} = P_{total}$ condition is not valid.

The first of these cannot be discounted because the disappearance of staurolite below the sillimanite-orthoclase isograd is commonplace in many parts of the world. Indeed, Hyndman, although he does not qualify it, chooses to place the breakdown of staurolite at 100°C lower. This could then effectively account for the absence of staurolite.

The second alternative is examined in Figure 7.11a under conditions where $P_{H_2O} = 0.6\ P_{fluid}$. Under such conditions, the breakdown of muscovite-quartz moves to lower temperatures (Kerrick, 1972) and the minimum melting of granite moves to higher temperatures. If the staurolite-muscovite-quartz breakdown is also moved to lower temperatures in line with the muscovite-quartz breakdown, and this should be consequential according to staurolite breakdown reactions (e.g. see Hoschek, 1969), then a situation is created whereby a muscovite-sillimanite-almandine-quartz association can exist yet both staurolite and cordierite are unstable. Whilst curves (3) and (1) have not been plotted

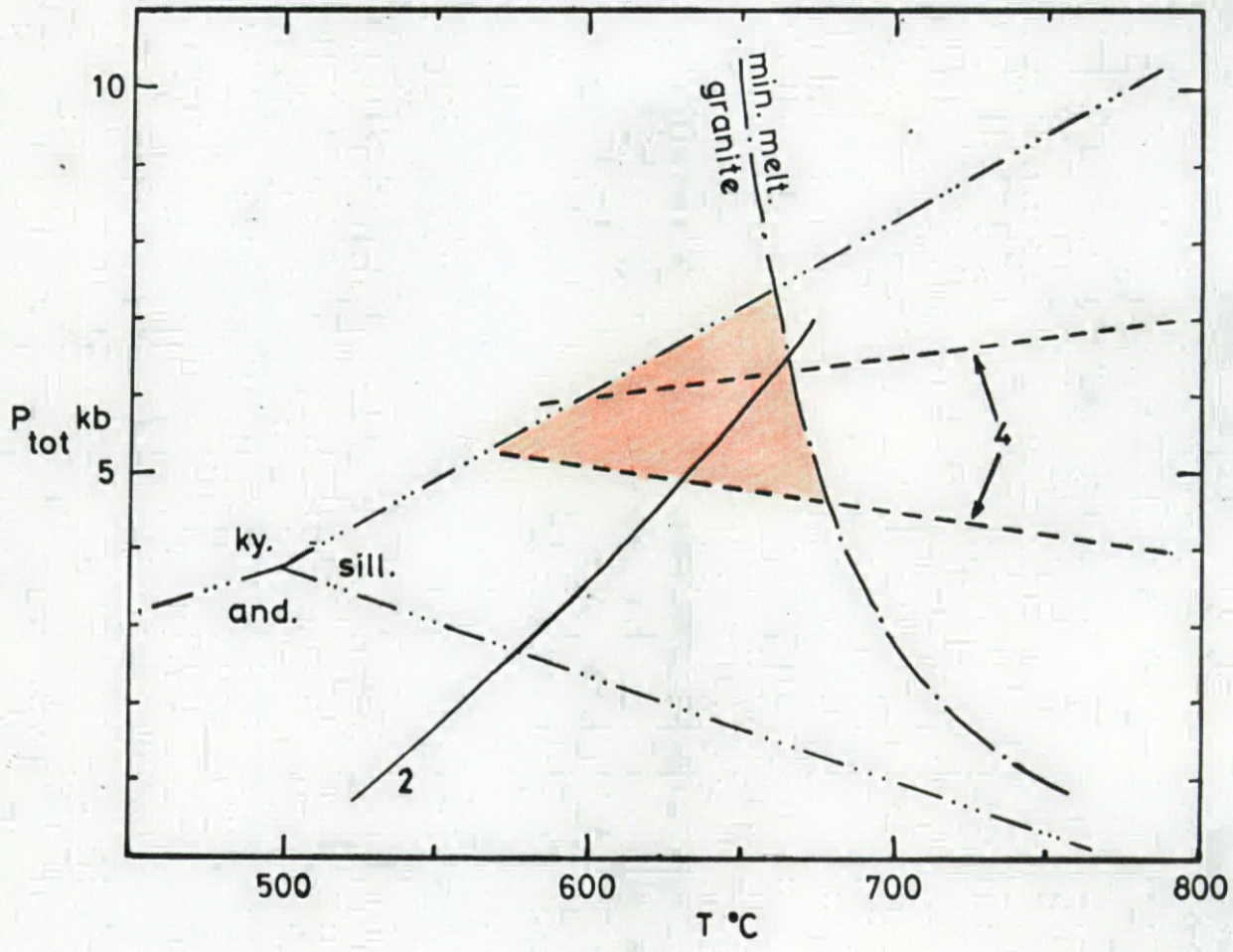
on Figure 7.11a, it can be assumed that they would lie at about the same relative positions to the minimum melting curve as they do on Figure 7.10. This is because water is essential as a reactant rather than a product and therefore any decrease in P_{H_2O} imposes a restriction on those reactions. The grunerite breakdown curve will move to lower temperatures in line with muscovite because water is a product of reaction.

In inferring that $P_{H_2O} < P_{fluid}$ yet $P_{fluid} = P_{total}$, it is necessary to account for the remainder of the fluid. Carbon dioxide is the natural assumption here because of the abundance of carbonates in the area and the nature of reactions (6) to (10). Therefore there definitely exists a prima facie case in support of this $P_{H_2O} < P_{fluid}$ model. The P-T regime implied by Figure 7.11 defines pressures of 5 - 7.5 Kb and temperatures for (a) the non-migmatite zone, of 620 - 660°C, and for (b) the migmatite zone, in excess of 660°C but no greater than about 700°C.

In concluding this discussion it is relevant to compare these T-P conditions with those inferred from the carbonate parageneses. In Figure 7.8, a temperature range from about 575°C to 625°C was inferred at a P_{total} = 3 Kb. Unfortunately, Skippen did not extend his work to higher pressures, but if his results are extrapolated to higher P total, they effectively move the curves and reactions up relative to the temperature scale (Fig. 7.11b). Such an extrapolation suggests temperatures of 620-630°C at P_T = 6.7 Kb. for the formation of forsterite. When this is compared to the boundary between the migmatite zone and non-migmatite zone which coincides closely with the first appearance of forsterite there is a very close correlation. That boundary which occurs at 650°C

FIG.7.12

P-T CONDITIONS for M_2



2) breakdown of muscovite + quartz (Kerrick, 1972)

4) cordierite / almandine topology at FeO/(FeO + MgO) = 0·6 (Currie, 1974)

Al_2SiO_5 polymorphs (Holdaway, 1971)

for $P_{total} = P_{H_2O}$ and 660° for $P_{H_2O} = 0.6\ P_{total}$ only represents a 20-30° discrepancy.

M_2 METAMORPHISM - Based on the absence of any migmatization during M_2 but continued growth of sillimanite and garnet with local orthoclase, the broad P-T conditions defined for M_{1-2} can be modified. Pressures ranges are bounded above by the sillimanite/kyanite tieline, below by the lower limit of almandine stability, and an upper temperature limit is defined by the minimum melting of granite. At $P_{H_2O} = 0.6\ P_{total}$, these restraints define P-T conditions ranging from 600-675°c and 5-7 Kb (Fig. 7.12). As previously discussed (Section 7.3.2.2), the alteration of M_1 carbonate parageneses does not necessarily require substantial changes in P-T conditions from those encountered in the initial M_1 metamorphism. Rather they require only a slight modification (hydration) of the fluid phase and they still maintain forsterite as a stable constituent.

If, as it has been suggested, the colour changes of hornblende in amphibolites reflect changing conditions during the M_2 event, a further control in the relevant P-T field is available. Binns (1964) defined the transition of colour from blue-green to green-brown as coincident with the breakdown of muscovite + quartz in the Broken Hill region. On this premise curve (2) in Figure 7.12 separates the higher temperature green-brown hornblende field from the blue-green hornblende field.

7.4 M_3 METAMORPHISM

The M_3 metamorphism was a major retrograde phase which encompassed the D_3 deformation. It was varied both in nature and in intensity and although there was some retrogression before the principal deformation, a close relationship

between intensely retrograded zones and intensely deformed zones suggests that the D_3 deformation was essential to the driving forces behind the reactions (or viceversa?). Two such examples are, specimen 331 (see Fig. 6.8a) which displays considerable retrogression of sillimanite and which is also tightly folded, and the mylonite zone where retrogression is locally complete.

However, with the exception of the mylonite zone and in particular the slaty mylonite, retrogressive reactions are only incipient. Consequently the observed assemblages consist essentially of metastable M_{1-2} remnants with minor alteration in zones of high deformation. There is therefore considerable ambiguity concerning the recognition of stable and metastable mineral associations.

7.4.1 Summary of Observed Mineral Associations

PELITIC AND SEMI-PELITIC ROCKS - Throughout most of the study area but in particular within the Mt. Millar/Morowie and Wangaraleednie sub-areas, muscovite, biotite and chlorite appear to coexist and all three have been observed to define S_3 schistosities. Chlorite is subordinant to muscovite and biotite, but locally pseudomorphs the biotite. Such pseudomorphs are associated with minute semi-opaque (high RI) inclusions which are presumed to be mainly epidote. This is confirmed in the slaty mylonites where chlorite-epidote-muscovite predominantes over biotite. M_3 biotite is, in most cases, dark green-brown in colour.

Almandine throughout the Mt. Millar/Morowie and Wangaraleedine sub-areas is essentially unaltered even when strongly fractured by S_3. However, within the deformed zone of the Narridy Creek granite it has been partially replaced by chlorite. Such replacement by chlorite is also

observed in parts of the Ullabidinie sub-area close (within 100-200 m) to the mylonite zone, while within the zone itself garnets are absent.

Sillimanite has remained as a metastable remnant of M_{1-2} throughout most of the study area. Locally, however, it has been retrogressed to sericite and quartz (e.g. Figure 6.8a).

In summary, M_3 assemblages, are, for the Mt. Millar/ Morowie and Wangaraleedinie sub-areas -

1) quartz-feldspar-muscovite-biotite/chlorite-epidote (-almandine)

and for the Mylonite Zone -

2) quartz-feldspar-muscovite-chlorite/biotite-epidote

CARBONATES - M_3 retrogression of M_{1-2} carbonate assemblages is confined to forsterite and diopside. Although a specific relationship could not be demonstrated between the serpentinization of forsterite and the D_3 deformation, the main reaction is an integral part of M_3 because the internal deformation of serpentine nodules (Fig. 6.21b), implies at least a pre D_4, possibly pre D_3, origin. Furthermore the presence of D_4 pressure shadow coronas around some nodules supports their pre D_4 existence.

Diopside alteration on the other hand was closely related to D_3 and was very specifically restricted to sub-grain/new grain and kink band boundaries (Fig. 6.22). It produced narrow irregular zones of tremolite-calcite-quartz.

The principal M_3 carbonate assemblages throughout the study area are,

3) tremolite-calcite-quartz

4) dolomite-calcite-serpentine

The occurrence of serpentine is necessarily restricted to

the formerly migmatized areas where M_{1-2} forsterite existed.

MAFIC ROCKS - There was no clear alteration of M_{1-2} parageneses within the amphibolites. Incipient sericitization of plagioclase is commonplace throughout the area, but could not be directly attributed to any particular event. Nevertheless, because it is associated with the formation of epidote and because M_4 retrogression is very local (see below), it conveniently fits in with the M_3 event. Hornblendes are not significantly altered during M_2 although they do have pale blue-green edges suggesting incipient retrogression. Amphibolites are not found in the mylonite zone of this study, but in the deformed zone of the Narridy Creek granite they have a strong L_3 lineation. The amphiboles defining that lineation are blue-green in colour hence supporting blue-green amphibole within the M_3 paragenesis. Such a paragenesis is believed to be,

5) hornblende/actinolite-plagioclase (-epidote-sericite-quartz)

7.4.2 Discussion

There are four main breakdown reactions that shall be discussed here. They are respectively, the breakdown of sillimanite, biotite/almandine, diopside and forsterite.

BREAKDOWN OF SILLIMANITE - Retrogression of sillimanite to sericite can be represented by either of the reactions,

12) 3 sillimanite + 3 quartz + $2K^+$ + $3H_2O$ → 2 muscovite + $2H^+$

13) sillimanite + K-feldspar + H_2O → muscovite + quartz

The second of these as it has been written here, represents the reversal of the M_{1-2} reaction (1) and requires the breakdown of K-feldspar. However it has been noted that K-feldspar has frequently undergone recrystallization during

D_3 to produce narrow zones of very fine new grains rather than completely breakdown to muscovite by reaction with sillimanite. Nevertheless, the occurrence of sericite in these recrystallized zones suggests that this reaction has had some effect.

The first reaction is one which has been commonly cited in literature as a step in the prograde reaction from either andalusite or kyanite to sillimanite (e.g. Carmichael, 1969). It was derived to explain the common occurrence of sillimanite within muscovite rims around andalusite or kyanite (e.g. Green, 1963; Chinner, 1966) rather than directly pseudomorphing them. It is used here as a retrogressive reaction, but because of the absence of andalusite or kyanite needed to balance out the anions, a source of K^+, in addition to water, is required to promote reaction. To this point it is no doubt significant that the principal localities of sillimanite retrogression are near to D_3 granite intrusions. Throughout the rest of the area, sillimanite pods etc. are largely unaltered even regardless of the close proximity of K-feldspar. This therefore constitutes circumstantial evidence in favour of the first of the sillimanite breakdown reactions. It underlines the importance of presence of reactants, particularly volatiles, in conjunction with the right P-T conditions to promote retrogression.

BREAKDOWN OF BIOTITE AND ALMANDINE - The principal effect of M_3 in the mylonite zone and adjacent gneisses is retrogression of biotite and almandine to chlorite and epidote. Initiation of this retrogression is first observed in the Mt. Millar/Morowie and Wangaraleednie sub-areas where garnet apparently remained stable yet biotite was locally retrograded. There

are several reactions, all hydration, which may lead to such retrogression, but the one favoured here is

14) biotite + plagioclase (An component) + water→chlorite + epidote + muscovite,

because of the commonly observed and related sericitization of plagioclase. Although there is no true experimental work on such a reaction, the reverse reaction, the widespread introduction of oligoclase instead of albite in the presence of epidote, has been well documented in field studies (e.g. Brown, 1962; Crawford, 1966) and in fact, has been used on many occasions as an indicator of the boundary between the greenschist and amphibolite facies (e.g. de Waard, 1959).

Allied to the sericitization of oligoclase in semi-pelites is the sericitization (sauseritization) of plagioclase within the amphibolites. In this case, however, hornblende is replaced by actinolite which accounts for the paler blue-green rims of the M_{1-2} hornblende.

The principal reactions leading to the breakdown of almandine are,

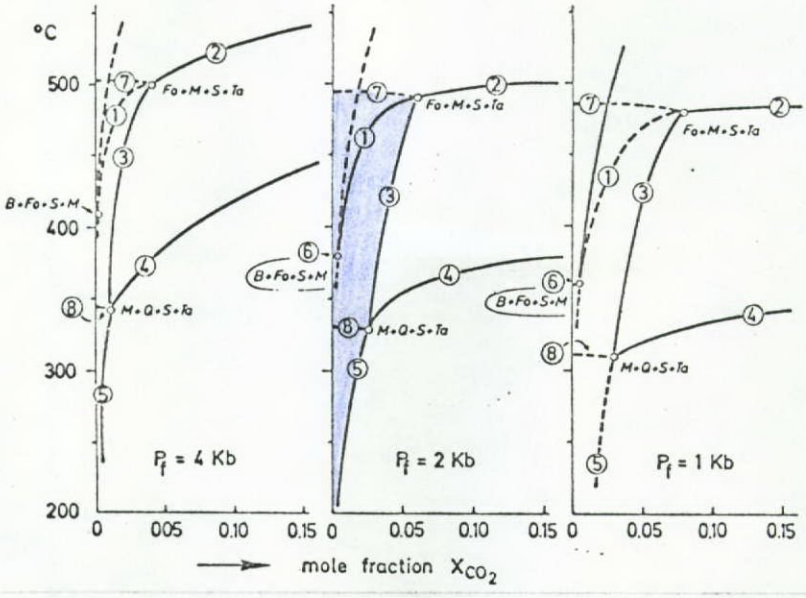
15) garnet + biotite + water→chlorite + muscovite + epidote

16) garnet + biotite + water→chlorite + muscovite + quartz

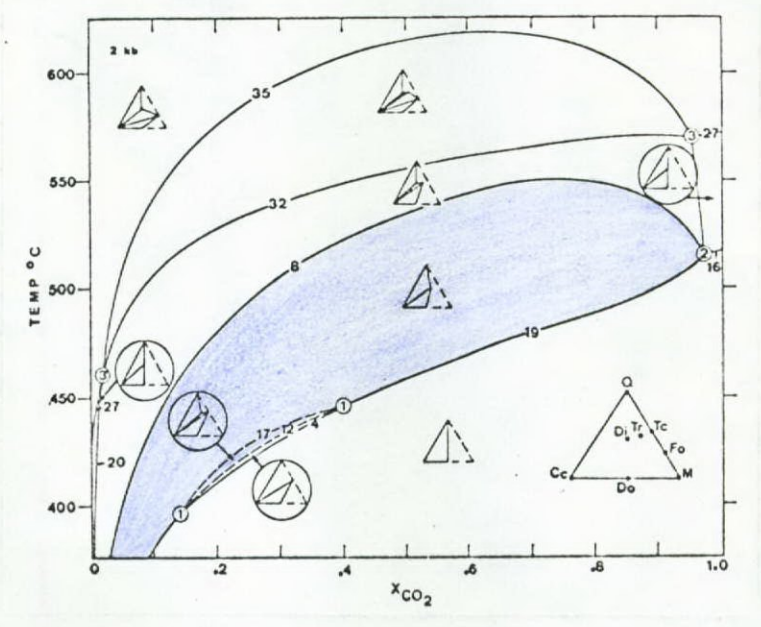
The reverse directions of these reactions have been widely used throughout the literature (e.g. Thompson and Norton, 1968; Hirschberg and Winkler, 1968; Brown, 1969) and although there are other possible reactions leading to the formation of almandine, they are considered as the most suitable (Winkler, 1976). This is supported by this study because of the widespread, concomitant breakdown of biotite and garnet, and the development of chlorite-epidote-sericite. These reactions are also fundamental in defining the boundary between the greenschist and amphibolite facies (Turner,

FIG. 7.13

T-X_{CO_2} TOPOLOGY for CARBONATE ROCKS during M_3



A) stability field for serpentine at low X_{CO_2} (Johannes, 1969). Curve 1) = reaction 17), curve 2) = breakdown of forsterite to talc + magnesite, curve 3) = hydration of talc to serpentine, and curve 7) = reaction 18).



B) stability field for tremolite without diopside (Skippen, 1974). Curve 8) = breakdown of diopside, and curve 19) = breakdown of tremolite.

1968; Miyashiro, 1973).

BREAKDOWN OF DIOPSIDE AND FORSTERITE - Two reactions, both hydration reactions, are considered to be important in the breakdown of forsterite;

17) 2 forsterite + 2 H_2O + CO_2 → serpentine + magnesite

18) 6 forsterite + talc + 9 H_2O → 5 serpentine

The first of these was recognized by Tilley (1920A) as the principal reaction representative of the formation of serpentine pseudomorphs after forsterite in southern Eyre Peninsula. Recently though it has been extensively studied by Johannes (1968, 1969) in relation to the breakdown of forsterite in ultramafic rocks. He has been able to demonstrate that the formation of serpentine requires very specific vapour compositions, namely, very high H_2O contents and correspondingly low CO_2 contents (Fig. 7.13a). At higher CO_2 contents, forsterite breaks down to talc and magnesite. This assemblage may subsequently convert to serpentine by hydration, (to very high H_2O contents) but the textures observed in this study do not support that transition because olivine relics are enclosed directly within the serpentine, there being no intermediary phase.

According to Johannes the first appearance of serpentine is associated with the second of the reactions cited above. It occurs at somewhat higher temperatures than the first reaction (Fig. 7.13) and as such represents the upper stability limit of serpentine. However it requires talc as a reactant and while it is certainly present in the region (e.g. in the Cowell jade province), talc has not been recorded in the actual study area.

Of equal importance to the serpentinization of forsterite but of more restricted occurrence, is the breakdown of

diopside. It can be represented by the reaction.

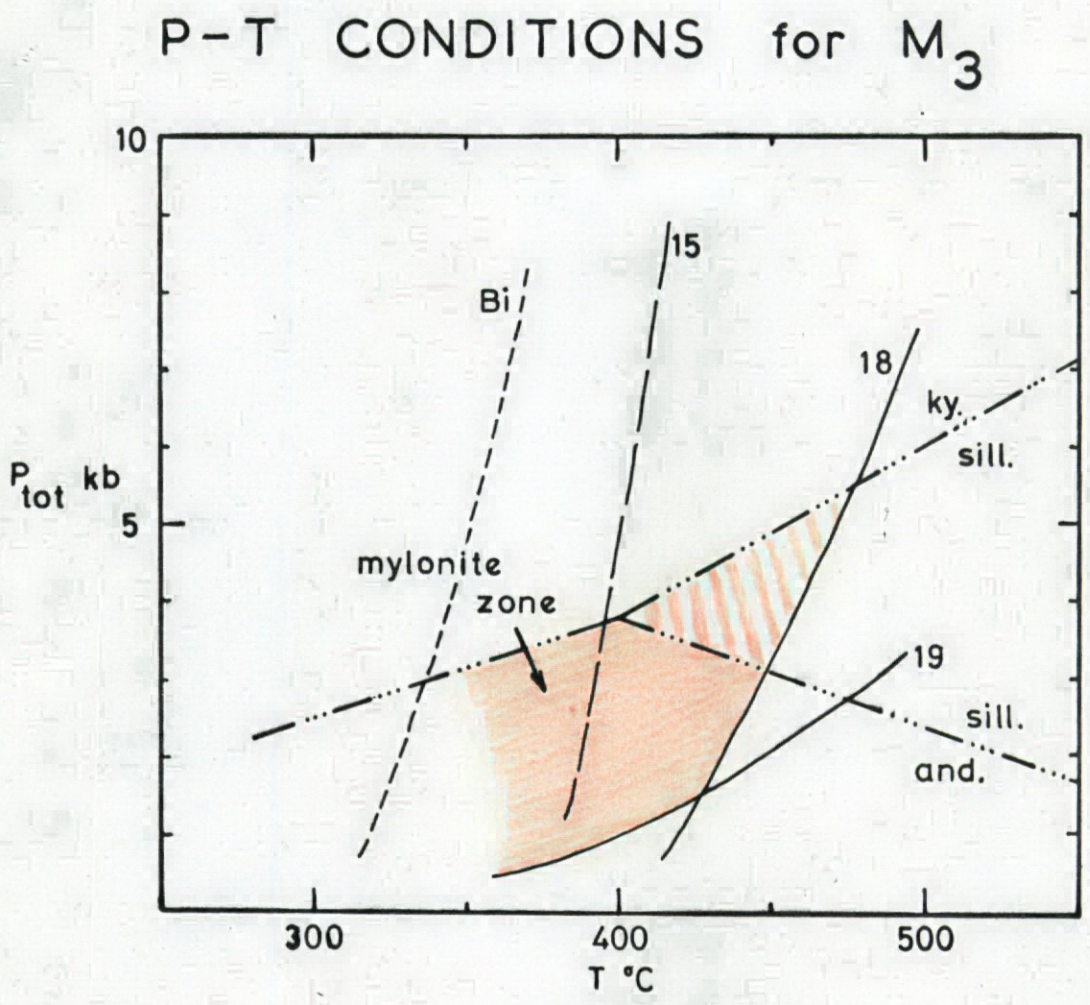
19) 5 diopside + $3CO_2$ + H_2O → tremolite + calcite + 2 quartz

The phase relationships of this reaction have been widely studied and the studies of Skippen (1974) and Slaughter et al (1975) have both emphasized the importance of the fluid composition (e.g. Fig. 7.13b). With very high water contents, as implied by the serpentinization model, diopside is quite resistant to breakdown even at temperatures down to and below 400°C. This represents a discrepancy in temperature between the breakdown reactions of diopside and forsterite, but in view of the very local alteration of diopside compared to forsterite and by its unique restriction to D_3 recovery features it is suggested that kinetic factors may have been more important in its breakdown.

7.4.3 P-T Conditions

The pressure-temperature conditions of the M_3 metamorphism are not clearly defined due to lack of complete parageneses and to lack of clear experimental data on many of the retrogressive changes observed. Nevertheless though, it is clear that the conditions involved are related to the greenschist/amphibolite facies boundary at moderate pressures. This can be deduced from the breakdown of biotite and almandine, by the sericitization of plagioclase, by the incipient retrogression of hornblende and by the widespread introduction of chlorite. Also, the observed M_3 mineral assemblages are characteristic of the upper greenschist facies (biotite zone) and lower amphibolite facies (almandine zone) of Turner (1968) and Miyashiro (1976). Specifically the Mt. Millar/Morowie and Wangaraleednie sub-areas would fall into the almandine zone whereas the mylonite zone and adjacent

FIG. 7.14



Al_2SiO_5 polymorphs (Holdaway, 1971)

Bi) lowest stability limit of prominent biotite (Winkler, 1976)

15) lower limit for almandine (Winkler, 1976)

18) breakdown of forsterite to serpentine (Johannes, 1975)

19) breakdown of diopside (Skippen, 1974)

gneisses would fall into the biotite zone.

With respect to specific restraints on the P-T conditions, the upper temperature limits of the M_3 metamorphism are sharply defined by the instability of sillimanite, by the first breakdown of forsterite (the forsterite + talc reaction) and by the first possible breakdown of diopside. P-T conditions necessarily straddle the boundary of the greenschist/amphibolite facies which is defined here by the almandine "in" (or "out") curve, and a lower limit is vaguely defined by the curve related to the first appearance of biotite (since biotite is still present in lesser quantities within the mylonite zone). Those restraints and the P-T conditions hence defined are shown in Figure 7.14. Restraints on the pressure are not clear but moderate pressures are inferred by the almost complete absence of biotite in parts of the mylonite zone. Miyashiro (1976) considers this to be characteristic of medium to high pressure metamorphism as opposed to low pressure metamorphism. Thus, the conditions believed to be most representative of M_3 are, P_{total} = 1-3 kb, and T = 490-525 for the Mt. Millar/Morowie and Wangaraleedine sub-areas, and T = 425-490 for the mylonite zone and adjacent areas. It is emphasized though that the apparently higher temperature for the Mt. Millar etc. areas may alternatively be a function of lower P_{H_2O} in that area. By reducing P_{H_2O} relative to P_{total}, the effect is to restrain hydration (i.e. retrogressive) reactions and hence to effectively move the almandine isograd to the left (i.e. to lower T).

7.5 M_4 METAMORPHISM

7.5.1 Summary of mineral parageneses

The principal features that characterize M_4 are.

1) adularia veinlets in semi-pelitic gneisses,

2) calcite veinlets in dolomites and less commonly in gneisses accompanied by intense sericitization of plagioclase (formerly oligoclase) on either side of them,

3) quartz-plagioclase (possibly albite) segregations often with coarse sphene in kink banded amphibolites,

and, adjacent to the Mt. Parapet lineament,

4) replacement of dolomite/calcite in the dolomite rocks by tremolite, and

5) replacement of biotite by actinolite adjacent to fractures in the Middle Camp granite.

7.5.2 Discussion

The very nature of M_4 reactions and their unique association to deformation structures suggests that the rate controlling factors are the availability and diffusion of essential components. This is evidenced by the presence of calcite and adularia in S_4 fractures, and by the intense sericitization of plagioclase immediately adjacent to such. All of the M_4 features require the introduction or dissipation of certain components (e.g. water or carbonate) and it is clear that D_4 structures have facilitated their mobility.

Sericitization of plagioclase was noted during the M_3 metamorphism and related there to hydration reactions accompanying biotite breakdown. A similar breakdown is envisaged here reflecting the instability of oligoclase under M_4 conditions.

Segregation banding in amphibolites does not suggest any volume changes and hence is mainly consequent to some sort of chemical transfer. Amphiboles have been depleted within these bands and have been substituted by various amounts of plagioclase, quartz, calcite/dolomite and to a

lesser extent, sphene, and other accessories. A reaction of the form of,

20) hornblende + plagioclase + vapour (CO_2)→quartz + carbonate + less calcic plagioclase + sphene

is suggested where much of the Ca+Mg of hornblende (and plagioclase) goes into carbonate, while excess components (e.g. TiO_2) go into accessories such as sphene.

Within the dolomites adjacent to the Mt. Parapet lineament in the Ullabidinie sub-area, the transition from a dolomite to a tremolite/actinolite rock is represented by the key reaction,

21) 8 quartz + 5 dolomite + H_2O→tremolite + calcite + 7 CO_2

It is suggested that quartz has been introduced and calcite (and CO_2) removed, along and immediately adjacent to the Mt. Parapet lineament. Remembering that quartz dykes and quartz pegmatites are frequent along this lineament, this is not unreasonable. Furthermore, the breakdown of biotite adjacent to S_4 fractures in nearby granite testifies to a high activity of calcium eminating from those features.

There has been very little study of the breakdown of biotite to actinolite although it has often been recorded. Brown (1971) described prograde reactions leading to the formation of biotite from actinolite within schists from western Otago, New Zealand, and noted that these reactions took place at or very near the boundary of the biotite and chlorite zones in conjunction with the breakdown of stilpnomelane. However, in northern America, other reactions leading to the biotite - actinolite transformation have been observed in micaceous limestones and in two cases these have defined a biotite to actinolite isograd which crosscuts sillimanite and biotite isograds in normal pelites (Hewitt,

1973; Carmichael, 1970). One such reaction which is relevant here, is

22) biotite + anorthite + calcite + quartz + H_2O→amphibole + muscovite + CO_2

Hewitt discusses this and other reactions but shows this particular one to be highly dependant on H_2O and CO_2 activities rather than temperature and pressure. However, the type of amphibole produced is dependant on the grade, and actinolite would imply greenschist conditions.

7.5.3 P-T Conditions

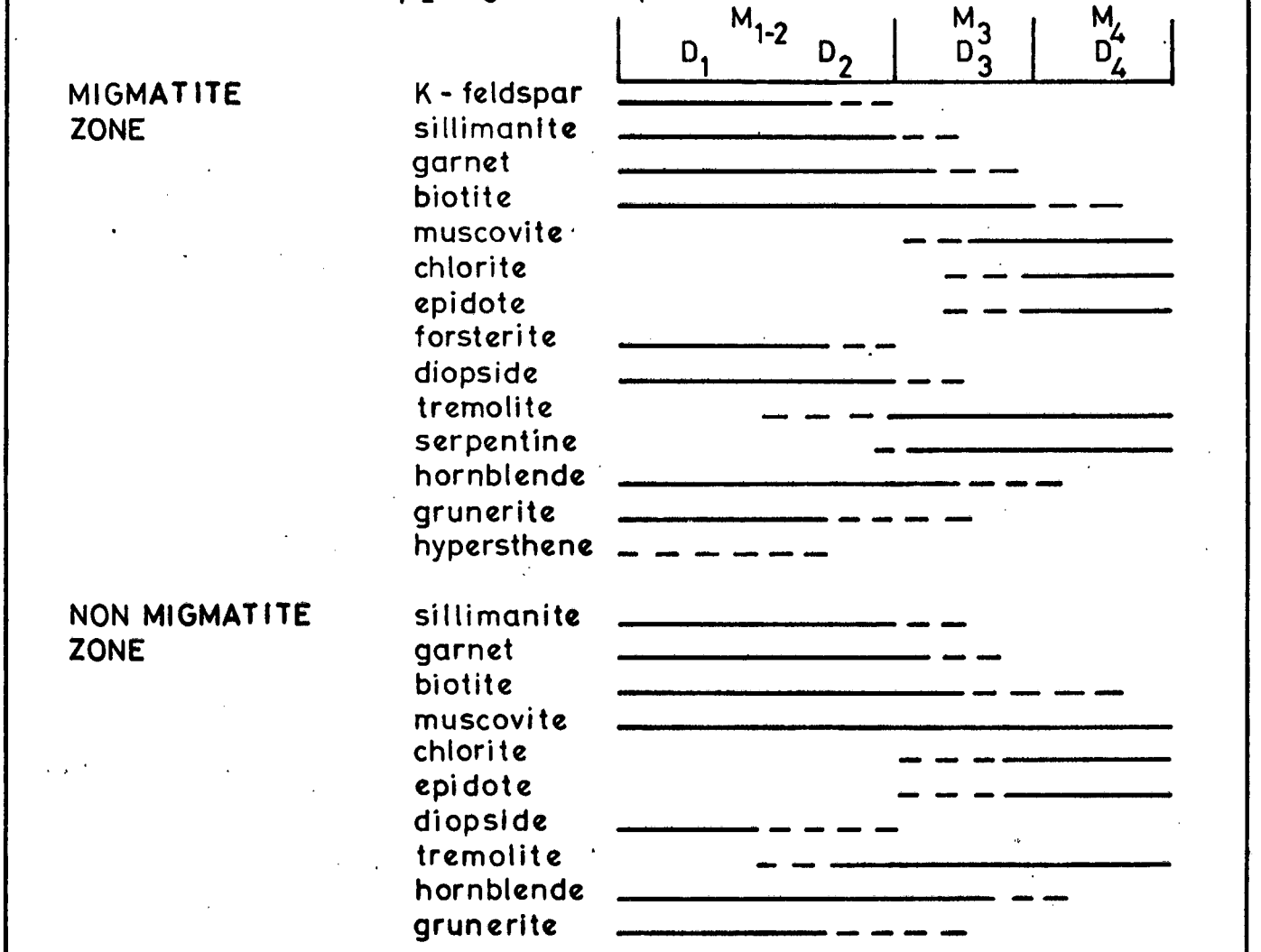
The metasomatic nature of the M_4 metamorphism and its incompleteness do not permit an accurate analysis of the physical conditions that prevailed during M_4/D_4. However, certain restraints can be placed on them. Because of the stability of tremolite within the carbonates, the T-X_{CO_2} diagrams of Skippen (1974) suggest that a lower limit of about 350°C (at 0.5 kb = P_{total}) can be estimated. An upper limit on the temperature is inferred by the upper stability of actinolite, namely the greenschist - amphibolite facies boundary. This is taken as about 490-500°C. The breakdown of biotite to actinolite might suggest temperatures below the biotite isograd (425°C) according to Brown (1971) but Hewitt (1973) has demonstrated that this is not a reliable guide. Rather it infers high H_2O and/or calcite activity.

7.6 SUMMARY OF METAMORPHISM

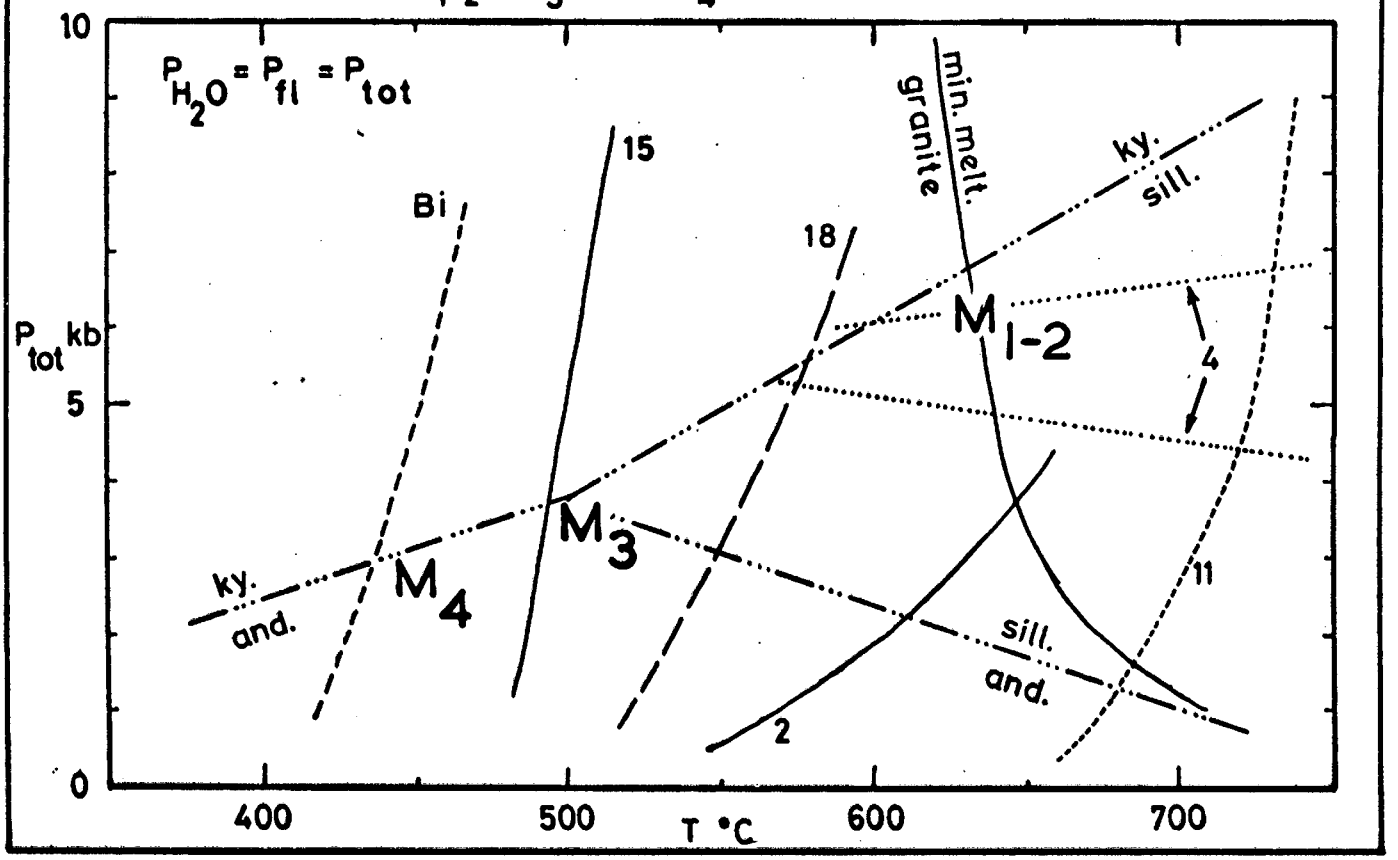
In the Cowell/Cleve district four major periods of metamorphism have been recognized which define a sequence of crystallization/recrystallization from high to low grade. The first two periods, grouped together as the M_{1-2} metamorphism, were both high grade, pervasive metamorphic events of the upper amphibolite facies. They variously affected

FIG. 7.15

A-B) synopsis of M_{1-2}, M_3 and M_4 mineral parageneses.



C) comparison of M_{1-2}, M_3 and M_4 P-T conditions (cf. Figs 7.10 & 7.14)



the area and a zone of migmatization corresponding to the sillimanite-orthoclase (-almandine) subfacies has been delineated from non-migmatized, quartz veined rocks of the sillimanite-muscovite (-almandine) subfacies. Although it was difficult to isolate the separate M_1 and M_2 components of this major event, it is considered that the principal migmatization episode was M_1. However the evidence for this is not conclusive and it is believed that the isograds were modified by the M_2 episode.

Distinct from the M_{1-2} metamorphism, the succeeding retrograde events, M_3 and M_4 were not as pervasive and were restricted mainly to areas of high strain. M_3 retrogression was clearly initiated prior to D_3 but its effects were most severe in regions of intense D_3 deformation, namely the mylonite zone. In that zone, upper greenschist facies conditions were encountered.

The M_4 event was very local in extent and restricted to D_4 structures. Middle greenschist facies conditions are inferred but the nature of M_4 alteration, particularly adjacent to the Mt. Parapet lineament, suggests that the mobility of volatiles (e.g. H_2O) played an essential role.

Development of the various minerals in relation to the metamorphic and structural events is outlined schematically in Figure 7.15 a-b and clearly illustrates the falling metamorphic grade from M_1 to M_4. This gradual decrease in grade is also reflected by the P-T conditions estimated for each event and is summarized in Figure 7.15 c. The P-T conditions indicated on that diagram for the M_{1-2} event when compared with P-T trajectories from various plate tectonic environments, represent an initial metamorphic evolution midway between those of plate interiors (e.g. Barrovian type meta-

morphism) and volcanic/plutonic complexes (e.g. Buchan or Abukuman type metamorphism; Ernst, 1975). They suggest either a somewhat higher thermal gradient of M_{1-2} (100-110°C/kb) than present day gradients (50-100°C/kb; Stewart, 1977); or else a local heat source superimposed on the normal regional gradient.

Comparing P-T conditions of M_3 with those of M_{1-2}, there is clearly a decrease in pressure and temperature of the order of 1.5-2 kb and 150°C respectively. A pressure decrease of this magnitude represents something like 5-8 km uplift either between the M_{1-2} and M_3 events or early during the M_3 event. With such an uplift there is undoubtedly going to be considerable erosion leading to deposition of a substantial pile of Carpentarian sediments. While there are minor exposures of younger Carpentarian sediments (e.g. Corunna Conglomerate and Moonabie Formation) no major sequences of Carpentarian rocks have yet been identified in South Australia. However it is surmised that low grade metasediments (dolomitic siltstones) underlying Adelaidean rocks on Yorke Peninsula (e.g. see Parker and Thomson, 1977) may perhaps be these missing sediments rather than Hutchison Group sediments as is currently believed (Thomson, 1976).

CHAPTER VIII

CONCLUSIONS AND TECTONIC IMPLICATIONS

8.1 SUMMARY OF CONCLUSIONS

In detailing the general geological framework of rocks in a small area of the Cleve Uplands between Cowell and Cleve, several very important conclusions have been reached which not only refer to the evolution of this particular area, but which also shed light on the geology of the whole Gawler orogenic domain (Glen et al, 1977).

8.1.1 Lithology

Detailed mapping of the Cowell/Cleve area has substantially modified the original South Australian Geological Survey mapping (Johns, 1957 and 1961). According to John's mapping, the area in question could be subdivided into two braod zones: a northwestern (Hutchison) "schist group" zone and a southeastern (Flinders) "gneiss group" zone, the difference between them being the level of metasomatism or granitization (Plan 1).

In the northwestern zone, mapping at the 1:20 000 scale has detailed a complexly folded, variously metamorphosed sequence of metasediments. John's reconnaissance type mapping is necessarily grossly over simplified and while he recognized most of the major lithologies (e.g. quartzite, dolomite, amphibolite, iron formation, schist and gneiss) he did not differentiate them. This study therefore has added considerably to his mapping for not only has it detailed the outcropping distribution of each lithology but it has also outlined variations within them. Specifically, a zone of partial migmatization accompanied by various mineralogical changes has been defined (Figs. 2.2 and 7.1).

In the southeastern zone detailed mapping has identified

two separate granite bodies and several remnants of metasediments. The granites have been differentiated on the basis of lithology and structure, and both are clearly of an intrusive nature. This zone of granites intruding metasediments is flanked on its southeastern side by a major mylonite zone recognized in this region for the first time.

8.1.2 Stratigraphy

No doubt one of the most important conclusions reached by this study is the definition of a working stratigraphy for the Cleve Uplands. Previous investigations because of their regional approach have never fully understood the detailed structural, plutonic and metamorphic evolution of the area and consequently have never been able to satisfactorily resolve the stratigrahical relationships between the various lithologies. However in this study by seeking a better understanding of the geological evolution of the rocks, it has been possible to erect a simple stratigraphy. Furthermore it has also enabled much of the confusion over terminology to be resolved.

In the Cowell/Cleve area all the metasedimentary rocks have been referred to a single group, the Hutchison Group. Although that term has been variously used (e.g. cf Tilley, 1920; Johns, 1961; Thomson, 1969; Webb and Thomson, 1977) with consequent confusion, it is significantly well entrenched in the literature to warrant its retention in the strict context implied by Tilley (1920) viz. to include all the (Proterozoic) metasediments. There is no justification to prefer any other name (e.g. Cleve Metamorphics (Thomson, 1969), or Middleback Group (Miles, 1954)) because they are either misrepresentative or they apply to only a part of the total succession.

The Hutchison Group as it has been described in this thesis (Chapter V, Fig. 5.7), consists of a thin basal calcsilicate unit, overlain successively by a major clastic quartzite unit tentatively equated with the Warrow Quartzite, dolomite, iron formation, semipelitic gneiss and schist with local interbanded amphibolite, a second iron formation (the Mt. Shannon iron formation), and finally more pelitic to semipelitic schist and gneiss. There is a good correlation of this sequence with other parts of the Cleve Uplands and furthermore, that part of the sequence beginning at the top of the Warrow Quartzite and going up to and including the Mt. Shannon iron formation also correlates well with the Middleback Group defined by Miles (1954). Therefore it is concluded that the Hutchison Group as detailed here is valid for all of northeastern Eyre Peninsula.

Related to the confusion over the definition of the Hutchison Group is the definition of Flinders Group. In this thesis the approach adopted by Coin (1976) has been adhered to in that all intrusive granites (and granite gneisses) have been called by their locality names whereas the name Flinders Group has been reserved strictly for those rocks considered as basement to the Hutchison Group. This is preferred over Miles' 'Gneiss Complex' although the two may prove to by synonymous.

Within the study area at Plug Range, a unit of granite gneiss has been tentatively labelled as the Flinders Group. It has been demonstrated that it lies structurally below the Warrow Quartzite and was probably formed at ca 2150 Ma.

8.1.3 Igneous, Metamorphic and Structural Evolution

Prior to this study, nothing much was known of the geological evolution of the Hutchison and Flinders Groups

in the Cleve Uplands. This study of their evolution has been based on a detailed structural analysis and the structure has been used as a datum to which both plutonism and metamorphism could be referred. Five principal deformation events have been recognized. The first was a fabric forming deformation possibly related to macroscopic isoclinal folding. It was a high grade deformation and produced pervasive planar fabrics. Overprinting it was a second intensive deformation D_2 producing macroscopic isoclinal folds and strong, axial planar, L-S type fabrics. High grade recrystallization and new grain growth were well advanced and dominated production of the observed fabrics. The third deformation D_3 was of somewhat lesser intensity producing in general tight, but not isoclinal, upright folds. However its intensity was varied and a gradual increase in strain recorded by meso- and microstructures has been documented going from northwest to southeast. Two zones of intense strain have been mapped and they are the deformed zone of the Narridy Creek granite and the eastern mylonite zone. In both zones strong L-S and S type fabrics have been produced by intense recrystallization and new grain growth. Elsewhere recrystallization is largely restricted although recovery processes are prominent. The final ductile deformation affecting the area, D_4, was only local in extent and did not produce many macroscopic effects. By contrast with the preceding deformations even recovery processes were of little importance.

Orientations of macroscopic features produced during the D_2 and D_3 events were largely north-south to northeast-southwest. D_2 structures were noticeably more constant in orientation (north-south) than the overprinting D_3 structures and this is seen as a consequence of the nature of those

deformations, D_2 being the more pervasive more intense deformation whereas D_3 was much more varied in style, intensity and orientation. D_4 structures represent a major change in the direction of strain and are oriented east-west and north-west - south-east. Subsequent to these ductile events, essentially brittle processes took over and are represented by north-south and northeast - south-west trending faults.

Allied to the deformational evolution, four principal stages of metamorphic evolution have been recognized. Collectively they represent a single cycle of metamorphism but with pulses of increased recrystallization consequent upon increased driving energy or mobility of components induced by each of the deformations. The first two metamorphic stages were difficult to separate but are believed to consist of a principal M_1 migmatization event which produced most of the observed parageneses, modified by a second M_2 event. Metamorphic grade was of upper amphibolite facies during both events with a peak during the M_1 stage. During that stage sillimanite was widespread and muscovite + quartz reacted to form orthoclase + sillimanite within the migmatized zone. However orthoclase + sillimanite was also produced during the M_2 episode and consequently the isogradic surfaces cut across macroscopic D_2 folds reflecting the combined effect of M_1 and M_2. The style of this M_{1-2} metamorphism has been described as midway between Barrovian and Buchan types indicating moderate pressure and a relatively high thermal gradient. Subsequent metamorphism was of retrograde character. Both the M_3 and M_4 stages were of much lower grade than the preceeding stages and their effects were only of very local extent. However within the highly deformed zones where there would have been a greater mobility of components and

more energy available, partial to almost complete alteration of the high grade assemblages was facilitated. In those zones greenschist facies conditions for M_3 and M_4 are implied.

Plutonism within the study area is represented by the syntectonic Middle Camp and Narridy Creek granites. These two igneous bodies are closely related spatially, but their lithology and structure easily distinguish them. In view of its S_2 fabric deformed by D_3 and D_4, the Middle Camp granite is believed to have been intruded either pre- or syn D_2. Its eastern phase contains numerous metasedimentary inclusions (mainly of altered dolomite) but its central phase at Middle Camp proper is largely massive and devoid of any such remnants. Compositionally it is granodioritic of quartz-plagioclase-microcline-biotite (-sphene) mineralogy. It was intruded at ca 1650 Ma.

By contrast to the Middle Camp granite, the Narridy Creek granite is slightly more alkaline. Much of it was deformed by the D_3 event so it must have been intruded either prior to or during that deformation. Its date of intrusion is estimated to be ca 1600 Ma.

8.1.4 Regional Correlation

Correlation of the geological evolution of the Cowell/Cleve area with adjacent areas of the Cleve Uplands, with the Middleback Ranges and with southern Eyre Peninsula is good. It has been demonstrated that the stratigraphy of the Hutchison Group as defined by this study is consistent over northeastern Eyre Peninsula and that there are many similarities with rocks of southern Eyre Peninsula.

Detailed structural studies are still very much in their infancy but again there are major similarities. In

both the Middleback Ranges and southern Eyre Peninsula tight, upright folds of identical character to F_3 of this study have been well documented. The major D_3 related mylonite zone described in this study has many similar characteristics with that in southern Eyre Peninsula and the presence of a major aeromagnetic anomaly connecting them further enhances their correlation (see Coin and Parker, in press). Earlier isoclinal folding perhaps corresponding to F_2, and later F_4 cross folding have been recorded in all areas but their details are still vague. Nevertheless it is clear that all of eastern Eyre Peninsula has been subjected to a complex fold history and that at least the D_3 and D_4 events were major widespread deformations.

Detailed metamorphic studies are also in their infancy, but a comparison of the metamorphic evolution of the Tumby Bay region with that envisaged here shows some very important parallels. These are the presence of an early pre-D_3, high grade event and its low pressure/high thermal gradient character. The highest grade rocks in the Tumby Bay region are in the east and likewise in the Cowell area a similar regional zonation has been recorded. Probably the most significant major discrepancy is the timing of metamorphism. On southern Eyre Peninsula dates of ca 1800 Ma have been variously quoted for the major metamorphic event whereas in the Cowell area ca 1700 Ma has been quoted. This implies either that rocks of the Cowell region remained deeper in the crust for a longer time than those of southern Eyre Peninsula, or alternatively, that the peak event was not synchronous in both areas.

The correlation of the geologic evolution of Eyre Peninsula with that of other parts of the Gawler sub-province

CHRONOLOGY OF EVENTS IN THE CLEVE UPLANDS

EASTERN EYRE PENINSULA

FIG. 8.1

AGE (million years)

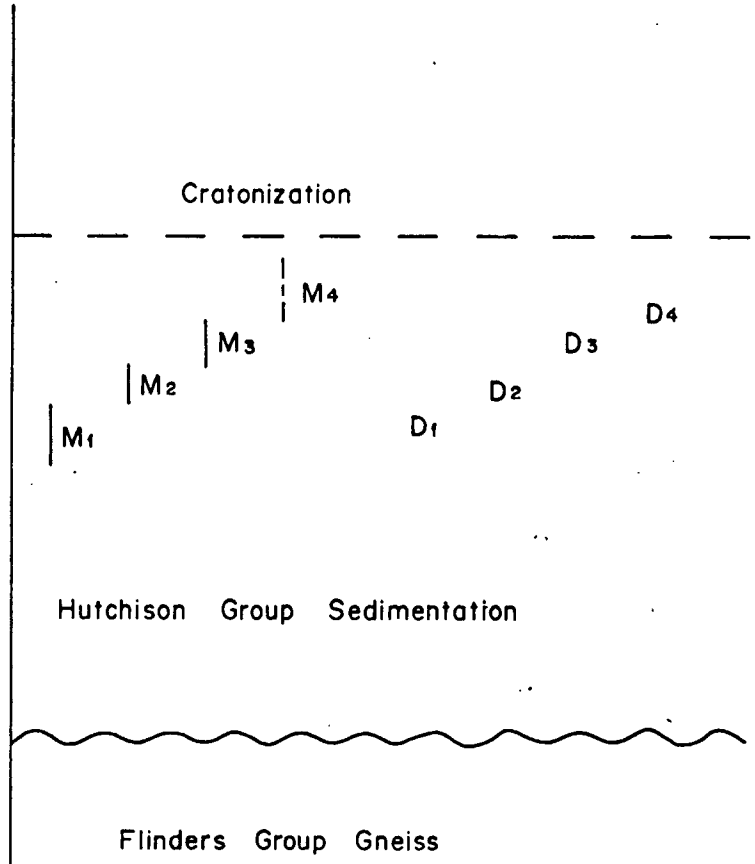
1000

1500

2000

2500

- Hiltaba and Charleston Granites.
  - Morowie Migmatite Gneiss (K–Ar)
- Gawler Range Volcanics.
  - Middlecamp Granite.
  - Metamorphism. (Plug Range Granite Gneiss & Mangalo Creek Schist)
- Kirton Point Granite Gneiss.
  - Plug Range Granite Gneiss.
- Glenloth Granite
- Whidbey Granite.
- Cape Carnot Augen Gneiss.



S13208

has been discussed by Glen et al (1977). That paper has been included as an appendix to this thesis (Appendix C).

8.2 TECTONIC IMPLICATIONS

It is beyond the means and scope of this thesis to comprehensively examine the tectonics of Eyre Peninsula in relation to well known tectonic regimes (e.g. with Phanerozoic tectonics). However since this thesis covers such a large part of the geological history of Eyre Peninsula it is valuable to record some observations.

The tectonic evolution of the Cowell/Cleve area is summarized in Figure 8.1. Sedimentation of the Hutchison Group occurred sometime during the interval 2100-1850 Ma and is believed to have been coeval with many of the world's major iron formations of the Hamersley or Lake Superior type. Sedimentation was on an older Precambrian basement, the Flinders Group, which has been variously dated at ca 2150-2600 Ma. That basement is locally exposed in the cores of anticlines.

Subsequent to sedimentation, the Hutchison Group was buried and underwent an extended period of intense deformation and metamorphism. The relative timing of the various stages of deformation, metamorphism and plutonism is illustrated in Figure 8.1. The metamorphic date of ca 1700 Ma obtained from the Plug Range granite gneiss and Mangalo Creek schist is believed to represent the terminal stage of the principle M_1/D_1 event. That event effected the homogenization of Rb and Sr and may well be related to the intrusion of the Kirton Point granite gneisses on southern Eyre Peninsula at ca 1820 Ma (Cooper et al, 1976).

From the available geochronology, the ensuing M_2/D_2 and M_3/D_3 events can be dated fairly specifically. The ca

1650 Ma age for the Middle Camp granite can be directly applied to the M_2/D_2 event since that granite was intruded during D_2. That figure can also be applied to the M_3/D_3 event since that event must postdate it. An upper constraint on the timing of the M_3/D_3 event is applied by the earliest extrusion of the Gawler Range Volcanics at ca 1550 Ma. The volcanics are relatively flat lying, lie unconformably on the folded Hutchison Group, and clearly postdate the D_3 deformation. Hence the major M_3/D_3 event occurred at ca 1650-1550 Ma. Specific timing of the M_4/D_4 event, however, is still partly obscure. Some parts of the Gawler Range Volcanics and Corunna Conglomerate have been weakly deformed about east-west axes and it is possible that this reflects D_4 movement within the basement. A K-Ar age of ca 1480 Ma for biotites from the migmatite gneisses at Morowie and from the Middle Camp granite certainly suggests that some mobility of components has been operative until that time. Therefore the M_4/D_4 event is considered to have occurred sometime around 1500-1550 Ma.

That ca 1480 Ma age also corresponds with the final episode of plutonism recorded in the Gawler domain (ca 1450-1500 Ma for the Charleston and Hiltaba granite suite). It heralds the cessation of major tectonic activity within the region. Subsequent events have been the deposition of thin, platformal Adelaidean sediments and minor block faulting. The Adelaidean sediments of the Stuart Shelf unlike their counterparts in the Adelaide Geosyncline and the platform areas of the Willyama domain, are not deformed (for a discussion see Glen et al, 1977).

Considering the Cowell/Cleve area in a much broader context as part of the Gawler domain, it belongs to the

major Proterozoic Arunta-Gawler Province (Rutland 1973, 1976). By comparison with the Phanerozoic, Rutland (1973) notes that the Proterozoic provinces of Australia are in many respects similar to the miotectonic (miogeosynclinal) belts of Phanerozoic cordilleran orogenies but with significant differences due to the greater mobility and higher geothermal gradients of the (?) thinner Precambrian lithosphere. In their concluding discussion, Glen et al (1977) also note the similarity between "the style of deformation and sequence of events in the Gawler sub-province" and "some high-grade zones of Phanerozoic orogenies." In particular though they draw an anology with the Omineca Crystalline Belt of the Canadian Cordillera.

The Omineca Crystalline Belt occupies the core zone of the Columbian Orogen which is the eastern, miotectonic section of the Canadian Cordillera (Wheeler et al, 1972). Characteristics of this zone are,

1) miogeosynclinal or platform type sedimentation - carbonates and quartzites abundant on the cratonic side passing laterally away from that (and also upwards) into more pelitic units. Basic volcanics (continental tholeites) are common and there are local iron formations of the Lake Superior type.
2) an older Precambrian crystalline basement represented by granitoid gneisses in the cores of gneiss domes.
3) complex polyphase deformation with considerable variation in style and shape. There is local recumbent folding and, in regions where deformation has outlasted metamorphism, there is also local mylonitization.

4) numerous granitic plutons - elongate, sinuous batholiths and smaller plutons, some post-tectonic, others syntectonic with the younger intrusions being more leucocratic and richer in quartz and K-feldspar.

5) greenschist to upper amphibolite facies metamorphism characteristic of moderate pressure Barrovian series (Slocan facies series, Read, 1973), high thermal gradients being characteristic.

As can be clearly seen, all of these features are remarkably similar to the geology of the Cowell/Cleve area. With the presence of an older PreCambrian basement now confirmed and particularly to the southwest and northwest (Webb and Thomson, 1977), the sedimentalogical model for eastern Eyre Peninsula consists of a miogeosynclinal or platformal sequence deposited on an older granitic basement. The deformational and plutonic evolution of the area as summarized in Figures 8.1 and 8.2 is also analogous to the miotectonic zone of a plate margin. Hence it is concluded that the rocks of the Cowell/Cleve area belong to a tectonic environment characterized by an active plate margin. That margin in this model would lie off to the east of Eyre Peninsula with an eutectonic zone beneath the Adelaide Geosyncline and/or Murray Basin. It confirms many of the Gondwanaland reconstructions that place its margins in such a position (e.g. Rutland, 1973; Goodwin, 1973).

REFERENCES CITED

Ashby, M.F. and Verall, R.A., 1973. Diffusion-accommodated flow and superplasticity. Acta Met., 21:149-163.

Asklund, B., Brown, W.L. and Smith, J.V., 1962. Hornblende - cummingtonite intergrowths. Am. Mineral., 47:160-163.

Ayrton, S.N. and Ramsay, J.G., 1974. Tectonic and metamorphic events in the Alps. Schweiz. Mineral. Petrogr. Mitt., 54:609-639.

Baeta, R.D., 1969. Slip systems in quartz: I Experiments. II Interpretation. Am. Mineral., 54:1551-1582.

Barclay, C.J., 1967. The petrology and geochemistry of some amphibolites from the Middleback Range. B. Sc. (Hons) thesis, Univ. Adelaide (unpubl.).

Bayley, R.W. and James, H.L., 1973. Precambrian iron formations of the United States. Econ. Geol., 68:934-959.

Bell, T.H. and Etheridge, M.A., 1973. Microstructure of mylonites and their descriptive terminology. Lithos, 6:337-348.

Bell, T.H. and Etherige, M.A., 1976. The deformation and recrystallization of quartz in a mylonite zone, Central Australia. Tectonophysics, 32:235-267.

Beukes, N.J., 1973. Precambrian iron formations of Southern Africa. Econ. Geol., 68:960-1004.

Binns, R.A., 1964. Zones of progressive regional metamorphism in the Willyama Complex, Broken Hill district, New South Wales. J. geol. Soc. Aust., 11:283-330.

Binns, R.A., 1965. The mineralogy of metamorphosed basic rocks from the Willyama Complex, Broken Hill district, New South Wales. Mineralog. Mag., 35:306-326.

Bonnischen, B., 1969. Metamorphic pyroxenes and amphiboles

in the Biwabik Iron Formation, Dunka River, Minnesota. Mineralog. Soc. Am. Spec. Paper 2:217-239.

Bouchez, J.L., 1977. Plastic deformation of quartzite at low temperature in an area of natural strain gradient. Tectonophysics, 39:25-50.

Boullier, A.M. and Gueguen, Y., 1975. SP Mylonites : origin of some mylonites by superplastic flow. Contrib. Mineral. Petrol., 50:93-104.

Bridges, M.C. and Etheridge, M.A., 1974. A computer program to contour orientation densities. Dept. of Geol. and Mineral., Univ. of Adelaide, unpubl. report.

Brown, E.H., 1969. Some zoned garnets from the greenschist facies. Am. Mineralog., 54:1662-1677.

Brown, E.H., 1971. Phase relations of biotite and stilpnomelane in the greenschist facies. Contrib. Mineral. Petrol., 31:275-299.

Brown, W.L., 1962. Peristerite unmixing in the plagioclases and metamorphic facies series. Norsk Geol. Tidsskr. (Feldspar vol.), 42:354-382.

Button, A., 1976. Iron formations as an end member in carbonate sedimentary cycles in the Transvaal Supergroup, South Africa. Econ. Geol., 71:193-201.

Carmichael, D.M., 1969. On the mechanism of prograde metamorphic reactions in quartz bearing pelitic rocks. Contrib. Mineral. Petrol., 20:244-267.

Carmichael, D.M., 1970. Intersecting isograds in the Whetstone Lake Area, Ontario. J. Petrol., 11:147-181.

Carter, N.L. and Raleigh, C.B., 1969. Principal stress directions from plastic flow in crystals. Geol.

Soc. Am. Bull., 80:1231-1264.

Chadwick, B., 1968. Deformation and metamorphism in the Lukmanier region, Central Switzerland. Geol. Soc. Am. Bull., 79:1123-1150.

Chinner, G.A., 1966. The significance of the aluminium silicates in metamorphism. Earth Sci. Rev., 2:111-126.

Chinner, G.A., 1966. The distribution of pressure and temperature during Dalradian metamorphism. Quart. J. Geol. Soc. London, 112:159-186.

Clarke, N.G., 1976. Structural analysis of the Port Neill mylonite zone and its country rocks, Port Neill, South Australia. B. Sc. (Hons) thesis, Univ. of Adelaide (unpub.).

Cloos, E., 1971. Microtectonics along the western edge of the Blue Ridge, Maryland and Virginia. John Hopkins Univ. Press, Baltimore, 234 pp.

Coin, C.D.A., 1976. A study of the Precambrian rocks in the vicinity of Tumby Bay, Southern Eyre Peninsula. Ph. D. thesis, Univ. Adelaide (unpubl.).

Coin, C.D.A. and Parker, A.J., (in prep.). A major mylonite zone on Eastern Eyre Peninsula, South Australia.

Collerson, K.D., 1974. Descriptive microstructural terminology for high-grade metamorphic tectonics. Geol. Mag., 111:313-318.

Compston, W. and Arriens, P.A., 1968. The Precambrian geochronology of Australia. Can. J. Earth Sci., 5:561-583.

Compston, W., Crawford, A.R. and Bofinger, V.M., 1966. A radiometric estimate of the duration of sedimentation in the Adelaide geosyncline, South Australia.

J. geol. Soc. Aust., 13:229-276.

Cooper, A.F., 1974. Multiphase deformation and its relationship to metamorphic crystallization at Haast River, South Westland, New Zealand. N.Z. J. of Geol. Geophys., 17:855-880.

Cooper, J.A., Fanning, C.M., Flook, M.M. and Oliver, R.L., 1976. Archaean and Proterozoic metamorphic rocks on southern Eyre Peninsula, South Australia. J. geol. Soc. Aust., 23:287-292.

Crawford, M.L., 1966. Composition of plagioclase and associated minerals in some schists from Vermont U.S.A., and South Westland, New Zealand, with inference about the Peristerite solvus. Contrib. Mineral. Petrol., 13:269-294.

Currie, K.L., 1971. The reaction 3 Cordierite = 2 Garnet + 4 Sillimanite + 5 quartz as a geological thermometer in the Opinicon Lake Region, Ontario. Contrib. Mineral. Petrol., 33:215-226.

Currie, K.L., 1974. A note on the calibration of the garnet-cordierite geothermometer and geobarometer. Contrib. Mineral. Petrol., 44:35-44.

Dallmeyer, R.D., 1972. Precambrian structural history of the Hudson Highlands near Bear Mountain, New York. Geol. Soc. Am. Bull., 83:895-904.

Daly, S., Webb, A.W. and Whitehead, S.G., 1978. Archaean to early Proterozoic banded iron formations in the Tarcoola region, South Australia. S. Aust. Dept. Mines report 77/148 (unpubl.).

Deelman, J.C., 1974. Granulo-mechanical aspects of lithification I. N. Jb. Geol. Paläout. Abh., 147;1-29.

Dieterich, J.H., 1969. Origin of cleavage in folded rocks. Am. J. Sci., 267;155-165.

Duncan, N., 1976. Exploration Licence No. 218 "Mount Messenger", South Australia, Relinquishment Report. S. Aust. Dept. Mines open file Env. 2732 (unpubl.).

Durney, D.W., 1972. Solution-transfer, an important geological deformation mechanism. Nature, 235:315-316.

Edgeworth, D.T.W., 1932. Notes to the Geological Map of Australia.

Edwards, A.B., 1936. The iron ores of the Middleback Ranges, South Australia. Proc. Aust. Inst. Min. Metall., 102:155-207.

Engel, A.E.J. and Engel, C.G., 1958. Progressive metamorphism and granitization of the major paragneiss, Northwest Adirondack Mountains, New York. Geol. Soc. Am. Bull., 69:1369-1414.

Ernst, W.G. (ed.), 1975. Subduction Zone Metamorphism. Dowden, Hutchinson and Ross, 445 pp.

Etheridge, M.A. and Hobbs, B.E., 1974. Chemical and deformational controls on recrystallization of mica. Contrib. Mineral. Petrol., 43:111-124.

Etheridge, M.A. and Lee, M.F., 1975. Microstructure of slate from Lady Loretta, Queensland, Australia. Geol. Soc. Am. Bull., 86:13-22.

Fanning, C.M., 1975. Petrology, structure and geochronology of some high grade metamorphic rocks at Fishery Bay and Cape Carnot, southern Eyre Peninsula. B. Sc. (Hons) thesis, Univ. Adelaide (unpubl.).

Flinn, D., 1965. Deformation in metamorphism. pp. 46-72 in Controls of Metamorphism, W.S. Pitcher and G.W. Flinn (eds). Oliver and Boyd, Edinburgh, 368 pp.

Flook, M.M., 1975. The geology and geochronology of high grade metamorphic rocks at Kirton Point and Cape Donnington, southern Eyre Peninsula. B. Sc. (Hons) thesis, Univ. Adelaide (unpubl.).

Forbes, W.C., 1977. Stability relations of grunerite, $Fe_7Si_8O_{22}(OH)_2$ Am. J. Sci., 277:735-749.

Frears, R.A., 1969. Petrology of the gneisses and associated amphibolites from Sleaford-Fishery Bay, southern Eyre Peninsula. B. Sc. (Hons) thesis, Univ. Adelaide (unpubl.).

Furber, D.V. and Cook, J.N., 1976. Middleback Range Iron Ores. In Knight, C.L. (ed), Economic Geology of Australia and Papua New Guinea. Australas. Inst. Min. Metall., Melbourne, pp. 945-951.

Ghosh, S.K. and Ramberg, H., 1976. Reorientation of inclusions by combination of pure shear and simple shear. Tectonophysics, 34:1-70.

Ghosh, S.K. and Sengupta, S., 1973. Compression and simple shear of test models with rigid and deformable inclusions. Tectonophysics, 17:133-176.

Giddings, J.W. and Embleton, B.J.J., 1976. Precambrian palaeomagnetism in Australia. II : Basic dykes from the Gawler Block. Tectonophysics, 30:109-118.

Glassley, W.E., 1975. High grade regional metamorphism of some carbonate bodies : significance for the orthopyroxene isograd. Am. J. Sci., 275:1133-1163.

Glen, R.A., Laing, W.P., Parker, A.J. and Rutland, R.W.R., 1977. Tectonic relationships between the Proterozoic Gawler and Willyama Orogenic Domains, Australia. J. geol. Soc. Aust., 24:125-150.

Goldich, S.S., 1973. Ages of Precambrian banded iron formations. Econ. Geol., 68:1126-1134.

Goodwin, A.M., 1973. Archaean iron formations and tectonic basins of the Canadian Shield. Econ. Geol., 68:915-933.

Green, H.W., Griggs, D.T. and Christie, J.M., 1970. Syntectonic and annealing recrystallization of fine grained quartz aggregates. In Paulitsch (ed.), Experimental and Natural Rock Deformation, Springer-Verlag, pp. 272-335.

Green, J.C., 1963. High level metamorphism of pelitic rocks in northern New Hampshire. Am. Mineralog., 48:991.

Guidotti, C.V., 1966. Prograde formation of muscovite pseudomorphs after staurolite and the formation of large megacrysts of muscovite. Geol. Soc. Am. Spec. Paper 87:206.

Hayden, H.W., Floreen, S. and Goodell, P.D., 1972. The deformation mechanism of superplasticity. Metal. Trans., 3:833-842.

Heinrich, E.W., 1965. Microscopic Identification of Minerals. McGraw-Hill, 414 pp.

Hensen, R.J. and Green, D.H., 1971. Experimental study of the stability of Cordierite and garnet in pelitic compositions at high pressures and temperatures. I. Contrib. Mineral. Petrol., 33:309-330.

Hewitt, D.A., 1973. The metamorphism of micaceous limestones from south-central Connecticut. Am. J. Sci., 273A:444-469.

Hirschberg, A. and Winkler, H.G.F., 1968. Stabilitatsbeziehungen Zwischen Chlorit, cordierit und Almandin bei der Metamorphose. Contrib. Mineral. Petrol., 18:17-42.

Hobbs, B.E., 1968. Recrystallization of single crystals of quartz. Tectonophysics, 6:353-401.

Hobbs, B.E., 1971. The analysis of strain in folded layers. Tectonophysics, 11:329-375.

Hobbs, B.E., McLaren, A.C. and Paterson, M.S., 1972. Plasticity of single crystals of synthetic quartz. In Heard et al (eds), Flow and Fracture of Rocks, Am. Geophys. Union, Monograph Ser. 16, pp. 29-53.

Hobbs, B.E., Means, W.D. and Williams, P.F., 1976. An outline of structural geology. John Wiley and Sons, 571 pp.

Holdaway, M.J., 1971. Stability of andalusite and the aluminium silicate phase diagram. Am. J. Sci., 271:97-131.

Hopwood, T., 1977. Conformable elongate orebodies and intrafolial folds parallel to a mineral streaking lineation. Geol. Soc. Sth. Africa Spec. Publ. No. 4.

Hoschek, G., 1967. Untersuchungen zum stabilitatsbereich von chloritoid und staurolith. Contrib. Mineral. Petrol., 14:123-162.

Hoschek, G., 1969. The stability of staurolite and chloritoid and their significance in metamorphism of pelitic rocks. Contrib. Mineral. Petrol., 22:208-232.

Hudleston, P.J., 1976. Early deformational history of Archaean rocks in the Vermilion district, northeast Minnesota. Can. J. Earth Sci., 13:579-592.

Hyndman, D.W., 1968. Petrology and structure of the Nakusp Map area, British Columbia. Geol. Survey Canada Bull. 161. 95 pp.

Hyndman, D.W., 1972. Petrology of Igneous and Metamorphic Rocks. McGraw-Hill, 533 pp.

I.U.G.S. Subcommission on the Systematics of Igneous Rocks, 1973. Classification and nomenclature of plutonic rocks. Recommendations. N. Jb. Miner. Mh., 4:149-164.

Jack, R.L., 1914. The geology of the County of Jervois, and of portions of the Counties of Buxton and York, with special reference to underground water supplies. Geol. Surv. S. Aust. Bull. 3, 47 pp.

Jack, R.L., 1922. The iron ore resources of South Australia. Geol. Surv. S. Aust. Bull. 9, 71 pp.

Jefferey, G.B., 1923. The motion of ellipsoidal particles immersed in a viscous fluid. Roy. Soc. London Proc, Ser. A, 102:161-177.

Johannes, W., 1968. Experimental investigation of the reaction forsterite + water = serpentine + brucite. Contrib. Mineral. Petrol., 19:309-315.

Johannes, W., 1969. An experimental investigation of the system $MgO-SiO_2-H_2O-CO_2$. Am. J. Sci., 267;1083-1104.

Johns, R.K., 1955. Serpentinized marble deposit near Cowell. S. Aust. Dept. Mines report 41/126 (unpubl.).

Johns, R.K., 1957. Cowell map sheet, Geological Atlas of South Australia, 1:63 360 series. Geol. Surv. S. Aust.

Johns, R.K., 1961. Geology and mineral resources of southern Eyre Peninsula. Geol. Surv. S. Aust. Bull. 37, 102 pp.

Johns, R.K., 1963. Limestone, dolomite and magnesite resources of South Australia. Geol. Surv. S. Aust. Bull. 38, 100 pp.

Johnson, M.R.W., 1970. Torridonian and Moinian. In Craig, G.Y. (ed), The Geology of Scotland. Oliver and Boyd, Edinburgh, 556 pp.

Jones, M.T., 1968. Structural geology of the South Middleback Range. B. Sc. (Hons) thesis, Univ. Adelaide (unpubl.).

Kamb, W.B., 1959. Theory of preferred orientation developed by crystallization under stress. J. Geol., 67:153-170.

Kerrick, D.M., 1972. Experimental determination of muscovite + quartz stability with $P_{H_2O} < P_{total}$. Am. J. Sci., 272:946-958.

Klein, C., 1966. Mineralogy and petrology of the metamorphosed Wabush Iron Formation, southwestern Labrador. J. Petrol. 7:246-305.

Klein, C., 1973. Changes in mineral assemblages with metamorphism of some banded Precambrian iron formations. Econ. Geol., 68:1075-1088.

Knipe, R.J. and White, S.H., 1977. Microstructural variation of an axial plane cleavage around a fold - a H.V.E.M. study. Tectonophysics, 39:355-380.

Kuno, H., 1968. Differentiation of basaltic magmas. In Hess, H.H. and Poldevaart, A. (eds), Basalts. J. Wiley and Sons.

Lapworth, C., 1885. The highland controversy in British geology : its causes, course, and consequences. Nature, 32:558-559.

Laut, P. et al (compilers), 1977. Environments of South Australia. Province 4, Eyre and Yorke Peninsulas. C.S.I.R.O., Division of Land Use Research, Canberra.

Leake, B.E., 1964. The chemical distinction between ortho- and para-amphibolites. J. Petrol., 5:238-254.

MacLeod, W.N., 1966. The geology and iron deposits of the Hamersley Range area, Western Australia. Geol. Surv. W. Aust. Bull. 117.

MacQueen, J.A. and Powell, D., 1977. Relationship between deformation and garnet growth in Moine (Precambrian) rocks of western Scotland. Geol. Soc. Am. Bull., 88:235-240.

Mancktelow, N.S., (in prep.). Strain variation between quartz grains of differing crystallographic orientation in a naturally deformed siltstone.

March, A., 1932. Mathematische Theorie der regulung nach der korngestalt bei affiner deformation. Z. Krist., 81: 285-297.

Marjoribanks, R.W., 1976. The relation between microfabric and strain in a progressively deformed quartzite sequence from Central Australia. Tectonophysics, 32:269-294.

Marjoribanks, R.W., 1976. Basement and cover relations on the northern margin of the Amadeus Basin, central Australia. Tectonophysics, 33:15-33.

Mason, M.G., 1968. Marble and nephrite jade, Hd. Minbrie, Sect. 116, Eyre Peninsula. S. Aust. Dept. Mines report 66/158 (unpubl.).

Masters, F., 1950. Saga of Wangaraleednie. Lutheran Publishing House, 223 pp.

Mawson, D., 1907. Geological features of part of Eyre Peninsula. Trans. R. Soc. S. Aust., 31:71-76.

Means, W.D., 1977. Experimental contributions to the study of foliations in rocks : a review of research since 1960. Tectonophysics, 39:329-354.

Mehnert, K.R., 1968. Migmatites and the origin of granitic rocks. Elsevier, Amsterdam, 393 pp.

Metz, P. and Trommsdorff, V., 1968. On phase equilibria in metamorphosed siliceous dolomites. Contrib. Mineral. Petrol., 18:305-309.

Miles, K.R., 1954. Geology and iron ore resources of the Middleback Range area. Geol. Surv. S. Aust. Bull. 33, 247 pp.

Miyashiro, A., 1973. Metamorphism and Metamorphic Belts. Allen and Unwin, 492 pp.

Moorbath, S., 1975. Evolution of Precambrian crust from stontium isotope evidence. Nature, 254:395-398.

Moore, A.C., 1970. Descriptive terminology for the textures of rocks in granulite facies terrains. Lithos, 3: 123-127.

Morrison-Smith, D.J., Paterson, M.S. and Hobbs, B.E., 1976. An electron microscope study of plastic deformation in single crystals of synthetic quartz. Tectonophysics, 33:43-79.

Nichol, D., 1974. Nephrite jade deposit near Cowell, Eyre Peninsula. Min. Resources Rev. S. Aust., 144: 11-26.

Oertel, G., 1970. Deformation of a slaty, lapillar tuff in the Lake district, England. Geol. Soc. Am. Bull., 81:1173-1188.

Parker, A.J., (in prep). Microstructural development of mylonite near Cowell, eastern Eyre Peninsula.

Parker, A.J. and Thomson, B.P., 1977. Preliminary report on stratigraphic drilling in E.L. 207 and adjacent areas, northern Yorke Peninsula. S. Aust. Dept. Mines report 1125/73 (unpubl.).

Philpotts, A.R., 1964. Origin of pseudotachylites. Am. J. Sci., 262:1008-1035.

Poldervaart, A., 1955. Chemistry of the earths crust. Geol. Soc. Am. Spec. Paper 62:119-144.

Ramberg, H., 1952. Origin of Igneous and Metamorphic Rocks. Univ. Chicago Press.

Ramsay, D.M. and Sturt, B.A., 1970. Polyphase deformation of a polymict Silurian conglomerate from Mageroy, Norway. J. Geol., 78:264-280.

Ramsay, J.G., 1958. Superimposed folding at Loch Monar, Inverness-shire and Ross-shire. Geol. Soc. London, Quart, J., 113:271-308.

Ramsay, J.G., 1967. Folding and Fracturing of Rocks. McGraw-Hill, New York, 568 pp.

Ramsay, J.G. and Wood, D.S., 1973. The geometric effects of volume change during deformation processes. Tectonophysics, 16:263-277.

Ransom, D.M., 1971. Host control of recrystallized quartz grains. Mineralog. Mag., 38:83-88.

Rast, N. and Platt, J.I., 1957. Cross-folds. Geol. Mag., 94:159-167.

Read, P.R., 1973. Petrology and structure of Poplar Creek map-area, British Columbia. Geol. Surv. Canada, Bull. 193, 144 pp.

Rickard, M.J., 1961. A note on cleavages in crenulated rocks. Geol. Mag., 98:324-332.

Roberts, D. and Stromgard, K.E., 1972. A comparison of natural and experimental strain patterns around fold hinge zones. Tectonophysics, 14:105-120.

Rooney, T.P., Riecker, R.E. and Gavasci, A.T., 1975. Hornblende deformation features. Geology, 3:364-366.

Rudd, E.A. and Miles, K.R., 1951. Iron ores of the Middleback Ranges, South Australia. S. Aust. Dept. Mines report 32/19 (unpubl.).

Rutland, R.W.R., 1973. Tectonic evolution of the continental crust in Australia. In Tarling, D.H. and Runcorn, S.K. (eds), Continental Drift, Sea Floor Spreading and Plate Tectonics : Implications to the Earth

Sciences, pp. 1003-1025. Academic Press, London.

Rutland, R.W.R., 1976. Orogenic evolution of Australia. Earth Sci. Rev., 12:161-196.

Rutland, R.W.R. and Etheridge, M.A., 1975. Two high grade schistosities at Broken Hill and their relation to major and minor structures. J. geol. Soc. Aust., 22:259-274.

Schwerdtner, W.M., 1970. Hornblende lineations in the Trout Lake area, Lac la Ronge map sheet, Saskatchewan. Can. J. Earth Sci., 7:884-899.

Seedsman, K.R., 1958. Gravity and magnetic traverses over aeromagnetic anomalies near Cowell, Eyre Peninsula. S. Aust. Dept. Mines report 46/101 (unpubl.).

Sibson, R.H., 1977. Fault rocks and fault mechanisms. J. Geol. Soc. London, 133:191-213.

Siddans, A.W.B., 1972. Slaty cleavage - a review of research since 1815. Earth Sci. Rev., 8:205-232.

Skippen, G., 1974. An experimental model for low pressure metamorphism of siliceous dolomitic marble. Am. J. Sci., 274;487-509.

Slaughter, J., Kerrick D.M. and Wall, V.J., 1975. Experimental and thermodynamic study of equilibria in the system $CaO-MgO-SiO_2-H_2O-CO_2$. Am. J. Sci., 275:143-162.

Soper, N.J. and Brown, P.E., 1971. Relationship between metamorphism and migmatization in the northern part of the Moine Nappe. Scott. J. Geol., 7: 305-325.

Spry, A., 1969. Metamorphic Textures. Pergamon Press, Oxford, 350 pp.

Storre, B. and Karotke, E., 1971. Experimentelle Anatexis von Glimmerschiefern in Modellsystemen. Fortschr. Mineral., 49:56-58.

Sturt, B.A., 1961. Preferred orientation of nepheline in deformed nepheline syenite gneisses, Sory, Northern Norway. Geol. Mag., 98:464-466.

Suzuki, T., 1970. X-Ray petrofabric analysis of quartz schists from central Shikoku, Japan, by X-Ray texture goniometer. In Paulitsch, P. (ed), Experimental and Natural Rock Deformation, pp. 1-18. Springer-Verlag.

Sylvester, A.G. and Christie, J.M., 1968. The origin of crossed girdle orientations of optic axes in deformed quartzites. J. Geol., 76:571-580.

Thompson, J.B., Robinson, P., Clifford, T.N. and Trask, N.J., 1968. Nappes and gneiss domes in west central New England. In Zen, E-An et al., (eds), Studies of Appalachian Geology : Northern and Maritime, pp. 203-218. Wiley-Interscience.

Thompson, J.B., Jn. and Norton, S.A., 1968. Palaeozoic regional metamorphism of pelitic schists. In Zen, E-An et al (eds), Studies of Appalachian Geology : Northern and Maritime pp. 319-327. Wiley-Interscience.

Thomson, B.P., 1969. The Precambrian crystalline basement. In Parkin, L.W. (ed), Handbook of South Australian Geology, pp. 21-48. Geol. Surv. S. Aust., Adelaide.

Thomson, B.P., 1976. Gawler craton - regional geology. In Knight, C.L. (ed), Economic Geology of Australia and Papua New Guinea, pp. 461-466. Australas. Inst. Min. Metall., Melbourne.

Tilley, C.E., 1920a. Metamorphism of Precambrian dolomites of southern Eyre Peninsula. Geol. Mag., 57:449-462.

Tilley, C.E., 1920b. The metamorphism of the Precambrian dolomites of southern Eyre Peninsula, South Australia. Geol. Mag., 57:492-500.

Tilley, C.E., 1921. The granite gneisses of southern Eyre Peninsula and their associated amphibolites. Geol. Soc. London, Quart, J., 77:75-134.

Tilley, C.E. 1921. Precambrian paragneisses of southern Eyre Peninsula, South Australia. Geol. Mag., 58:251-259.

Tilley, C.E., 1925. Petrographical notes on some chloritoid rocks. Geol. Mag., 62:309-318.

Tobisch, P.T., Fleuty, M.J., Merh, S.S., Mulhopadhyay, D. and Ramsay, J.G., 1970. Deformational and metamorphic history of the Moinian and Lewisian rocks between Strathconan and Glen Afric. Scott. J. Geol., 6: 243-265.

Tonkin, D.G., 1971. Exploration of S.M.L. 383, Franklin Harbour, South Australia. S. Aust. Dept. Mines open file Env. 1355 (unpubl.).

Toogood, D.J., 1976. Structural and metamorphic evolution of a gneiss terrain in the Namaqua Belt near Onseepkans, South West Africa. Univ. Cape Town, Chamber Mines Precambrian Res. Unit, Bull. 19, 189 pp.

Tullis, J., Christie, J.M. and Griggs, D.T., 1973. Microstructures and preferred orientations of experimentally deformed quartzites. Geol. Soc. Am. Bull., 84:297-314.

Tullis, T.E., 1976. Experiments on the origin of slaty cleavage and schistosity. Geol. Soc. Am. Bull.,

87:745-753.

Turner, F.J., 1941. The development of pseudo-stratification by metamorphic differentiation in the schists of Otago, New Zealand. Am. J. Sci., 239:1-16.

Turner, F.J., 1968. Metamorphic Petrology. McGraw-Hill, New York, 403 pp.

Turner, F.J. and Weiss, L.E., 1963. Structural Analysis of Metamorphic Tectonites. McGraw-Hill, New York, 545 pp.

Van de Kamp, P.C., 1968. Geochemistry and origin of metasediments in the Haliburton-Madoc area, southeastern Ontario. Can. J. Earth Sci., 5:1337-1370.

Vernon, R.H., 1962. Coexisting cummingtonite and hornblende in an amphibolite from Duchess, Queensland, Australia. Am. Mineral., 47:860-370.

Vernon, R.H., 1976. Metamorphic Processes. Allen and Unwin, 247 pp.

Vernon, R.H., 1977. Microfabric of mica aggregates in partly recrystallized biotite. Contrib. Mineral. Petrol., 61:175-185.

Vernon, R.H. and Ransom, D.M., 1971. Retrograde schists of the amphibolite facies at Broken Hill, New South Wales. J. geol. Soc. Aust., 18:267-278.

Waard, D. de, 1959. Anorthite content of plagioclase in basic and pelitic schists as related to metamorphic zoning in the Usamassif, Timor. Am. J. Sci., 257: 553-562.

Waters, A.C. and Campbell, C.O., 1935. Mylonites from the San Andreas fault zone. Am. J. Sci. 5th Ser., 29:473-503.

Webb, A.W. and Thomson, B.P., 1977. Archaean basement rocks in the Gawler Craton, South Australia. Search, 8:34-36.

Wenk, E., 1970. Zur regional metamorphose und ultrametamorphose im Lepontin. Fortschr. Mineral., 47: 34-51.

Wheeler, J.O., Aitken, J.D., Berry, M.J., Gabrielse, H., Hutchinson, W.W., Jacoby, W.R., Monger, J.W.H., Niblett, E.R., Norris, D.K., Price, R.A., and Stacey, R.A., 1972. The Cordilleran structural province. In Price, R.A. and Douglas, R.J.W., Variations in Tectonic Styles in Canada, pp. 1-82. Geol. Assoc. Canada, Spec. Paper 11.

White, S., 1973. The dislocation structures responsible for the optical effects in some naturally deformed quartzites. J. Mater. Sci., 9:490-499.

White, S., 1976. The effects of strain on the microstructures, fabrics and deformation mechanisms in quartzite. Phil. Trans. R. Soc., London, Ser. A.

White, S., 1977. Geological significance of recovery and recrystallization processes in quartz. Tectonophysics, 39:143-170.

Whitten, G.F., 1964. Report on the geology, geophysics and drilling, Hd. Miltalie, Sec. 60, Eyre Peninsula. S. Aust. Dept. Mines report 59/105 (unpubl.).

Whitten, G.F., 1966. Geology of South Australian iron deposits M. Sc. thesis, Univ. Adelaide (unpubl.).

Whitten, G.F., 1966. Suggested correlation of iron ore deposits within South Australia. Q. geol. Notes, geol. Surv. S. Aust., 18:7-11.

Williams, P.F., 1972a. Development of metamorphic layering and cleavage in low-grade metamorphic rocks at Bermagui, Australia. Am. J. Sci., 272:1-47.

Williams, P.F., 1972b. "Pressure shadow" structures in foliated rocks from Bermagui, New South Wales. J. geol. Soc. Aust., 18:371-377.

Williams, P.F., 1977. Foliations : a review and discussion. Tectonophysics, 39:305-328.

Williams, P.F., Collins, A.R. and Wiltshire, R.G., 1969. Cleavage and penecontemporaneous deformation structures in sedimentary rocks. J. Geol. 77: 415-425.

Wilson, C.J.L., 1973. The prograde microfabric in a deformed quartzite sequence, Mount Isa, Australia. Tectonophysics, 19:39-81.

Wilson, C.J.L., 1975. Preferred orientation in quartz ribbon mylonites. Geol. Soc. Am. Bull., 86:968-974.

Winkler, H.G.F., 1967. Petrogenesis of Metamorphic Rocks, 2nd ed. Springer-Verlag, New York, 320 pp.

Winkler, H.G.F., 1976. Petrogenesis of Metamorphic Rocks, 4th ed. Springer-Verlag, New York, 334 pp.

Wood, D.S., 1974. Current views of the development of slaty cleavage. Ann. Rev. Earth Sci., 2:1-35.

Zwart, H.J., 1963. Some examples of the relations between deformation and metamorphism from the central Pyrenees. Geol. Mijnbouw, 42:143-154.

APPENDIX C

in enclosure at the rear of

this volume.

Tectonic relationships between the Proterozoic Gawler and Willyama Orogenic Domains, Australia.

By R.A. Glen, W.P. Laing,

A.J. Parker and R.W.R. Rutland.

Reprint from

Journal of the Geological Society of Australia

Vol. 24, Pt. 3

pp. 125-150

June, 1977

LIST OF FIGURES

Enclosed in pocket at rear of Volume II		SADME	Plan No.
Plan 1	Geological Map: Portion of Eyre Peninsula (Scale 1:253 4400)	78-48	
Plan 2	Geological Map of the Cowell/Cleve District, Eyre Peninsula (Scale 1:20 000)	78-161	

VOLUME I

Figure No.		SADME	Plan No.
1.1	Locality plan	S13210	
1.2	Synopsis of previous stratigraphic nomenclature on Eyre Peninsula	78-855	
2.1	Regional variation in quartzite lithology	78-130	
2.2	Distribution of migmatite gneisses	78-62	
2.3	Modal compositions of semipelitic gneisses	S13211	
2.4	Modal compositions of amphibolites	S13212	
2.5	Modal compositions of granitic rocks	S13740	
3.1	Location of subarears and simplified geology	78-64	
3.2	Plate - F_2 folds in semipelitic rocks		
3.3	t' plots for various F_2 and F_3 folds	S13232	
3.4	Plate - L_2 lineations in semipelitic gneisses		
3.5	Plate - L_2 quartz rodding in quartzites		
3.6	Plate - F_2 folds in calcsilicates, amphibolite and Plug Range granite gneiss		
3.7	Plate - F_3 folds in semipelitic rocks		
3.8	Plate - F_3 folds in quartzite, Plug Range granite gneiss and Middle Camp granite		
3.9	Plate - Narridy Creek granite		
3.10	Plate - Mylonite zone - F_3 folds and slaty mylonite		
3.11	Plate - Mylonite zone in Mindrow Creek		
3.12	Plate - D_4 structures		
4.1	Structural map and stereodiagrams of the Wangaraleednie Subarea	78-856 and S13779	
4.2	Structural cross sections of the Wangaraleednie Subarea	s13744	
4.3	Structural map and stereodiagrams of the Mt. Millar/Morowie Subarea	78-857 and S13780	

		SADME Plan No.
4.4	Structural cross sections of the Mt. Millar/Morowie Subarea	S13748
4.5	Deformation of F_2 and L_2 lineations in the Mt. Millar/Morowie Subarea	S13745
4.6	Structural geology of the Calcookara Subarea	78-858 and S13781
4.8	Fabric elements in the Narridy Creek Subarea	78-859
4.9	Structural map and stereodiagrams of the Middle Camp Subarea	78-860
4.10	Structural cross sections of the Mattum area	S13749
4.11	Structural geology of the Ullabidinie Subarea	S13746
4.12	D_4 features in the Ullabidinie Subarea	S13750
4.13	Structural map of the Plug Range Subarea	S13747 and S13782
4.14	Structural cross sections of the Plug Range Subarea	S13751
4.15	Synoptic stereodiagrams and the assumed style of F_3 in the Cowell/Cleve district	S13225
4.16	Synoptic stereodiagram and deformation of F_2 and L_2 structures by F_3	S13752
4.17	Regional correlation of the structural evolution	S13743
5.1	Location of key stratigraphic cross sections	78-65
5.2	Geological cross-sections in the Wangaraleednie Subarea	S13227
5.3	Geological cross sections in the Mt. Millar Subarea	S13228
5.4	Geological cross sections in the Morowie Subarea	S13229
5.5	Geological cross sections in the Middle Camp Subarea	S13230
5.6	Geological cross sections in the Plug Range Subarea	S13231
5.7	Comparative stratigraphy of the sub-areas	S13207
5.8	Geochemistry of amphibolites	78-853

		SADME Plan No.
5.9	Geological Plan and cross section of the Cleveley/Glenhaven area	S13162
5.10A	Stratigraphic correlation in the Cleve Uplands	78-854
5.10B	Stratigraphy of the Middleback Ranges	S13741
5.10C	Inferred stratigraphy of southern Eyre Peninsula	S13742
5.11	Interpretative geological map and sections	78-153
Appendix A		
A1	Location of geochemical samples	
A2	Location of geochemical samples	S13771
Appendix B		
B1	Location of geochronology samples	78-862
VOLUME II		
6.1	Plate - S_1 mica	
6.2	Plate - S_1 sillimanite and M_1 garnet	
6.3	Plate - F_1 folds	
6.4	Typical F_2 folds	S13213
6.5	Plate - F_2 fold hinges in semipelitic rocks	
6.6	Plate - S_2 fibrolite beards and M_2 feldspar	
6.7	M_2 garnet and L_2 mica lineation	S13754
6.8	Plate - elongate fibrolite pods and dominal S_2 in quartzites	
6.9	Plate - L_2 parallel quartz pods	
6.10	Plate - D_2 fabrics in amphibolites	
6.11	Distribution of strain in idealized folds	S13753
6.12	Development of L_2 lineations	S13755
6.13	Plate - porgressive development of S_2 dominal schistosity	
6.14	F_3 folds in semipelites	S13756
6.15	Plate - F_3 hinges in semipelites	
6.16	Plate - quartz, mica and feldspar textures in tight F_3 folds	
6.17	Plate - S_3 mica	
6.18	Plate - F_3 folds in banded diopside quartzite	

		SADME	Plan No
6.19	Textural categories of quartzites	S13757	
6.20	Regional variation in D_3 quartz textures		
6.21	Plate - dolomite, phlogopite and serpentine textures		
6.22	Plate - clinopyroxene deformation, recovery and recrystallization		
6.23	Plate - D_3 fabrics in the Narridy Creek granite		
6.24	Plate - D_3 recovery and recrystallization of plagioclase		
6.25	Plate - S_3 mica films and tension veins		
6.26	The crystallographic preferred orientation of quartz	78-861	
6.27	Old and new grain relationships in quartzites	S13214	
6.28	Plate - F_m fold hinges and S_m mica		
6.29	Plate - mylonite specimens MY-1 and 2		
6.30	Plate - D_m plagioclase		
6.31	Plate - mylonite specimens MY-3 and 4		
6.32	Plate - slaty mylonit specimens MY-5 and 6		
6.33	Plate - D_m plagioclase and microcline recrystallization		
6.34	Plate - mylonitic "fluid" phase		
6.35	Plate - D_4 features		
7.1	MIneral parageneses of pelitic and semi-pelitic rocks	78-63	
7.2	ACF and AKF diagrams for M_{1-2}	S13758	
7.3	The migmatite zone in relationship to macroscopic folding	S13759	
7.4	Comparative summary of migmatitic and non migmatitic semi-pelites	S13760	
7.5	Chemical restrictions on rocks containing staurolite	S13761	
7.6	M_{1-2} carbonate parageneses	S13762	
7.7	Plate - dolomite-calcsilicate association		
7.8	$T\text{-}X_{CO_2}$ topology for reactions (6) to (10)	S13763	
7.9	Zonation of hornblende colour	78-61	
7.10	P-T conditions of M_1	S13764	
7.11	P-T conditions for M_1 - II	S13765	
7.12	P-T conditons for M_2	S13766	
7.13	$T\text{-}X_{CO_2}$ topology for carbonate rocks during M_3	S13767	

		SAMDE Plan No.
7.14	P-T conditions for M_3	S13768
7.15	Synopsis of M_{1-2}, M_3 and M_4 mineral parageneses and P-T conditions	S13769
8.1	Chronology of events in the Cleve Uplands	S13208
8.2	Interpretative cross section through Middle Camp, Mt. Millar and Mt. Desperate	S13770

Glen, R.A., Laing, W.P., Parker, A.J., and Rutland, R.W.R., (1977) Tectonic relationships between the Proterozoic Gawler and Willyama orogenic domains, Australia.
Journal of the Geological Society of Australia, v. 24 (3-4), pp. 125-150.

NOTE:
This publication is included in the print copy
of the thesis held in the University of Adelaide Library.

It is also available online to authorised users at:

http://dx.doi.org/10.1080/00167617708728975

PORTION OF

EYRE PENINSULA

GEOLOGICAL MAP

PLAN I

BULLETIN No. 37

Map Corners from data available at publication.

136° 00′ 30′ 137° 00′

33° 15′ 30′ 45′ 34° 00′

Bunora R.S. · CARALUE BLUFF · Waddikee R.S. · Caralue R.S. · CARPIE · ROLLER POINT · MT. BOSANQUET · CARAPPEE HILL · DARKE PEAK · DARKE PEAK RANGE · Darke Peak · Konanda R.S. · Mangalo · MT. OLINTHUS · POOTINNIE HILL · Kilroo · Kirkpa R.S. · Karkarook R.S. · Tuckey · Rudall · CLEVE · COWELL · Carpa · Elbow Hill · Germein Point · Taragoro R.S. · Boothby · MT. PRISCILLA · Port Gibbon · Gibbon Point · VERRAN HILL · Verran R.S. · ARNO BAY · Cape Driver · CAPE DRIVER TRIG. · Wharminda R.S. · BLUE RANGE · WHEARE RIDGE · SPENCER GULF · LINCOLN HIGHWAY · FRANKLIN HARBOUR

Qrs · Qtz. · As · Ag · Ac

REFERENCE

PALAEOZOIC CAINOZOIC — QUATERNARY

Qrs — Alluvium, soils, clays, sands and gravels, capped by travertine in parts. Sand dunes.

Conglomerates, grits and sandstone.

? CAMBRIAN

ARCHAEAN — HUTCHISON GROUP

As — Haematite Quartzite: quartzites and cherts with interbedded schist and dolomite.

Quartzite: flaggy to massive and often sericitic.

Undifferentiated Mica schists with minor quartzites, amphibolites, graphite schists, micaceous quartzites and quartz-felspar gneisses; pegmatites abundant.

Dolomites.

FLINDERS GROUP — Undifferentiated Quartz-felspar gneisses; metasediments with minor quartzites, migmatites, schists and amphibolites. Pegmatites abundant.

Quartzite, quartz sericite schists.

Dolomites.

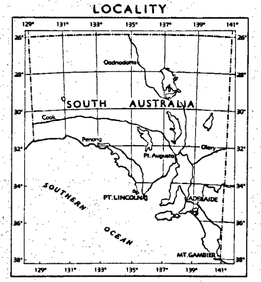
Qtz. — Quartz reefs.

GEOLOGICAL BOUNDARIES
- OBSERVED
- APPROXIMATE
- FAULT SCARP
- BEDDING
- STRIKE AND DIP
- STRUCTURE FORM LINES
- GNEISSOSITY, SCHISTOSITY
- MAIN ROAD
- ROAD
- RAILWAY
- TRIANGULATION STATION
- RIVER OR CREEK
- SWAMP

INDEX TO 1 MILE GEOLOGICAL MAPS

DARKE	GLYNN
RUDALL	COWELL
VERRAN	ARNO

LOCALITY



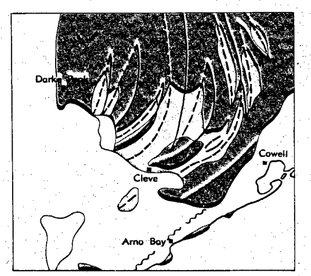
SCALE
4 MILES TO 1 INCH

MILES 2 1 0 2 4 6 8 10 12 14 16 18 20 MILES

KILOMETRES 5 0 5 10 15 20 25 KILOMETRES

H.J. WALL, GOVERNMENT PHOTOLITHOGRAPHER, ADELAIDE

TECTONIC SKETCH



- Quaternary
- ? Cambrian
- Archaean
- Hutchison Group
- Flinders Group
- Anticline
- Syncline
- Fault (inferred)

Geology by R. K. Johns, B.Sc., Senior Geologist.

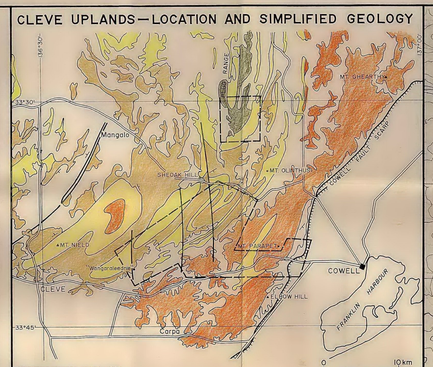
Compiled from published 1 inch to 1 mile geological maps.

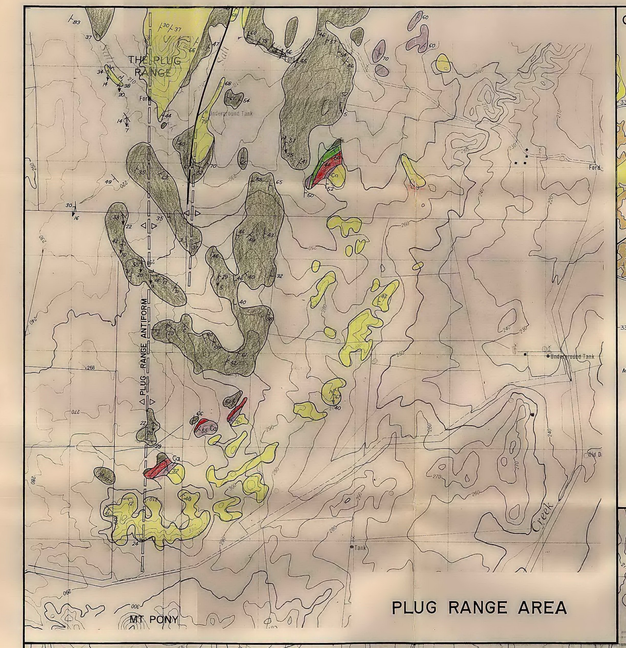
Cartography by Geological Drafting Section, Dept. Mines, S.A.

Published 1959.

78-48

CLEVE UPLANDS—LOCATION AND SIMPLIFIED GEOLOGY





REFERENCE

QUATERNARY

- Alluvium
- Fault breccia
- Quartz dyke

MIDDLE PROTEROZOIC

- Pegmatite and aplite
- NARRIDY CREEK GRANITE: Massive granite in Narridy Creek but granite gneiss west of there.
- MIDDLE CAMP GRANITE: Granite gneiss and granodiorite gneiss.

LOWER PROTEROZOIC — HUTCHISON GROUP

Ferns area
- Massive dolomite.
- (?) Upper Iron Formation: Banded diopside quartzite.
- Semipelite unit.

- Amphibolite.
- Semipelite unit: (?Cook Gap Schist), layered migmatite gneiss (in Mt. Millar, Ferns, Morowie, Mindrow Ck areas) quartzo-feldspathic gneiss and schist (in Wangaraleednie, Sheoak Hill, Yalpoudnie areas).
- Amphibolite; massive, medium grained schistose amphibolite and minor porphyroblastic amphibolite.
- Lower (?Middleback) Iron Formation: Banded diopside quartzite and grunerite schist.
- Dolomite: Massive to poorly layered.
- Pelitic schist.
- WARROW QUARTZITE: Massive to flaggy muscovite-feldspar quartzite with minor interbanded pelitic schist and gneiss.
- Pelitic sillimanite gneiss (podded).
- Well layered calc-silicate (Ca) and massive dolomite.
- Diopside-tremolite rock.
- Migmatite gneiss.

?ARCHAEAN

- (?) FLINDERS GROUP: Granite and augen gneiss with conformable amphibolite bands.

Faults
F3 Fold axes
Antiform
Synform
Dominant foliation
Si-2 (Hutchison Group)
S2 (Middle Camp Granite)
S3 (Narridy Creek Granite)
Mesoscopic F3 Folds (with vergence)
L3 Lineations (Narridy Creek Granite)
Abandoned mine

KILOMETRES 0 2 3 4 KILOMETRES
CONTOUR VALUES IN METRES

GEOLOGICAL MAP OF THE COWELL—CLEVE DISTRICT EASTERN EYRE PENINSULA

Drawn · A.F. DEPARTMENT OF MINES AND ENERGY — SOUTH AUSTRALIA J. Parker · Jan. 1978

Plan No. 2

78-161